Regulation and signalling of endothelial RHO GTPases

Inaugural-Dissertation

Zur

Erlangung des Doktorgrades der
Mathematisch-Naturwisshenschaftlichen Fakultät
der Heinrich-Heine-Universität Düsseldorf

vorgelegt von

Ehsan AMIN

Aus Esfahan, Iran

Düsseldorf, December 2016

Aus dem Institute für Biochemie und Molekularbiologie II
der Heinrich-Heine-Universität Düsseldorf

Gedruckt mit der Genehmigung der
Mathematisch-Naturwisshenschaftlichen Fakultät der
Heinrich-Heine-Universität Düsseldorf

Supervisor: Prof. Mohammad Reza AHMADIAN
Co-supervisor: Prof. Georg GROTH

Tag der mündlichen Prüfung: 22.12.2016

Eidesstattliche Erklärung

Hiermit erkläre ich, Ehsan AMIN, an Eides statt, dass ich die hier vorgelegte Dissertation eigenständig und ohne unerlaubte Hilfe angefertigt habe. Es wurden keinerlei andere Quellen und Hilfsmittel, außer den angegebenen, benutzt. Zitate aus anderen Arbeiten wurden kenntlich gemacht. Diese Dissertation wurde in der vorgelegten oder einer ähnlichen Form noch bei keiner anderen Institution eingereicht und es wurden bisher keine erfolglosen Promotionsversuche von mir unternommen.

Signed: Ehsan AMIN

Date: Düsseldorf, December 2016

"Science is a way of life. Science is a perspective. Science is the process that takes us from confusion to understanding in a manner that's precise, predictive and reliable - a transformation, for those lucky enough to experience it, that is empowering and emotional."

Brian Greene

Abstract

Small GTPases of RHO and RAS families tune timing of signal transduction and regulate many biological functions, such as actin dynamics, proliferation and differentiation. Their abnormal activation plays a crucial role especially in cardiovascular diseases and cancer. Strikingly, 26 human RAS and 20 RHO proteins together with numerous regulators (GEFs, GAPs and GDIs) and effectors make the study of biological pathways rather versatile. To gain new insights into disease treatment strategies, comprehensive study of the interaction networks of these GTPases is required, as aimed of the present dissertation. It has been shown that RAC1 pathway regulates platelet activation, which has been proposed to be blocked by RAC1 inhibitors. But here, we demonstrated that this effect arises partly from inhibition of PAK1, a RAC1 effector. Similarly, Roc-A, a RAF inhibitor that blocks cancer cell proliferation, also inhibits cancer cell migration and invasion by interfering with the activities of RHOA, RAC1 and CDC42, the master regulators of cellular migration. We provide evidence that these inhibitory effects may emerge from early upstream events and not from inhibition of GEFs, GAPs or GDIs. p115RhoGEF, a specific RHOA GEF, plays a critical role in increasing endothelial permeability. Measuring rate constants of all steps of p115-catalyzed nucleotide exchange reaction and the cellular concentrations of RHOA and p115 enabled us to estimate the lifetime of RHOA activation in endothelial cells. RHOGAPs play a critical role in regulation of endothelial permeability but only a few of them are studied. Existence of 66 RHOGAPs in human proteome and availability of large structural data guided us to investigate their specificities for RHO proteins. Our meta-analysis demonstrates a broad range of catalytic efficiencies of RHOGAPs towards RHO proteins. Moreover, we have proposed that p190RHOGAP, a central enhancer of endothelial barrier function, is also able to inactivate RHOD. In addition, we describe how the GAP activity of DLC tumor suppressors is physically inhibited by p120RASGAP. We have accomplished a similar study describing the binding modes of various effectors with different members of RAS family. Hence, five distinct regions determine RAS binding to RAS associating (RA) and RAS binding (RB) domains of various effectors. ROCK is a main regulator of actin-myosin contraction by phosphorylating and inactivating MLCP. Its hyper-activation leads to various cardiovascular diseases, such as cerebral vasospasm and hypertension. Using electron microscopy, we provide structural insights into an elongated parallel dimer of purified ROCK full-length. We propose that scaffold proteins may modulate ROCK autoregulation in the cellular context. Notably, we found that deficiency of CNTF, a cytokine, protects against AngII-dependent hypertension, through phosphorylation of MLCP. One of the scaffold proteins is NPM, which is known to regulate centrosome duplication triggered by RAN activation. Our biochemical data reveal for the first time direct interaction of NPM with viral proteins and may thus promote infection. Another vital scaffold protein is IQGAP1, which regulates endothelial barrier functions via physical association with GTP-bound, active RAC1 and CDC42 proteins. Here we provide insights into the mechanism of these interactions. It seems that in order to understand the complexity of signal transduction mediated through molecular switches of RAS and RHO families, the functions of their poorly characterized members needs detailed investigations.

Zusammenfassung

Kleine GTPasen der RHO und RAS Familie sind zentrale Schalter zur zeitlichen Feinabstimmung von Signaltransduktionsprozessen. Sie regulieren somit wichtige biologische Prozesse wie Aktin-dynamik, Proliferation und Differenzierung. Eine abnormale Aktivierung dieser Proteine spielt vor allem eine maßgebliche Rolle bei kardiovaskulären Erkrankungen und Krebs. Die genaue Analyse der zugrunde liegenden Signalwege wird durch die Anzahl verschiedener RAS (26) und RHO (20) Proteine und ihr Zusammenspiel mit einer Vielzahl an Regulatoren (GEFs, GAPs und GDIs) und Effektoren erschwert. Um Erkenntnisse für die Entwicklung neuartiger Behandlungsstrategien zu gewinnen, ist es nötig, die Interaktionsnetzwerke dieser kleinen GTPasen aufzuklären. Die Unter-suchung dieser Interaktionen war Ziel dieser Dissertation. Es ist gezeigt worden, dass eine RAC1-vermittelte Regulation der Plättchen-Aktivierung durch RAC1-Inhibitoren blockiert wird. In dieser Arbeit zeigen wir, dass dieser Effekt zum Teil auf einer Inhibition von PAK1, einem RAC1 Effek-tor, beruht. Gleichermaßen hemmt Roc-A, ein Inhibitor der RAF-Kinase nicht nur die Proliferation von Krebszellen, sondern darüber hinaus auch die Krebszellmigration und -Invasion via RHOA, RAC1 und CDC42 als Hauptregulatoren der Zellmigration. Die Wirkung von Roc-A beruht sehr wahrscheinlich auf der Inhibition von Upstream-Signalen und nicht auf der Inhibition von Rho-spezifischen Regulatoren, wie GEFs, GAPs oder GDIs. P115RhoGEF, ein spezifischer GEF von RHOA, spielt eine wichtige Rolle in der endothelialen Permeabilität. Durch die Bestimmung der Geschwindigkeitskonstanten einzelner Schritte der p115-katalysierten Nukelotidaustauschreak-tion, sowie der zellulären Konzentrationen von RHOA und p115, haben wir die Dauer der RHOA-Aktivierung in Endothelzellen ermittelt. Trotz ihrer Schlüsselrolle bei der Regulation der endothe-lialen Permeabilität sind nur einige wenige der 66 RHOGAPs untersucht. Aufgrund der zahlreich vorliegenden Strukturdaten für die RHOAGAPs im humanen Proteom, haben wir deren Aktiv-ität und Spezifität für verschiedene RHO-Proteine untersucht. Unsere Metaanalyse zeigt eine bre-ite katalytische Effizienz von RHOGAPs für die RHO-Proteinen. Des Weiteren schlagen wir vor, dass p190RHOGAP (ein zentraler Regulator der endothelialen Permeabilität) neben RHOA auch RHOD inaktiviert. Wir beschreiben zusätzlich die direkte Inhibition der GAP-Aktivität von DLC-Tumorsuppressoren durch p120RASGAP. In einer weiteren Studie beschreiben wir die Spezifität von verschiedenen RAS-Effektoren, die durch ihre RAS-Assoziation- (RA-) und RAS-Bindungs- (RB-) Domänen an fünf definierte Regionen an der Oberfläche von RAS-Proteinen binden. Der RHOA-Effektor ROCK reguliert die Kontraktion vom Actomyosin durch MLCP-Phosphorylierung und -Inaktivierung, und führt somit bei einer Hyperaktivierung zu kardiovaskulären Erkrankun-gen, wie Vasospasmen zerebraler Gefäße und Bluthochdruck. Elektronenmikroskopische Unter-suchungen zeigten ein langgestrecktes paralleles Dimer von gereinigtem volle-Länge ROCK. Diese Daten legen die Hypothese nahe, dass ROCK-Aktivität in der Zelle zusätzlich durch Scaffold-Proteine moduliert wird. In einer anderen Arbeit zeigen wir, dass eine CNTF-defizienz durch MLCP-Phosphorylierung vor dem Angiotensin II-induzierten Bluthochdruck schützt. Ein anderes, wichtiges Scaffold-Protein ist NPM, welches die RAN-aktivierte Zentrosomduplikation reguliert. In einer biochemischen Studie beschreiben wir erstmalig die direkte Interaktion von NMP mit viralen Proteinen. Ein weiteres für die Aufrechterhaltung der endothelialen Barriere wichtiges Scaffold-Protein ist IQGAP1, das durch physikalische Interaktionen mit den GTP-gebundenen Formen von RAC1 und CDC42 reguliert wird. Um die Komplexität der Signaltransduktion, die durch die molekularen Schalter der RAS und RHO Familien vermittelt wird, besser zu verstehen, scheint eine detailliertere Untersuchung der Funktionen von bisher noch nicht charakterisierten Mitgliedern dieser Proteinfamilien unerlässlich zu sein.

Acknowledgements

Firstly, I would like to express my sincere gratitude to my advisor Prof. Mohammad Reza Ahmadian for the continuous support of my PhD study and related research, for his patience, motivation, and immense knowledge. His guidance helped me in all the time of research and writing of this thesis. I could not have imagined having a better advisor and mentor for my Ph.D study. I thank Prof. Georg Groth for his guidances during whole time of my study as a PhD student. Besides my advisor, I would like to thank Dr. Radovan Dvorsky for great bioinformatic helping and discussions during my PhD work. I thank my friends in Düsseldorf for the stimulating discussions, for the sleepless nights we were working together, and for all the fun we have had in the last five years. Especially friends with whom I have started my PhD, Hossein nakhaeizadeh, Kazem Nouri and Saeideh Nakhaeirad. We were really a team together and I had always their supports.

I owe a special thanks to my family, my mom and dad, my brother javad and my sisters Shanhnaz and Mahnaz who supported me and helped me throughout my life and during this study. Mom, dad I do not know how to thank you enough for providing me all supports to be where I am today. I love you so much.

I greatly appreciate the manner, patience and help of my mother and father in law who always supported me and kept my heart warm.

I also dedicate this PhD thesis to my lovely son, Saman who is the pride and joy of my life. I love you more than anything and I appreciate all your patience during baba's Ph.D. studies.

Finally, and most importantly, I would like to thank my wife Leila. Her support, encouragement, quiet patience and unwavering love were undeniably the bedrock upon which the past ten years of my life have been built. Her tolerance of my occasional vulgar moods is a testament in itself of her unyielding devotion and love. I love you for everything, for being so understanding and for putting up with me through the toughest moments of my life.

Contents

List of Figures

List of Tables

List of Abbreviations

aa	amino acids
ACK	CDC42-associated tyrosine kinase
AD	acidic domain
AEDANS	(5-(2-[(iodoacetyl)amino]ethylamino)naphthalene-1-sulfonic acid)
AID	Auto inhibitory domain
AJs	Adherent junctions
ARF	ADP ribosylation factor
Arp2 /3	actin-related proteins 2/3
aSEC	analytical SEC
CBB	coomassie brilliant blue
CDC42	cell division control protein 42 homolog
CHD	calponine homology domain
CNTF	Ciliary neurotrophic factor
CRD	Cysteine rich domain
CRIB	CDC42/RAC-interactive binding
DLC	Deleted in liver cancer
DNA	deoxyribonucleic acid
e.g.	exempli gratia, for example
EC	Endothelial cells
EP	Endothelial permeability
ERK	extracellular regulated kinase
FAK	Focal adhesion kinase
FL	full-length
FMRP	fragile X mental retardation protein
FTIs	Farnesyl transferase inhibitors
GAP	GTPase-activating protein
GDI	guanine nucleotide dissociation inhibitor
GDP	guanosine diphosphate
GEF	guanine-nucleotide-exchange factor
GGTIs	GeranylGeranyl trasnferase inhibitors
GTP	guanosine triphosphate

GTPases	guanosine triphosphatases
HR1	Homology region 1
HVR	hypervariable region
IP	Immunoprecipitation
IQ	protein sequences containing Iso/Leu and Gln residues
IQGAPs	IQ-domain GTPase- activating proteins
ITC	Isothermal titration calorimetry
kDa	kilo dalton
KRAS	kirsten rat sarcoma
Lis1	lissencephaly 1
MALS	multi angle light scattering
MAPK	mitogen-activated protein kinase
mDia1	mammalian homolog of Drosophila diaphanous
MEK	MAPK/ERK kinase
MLC	Myosin light chain
MLCK	Myosin light chain kinase
MLCP	Myosin light chain phosphatase
NCL	nucleolin
NES	nuclear export signal
NF1	neurofibromatosis type 1
NLS	nuclear localization signals
NoLS	nucleolar localization signal
NPM1	nucleophosmin
OD	oligomerization domain
PAK	p21-activated kinase
PD	pull-down
PDZ	PSD-95, Dlg, and ZO-1/2
PH	Pleckstrin homology
PKC	protein kinase C
RAC	RAS-related C3 botulinum toxin substrate
RAF	rapidly accelerated fibrosarcoma
RAN	RAS-related nuclear protein
RAS	rat sarcoma
RBD	RNA binding domain
RHO	RAS homolog
RNA	ribonucleic acid
ROCK	Rho-associated coiled-coil kinase

RRM	RNA recognition motifs
SBD	Shroom binding doamin
SEC	size exclusion chromatography
SOS	Son of Sevenless
VE	Vascular endothelial
WASP	wiskott?aldrich-syndrome protein
WT	wild type
WW	tryptophan-containing protein domain

Amino acid abbreviations

Ala (A)	Alanine
Arg (R)	Arginine
Asn (N)	Asparagine
Asp (D)	Aspartic Acid
Cys (C)	Cysteine
Gln (Q)	Glutamine
Glu (E)	Glutamic Acid
Gly (G)	Glycine
His (H)	Histidine
Ile (I)	Isoleucine
Leu (L)	Leucine
Lys (K)	Lysine
Met (M)	Methionine
Phe (F)	Phenylalanine
Pro (P)	Proline
Ser (S)	Serine
Thr (T)	Threonine
Trp (W)	Tryptophan
Tyr (Y)	Tyrosine
Val (V)	Valine

Dedicated to my wife Leila and my son Saman

Chapter 1

General Introduction

1.1 Ras superfamily

During the 1960s Jennifer Harvey (Harvey, 1964) and Werner Kirsten (Kirsten et al., 1970) discovered two viruses causing tumors in Rat. The tumor-causing viral genes were named *HRAS* and *KRAS*, for their discoverers (Harvey and Kirsten) and for their ability to cause rat sarcomas. Twenty years later, the activated form of these genes has been found in human bladder carcinoma as first oncogenes (Goldfarb et al., 1982; Pulciani et al., 1982; Shih et al., 1982). Up to date over 150 human members of homologues proteins has been identified as the members of the co-called RAS superfamily, which is divided into five major families on the basis of sequence, structure and functional similarities: RAS, RHO, RAB, ARF and RAN (Wennerberg et al., 2005). Ras superfamily proteins are small (21-25 kDa) GTP-binding proteins, which hydrolyze GTP and function as molecular switches between the GDP-bound OFF and the GTP-bound ON state (Vetter et al., 2001). These small GTPases involve in signal transduction and provide a critical link between receptors at the cell surface and various signaling pathways that regulate a variety of cellular processes. The RAS GTPases involved in regulation of gene expression, cell proliferation, survival and differentiation. RHO GTPases are involved in regulation of actin organization and cytoskeleton. RAB and ARF GTPases are involved in vesicular trafficking, regulating endocytosis and secretory pathways. RAN is involved in nuclear–cytoplasmic transport and mitotic spindle organization (Vigil et al., 2010). Structurally small GTPases contain a 20 kDa core G domain, which is conserved among all Ras superfamily proteins and is involved in GTP binding and hydrolysis (Wittinghofer et al., 2011). GTPases have additional carboxy-terminal hyper-variable region (HVR) that commonly undergo post-translational modification to be involved in membrane interaction (Konstantinopoulos et al., 2007).

1.1.1 Mechanism of GTPase activity

The first three dimensional structure of HRAS has been solved by X-Ray crystallography by group of Wittinghofer in 1990 (Pai et al., 1990). The mechanism of GTP hydrolysis of

HRAS has been elucidated in details. Water molecule in active site is activated for the nucleophilic attack to γ-phosphate by polarization via hydrogen bonding from the carbonyl part of Q61 side chain. The magnesium ion (Mg^{2+}) coordinated to β- and γ-phosphates and therefore assists GTP hydrolysis either by increasing the electrophilicity of the γ-phosphate group or by increasing the acidity of the leaving group, GDP (Figure 1.1) (Pai et al., 1990). The GDP/GTP exchange and GTP hydrolysis reactions lead to conformational changes at two regions, called switch I and II. These regions in the GTP-bound RAS are also involved in signal transduction by physically contacting the downstream effectors (Scheffzek et al., 1997).
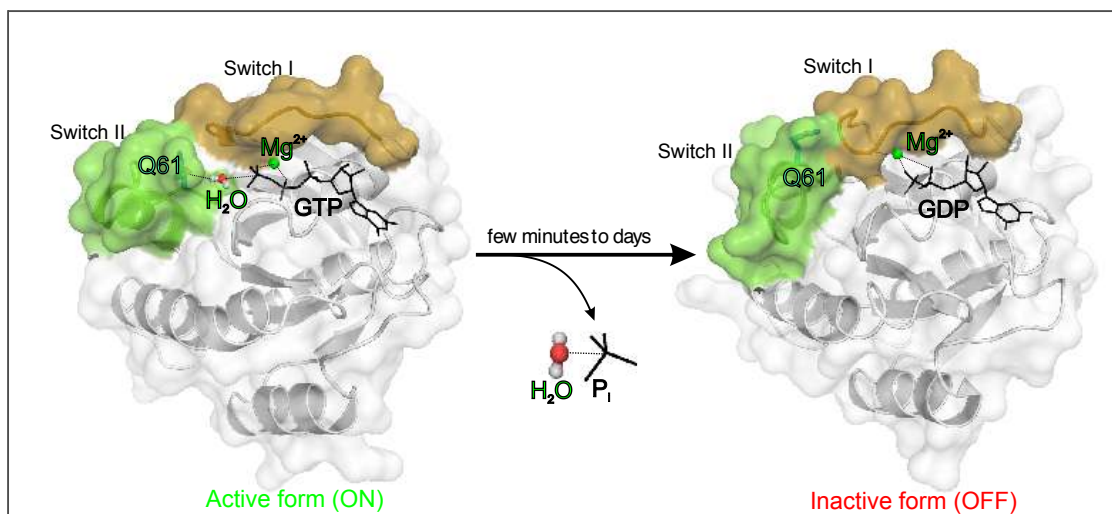
FIGURE 1.1: The mechanism of the GTP hydrolysis by RAS. Left panel shows the active (ON) form of HRAS (GTP form; protein data base or PDB ID: 5p21). Switch regions (green and brown) in this state are favorable to bond to effector proteins. Water molecule and γ-phosphate are coordinated by Mg^{2+} ion and carbonyl group of Q61 side chain for both nucleophilic attack and hydrolysis of γ-phosphate. Right panel shows the inactive (OFF) form of H-RAS (GDP form; PDB ID: 1aa9). GDP/GTP exchange and GTP hydrolysis control the conformational switch of the proteins.

1.1.2 Regulation of GTPases

GTPases are molecular switches, which are timely regulated between ON and OFF states. Their GDP/GTP cycle is tightly controlled by two classes of proteins (Figure 1.2): i) Guanine nucleotide Exchange Factors (GEFs) catalyze the exchange of bound GDP for the more abundant GTP and switch on GTPases; ii) GTPase Activating Proteins (GAPs) stimulate the low intrinsic GTP hydrolysis and thus switch off GTPases. In their active GTP-bound state, they have the ability to interact with a large variety of so-called effector proteins, which are responsible for their various effects (Figure 1.2) (S.-C. Zhang et al.,

2014). Intrinsic rate of GTP hydrolysis can be accelerated by GAP proteins by a factor of 10^5 (Rensland et al., 1991; Ahmadian et al., 1997b; Ahmadian et al., 1997a). On the other hand, intrinsic life time of GTPases inactivation, 16 hours, drops to 30 mili-seconds. Also, the acceleration of GDP dissociation from Ras by GEFs is more than 105 fold. For example life time activation of HRAS could be shortened from 9 hours to 140 ms in the presence of its GEF Son of sevenless (SOS) (Lenzen et al., 1998). So, in this way GTPase regulation is critical point in timing of signal transductions in the cell.
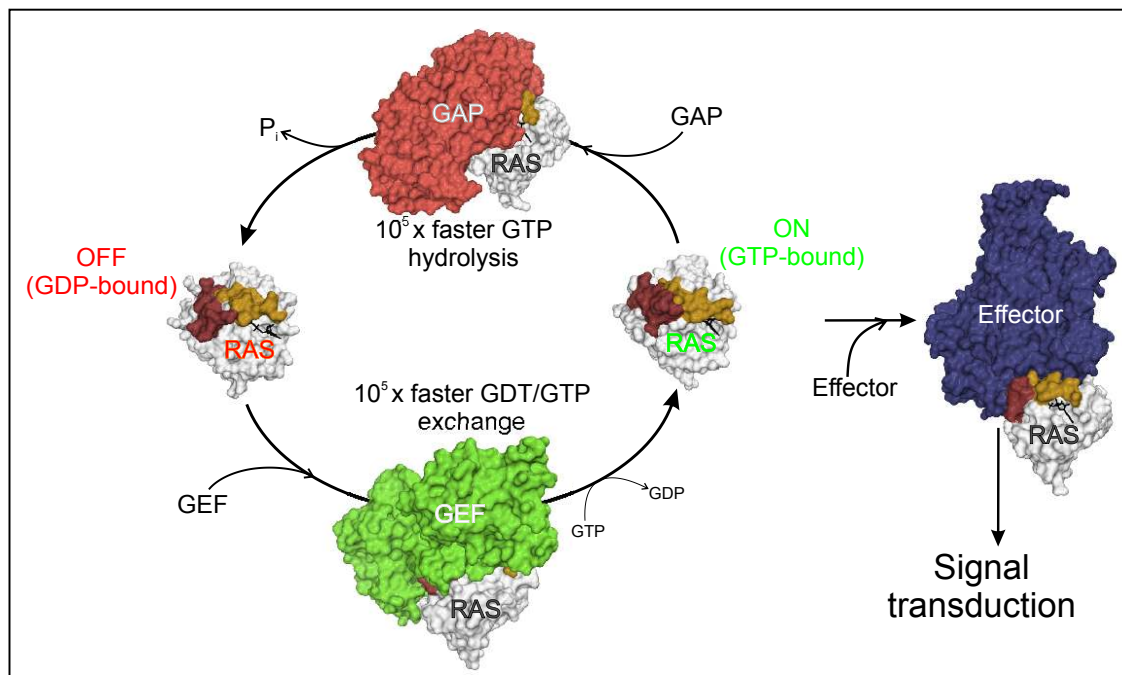
FIGURE 1.2: RAS GTPase regulation cycle. Switch I and II regions of HRAS are colored brown and orange (HRAS-GDP; Protein Data Bank Acc No.: 1aa9) (Ito et al., 1997). Binding of p120GAP (colored red) to HRAS accelerates GTP hydrolysis by 5 order of magnitude (HRAS-p120GAP; 1WQ1) (Scheffzek et al., 1997). GEF association of HRAS speeds up nucleotide exchange up to xxx orders (HRAS-SOS; 4URU) (Winter et al., 2015). GTP-bound HRAS binds to effector proteins and promotes downstream signaling (HRAS-PI3K; 1he8) (Pacold et al., 2000).

1.1.3 Mechanism of GAP-stimulated GTPase reaction

Stimulation of the intrinsic GTPase activity of GTP-binding proteins by GAPs is a basic principle of GTP-binding protein down-regulation. The molecular mechanism behind this reaction has been elucidated. GAP provides an arginine (the arginine finger) to stabilize the partial negative charges that develop at the transition state, and it positions the conserved glutamine from the switch II (Gln61 in RAS) to activate a water molecule

for in-line nucleophilic attack of the γ-phosphate of GTP, eventually establishing a bona fide enzymatic active site (Ahmadian et al., 1997b; Cherfils et al., 2013). AlF$_3$ activates GTPases, like RAS, in their inactive GDP-bound state, mimicking γ-phosphate of GTP in the transition state only in the presence of GAP (Mittal et al., 1996). Crystal structure of GDP-AlF$_3$-bound HRAS-p120RASGAP shows complementation of the HRAS active site (Figure 1.3) (Scheffzek et al., 1997).
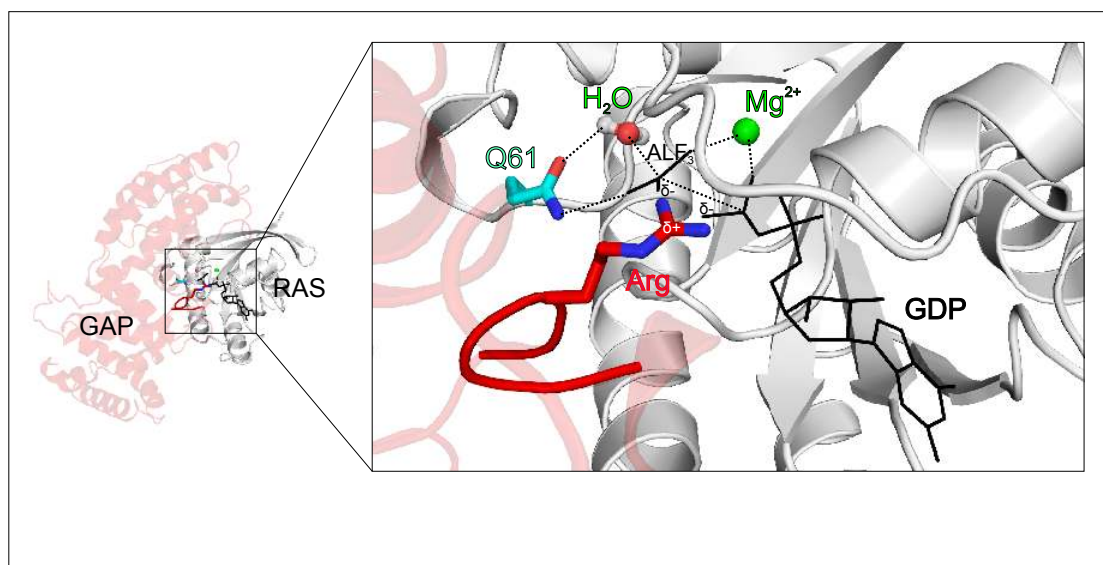
FIGURE 1.3: Mechanism of GAP-stimulated GTP hydrolysis explored by the crystal structure of the RAS-GDP-AlF$_3$-p120RASGAP complex (1WQ1). ALF$_3$ (γ-phosphate) is coordinated with Mg^{2+} ion and undergoes nucleophilic attack by water with contribution of glutamine residue of HRAS. Arginine finger of GAP with partially positive charges stabilizes partial negative charges of β- and γ-phosphates and lower down the energy level leads to acceleration of GTP hydrolysis.

1.1.4   Mechanism of Guanine nucleotide exchange factors

The biochemical roles of GEFs are postulated as stimulating the release of the bound GDP and stabilizing a nucleotide-free transition state of RAS (Bos et al., 2007). The crystal structure of human HRAS in complex with the catalytic GEF domain of the SOS protein has been determined. The normally picomolar affinity of nucleotides with RAS is disrupted by SOS in two ways: i) the insertion of a α-helix from SOS into RAS opens the nucleotide binding site as a result of the switch I displacement, ii) side chains presented by this helix and by a distorted conformation of the switch II region of RAS alter the chemical environment of the binding site for the phosphate groups of the nucleotide

and the associated magnesium ion, such that their binding is no longer favored (Figure 1.4). The RAS-SOS complex adopts a structure that allows nucleotide release and rebinding (Boriack-Sjodin et al., 1998). Cellular GTP concentration is approximately ten times higher than GDP, resulting in a GTP-bound state in cells upon interaction with GEF (Bennett et al., 2009).
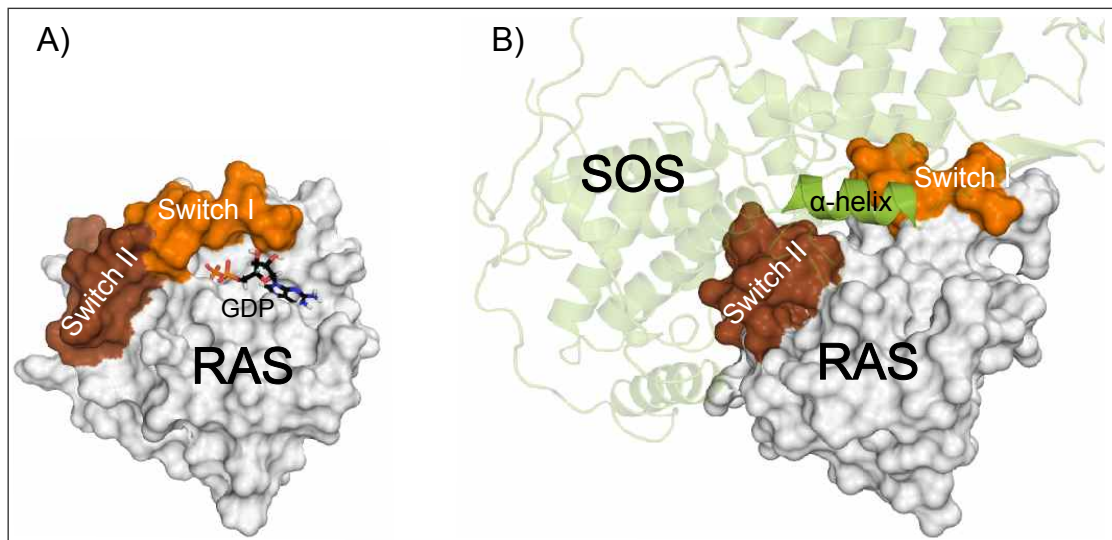
FIGURE 1.4: Mechanism of the GEF-catalyzed nucleotide exchange of HRAS. A) GDP-bound HRAS structure (1aa9). B) HRAS-SOS complex structure (1bkd). Highlighted α-helix (green) is inserted to the switch regions, which leads to their conformational change and causes a strong decrease in nucleotide dissociation.

1.2 Ras subfamily

RAS is the prototypical member of the RAS superfamily. These proteins are usually small GTPases involved in a variety of cellular processes, ranging from intracellular metabolisms to proliferation and differentiation as well as embryogenesis and normal development (Brossier et al., 2015; Karnoub et al., 2008; Nakhaei-Rad et al., 2016). The most characterized RAS proteins are HRAS, KRAS and NRAS, which are the most common oncogenes in human cancer. When RAS is switched on by extracellular signals, it subsequently activates cascades involved in cell growth, survival and differentiation (Coleman et al., 2004; Wittinghofer et al., 1997). Therefore, its mutation, found human cancers, cause hyperactive RAS proteins following constitutive signal transduction inside the cell, which result in cell growth and division and consequently to cancer even in the absence of extracellular signals. In addition to RAS isoforms there are other members

of the RAS family, including the RRAS proteins (RRAS, RRAS2/TC21, RRAS3/MRAS), the RAL proteins (A and B), the RAPs (1A, 1B, 2A, and 2B) and RHEB (**Reuther00**).

1.2.1   RAS effectors

In their GTP-bound state, RAS proteins physically interact with their downstream effector proteins, triggering activation of multiple signaling pathways with complex and divergent effects ([Figure 1.5](#)) (Kyriakis, [2009](#)). RAS effectors have been reported to contain conserved regions, designated as RAS binding (RB) or RAS association (RA) domains, which interact with switch regions of RAS (Fiegen et al., [2006](#)). Best-studied effectors are the RAF (named for Rapidly Accelerated Fibrosarcoma) kinases, phosphatidyl inositol 3'-OH kinase (PI3K), RAL Guanine nucleotide dissociation stimulator (RALGDS), PLC-ε as an isozyme of phospholipase C (PLC) family, and the RAS-association domain family (RASSF5) (Donninger et al., [2016](#); Katz et al., [1997](#)).

The RAF kinases (A, B and C) are Ser/Thr protein kinases that function as direct activators of MAPK (Mitogen-Activated Protein Kinases) pathway (Matallanas et al., [2011](#)). MAPK pathway is evolutionarily conserved and represents a major mechanism by which mitogens stimulate cell proliferation.

The PI3Ks are lipid kinases that phosphorylate phosphatidyl inositol specifically on the inositol 3'-OH group thereby generating for example PI-3,4,5- trisphosphate (PIP3). PIP3 is an important second messenger with which plekstrin homology (PH) domain-containing proteins, thereby fostering the assembly of signaling complexes. Typically, PI3Ks are recruited to the membrane by their Src homology-2 (SH2) domains (binding to p-Tyr), and bind via their RBD domains to active RAS proteins. PI3K activity is required for the activation of Ser/Thr kinases of the AKT family, which various processes, including apoptosis and survival (Castellano et al., [2011b](#); Castellano et al., [2011a](#); P. Liu et al., [2009](#)).

PLC-ε contains a C-terminal RAS association (RA) domain and an N-terminal RASGEF domain, which suggests its bifunctional regulatory potential as both an activator and an effector of RAS (Wing et al., [2003](#)).

RALGDS is a GEF specific for the RAL proteins, RALA and RALB. RAL proteins regulate vesicular trafficking within the cell. RAS, through RAL, triggers activation of RALBP1 and regulates receptor-mediated endocytosis (Neel et al., [2011](#)).

RASSF had been described as RA-containing RAS effectors, characterized by their ability to inhibit cell growth and proliferation while promoting cell death. RASSF1 isoform A is an established tumor suppressor and is frequently silenced in a variety of tumors (Gordon et al., [2012](#)).

It is evident that RAS proteins are part of a complex network of signaling nodes, rather than discrete components of linear pathways. The complexity of RAS protein regulation,

and the continuing identification and characterization of RAS targets with novel functions have cast aside old models of signal transduction.
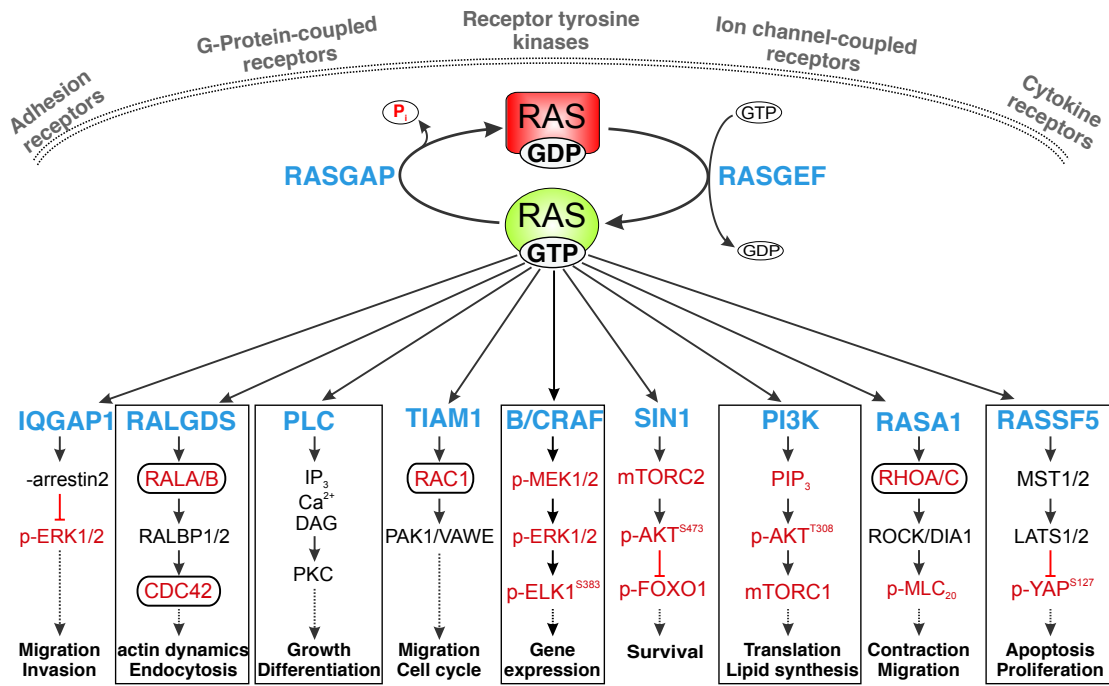
FIGURE 1.5: RAS effectors and downstream pathways. Once activated by diverse stimuli at the plasma membrane, RAS proteins signal through multiple effectors and activate various different signaling pathways. Most of these pathways are involved in proliferation, differentiation and apoptosis. The best-characterized pathways are the RAF-MEK-ERK (MAPK) pathway, the PI3K pathway and the RAL pathway, as described in text. MEK: MAPK/ERK kinase; ERK: extracellular signal-regulated kinase.

1.3 RHO subfamily

RHO (Ras Homologue) GTPases, another family of the RAS superfamily, are ubiquitously expressed and 20 classical members have been identified in human (Table 1.1) (Consortium, 2015). In terms of structure RHO proteins have an extra α-helix (called insert region) as compared to the RAS structure. Its function is not fully understood, yet (Zong et al., 2001). RHO GTPases mostly are molecular switches that control a wide variety of signal transduction pathways in all eukaryotic cells, regulating the actin cytoskeleton, cell polarity, microtubule dynamics, membrane transport pathways and transcription factor activity (Jaffe et al., 2005; Raftopoulou et al., 2004). RHOA, RAC1 and CDC42 are the best-characterized members so far. RHOA regulates the assembly of contractile, actin myosin filaments, while RAC1 and CDC42 regulate the polymerization of

actin to form peripheral lamellipodial and filopodial protrusions, respectively (Etienne-Manneville et al., 2002; Raftopoulou et al., 2004). In addition, all three GTPases promote integrin engagement with adhesion complexes (Lawson et al., 2014). Therefore, these regulatory proteins play a critical role in controlling cell migration. Most notably, CDC42 is required for the establishment of cell polarity and cooperates with other GTPases to affect cell adhesion and stress fibers to promote cell movement (Nobes et al., 1999).

The RHO GTPase cycle is tightly regulated by three groups of proteins as discussed before. RHOGEFs promote the exchange of GDP for GTP to activate the GTPase and RHOGAPs negatively regulate the switch by enhancing its intrinsic GTPase activity. GDP-dissociation inhibitors (GDIs) are third regulators and thought to block the GTPase cycle by sequestering the GDP-bound form from membrane (Dovas et al., 2005). Extracellular signals could regulate the switch by modifying any of these proteins, predominantly acting through GEFs. Once activated, RHO GTPases interact with cellular target proteins (effectors) to generate a downstream response (Raftopoulou et al., 2004). To date, more than 100 effectors, 70 GEFs and 60 GAPs have been described for the human RHO family (Amin et al., 2016; Consortium, 2015; Jaiswal et al., 2013).

1.3.1   RHOGDIs

Interestingly, in contrast to other regulators there are only three RHO-specific GDI members in human proteome (Table 1.2) (Consortium, 2015). At any given time, only a small fraction of all RHO GTPases present in the cell are in the active state and are associated with membranes. The inactive pool is maintained in the cytosol by associating with RHOGDIs (Garcia-Mata et al., 2011). It has been shown that depletion of RHOGDI promotes misfolding and degradation of the cytosolic geranylgeranylated pool of RHO GTPases (Boulter et al., 2010). So, RHOGDI system plays an important role in spatial determination in the actin cytoskeletal control (Sasaki et al., 1998).

1.3.2   RHOGAPs

Slow intrinsic GTPase activity of RHO proteins is greatly enhanced by RHOGAPs, thus inactivation RHO GTPases and terminating the signal (Cherfils et al., 2013; Scheffzek et al., 1998). 66 RHOGAPs exist in human proteome (Table 1.3) (Amin et al., 2016). Large number of RHOGAPs and their structural complexity demonstrate that we are still far from fully understanding where, when and how they operate (Tcherkezian et al., 2007; Amin et al., 2016). Cellular processes are complex because they involve several interacting components, sometimes located in different organelles. Cellular events involve many scales of distance and time. Events such as activation of cell surface receptors and

TABLE 1.1: Human RHO family proteins

Nr.	Entry	Gene names	Protein names	Length
1	P60953	CDC42	Cell division control protein 42 homolog (G25K GTP-binding protein)	191
2	P63000	RAC1	Ras-related C3 botulinum toxin substrate 1 (Cell migration-inducing gene 5 protein) (Ras-like protein TC25) (p21-Rac1)	192
3	P15153	RAC2	Ras-related C3 botulinum toxin substrate 2 (GX) (Small G protein) (p21-Rac2)	192
4	P60763	RAC3	Ras-related C3 botulinum toxin substrate 3 (p21-Rac3)	192
5	O94844	RHOBTB1	Rho-related BTB domain-containing protein 1	696
6	Q9BYZ6	RHOBTB2	Rho-related BTB domain-containing protein 2 (Deleted in breast cancer 2 gene protein) (p83)	727
7	P61586	RHOA	Transforming protein RhoA (Rho cDNA clone 12) (h12)	193
8	P62745	RHOB	Rho-related GTP-binding protein RhoB (Rho cDNA clone 6) (h6)	196
9	P08134	RHOC	Rho-related GTP-binding protein RhoC (Rho cDNA clone 9) (h9)	193
10	O00212	RHOD	Rho-related GTP-binding protein RhoD (Rho-related protein HP1) (RhoHP1)	210
11	Q9HBH0	RHOF	Rho-related GTP-binding protein RhoF (Rho family GTPase Rif) (Rho in filopodia)	211
12	P84095	RHOG	Rho-related GTP-binding protein RhoG	191
13	Q15669	RHOH	Rho-related GTP-binding protein RhoH (GTP-binding protein TTF) (Translocation three four protein)	191
14	Q9H4E5	RHOJ	Rho-related GTP-binding protein RhoJ (Ras-like protein family member 7B) (Tc10-like GTP-binding protein)	214
15	P17081	RHOQ	Rho-related GTP-binding protein RhoQ (Ras-like protein TC10) (Ras-like protein family member 7A)	205
16	Q7L0Q8	RHOU	Rho-related GTP-binding protein RhoU (CDC42-like GTPase 1) (GTP-binding protein-like 1) (Rho GTPase-like protein ARHU) (Ryu GTPase) (Wnt-1 responsive Cdc42 homolog 1) (WRCH-1)	258
17	Q96L33	RHOV	Rho-related GTP-binding protein RhoV (CDC42-like GTPase 2) (GTP-binding protein-like 2) (Rho GTPase-like protein ARHV) (Wnt-1 responsive Cdc42 homolog 2) (WRCH-2)	236
18	Q92730	RND1	Rho-related GTP-binding protein Rho6 (Rho family GTPase 1) (Rnd1)	232
19	P52198	RND2	Rho-related GTP-binding protein RhoN (Rho family GTPase 2) (Rho-related GTP-binding protein Rho7) (Rnd2)	227
20	P61587	RND3	Rho-related GTP-binding protein RhoE (Protein MemB) (Rho family GTPase 3) (Rho-related GTP-binding protein Rho8) (Rnd3)	244

TABLE 1.2: Human RHOGDI proteins

	Entry	Gene names	Protein names	Length
1	P52565	ARHGDIA	Rho GDP-dissociation inhibitor 1 (Rho GDI 1) (Rho-GDI alpha), GDIR1	204
2	P52566	ARHGDIB	Rho GDP-dissociation inhibitor 2 (Rho GDI 2) (Ly-GDI) (Rho-GDI beta), GDIR2	201
3	Q99819	ARHGDIG	Rho GDP-dissociation inhibitor 3 (Rho GDI 3) (Rho-GDI gamma), GDIR3	225

other individual signaling reactions are very fast and happen within from fraction of seconds to several seconds. Cascades of individual intracellular signaling pathways, mostly within the cytosol, operate at the time scale of from several seconds to minutes. Finally, nuclear signaling events such as activation of transcription factors and translocation of such molecules to the nucleus also occur within minutes. Events such as gene expression, translation and protein translocation occur on a time scale of several hours, and sometimes days (Maurya et al., 2010). RHOGAPs as timing regulators are present at various levels.

Photo-transduction in retinal rods is one of fastest processes. The time to peak of the flash response is about 100 ms and the recovery time constant about 200 ms. RGS9 as a GAP for G-proteins is essential for the normal recovery of the light response in rods (Burns et al., 2010). Rate constant of RGS9, which stimulates GTP hydrolysis of Transducin, is about 50 s^{-1} (Burns et al., 2010).

Propagation of neuronal pulses is another fast process. Synaptic terminal in the brain typically contains only 100–200 synaptic vesicles and they must be recycled to maintain efficient neurotransmitter release during ongoing activity. Vesicle recycling lasts from few hundred milliseconds to few seconds. OPHN1 (as a RHOAGP) impairment links to defects in efficient synaptic vesicle retrieval (Gandhi et al., 2003; Nakano-Kobayashi et al., 2009).

Transferrin is an iron-binding protein that facilitates iron-uptake in cells. Its trafficking is an essential process and takes around ten minutes. Depletion of DLC3 (another RHOGAP) impairs the transport of internalized transferrin to the endocytic recycling compartment (ERC) (Braun et al., 2015; Geissbuehler et al., 2012).

Therefore, GAP proteins especially RHOGAPs coordinate many timing processes in cells either by turning off the main cascade to function as a recovery process or opposing signaling pathways to provide stability of main cascade transmission. Hence understanding the efficiency, selectivity and specificity of this family of proteins will unravel many questions of biological processes.

1.3.3 RHOGEFs

The largest family of RHOGEFs is comprised of the DBL family RHOGEFs with 70 human members (Table 1.4)(Jaiswal et al., 2013). They contain a DBL homology (DH) domain, which is the catalytic domain for nucleotide exchange of RHO proteins and activates them within particular spatio-temporal contexts in concert with other domains. The failure to do so can have significant consequences and is reflected in some human diseases (Rossman et al., 2005; Sahai et al., 2002). Recent evidence suggests that these proteins may be potential therapeutic targets for developing drugs to treat various diseases, including cancer (Bos et al., 2007). PDZ-RHOGEF (PRG), leukemia-associated RHOGEF (LARG) and p115RHOGEF (p115) are the best-characterized RHOGEFs, which link GPCRs to RHO activation and are essential for various functions, such as neurite outgrowth, embryonic development, platelet activation and thrombosis and regulation of vascular tone and blood pressure (Guilluy et al., 2010; Lin et al., 2011; Mikelis et al., 2013; Williams et al., 2015).

P115RHOGEF also called ARHGEF1 was identified as a RHOA nucleotide exchange factor involved in angiotensin II –mediated regulation of vascular tone and hypertension (Carbone et al., 2015). Through phosphorylation by protein kinase C, it is responsible for thrombin-induced RHOA activation and downstream signaling toward the endothelial permeability. Similarly, it mediates lipopolysaccharide (LPS-) induced RHOA activation and permeability in brain endothelial cells. p115 is in crosstalk between endothelial integrin and cadherin adhesions, as its enhanced interaction with RHOA, reduced junctional integrity (Buul et al., 2014). In another hand, p115 is required for apical extrusion of apoptotic cells from an epithelium (Slattum et al., 2009). It has been discussed that RHO activity fluctuates on time and length scales of tens of seconds and micrometers (Fritz et al., 2016). Hence, how p115 as a main activator of RHOA is regulating this timing has a crucial importance.

1.3.4 RHO effectors

RHO GTPases physically interact with multiple effector proteins and regulates their activity which contribute to cellular responses (Bishop et al., 2000). Kinases form an important class of RHO effector and result downstream phosphorylation cascades. Different RHO-associated serine/threonine kinases, such as PAK (p21-activated kinase), ROCK (RHO-associated coiled-coil kinase), CRIK (citron kinase) and PKN (protein kinase novel), interact with and are regulated by their partner GTPases (Amin et al., 2013; Narumiya et al., 2009; Zhao et al., 2005). Another group of effectors are scaffolding proteins, probably making a framework for signaling cascades, especially the dynamics of

TABLE 1.3: Human RHOGAP proteins

Nr.	Entry	Gene names	Protein names	Length
1	P27986	PIK3R1	Phosphatidylinositol 3-kinase regulatory subunit alpha (PI3-kinase regulatory subunit alpha) (PI3K regulatory subunit alpha) (PtdIns-3-kinase regulatory subunit alpha) (Phosphatidylinositol 3-kinase 85 kDa regulatory subunit alpha) (PI3-kinase subunit p85-alpha) (PtdIns-3-kinase regulatory subunit p85-alpha)	724
2	Q01968	OCRL	Inositol polyphosphate 5-phosphatase OCRL-1 (EC 3.1.3.36) (Lowe oculocerebrorenal syndrome protein)	901
3	Q9H0H5	RACGAP1	Rac GTPase-activating protein 1 (Male germ cell RacGap) (MgcRacGAP) (Protein CYK4 homolog) (CYK4) (HsCYK-4)	632
4	Q96QB1	DLC1	Rho GTPase-activating protein 7 (Deleted in liver cancer 1 protein) (DLC-1) (HP protein) (Rho-type GTPase-activating protein 7) (START domain-containing protein 12) (StARD12) (StAR-related lipid transfer protein 12)	1528
5	P11274	BCR	Breakpoint cluster region protein (EC 2.7.11.1) (Renal carcinoma antigen NY-REN-26)	1271
6	O00459	PIK3R2	Phosphatidylinositol 3-kinase regulatory subunit beta (PI3-kinase regulatory subunit beta) (PI3K regulatory subunit beta) (PtdIns-3-kinase regulatory subunit beta) (Phosphatidylinositol 3-kinase 85 kDa regulatory subunit beta) (PI3-kinase subunit p85-beta) (PtdIns-3-kinase regulatory subunit p85-beta)	728
7	Q13459	MYO9B	Unconventional myosin-IXb (Unconventional myosin-9b)	2157
8	P32019	INPP5B	Type II inositol 1,4,5-trisphosphate 5-phosphatase (EC 3.1.3.36) (75 kDa inositol polyphosphate-5-phosphatase) (Phosphoinositide 5-phosphatase) (5PTase)	993
9	O75044	SRGAP2	SLIT-ROBO Rho GTPase-activating protein 2 (srGAP2) (Formin-binding protein 2) (Rho GTPase-activating protein 34)	1071
10	Q15311	RALBP1	RalA-binding protein 1 (RalBP1) (76 kDa Ral-interacting protein) (Dinitrophenyl S-glutathione ATPase) (DNP-SG ATPase) (Ral-interacting protein 1)	655
11	A7KAX9	ARHGAP32	Rho GTPase-activating protein 32 (Brain-specific Rho GTPase-activating protein) (GAB-associated Cdc42/Rac GTPase-activating protein) (GC-GAP) (GTPase regulator interacting with TrkA) (Rho-type GTPase-activating protein 32) (Rho/Cdc42/Rac GTPase-activating protein RICS) (RhoGAP involved in the beta-catenin-N-cadherin and NMDA receptor signaling) (p200RhoGAP) (p250GAP)	2087
12	Q96P48	ARAP1	Arf-GAP with Rho-GAP domain, ANK repeat and PH domain-containing protein 1 (Centaurin-delta-2) (Cnt-d2)	1450
13	Q5T5U3	ARHGAP21	Rho GTPase-activating protein 21 (Rho GTPase-activating protein 10) (Rho-type GTPase-activating protein 21)	1957
14	Q9NRY4	ARHGAP35	Rho GTPase-activating protein 35 (Glucocorticoid receptor DNA-binding factor 1) (Glucocorticoid receptor repression factor 1) (GRF-1) (Rho GAP p190A) (p190-A)	1499
15	Q8N264	ARHGAP24	Rho GTPase-activating protein 24 (Filamin-A-associated RhoGAP) (FilGAP) (RAC1- and CDC42-specific GTPase-activating protein of 72 kDa) (RC-GAP72) (Rho-type GTPase-activating protein 24) (RhoGAP of 73 kDa) (Sarcoma antigen NY-SAR-88) (p73RhoGAP)	748
16	Q9Y3M8	STARD13	StAR-related lipid transfer protein 13 (46H23.2) (Deleted in liver cancer 2 protein) (DLC-2) (Rho GTPase-activating protein) (START domain-containing protein 13) (StARD13)	1113
17	P15882	CHN1	N-chimaerin (A-chimaerin) (Alpha-chimerin) (N-chimerin) (NC) (Rho GTPase-activating protein 2)	459
18	B2RTY4	MYO9A	Unconventional myosin-IXa (Unconventional myosin-9a)	2548
19	Q8WWN8	ARAP3	Arf-GAP with Rho-GAP domain, ANK repeat and PH domain-containing protein 3 (Centaurin-delta-3) (Cnt-d3)	1544
20	O43182	ARHGAP6	Rho GTPase-activating protein 6 (Rho-type GTPase-activating protein 6) (Rho-type GTPase-activating protein RhoGAPX-1)	974
21	Q68EM7	ARHGAP17	Rho GTPase-activating protein 17 (Rho-type GTPase-activating protein 17) (RhoGAP interacting with CIP4 homologs protein 1) (RICH-1)	881
22	O43295	SRGAP3	SLIT-ROBO Rho GTPase-activating protein 3 (srGAP3) (Mental disorder-associated GAP) (Rho GTPase-activating protein 14) (WAVE-associated Rac GTPase-activating protein) (WRP)	1099
23	O60890	OPHN1	Oligophrenin-1	802
24	P98171	ARHGAP4	Rho GTPase-activating protein 4 (Rho-GAP hematopoietic protein C1) (Rho-type GTPase-activating protein 4) (p115)	946
25	Q13017	ARHGAP5	Rho GTPase-activating protein 5 (Rho-type GTPase-activating protein 5) (p190-B)	1502
26	Q07960	ARHGAP1	Rho GTPase-activating protein 1 (CDC42 GTPase-activating protein) (GTPase-activating protein rhoGAP) (Rho-related small GTPase protein activator) (Rho-type GTPase-activating protein 1) (p50-RhoGAP)	439
27	Q9Y3L3	SH3BP1	SH3 domain-binding protein 1 (3BP-1)	701
28	Q12979	ABR	Active breakpoint cluster region-related protein	859
29	Q8WZ64	ARAP2	Arf-GAP with Rho-GAP domain, ANK repeat and PH domain-containing protein 2 (Centaurin-delta-1) (Cnt-d1) (Protein PARX)	1704
30	P52757	CHN2	Beta-chimaerin (Beta-chimerin) (Rho GTPase-activating protein 3)	468
31	Q5TB30	DEPDC1	DEP domain-containing protein 1A	811
32	Q8WUY9	DEPDC1B	DEP domain-containing protein 1B (HBV X-transactivated gene 8 protein) (HBV XAg-transactivated protein 8)	529
33	Q9NYF5	FAM13B	Protein FAM13B (GAP-like protein N61)	915
34	O94988	FAM13A	Protein FAM13A	1023
35	Q9P107	GMIP	GEM-interacting protein (GMIP)	970
36	Q92619	HMHA1	Minor histocompatibility protein HA-1 [Cleaved into: Minor histocompatibility antigen HA-1 (mHag HA-1)]	1136
37	P85298	ARHGAP8	Rho GTPase-activating protein 8 (Rho-type GTPase-activating protein 8)	464
38	Q53QZ3	ARHGAP15	Rho GTPase-activating protein 15 (ArhGAP15) (Rho-type GTPase-activating protein 15)	475
39	Q9P227	ARHGAP23	Rho GTPase-activating protein 23 (Rho-type GTPase-activating protein 23)	1491
40	Q6ZUM4	ARHGAP27	Rho GTPase-activating protein 27 (CIN85-associated multi-domain-containing Rho GTPase-activating protein 1) (Rho-type GTPase-activating protein 27) (SH3 domain-containing protein 20)	889
41	O14559	ARHGAP33	Rho GTPase-activating protein 33 (Rho-type GTPase-activating protein 33) (Sorting nexin-26) (Tc10/CDC42 GTPase-activating protein)	1287
42	Q9C0H5	ARHGAP39	Rho GTPase-activating protein 39	1083
43	Q6P4F7	ARHGAP11A	Rho GTPase-activating protein 11A (Rho-type GTPase-activating protein 11A)	1023
44	Q14CB8	ARHGAP19	Rho GTPase-activating protein 19 (Rho-type GTPase-activating protein 19)	494
45	Q7Z5H3	ARHGAP22	Rho GTPase-activating protein 22 (Rho-type GTPase-activating protein 22)	698
46	Q9P2N2	ARHGAP28	Rho GTPase-activating protein 28 (Rho-type GTPase-activating protein 28)	729
47	Q2M1Z3	ARHGAP31	Rho GTPase-activating protein 31 (Cdc42 GTPase-activating protein)	1444
48	Q5TG30	ARHGAP40	Rho GTPase-activating protein 40 (Rho-type GTPase-activating protein 40)	622
49	Q17R89	ARHGAP44	Rho GTPase-activating protein 44 (NPC-A-10) (Rho-type GTPase-activating protein RICH2) (RhoGAP interacting with CIP4 homologs protein 2) (RICH-2)	818
50	Q3KRB8	ARHGAP11B	Rho GTPase-activating protein 11B (Protein FAM7B1) (Rho-type GTPase-activating protein 11B)	267
51	Q7Z6I6	ARHGAP30	Rho GTPase-activating protein 30 (Rho-type GTPase-activating protein 30)	1101
52	A1A4S6	ARHGAP10	Rho GTPase-activating protein 10 (GTPase regulator associated with focal adhesion kinase 2) (Graf-related protein 2) (Rho-type GTPase-activating protein 10)	786
53	Q8IWW6	ARHGAP12	Rho GTPase-activating protein 12 (Rho-type GTPase-activating protein 12)	846
54	Q8N392	ARHGAP18	Rho GTPase-activating protein 18 (MacGAP) (Rho-type GTPase-activating protein 18)	663
55	Q9P2F6	ARHGAP20	Rho GTPase-activating protein 20 (Rho-type GTPase-activating protein 20)	1191
56	P42331	ARHGAP25	Rho GTPase-activating protein 25 (Rho-type GTPase-activating protein 25)	645
57	A6NI28	ARHGAP42	Rho GTPase-activating protein 42 (Rho GTPase-activating protein 10-like) (Rho-type GTPase-activating protein 42)	874
58	Q9BRR9	ARHGAP9	Rho GTPase-activating protein 9 (Rho-type GTPase-activating protein 9)	750
59	Q9UNA1	ARHGAP26	Rho GTPase-activating protein 26 (GTPase regulator associated with focal adhesion kinase) (Oligophrenin-1-like protein) (Rho-type GTPase-activating protein 26)	814
60	Q6ZRI8	ARHGAP36	Rho GTPase-activating protein 36	547
61	Q52LW3	ARHGAP29	Rho GTPase-activating protein 29 (PTPL1-associated RhoGAP protein 1) (Rho-type GTPase-activating protein 29)	1261
62	Q7Z6B7	SRGAP1	SLIT-ROBO Rho GTPase-activating protein 1 (srGAP1) (Rho GTPase-activating protein 13)	1085
63	Q92502	STARD8	StAR-related lipid transfer protein 8 (Deleted in liver cancer 3 protein) (DLC-3) (START domain-containing protein 8) (StARD8) (START-GAP3)	1023
64	Q5VT97	SYDE2	Rho GTPase-activating protein SYDE2 (Synapse defective protein 1 homolog 2) (Protein syd-1 homolog 2)	1194
65	Q6ZW31	SYDE1	Rho GTPase-activating protein SYDE1 (Synapse defective protein 1 homolog 1) (Protein syd-1 homolog 1)	735
66	Q8N103	TAGAP	T-cell activation Rho GTPase-activating protein (T-cell activation GTPase-activating protein)	731

TABLE 1.4: Human RHOGEF proteins

Nr.	Entry	Gene names	Protein names	Length
1	Q12979	ABR	Active breakpoint cluster region-related protein	859
2	Q12802	AKAP13	A-kinase anchor protein 13 (AKAP-13) (AKAP-Lbc) (Breast cancer nuclear receptor-binding auxiliary protein) (Guanine nucleotide exchange factor Lbc) (Human thyroid-anchoring protein 31) (Lymphoid blast crisis oncogene) (LBC oncogene) (Non-oncogenic Rho GTPase-specific GTP exchange factor) (Protein kinase A-anchoring protein 13) (PRKA13) (p47)	2813
3	Q96Q42	ALS2	Alsin (Amyotrophic lateral sclerosis 2 chromosomal region candidate gene 6 protein) (Amyotrophic lateral sclerosis 2 protein)	1657
4	Q8N1W1	ARHGEF28	Rho guanine nucleotide exchange factor 28 (190 kDa guanine nucleotide exchange factor) (p190-RhoGEF) (p190RhoGEF) (Rho guanine nucleotide exchange factor)	1705
5	A8MVX0	ARHGEF33	Rho guanine nucleotide exchange factor 33	844
6	Q8N4T4	ARHGEF39	Rho guanine nucleotide exchange factor 39	335
7	Q9HCE6	ARHGEF10L	Rho guanine nucleotide exchange factor 10-like protein (GrinchGEF)	1279
8	A1IGU5	ARHGEF37	Rho guanine nucleotide exchange factor 37	675
9	Q9NXL2	ARHGEF38	Rho guanine nucleotide exchange factor 38	777
10	Q8TER5	ARHGEF40	Rho guanine nucleotide exchange factor 40 (Protein SOLO)	1519
11	Q92888	ARHGEF1	Rho guanine nucleotide exchange factor 1 (115 kDa guanine nucleotide exchange factor) (p115-RhoGEF) (p115RhoGEF) (Sub1.5)	912
12	Q92974	ARHGEF2	Rho guanine nucleotide exchange factor 2 (Guanine nucleotide exchange factor H1) (GEF-H1) (Microtubule-regulated Rho-GEF) (Proliferating cell nucleolar antigen p40)	986
13	Q9NR81	ARHGEF3	Rho guanine nucleotide exchange factor 3 (Exchange factor found in platelets and leukemic and neuronal tissues) (XPLN)	526
14	Q9NR80	ARHGEF4	Rho guanine nucleotide exchange factor 4 (APC-stimulated guanine nucleotide exchange factor 1) (Asef) (Asef1)	690
15	Q12774	ARHGEF5	Rho guanine nucleotide exchange factor 5 (Ephexin-3) (Guanine nucleotide regulatory protein TIM) (Oncogene TIM) (Transforming immortalized mammary oncogene) (p60 TIM)	1597
16	Q15052	ARHGEF6	Rho guanine nucleotide exchange factor 6 (Alpha-Pix) (COOL-2) (PAK-interacting exchange factor alpha) (Rac/Cdc42 guanine nucleotide exchange factor 6)	776
17	Q14155	ARHGEF7	Rho guanine nucleotide exchange factor 7 (Beta-Pix) (COOL-1) (PAK-interacting exchange factor beta) (p85)	803
18	Q7Z628	NET1	Neuroepithelial cell-transforming gene 1 protein (Proto-oncogene p65 Net1) (Rho guanine nucleotide exchange factor 8)	596
19	O43307	ARHGEF9	Rho guanine nucleotide exchange factor 9 (Collybistin) (PEM-2 homolog) (Rac/Cdc42 guanine nucleotide exchange factor 9)	516
20	O15013	ARHGEF10	Rho guanine nucleotide exchange factor 10	1369
21	O15085	ARHGEF11	Rho guanine nucleotide exchange factor 11 (PDZ-RhoGEF)	1522
22	Q9NZN5	ARHGEF12	Rho guanine nucleotide exchange factor 12 (Leukemia-associated RhoGEF)	1544
23	O94989	ARHGEF15	Rho guanine nucleotide exchange factor 15 (Ephexin-5) (E5) (Vsm-RhoGEF)	841
24	Q5VV41	ARHGEF16	Rho guanine nucleotide exchange factor 16 (Ephexin-4)	709
25	Q96PE2	ARHGEF17	Rho guanine nucleotide exchange factor 17 (164 kDa Rho-specific guanine-nucleotide exchange factor) (p164-RhoGEF) (p164RhoGEF) (Tumor endothelial marker 4)	2063
26	Q6ZSZ5	ARHGEF18	Rho guanine nucleotide exchange factor 18 (114 kDa Rho-specific guanine-nucleotide exchange factor) (p114-Rho-GEF) (p114RhoGEF) (Septin-associated RhoGEF) (SA-RhoGEF)	1173
27	Q8IW93	ARHGEF19	Rho guanine nucleotide exchange factor 19 (Ephexin-2)	802
28	Q86VW2	ARHGEF25	Rho guanine nucleotide exchange factor 25 (Guanine nucleotide exchange factor GEFT) (Rac/Cdc42/Rho exchange factor GEFT) (RhoA/Rac/Cdc42 guanine nucleotide exchange factor GEFT) (p63RhoGEF)	580
29	Q96DR7	ARHGEF26	Rho guanine nucleotide exchange factor 26 (SH3 domain-containing guanine exchange factor)	871
30	P11274	BCR	Breakpoint cluster region protein (EC 2.7.11.1) (Renal carcinoma antigen NY-REN-26)	1271
31	Q6XZF7	DNMBP	Dynamin-binding protein (Scaffold protein Tuba)	1577
32	Q9H8V3	ECT2	Protein ECT2 (Epithelial cell-transforming sequence 2 oncogene)	914
33	Q008S8	ECT2L	Epithelial cell-transforming sequence 2 oncogene-like (Lung-specific F-box and DH domain-containing protein) (Putative guanine nucleotide exchange factor LFDH)	904
34	Q9Y4F1	FARP1	FERM, RhoGEF and pleckstrin domain-containing protein 1 (Chondrocyte-derived ezrin-like protein) (Pleckstrin homology domain-containing family C member 2) (PH domain-containing family C member 2)	1045
35	O94887	FARP2	FERM, RhoGEF and pleckstrin domain-containing protein 2 (FERM domain including RhoGEF) (FIR) (Pleckstrin homology domain-containing family C member 3) (PH domain-containing family C member 3)	1054
36	P98174	FGD1	FYVE, RhoGEF and PH domain-containing protein 1 (Faciogenital dysplasia 1 protein) (Rho/Rac guanine nucleotide exchange factor FGD1) (Rho/Rac GEF) (Zinc finger FYVE domain-containing protein 3)	961
37	Q7Z6J4	FGD2	FYVE, RhoGEF and PH domain-containing protein 2 (Zinc finger FYVE domain-containing protein 4)	655
38	Q5JSP0	FGD3	FYVE, RhoGEF and PH domain-containing protein 3 (Zinc finger FYVE domain-containing protein 5)	725
39	Q96M96	FGD4	FYVE, RhoGEF and PH domain-containing protein 4 (Actin filament-binding protein frabin) (FGD1-related F-actin-binding protein) (Zinc finger FYVE domain-containing protein 6)	766
40	Q6ZNL6	FGD5	FYVE, RhoGEF and PH domain-containing protein 5 (Zinc finger FYVE domain-containing protein 23)	1462
41	Q6ZV73	FGD6	FYVE, RhoGEF and PH domain-containing protein 6 (Zinc finger FYVE domain-containing protein 24)	1430
42	Q15811	ITSN1	Intersectin-1 (SH3 domain-containing protein 1A) (SH3P17)	1721
43	Q9NZM3	ITSN2	Intersectin-2 (SH3 domain-containing protein 1B) (SH3P18) (SH3P18-like WASP-associated protein)	1697
44	O60229	KALRN	Kalirin (EC 2.7.11.1) (Huntingtin-associated protein-interacting protein) (Protein Duo) (Serine/threonine-protein kinase with Dbl- and pleckstrin homology domain)	2985
45	P10911	MCF2	Proto-oncogene DBL (Proto-oncogene MCF-2) [Cleaved into: MCF2-transforming protein; DBL-transforming protein]	925
46	O15068	MCF2L	Guanine nucleotide exchange factor DBS (DBL's big sister) (MCF2-transforming sequence-like protein)	1137
47	Q86YR7	MCF2L2	Probable guanine nucleotide exchange factor MCF2L2 (Dbs-related Rho family guanine nucleotide exchange factor) (MCF2-transforming sequence-like protein 2)	1114
48	Q8N5V2	NGEF	Ephexin-1 (Eph-interacting exchange protein) (Neuronal guanine nucleotide exchange factor)	710
49	Q5VST9	OBSCN	Obscurin (EC 2.7.11.1) (Obscurin-RhoGEF) (Obscurin-myosin light chain kinase) (Obscurin-MLCK)	7968
50	Q96PX9	PLEKHG4B	Pleckstrin homology domain-containing family G member 4B (PH domain-containing family G member 4B)	1271
51	Q9ULL1	PLEKHG1	Pleckstrin homology domain-containing family G member 1	1385
52	Q9H7P9	PLEKHG2	Pleckstrin homology domain-containing family G member 2 (PH domain-containing family G member 2)	1386
53	A1L390	PLEKHG3	Pleckstrin homology domain-containing family G member 3 (PH domain-containing family G member 3)	1219
54	Q58EX7	PLEKHG4	Puratrophin-1 (Pleckstrin homology domain-containing family G member 4) (PH domain-containing family G member 4) (Purkinje cell atrophy-associated protein 1)	1191
55	O94827	PLEKHG5	Pleckstrin homology domain-containing family G member 5 (PH domain-containing family G member 5) (Guanine nucleotide exchange factor 720) (GEF720)	1062
56	Q3KR16	PLEKHG6	Pleckstrin homology domain-containing family G member 6 (PH domain-containing family G member 6) (Myosin-interacting guanine nucleotide exchange factor) (MyoGEF)	790
57	Q6ZR37	PLEKHG7	Pleckstrin homology domain-containing family G member 7 (PH domain-containing family G member 7)	379
58	Q8TCU6	PREX1	Phosphatidylinositol 3,4,5-trisphosphate-dependent Rac exchanger 1 protein (P-Rex1) (PtdIns(3,4,5)-dependent Rac exchanger 1)	1659
59	Q70Z35	PREX2	Phosphatidylinositol 3,4,5-trisphosphate-dependent Rac exchanger 2 protein (P-Rex2) (PtdIns(3,4,5)-dependent Rac exchanger 2) (DEP domain-containing protein 2)	1606
60	Q13972	RASGRF1	Ras-specific guanine nucleotide-releasing factor 1 (Ras-GRF1) (Guanine nucleotide-releasing protein) (GNRP) (Ras-specific nucleotide exchange factor CDC25)	1273
61	O14827	RASGRF2	Ras-specific guanine nucleotide-releasing factor 2 (Ras-GRF2) (Ras guanine nucleotide exchange factor 2)	1237
62	Q07889	SOS1	Son of sevenless homolog 1 (SOS-1)	1333
63	Q07890	SOS2	Son of sevenless homolog 2 (SOS-2)	1332
64	Q96N96	SPATA13	Spermatogenesis-associated protein 13 (APC-stimulated guanine nucleotide exchange factor 2) (Asef2)	652
65	Q13009	TIAM1	T-lymphoma invasion and metastasis-inducing protein 1 (TIAM-1)	1591
66	Q8IVF5	TIAM2	T-lymphoma invasion and metastasis-inducing protein 2 (TIAM-2) (SIF and TIAM1-like exchange factor)	1701
67	O75962	TRIO	Triple functional domain protein (EC 2.7.11.1) (PTPRF-interacting protein)	3097
68	P52735	VAV2	Guanine nucleotide exchange factor VAV2 (VAV-2)	878
69	Q9UKW4	VAV3	Guanine nucleotide exchange factor VAV3 (VAV-3)	847
70	P15498	VAV1	Proto-oncogene vav	845

filamentous actin. IQ motif containing GTPase activating protein 1 (IQGAP1) (Hedman et al., 2015), mammalian homolog of Drosophila diaphanous (mDia1), Wiskott-Aldrich syndrome protein (WASP) and Rhotekin (RTKN) are best investigated effectors in this regard and facilitate complex formations in cells (Figure 1.6) (C.-A. Liu et al., 2004).
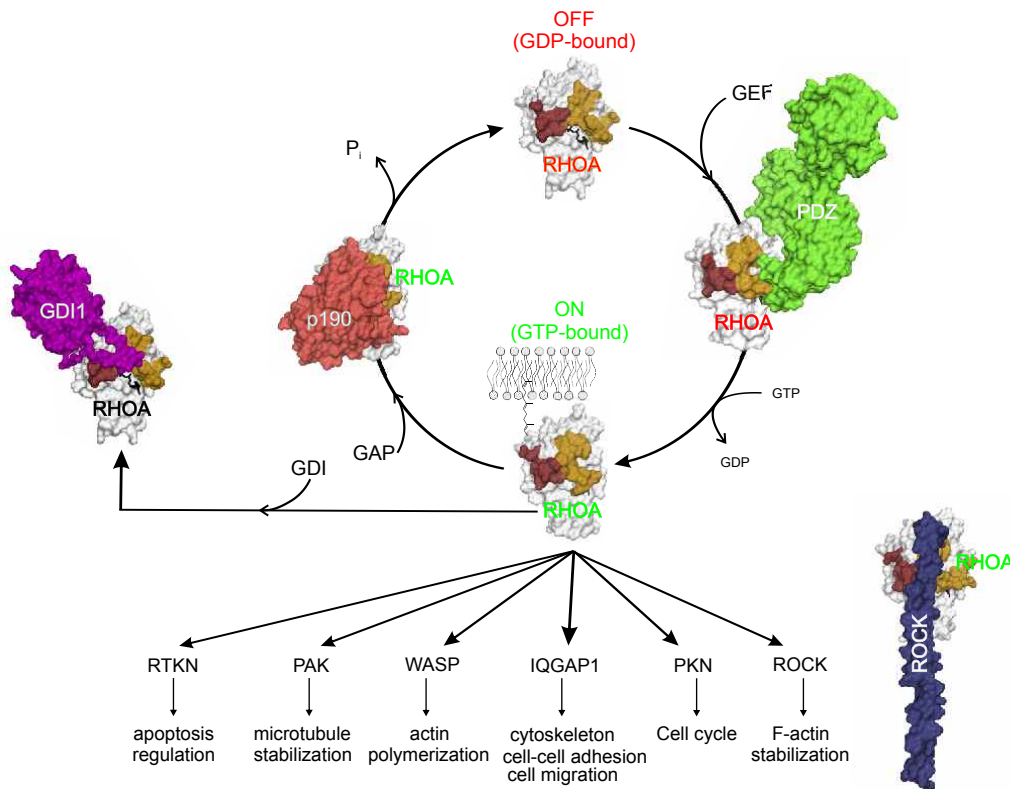

FIGURE 1.6: RHOA activation and inactivation cycle and its downstream effectors. Switch I and II regions of RHOA are colored brown and orange. (RHOA.GDP; Protein Data Bank Acc No.: 1ftn). Binding of p190 (colored red) to RHOA accelerates GTP hydrolysis (RHOA-p190; 5irc). Association of RHOA with PDZ-RHOGEF speeds up nucleotide exchange (RHOA-PDZGEF; 3kz1). GTP-bound RHOA binds to different effector proteins and promotes downstream signaling to fulfill diverse biological functions (RHOA-ROCK; 1s1c).

ROCK

RHO-associating coiled-coil kinase 1 (ROCK1, also called RHO kinase) is a well-defined effector for RHOA and key regulator of actin cytoskeleton (Amin et al., 2013). It is a 160-kDa protein that contains an N-terminal kinase domain, a central coiled-coil region and C-terminal pleckstrin homology (PH) domain (Figure 1.7). Central coiled-coil is composed of RHO binding domain (RBD) and homology region 1 (HR1), responsible for

RHOA binding. The Shroom binding domain has been proposed to regulate ROCK cellular distribution (Mohan et al., 2013). Split PH domain and squeezed cycteine-rich domain (CRD) represent membrane binding domains (Wen et al., 2008). It is thought that ROCK is in an auto-inhibited conformation via intramolecular or even intermolecular interaction of PH domain to kinase domain of a dimeric protein and inhibiting the kinase activity (Couzens et al., 2009). Binding of active RHOA to RBD domain has been suggested to release its auto-inhibited state and exposed kinase domain to its substrates. Proteolytic cleavage of ROCK or binding of lipids to PH domain are also discussed to activate ROCK (Schofield et al., 2013). Up to date various phosphorylation sites on ROCK has been observed but the exact roles are not well understood yet.
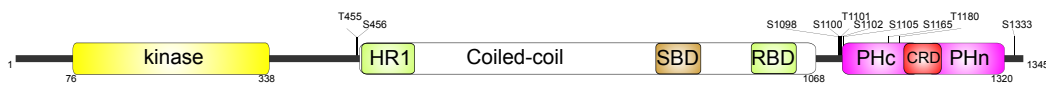

FIGURE 1.7: Domain organization of RHO kinase. HR1: homology region 1; SBD: shroom binding domain; RBD: RHO binding domain; PH: pleckstrin homology; CRD: cysteine-rich domain.

PAK

p21-activated kinase (PAK1) is a downstream effector of RAC1 and CDC42. It consists of a conserved C-terminal kinase domain, an N-terminal regulatory region, consisting of a GTPase-binding domain (GBD) and an autoinhibitory domain (AID) (Figure 1.8) (Rane et al., 2014). Several Proline-rich motifs appear to be responsible for bindind to SH3 domain-containing adapter proteins (Parrini, 2012). Inactive PAK1 is trans-inhibited in a form of homodimer. AID of one PAK molecule binds and inhibits the kinase domain of the other one. GTP-loaded RAC1 or CDC42 binds to the GBD domain, leading to disruption of dimerization, removal of the trans-inhibitory (Ha et al., 2012). Different studies, using cell culture, transgenic mice, and knockout mice, have revealed important roles for the PAKs in cytoskeletal organization and in many aspects of cell growth and development (Rane et al., 2014). PAK functions include proper morphogenesis and conductance of the heart, cardiac contractility, and development and integrity of the vasculature (Kelly et al., 2013). PAK regulates the contractility of smooth muscle by regulating actin polymerization (W. Zhang et al., 2016). It also mediates activation of downstream MAPK pathway by MEK1 and RAF1 phosphorylation (Wang et al., 2013).

IQGAP

IQ motif-containing GTPase-activating protein (IQGAP) contains several domains that mediate protein–protein interactions and scaffolds diverse cellular pathways (Figure 1.9).
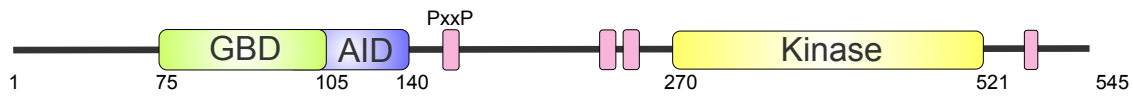
FIGURE 1.8: Domain organization of PAK1. GBD: GTPase binding domain; AID: auto inhibitory domain; P: Proline; x: any amino acid

It integrates protein complexes required for cellular processes. Calponin homology domain (CHD) is an F-actin binding domain and so integrate protein complexes to cytoskeletal reorganizational events (Mateer et al., 2004; Schmidt, 2012). GAP-related domain (GRD) is identified as a RASGAP domain but lacks catalytic activity and binds preferentially to CDC42 and RAC1 (Owen et al., 2008). IQ motifs are calmodolin binding motifs. Coiled-coil region leads to dimerization of IQGAP proteins. WW domain contains several tryptophan residues and binds to polyproline regions. IQGAP1 integrates microtubules and actin cytoskeleton together and enhances endothelial barrier function by bringing RAC1 and CDC42 to microtubules (Tian et al., 2014).
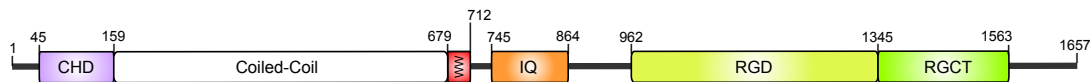

FIGURE 1.9: Domain organization of IQGAP1. CHD: calponin homology domain; GRD: GAP-related domain; RGCT: RASGAP related C-terminus; WW: polyproline binding domain; CRAD: CDC42/RAC associated domain. IQ refers to the first two conserved amino acids (Isoleucine and Glutamine) of IQ-motif.

1.4   (Patho) Biochemical Pathways

RHO GTPases control various signal transduction pathways that leads to both the formation and the organization of actin filaments (Jaffe et al., 2005). One of the major biological functions at cellular level, regulated by RHO GTPases, is endothelial barrier function. Changes in fine-tuning of this property leads to different cardiovascular diseases (Chistiakov et al., 2015). When the continuity of endothelial layer is disrupted and the underlying sub-endothelial matrix is exposed, a coordinated series of events are set in motion to seal the defect. Platelets aggregation plays the primary role in this process and they adhere to the vascular wall in response to injury (Rumbaut et al., 2010). RHO GTPases have emerged as key regulators in the dynamics of the actin cytoskeleton in platelets and play key roles in platelet aggregation, secretion, spreading and thrombus formation (Aslan et al., 2013; Elvers, 2016). Another pathological process is cancer cell metastasis and transmigration through endothelial barrier. It has been shown that RHO GTPases

are one of key regulators of cancer cell migrations (Vega et al., 2008).

1.4.1 Endothelial barrier (dys)function

Endothelial cells form a monolayer that cover the internal surface of blood vessels and is actively involved in vital functions of the cardiovascular system, including regulation of fluid and solute exchange, haemostasis and coagulation, inflammatory responses, vasculogenesis and angiogenesis (Rodrigues et al., 2015). Endothelial cells (ECs) make a barrier between lumen and inner tissues and actively regulate the extravasation of blood (Komarova et al., 2010). When junctions are disrupted, the permeability is increased and the vascular integrity is altered. Several processes change the junctional integrity of endothelium: i) vasoactive agents, ii) leukocyte-derived mediators and iii) induction of angiogenesis. This intuitive processes, however, appears to be complex, and it is influenced by several signaling pathways. RHO GTPases are the key regulators of endothelial barrier functions and contribute to the fine-tuning of vascular permeability under both physiological and pathological conditions (Amado-Azevedo et al., 2014). RAC1 and CDC42 are generally thought to spatially control the formation of filopodia and lamellipodia, which favors barrier improvement, whereas RHOA is mainly involved in the organization of stress fibers during cell contraction and also impairs barrier integrity. However, recent studies have highlighted a more complex involvement of RHO GTPases in positive and negative regulation of the endothelial barrier (Figure 1.10) (Giannotta et al., 2013; Szulcek et al., 2013).

Induction of endothelial permeability

Two independent mechanisms are involved in endothelial permeability: i) Destabilization of adherent junctions (AJs) via phosphorylation of its constituents, which in most cases leads to VE-cadherin internalization, and ii) activation of actin-myosin contractility, thus applying mechanical forces to AJs that break apart the junctions (Komarova et al., 2010). Thrombin, a pro-coagulant serine protease, mediates a transient increase in endothelial permeability and is well studied (Vouret-Craviari et al., 1998). RHOA activity increases upon thrombin stimulation. Activated ROCK axis inactivates myosin light chain (MLC) phosphatase, which leads to increased MLC phosphorylation. ROCK also phosphorylates MLC directly and consequently leads to actin-myosin contractility (Amin et al., 2013). PKC-α regulates RHOGDI by phosphorylation and cause RHO-dependent endothelial barrier dysfunction (Mehta et al., 2001). Nitrite oxide (NO) selectively nitrates p190RHOGAP at Tyr-1105 and results its inactivation and consequent activation of

RHOA and its pathways (Siddiqui et al., 2011). FAK phosphorylation of β-catenin disassemble AJs by promoting VE-Cadherin internalization (Chen et al., 2012).
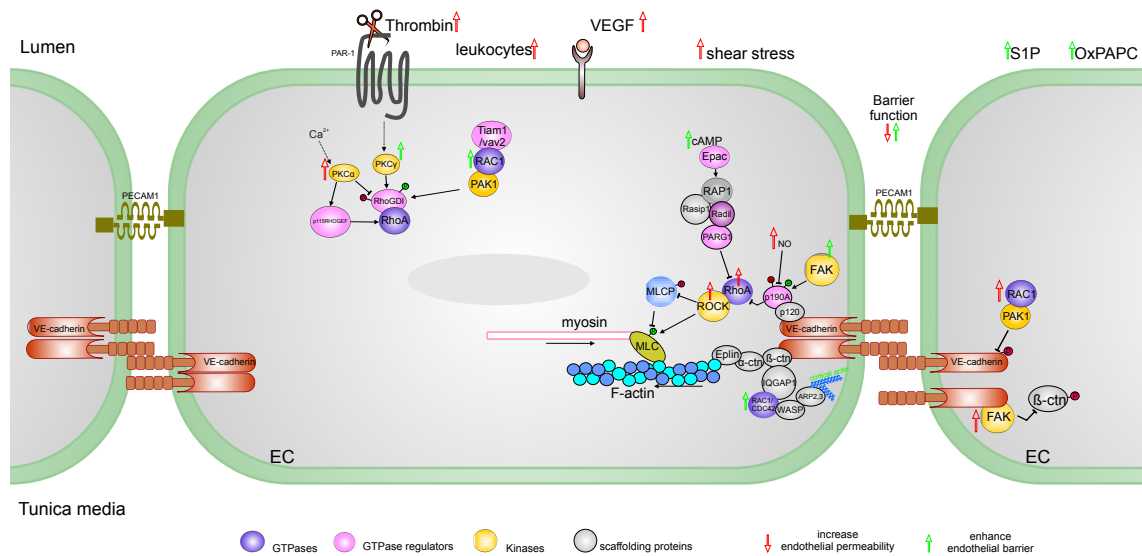

FIGURE 1.10: Endothelial barrier regulation. RHO GTPases are key regulators of barrier function downstream of receptor activation by external stimuli. Red and green phosphorylations are inhibitory and activation, respectively. Red and green arrows represents either decrease or protect barrier function, respectively.

Enhancement of endothelial barrier function

Elevation of cyclic AMP (cAMP) protects endothelial barrier function (Moy et al., 1998). It has been reported that RAP and RHO crosstalk enhance endothelial barrier function in resting conditions (Cullere et al., 2005; Post et al., 2013). RAP1 induces translocations of RASip1 and a RADil-PARG1 complex to the plasma membrane. This results in inhibition of RHO signaling and increased endothelial barrier function (Post et al., 2015). In this pathway RAP1 is activated by cAMP dependent activation of EPAC as a GEF for RAP1 (Post et al., 2013). Also, FAK via phosphorylation of p190RHOGAP, has a crucial role in barrier restoration after thrombin induced increase in endothelial permeability (Holinstat et al., 2006). One important aspect to stabilize barrier function is cortical actin polymerization at the site of plasma membrane. IQGAP1 promotes cortical cytoskeletal remodeling and adherens junctions via RAC1/CDC42 signaling and enhance EC barrier protective effect of oxidized phospholipids (Tian et al., 2016).

Therefore, investigation of RHO GTPase regulation is highly needed to understand tuning mechanism of endothelial barrier (dys)function, considering the existence of 66 RHOGAP

and 20 RHO GTPases. This could leads to identify drug targets to inhibit barrier permeability in disease conditions. Notably, sometimes a controlled, temporal, and local increase in permeability can also be desired, for example, with the aim to enhance drug delivery (Nieuw Amerongen et al., 2002).

1.4.2 Platelet aggregation

As the guardians of vascular integrity, platelets patrol the circulation for vessel leakage in a quiescent shape. Upon detecting molecular cues of vessel damage, platelets undergo a dramatic change in shape, bind to adhesive protein substrates and aggregate to form vascular plugs to ultimately halt bleeding (Aslan et al., 2013). Besides physiological functions, platelet activation is a contributing factor to atherothrombosis. The activities of RHO GTPase proteins are central to many of the processes which leads to activation and aggregation of platelets (Elvers, 2016; Goggs et al., 2015). CDC42 activation by release of stimulus from endothelial cells leads to filopodia formation in platelets. Activation of RAC1 and following PAK1 causes p-selectin and integrins activation and undergoes platelets aggregations (Figure 1.11) (**Dutting15**).

1.4.3 Cancer cell metastasis

RHO signaling pathways regulate the growth, motility, invasion and metastasis of a variety of cancer cells (Etienne-Manneville et al., 2002). Aberrant RHO signaling, such as over-expression or hyper-activation by gain-of-function of GEFs or loss-of-function of GAPs, provokes cancer cells to increase invasive and metastasis activities (Parri et al., 2010). In contrast to RAS proteins, to date, no oncogenic mutations have been found in genes related to RHO proteins. RHOH has been reported to be mutated in non-Hodgkin's lymphomas and multiple myeloma (Pasqualucci et al., 2001). Furthermore, CDC42 mutations has been reported in patients with macrothrombocytopenia (Takenouchi et al., 2015; Takenouchi et al., 2016). RHOA and RHOC expression and activity is increased in human tumors, but RHOB is down regulated (Ridley, 2013). Notably, RAC1 signaling is important for malignant transformation and mice lacking the TIAM1 (a RAC1 GEF) are protective against induced skin cancer (Bid et al., 2013). But, the exact mechanisms and involving other RHO proteins are not fully investigated. So, further investigations are required for development of novel strategies targeting the RHO GTPase signaling pathways to inhibit invasion and metastasis of cancer cells.
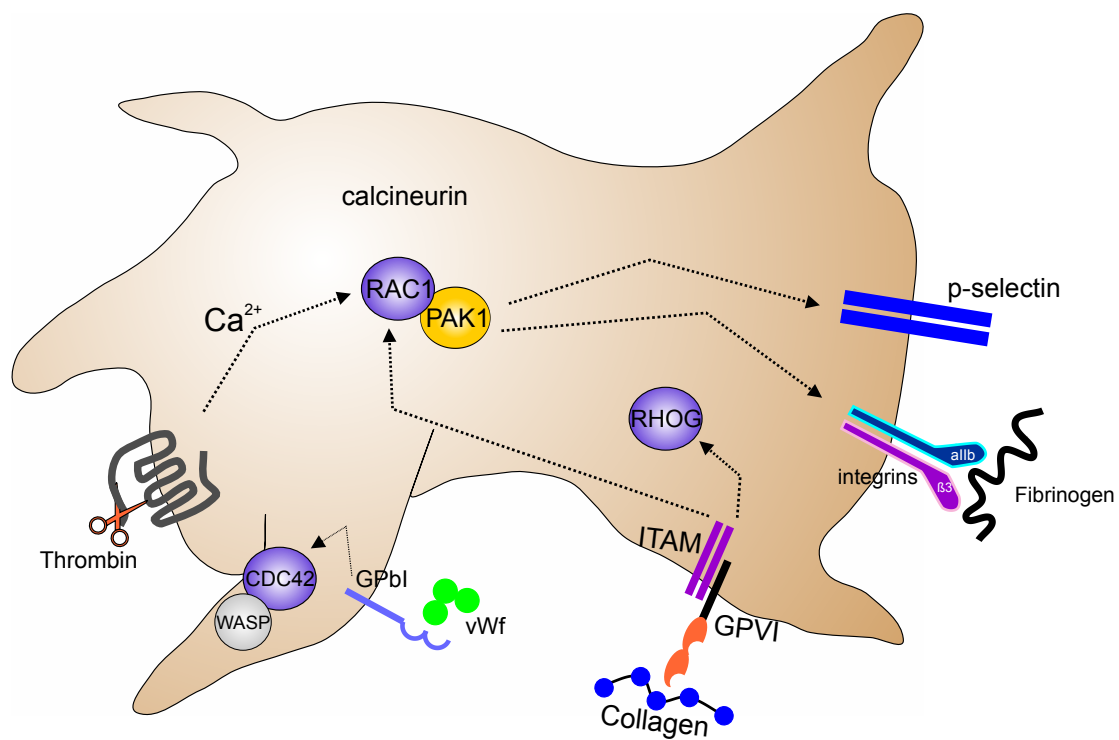
FIGURE 1.11: Platelet activation and aggregation. RHO GTPases fine tune timing of platelet functions. Activation of platelets by external stimuli from endothelial cells or circulatory substances is tuned. Also thrombin induced aggregations are promoted mainly by RAC1 and its effector PAK1 via activation integrins and p-selectins.

Chapter 2

Classical RHO Proteins (book chapter)

Classical RHO Proteins: Biochemistry of Molecular Switch Function and Regulation
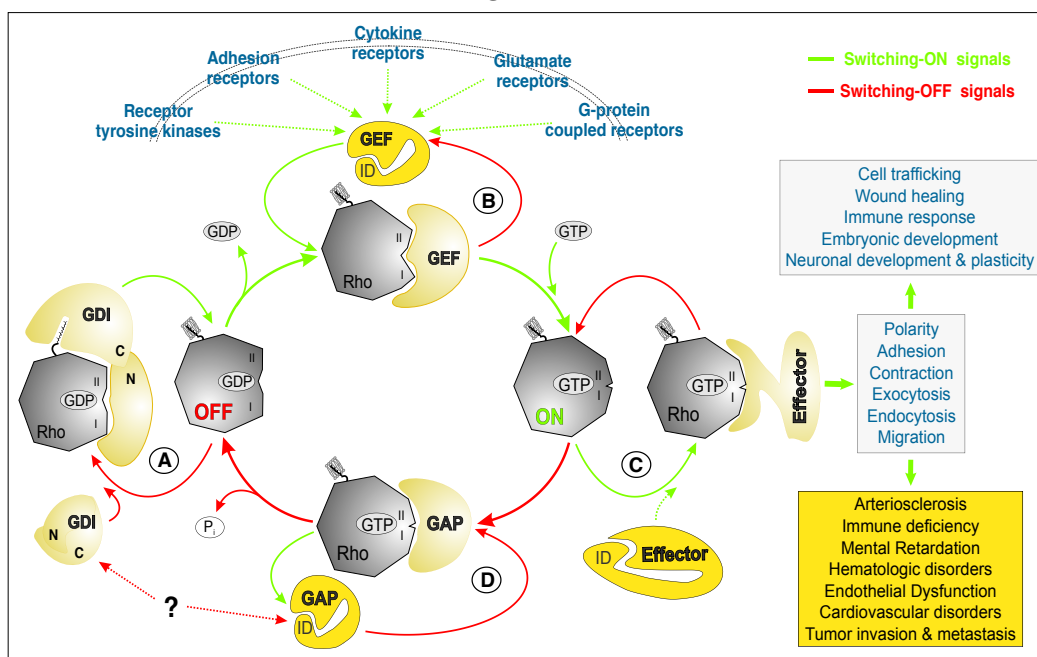
Status:	Published in Wittinghofer, A (ed) RAS Superfamily small G Proteins, Biology and Mechanism, Vol. 1 Springer (2014), Chapter 14, pp 327-340
Own Proportion to this work:	20 %; writing the GAPs section

Chapter 14
Classical Rho Proteins: Biochemistry of Molecular Switch Function and Regulation

**Si-Cai Zhang, Kazem Nouri, Ehsan Amin, Mohamed S. Taha,
Hossein Nakhaeizadeh, Saeideh Nakhaei-Rad, Radovan Dvorsky,
and Mohammad Reza Ahmadian**

Abstract Rho family proteins are involved in an array of cellular processes by modulating cytoskeletal organization, transcription, and cell cycle progression. The signaling functions of Rho family proteins are based on the formation of distinctive protein–protein complexes with their regulators and effectors. A necessary precondition for such differential interactions is an intact molecular switch function, which is a hallmark of most members of the Rho family. Such classical Rho proteins cycle between an inactive GDP-bound state and an active GTP-bound state. They specifically interact via a consensus-binding sites called switch I and II with three structurally and functionally unrelated classes of regulatory proteins, such as guanine nucleotide dissociation inhibitors (GDIs), guanine nucleotide exchange factors (GEFs), and GTPase-activating proteins (GAPs). Extensive studies in the last 25 years have provided invaluable insights into the molecular mechanisms underlying regulation and signal transduction of the Rho family proteins. In this chapter, we will review common features of Rho protein regulations and highlight specific aspects of their structure–function relationships.

Keywords Effector • GAP • GDI • GEF • Rho GTPase • Switch region

Abbreviations

A	Aliphatic amino acid
Bcr	Breakpoint cluster region protein
C	Cysteine
CZH	CDM-zizimin homology

S.-C. Zhang • K. Nouri • E. Amin • M.S. Taha • H. Nakhaeizadeh • S. Nakhaei-Rad •
R. Dvorsky • M.R. Ahmadian (✉)
Institute of Biochemistry and Molecular Biology II, Medical Faculty, Heinrich-Heine-University, 40225 Düsseldorf, Germany
e-mail: reza.ahmadian@uni-duesseldorf.de

Db1   Diffuse B-cell lymphoma
DH   Dbl homology domain
DHR1&2   DOCK-homology regions 1 and 2
ERM   Ezrin/radixin/moesin
GAPs   GTPase-activating proteins
GDIs   Guanine nucleotide dissociation inhibitors
GDP   Guanosine diphosphate
GEFs   Guanine nucleotide exchange factors
Gln   Glutamine
Gly   Glycine
GTP   Guanosine triphosphate
$p75^{NTR}$ Neurotrophin receptor p75
PAK1   p21-activated kinase 1
PH   Pleckstrin homology domain
PKA   Protein kinase A
PKC   Protein kinase C
P-loop   Phosphate-binding loop
X   Any amino acid

14.1   General Introduction

The role of the Rho family proteins as signaling molecules in controlling a large number of fundamental cellular processes is largely dependent on a functional molecular switch between a GDP-bound, inactive state and a GTP-bound, active state (Dvorsky and Ahmadian 2004). This function underlies a so-called GTPase cycle consisting of two different, slow biochemical reactions, the GDP/GTP exchange and the GTP hydrolysis. The cellular regulation of this cycle involves guanine nucleotide exchange factors (GEFs), which accelerate the intrinsic nucleotide exchange, and GTPase-activating proteins (GAPs), which stimulate the intrinsic GTP hydrolysis activity (Cherfils and Zeghouf 2013). Rho protein function requires both posttranslational modification by isoprenyl groups and membrane association. Therefore, Rho proteins underlie a third control mechanism that directs their membrane targeting to specific subcellular sites. This mechanism is achieved by the function of guanine nucleotide dissociation inhibitors (GDIs), which bind selectively to prenylated Rho proteins and control their cycle between cytosol and membrane. Activation of Rho proteins results in their association with effector molecules that subsequently activate a wide variety of downstream signaling cascades (Bishop and Hall 2000; Burridge and Wennerberg 2004), thereby regulating many important physiological and pathophysiological processes in eukaryotic cells (Etienne-Manneville and Hall 2002; Heasman and Ridley 2008) (see Chap. 16). In the following, the biochemical properties of the Rho proteins and their regulatory cycles will be described in detail. Figure 14.1 schematically summarizes the regulatory mechanism of the Rho proteins.
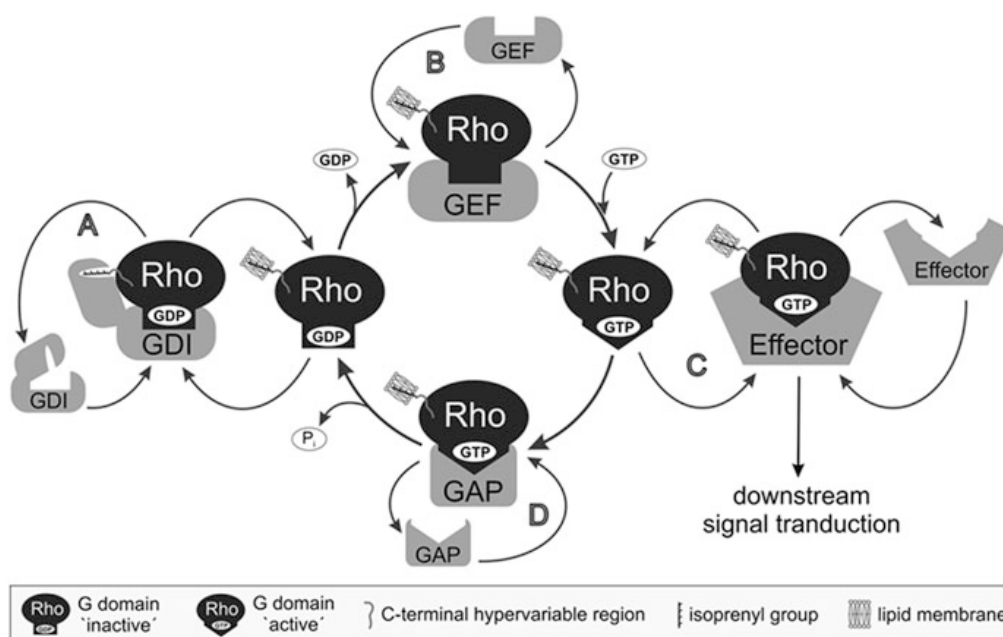
Fig. 14.1 Molecular principles of regulation and signaling of Rho Proteins. Most members of the Rho family act as molecular switches by cycling between an inactive, GDP-bound state and an active GTP-bound state. They interact specifically with four structurally and functionally unrelated classes of proteins: (**a**) In resting cells, guanine nucleotide dissociation inhibitors (GDIs) sequestrate the Rho proteins from the membrane by binding to the lipid anchor and create an inactivated cytosolic pool. (**b**) In stimulated cells, different classes of membrane receptors activate guanine nucleotide exchange factors (GEFs), which in turn activate their substrate Rho proteins by accelerating the slow intrinsic exchange of GDP for GTP and turn on the signal transduction. (**c**) The active GTP-bound Rho proteins interact with and activate their targets (the downstream effectors) to evoke a variety of intracellular responses. (**d**) GTPase-activating proteins (GAPs) negatively regulate the switch by stimulating the slow intrinsic GTP hydrolysis activity of the Rho proteins and turn off the signal transduction

14.2   Rho Family and the Molecular Switch Mechanism

Members of the GTP-binding proteins of the Rho family have emerged as key regulatory molecules that couple changes in the extracellular environment to intracellular signal transduction pathways. So far, 20 human members of the Rho family have been identified, which can be divided into six distinct subfamilies based on their sequence homology: (1) Rho (RhoA, RhoB, RhoC); (2) Rac (Rac1, Rac1b, Rac2, Rac3, RhoG); (3) Cdc42 (Cdc42, G25K, TC10, TCL, RhoU/Wrch1, RhoV/Chp); (4) RhoD (RhoD, Rif); (5) Rnd (Rnd1, Rnd2, Rnd3); (6) RhoH/TTF (Boureux et al. 2007; Jaiswal et al. 2013a, b; Wennerberg and Der 2004).

Rho family proteins are approximately 21–25 kDa in size typically containing a conserved GDP/GTP-binding domain (called G domain) and a C-terminal hyper-variable region ending with a consensus sequence known as CAAX (C is cysteine, A is any aliphatic amino acid, and X is any amino acid). The G domain consists of five conserved sequence motifs (G1-G5) that are involved in nucleotide binding and

hydrolysis (Wittinghofer and Vetter 2011). In the cycle between the inactive and active states at least two regions of the protein, switch I (G2) and Switch II (G3), undergo structural rearrangements and transmit the "OFF" to "ON" signal to downstream effectors (Fig. 14.1) (Dvorsky and Ahmadian 2004). Subcellular localization of Rho proteins at different cellular membranes, that is known to be critical for their biological activity, is achieved by a series of posttranslational modifications at a cysteine residue in the CAAX motif, including isoprenylation (geranylgeranyl or farnesyl), endoproteolysis, and carboxyl methylation (Roberts et al. 2008).

A characteristic region of Rho family GTPases is the insert helix (amino acids 124–136, RhoA numbering) that may play a role in effector activation and downstream process (Thapar et al. 2002). Although the function of the insert helix has not been elucidated yet, it has been reported to be involved in the Rho-dependent activation of ROCK (Zong et al. 2001), phospholipase D (Walker and Brown 2002) and mDia (Lammers et al. 2008; Rose et al. 2005), and in the Rac-dependent activation of p67phox (Joneson and Bar-Sagi 1997; Karnoub et al. 2001; Nisimoto et al. 1997) and Plexin B1 (Bouguet-Bonnet and Buck 2008).

Although the majority of the Rho family proteins are remarkably inefficient GTP hydrolyzing enzymes, in quiescent cells they rest in an inactive state because the GTP hydrolysis is in average two orders of magnitude faster than the GDP/GTP exchange (Jaiswal et al. 2013a, b). Such different intrinsic activities provide the basis for a two-state molecular switch mechanism, which highly depends on the regulatory functions of GEFs and GAPs that directly control ON and OFF states of classical type of Rho proteins (Fig. 14.1). Eleven out of twenty members of the Rho family belong to these classical molecular switches, namely RhoA, RhoB, RhoC, Rac1, Rac2, Rac3, RhoG, Cdc42, G25K, TC10, and TCL (Jaiswal et al. 2013a, b).

The atypical Rho family members, including Rnd1, Rnd2, Rnd3, Rac1b, RhoH/TTF, Wrch1, RhoD, and Rif, have been proposed to accumulate in the GTP-bound form in cells due to various biochemical properties (Jaiswal et al. 2013a, b). Rnd1, Rnd2, Rnd3, and RhoH/TTF represent a completely distinct group of proteins within the Rho family (Riou et al. 2010; Troeger et al. 2013), as they do not share several conserved and essential amino acids, including Gly-12 (Rac1 numbering) in the G1 motif (also called phosphate-binding loop or P-loop) and Gln-61 (Rac1 numbering) in the G3 motif or switch II region. The role of these residues in GTP hydrolysis is well described for Ras oncogene in human cancers (Chaps. 6 and 7). Thus, they can be considered as GTPase-deficient Rho-related GTP-binding proteins (Fiegen et al. 2002; Garavini et al. 2002; Gu et al. 2005; Li et al. 2002) (see also Chap. 15). Another example is Rac1b, which is an alternative splice variant of Rac1 and contains a 19-amino acid insertion next to the switch II region (Jordan et al. 1999). Rac1b exhibits different biochemical properties as compared to the other Rac isoforms (Fiegen et al. 2004; Haeusler et al. 2006), including an accelerated GEF-independent GDP/GTP exchange and an impaired GTP hydrolysis (Fiegen et al. 2004). RhoD and Rif are involved in the regulation of actin dynamics (Fan and Mellor 2012; Gad and Aspenstrom 2010) and exhibit a strikingly faster nucleotide exchange than GTP hydrolysis similarly to Rac1b and thus persist

mainly in the active state under resting conditions (Jaiswal et al. 2013a, b). Wrch1, a Cdc42-like protein that has been reported to be a fast cycling protein (Shutes et al. 2006), resembles in this context Rac1b, RhoD, and Rif (Jaiswal et al. 2013a, b). These atypical members of the Rho family with their distinctive biochemical features do not follow the classical switch mechanism and may thus require additional forms of regulation.

14.3   Guanine Nucleotide Dissociation Inhibitors

Multiple functions have been originally described for the Rho-specific GDIs, including the inhibition of the GDP/GTP exchange (Hiraoka et al. 1992; Ohga et al. 1989), the intrinsic and GAP-stimulated GTP hydrolysis (Chuang et al. 1993; Hancock and Hall 1993; Hart et al. 1992), and the interaction with the downstream effectors (Pick et al. 1993). However, it is generally accepted that in resting cells, RhoGDIs target the isoprenyl anchor and sequester Rho proteins from their site of action at the membrane in the cytosol (Boulter and Garcia-Mata 2010; Garcia-Mata et al. 2011).

RhoGDIs undergo a high affinity interaction with the Rho proteins using an N-terminal regulatory arm contacting the switch regions and a C-terminal domain binding the isoprenyl group (Tnimov et al. 2012). In contrast to the large number of RhoGEFs and RhoGAPs, there are only three known RhoGDIs in human (DerMardirossian and Bokoch 2005). RhoGDI-1 (also called RhoGDIα) is ubiqui-tously expressed (Fukumoto et al. 1990), whereas RhoGDI-2 (also called RhoGDIβ, LyGDI, or D4GDI) is predominantly found in hematopoietic tissues and lympho-cytes (Leonard et al. 1992; Scherle et al. 1993) and RhoGDI-3 (also called RhoGDIγ) in lung, brain, and testis (Adra et al. 1997; Zalcman et al. 1996).

Despite intensive research over the last two decades, the molecular basis by which GDI proteins associate and extract the Rho GTPases from the membrane remains to be investigated. The neurotrophin receptor p75 (p75[NTR]) and ezrin/radixin/moesin (ERM) proteins have been proposed to displace the Rho proteins from the RhoGDI complex resulting in reassociation with the cell membrane (Takahashi et al. 1997; Yamashita and Tohyama 2003). Another regulatory mech-anism is RhoGDI phosphorylation. RhoGDI has been shown to be phosphorylated by serine/threonine p21-activated kinase 1 (PAK1), protein kinase A (PKA), protein kinase C (PKC), and the tyrosine kinase Src, thereby decreasing the ability of RhoGDI to form a complex with the Rho proteins, including RhoA, Rac1, and Cdc42 (DerMardirossian et al. 2004, 2006).

14.4 Guanine Nucleotide Exchange Factors

GEFs are able to selectively bind to their respective Rho proteins and accelerate the exchange of tightly bound GDP for GTP. A common mechanism utilized by GEFs is to strongly reduce the affinity of the bound GDP, leading to its displacement and the subsequent association with GTP (Cherfils and Chardin 1999; Guo et al. 2005). This reaction involves several stages, including an intermediate state of the GEF in the complex with the nucleotide-free Rho protein. This intermediate does not accumulate in the cell and rapidly dissociates because of the high intracellular GTP concentration leading to the formation of the active Rho·GTP complex. The main reason therefore is that the binding affinity of nucleotide-free Rho protein is significantly higher for GTP than for the GEF proteins (Cherfils and Chardin 1999; Hutchinson and Eccleston 2000). Cellular activation of the Rho proteins and their cellular signaling can be selectively uncoupled from the GEFs by overexpressing dominant negative mutants of the Rho proteins (e.g., threonine 17 in Rac1 and Cdc42 or threonine 19 in RhoA to asparagine) (Heasman and Ridley 2008). Such mutations decrease the affinity of the Rho protein to nucleotide resulting in a so-called dominant negative behavior (Rossman et al. 2002). As a consequence, dominant negative mutants form a tight complex with their cognate GEFs and thus prevent them from activating the endogenous Rho proteins.

RhoGEFs of the diffuse B-cell lymphoma (Dbl) family directly activate the proteins of the Rho family (Cook et al. 2013; Jaiswal et al. 2013a, b). The prototype of this GEF family is the Dbl protein, which was isolated as an oncogenic product from diffuse B-cell lymphoma cells in an oncogene screen (Eva et al. 1988; Srivastava et al. 1986), and has been later reported to act on Cdc42 (Hart et al. 1991). The Dbl family consists of 74 members in human (Jaiswal et al. 2013a, b) with evolutionary conserved orthologs in fly (23 members), yeast (6 members), worm (18 members) (Schmidt and Hall 2002; Venter et al. 2001), and slime mold (45 members) (Vlahou and Rivero 2006). Human Dbl family proteins have recently been grouped into functionally distinct categories based on both their catalytic efficiencies and their sequence–structure relationship (Jaiswal et al. 2013a, b). The members of the Dbl family are characterized by a unique Dbl homology (DH) domain (Aittaleb et al. 2010; Erickson and Cerione 2004; Hoffman and Cerione 2002; Jaiswal et al. 2011; Viaud et al. 2012). The DH domain is a highly efficient catalytic machine (Rossman et al. 2005) that is able to accelerate the nucleotide exchange of Rho proteins up to 10^7-fold (Jaiswal et al. 2011, 2013a, b), as efficiently as the RanGEF RCC1 (Klebe et al. 1995) and *Salmonella typhimurium* effector SopE (see below) (Bulgin et al. 2010; Rudolph et al. 1999). The DH domain is often preceded by a pleckstrin homology (PH) domain indicating an essential and conserved function. A model for PH domain-assisted nucleotide exchange has been proposed for some GEFs, such as Dbl, Dbs, and Trio (Rossman et al. 2005). Herein the PH domain serves multiple roles in signaling events anchoring GEFs to the membrane (via phosphoinositides) and directing them

towards their interacting GTPases which are already localized to the membrane (Rossman et al. 2005).

In addition to the DH-PH tandem, Dbl family proteins are highly diverse and contain additional domains with different functions, including SH2, SH3, CH, RGS, PDZ, and IQ domains for interaction with other proteins; BAR, PH FYVE, C1, and C2 domains for interaction with membrane lipids; and other functional domains like Ser/Thr kinase, RasGEF, RhoGAP, and RanGEF (Cook et al. 2013). These additional domains have been implicated in autoregulation, subcellular localization, and connection to upstream signals (Dubash et al. 2007; Rossman et al. 2005). Spatiotemporal regulation of the Dbl proteins has been implicated to specifically initiate activation of substrate Rho proteins (Jaiswal et al. 2013a, b) and to control a broad spectrum of normal and pathological cellular functions (Dubash et al. 2007; Hall and Lalli 2010; Mulinari and Hacker 2010; Mulloy et al. 2010; Schmidt and Hall 2002). Thus, it is evident that members of the Dbl protein family are attractive therapeutic targets for a variety of diseases (Bos et al. 2007; Loirand et al. 2008; Vigil et al. 2010).

Apart from conventional Dbl family RhoGEFs there are two additional proteins families, which do not share any sequence and structural similarity with each other. The dedicator of cytokinesis (DOCK) or CDM-zizimin homology (CZH) family RhoGEFs are characterized by two conserved regions, known as the DOCK-homology regions 1 and 2 (DHR1 and DHR2) domains (Meller et al. 2005; Rittinger 2009). This type of GEFs employs their DHR2 domain to activate specially Rac and Cdc42 proteins (Meller et al. 2005). Another Rho protein-specific GEF family, represented by the SopE/WxxxE-type exchange factors, is classified as type III effector proteins of bacterial pathogens (Bulgin et al. 2010). They mimic functionally, but not structurally, eukaryotic GEFs by efficiently activating Rac1 and Cdc42 and thus induce "the trigger mechanism of cell entry" (see Chap. 4) (Bulgin et al. 2010; Rudolph et al. 1999).

14.5   GTPase-Activating Proteins

Hydrolysis of the bound GTP is the timing mechanism that terminates signal transduction of the Rho family proteins and returns them to their GDP-bound inactive state (Jaiswal et al. 2012). The intrinsic GTP hydrolysis (GTPase) reaction is usually slow, but can be stimulated by several orders of magnitude through interaction with Rho-specific GAPs (Eberth et al. 2005; Fidyk and Cerione 2002; Zhang and Zheng 1998). The RhoGAP family is defined by the presence of a conserved catalytic GAP domain which is sufficient for the interaction with Rho proteins and mediating accelerated catalysis (Scheffzek and Ahmadian 2005). The GAP domain supplies a conserved arginine residue, termed "arginine finger", into the GTP-binding site of the cognate Rho protein, in order to stabilize the transition state and catalyze the GTP hydrolysis reaction (Nassar et al. 1998; Rittinger et al. 1997). A similar mechanism is utilized by other small GTP-binding proteins

(Scheffzek and Ahmadian 2005), including Ras, Rab, and Arf, although the sequence and folding of the respective GAP families are different (Ismail et al. 2010; Pan et al. 2006; Scheffzek et al. 1997). Masking the catalytic arginine finger is an elegant mechanism for the inhibition of the GAP activity. This has been recently shown for the tumor suppressor protein DLC1, a RhoGAP, which is competitively and selectively inhibited by the SH3 domain of p120RasGAP (Jaiswal et al. 2014).

RhoGAP insensitivity can be achieved by the substitution of either the catalytic arginine of the GAP domain (Fidyk and Cerione 2002; Graham et al. 1999) or amino acids critical for the GTP hydrolysis in Rho proteins, e.g., Glycine 12 and Glutamine 61 in Rac1 and Cdc42 or Glycine 14 and Glutamine 63 in RhoA, which are known as the constitutive active mutants (Ahmadian et al. 1997; Graham et al. 1999). Most remarkably, a similar mechanistic strategy has been mimicked by bacterial GAPs (see Chap. 4), such as the *Salmonella typhimurium* virulence factor SptP, the *Pseudomonas aeruginosa* cytotoxin ExoS, and *Yersinia pestis* YopE, even though they do not share any sequence or structural similarity to eukaryotic RhoGAP domains (Evdokimov et al. 2002; Stebbins and Galan 2000; Wurtele et al. 2001).

The first RhoGAP, p50RhoGAP, was identified by biochemical analysis of human spleen cell extracts in the presence of recombinant RhoA (Garrett et al. 1989). Since then more than 80 RhoGAP containing proteins have been identified in eukaryotes, ranging from yeast to human (Lancaster et al. 1994; Moon and Zheng 2003). The RhoGAP domain (also known as Bcr-homology, BH domain) containing proteins are present throughout the genome and rarely cluster in specific chromosomal regions (Peck et al. 2002). The majority of the RhoGAP family members are frequently accompanied by several other functional domains and motifs implicated in tight regulation and membrane targeting (Eberth et al. 2009; Moon and Zheng 2003; Tcherkezian and Lamarche-Vane 2007). Numerous mechanisms have been shown to affect the specificity and the catalytic activity of the RhoGAPs, e.g., intramolecular autoinhibition (Eberth et al. 2009), posttranslational modification (Minoshima et al. 2003), and regulation by interaction with lipid membrane (Ligeti et al. 2004) and proteins (Yang et al. 2009).

14.6   Conclusions

Abnormal activation of Rho proteins has been shown to play a crucial role in cancer, infectious and cognitive disorders, and cardiovascular diseases. However, several tasks have to be yet accomplished in order to understand the complexity of Rho proteins signaling: (1) The Rho family comprises of 20 signaling proteins, of which only RhoA, Rac1, and Cdc42 have been comprehensively studied so far. The functions of the other less-characterized members of this protein family await detailed investigation. (2) Despite intensive research over the last two decades, the mechanisms by which RhoGDIs associate and extract the Rho proteins from the

membrane and the factors displacing the Rho protein from the complex with RhoGDI remain to be elucidated. (3) For the regulation of the 22 Rho proteins, a tremendous number of their regulatory proteins (>74 GEFs and >80 GAPs) exist in the human genome. How these regulators selectively recognize their Rho protein targets is not well understood and majority of GEFs and GAPs in humans so far remain uncharacterized. (4) Most of the GEFs and GAPs themselves need to be regulated and require activation through the relief of autoinhibitory elements (Chow et al. 2013; Eberth et al. 2009; Jaiswal et al. 2011; Mitin et al. 2007; Moskwa et al. 2005; Rojas et al. 2007; Yohe et al. 2008). With a few exceptions (Cherfils and Zeghouf 2013; Mayer et al. 2013), it is conceptually still unclear how such autoregulatory mechanisms are operated. A better understanding of the specificity and the mode of action of these regulatory proteins is not only fundamentally important for many aspects of biology but is also a master key for the development of drugs against a variety of diseases caused by aberrant functions of Rho proteins.

References

Adra CN, Manor D, Ko JL et al (1997) RhoGDIgamma: a GDP-dissociation inhibitor for Rho proteins with preferential expression in brain and pancreas. Proc Natl Acad Sci USA 94:4279–4284

Ahmadian MR, Mittal R, Hall A et al (1997) Aluminum fluoride associates with the small guanine nucleotide binding proteins. FEBS Lett 408:315–318

Aittaleb M, Boguth CA, Tesmer JJ (2010) Structure and function of heterotrimeric G protein-regulated Rho guanine nucleotide exchange factors. Mol Pharmacol 77:111–125

Bishop AL, Hall A (2000) Rho GTPases and their effector proteins. Biochem J 348(Pt 2):241–255

Bos JL, Rehmann H, Wittinghofer A (2007) GEFs and GAPs: critical elements in the control of small G proteins. Cell 129:865–877

Bouguet-Bonnet S, Buck M (2008) Compensatory and long-range changes in picosecond-nanosecond main-chain dynamics upon complex formation: 15N relaxation analysis of the free and bound states of the ubiquitin-like domain of human plexin-B1 and the small GTPase Rac1. J Mol Biol 377:1474–1487

Boulter E, Garcia-Mata R (2010) RhoGDI: a rheostat for the Rho switch. Small GTPases 1:65–68

Boureux A, Vignal E, Faure S et al (2007) Evolution of the Rho family of ras-like GTPases in eukaryotes. Mol Biol Evol 24:203–216

Bulgin R, Raymond B, Garnett JA et al (2010) Bacterial guanine nucleotide exchange factors SopE-like and WxxxE effectors. Infect Immun 78:1417–1425

Burridge K, Wennerberg K (2004) Rho and Rac take center stage. Cell 116:167–179

Cherfils J, Chardin P (1999) GEFs: structural basis for their activation of small GTP-binding proteins. Trends Biochem Sci 24:306–311

Cherfils J, Zeghouf M (2013) Regulation of small GTPases by GEFs, GAPs, and GDIs. Physiol Rev 93:269–309

Chow CR, Suzuki N, Kawamura T et al (2013) Modification of p115RhoGEF Ser(330) regulates its RhoGEF activity. Cell Signal 25:2085–2092

Chuang TH, Xu X, Knaus UG et al (1993) GDP dissociation inhibitor prevents intrinsic and GTPase activating protein-stimulated GTP hydrolysis by the Rac GTP-binding protein. J Biol Chem 268:775–778

Cook DR, Rossman KL, Der CJ (2013) Rho guanine nucleotide exchange factors: regulators of Rho GTPase activity in development and disease. Oncogene 16:362

336   S.-C. Zhang et al.

DerMardirossian C, Bokoch GM (2005) GDIs: central regulatory molecules in Rho GTPase
    activation. Trends Cell Biol 15:356–363
DerMardirossian C, Schnelzer A, Bokoch GM (2004) Phosphorylation of RhoGDI by Pak1
    mediates, dissociation of Rac GTPase. Mol Cell 15:117–127
DerMardirossian C, Rocklin G, Seo JY et al (2006) Phosphorylation of RhoGDI by Src regulates
    Rho GTPase binding and cytosol-membrane cycling. Mol Biol Cell 17:4760–4768
Dubash AD, Wennerberg K, Garcia-Mata R et al (2007) A novel role for Lsc/p115 RhoGEF and
    LARG in regulating RhoA activity downstream of adhesion to fibronectin. J Cell Sci
    120:3989–3998
Dvorsky R, Ahmadian MR (2004) Always look on the bright site of Rho: structural implications
    for a conserved intermolecular interface. EMBO Rep 5:1130–1136
Eberth A, Dvorsky R, Becker CF et al (2005) Monitoring the real-time kinetics of the hydrolysis
    reaction of guanine nucleotide-binding proteins. Biol Chem 386:1105–1114
Eberth A, Lundmark R, Gremer L et al (2009) A BAR domain-mediated autoinhibitory mecha-
    nism for RhoGAPs of the GRAF family. Biochem J 417:371–377
Erickson JW, Cerione RA (2004) Structural elements, mechanism, and evolutionary convergence
    of Rho protein-guanine nucleotide exchange factor complexes. Biochemistry 43:837–842
Etienne-Manneville S, Hall A (2002) Rho GTPases in cell biology. Nature 420:629–635
Eva A, Vecchio G, Rao CD et al (1988) The predicted DBL oncogene product defines a distinct
    class of transforming proteins. Proc Natl Acad Sci USA 85:2061–2065
Evdokimov AG, Tropea JE, Routzahn KM et al (2002) Crystal structure of the Yersinia pestis
    GTPase activator YopE. Protein Sci 11:401–408
Fan L, Mellor H (2012) The small Rho GTPase Rif and actin cytoskeletal remodelling. Biochem
    Soc Trans 40:268–272
Fidyk NJ, Cerione RA (2002) Understanding the catalytic mechanism of GTPase-activating
    proteins: demonstration of the importance of switch domain stabilization in the stimulation
    of GTP hydrolysis. Biochemistry 41:15644–15653
Fiegen D, Blumenstein L, Stege P et al (2002) Crystal structure of Rnd3/RhoE: functional
    implications. FEBS Lett 525:100–104
Fiegen D, Haeusler LC, Blumenstein L et al (2004) Alternative splicing of Rac1 generates Rac1b,
    a self-activating GTPase. J Biol Chem 279:4743–4749
Fukumoto Y, Kaibuchi K, Hori Y et al (1990) Molecular-cloning and characterization of a novel
    type of regulatory protein (Gdi) for the Rho proteins, Ras P21-Like small Gtp-binding proteins.
    Oncogene 5:1321–1328
Gad AK, Aspenstrom P (2010) Rif proteins take to the RhoD: Rho GTPases at the crossroads of
    actin dynamics and membrane trafficking. Cell Signal 22:183–189
Garavini H, Riento K, Phelan JP et al (2002) Crystal structure of the core domain of RhoE/Rnd3: a
    constitutively activated small G protein. Biochemistry 41:6303–6310
Garcia-Mata R, Boulter E, Burridge K (2011) The 'invisible hand': regulation of RHO GTPases by
    RHOGDIs. Nat Rev Mol Cell Biol 12:493–504
Garrett MD, Self AJ, van Oers C et al (1989) Identification of distinct cytoplasmic targets for ras/
    R-ras and rho regulatory proteins. J Biol Chem 264:10–13
Graham DL, Eccleston JF, Lowe PN (1999) The conserved arginine in rho-GTPase-activating
    protein is essential for efficient catalysis but not for complex formation with Rho.GDP and
    aluminum fluoride. Biochemistry 38:985–991
Gu Y, Zheng Y, Williams DA (2005) RhoH GTPase: a key regulator of hematopoietic cell
    proliferation and apoptosis? Cell Cycle 4:201–202
Guo Z, Ahmadian MR, Goody RS (2005) Guanine nucleotide exchange factors operate by a simple
    allosteric competitive mechanism. Biochemistry 44:15423–15429
Haeusler LC, Hemsath L, Fiegen D et al (2006) Purification and biochemical properties of Rac1,
    2, 3 and the splice variant Rac1b. Methods Enzymol 406:1–11
Hall A, Lalli G (2010) Rho and Ras GTPases in axon growth, guidance, and branching. Cold
    Spring Harb Perspect Biol 2:a001818

Hancock JF, Hall A (1993) A novel role for RhoGDI as an inhibitor of GAP proteins. EMBO J 12:1915–1921

Hart MJ, Eva A, Evans T et al (1991) Catalysis of guanine nucleotide exchange on the CDC42Hs protein by the dbl oncogene product. Nature 354:311–314

Hart MJ, Maru Y, Leonard D et al (1992) A GDP dissociation inhibitor that serves as a GTPase inhibitor for the Ras-like protein CDC42Hs. Science 258:812–815

Heasman SJ, Ridley AJ (2008) Mammalian Rho GTPases: new insights into their functions from in vivo studies. Nat Rev Mol Cell Biol 9:690–701

Hiraoka K, Kaibuchi K, Ando S et al (1992) Both stimulatory and inhibitory GDP/GTP exchange proteins, smg GDS and rho GDI, are active on multiple small GTP-binding proteins. Biochem Biophys Res Commun 182:921–930

Hoffman GR, Cerione RA (2002) Signaling to the Rho GTPases: networking with the DH domain. FEBS Lett 513:85–91

Hutchinson JP, Eccleston JF (2000) Mechanism of nucleotide release from Rho by the GDP dissociation stimulator protein. Biochemistry 39:11348–11359

Ismail SA, Vetter IR, Sot B et al (2010) The structure of an Arf-ArfGAP complex reveals a Ca2+ regulatory mechanism. Cell 141:812–821

Jaiswal M, Gremer L, Dvorsky R et al (2011) Mechanistic insights into specificity, activity, and regulatory elements of the regulator of G-protein signaling (RGS)-containing Rho-specific guanine nucleotide exchange factors (GEFs) p115, PDZ-RhoGEF (PRG), and leukemia-associated RhoGEF (LARG). J Biol Chem 286:18202–18212

Jaiswal M, Dubey BN, Koessmeier KT et al (2012) Biochemical assays to characterize Rho GTPases. Methods Mol Biol 827:37–58

Jaiswal M, Dvorsky R, Ahmadian MR (2013a) Deciphering the molecular and functional basis of Dbl family proteins: a novel systematic approach toward classification of selective activation of the Rho family proteins. J Biol Chem 288:4486–4500

Jaiswal M, Fansa EK, Dvorsky R et al (2013b) New insight into the molecular switch mechanism of human Rho family proteins: shifting a paradigm. Biol Chem 394:89–95

Jaiswal M, Dvorsky R, Amin E et al (2014) Functional crosstalk between Ras and Rho pathways: p120RasGAP competitively inhibits the RhoGAP activity of Deleted in Liver Cancer (DLC) tumor suppressors by masking its catalytic arginine finger. J Biol Chem 289:6839–6849

Joneson T, Bar-Sagi D (1997) Ras effectors and their role in mitogenesis and oncogenesis. J Mol Med (Berl) 75:587–593

Jordan P, Brazao R, Boavida MG et al (1999) Cloning of a novel human Rac1b splice variant with increased expression in colorectal tumors. Oncogene 18:6835–6839

Karnoub AE, Der CJ, Campbell SL (2001) The insert region of Rac1 is essential for membrane ruffling but not cellular transformation. Mol Cell Biol 21:2847–2857

Klebe C, Prinz H, Wittinghofer A et al (1995) The kinetic mechanism of Ran–nucleotide exchange catalyzed by RCC1. Biochemistry 34:12543–12552

Lammers M, Meyer S, Kuhlmann D et al (2008) Specificity of interactions between mDia isoforms and Rho proteins. J Biol Chem 283:35236–35246

Lancaster CA, Taylor-Harris PM, Self AJ et al (1994) Characterization of rhoGAP. A GTPase-activating protein for rho-related small GTPases. J Biol Chem 269:1137–1142

Leonard D, Hart MJ, Platko JV et al (1992) The identification and characterization of a GDP-dissociation inhibitor (GDI) for the CDC42Hs protein. J Biol Chem 267:22860–22868

Li X, Bu X, Lu B et al (2002) The hematopoiesis-specific GTP-binding protein RhoH is GTPase deficient and modulates activities of other Rho GTPases by an inhibitory function. Mol Cell Biol 22:1158–1171

Ligeti E, Dagher MC, Hernandez SE et al (2004) Phospholipids can switch the GTPase substrate preference of a GTPase-activating protein. J Biol Chem 279:5055–5058

Loirand G, Scalbert E, Bril A et al (2008) Rho exchange factors in the cardiovascular system. Curr Opin Pharmacol 8:174–180

Mayer S, Kumar R, Jaiswal M et al (2013) Collybistin activation by GTP-TC10 enhances postsynaptic gephyrin clustering and hippocampal GABAergic neurotransmission. Proc Natl Acad Sci USA 110:20795–20800

Meller N, Merlot S, Guda C (2005) CZH proteins: a new family of Rho-GEFs. J Cell Sci 118:4937–4946

Minoshima Y, Kawashima T, Hirose K et al (2003) Phosphorylation by aurora B converts MgcRacGAP to a RhoGAP during cytokinesis. Dev Cell 4:549–560

Mitin N, Betts L, Yohe ME et al (2007) Release of autoinhibition of ASEF by APC leads to CDC42 activation and tumor suppression. Nat Struct Mol Biol 14:814–823

Moon SY, Zheng Y (2003) Rho GTPase-activating proteins in cell regulation. Trends Cell Biol 13:13–22

Moskwa P, Paclet MH, Dagher MC et al (2005) Autoinhibition of p50 Rho GTPase-activating protein (GAP) is released by prenylated small GTPases. J Biol Chem 280:6716–6720

Mulinari S, Hacker U (2010) Rho-guanine nucleotide exchange factors during development: Force is nothing without control. Small GTPases 1:28–43

Mulloy JC, Cancelas JA, Filippi MD et al (2010) Rho GTPases in hematopoiesis and hemopathies. Blood 115:936–947

Nassar N, Hoffman GR, Manor D et al (1998) Structures of Cdc42 bound to the active and catalytically compromised forms of Cdc42GAP. Nat Struct Biol 5:1047–1052

Nisimoto Y, Freeman JL, Motalebi SA et al (1997) Rac binding to p67(phox). Structural basis for interactions of the Rac1 effector region and insert region with components of the respiratory burst oxidase. J Biol Chem 272:18834–18841

Ohga N, Kikuchi A, Ueda T et al (1989) Rabbit intestine contains a protein that inhibits the dissociation of GDP from and the subsequent binding of GTP to rhoB p20, a ras p21-like GTP-binding protein. Biochem Biophys Res Commun 163:1523–1533

Pan X, Eathiraj S, Munson M et al (2006) TBC-domain GAPs for Rab GTPases accelerate GTP hydrolysis by a dual-finger mechanism. Nature 442:303–306

Peck J, Douglas Gt WCH et al (2002) Human RhoGAP domain-containing proteins: structure, function and evolutionary relationships. FEBS Lett 528:27–34

Pick E, Gorzalczany Y, Engel S (1993) Role of the rac1 p21-GDP-dissociation inhibitor for rho heterodimer in the activation of the superoxide-forming NADPH oxidase of macrophages. Eur J Biochem 217:441–455

Riou P, Villalonga P, Ridley AJ (2010) Rnd proteins: multifunctional regulators of the cytoskeleton and cell cycle progression. Bioessays 32:986–992

Rittinger K (2009) Snapshots form a big picture of guanine nucleotide exchange. Sci Signal 2:pe63

Rittinger K, Walker PA, Eccleston JF et al (1997) Structure at 1.65 A of RhoA and its GTPase-activating protein in complex with a transition-state analogue. Nature 389:758–762

Roberts PJ, Mitin N, Keller PJ et al (2008) Rho Family GTPase modification and dependence on CAAX motif-signaled posttranslational modification. J Biol Chem 283:25150–25163

Rojas RJ, Yohe ME, Gershburg S et al (2007) Galphaq directly activates p63RhoGEF and Trio via a conserved extension of the Dbl homology-associated pleckstrin homology domain. J Biol Chem 282:29201–29210

Rose R, Weyand M, Lammers M et al (2005) Structural and mechanistic insights into the interaction between Rho and mammalian Dia. Nature 435:513–518

Rossman KL, Worthylake DK, Snyder JT et al (2002) Functional analysis of cdc42 residues required for Guanine nucleotide exchange. J Biol Chem 277:50893–50898

Rossman KL, Der CJ, Sondek J (2005) GEF means go: turning on RHO GTPases with guanine nucleotide-exchange factors. Nat Rev Mol Cell Biol 6:167–180

Rudolph MG, Weise C, Mirold S et al (1999) Biochemical analysis of SopE from Salmonella typhimurium, a highly efficient guanosine nucleotide exchange factor for RhoGTPases. J Biol Chem 274:30501–30509

Scheffzek K, Ahmadian MR (2005) GTPase activating proteins: structural and functional insights 18 years after discovery. Cell Mol Life Sci 62:3014–3038

Scheffzek K, Ahmadian MR, Kabsch W et al (1997) The Ras-RasGAP complex: structural basis for GTPase activation and its loss in oncogenic Ras mutants. Science 277:333–338

Scherle P, Behrens T, Staudt LM (1993) Ly-GDI, a GDP-dissociation inhibitor of the RhoA GTP-binding protein, is expressed preferentially in lymphocytes. Proc Natl Acad Sci USA 90:7568–7572

Schmidt A, Hall A (2002) Guanine nucleotide exchange factors for Rho GTPases: turning on the switch. Genes Dev 16:1587–1609

Shutes A, Berzat AC, Chenette EJ et al (2006) Biochemical analyses of the Wrch atypical Rho family GTPases. Methods Enzymol 406:11–26

Srivastava SK, Wheelock RH, Aaronson SA et al (1986) Identification of the protein encoded by the human diffuse B-cell lymphoma (dbl) oncogene. Proc Natl Acad Sci USA 83:8868–8872

Stebbins CE, Galan JE (2000) Modulation of host signaling by a bacterial mimic: structure of the Salmonella effector SptP bound to Rac1. Mol Cell 6:1449–1460

Takahashi K, Sasaki T, Mammoto A et al (1997) Direct interaction of the Rho GDP dissociation inhibitor with ezrin/radixin/moesin initiates the activation of the Rho small G protein. J Biol Chem 272:23371–23375

Tcherkezian J, Lamarche-Vane N (2007) Current knowledge of the large RhoGAP family of proteins. Biol Cell 99:67–86

Thapar R, Karnoub AE, Campbell SL (2002) Structural and biophysical insights into the role of the insert region in Rac1 function. Biochemistry 41:3875–3883

Tnimov Z, Guo Z, Gambin Y et al (2012) Quantitative analysis of prenylated RhoA interaction with its chaperone, RhoGDI. J Biol Chem 287:26549–26562

Troeger A, Chae HD, Senturk M et al (2013) A unique carboxyl-terminal insert domain in the hematopoietic-specific, GTPase-deficient Rho GTPase RhoH regulates post-translational processing. J Biol Chem 288:36451–36462

Venter JC, Adams MD, Myers EW et al (2001) The sequence of the human genome. Science 291:1304–1351

Viaud J, Gaits-Iacovoni F, Payrastre B (2012) Regulation of the DH-PH tandem of guanine nucleotide exchange factor for Rho GTPases by phosphoinositides. Adv Biol Regul 52:303–314

Vigil D, Cherfils J, Rossman KL et al (2010) Ras superfamily GEFs and GAPs: validated and tractable targets for cancer therapy? Nat Rev Cancer 10:842–857

Vlahou G, Rivero F (2006) Rho GTPase signaling in Dictyostelium discoideum: insights from the genome. Eur J Cell Biol 85:947–959

Walker SJ, Brown HA (2002) Specificity of Rho insert-mediated activation of phospholipase D1. J Biol Chem 277:26260–26267

Wennerberg K, Der CJ (2004) Rho-family GTPases: it's not only Rac and Rho (and I like it). J Cell Sci 117:1301–1312

Wittinghofer A, Vetter IR (2011) Structure-function relationships of the G domain, a canonical switch motif. Annu Rev Biochem 80:943–971

Wurtele M, Wolf E, Pederson KJ et al (2001) How the Pseudomonas aeruginosa ExoS toxin downregulates Rac. Nat Struct Biol 8:23–26

Yamashita T, Tohyama M (2003) The p75 receptor acts as a displacement factor that releases Rho from Rho-GDI. Nat Neurosci 6:461–467

Yang XY, Guan M, Vigil D et al (2009) p120Ras-GAP binds the DLC1 Rho-GAP tumor suppressor protein and inhibits its RhoA GTPase and growth-suppressing activities. Oncogene 28:1401–1409

Yohe ME, Rossman K, Sondek J (2008) Role of the C-terminal SH3 domain and N-terminal tyrosine phosphorylation in regulation of Tim and related Dbl-family proteins. Biochemistry 47:6827–6839

Zalcman G, Closson V, Camonis J et al (1996) RhoGDI-3 is a new GDP dissociation inhibitor (GDI). Identification of a non-cytosolic GDI protein interacting with the small GTP-binding proteins RhoB and RhoG. J Biol Chem 271:30366–30374

Zhang B, Zheng Y (1998) Regulation of RhoA GTP hydrolysis by the GTPase-activating proteins p190, p50RhoGAP, Bcr, and 3BP-1. Biochemistry 37:5249–5257

Zong H, Kaibuchi K, Quilliam LA (2001) The insert region of RhoA is essential for Rho kinase activation and cellular transformation. Mol Cell Biol 21:5287–5298

Chapter 3

RHO Kinase regulation (review)

RHO-kinase: regulation, (dys)function and inhibition
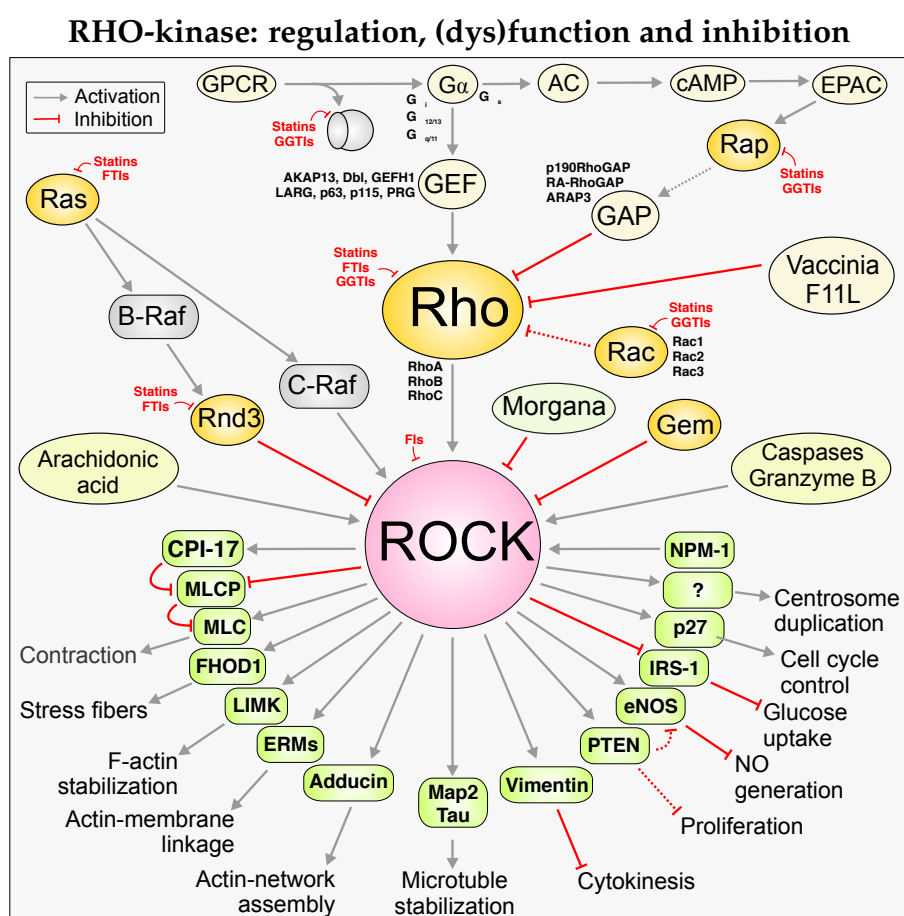
Status:	Published in Biological Chemistry journal 2013; 394(11): 1399–1410
Impact factor:	3.27
Own Proportion to this work:	70 %; documenting literatures and writing manuscript

Review

Ehsan Amin, Badri Nath Dubey[a], Si-Cai Zhang, Lothar Gremer, Radovan Dvorsky, Jens M. Moll, Mohamed S. Taha, Luitgard Nagel-Steger, Roland P. Piekorz, Avril V. Somlyo and Mohammad R. Ahmadian*

Rho-kinase: regulation, (dys)function, and inhibition

Abstract: In a variety of normal and pathological cell types, Rho-kinases I and II (ROCKI/II) play a pivotal role in the organization of the nonmuscle and smooth muscle cytoskeleton and adhesion plaques as well as in the regulation of transcription factors. Thus, ROCKI/II activity regulates cellular contraction, motility, morphology, polarity, cell division, and gene expression. Emerging evidence suggests that dysregulation of the Rho-ROCK pathways at different stages is linked to cardiovascular, metabolic, and neurodegenerative diseases as well as cancer. This review focuses on the current status of understanding the multiple functions of Rho-ROCK signaling pathways and various modes of regulation of Rho-ROCK activity, thereby orchestrating a concerted functional response.

Keywords: coiled-coil-containing protein kinase; drug target; RhoA; Rho-associated; Rho-kinase; ROCK.

[a]Present address: Biozentrum, University of Basel, Basel, Switzerland.
*Corresponding author: Mohammad R. Ahmadian, Institut für Biochemie und Molekularbiologie II, Medizinische Fakultät der Heinrich-Heine-Universität, D-40255 Düsseldorf, Germany, e-mail: reza.ahmadian@uni-duesseldorf.de
Ehsan Amin, Badri Nath Dubey, Si-Cai Zhang, Radovan Dvorsky, Jens M. Moll, Mohamed S. Taha and Roland P. Piekorz: Institut für Biochemie und Molekularbiologie II, Medizinische Fakultät der Heinrich-Heine-Universität, D-40255 Düsseldorf, Germany
Lothar Gremer and Luitgard Nagel-Steger: Institut für Strukturbiochemie (ICS-6), Forschungszentrum Jülich, Jülich, Germany; and Institut für Physikalische Biologie, Mathematisch-Naturwissenschaftliche Fakultät der Heinrich-Heine-Universität, D-40255 Düsseldorf, Germany
Avril V. Somlyo: Department of Molecular Physiology and Biological Physics, University of Virginia, Charlottesville, VA 22908, USA

Introduction

A hallmark of small GTPases, including Rho proteins, is the ability to undergo conformational changes in response to alternate binding of GDP and GTP. They act as molecular switches in the cell by cycling between a GDP-bound inactive state and a GTP-bound active state (Wittinghofer and Vetter, 2011). With a few exceptions (Jaiswal et al., 2013b), the conformational state and localization of Rho GTPases is regulated by three kinds of interacting molecules, guanine nucleotide exchange factors (GEFs), GTPase-activating proteins (GAPs), and guanine nucleotide dissociation inhibitors (Dvorsky and Ahmadian, 2004).

Rho GTPases, in their activated states, regulate cellular structures by controlling the dynamics of microfilaments and microtubules through the binding and activation of their specific downstream effector proteins (Bishop and Hall, 2000; Dvorsky and Ahmadian, 2004). For RhoA, two classes of effector molecules have been described so far. These are scaffold proteins such as Rhophilin, Rhotekin, Kinectin, and Diaphanous (Dia), as well as serine/threonine protein kinases like protein kinase C-related kinase (PRK1, also called PKNα), citron kinase, and the Rho-associated coiled-coil kinases I (ROCKI, also called ROKβ/p160ROCK) and II (ROCKII, also known as ROKα/Rho-kinase) (Amano et al., 2010; Zou and Teitelbaum, 2010; Rath and Olson, 2012). Although both isoforms are ubiquitously expressed, ROCKI expression is enriched in the lung, liver, spleen, kidneys, and testes, whereas ROCKII is more prominent in the brain and heart (Morgan-Fisher et al., 2013). Although ROCKI and ROCKII share many downstream targets, some functional differences have been reported, such as the inhibition of pressure overload-induced cardiac fibrosis in ROCKI null mice (Zhang et al., 2006) or the ability to bind myosin; the regulatory subunit of myosin phosphatase binds ROCKII but not ROCKI, yet both can regulate myosin phosphatase and regulatory light-chain phosphorylation (Wang et al., 2009). For convenience, we do not distinguish between the ROCK isoforms and generally refer to ROCK in this review.

More than 8000 articles on Rho-ROCK are currently available in the PubMed database, including approximately 900 reviews. Here, we summarize the current

knowledge about the crucial role of the Rho-ROCK pathways in human diseases and therapeutic strategies to interfere with their functions. In this review, we will point out various, in part reciprocal, control mechanisms orchestrating a concerted functional response as collectively shown in Figure 1.

Functional repertoire and molecular pathways

Following activation by Rho, ROCK becomes a regulator, especially of cytoskeletal remodeling, for example, actin filament stabilization, assembly of the actin network and the actomyosin fibers, actin-membrane linkage, and microtubule dynamics through the phosphorylation of a number of downstream target proteins (Figure 1).

Smooth muscle and nonmuscle myosin II actomyosin ATPase activity and myosin cross-bridge cycling are regulated by Ca^{2+}-calmodulin-activated myosin light-chain kinase (MLCK) phosphorylation of the regulatory myosin light chain (MLC_{20}) and its dephosphorylation by myosin phosphatase (MLCP). At constant agonist-induced MLCK activity, the extent of MLC_{20} phosphorylation and contraction can be modulated through concomitant activation of RhoA/ROCK signaling, which regulates MLCP activity to Ca^{2+}-sensitize or Ca^{2+}-desensitize contraction (Somlyo and Somlyo, 2003). Indeed, one of the best investigated ROCK functions is the inhibitory phosphorylation of the myosin phosphatase-targeting subunit isoform 1 (MYPT1) at both Thr696 and Thr853 (Kimura et al., 1996; Somlyo and Somlyo, 2003; Loirand et al., 2006; Nunes et al., 2010; Walsh, 2011). This leads to an increase in MLC_{20} phosphorylation to promote contraction of smooth muscle and the formation of contractile actomyosin stress fibers in cultured cells (Somlyo and Somlyo, 2004). ROCK also inhibits MLCP activity by indirectly phosphorylating CPI-17, a potent inhibitor of the catalytic subunit of type 1 protein phosphatase (PP1c) that is not dependent on the phosphorylation of MYPT1 (Eto et al., 1995; Koyama et al., 2000). ROCK has been shown to directly phosphorylate
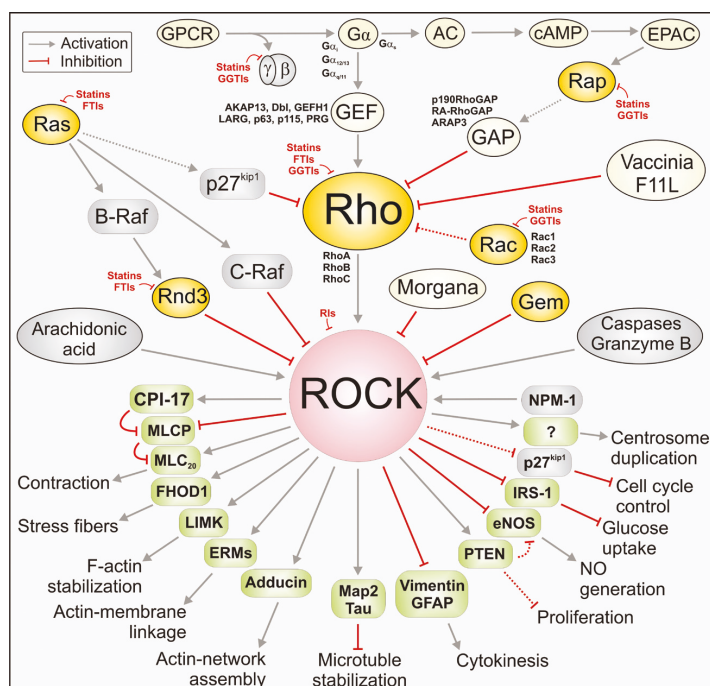
Figure 1 Regulation, functions, and inhibition of the Rho-ROCK-controlled cellular processes.
Broad ranges of ROCK substrates are responsible for diverse cellular functions, which are controlled both positively and negatively by multiple mechanisms. As indicated, statin, GGTI, and FTI treatments as therapeutic strategies abrogate membrane localization of various proteins, including Rho, Rac, Ras, Rnd, and Gγ subunit, and thus interfere with the Rho-ROCK signaling in various types of cells and diseases. Solid arrows are known direct signal cascades, whereas dashed line arrows indicate the putative ones.

MLC_{20} (Amano et al., 1996), but this contribution to total MLC_{20} phosphorylation *in vivo* is not clear.

ROCK controls the stabilization of actin filaments by phosphorylating LIM (LIN-11, ISL1, and MEC-3) kinases 1 and 2 at conserved threonines localized in their respective activation loops. LIM kinases phosphorylate cofilin, thereby inhibiting cofilin-mediated actin filament disassembly. Another ROCK substrate is adducin, a membrane skeletal phosphoprotein that associates with and promotes the association of spectrin with actin filaments, thereby increasing the contractile response (Kimura et al., 1998). The phosphorylation of formin homology domain protein 1 (FHOD1), a major endothelial formin leads to the formation of stress fibers (Takeya et al., 2008). ROCK activates ezrin/radixin/moesin proteins (ERMs) through phosphorylation in the actin-binding domain (Matsui et al., 1998), which in turn directly cross-link the actin cytoskeleton to the plasma membrane and allow the recruitment of multiple signaling proteins.

During cytokinesis, Rho and ROCK are involved in both the progression of the cleavage furrow formation and the disassembly of intermediate filaments such as vimentin and glial fibrillary acidic protein (GFAP) through the phosphorylation of their head domains, which ensures furrow completion (Goto et al., 1998; Yasui et al., 1998; Amano et al., 2010). Other ROCK substrates are the microtubule-associated proteins Tau and MAP2, which modulate microtubule structure and dynamics (Amano et al., 2010). By controlling these events, ROCK directly contributes to a number of cytoskeleton-mediated processes, including adhesion, contraction, polarity, cytokinesis, motility, permeability, phagocytosis, and neurite retraction (Somlyo and Somlyo, 2003; Tan et al., 2011; Tonges et al., 2011).

Further downstream effects of the Rho-ROCK pathway include the negative regulation of endothelial NO synthase (eNOS) and therefore the suppression of NO production in the endothelium, leading to an increase in vascular tone (Rikitake and Liao, 2005). ROCK directly phosphorylates eNOS at Thr495, thereby inhibiting its enzymatic activity (Sugimoto et al., 2007). In addition, Rho-ROCK signal transduction also regulates eNOS gene expression by affecting its mRNA stability (Eto et al., 2001). An indirect effect of ROCK on NO production is achieved by the negative regulation of the PI3K-Akt-eNOS-mediated signaling cascade. Here, phosphatase activity of phosphatase and tensin homologue (PTEN) is stimulated through phosphorylation (Li et al., 2005). Accumulated evidence also suggests that ROCK plays a pivotal role in the regulation of insulin- and PI3K-dependent translocation of glucose transporter 4 (GLUT4) to the plasma membrane, for example, in skeletal muscles (Lee et al., 2009). ROCK activation is essential for the normal action of insulin on glucose uptake, most likely due to ROCK-mediated phosphorylation and inhibition of insulin receptor substrate 1 (IRS-1) (Begum et al., 2002; Furukawa et al., 2005). A targeted disruption of ROCK causes insulin resistance *in vivo* (Lee et al., 2009).

In addition, Rho-ROCK signaling plays an important function in gene expression, cell cycle progression, proliferation, differentiation, and apoptosis (Olson, 2008; Fukasawa, 2011; Street and Bryan, 2011; David et al., 2012). ROCK regulates the level of the cell cycle regulatory proteins, e.g., by elevating cyclin D1 and reducing $p27^{Kip1}$ protein levels (Croft and Olson, 2006). Another remarkable link of ROCK to cell cycle progression has been implicated by the interaction between ROCK and the multifaceted nucleolar phosphoprotein nucleophosmin (NPM-1). Following phosphorylation by cyclin-dependent kinase 2 (CDK2)/cyclin E, NPM-1 tightly associates with and activates ROCK, a critical event for the timely initiation of centrosome duplication and the coupling of centrosome duplication and DNA replication during S-phase (Ma et al., 2006; Hanashiro et al., 2011). Interestingly, Morgana (also called cysteine- and histidine-rich domain-containing protein 1), which is strongly downregulated in breast and lung cancer samples, directly binds ROCK in a complex with heat shock protein 90 (HSP90) and thereby inhibits centrosome duplication and tumorigenesis (Ferretti et al., 2010).

The selectivity of Rho/ROCK inhibition in human diseases

The strong interest in the Rho-ROCK pathway for drug targeting is based on the observation that the abnormal activation of this pathway plays a crucial role in numerous and diverse human diseases. These include tumor invasion, angiogenesis, and metastasis (Narumiya et al., 2009; Baranwal and Alahari, 2011; Mardilovich et al., 2012; Morgan-Fisher et al., 2013; Schofield and Bernard, 2013); cardiovascular disorders such as coronary vasospasm, cerebral cavernous malformation, hypertension, atherosclerosis, pulmonary hypertension, cardiac hypertrophy, and stroke (Shimokawa and Rashid, 2007; Olson, 2008; Nunes et al., 2010; Satoh et al., 2011; Shi et al., 2011; Zhou et al., 2011; Noma et al., 2012; Wang and Liao, 2012); insulin resistance, metabolic diseases, and diabetic nephropathy (Komers, 2011; Zhou and Li, 2012; Richardson et al., 2013); and neurodegenerative disorders (Mueller et al., 2005; Schmandke and Strittmatter, 2007; Salminen et al., 2008; Tonges et al., 2011). Advances in understanding the role of Rho-ROCK signaling in various human disorders

originate from extensive experimental studies using predominantly different pharmacological inhibitors (Somlyo, 1997; Uehata et al., 1997; Olson, 2008; Hahmann and Schroeter, 2010; Miyamoto et al., 2010; Zhou and Liao, 2010; Tonges et al., 2011; Mardilovich et al., 2012) and also to some extent from other independent tools, including the use of bacterial toxins and dominant negative variants of Rho GTPases (Bishop and Hall, 2000). Moreover, ROCK inhibitors have been shown to be useful tools for cultivation of human embryonic stem cells and induced pluripotent stem cells (Rizzino, 2010; Ohgushi and Sasai, 2011).

The activation process of the Rho-ROCK pathway underlies several different regulatory mechanisms: (i) posttranslational lipid modification and translocation of Rho to the cellular membrane, (ii) receptor-dependent GEF-catalyzed GDP/GTP exchange of Rho, (iii) allosteric mode of ROCK activation upon direct association with Rho, and (iv) ATP-dependent phosphorylation of various ROCK substrates. Interference with any of the above processes has been proven to inhibit Rho-ROCK-stimulated cellular responses (Mardilovich et al., 2012). The most frequently used pharmacological inhibitors for the Rho-ROCK pathway can be categorized into three classes, including substances inhibiting ROCK [ROCK inhibitors (RIs)], geranylgeranyl transferase 1 (GGTase), or 3-hydroxy-3-methylglutaryl-coenzyme A (HMG-CoA) reductase (also known as statins). An issue of debate, however, is that in many studies, these compounds, especially statins and GGTase inhibitors (GGTIs), have been often regarded as 'specific' inhibitors of the Rho-ROCK activity, which is actually rather improper.

Y-27632 and fasudil (also known as HA-1077) are by far the most widely used ROCK inhibitors that target its ATP-binding site of the kinase domain and competitively inhibit phosphorylation of various substrates (Uehata et al., 1997; Somlyo, 1997; Suzuki et al., 1999; Mueller et al., 2005; Liao et al., 2007; Hahmann and Schroeter, 2010; Miyamoto et al., 2010; Mardilovich et al., 2012). A systematic *in vitro* analysis of Y-27632 and fasudil targets has revealed that they also inhibit PRK2/PKNγ, another Rho-regulated kinase, almost as potently as ROCK itself (Davies et al., 2000). Y-27632 had a minimal effect on other kinases in this screen of a large panel of protein kinases. However, at high concentrations, Y-27632 inhibits several other serine/threonine-specific protein kinases with wide cellular functions, including ERK2, GSK3β, JNK1α, p38α, PKA, PKBα, PKCα, and S6K1 (Davies et al., 2000). Therefore, the judicious use of low concentrations of Y-27632 and fasudil as well as the evaluation of the activity of these possible off-target kinases is important. Of note, fasudil is known as a prodrug, which has to be metabolized to hydroxyfasudil *in*

vivo that then displays a more potent inhibitory effect than its precursor fasudil (Rikitake et al., 2005).

Subcellular localization of Rho proteins to different cellular membranes, which is known to be critical for their biological activity, is achieved by posttranslational modifications at a distinct cysteine residue in the C-terminal CAAX motif (C is cysteine, A is any aliphatic amino acid, and X is any amino acid) (Roskoski, 2003; Roberts et al., 2008). Thus, Rho proteins serve as substrates for isoprenyl-transferring enzymes, such as GGTase 1 and in a few cases also farnesyl transferase (FTase). A covalent and irreversible attachment of a 20-carbon geranylgeranyl or a 15-carbon farnesyl moiety by these enzymes to the cysteine residue of the CAAX motif, which is present in more than 100 proteins, is necessary for eukaryotic cell growth, differentiation, and morphology (Lane and Beese, 2006). These two lipids are synthesized from the activated cholesterol precursors, farnesylpyrophosphate (FPP) and geranylgeranylpyrophosphate (GGPP) by the mevalonate pathway. Two post-prenylation enzymatic steps are critical for proper localization, including proteolytic cleavage of the AAX residues by the protease Rce1 and methylation of the terminal isoprenylcysteine by the methyltransferase ICMT (Winter-Vann and Casey, 2005).

Geranylgeranylation is required for Rho protein functions and is thus a prerequisite for their involvement in pathogenesis of human diseases. This prompted the development of potential GGTase 1 inhibitors (GGTIs) (Gelb et al., 2006; Triola et al., 2012). By preventing geranylgeranylation, GGTIs are able to inhibit proliferation and induce apoptosis in various biological systems (Sebti and Hamilton, 2000a; Khwaja et al., 2006) and to interfere with the progression of atherosclerosis *via* the inhibition of plaque angiogenesis (Park et al., 2006). GGTIs have been shown to block subcellular localization and consequently the signaling function of several Rho proteins, including RhoA, Cdc42, and Rac1 (Sebti and Hamilton, 2000b; Joyce and Cox, 2003; Khan et al., 2011). Importantly, the fact that a range of geranylgeranylated proteins besides Rho proteins, for example, the γ-subunits of heterotrimeric G proteins represent substrates of GGTase 1 (Marrari et al., 2007), scale down the selectivity spectrum of GGTIs (Konstantinopoulos et al., 2007).

Major recent efforts focused on blocking prenylation of Ras oncogenes have been first directed to the development of FTase inhibitors (FIs) (Blum et al., 2008; Mardilovich et al., 2012). By blocking the FTase activity, Ras was instead geranylgeranylated. This stimulated the development of dual-targeting FTase and GGTase 1 inhibitors, such as AZD3409, which has been shown to inhibit farnesylation to a higher extent than geranylgeranylation

(Appels et al., 2011). However, the inhibition of both farnesylation and geranylgeranylation could not be correlated with the antiproliferative activity of this drug (Appels et al., 2011).

In addition, it was recently shown that protein geranylgeranylation is required for the dimerization and activation of the epidermal growth factor receptor, a key player in a signaling pathway, whose activity is upregulated in more than 30% of human cancers (Zhao et al., 2010). Another example is geranylgeranylation of Rab27B, which has been shown to be required for breast cancer growth, invasion, and metastasis (Hendrix et al., 2010). Thus, geranylgeranyl pyrophosphate (GGPP) synthase has emerged as a new therapeutic target that has been suggested to provide another platform for interfering with protein prenylation in cells (Wiemer et al., 2011). Cellular GG-PP depletion, by inhibiting this enzyme, affects all geranylgeranylated proteins, including also the regulatory functions of Rab proteins in vesicle trafficking (Stenmark, 2009). Rab GTPases consisting of at least 60 different family members are modified by GGTase 2, which recognizes C-terminal CCXX, CC, or CXC motifs (Brunsveld et al., 2006; Itzen and Goody, 2011). It will be interesting to see whether GG-PP synthase inhibitors will develop also into widely used drugs comparable to the HMG-CoA reductase inhibitors (statins).

Statins are clinically approved for the treatment of hypercholesterolemia (Faiz et al., 2012; Raper et al., 2012). However, increasing clinical and experimental evidence demonstrates a variety of beneficial effects beyond the reduction of serum cholesterol (Lopez-Pedrera et al., 2012). These cholesterol-independent 'pleiotropic' effects are mediated by the depletion of crucial isoprenoid intermediates of the cholesterol biosynthetic pathway, namely FPP and GGPP. Statin treatment has been shown to abrogate membrane localization of small GTPases and interfere with, among others, Rho-ROCK signaling in various types of cells and diseases, including cancer (Riganti et al., 2008; Wiemer et al., 2009; Roy et al., 2011; Mardilovich et al., 2012), diabetes (Zhou and Li, 2011), cardiovascular disease (Reddy et al., 2005; Nakamura et al., 2006; Zhou and Liao, 2009; Zhou et al., 2011; Lopez-Pedrera et al., 2012), endothelial dysfunction (Tesfamariam, 2006; Noma et al., 2012), pulmonary hypertension (Oka et al., 2008; Antoniu, 2012), heart failure and ischemic stroke (Sawada and Liao, 2009; Miyamoto et al., 2010), bronchial asthma (Chiba et al., 2010), Alzheimer disease (Tang, 2005), and kidney disease (Fried, 2008). To what extent Rho-ROCK activity is inhibited in these respective patients upon statin therapy is unclear. It is a fact that inhibition of HMG-CoA reductase and consequently the depletion of

GGPP and FPP may conceivably compromise diverse cellular functions and processes controlled by the families of Ras, Rho, and Rab GTPases; the γ subunits of the heterotrimeric G proteins involved in signaling by G-protein-coupled receptors (GPCRs); and many other prenylated proteins (Figure 1).

It is important to note that targeting protein prenylation in human diseases, despite the large number of different prenylated proteins, has reached an immense area of applications, ranging from cancer and cardiovascular diseases to also very rare genetic disorders, for example, Hutchinson-Gilford progeria syndrome (Resh, 2012; Young et al., 2013). The usefulness of such a clinical approach remains in many cases a matter of debate. In this context, it is important to note that statins have negative side effects on mood states, including depression, anxiety, anger, hostility, fatigue, confusion, skeletal muscle pain, and vigor (While and Keen, 2012).

Control mechanisms regulating the activity of the Rho-ROCK pathway

As discussed above, the Rho-ROCK pathway is involved in multiple biochemical and pathobiochemical processes, and not surprisingly, Rho and ROCK proteins are subjected to several regulatory mechanisms that influence their activation, thereby controlling the kinase activity of ROCK. The first step is a proper subcellular localization of these proteins that is highly dependent on the cell type and consequently on the controlled process, ranging from changes in contractility, permeability, motility, proliferation, to apoptosis.

The activity of Rho proteins is controlled through the activation of various cell surface receptors, including tyrosine kinase receptors, GPCRs, and cell-cell and cell-matrix adhesion molecules, such as cadherins and integrins (Wettschureck and Offermanns, 2002; Iden and Collard, 2008; Tybulewicz and Henderson, 2009; Zou and Teitelbaum, 2010; Litosch, 2011; Raptis et al., 2011; Momotani and Somlyo, 2012). Receptor signaling recruits and activates a large variety of the Dbl family proteins (so-called RhoGEFs), which have been recently classified on the basis of their selectivity for different Rho proteins as substrate into distinct subfamilies (Jaiswal et al., 2013a). In this regard, multiple Rho-selective members of the Dbl family have been reported to specifically link G-protein-coupled signals to Rho activation, including AKAP13/Lbc, Dbl, GEFH1/Lfc, LARG, p63, p115, and PRG (Jin and Exton, 2000; Diviani et al., 2001; Loirand et al., 2006; Vanni

et al., 2007; Wirth et al., 2008; Meiri et al., 2009; Momotani et al., 2011; Momotani and Somlyo, 2012; Mikelis et al., 2013; Takefuji et al., 2013). Dbl proteins catalyze the GDP/GTP exchange of the three Rho isoforms, RhoA, RhoB, and RhoC, and therefore act as positive regulators (Jaiswal et al., 2011, 2013a; Rossman et al., 2005).

The interaction of the active (GTP-bound) Rho isoforms with a large and functionally diverse number of effectors is the basis for signal transduction into different pathways (Bishop and Hall, 2000; Karnoub et al., 2004). It is very likely that different RhoGEFs contribute to directing Rho signaling to these different pathways (Wirth et al., 2008; Momotani et al., 2011). In addition to the competition of multiple effectors in binding to a single GTPase, the utilization of multiple contact sites adds another level of complexity toward comprehending the molecular mechanisms underlying RhoA-mediated effector activation (Blumenstein and Ahmadian, 2004). The most common mechanism of effector activation by RhoA appears to be the disruption of intramolecular autoinhibitory interactions to release functional domains within the effector protein. The activity of the kinase domain of ROCK, for example, has been proposed to be autoinhibited by a segment at the C-terminus of ROCK, encompassing a Rho-binding domain (RBD) (Dvorsky et al., 2004) and a split PH domain that is bisected by a cysteine-rich C1 domain (PHn-C1-PHc) (Amano et al., 1999). Under resting conditions, inactive ROCK may exist in a tetrameric state (Chen et al., 2002; Doran et al., 2004). Activated RhoA has been shown to bind to three different domains in the central coiled-coil region of ROCK, such as the RBD, the Rho-interacting domain (RID), and the homology region 1 (HR1) (Blumenstein and Ahmadian, 2004). Therefore, it has been proposed that Rho-mediated activation of ROCK may operate through an allosteric binding mechanism. Accordingly, Rho might successively associate with RBD, RID, and HR1, inducing a conformational change that displaces the autoinhibitory C-terminus, generating ROCK dimers. The activity of the released kinase domain is most probably further potentiated *via* transphosphorylation and other components, including arachidonic acid binding and lipid membrane binding *via* the unconventional C-terminal PHn-C1-PHc (Somlyo and Somlyo, 2000; Riento and Ridley, 2003; Wen et al., 2008; Morgan-Fisher et al., 2013). ROCK is a substrate of proteases, such as granzyme B or caspases 3 and 8, which cleave off the PH domain and generate a constitutively active ROCK (Morgan-Fisher et al., 2013). ROCK cleavage by caspase-3 during apoptosis generates a truncated active form and induces MLC phosphorylation and apoptotic membrane blebbing (Coleman et al., 2001). Caspase-8-mediated ROCK cleavage leads to

the remodeling of the actin cytoskeleton, resulting in an amoeboid-shaped cell associated with cell migration and in enhanced invasiveness of tumor cells in response to constitutively active PI3K signaling, which regulates cell proliferation, growth and mobility, and signaling through the cell death ligands, TRAIL and CD95L (Ehrenschwender et al., 2010).

In contrast to activating upstream regulators, there are only a few signaling pathways known that negatively control Rho-ROCK-mediated cellular processes through the activation of inactivating regulatory molecules, including the Rho GTPase-activating proteins (RhoGAPs) (Ligeti et al., 2012). p190RhoGAP, for example, antagonizes the Rho-ROCK-mediated regulation of actomyosin contractility by stimulating GTP hydrolysis and reducing the activity of RhoA in tumor cells. This mechanism has been shown to depend on the association of p190RhoGAP with Rnd3/RhoE, a Rho-related GTP-binding protein (Jaiswal et al., 2013b), which is controlled by the assembly of the DDR1-Par3/Par6 complex (Hidalgo-Carcedo et al., 2011). p190RhoGAP has been also shown to be an integral component in the Rac1-induced inactivation of Rho signaling (Nimnual et al., 2003; Herbrand and Ahmadian, 2006). Contrary to Rho-induced cell contractility, Rac promotes rather cellular protrusion and thus counteracts Rho signaling. In this regard, the reciprocal balance between these GTPases determines morphology and migratory behavior of cells (Heasman and Ridley, 2008). Recently, a cAMP-mediated PKA-independent signaling through the Epac/Rap1 pathway has been shown to induce a significant relaxation of RhoA-mediated smooth muscle contraction (Zieba et al., 2011). In this context, the Rap1-activated RhoGAPs, such as RA-RhoGAP or ARAP3, have been suggested to downregulate RhoA activity in the smooth muscle (Zieba et al., 2011). Moreover, blocking Rho-ROCK interaction and signaling by directly targeting Rho protein is another mechanism. Phosphorylation of the cell cycle inhibitor p27[Kip1] by p90 ribosomal S6 kinase (RSK1) downstream of Ras, has been shown to directly bind RhoA and inhibit Rho-ROCK pathway (Larrea et al., 2009). Vaccinia virus utilizes its F11L protein to interfere with the Rho interaction with ROCK. This virus blocks stress fiber formation of the host cells through its F11L protein, reported to directly bind RhoA and inhibit RhoA-mediated ROCK activation (Valderrama et al., 2006).

Rho-ROCK signaling can be specifically abrogated by the inhibition of the kinase domain of ROCK. This Ras-dependent mechanism includes a link between C-Raf and ROCK (Niault and Baccarini, 2010). Accordingly, the N-terminal regulatory domain of C-Raf binds physically to the kinase domain of ROCK and directly inhibits its

enzymatic activity. ROCK inhibition by C-Raf has been proposed to be necessary for the development and maintenance of Ras-induced epidermal tumors. In addition, B-Raf has been shown to positively control Rnd3/RhoE expression, which in turn regulates the cross-talk between the RAF/MEK/ERK and Rho/ROCK signaling pathways and contributes to oncogene-mediated reorganization of the actin cytoskeleton (Klein et al., 2008). Rnd3/RhoE induces stress fiber disassembly by directly binding ROCK and inhibiting it from phosphorylating downstream targets (Riento et al., 2003). ROCK can in turn phosphorylate Rnd3/RhoE as well as p190RhoGAP to downregulate GAP activity, leading to a further increase in RhoA activity (Madigan et al., 2009). Gem and Rad are other GTP-binding proteins that act as negative regulators of the Rho-ROCK pathway (Ward et al., 2002). Gem binds to the coiled-coil region of ROCK independently of RhoA and modifies the substrate specificity of ROCK. Taken together, RhoA, RhoB, and RhoC associate with and activate ROCK, whereas other GTP-binding proteins inhibit ROCK either directly, as has been found for Rnd3/RhoE and Gem, or indirectly, as has been reported for Rac and Ras signals.

Conclusion

RhoA-ROCK has emerged as a central signal-integrating node that senses and responds to extracellular and intracellular cues and thus regulates a wide range of fundamental cell functions such as contraction, motility, proliferation, and apoptosis. Abnormal activation of the RhoA-ROCK pathway has been observed in cancer, neurodegenerative diseases, and notably in major cardiovascular disorders, including hypertension, atherosclerosis, cerebral cavernous malformations leading to stroke, postangioplasty restenosis, pulmonary hypertension, and cardiac hypertrophy. Great effort has been expended over the past years in the development of pharmacological inhibitors interfering with RhoA-ROCK signal transduction. A large number of studies have shown that statins, GGTIs, FIs, and RIs are valuable tools for elucidating the physiological and pathophysiological roles of pathways and processes involving prenylated proteins, such as RhoA, B, and C and protein kinases, including ROCK.

Despite almost 20 years of intensive research on therapeutic-relevant small GTPase signaling, only two approaches for drug design have been thoroughly exploited, which are kinase and prenylation inhibitors. A common problem with kinase inhibitors is their tendency toward nonselectivity because the majority of these inhibitors interact with highly conserved proteins domains, in particular the catalytic domain. For known reasons, the structure-function relationship of the kinase domains has been very well investigated in the last decade, and other mechanisms have been largely disregarded. Targeting protein prenylation in human diseases, despite the large number of different prenylated proteins, has been mostly described for Ras and Rho proteins. There is, therefore, an urgent need for alternative approaches that specifically target Rho-ROCK signal transduction. Although ROCK belongs to one of the best investigated small GTPase effectors in both fundamental and clinical research, the molecular basis of its regulation has remained a matter of speculation. Thus, it is required to identify new mechanisms, which may offer great potential for defining new drug target sites and for attempting a novel strategy for more selective therapeutic intervention.

It is of major importance to note that apart from Rho isoforms, which bind to and activate ROCK, there are, in addition to the RhoGEFs and RhoGAPs, also Rnd3/RhoE, Gem, C-Raf, p27[Kip1], F11L, Morgana, NPM-1, and the Gγ subunits as well as Rac and Ras isoforms that directly or indirectly control the activity of Rho-ROCK signaling pathways (Figure 1). Thus, understanding the mechanisms underlying the negative regulation of Rho-ROCK signaling could lead to the development of novel therapeutic approaches for the treatment of these diseases. In addition, one has to take into account the fact that the function of these negative regulators, except for Rad, also depends on prenylation. Rnd3 and Ras proteins are farnesylated, whereas RhoA, RhoC, and the Rac isoforms as well as Gγ proteins are geranylgeranylated. RhoB exists in two populations that are either farnesylated or geranylgeranylated. It is therefore crucial that future studies examining associations between prenylation inhibitors and various ROCK-associated human diseases also focus on small GTPases other than only the Rho isoforms.

References

Amano, M., Ito, M., Kimura, K., Fukata, Y., Chihara, K., Nakano, T., Matsuura, Y., and Kaibuchi, K. (1996). Phosphorylation and activation of myosin by Rho-associated kinase (Rho-kinase). J. Biol. Chem. *271*, 20246–20249.

Amano, M., Chihara, K., Nakamura, N., Kaneko, T., Matsuura, Y., and Kaibuchi, K. (1999). The COOH-terminus of Rho-kinase negatively regulates rho-kinase activity. J. Biol. Chem. *274*, 32418–32424.

Amano, M., Nakayama, M., and Kaibuchi, K. (2010). Rho-kinase/ROCK: a key regulator of the cytoskeleton and cell polarity. Cytoskeleton *67*, 545–554.

Antoniu, S.A. (2012). Targeting RhoA/ROCK pathway in pulmonary arterial hypertension. Expert Opin. Ther. Targets *16*, 355–363.

Appels, N.M., Bolijn, M.J., van Eijndhoven, M.A., Stephens, T.C., Beijnen, J.H., and Schellens, J.H. (2011). Characterization of the *in vitro* activity of AZD3409, a novel prenyl transferase inhibitor. Cancer Chemother. Pharmacol. *67*, 137–145.

Baranwal, S. and Alahari, S.K. (2011). Rho GTPase effector functions in tumor cell invasion and metastasis. Curr. Drug Targets *12*, 1194–1201.

Begum, N., Sandu, O.A., Ito, M., Lohmann, S.M., and Smolenski, A. (2002). Active Rho kinase (ROK-α) associates with insulin receptor substrate-1 and inhibits insulin signaling in vascular smooth muscle cells. J. Biol. Chem. *277*, 6214–6222.

Bishop, A.L. and Hall, A. (2000). Rho GTPases and their effector proteins. Biochem. J. *348*, 241–255.

Blum, R., Cox, A.D., and Kloog, Y. (2008). Inhibitors of chronically active ras: potential for treatment of human malignancies. Recent Pat. Anticancer Drug Discov. *3*, 31–47.

Blumenstein, L. and Ahmadian, M.R. (2004). Models of the cooperative mechanism for Rho effector recognition: implications for RhoA-mediated effector activation. J. Biol. Chem. *279*, 53419–53426.

Brunsveld, L., Kuhlmann, J., Alexandrov, K., Wittinghofer, A., Goody, R.S., and Waldmann, H. (2006). Lipidated ras and rab peptides and proteins – synthesis, structure, and function. Angew. Chem. *45*, 6622–6646.

Chen, X.Q., Tan, I., Ng, C.H., Hall, C., Lim, L., and Leung, T. (2002). Characterization of RhoA-binding kinase ROKα implication of the pleckstrin homology domain in ROKα function using region-specific antibodies. J. Biol. Chem. *277*, 12680–12688.

Chiba, Y., Matsusue, K., and Misawa, M. (2010). RhoA, a possible target for treatment of airway hyperresponsiveness in bronchial asthma. J. Pharmacol. Sci. *114*, 239–247.

Coleman, M.L., Sahai, E.A., Yeo, M., Bosch, M., Dewar, A., and Olson, M.F. (2001). Membrane blebbing during apoptosis results from caspase-mediated activation of ROCK I. Nat. Cell Biol. *3*, 339–345.

Croft, D.R. and Olson, M.F. (2006). The Rho GTPase effector ROCK regulates cyclin A, cyclin D1, and p27Kip1 levels by distinct mechanisms. Mol. Cell. Biol. *26*, 4612–4627.

David, M., Petit, D., and Bertoglio, J. (2012). Cell cycle regulation of Rho signaling pathways. Cell Cycle *11*, 3003–3010.

Davies, S.P., Reddy, H., Caivano, M., and Cohen, P. (2000). Specificity and mechanism of action of some commonly used protein kinase inhibitors. Biochem. J. *351*, 95–105.

Diviani, D., Soderling, J., and Scott, J.D. (2001). AKAP-Lbc anchors protein kinase A and nucleates Gα 12-selective Rho-mediated stress fiber formation. J. Biol. Chem. *276*, 44247–44257.

Doran, J.D., Liu, X., Taslimi, P., Saadat, A., and Fox, T. (2004). New insights into the structure-function relationships of Rho-associated kinase: a thermodynamic and hydrodynamic study of the dimer-to-monomer transition and its kinetic implications. Biochem. J. *384*, 255–262.

Dvorsky, R. and Ahmadian, M.R. (2004). Always look on the bright site of Rho: structural implications for a conserved intermo-lecular interface. EMBO Rep. *5*, 1130–1136.

Dvorsky, R., Blumenstein, L., Vetter, I.R., and Ahmadian, M.R. (2004). Structural insights into the interaction of ROCKI with the switch regions of RhoA. J. Biol. Chem. *279*, 7098–7104.

Ehrenschwender, M., Siegmund, D., Wicovsky, A., Kracht, M., Dittrich-Breiholz, O., Spindler, V., Waschke, J., Kalthoff, H., Trauzold, A., and Wajant, H. (2010). Mutant PIK3CA licenses TRAIL and CD95L to induce non-apoptotic caspase-8-mediated ROCK activation. Cell Death Differ. *17*, 1435–1447.

Eto, M., Ohmori, T., Suzuki, M., Furuya, K., and Morita, F. (1995). A novel protein phosphatase-1 inhibitory protein potentiated by protein kinase C. Isolation from porcine aorta media and characterization. J. Biochem. (Tokyo) *118*, 1104–1107.

Eto, M., Barandier, C., Rathgeb, L., Kozai, T., Joch, H., Yang, Z., and Luscher, T.F. (2001). Thrombin suppresses endothelial nitric oxide synthase and upregulates endothelin-converting enzyme-1 expression by distinct pathways: role of Rho/ROCK and mitogen-activated protein kinase. Circ. Res. *89*, 583–590.

Faiz, F., Hooper, A.J., and van Bockxmeer, F.M. (2012). Molecular pathology of familial hypercholesterolemia, related dyslipidemias and therapies beyond the statins. Crit. Rev. Clin. Lab. Sci. *49*, 1–17.

Ferretti, R., Palumbo, V., Di Savino, A., Velasco, S., Sbroggio, M., Sportoletti, P., Micale, L., Turco, E., Silengo, L., Palumbo, G., et al. (2010). Morgana/chp-1, a ROCK inhibitor involved in centrosome duplication and tumorigenesis. Dev. Cell *18*, 486–495.

Fried, L.F. (2008). Effects of HMG-CoA reductase inhibitors (statins) on progression of kidney disease. Kidney Int. *74*, 571–576.

Fukasawa, K. (2011). Aberrant activation of cell cycle regulators, centrosome amplification, and mitotic defects. Horm. Cancer *2*, 104–112.

Furukawa, N., Ongusaha, P., Jahng, W.J., Araki, K., Choi, C.S., Kim, H.J., Lee, Y.H., Kaibuchi, K., Kahn, B.B., Masuzaki, H., et al. (2005). Role of Rho-kinase in regulation of insulin action and glucose homeostasis. Cell Metab. *2*, 119–129.

Gelb, M.H., Brunsveld, L., Hrycyna, C.A., Michaelis, S., Tamanoi, F., Van Voorhis, W.C., and Waldmann, H. (2006). Therapeutic intervention based on protein prenylation and associated modifications. Nat. Chem. Biol. *2*, 518–528.

Goto, H., Kosako, H., Tanabe, K., Yanagida, M., Sakurai, M., Amano, M., Kaibuchi, K., and Inagaki, M. (1998). Phosphorylation of vimentin by Rho-associated kinase at a unique amino-terminal site that is specifically phosphorylated during cytokinesis. J. Biol. Chem. *273*, 11728–11736.

Hahmann, C. and Schroeter, T. (2010). Rho-kinase inhibitors as therapeutics: from pan inhibition to isoform selectivity. Cell. Mol. Life Sci. *67*, 171–177.

Hanashiro, K., Brancaccio, M., and Fukasawa, K. (2011). Activated ROCK II by-passes the requirement of the CDK2 activity for centrosome duplication and amplification. Oncogene *30*, 2188–2197.

Heasman, S.J. and Ridley, A.J. (2008). Mammalian Rho GTPases: new insights into their functions from *in vivo* studies. Nat. Rev. Mol. Cell Biol. *9*, 690–701.

Hendrix, A., Maynard, D., Pauwels, P., Braems, G., Denys, H., Van den Broecke, R., Lambert, J., Van Belle, S., Cocquyt, V., Gespach, C., et al. (2010). Effect of the secretory small GTPase Rab27B on breast cancer growth, invasion, and metastasis. J. Natl. Cancer Inst. *102*, 866–880.

Herbrand, U. and Ahmadian, M.R. (2006). p190-RhoGAP as an integral component of the Tiam1/Rac1-induced downregulation of Rho. Biol. Chem. *387*, 311–317.

Hidalgo-Carcedo, C., Hooper, S., Chaudhry, S.I., Williamson, P., Harrington, K., Leitinger, B., and Sahai, E. (2011). Collective cell migration requires suppression of actomyosin at cell-cell contacts mediated by DDR1 and the cell polarity regulators Par3 and Par6. Nat. Cell Biol. *13*, 49–58.

Iden, S. and Collard, J.G. (2008). Crosstalk between small GTPases and polarity proteins in cell polarization. Nat. Rev. Mol. Cell Biol. *9*, 846–859.

Itzen, A. and Goody, R.S. (2011). Covalent coercion by *Legionella pneumophila*. Cell Host Microbe *10*, 89–91.

Jaiswal, M., Gremer, L., Dvorsky, R., Haeusler, L.C., Cirstea, I.C., Uhlenbrock, K., and Ahmadian, M.R. (2011). Mechanistic insights into specificity, activity, and regulatory elements of the regulator of G-protein signaling (RGS)-containing Rho-specific guanine nucleotide exchange factors (GEFs) p115, PDZ-RhoGEF (PRG), and leukemia-associated RhoGEF (LARG). J. Biol. Chem. *286*, 18202–18212.

Jaiswal, M., Dvorsky, R., and Ahmadian, M.R. (2013a). Deciphering the molecular and functional basis of Dbl family proteins: a novel systematic approach toward classification of selective activation of the Rho family proteins. J. Biol. Chem. *288*, 4486–4500.

Jaiswal, M., Fansa, E.K., Dvorsky, R., and Ahmadian, M.R. (2013b). New insight into the molecular switch mechanism of human Rho family proteins: shifting a paradigm. Biol. Chem. *394*, 89–95.

Jin, S. and Exton, J.H. (2000). Activation of RhoA by association of Gα(13) with Dbl. Biochem. Biophys. Res. Commun. *277*, 718–721.

Joyce, P.L. and Cox, A.D. (2003). Rac1 and Rac3 are targets for geranylgeranyltransferase I inhibitor-mediated inhibition of signaling, transformation, and membrane ruffling. Cancer Res. *63*, 7959–7967.

Karnoub, A.E., Symons, M., Campbell, S.L., and Der, C.J. (2004). Molecular basis for Rho GTPase signaling specificity. Breast Cancer Res. Treat. *84*, 61–71.

Khan, O.M., Ibrahim, M.X., Jonsson, I.M., Karlsson, C., Liu, M., Sjogren, A.K., Olofsson, F.J., Brisslert, M., Andersson, S., Ohlsson, C., et al. (2011). Geranylgeranyltransferase type I (GGTase-I) deficiency hyperactivates macrophages and induces erosive arthritis in mice. J. Clin. Invest. *121*, 628–639.

Khwaja, A., Sharpe, C.C., Noor, M., and Hendry, B.M. (2006). The role of geranylgeranylated proteins in human mesangial cell proliferation. Kidney Int. *70*, 1296–1304.

Kimura, K., Ito, M., Amano, M., Chihara, K., Fukata, Y., Nakafuku, M., Yamamori, B., Feng, J., Nakano, T., Okawa, K., et al. (1996). Regulation of myosin phosphatase by Rho and Rho-associated kinase (Rho-kinase). Science *273*, 245–248.

Kimura, K., Fukata, Y., Matsuoka, Y., Bennett, V., Matsuura, Y., Okawa, K., Iwamatsu, A., and Kaibuchi, K. (1998). Regulation of the association of adducin with actin filaments by Rho-associated kinase (Rho-kinase) and myosin phosphatase. J. Biol. Chem. *273*, 5542–5548.

Klein, R.M., Spofford, L.S., Abel, E.V., Ortiz, A., and Aplin, A.E. (2008). B-RAF regulation of Rnd3 participates in actin cytoskeletal and focal adhesion organization. Mol. Biol. Cell *19*, 498–508.

Komers, R. (2011). Rho kinase inhibition in diabetic nephropathy. Curr. Opin. Nephrol. Hypertens. *20*, 77–83.

Konstantinopoulos, P.A., Karamouzis, M.V., and Papavassiliou, A.G. (2007). Post-translational modifications and regulation of the RAS superfamily of GTPases as anticancer targets. Nat. Rev. Drug Discov. *6*, 541–555.

Koyama, M., Ito, M., Feng, J., Seko, T., Shiraki, K., Takase, K., Hartshorne, D.J., and Nakano, T. (2000). Phosphorylation of CPI-17, an inhibitory phosphoprotein of smooth muscle myosin phosphatase, by Rho-kinase. FEBS Lett. *475*, 197–200.

Lane, K.T. and Beese, L.S. (2006). Thematic review series: lipid posttranslational modifications. Structural biology of protein farnesyltransferase and geranylgeranyltransferase type I. J. Lipid Res. *47*, 681–699.

Larrea, M.D., Hong, F., Wander, S.A., da Silva, T.G., Helfman, D., Lannigan, D., Smith, J.A., and Slingerland, J.M. (2009). RSK1 drives p27Kip1 phosphorylation at T198 to promote RhoA inhibition and increase cell motility. Proc. Natl. Acad. Sci. USA *106*, 9268–9273.

Lee, D.H., Shi, J., Jeoung, N.H., Kim, M.S., Zabolotny, J.M., Lee, S.W., White, M.F., Wei, L., and Kim, Y.B. (2009). Targeted disruption of ROCK1 causes insulin resistance *in vivo*. J. Biol. Chem. *284*, 11776–11780.

Li, Z., Dong, X., Wang, Z., Liu, W., Deng, N., Ding, Y., Tang, L., Hla, T., Zeng, R., Li, L., et al. (2005). Regulation of PTEN by Rho small GTPases. Nat. Cell Biol. *7*, 399–404.

Liao, J.K., Seto, M., and Noma, K. (2007). Rho kinase (ROCK) inhibitors. J. Cardiovasc. Pharmacol. *50*, 17–24.

Ligeti, E., Welti, S., and Scheffzek, K. (2012). Inhibition and termination of physiological responses by GTPase activating proteins. Physiol. Rev. *92*, 237–272.

Litosch, I. (2011). RhoA co-ordinates with heterotrimeric G proteins to regulate efficacy. Biochem. Biophys. Res. Commun. *415*, 215–219.

Loirand, G., Guerin, P., and Pacaud, P. (2006). Rho kinases in cardiovascular physiology and pathophysiology. Circ. Res. *98*, 322–334.

Lopez-Pedrera, C., Ruiz-Limon, P., Valverde-Estepa, A., Barbarroja, N., and Rodriguez-Ariza, A. (2012). To cardiovascular disease and beyond: new therapeutic perspectives of statins in autoimmune diseases and cancer. Curr. Drug Targets *13*, 829–841.

Ma, Z., Kanai, M., Kawamura, K., Kaibuchi, K., Ye, K., and Fukasawa, K. (2006). Interaction between ROCK II and nucleophosmin/B23 in the regulation of centrosome duplication. Mol. Cell. Biol. *26*, 9016–9034.

Madigan, J.P., Bodemann, B.O., Brady, D.C., Dewar, B.J., Keller, P.J., Leitges, M., Philips, M.R., Ridley, A.J., Der, C.J., and Cox, A.D. (2009). Regulation of Rnd3 localization and function by protein kinase Ca-mediated phosphorylation. Biochem. J. *424*, 153–161.

Mardilovich, K., Olson, M.F., and Baugh, M. (2012). Targeting Rho GTPase signaling for cancer therapy. Future Oncol. *8*, 165–177.

Marrari, Y., Crouthamel, M., Irannejad, R., and Wedegaertner, P.B. (2007). Assembly and trafficking of heterotrimeric G proteins. Biochemistry (Mosc.) *46*, 7665–7677.

Matsui, T., Maeda, M., Doi, Y., Yonemura, S., Amano, M., Kaibuchi, K., and Tsukita, S. (1998). Rho-kinase phospho-rylates COOH-terminal threonines of ezrin/radixin/moesin (ERM) proteins and regulates their head-to-tail association. J. Cell Biol. *140*, 647–657.

Meiri, D., Greeve, M.A., Brunet, A., Finan, D., Wells, C.D., LaRose, J., and Rottapel, R. (2009). Modulation of Rho guanine exchange factor Lfc activity by protein kinase A-mediated phospho-rylation. Mol. Cell. Biol. *29*, 5963–5973.

Mikelis, C.M., Palmby, T.R., Simaan, M., Li, W., Szabo, R., Lyons, R., Martin, D., Yagi, H., Fukuhara, S., Chikumi, H., et al. (2013). PDZ-RhoGEF and LARG are essential for embryonic development and provide a link between thrombin and LPA receptors and Rho activation. J. Biol. Chem. *288*, 12232–12243.

Miyamoto, S., Del Re, D.P., Xiang, S.Y., Zhao, X., Florholmen, G., and Brown, J.H. (2010). Revisited and revised: is RhoA always a villain in cardiac pathophysiology? J Cardiovasc. Transl. Res. *3*, 330–343.

Momotani, K. and Somlyo, A.V. (2012). p63RhoGEF: a new switch for G$_q$-mediated activation of smooth muscle. Trends Cardiovasc. Med. *22*, 122–127.

Momotani, K., Artamonov, M.V., Utepbergenov, D., Derewenda, U., Derewenda, Z.S., and Somlyo, A.V. (2011). p63RhoGEF couples Ga(q/11)-mediated signaling to Ca^{2+} sensitization of vascular smooth muscle contractility. Circ. Res. *109*, 993–1002.

Morgan-Fisher, M., Wewer, U.M., and Yoneda, A. (2013). Regulation of ROCK activity in cancer. J. Histochem. Cytochem. *61*, 185–198.

Mueller, B.K., Mack, H., and Teusch, N. (2005). Rho kinase, a promising drug target for neurological disorders. Nat. Rev. Drug Discov. *4*, 387–398.

Nakamura, H., Arakawa, K., Itakura, H., Kitabatake, A., Goto, Y., Toyota, T., Nakaya, N., Nishimoto, S., Muranaka, M., Yamamoto, A., et al. (2006) Primary prevention of cardiovascular disease with pravastatin in Japan (MEGA Study): a prospective randomised controlled trial. Lancet *368*, 1155–1163.

Narumiya, S., Tanji, M., and Ishizaki, T. (2009). Rho signaling, ROCK and mDia1, in transformation, metastasis and invasion. Cancer Metastasis Rev. *28*, 65–76.

Niault, T.S. and Baccarini, M. (2010). Targets of Raf in tumori-genesis. Carcinogenesis *31*, 1165–1174.

Nimnual, A.S., Taylor, L.J., and Bar-Sagi, D. (2003). Redox-dependent downregulation of Rho by Rac. Nat. Cell Biol. *5*, 236–241.

Noma, K., Kihara, Y., and Higashi, Y. (2012). Striking crosstalk of ROCK signaling with endothelial function. J. Cardiol. *60*, 1–6.

Nunes, K.P., Rigsby, C.S., and Webb, R.C. (2010). RhoA/Rho-kinase and vascular diseases: what is the link? Cell. Mol. Life Sci. *67*, 3823–3836.

Ohgushi, M. and Sasai, Y. (2011). Lonely death dance of human pluripotent stem cells: ROCKing between metastable cell states. Trends Cell Biol. *21*, 274–282.

Oka, M., Fagan, K.A., Jones, P.L., and McMurtry, I.F. (2008). Therapeutic potential of RhoA/Rho kinase inhibitors in pulmonary hypertension. Br. J. Pharmacol. *155*, 444–454.

Olson, M.F. (2008). Applications for ROCK kinase inhibition. Curr. Opin. Cell Biol. *20*, 242–248.

Park, H.J., Zhang, Y., Georgescu, S.P., Johnson, K.L., Kong, D., and Galper, J.B. (2006). Human umbilical vein endothelial cells and human dermal microvascular endothelial cells offer new insights into the relationship between lipid metabolism and angiogenesis. Stem Cell Rev. *2*, 93–102.

Raper, A., Kolansky, D.M., and Cuchel, M. (2012). Treatment of familial hypercholesterolemia: is there a need beyond statin therapy? Curr. Atheroscler. Rep. *14*, 11–16.

Raptis, L., Arulanandam, R., Geletu, M., and Turkson, J. (2011). The R(h)oads to Stat3: Stat3 activation by the Rho GTPases. Exp. Cell Res. *317*, 1787–1795.

Rath, N. and Olson, M.F. (2012). Rho-associated kinases in tumori-genesis: re-considering ROCK inhibition for cancer therapy. EMBO Rep. *13*, 900–908.

Reddy, R., Chahoud, G., and Mehta, J.L. (2005). Modulation of cardiovascular remodeling with statins: fact or fiction? Curr. Vasc. Pharmacol. *3*, 69–79.

Resh, M.D. (2012). Targeting protein lipidation in disease. Trends Mol. Med. *18*, 206–214.

Richardson, B.T., Dibble, C.F., Borikova, A.L., and Johnson, G.L. (2013). Cerebral cavernous malformation is a vascular disease associated with activated RhoA signaling. Biol. Chem. *394*, 35–42.

Riento, K. and Ridley, A.J. (2003). Rocks: multifunctional kinases in cell behaviour. Nat. Rev. Mol. Cell Biol. *4*, 446–456.

Riento, K., Guasch, R.M., Garg, R., Jin, B., and Ridley, A.J. (2003). RhoE binds to ROCK I and inhibits downstream signaling. Mol. Cell. Biol. *23*, 4219–4229.

Riganti, C., Aldieri, E., Doublier, S., Bosia, A., and Ghigo, D. (2008). Statins-mediated inhibition of rho GTPases as a potential tool in anti-tumor therapy. Mini Rev. Med. Chem. *8*, 609–618.

Rikitake, Y. and Liao, J.K. (2005). Rho GTPases, statins, and nitric oxide. Circ. Res. *97*, 1232–1235.

Rikitake, Y., Kim, H.H., Huang, Z., Seto, M., Yano, K., Asano, T., Moskowitz, M.A., and Liao, J.K. (2005). Inhibition of Rho kinase (ROCK) leads to increased cerebral blood flow and stroke protection. Stroke *36*, 2251–2257.

Rizzino, A. (2010). Stimulating progress in regenerative medicine: improving the cloning and recovery of cryopreserved human pluripotent stem cells with ROCK inhibitors. Regen. Med. *5*, 799–807.

Roberts, P.J., Mitin, N., Keller, P.J., Chenette, E.J., Madigan, J.P., Currin, R.O., Cox, A.D., Wilson, O., Kirschmeier, P., and Der, C.J. (2008). Rho Family GTPase modification and dependence on CAAX motif-signaled posttranslational modification. J. Biol. Chem. *283*, 25150–25163.

Roskoski, R., Jr. (2003). Protein prenylation: a pivotal posttranslational process. Biochem. Biophys. Res. Commun. *303*, 1–7.

Rossman, K.L., Der, C.J., and Sondek, J. (2005). GEF means go: turning on RHO GTPases with guanine nucleotide-exchange factors. Nat. Rev. Mol. Cell Biol. *6*, 167–180.

Roy, M., Kung, H.J., and Ghosh, P.M. (2011). Statins and prostate cancer: role of cholesterol inhibition vs. prevention of small GTP-binding proteins. Am. J. Cancer Res. *1*, 542–561.

Salminen, A., Suuronen, T., and Kaarniranta, K. (2008). ROCK, PAK, and Toll of synapses in Alzheimer's disease. Biochem. Biophys. Res. Commun. *371*, 587–590.

Satoh, K., Fukumoto, Y., and Shimokawa, H. (2011). Rho-kinase: important new therapeutic target in cardiovascular diseases. Am. J. Physiol. Heart Circ. Physiol. *301*, H287–H296.

Sawada, N. and Liao, J.K. (2009). Targeting eNOS and beyond: emerging heterogeneity of the role of endothelial Rho proteins in stroke protection. Expert Rev. Neurother. *9*, 1171–1186.

Schmandke, A. and Strittmatter, S.M. (2007). ROCK and Rho: biochemistry and neuronal functions of Rho-associated protein kinases. Neuroscientist *13*, 454–469.

Schofield, A.V. and Bernard, O. (2013). Rho-associated coiled-coil kinase (ROCK) signaling and disease. Crit. Rev. Biochem. Mol. Biol. *48*, 301–316.

Sebti, S.M. and Hamilton, A.D. (2000a). Farnesyltransferase and geranylgeranyltransferase I inhibitors in cancer therapy: important mechanistic and bench to bedside issues. Expert. Opin. Invest. Drugs *9*, 2767–2782.

Sebti, S.M. and Hamilton, A.D. (2000b). Inhibition of Rho GTPases using protein geranylgeranyltransferase I inhibitors. Methods Enzymol. *325*, 381–388.

Shi, J., Zhang, L., and Wei, L. (2011). Rho-kinase in development and heart failure: insights from genetic models. Pediatr. Cardiol. *32*, 297–304.

Shimokawa, H. and Rashid, M. (2007). Development of Rho-kinase inhibitors for cardiovascular medicine. Trends Pharmacol. Sci. *28*, 296–302.

Somlyo, A.P. (1997). Signal transduction. Rhomantic interludes raise blood pressure. Nature *389*, 908–909, 911.

Somlyo, A.P. and Somlyo, A.V. (2000). Signal transduction by G-proteins, rho-kinase and protein phosphatase to smooth muscle and non-muscle myosin II. J. Physiol. *522 Pt 2*, 177–185.

Somlyo, A.P. and Somlyo, A.V. (2003). Ca²⁺ sensitivity of smooth muscle and nonmuscle myosin II: modulated by G proteins, kinases, and myosin phosphatase. Physiol. Rev. *83*, 1325–1358.

Somlyo, A.P. and Somlyo, A.V. (2004). Signal transduction through the RhoA/Rho-kinase pathway in smooth muscle. J. Muscle Res. Cell Motil. *25*, 613–615.

Stenmark, H. (2009). Rab GTPases as coordinators of vesicle traffic. Nat. Rev. Mol. Cell Biol. *10*, 513–525.

Street, C.A. and Bryan, B.A. (2011). Rho kinase proteins – pleiotropic modulators of cell survival and apoptosis. Anticancer Res. *31*, 3645–3657.

Sugimoto, M., Nakayama, M., Goto, T.M., Amano, M., Komori, K., and Kaibuchi, K. (2007). Rho-kinase phosphorylates eNOS at threonine 495 in endothelial cells. Biochem. Biophys. Res. Commun. *361*, 462–467.

Suzuki, Y., Yamamoto, M., Wada, H., Ito, M., Nakano, T., Sasaki, Y., Narumiya, S., Shiku, H., and Nishikawa, M. (1999). Agonist-induced regulation of myosin phosphatase activity in human platelets through activation of Rho-kinase. Blood *93*, 3408–3417.

Takefuji, M., Kruger, M., Sivaraj, K.K., Kaibuchi, K., Offermanns, S., and Wettschureck, N. (2013). RhoGEF12 controls cardiac remodeling by integrating G protein- and integrin-dependent signaling cascades. J. Exp. Med. *210*, 665–673.

Takeya, R., Taniguchi, K., Narumiya, S., and Sumimoto, H. (2008). The mammalian formin FHOD1 is activated through phospho-rylation by ROCK and mediates thrombin-induced stress fibre formation in endothelial cells. EMBO J. *27*, 618–628.

Tan, H.B., Zhong, Y.S., Cheng, Y., and Shen, X. (2011). Rho/ROCK pathway and neural regeneration: a potential therapeutic target for central nervous system and optic nerve damage. Int. J. Ophthalmol. *4*, 652–657.

Tang, B.L. (2005). Alzheimer's disease: channeling APP to non-amyloidogenic processing. Biochem. Biophys. Res. Commun. *331*, 375–378.

Tesfamariam, B. (2006). The effects of HMG-CoA reductase inhibitors on endothelial function. Am. J. Cardiovasc. Drugs *6*, 115–120.

Tonges, L., Koch, J.C., Bahr, M., and Lingor, P. (2011). ROCKing regeneration: Rho kinase inhibition as molecular target for neurorestoration. Front. Mol. Neurosci. *4*, 39.

Triola, G., Waldmann, H., and Hedberg, C. (2012). Chemical biology of lipidated proteins. ACS Chem. Biol. *7*, 87–99.

Tybulewicz, V.L. and Henderson, R.B. (2009). Rho family GTPases and their regulators in lymphocytes. Nat. Rev. Immunol. *9*, 630–644.

Uehata, M., Ishizaki, T., Satoh, H., Ono, T., Kawahara, T., Morishita, T., Tamakawa, H., Yamagami, K., Inui, J., Maekawa, M., et al. (1997). Calcium sensitization of smooth muscle mediated by a Rho-associated protein kinase in hypertension. Nature *389*, 990–994.

Valderrama, F., Cordeiro, J.V., Schleich, S., Frischknecht, F., and Way, M. (2006). Vaccinia virus-induced cell motility requires F11L-mediated inhibition of RhoA signaling. Science *311*, 377–381.

Vanni, C., Mancini, P., Ottaviano, C., Ognibene, M., Parodi, A., Merello, E., Russo, C., Varesio, L., Zheng, Y., Torrisi, M.R., et al. (2007). Gα13 regulation of proto-Dbl signaling. Cell Cycle *6*, 2058–2070.

Walsh, M.P. (2011). Vascular smooth muscle myosin light chain diphosphorylation: mechanism, function, and pathological implications. IUBMB Life *63*, 987–1000.

Wang, Q.M. and Liao, J.K. (2012). ROCKs as immunomodulators of stroke. Expert Opin. Ther. Targets *16*, 1013–1025.

Wang, Y., Zheng, X.R., Riddick, N., Bryden, M., Baur, W., Zhang, X., and Surks, H.K. (2009). ROCK isoform regulation of myosin phosphatase and contractility in vascular smooth muscle cells. Circ. Res. *104*, 531–540.

Ward, Y., Yap, S.F., Ravichandran, V., Matsumura, F., Ito, M., Spinelli, B., and Kelly, K. (2002). The GTP binding proteins Gem and Rad are negative regulators of the Rho-Rho kinase pathway. J. Cell Biol. *157*, 291–302.

Wen, W., Liu, W., Yan, J., and Zhang, M. (2008). Structure basis and unconventional lipid membrane binding properties of the PH-C1 tandem of rho kinases. J. Biol. Chem. *283*, 26263–26273.

Wettschureck, N. and Offermanns, S. (2002). Rho/Rho-kinase mediated signaling in physiology and pathophysiology. J. Mol. Med. *80*, 629–638.

While, A. and Keen, L. (2012). The effects of statins on mood: a review of the literature. Eur. J. Cardiovasc. Nurs. *11*, 85–96.

Wiemer, A.J., Hohl, R.J., and Wiemer, D.F. (2009). The intermediate enzymes of isoprenoid metabolism as anticancer targets. Anticancer Agents Med. Chem. *9*, 526–542.

Wiemer, A.J., Wiemer, D.F., and Hohl, R.J. (2011). Geranylgeranyl diphosphate synthase: an emerging therapeutic target. Clin. Pharmacol. Ther. *90*, 804–812.

Winter-Vann, A.M. and Casey, P.J. (2005). Post-prenylation-processing enzymes as new targets in oncogenesis. Nat. Rev. Cancer *5*, 405–412.

Wirth, A., Benyo, Z., Lukasova, M., Leutgeb, B., Wettschureck, N., Gorbey, S., Orsy, P., Horvath, B., Maser-Gluth, C., Greiner, E., et al. (2008). G12-G13-LARG-mediated signaling in vascular smooth muscle is required for salt-induced hypertension. Nat. Med. *14*, 64–68.

Wittinghofer, A. and Vetter, I.R. (2011). Structure-function relationships of the G domain, a canonical switch motif. Annu. Rev. Biochem. *80*, 943–971.

Yasui, Y., Amano, M., Nagata, K., Inagaki, N., Nakamura, H., Saya, H., Kaibuchi, K., and Inagaki, M. (1998). Roles of Rho-associated kinase in cytokinesis; mutations in Rho-associated kinase phosphorylation sites impair cytokinetic segregation of glial filaments. J. Cell Biol. *143*, 1249–1258.

Young, S.G., Yang, S.H., Davies, B.S., Jung, H.J., and Fong, L.G. (2013). Targeting protein prenylation in progeria. Sci. Transl. Med. *5*, 171–173.

Zhang, H., Sawashita, J., Fu, X., Korenaga, T., Yan, J., Mori, M., and Higuchi, K. (2006). Transmissibility of mouse AApoAII amyloid fibrils: inactivation by physical and chemical methods. FASEB J. *20*, 1012–1014.

Zhao, T.T., Le Francois, B.G., Goss, G., Ding, K., Bradbury, P.A., and Dimitroulakos, J. (2010). Lovastatin inhibits EGFR dimerization and AKT activation in squamous cell carcinoma cells: potential regulation by targeting rho proteins. Oncogene *29*, 4682–4692.

Zhou, H. and Li, Y. (2011). Long-term diabetic complications may be ameliorated by targeting Rho kinase. Diabetes Metab. Res. Rev. *27*, 318–330.

Zhou, H. and Li, Y.J. (2012). Rho kinase inhibitors: potential treatments for diabetes and diabetic complications. Curr. Pharm. Des. *18*, 2964–2973.

Zhou, Q. and Liao, J.K. (2009). Statins and cardiovascular diseases: from cholesterol lowering to pleiotropy. Curr. Pharm. Des. *15*, 467–478.

Zhou, Q. and Liao, J.K. (2010). Pleiotropic effects of statins. Basic research and clinical perspectives. Circ. J. *74*, 818–826.

Zhou, Q., Gensch, C., and Liao, J.K. (2011). Rho-associated coiled-coil-forming kinases (ROCKs): potential targets for the treatment of atherosclerosis and vascular disease. Trends Pharmacol. Sci. *32*, 167–173.

Zieba, B.J., Artamonov, M.V., Jin, L., Momotani, K., Ho, R., Franke, A.S., Neppl, R.L., Stevenson, A.S., Khromov, A.S., Chrzanowska-Wodnicka, M., et al. (2011). The cAMP-responsive Rap1 guanine nucleotide exchange factor, Epac, induces smooth muscle relaxation by down-regulation of RhoA activity. J. Biol. Chem. *286*, 16681–16692.

Zou, W. and Teitelbaum, S.L. (2010). Integrins, growth factors, and the osteoclast cytoskeleton. Ann. NY Acad. Sci. *1192*, 27–31.
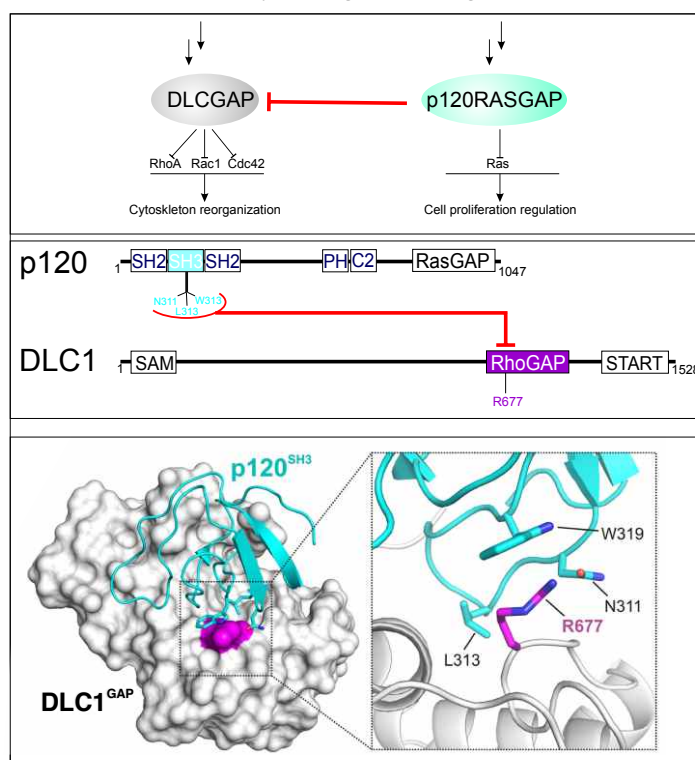
Chapter 4

RHO-RAS crosstalk

Functional Cross-talk between RAS and RHO Pathways
A RAS-specific GTPase-activating protein (p120RasGAP) completely inhibits the
RHOGAP activity of deleted in liver cancer (DLC) tumor suppresor by masking the
catalytic arginine finger

Functional Cross-talk between Ras and Rho Pathways

A Ras-SPECIFIC GTPase-ACTIVATING PROTEIN (p120RasGAP) COMPETITIVELY INHIBITS THE RhoGAP ACTIVITY OF DELETED IN LIVER CANCER (DLC) TUMOR SUPPRESSOR BY MASKING THE CATALYTIC ARGININE FINGER[*]

Mamta Jaiswal[‡1], **Radovan Dvorsky**[‡], **Ehsan Amin**[‡], **Sarah L. Risse**[‡], **Eyad K. Fansa**[‡], **Si-Cai Zhang**[‡], **Mohamed S. Taha**[‡], **Aziz R. Gauhar**[‡2], **Saeideh Nakhaei-Rad**[‡], **Claus Kordes**[§], **Katja T. Koessmeier**[‡], **Ion C. Cirstea**[‡¶], **Monilola A. Olayioye**[‖3], **Dieter Häussinger**[§], and **Mohammad R. Ahmadian**[‡4]

From the ‡Institute of Biochemistry and Molecular Biology II and §Clinic for Gastroenterology, Hepatology and Infectiology, Medical Faculty, Heinrich Heine University, 40225 Düsseldorf, ¶Leibniz Institute for Age Research, 07745 Jena, and ‖Institute of Cell Biology and Immunology, University of Stuttgart, 70569 Stuttgart, Germany

Background: The regulatory mechanism of the DLC1 tumor suppressor protein is unclear.
Results: Structure-function analysis revealed determinants for the selectivity, activity, and inhibition of DLC1 RhoGAP function.
Conclusion: p120RasGAP competitively and selectively inhibits DLC1 by targeting its catalytic arginine finger.
Significance: This mechanistic study emphasizes the importance of the functional inter-relationships of GTPase-activating proteins mediating cross-talk between the Ras and Rho pathways.

The three deleted in liver cancer genes (DLC1–3) encode Rho-specific GTPase-activating proteins (RhoGAPs). Their expression is frequently silenced in a variety of cancers. The RhoGAP activity, which is required for full DLC-dependent tumor suppressor activity, can be inhibited by the Src homology 3 (SH3) domain of a Ras-specific GAP (p120RasGAP). Here, we comprehensively investigated the molecular mechanism underlying cross-talk between two distinct regulators of small GTP-binding proteins using structural and biochemical methods. We demonstrate that only the SH3 domain of p120 selectively inhibits the RhoGAP activity of all three DLC isoforms as compared with a large set of other representative SH3 or RhoGAP proteins. Structural and mutational analyses provide new insights into a putative interaction mode of the p120 SH3 domain with the DLC1 RhoGAP domain that is atypical and does not follow the classical P*XX*P-directed interaction. Hence, p120 associates with the DLC1 RhoGAP domain by targeting the catalytic argi-

nine finger and thus by competitively and very potently inhibiting RhoGAP activity. The novel findings of this study shed light on the molecular mechanisms underlying the DLC inhibitory effects of p120 and suggest a functional cross-talk between Ras and Rho proteins at the level of regulatory proteins.

The Ras and Rho families of small GTP-binding proteins are key transducers of a variety of cellular processes ranging from reorganization of the cytoskeleton to transcriptional regulation and control of cell growth and survival (1). Loss of the control mechanisms and aberrant activation of Ras and Rho proteins are one of the most common molecular alterations found in cancer cells promoting tumor growth and metastasis (2–5). Ras signaling stimulates diverse pathways and signals toward Rho proteins, which are known to be required for cell transformation by oncogenic Ras (6–8). Emerging evidence suggests that the GTPase-activating proteins (GAPs),[5] in particular p120RasGAP (also known as RAS p21 protein activator 1 or RASA1; here called p120) and the Rho-specific p190ARhoGAP (also known as ARHGAP35; here called p190), p200RhoGAP (also known as ARHGAP32, p250GAP, GC-GAP, Rics, or Grit) and deleted in liver cancer 1 (DLC1; also known as ARHGAP7, p122RhoGAP, or STARD12), act as a linker between Ras and Rho signaling pathways (9–11). GAPs are multifaceted and multifunctional molecules (12, 13) and are the principal inactivators of Ras and Rho signaling. They utilize a catalytic "arginine finger" to stimulate the inefficient intrinsic GTP hydrolysis reaction of these small GTP-binding proteins by several orders of magnitude (14).

p120RasGAP Competitively Inhibits DLC RhoGAP

Frequent loss of *DLC1* gene expression was first described in liver cancer (15) and later in breast, colon, gastric, prostate, cervical, esophageal, and other cancers (16–18). DLC1 RhoGAP function is required for the maintenance of cell morphology and the coordination of cell migration (11, 19–21). DLC1 and its isoforms DLC2 (also known as ARHGAP37 or STARD13) and DLC3 (also known as ARHGAP38 or STARD8) consist of an N-terminal sterile α motif (SAM) domain, a central phosphorylation region followed by the catalytic RhoGAP domain, and a C-terminal steroidogenic acute regulatory related lipid transfer (START) domain (see Fig. 1*A*) (22, 23). The SAM and GAP domains are linked by a serine-containing region, which contains a recognition motif for the phosphoserine/phosphothreonine-binding 14-3-3 adaptor proteins (22). DLC1 has been reported to interact with tensin, talin, focal adhesion kinase, and α-catenin (22, 24–29) and with lipids (30). However, the precise mechanism of DLC1 regulation remains unclear.

An emerging theme is that RhoGAPs, such as the OPHN1 and GRAF1 (31, 32) and p50RhoGAP (33–36), require activation through the relief of autoinhibitory elements. These elements are collectively membrane-binding modules, including BAR (Bin/Amphiphysin/Rvs), PH (pleckstrin homology), C1, and Sec14 domains (31–33, 36). The SAM domain of DLC1 has been suggested to act as an autoinhibitory domain of DLC1 RhoGAP activity *in vitro* and *in vivo*. SAM domain-deleted DLC1 displayed enhanced catalytic activity for RhoA (20). However, it is still unclear how such an autoregulatory mechanism of DLC1 may operate.

p120 contains multiple domains with different functions (see Fig. 1*B*) (37). Whereas the C terminus of p120 with the catalytic GAP activity is responsible for Ras inactivation (38–40), its N-terminal Src homology 2 and 3 (SH2 and SH3) domains have been suggested to possess an effector function (41–44). p120 functionally modulates Rho signaling by direct binding to two Rho-specific GAPs, p190 and DLC1 (9, 11, 45). The association of p120 with the tyrosine phosphorylated p190 via its SH2 domain promotes Rho inactivation (45–47). Thus, p120 positively regulates the RhoGAP function of p190. Another mechanism, which connects the Ras and Rho pathways and regulates the actin cytoskeleton, is dependent on the p120 SH3 domain and controls Rho activation (41). This mechanism was later revealed to involve DLC1 but not p190 (11). Here, the p120 SH3 domain (called p120^{SH3}) binds to the RhoGAP domain of DLC1 (called DLC1^{GAP}) and inhibits the DLC1-dependent Rho inactivation (11). Hereby, p120 acts as a negative regulator not only for Ras but also for the GAP activity of DLC1. However, the molecular mechanisms underlying these cross-talk phenomena have not yet been elucidated.

In this study, we have explored the regulatory mechanism of DLC1 at the molecular level, in particular its *trans*-inhibition by p120^{SH3}. We have characterized the selectivity of the interaction between the DLC1^{GAP} and p120^{SH3} using a large number of purified SH3 and RhoGAP proteins and identified structural and functional determinants for the DLC1-p120 interaction. This study provides deep insights into the underlying regulatory cross-talk between the Rho and Ras family of small GTP-binding proteins.

EXPERIMENTAL PROCEDURES

Constructs—Human Abr^{GAP} (aa 559–822), DLC1^{fl} (aa 1–1091), DLC1^{GAP} (aa 609–878), DLC1^{SAM} (aa 1–96), DLC1^{START} (aa 880–1079), DLC2^{GAP} (aa 644–916), DLC3^{GAP} (aa 620–890), GRAF1^{GAP} (aa 383–583), MgcRac^{GAP} (aa 343–620), Nadrin^{GAP} (aa 245–499), OPHN1^{GAP} (aa 375–583), p50^{GAP} (aa 198–439), p190^{GAP} (aa 1250–1513), N-terminal truncated p120$^{\Delta n128}$ (aa 129–1047); SH2-SH3-SH2-encoding p120$^{SH2-3-2}$ (aa 129–447), p120^{SH3} (aa 275–350), Src^{SH3} (aa 77–140), and human RhoA (aa 1–181), Cdc42 (aa 1–178), and Rac1 (aa 1–184) were amplified by standard PCR and cloned in pGEX-4T1 and pGEX-4T1-NTEV, respectively. Constructs of SH3 domain of Crk1^{SH3} (aa 131–191), Grb2^{SH3-1} (aa 1–55), Grb2^{SH3-2} (aa 159–217), Nck1^{SH3-1} (aa 5–60), Nck1^{SH3-2} (aa 109–163), and Nck1^{SH3-3} (aa 173–262) were created as described previously (48).

Site-directed Mutagenesis—Point mutations N311R; L313A; W319G; and N311R,L313A,W319G in p120^{SH3} and R677A in DLC1^{GAP} were generated using the QuikChange^{TM} site-directed mutagenesis kit (Stratagene) and confirmed by DNA sequencing.

Proteins—*Escherichia coli* BL21(DE3) pLysS, BL21(DE3) CodonPlus-RIL, and Rosetta(DE3) strains containing the respective plasmids (see constructs) were grown to an A_{600} of 0.7 (37 °C at 140 rpm) and induced with 0.1 mM isopropyl β-D-thiogalactopyranoside overnight at 25 °C as described before (49, 50). All proteins were isolated in a first step as glutathione *S*-transferase (GST) fusion proteins by affinity chromatography on a GSH-agarose column and in a second step by size exclusion chromatography (Superdex S75 or S200) after proteolytic cleavage of GST. GTP-binding proteins without nucleotide (nucleotide-free form) or with tetramethylrhodamine-conjugated GTP (tamraGTP) were prepared as described before (49, 50). Concentrations of proteins were determined by Bradford assay or absorbance at 280 nm using the extinction coefficient deduced from the protein sequence. Purified proteins were snap frozen in liquid nitrogen and stored at −80 °C.

Analytical Size Exclusion Chromatography (aSEC)—aSEC for the detection of complex formation was performed for DLC1^{GAP} and p120^{SH3} on a Superdex 75 column (10/300) using buffer containing 30 mM HEPES, pH 7.6, 5 mM MgCl$_2$, 150 mM NaCl, and 3 mM DTT. 10 μM DLC1^{GAP} was incubated with 15 μM p120^{SH3} for 5 min at 4 °C in the same buffer in a total volume of 150 μl. Before loading to an aSEC column, samples were spun at 13,000 rpm at 4 °C to remove any particulate impurities. The flow rate was maintained at 0.5 ml/min, and 500-μl fractions were collected. Peak fractions were visualized by 15% SDS-PAGE and subsequent Coomassie Blue staining.

Kinetics Measurements—All fluorescence measurements were performed at 25 °C in a buffer containing 30 mM Tris-HCl, pH 7.5, 10 mM K$_2$HPO$_4$/KH$_2$PO$_4$, pH 7.4, 10 mM MgCl$_2$, and 3 mM DTT. The tamraGTP hydrolysis of Rho proteins (0.2 μM) was measured in the absence and presence of different amounts of respective GAP proteins as described previously (49, 52). Fast kinetics (<1000 s) were performed with a Hi-Tech Scientific SF-61 stopped-flow instrument with a mercury xenon light source and TgK Scientific Kinetic Studio software (version

2.19). An excitation wavelength of 545 nm was used for tamra. Emission was detected through a cutoff filter of 570 nm. Slow kinetics (>1000 s) were measured on a PerkinElmer Life Sciences spectrofluorometer (LS50B) using an excitation wavelength of 545 nm and an emission wavelength of 583 nm. Data were evaluated by single exponential fitting with the GraFit program to obtain the observed rate constant (k_{obs}) for the respective reaction as described before (49, 52).

Isothermal Titration Calorimetry (ITC) Measurements—The interaction of DLC1^{GAP} and p120^{SH3} and analysis of DLC1^{GAP} variant and different p120^{SH3} variants were studied by ITC (MicroCal^{TM} VP-ITC microcalorimeter) as described (48). All measurements were carried out in 30 mM Tris-HCl, pH 7.5, 150 mM NaCl, 5 mM MgCl$_2$, and 1 mM tris(2-carboxyethyl)phosphine hydrochloride. The data were analyzed using Origin 7.0 software provided by the manufacturer.

Structural Analysis—To obtain insight into the residues responsible for the binding of the SH3 domain of p120 and RhoGAP domain of DLC1, docking of their corresponding structures (Protein Data Bank code 2J05 (53) and Protein Data Bank code 3KUQ, respectively), was performed with the program PatchDock (54). From the 20 best scored models, we selected the lowest energy model, which also has the Arg finger Arg-677 at the interface, and used it for further refinement with the program CHARMM (55). As the arginine finger is assumed to be crucial for the formation of the complex, we thoroughly explored its conformation in the course of refinement. Torsion angles of its side chain were additionally set up according to the Dynameomics rotamer library (56), and the energy of each complex was minimized by 2000 steps using the adapted basis Newton-Raphson method.

RESULTS

Low GAP Activities of the DLC Isoforms—Real time kinetic measurements of the RhoGAP activities of the DLC isoforms toward Cdc42, Rac1, and RhoA were performed using purified RhoGAP domains of the DLC proteins (Fig. 1) and fluorescent tamraGTP. This GTP analog is sensitive toward conformational changes induced by GTP hydrolysis (52). As shown in Fig. 2A, the very slow intrinsic tamraGTP hydrolysis of Cdc42 (*inset*) was markedly increased in the presence of the RhoGAP domain of DLC1 (DLC1^{GAP}). Similar experiments were performed under the same conditions with Rac1 and RhoA (Fig. 2B). Observed rate constants (k_{obs}) of respective DLC1^{GAP} activities are presented in comparison with intrinsic hydrolysis rates as *bars* in Fig. 2B. DLC1^{GAP} exhibited the highest activity for RhoA (1,650-fold) and Cdc42 (332-fold) and the lowest activity for Rac1 (75-fold). We next focused on the differences among the DLC isoforms and measured the activities of DLC2 and DLC3 for Cdc42 (Fig. 2C). Obtained data show that DLC2 and DLC3 exhibit 78- and 11-fold lower GAP activities, respectively, as compared with that of DLC1. Our results indicate that the DLC family members are inefficient GAPs, at least *in vitro*, with catalytic activities that are several orders of magnitude lower than the activities of the RhoGAPs p50 and p190 (Fig. 2C) or other highly efficient RhoGAPs, such as GRAF1 or OPHN1 (32).

p120RasGAP Competitively Inhibits DLC RhoGAP

A comparison of the obtained data on the DLC isoforms with those of other RhoGAP family members raised the question of whether the extremely low GAP activities of DLC proteins stem from effects on either binding affinity (K_d) or catalytic activity (k_{cat}). Therefore, we measured the kinetics of tamraGTP hydrolysis of Cdc42 at increasing concentrations of DLC1^{GAP} and GRAF1^{GAP}. The rate constants (k_{obs}) of the fitted single exponential decays increased in a hyperbolic manner as a function of GAP concentrations as described previously (52, 57). We used Cdc42 in most experiments because of a large change in fluorescence upon tamraGTP hydrolysis as compared with Rac1 and RhoA. Fitting a hyperbolic curve to the points according to Equation 1 led to the corresponding kinetic parameters K_d and k_{cat} (Fig. 2D).

$$k_{obs} = \frac{k_{cat}}{1 + \dfrac{K_d}{[\text{DLC1}]}} \qquad \text{(Eq. 1)}$$

Unlike the relatively similar K_d values, there was a large difference in the k_{cat} values for the GTP hydrolysis reaction: 6.26 s^{-1} for DLC1^{GAP} compared with 289 s^{-1} for the highly efficient GRAF1^{GAP}. These data clearly indicate that the very low GAP activity of the DLC proteins relies more on the catalytic activity than on the binding affinity to Cdc42.

Insights into cis-Regulatory Modules of DLC1 Function—To examine the influence of other domains of DLC1 (Fig. 1A) on its GAP activity, we further measured tamraGTP hydrolysis of Cdc42 stimulated by full-length DLC1 (DLC1^{fl}). As shown in Fig. 3A, DLC1^{fl} exhibited a strongly reduced GAP activity as compared with the isolated DLC1^{GAP}. The k_{obs} values obtained from single turnover kinetic data were 0.02 and 0.47 s^{-1}, respectively, and reveal that the DLC1^{fl} activity was 23.5-fold lower than that of DLC1^{GAP} (Fig. 3B). This result strongly supports the previous notion that other regions of DLC1, such as the SAM domain (20), may undergo an intramolecular interaction with the GAP domain and thus contribute to its autoinhibition in a *cis*-inhibitory manner.

To analyze whether the autoinhibitory effect is caused by N- and C-terminal SAM and/or START domains of DLC1 (Fig. 1A), we purified these domains and measured their effects on the DLC1^{GAP} activity *in vitro*. Using high concentrations of SAM, START, or both (up to a 100-fold molar excess above the GAP domain), we did not observe any significant inhibition of the DLC1^{GAP} activity using tamraGTP hydrolysis of Cdc42 (Fig. 3C). The fact that the isolated SAM and START domains did not reveal any GAP-inhibitory activity strongly suggests that the autoinhibitory mechanism of DLC1 may require additional regions of the full-length protein. One possibility is the serine-rich 14-3-3 binding region between the SAM and the GAP domains (Fig. 1A).

p120 SH3 as a Potent trans-Inhibitory Factor of the DLC1^{GAP} Activity—The SH3 domain of p120 has been reported as a novel binding partner of DLC1 with GAP-inhibitory and growth suppression activity (11). To monitor this effect in real time, DLC1^{GAP} activity was measured in the absence and presence of purified p120^{SH3} under the same conditions as in the experiments described above (Fig. 2). As shown in Fig. 4A, DLC1^{GAP}-

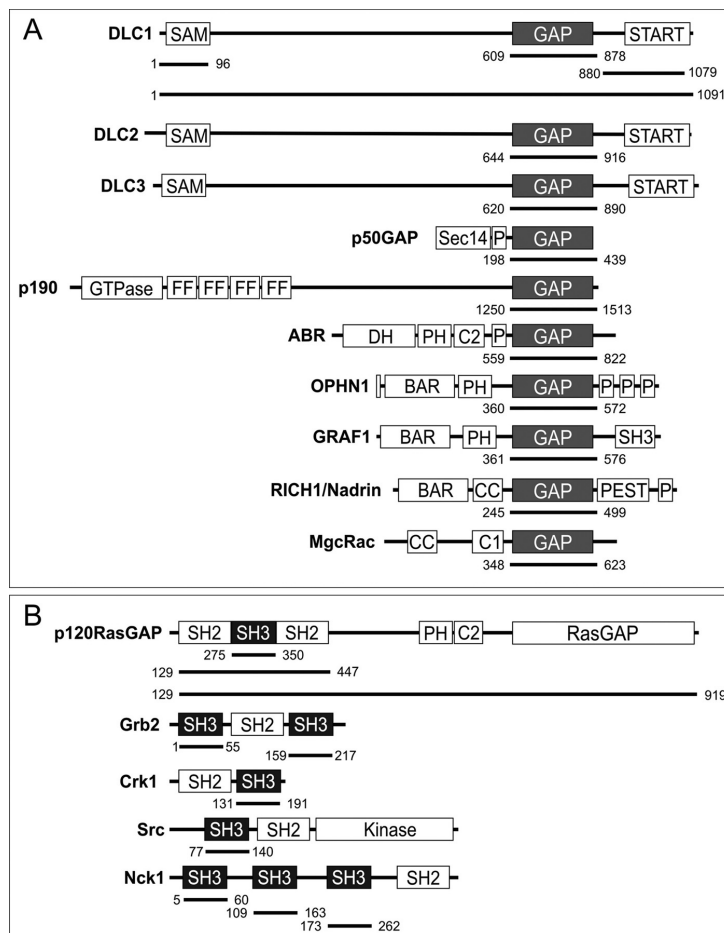*p120RasGAP Competitively Inhibits DLC RhoGAP*

FIGURE 1. **Schematic representation of domain organization and designed fragments of GAP (*A*) and SH3 domain-containing proteins (*B*) used in this study.** The *numbers* indicate the N and C termini of the amino acids of the respective fragments. *BAR*, Bin/Amphiphysin/Rvs; *C1*, cysteine-rich region; *CC*, coiled coil; *DH*, Dbl homology domain; *FF*, double phenylalanine; *P*, proline-rich; *PH*, pleckstrin homology; *PSET*, proline, serine, glutamic acid, and threonine; *RGS*, regulator of G-protein signaling; *Sec14*, secretion and cell surface growth 14.

stimulated tamraGTP hydrolysis of Cdc42 was drastically reduced using a 10-fold excess of p120[SH3] over the DLC1[GAP] concentration. The respective k_{obs} value of 0.63 for DLC1[GAP] activity was reduced by 83-fold in the presence of p120[SH3] to 0.0076 s^{-1} (Fig. 4*B*), which is close to the intrinsic tamraGTP hydrolysis of Cdc42 (0.02 s^{-1}). These measurements were also performed for RhoA and Rac1 using the same conditions as for Cdc42 (Fig. 4*B*). Similarly, 247- and 15.5-fold reductions of the DLC1[GAP] activity for RhoA and Rac1, respectively, were determined in the presence of a 10-fold molar excess of p120[SH3]. An explanation for this large variation may be the significant differences in DLC1[GAP] binding affinity for the three members of the Rho family.

In the next step, we analyzed the inhibitory effect of p120[SH3] on the GAP activity of DLC2 and DLC3 toward Cdc42. Fig. 4*C* shows that the catalytic GAP activity of purified DLC2[GAP] and DLC3[GAP] was also inhibited in the presence of p120[SH3] but not

as drastically as in the case of DLC1[GAP]. The next question we addressed was whether the SH3 domain is freely accessible to exert its inhibitory effect or whether other domains of p120 also play a role in the inhibition of DLC GAP activity (Fig. 1). Therefore, we purified the SH2-SH3-SH2-encompassing p120[SH2-3-2] and N-terminal truncated p120[Δn128] proteins and analyzed their DLC1[GAP] inhibitory effects in direct comparison with isolated p120[SH3]. Larger p120 fragments inhibited the DLC1[GAP] activity but to a 19- and 10-fold lower extent than p120[SH3] (Fig. 4*D*).

Taken together, our *in vitro* data demonstrate that (i) p120[SH3] acts as a potent *trans*-inhibitory factor of the GAP activity of the DLC isoforms and (ii) the SH3 domain of p120 is not completely unmasked (freely accessible) in the presence of other p120 domains, especially the adjacent SH2 domains. Whether the N-terminal 128 amino acids play a role in this regard remains unclear. Full-length p120 could not be purified due to its instability.
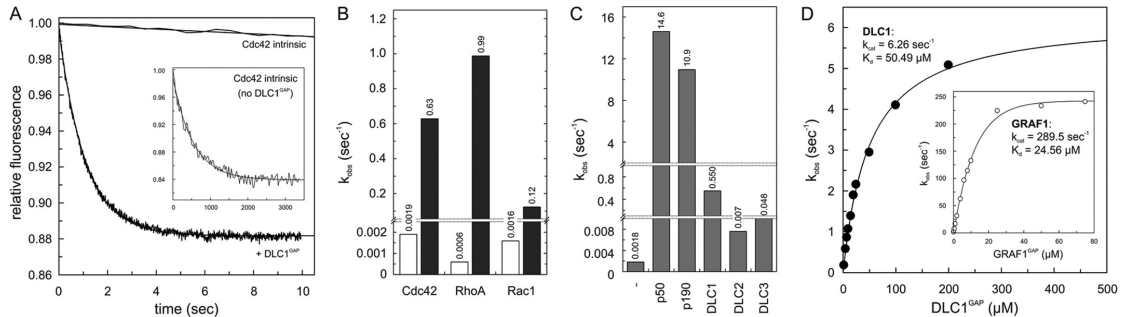
FIGURE 2. **Inefficient GAP activities of the DLC isoforms.** *A*, Cdc42-tamraGTP (0.2 μM) was rapidly mixed with 5 μM DLC1^{GAP} to monitor the GAP-stimulated tamraGTP hydrolysis reaction of Cdc42 in real time. Note the very slow intrinsic GTPase reaction of Cdc42 (*inset*) that was measured in the absence of GAP. Rate constants (k_{obs}) were obtained by single exponential fitting of the data. *B*, the k_{obs} values of GTP hydrolysis of Rho proteins (0.2 μM) measured in the presence of DLC1^{GAP} (5 μM) are represented as a column chart. Calculated -fold activation values were obtained by dividing the k_{obs} values of GAP-stimulated reactions by the k_{obs} values of the intrinsic reactions of respective GTPases. For convenience, the k_{obs} values are given above the *bar charts*. *C*, measured GAP activities of DLC1, DLC2, and DLC3 (5 μM, respectively) toward Cdc42 (0.2 μM) were very low as compared with p150 and p190. *D*, the GTP hydrolysis of Cdc42 (0.2 μM) was measured in the presence of increasing concentrations of the respective GAP domains of DLC1 and GRAF1 (*inset*). The dependence of the k_{obs} values of the GAP-stimulated GTP hydrolysis plotted on the concentrations of DLC1^{GAP} and GRAF1 was fitted by a hyperbolic curve to obtain the kinetic parameters (k_{cat} and K_d).
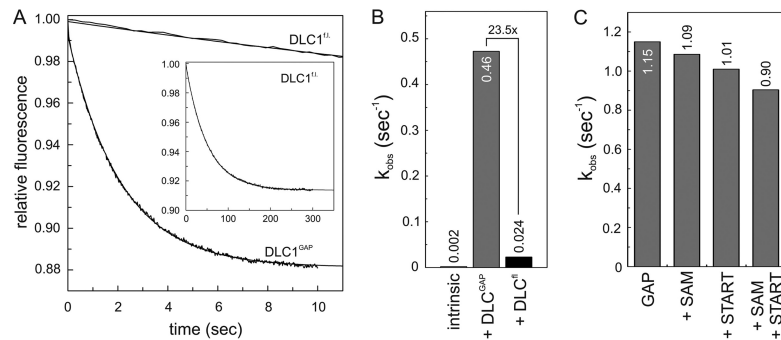
FIGURE 3. **cis-Acting regulation of DLC1^{GAP} activity.** *A*, kinetics of the tamraGTP hydrolysis reaction of Cdc42 (0.2 μM) stimulated by DLC1^{fl} (5 μM) was much slower (*inset*) than that stimulated by DLC^{GAP} (5 μM). *B*, the k_{obs} values, illustrated as a bar chart, showed that the GAP activity of DLC1^{fl} is reduced by 23.5-fold as compared with that of the DLC1^{GAP} but not completely inhibited as compared with the intrinsic GTPase reaction. For convenience, the k_{obs} values are given above the *bar charts*. *C*, the activity of DLC1^{GAP} (10 μM) on tamraGTP hydrolysis of Cdc42 (0.2 μM) was not significantly changed in the presence of a 100-fold excess of SAM, START, or both domains (1 mM, respectively).
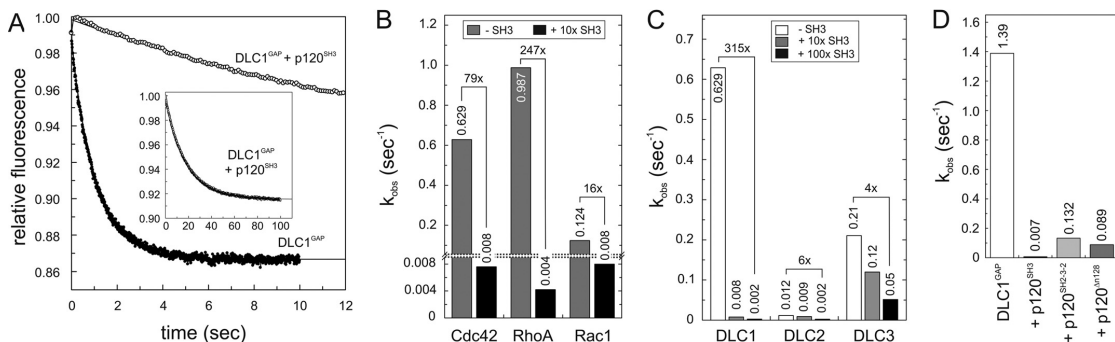
FIGURE 4. **p120^{SH3} as a potent inhibitor of the DLC GAP function.** *A*, kinetics of the tamraGTP hydrolysis reaction of Cdc42 (0.2 μM) stimulated by DLC1^{GAP} (5 μM) was reduced in the presence of a 10-fold excess of p120^{SH3} (50 μM). The complete reaction is shown in the *inset*. *B*, DLC1^{GAP} activities toward Cdc42, RhoA, and Rac1, measured under the same conditions as in *A*, are strongly inhibited by p120^{SH3}. For convenience, the k_{obs} values are given above the *bar charts*. *C*, DLC3^{GAP} (5 μM) was not inhibited by p120^{SH3} (50 and 500 μM) as efficiently as DLC1^{GAP} and DLC2^{GAP} (5 μM, respectively). *D*, p120$^{SH2-3-2}$ and p120$^{\Delta n128}$ (40 μM) inhibited the activity of DLC^{GAP} (10 μM) but not as efficiently as p120^{SH3} (40 μM).

Highly Selective Interaction between p120^{SH3} and DLC1^{GAP}— The next issue we addressed was the selectivity of the p120^{SH3} toward DLC1^{GAP}. Therefore, we purified seven additional

RhoGAP and SH3 domains of other proteins (Fig. 1). We measured the effect of p120^{SH3} on the GAP activity of Abr, GRAF1, MgcRacGAP, Nadrin, OPHN1, p50, and p190 on the one hand

p120RasGAP Competitively Inhibits DLC RhoGAP
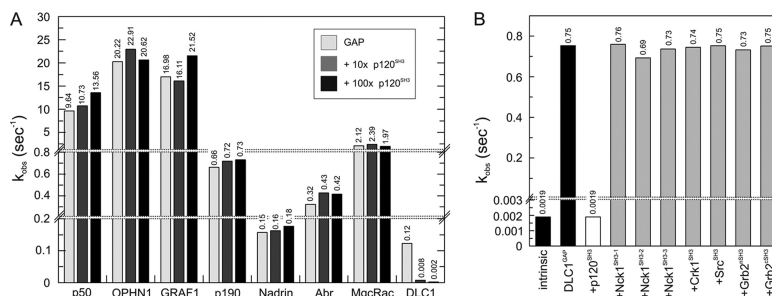
FIGURE 5. **Highly selective interaction between p120^{SH3} and DLC1^{GAP}.** *A*, p120^{SH3}-inhibiting effect on seven additional RhoGAPs (2 μM, respectively) was measured using the tamraGTP hydrolysis reaction of Cdc42 (0.2 μM) and p120^{SH3} (20 and 200 μM, respectively). p120^{SH3} inhibited only DLC1^{GAP} but not the other RhoGAPs. For convenience, the k_{obs} values are given above the *bar charts*. *B*, the effect of seven additional SH3 proteins (100 μM, respectively) on inhibiting DLC1^{GAP} (10 μM) was measured. Only p120^{SH3} inhibited DLC1^{GAP} but not the other SH3 domains.

and the effects of the SH3 domains of Crk1, c-Src, Grb2 (N- and C-terminal SH3 domains), and Nck1 (all three SH3 domains) on the DLC1^{GAP} activity on the other hand. As summarized in Fig. 5, neither did p120^{SH3} inhibit the activity of other GAPs of the Rho family (Fig. 5A) nor was the DLC1^{GAP} activity affected by the presence of other SH3 domains (Fig. 5B). These data clearly demonstrate that the p120^{SH3}-mediated *trans*-inhibition of DLC isoforms is highly selective.

Potent DLC1 Inhibition Due to High Affinity p120^{SH3}-DLC1^{GAP} Complex Formation—In the next step, we characterized in more detail the interaction between p120^{SH3} and DLC1^{GAP} as well as the inhibition of the DLC1^{GAP} activity induced by p120^{SH3} using different qualitative and quantitative biophysical and biochemical methods. aSEC is an accurate and simple method to visualize high affinity protein-protein interactions. p120$^{SH3}$ (9 kDa) and DLC1^{GAP} (31 kDa) alone and a mixture of both proteins were loaded on a Superdex 75 (10/300) column, and eluted peak fractions were analyzed by SDS-PAGE. Data summarized in Fig. 6A clearly illustrate that a mixture of p120^{SH3} and DLC1^{GAP} shift the elution profile of the respective protein domains to an elution volume of 10.5 ml, indicating the formation of a complex between both proteins. We next determined the inhibitory potency of p120^{SH3} by measuring DLC1^{GAP} activity at increasing concentrations of p120^{SH3}. An inhibitory constant (K_i) of 0.61 μM was calculated by fitting the Morrison equation for a tight binding inhibitor (58) to individual k_{obs} values plotted against different p120^{SH3} concentrations (Fig. 6B). Furthermore, we measured the dissociation constant of the p120^{SH3}-DLC1^{GAP} interaction using ITC. The results shown in Fig. 6C allowed the determination of a stoichiometry of 1:1 and a dissociation constant (K_d) of 0.6 μM for the binding of p120^{SH3} to DLC1^{GAP} (Fig. 6C); this value nicely resembles the K_i value obtained from inhibition kinetics (Fig. 6B). This binding affinity is remarkably high and unexpected considering the low micromolar range affinities of SH3 domains for their PXXP-containing proteins (59). Taken together, these data strongly suggest that the mode of the p120^{SH3}-DLC1^{GAP} interaction most likely differs from the conventional SH3 interaction with PXXP loop motifs as recently published (48).

Structural Insight into a Putative Binding Mode between p120^{SH3} and DLC1^{GAP}—The high nanomolar affinity of p120^{SH3} for DLC1^{GAP} and the absence of a PXXP motif in DLC1^{GAP} strongly support the notion that the p120^{SH3}-DLC1^{GAP} interaction is mediated via a novel binding mechanism. To gain insight into the structural basis of this interaction, we first performed protein-protein docking of available crystal structures of p120^{SH3} (Protein Data Bank code 2J05) (53) and DLC1^{GAP} (Protein Data Bank code 3KUQ) using the Patch-Dock program (54). The model of the complex ranked as the first among 20 resulting models fulfilled the criteria for a close proximity of p120^{SH3} to the catalytic arginine finger (Arg-677) of the DLC1^{GAP} domain and was thus selected for refinement by molecular modeling methods. Inspecting the refined model, we identified three potential DLC1^{GAP} binding residues of p120^{SH3} (Asn-311, Leu-313, and Trp-319) that were closest to the catalytic Arg-677 of DLC1^{GAP} (Fig. 7A). We proposed that mutation of these residues may impair binding of the SH3 domain, which otherwise masks the arginine finger of DLC1^{GAP}. Catalytic arginine is known to stabilize the transition intermediate state of the hydrolysis reaction in the active center of Rho proteins (Fig. 7B) (14, 60). This assumption also suggests that p120 competitively inhibits DLC1 GAP function.

To validate our assumption, we performed mutational analysis of the above mentioned key residues at the p120^{SH3}-DLC1^{GAP} interface: N311R, L313A, and W319G in p120^{SH3} (single, double, and triple single point mutations) and R677A in DLC1^{GAP}. Expectedly, DLC1^{GAP} with the catalytic arginine finger substituted to alanine was deficient in stimulating tamraGTP hydrolysis of Cdc42 (data not shown) and most remarkably in associating with p120^{SH3} (Fig. 8, A and B). The latter was examined using two independent methods, ITC and aSEC. Reciprocally, p120$^{SH3(N311R,L313A,W319G)}$ was almost disabled in inhibiting DLC1^{GAP} activity (Fig. 8E), most probably due to its inability to bind to DLC1^{GAP} (Fig. 8, C and D). The analysis of the single point mutations revealed that W319G substitution had a minor effect on the association with (data not shown) and on the inhibition of DLC^{GAP} (Fig. 8E). p120$^{SH3(N311R,L313A)}$ on the other hand significantly abolished both the inhibitory effect of p120^{SH3} (Fig. 8E) and the complex formation with DLC1^{GAP} (data not shown) as compared with wild-type p120^{SH3}. Taken together,
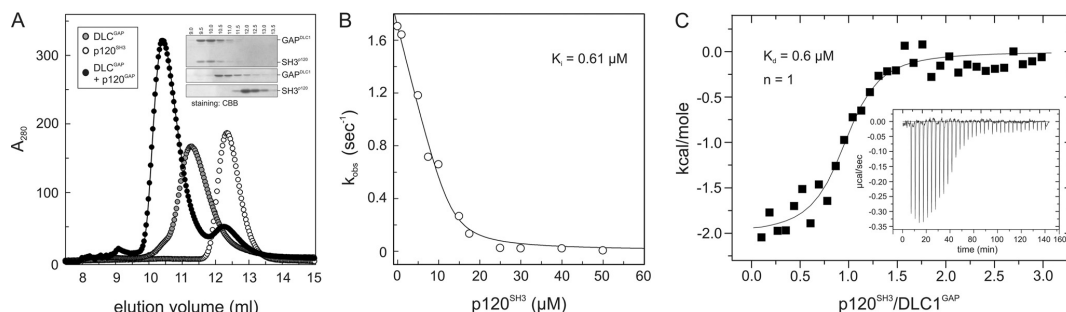
FIGURE 6. **High affinity interaction between p120^{SH3} and DLC1^{GAP}.** *A*, co-elution of a mixture of DLC1^{GAP} (10 μM) and p120^{SH3} (15 μM) (*open circles*) from a Superdex 75 (10/300) as shown by SDS-PAGE (15%) and Coomassie Brilliant Blue (*CBB*) staining (*inset*) indicates their complex formation. *B*, the activity of DLC1^{GAP} (20 μM) toward Cdc42 (0.2 μM) was measured at increasing concentrations of p120^{SH3}, and the obtained k_{obs} values were plotted against increasing concentrations of the inhibitor p120^{SH3}. The K_i value was obtained by non-linear regression based on the Morrison equation for tight binding inhibitors (58). *C*, ITC analysis was performed by titrating DLC1^{GAP} (20 μM) with p120^{SH3} (400 μM). K_d is the dissociation constant, and *n* is the stoichiometry.
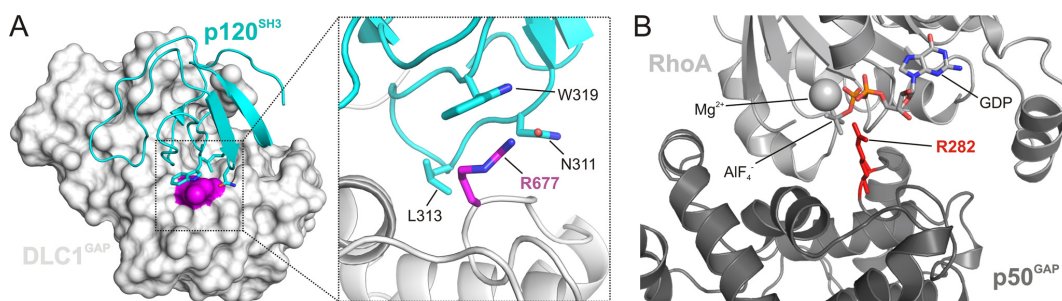
FIGURE 7. **Structural insight into a putative binding mode between p120^{SH3} and DLC1^{GAP}.** *A*, molecular docking analyses were performed between the available crystal structures of p120^{SH3} (Protein Data Bank code 2J05) (53) and DLC1^{GAP} (Protein Data Bank code 3KUQ) using the program PatchDock (54). In the best ranked and refined model, p120^{SH3} was located in close proximity of the catalytic arginine finger (Arg-677; *magenta*) of DLC1^{GAP}. In this model, p120^{SH3} supplied three amino acids (Asn-311, Leu-313, and Trp-319) to directly contact the catalytic core of DLC1^{GAP}, especially Arg-677, and mask its accessibility to the Rho proteins. *B*, p50GAP provides an arginine finger (Arg-282; *red*) in the active site of RhoA to stabilize the transition state of the GTP hydrolysis reaction (Protein Data Bank code 1TX4) (60). GDP-AlF$_4^-$ mimics the transition state of the GTP hydrolysis reaction.

our mutational and biochemical analyses support the *in silico* structural model (Fig. 7*A*) and provide new insight into how p120^{SH3} may bind and inhibit the catalytic activity of DLC1^{GAP}.

DISCUSSION

In this study, we have elucidated the molecular mechanism of how the RasGAP p120 selectively acts as a negative regulator of the RhoGAP activity of DLC1. We have shown that p120^{SH3}, by utilizing a novel binding mode, selectively undergoes a high affinity interaction with the RhoGAP domain of DLC1 and effectively inhibits its GAP activity by targeting its catalytic arginine finger. Interestingly, p120^{SH3} acts on the DLC isoforms but not on seven other representative members of the RhoGAP family. Our data together support the notion of a functional cross-talk between Ras and Rho proteins at the level of regulatory proteins (11, 45).

In contrast to the molecular mechanism of Rho protein inactivation by GAPs, which is well established (14, 61), it is still unclear how GAPs themselves are regulated. Different mechanisms are implicated in the regulation of GAPs, such as regulation by protein phosphorylation, proteolytic degradation, intramolecular autoinhibition, and changes in subcellular localization or protein complex formation (62, 63). "Intramolecular inhibition" (also called "autoinhibition," "*cis*-inhibition," "autoinhibitory

loop," "autoregulation," and "bistable switch") of biological molecules is a fundamental control mechanism in nature and is an emerging theme in the regulation of different kinds of proteins, including the regulators of small GTP-binding proteins themselves. Besides the guanine nucleotide exchange factors (64–69), GAPs also have been reported to require activation through the relief of autoinhibitory elements (20, 31–33, 35, 36). Kim *et al.* (20) have shown that DLC1^{fl} has a reduced GAP activity and have proposed that the N-terminal SAM domain may be a *cis*-inhibitory element contributing to DLC1 autoinhibition. Our real time kinetic experiments, however, have shown that neither isolated SAM or START alone nor both domains in combination are directly responsible for the observed DLC1^{fl} autoinhibition in a cell-free system (Fig. 3). Taken together, it rather seems plausible that other regions, probably together with SAM and START domains, are involved in the autoinhibition of DLC1. In addition, it is important to note that release of the autoinhibitory loop of DLC1 is most likely subjected to posttranslational modifications (21, 70) and interactions with other proteins (16, 28, 34) along with changes in subcellular localization (30), collectively contribute to the regulation of DLC1 GAP activity in intact cells. In this context, PKD-mediated phosphorylation (70) and 14-3-3 binding and

p120RasGAP Competitively Inhibits DLC RhoGAP
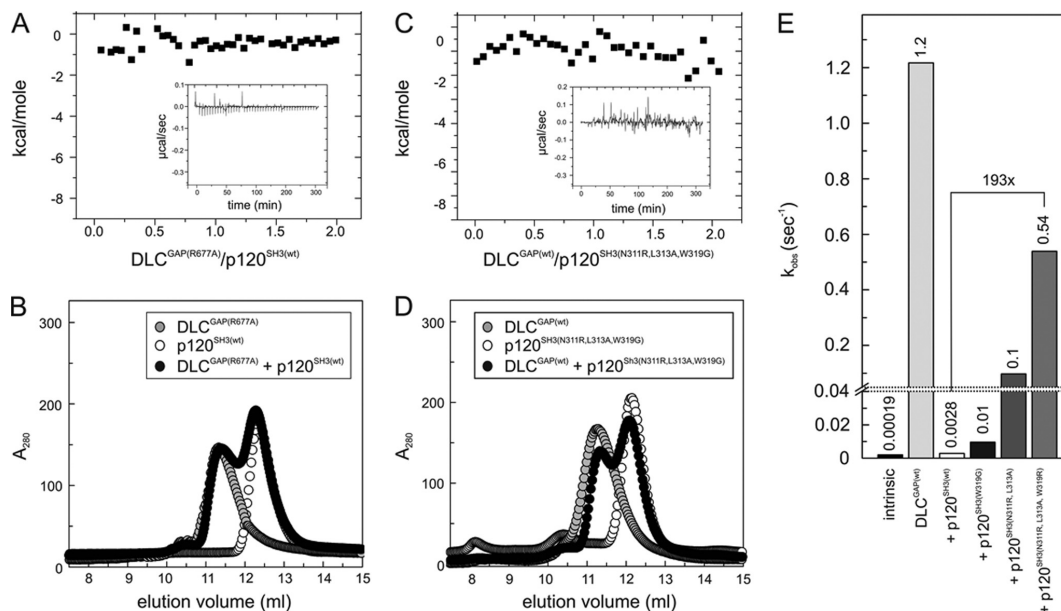

FIGURE 8. **Loss of p120-DLC1 interaction by mutational analysis.** No interaction was observed between DLC1$^{GAP(R677A)}$ and p120$^{SH3(WT)}$ (*A* and *B*) and DLC1$^{GAP(WT)}$ and p120$^{SH3(N311R,L313A,W319G)}$ (*C* and *D*). Loss of interaction and of inhibition was measured by ITC (*A* and *C*) and aSEC (*B* and *D*) as compared with the p120$^{SH3(WT)}$-DLC1$^{GAP(WT)}$ interaction shown in Fig. 6. *E*, the activity of DLC1^{GAP} (25 μM) in stimulating tamraGTP hydrolysis of Cdc42 (0.2 μM) was measured in the presence of p120^{SH3} variants (125 μM), respectively. For convenience, the k_{obs} values are given above the *bar charts*.

cytosolic sequestration (22) are good examples for the regulation DLC1 function.

Functional characterization and structural elucidation of the *trans*-inhibitory mechanism of DLC1 mediated by the Ras-specific GAP p120 protein (11) was the central theme of this study. Our data clearly revealed that the GAP activity of not only DLC1 but also that of DLC2 and DLC3 was almost completely abolished in the presence of the SH3 domain of p120 (Fig. 4). We showed that larger fragments of p120, such as p120$^{SH2-3-2}$ and the almost full-length p120$^{\Delta n128}$, inhibit the DLC GAP function but strikingly not to the same extent as seen for the isolated SH3 domain (Fig. 4*D*). These data indicate that only a freely accessible and exposed SH3 domain of p120, most probably following an upstream signal and in a defined subcellular environment (11, 37), is able to potently inhibit DLC proteins. One of the p120 binding partners is p190, which has been proposed to induce a conformational change in p120 by binding to its SH2 domains and exposing the adjacent SH3 domain for additional protein interactions with additional proteins (47), one of which is most likely DLC1.

Several studies have shown that DLC1 is able to inactivate Cdc42 and the Rho isoforms (RhoA, RhoB, and RhoC) but not Rac1 *in vitro* (20, 71–73). DLC1^{GAP} activity toward other members of the Rho family has not yet been published. Our preliminary data showed that the DLC proteins are active *in vitro* on almost all members of the Rho family that are able to hydrolyze GTP.[6]

Chan *et al.* (74) have shown an increased level of RhoA-GTP in DLC2-null mice but not in samples from control mice. Consistently, the overexpression of DLC isoforms has been shown to lead to inactivation of RhoA and to the reduction of actin stress fiber formation (75, 76), suggesting that DLC proteins are Rho-selective GAPs and the role of the DLC *trans*-inhibitory protein p120 is to retain Rho proteins in their active GTP-bound states. Contrary to DLC proteins, p120 binding is part of the p190 activation process that controls inactivation of Rho-type proteins (45, 47, 77). A prerequisite for this interaction is phosphorylation of p190 at tyrosine 1105, which is a target of the p120 SH2 domains (77). In this regard, p120 oppositely controls the activities of two different RhoGAPs and obviously two different Rho/Rho effector systems; one is left activated, and the other is switched off.

SH3 domain-containing cellular signaling proteins mediate interactions via specific proline-containing peptides. The SH3 domain of p120 has been discussed recently to interact with other proteins in a P*XX*P motif-independent manner (48). *In silico* analysis revealed that the GAP domain of DLC1 does not possess a proline-rich region and therefore, unlike classical P*XX*P motif-recognizing SH3 domains, the interaction mode of the p120 SH3 domain is atypical and utilizes different amino acids to bind and mask the catalytic arginine finger of the GAP domain of DLC1. The Ser/Thr kinases Aurora A and Aurora B are other examples in addition to DLC1 for negative modulation of biological processes by p120 (78). The SH3 domain of p120 binds to the catalytic domain of Aurora kinases that inhibits their kinase activity. These interactions also do not involve a

---

[6] M. Jaiswal, E. Amin, and R. Dvorsky, unpublished data.

proline-rich consensus sequence. Two accessible hydrophobic regions of p120 SH3 have been suggested to function as binding sites for protein interaction (79). Our study supports this notion as we have shown that mutation of three amino acids close to one of these proposed binding sites indeed diminished the DLC1^{GAP} binding and inhibiting ability of p120 SH3.

We demonstrated that the interaction between p120^{SH3} and DLC1^{GAP} displays at least three remarkable characteristics, namely high affinity, high selectively, and a non-canonical binding mode. The high affinity interaction of 0.6 μM is striking because the binding constants of SH3 domains for proline-rich motifs in their target proteins are mostly in the micromolar range (48, 59). The very few examples of high affinity binding of SH3 domains are those between Mona/Gads and SLP-76 (80), C3G and c-Crk (51), and Grb2 and Wrch1 (48).

CONCLUSION

Mechanistic and structural insights into selectivity, activity, and regulation of DLC1 presented in this study shed light on the role of the multifunctional, regulatory signaling molecule p120RasGAP. It is evident that p120 acts in addition to its RasGAP domain, which is required to switch off Ras signal transduction, as an "effector" conversely controlling, via its SH2 domains and a non-canonical SH3 domain, the RhoGAP activities of the DLC and p190 proteins and hence Rho signal transduction. Interestingly, p120 interacts, in addition to DLC1 and p190, with a third RhoGAP, called p200RhoGAP. In contrast to p190 and DLC1, which are downstream of p120, p200RhoGAP has been proposed to bind to the p120 SH3 domain via its very C-terminal proline-rich region and to sequester its RasGAP function from inactivating Ras (10). These examples nicely illustrate the interdependence of the Ras and Rho signaling pathways and underline the multifunctional and multifaceted nature of regulatory proteins beyond their critical GAP functions.

REFERENCES

1. Aznar, S., and Lacal, J. C. (2001) Searching new targets for anticancer drug design: the families of Ras and Rho GTPases and their effectors. *Prog. Nucleic Acid Res. Mol. Biol.* **67,** 193–234
2. Fritz, G., Just, I., and Kaina, B. (1999) Rho GTPases are over-expressed in human tumors. *Int. J. Cancer* **81,** 682–687
3. Pruitt, K., and Der, C. J. (2001) Ras and Rho regulation of the cell cycle and oncogenesis. *Cancer Lett.* **171,** 1–10
4. Zondag, G. C., Evers, E. E., ten Klooster, J. P., Janssen, L., van der Kammen, R. A., and Collard, J. G. (2000) Oncogenic Ras downregulates Rac activity, which leads to increased Rho activity and epithelial-mesenchymal transition. *J. Cell Biol.* **149,** 775–782
5. Sahai, E., and Marshall, C. J. (2002) RHO-GTPases and cancer. *Nat. Rev. Cancer* **2,** 133–142
6. Khosravi-Far, R., Campbell, S., Rossman, K. L., and Der, C. J. (1998) Increasing complexity of Ras signal transduction: involvement of Rho family proteins. *Adv. Cancer Res.* **72,** 57–107
7. Coleman, M. L., Marshall, C. J., and Olson, M. F. (2004) RAS and RHO GTPases in G1-phase cell-cycle regulation. *Nat. Rev. Mol. Cell Biol.* **5,** 355–366
8. Karnoub, A. E., and Weinberg, R. A. (2008) Ras oncogenes: split personalities. *Nat. Rev. Mol. Cell Biol.* **9,** 517–531
9. Asnaghi, L., Vass, W. C., Quadri, R., Day, P. M., Qian, X., Braverman, R., Papageorge, A. G., and Lowy, D. R. (2010) E-cadherin negatively regulates neoplastic growth in non-small cell lung cancer: role of Rho GTPases. *Oncogene* **29,** 2760–2771
10. Shang, X., Moon, S. Y., and Zheng, Y. (2007) p200 RhoGAP promotes cell proliferation by mediating cross-talk between Ras and Rho signaling pathways. *J. Biol. Chem.* **282,** 8801–8811
11. Yang, X. Y., Guan, M., Vigil, D., Der, C. J., Lowy, D. R., and Popescu, N. C. (2009) p120Ras-GAP binds the DLC1 Rho-GAP tumor suppressor protein and inhibits its RhoA GTPase and growth-suppressing activities. *Oncogene* **28,** 1401–1409
12. Scheffzek, K., and Ahmadian, M. R. (2005) GTPase activating proteins: structural and functional insights 18 years after discovery. *Cell. Mol. Life Sci.* **62,** 3014–3038
13. Ligeti, E., Welti, S., and Scheffzek, K. (2012) Inhibition and termination of physiological responses by GTPase activating proteins. *Physiol. Rev.* **92,** 237–272
14. Scheffzek, K., Ahmadian, M. R., and Wittinghofer, A. (1998) GTPase-activating proteins: helping hands to complement an active site. *Trends Biochem. Sci.* **23,** 257–262
15. Yuan, B. Z., Miller, M. J., Keck, C. L., Zimonjic, D. B., Thorgeirsson, S. S., and Popescu, N. C. (1998) Cloning, characterization, and chromosomal localization of a gene frequently deleted in human liver cancer (DLC-1) homologous to rat RhoGAP. *Cancer Res.* **58,** 2196–2199
16. Durkin, M. E., Yuan, B. Z., Zhou, X., Zimonjic, D. B., Lowy, D. R., Thorgeirsson, S. S., and Popescu, N. C. (2007) DLC-1: a Rho GTPase-activating protein and tumour suppressor. *J. Cell. Mol. Med.* **11,** 1185–1207
17. Liao, Y. C., and Lo, S. H. (2008) Deleted in liver cancer-1 (DLC-1): a tumor suppressor not just for liver. *Int. J. Biochem. Cell Biol.* **40,** 843–847
18. Zimonjic, D. B., and Popescu, N. C. (2012) Role of DLC1 tumor suppressor gene and MYC oncogene in pathogenesis of human hepatocellular carcinoma: potential prospects for combined targeted therapeutics (review). *Int. J. Oncol.* **41,** 393–406
19. Holeiter, G., Heering, J., Erlmann, P., Schmid, S., Jähne, R., and Olayioye, M. A. (2008) Deleted in liver cancer 1 controls cell migration through a Dia1-dependent signaling pathway. *Cancer Res.* **68,** 8743–8751
20. Kim, T. Y., Healy, K. D., Der, C. J., Sciaky, N., Bang, Y. J., and Juliano, R. L. (2008) Effects of structure of Rho GTPase-activating protein DLC-1 on cell morphology and migration. *J. Biol. Chem.* **283,** 32762–32770
21. Kim, T. Y., Vigil, D., Der, C. J., and Juliano, R. L. (2009) Role of DLC-1, a tumor suppressor protein with RhoGAP activity, in regulation of the cytoskeleton and cell motility. *Cancer Metastasis Rev.* **28,** 77–83
22. Scholz, R. P., Regner, J., Theil, A., Erlmann, P., Holeiter, G., Jähne, R., Schmid, S., Hausser, A., and Olayioye, M. A. (2009) DLC1 interacts with 14-3-3 proteins to inhibit RhoGAP activity and block nucleocytoplasmic shuttling. *J. Cell Sci.* **122,** 92–102
23. Lukasik, D., Wilczek, E., Wasiutynski, A., and Gornicka, B. (2011) Deleted in liver cancer protein family in human malignancies (review). *Oncol. Lett.* **2,** 763–768
24. Yam, J. W., Ko, F. C., Chan, C. Y., Jin, D. Y., and Ng, I. O. (2006) Interaction of deleted in liver cancer 1 with tensin2 in caveolae and implications in tumor suppression. *Cancer Res.* **66,** 8367–8372
25. Liao, Y. C., Si, L., deVere White, R. W., and Lo, S. H. (2007) The phosphotyrosine-independent interaction of DLC-1 and the SH2 domain of cten regulates focal adhesion localization and growth suppression activity of DLC-1. *J. Cell Biol.* **176,** 43–49
26. Qian, X., Li, G., Asmussen, H. K., Asnaghi, L., Vass, W. C., Braverman, R., Yamada, K. M., Popescu, N. C., Papageorge, A. G., and Lowy, D. R. (2007) Oncogenic inhibition by a deleted in liver cancer gene requires cooperation between tensin binding and Rho-specific GTPase-activating protein activities. *Proc. Natl. Acad. Sci. U.S.A.* **104,** 9012–9017
27. Chan, L. K., Ko, F. C., Ng, I. O., and Yam, J. W. (2009) Deleted in liver cancer 1 (DLC1) utilizes a novel binding site for Tensin2 PTB domain interaction and is required for tumor-suppressive function. *PLoS One* **4,** e5572

p120RasGAP Competitively Inhibits DLC RhoGAP

28. Tripathi, V., Popescu, N. C., and Zimonjic, D. B. (2013) DLC1 induces expression of E-cadherin in prostate cancer cells through Rho pathway and suppresses invasion. *Oncogene* **4,** 1–10

29. Li, G., Du, X., Vass, W. C., Papageorge, A. G., Lowy, D. R., and Qian, X. (2011) Full activity of the deleted in liver cancer 1 (DLC1) tumor suppressor depends on an LD-like motif that binds talin and focal adhesion kinase (FAK). *Proc. Natl. Acad. Sci. U.S.A.* **108,** 17129–17134

30. Erlmann, P., Schmid, S., Horenkamp, F. A., Geyer, M., Pomorski, T. G., and Olayioye, M. A. (2009) DLC1 activation requires lipid interaction through a polybasic region preceding the RhoGAP domain. *Mol. Biol. Cell* **20,** 4400–4411

31. Fauchereau, F., Herbrand, U., Chafey, P., Eberth, A., Koulakoff, A., Vinet, M. C., Ahmadian, M. R., Chelly, J., and Billuart, P. (2003) The RhoGAP activity of OPHN1, a new F-actin-binding protein, is negatively controlled by its amino-terminal domain. *Mol. Cell. Neurosci.* **23,** 574–586

32. Eberth, A., and Ahmadian, M. R. (2009) *In vitro* GEF and GAP assays. *Curr. Protoc. Cell Biol.* **Chapter 14,** Unit 14.19

33. Colón-González, F., Leskow, F. C., and Kazanietz, M. G. (2008) Identification of an autoinhibitory mechanism that restricts C1 domain-mediated activation of the Rac-GAP α2-chimaerin. *J. Biol. Chem.* **283,** 35247–35257

34. Jian, X., Brown, P., Schuck, P., Gruschus, J. M., Balbo, A., Hinshaw, J. E., and Randazzo, P. A. (2009) Autoinhibition of Arf GTPase-activating protein activity by the BAR domain in ASAP1. *J. Biol. Chem.* **284,** 1652–1663

35. Zhou, Y. T., Chew, L. L., Lin, S. C., and Low, B. C. (2010) The BNIP-2 and Cdc42GAP homology (BCH) domain of p50RhoGAP/Cdc42GAP sequesters RhoA from inactivation by the adjacent GTPase-activating protein domain. *Mol. Biol. Cell* **21,** 3232–3246

36. Moskwa, P., Paclet, M. H., Dagher, M. C., and Ligeti, E. (2005) Autoinhibition of p50 Rho GTPase-activating protein (GAP) is released by prenylated small GTPases. *J. Biol. Chem.* **280,** 6716–6720

37. Pamonsinlapatham, P., Hadj-Slimane, R., Lepelletier, Y., Allain, B., Toccafondi, M., Garbay, C., and Raynaud, F. (2009) p120-Ras GTPase activating protein (RasGAP): a multi-interacting protein in downstream signaling. *Biochimie* **91,** 320–328

38. Ahmadian, M. R., Hoffmann, U., Goody, R. S., and Wittinghofer, A. (1997) Individual rate constants for the interaction of Ras proteins with GTPase-activating proteins determined by fluorescence spectroscopy. *Biochemistry* **36,** 4535–4541

39. Ahmadian, M. R., Stege, P., Scheffzek, K., and Wittinghofer, A. (1997) Confirmation of the arginine-finger hypothesis for the GAP-stimulated GTP-hydrolysis reaction of Ras. *Nat. Struct. Biol.* **4,** 686–689

40. Scheffzek, K., Ahmadian, M. R., Kabsch, W., Wiesmüller, L., Lautwein, A., Schmitz, F., and Wittinghofer, A. (1997) The Ras-RasGAP complex: structural basis for GTPase activation and its loss in oncogenic Ras mutants. *Science* **277,** 333–338

41. Leblanc, V., Tocque, B., and Delumeau, I. (1998) Ras-GAP controls Rho-mediated cytoskeletal reorganization through its SH3 domain. *Mol. Cell. Biol.* **18,** 5567–5578

42. Chan, P. C., and Chen, H. C. (2012) p120RasGAP-mediated activation of c-Src is critical for oncogenic Ras to induce tumor invasion. *Cancer Res.* **72,** 2405–2415

43. Clark, G. J., and Der, C. J. (1995) Aberrant function of the Ras signal transduction pathway in human breast cancer. *Breast Cancer Res. Treat.* **35,** 133–144

44. Clark, G. J., Westwick, J. K., and Der, C. J. (1997) p120 GAP modulates Ras activation of Jun kinases and transformation. *J. Biol. Chem.* **272,** 1677–1681

45. Herbrand, U., and Ahmadian, M. R. (2006) p190-RhoGAP as an integral component of the Tiam1/Rac1-induced downregulation of Rho. *Biol. Chem.* **387,** 311–317

46. Wang, Z., Tung, P. S., and Moran, M. F. (1996) Association of p120 ras GAP with endocytic components and colocalization with epidermal growth factor (EGF) receptor in response to EGF stimulation. *Cell Growth Differ.* **7,** 123–133

47. Hu, K. Q., and Settleman, J. (1997) Tandem SH2 binding sites mediate the RasGAP-RhoGAP interaction: a conformational mechanism for SH3 domain regulation. *EMBO J.* **16,** 473–483

48. Risse, S. L., Vaz, B., Burton, M. F., Aspenström, P., Piekorz, R. P., Brunsveld, L., and Ahmadian, M. R. (2013) SH3-mediated targeting of Wrch1/RhoU by multiple adaptor proteins. *Biol. Chem.* **394,** 421–432

49. Jaiswal, M., Dubey, B. N., Koessmeier, K. T., Gremer, L., and Ahmadian, M. R. (2012) Biochemical assays to characterize Rho GTPases. *Methods Mol. Biol.* **827,** 37–58

50. Eberth, A., Lundmark, R., Gremer, L., Dvorsky, R., Koessmeier, K. T., McMahon, H. T., and Ahmadian, M. R. (2009) A BAR domain-mediated autoinhibitory mechanism for RhoGAPs of the GRAF family. *Biochem. J.* **417,** 371–377

51. Wu, X., Knudsen, B., Feller, S. M., Zheng, J., Sali, A., Cowburn, D., Hanafusa, H., and Kuriyan, J. (1995) Structural basis for the specific interaction of lysine-containing proline-rich peptides with the N-terminal SH3 domain of c-Crk. *Structure* **3,** 215–226

52. Eberth, A., Dvorsky, R., Becker, C. F., Beste, A., Goody, R. S., and Ahmadian, M. R. (2005) Monitoring the real-time kinetics of the hydrolysis reaction of guanine nucleotide-binding proteins. *Biol. Chem.* **386,** 1105–1114

53. Ross, B., Kristensen, O., Favre, D., Walicki, J., Kastrup, J. S., Widmann, C., and Gajhede, M. (2007) High resolution crystal structures of the p120 RasGAP SH3 domain. *Biochem. Biophys. Res. Commun.* **353,** 463–468

54. Schneidman-Duhovny, D., Inbar, Y., Nussinov, R., and Wolfson, H. J. (2005) PatchDock and SymmDock: servers for rigid and symmetric docking. *Nucleic Acids Res.* **33,** W363–W367

55. Brooks, B. R., Brooks, C. L., 3rd, Mackerell, A. D., Jr., Nilsson, L., Petrella, R. J., Roux, B., Won, Y., Archontis, G., Bartels, C., Boresch, S., Caflisch, A., Caves, L., Cui, Q., Dinner, A. R., Feig, M., Fischer, S., Gao, J., Hodoscek, M., Im, W., Kuczera, K., Lazaridis, T., Ma, J., Ovchinnikov, V., Paci, E., Pastor, R. W., Post, C. B., Pu, J. Z., Schaefer, M., Tidor, B., Venable, R. M., Woodcock, H. L., Wu, X., Yang, W., York, D. M., and Karplus, M. (2009) CHARMM: the biomolecular simulation program. *J. Comput. Chem.* **30,** 1545–1614

56. Scouras, A. D., and Daggett, V. (2011) The Dynameomics rotamer library: amino acid side chain conformations and dynamics from comprehensive molecular dynamics simulations in water. *Protein Sci.* **20,** 341–352

57. Eccleston, J. F., Moore, K. J., Morgan, L., Skinner, R. H., and Lowe, P. N. (1993) Kinetics of interaction between normal and proline 12 Ras and the GTPase-activating proteins, p120-GAP and neurofibromin. The significance of the intrinsic GTPase rate in determining the transforming ability of *ras*. *J. Biol. Chem.* **268,** 27012–27019

58. Morrison, J. F. (1969) Kinetics of the reversible inhibition of enzyme-catalysed reactions by tight-binding inhibitors. *Biochim. Biophys. Acta* **185,** 269–286

59. Kärkkäinen, S., Hiipakka, M., Wang, J. H., Kleino, I., Vähä-Jaakkola, M., Renkema, G. H., Liss, M., Wagner, R., and Saksela, K. (2006) Identification of preferred protein interactions by phage-display of the human Src homology-3 proteome. *EMBO Rep.* **7,** 186–191

60. Rittinger, K., Walker, P. A., Eccleston, J. F., Smerdon, S. J., and Gamblin, S. J. (1997) Structure at 1.65 Å of RhoA and its GTPase-activating protein in complex with a transition-state analogue. *Nature* **389,** 758–762

61. Dvorsky, R., and Ahmadian, M. R. (2004) Always look on the bright site of Rho: structural implications for a conserved intermolecular interface. *EMBO Rep.* **5,** 1130–1136

62. Moon, S. Y., and Zheng, Y. (2003) Rho GTPase-activating proteins in cell regulation. *Trends Cell Biol.* **13,** 13–22

63. Tcherkezian, J., and Lamarche-Vane, N. (2007) Current knowledge of the large RhoGAP family of proteins. *Biol. Cell* **99,** 67–86

64. Rossman, K. L., Der, C. J., and Sondek, J. (2005) GEF means go: turning on RHO GTPases with guanine nucleotide-exchange factors. *Nat. Rev. Mol. Cell Biol.* **6,** 167–180

65. Aittaleb, M., Boguth, C. A., and Tesmer, J. J. (2010) Structure and function of heterotrimeric G protein-regulated Rho guanine nucleotide exchange factors. *Mol. Pharmacol.* **77,** 111–125

66. DiNitto, J. P., Lee, M. T., Malaby, A. W., and Lambright, D. G. (2010) Specificity and membrane partitioning of Grsp1 signaling complexes with Grp1 family Arf exchange factors. *Biochemistry* **49,** 6083–6092

67. Gureasko, J., Kuchment, O., Makino, D. L., Sondermann, H., Bar-Sagi, D., and Kuriyan, J. (2010) Role of the histone domain in the autoinhibition and activation of the Ras activator Son of Sevenless. *Proc. Natl. Acad. Sci.*

U.S.A. **107,** 3430–3435

68. Jaiswal, M., Gremer, L., Dvorsky, R., Haeusler, L. C., Cirstea, I. C., Uhlen-
    brock, K., and Ahmadian, M. R. (2011) Mechanistic insights into specific-
    ity, activity, and regulatory elements of the regulator of G-protein signal-
    ing (RGS)-containing Rho-specific guanine nucleotide exchange factors
    (GEFs) p115, PDZ-RhoGEF (PRG), and leukemia-associated RhoGEF
    (LARG). *J. Biol. Chem.* **286,** 18202–18212

69. Mitin, N., Betts, L., Yohe, M. E., Der, C. J., Sondek, J., and Rossman, K. L.
    (2007) Release of autoinhibition of ASEF by APC leads to CDC42 activa-
    tion and tumor suppression. *Nat. Struct. Mol. Biol.* **14,** 814–823

70. Scholz, R. P., Gustafsson, J. O., Hoffmann, P., Jaiswal, M., Ahmadian, M. R.,
    Eisler, S. A., Erlmann, P., Schmid, S., Hausser, A., and Olayioye, M. A.
    (2011) The tumor suppressor protein DLC1 is regulated by PKD-medi-
    ated GAP domain phosphorylation. *Exp. Cell Res.* **317,** 496–503

71. Ching, Y. P., Wong, C. M., Chan, S. F., Leung, T. H., Ng, D. C., Jin, D. Y.,
    and Ng, I. O. (2003) Deleted in liver cancer (DLC) 2 encodes a RhoGAP
    protein with growth suppressor function and is underexpressed in hepa-
    tocellular carcinoma. *J. Biol. Chem.* **278,** 10824–10830

72. Wong, C. M., Lee, J. M., Ching, Y. P., Jin, D. Y., and Ng, I. O. (2003) Genetic
    and epigenetic alterations of DLC-1 gene in hepatocellular carcinoma.
    Cancer Res. **63,** 7646–7651

73. Healy, K. D., Hodgson, L., Kim, T. Y., Shutes, A., Maddileti, S., Juliano,
    R. L., Hahn, K. M., Harden, T. K., Bang, Y. J., and Der, C. J. (2008) DLC-1
    suppresses non-small cell lung cancer growth and invasion by RhoGAP-
    dependent and independent mechanisms. *Mol. Carcinog.* **47,** 326–337

74. Chan, F. K., Chung, S. S., Ng, I. O., and Chung, S. K. (2012) The RhoA
    GTPase-activating protein DLC2 modulates RhoA activity and hyperal-

p120RasGAP Competitively Inhibits DLC RhoGAP

gesia to noxious thermal and inflammatory stimuli. *Neurosignals* **20,**
112–126

75. Leung, T. H., Ching, Y. P., Yam, J. W., Wong, C. M., Yau, T. O., Jin, D. Y.,
    and Ng, I. O. (2005) Deleted in liver cancer 2 (DLC2) suppresses cell
    transformation by means of inhibition of RhoA activity. *Proc. Natl. Acad.
    Sci. U.S.A.* **102,** 15207–15212

76. Kawai, K., Kiyota, M., Seike, J., Deki, Y., and Yagisawa, H. (2007) START-
    GAP3/DLC3 is a GAP for RhoA and Cdc42 and is localized in focal adhe-
    sions regulating cell morphology. *Biochem. Biophys. Res. Commun.* **364,**
    783–789

77. Roof, R. W., Haskell, M. D., Dukes, B. D., Sherman, N., Kinter, M., and
    Parsons, S. J. (1998) Phosphotyrosine (p-Tyr)-dependent and -indepen-
    dent mechanisms of p190 RhoGAP-p120 RasGAP interaction: Tyr 1105 of
    p190, a substrate for c-Src, is the sole p-Tyr mediator of complex forma-
    tion. *Mol. Cell. Biol.* **18,** 7052–7063

78. Gigoux, V., L'Hoste, S., Raynaud, F., Camonis, J., and Garbay, C. (2002)
    Identification of Aurora kinases as RasGAP Src homology 3 domain-bind-
    ing proteins. *J. Biol. Chem.* **277,** 23742–23746

79. Yang, Y. S., Garbay, C., Duchesne, M., Cornille, F., Jullian, N., Fromage, N.,
    Tocque, B., and Roques, B. P. (1994) Solution structure of GAP SH3 do-
    main by ¹H NMR and spatial arrangement of essential Ras signaling-in-
    volved sequence. *EMBO J.* **13,** 1270–1279

80. Harkiolaki, M., Lewitzky, M., Gilbert, R. J., Jones, E. Y., Bourette, R. P.,
    Mouchiroud, G., Sondermann, H., Moarefi, I., and Feller, S. M. (2003)
    Structural basis for SH3 domain-mediated high-affinity binding between
    Mona/Gads and SLP-76. *EMBO J.* **22,** 2571–2582

Chapter 5

Rocaglamide inhibits RHO GTPase activity and cancer cell migration

The anticancer phytochemical Rocaglamide inhibits RHO GTPase activity and cancer cell migration
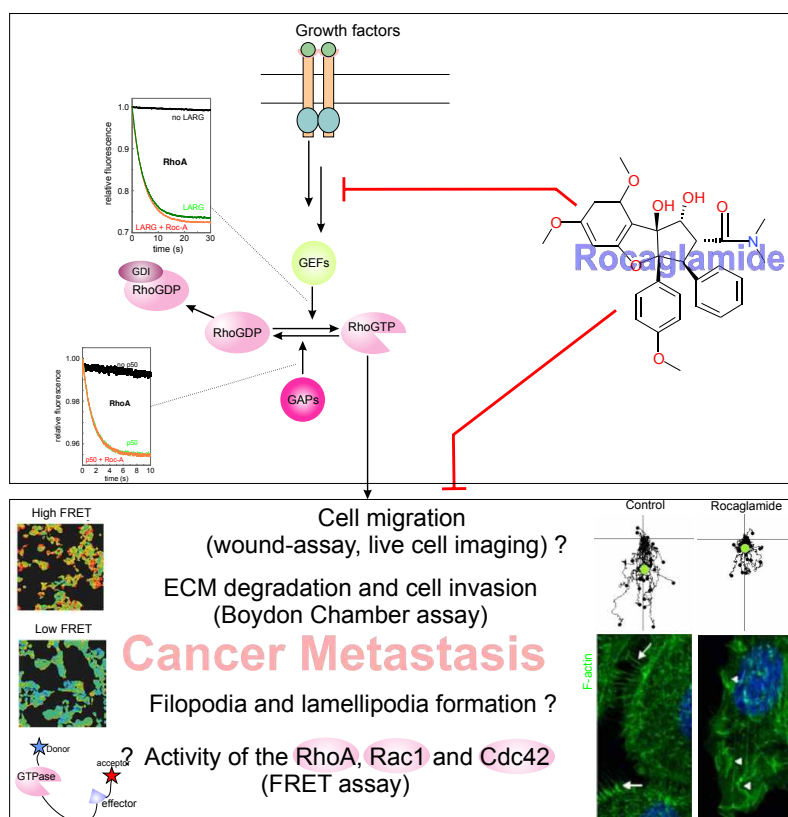
Status:	Published in Oncotarget. 7(32): 51908-51921
Impact factor:	6.34
Own Proportion to this work:	15 %; investigating inhibitory effects of Rocaglamide on GEFs and GAPs in vitro (Figure 6)

The anticancer phytochemical rocaglamide inhibits Rho GTPase activity and cancer cell migration

Michael S. Becker[1], Paul M. Müller[2], Jörg Bajorat[1], Anne Schroeder[1], Marco Giaisi[1], Ehsan Amin[3], Mohammad R. Ahmadian[3], Oliver Rocks[2], Rebecca Köhler[1], Peter H. Krammer[1], Min Li-Weber[1]

[1]Tumorimmunology Program (D030), German Cancer Research Center (DKFZ), INF-280, Heidelberg, Germany

[2]Max Delbrück Center for Molecular Medicine Berlin-Buch, Berlin, Germany

[3]Institute of Biochemistry and Molecular Biology II, Medical Faculty of the Heinrich-Heine University, Düsseldorf, Germany

Correspondence to: Min Li-Weber, *email:* m.li-weber@dkfz-heidelberg.de

ABSTRACT

Chemotherapy is one of the pillars of anti-cancer therapy. Although chemotherapeutics cause regression of the primary tumor, many chemotherapeutics are often shown to induce or accelerate metastasis formation. Moreover, metastatic tumors are largely resistant against chemotherapy. As more than 90% of cancer patients die due to metastases and not due to primary tumor formation, novel drugs are needed to overcome these shortcomings. In this study, we identified the anticancer phytochemical Rocaglamide (Roc-A) to be an inhibitor of cancer cell migration, a crucial event in metastasis formation. We show that Roc-A inhibits cellular migration and invasion independently of its anti-proliferative and cytotoxic effects in different types of human cancer cells. Mechanistically, Roc-A treatment induces F-actin-based morphological changes in membrane protrusions. Further investigation of the molecular mechanisms revealed that Roc-A inhibits the activities of the small GTPases RhoA, Rac1 and Cdc42, the master regulators of cellular migration. Taken together, our results provide evidence that Roc-A may be a lead candidate for a new class of anticancer drugs that inhibit metastasis formation.

INTRODUCTION

Many chemotherapeutics currently used in anti-cancer treatment mainly act by cytotoxicity. Although, chemotherapy frequently leads to shrinkage in primary tumor volume, several studies have shown that it may also induce or accelerate metastasis formation [1, 2]. One strategy to overcome this shortcoming is to develop small molecule drugs with antimetastatic activity in addition to the cytotoxicity towards cancer cells.

Cancer cell migration is a crucial process in metastasis formation. The first step in cellular migration is polarization of the cell. A leading and trailing edge form in response to an external gradient of signal molecules. In a second step the cell body at the leading edge protrudes and subsequently attaches to the underlying substratum. Eventually, the trailing edge detaches from the substratum and is pulled forward. The migration of the cell and the

development of cellular protrusions are largely driven by the reorganization of the actin cytoskeleton [3]. Whereas actin polymerizes at the leading edge of the cell into F-actin, bundled F-actin fibers at the rear of the cell depolymerize. The forming actin meshwork at the leading edge of the cell is the driving force for membrane protrusions, such as the flat and elongated lamellipodia, which play a crucial part in directed cellular migration [4]. Among the main regulators of actin reorganization are the Rho GTPases RhoA, Rac1 and Cdc42 [5, 6]. Rho GTPases shuttle between a GTP-bound active and a GDP-bound inactive form. Loss-of function of any of these molecules has been described to largely inhibit the migratory behavior of cells [7].

The phytochemical Rocaglamide-A (Roc-A) belongs to the chemical class of cyclopenta[b]-tetrahydrobenzofurans, collectively referred to as flavaglines or rocaglamides [8, 9]. *In vivo* and *in vitro*

studies have shown that flavaglines/rocaglamides are new candidate drugs for the treatment of cancer [10-14]. So far, the anti-tumor activities of these compounds have been documented to be largely due to inhibition of the eukaryotic translation initiation resulting in blockage of protein translation [12, 15-17]. In addition, a screen involving over 300,000 chemical compounds showed that Roc-A is also a potent inhibitor of HSF1 activation which is involved in cancer glucose uptake [13]. However, whether flavaglines could affect cancer cell migration and metastasis formation has not been thoroughly studied. In this study, we show that Roc-A inhibits cellular migration independent of its anti-proliferative and cytotoxic effects. We show that Roc-A treatment leads to major morphological changes in the organization of F-actin-based protrusions, such as lamellipodia. By applying Förster resonance energy transfer (FRET)-microscopy we revealed that Roc-A reduces the activity of Rho GTPases RhoA, Rac1 and Cdc42. Taken together, our study suggests that Roc-A may be a promising candidate compound for preventing metastasis.

RESULTS

Roc-A inhibits cellular migration independent of its cytotoxic and anti-proliferative effects

We and others have previously shown that Roc-A and its derivatives exert their anticancer effects by inducing apoptosis as well as proliferation arrest (for review see [8]). Along with the study of the anti-proliferative effect of Roc-A [10], we have also observed marked changes in cellular morphology in the prostate cancer cell line PC-3. Under Roc-A treatment, PC-3 cells were less elongated and frequently increased in diameter. To further investigate the influence of Roc-A in cellular morphology, we cultured PC-3 cells in a gradient of FCS ranging from 0 to 10 % in the presence or absence (solvent DMSO) of Roc-A. To exclude the possibility that the observed changes in cellular morphology were due to inhibition of protein synthesis or induction of apoptosis we first examined which doses of Roc-A have no or little effect on translation and cell death. Using an *in vitro* protein synthesis assay, we determined that Roc-A at the concentrations below or equal to 30 nM has no substantial effect on translation inhibition in PC3 cells (Figure 1A). Significant inhibition of protein synthesis by Roc-A was observed at 100 nM and higher (Supplementary Figure S1A). Roc-A also has little effect on apoptosis induction at concentrations below 50 nM (Supplementary Figure S1B). Therefore, we carried out all assays with 15 or 30 nM of Roc-A in PC3 cells.

Consistent with our initial observations, PC3 cells were less elongated when treated with Roc-A (Figure 1B). In addition, Roc-A treatment decreased cell polarity by more than two-fold as determined by the number of

cells aligned along the FCS gradient (Figure 1B and 1C). Cell polarity is a crucial and first step in directed cellular migration. Therefore, we hypothesized that Roc-A treatment would prevent cellular migration. To test this hypothesis we first performed a wound-assay. In this assay, confluent cell layers are separated by a gap. Due to the lack of adjacent cells, cells migrate towards each other and close the gap over time. We observed that Roc-A treatment resulted in prevention of gap closure in a dose-dependent manner at concentrations of 15 – 30 nM in PC3 cells (Figure 1D and 1E). As Roc-A can block cellular proliferation by activation of the Chk1/2 signaling pathway [10], we treated PC-3 cells with the anti-proliferative drug Mitomycin C (MC) to exclude the possibility that delayed gap closure was due to inhibition of cellular proliferation. Although MC treatment (5 μg/ml for 1h) led to a stronger inhibition of proliferation than Roc-A treatment (Figure 1F) it did not inhibit gap closure (Figure 1D and 1E). Increased exposure to cells with MC for more than 1h caused a similar level of cell death as Roc-A (Supplementary Figure S1B and S1C). These experiments exclude that the Roc-A-mediated delay in gap closure was due to inhibition of cellular proliferation. In addition to its anti-proliferative effects, Roc-A is also known to be cytotoxic to various cancer cell lines and primary cancer cells by induction of apoptotic cell death. To rule out that the observed delay in gap closure was caused by Roc-A-induced cell death, cell viability was examined by AnxV and 7-AAD staining after treatment. The experiments showed that Roc-A decreased PC3 cell viability by only 5 % when used at 30 nM (Figure 1G). However, gap closure was inhibited by approximately 60% at the same concentration (Figure 1E). In addition, we used the pan-caspase inhibitor zVAD-fmk to block any occurring apoptosis in the assay. In the presence of zVAD-fmk, Roc-A-induced apoptosis was completely blocked (Figure 1G). However, inhibition of apoptosis did not significantly affect the gap closure (Figure 1D and 1E). Taken together, these experiments demonstrate that Roc-A can inhibit cell migration independent from its anti-proliferative and cytotoxic effects.

To investigate whether Roc-A can inhibit cell migration in general, we tested one normal (non-tumor) fibroblast cell line NIH-3T3 and four additional human cancer cell lines: transformed human embryonic kidney cell line 293T, breast cancer cell line MDA-MB-231, human colon cancer cell line HCT116, and human cervical cancer cell line HeLa. Consistent with the above results, Roc-A blocked gap closures in all cell lines tested in a dose-dependent manner (Figure 2A and 2B; Supplementary Figure S2 and S3). High doses of Roc-A can induce significant apoptotic cell death (Supplementary Figure S4). However, the concentrations of Roc-A used in the wound assays caused only 3-10% cell death (Supplementary Figure S4). In 293T and MDA-MB-231 cells, for instance, Roc-A inhibited gap closure

by approximately 70-80% (Figure 2A and 2B). While MC treatment had no effect on gap closure (Figure 2A and 2B), it inhibited cellular proliferation stronger (in 293T cells) or equipotent (in MDA-MB-231 cells) to Roc-A (Figure 2A-2C) and caused higher cell death (10-20%) than Roc-A (Supplementary Figure S5). Cell viability of 293T cells was not affected by Roc-A at concentrations of 15 - 30 nM (Figure 2D; Supplementary Figure S3).

In MDA-MB-231 cells, Roc-A treatment resulted in a decrease in cell viability of less than 5%, which could be blocked completely by zVAD-fmk (Figure 2D). Inhibition of apoptosis only marginally affected Roc-A-mediated inhibition of MDA-MB-231 cell migration (Figure 2B). Thus, the anti-migratory effect of Roc-A on PC-3 cells could be reproduced in other cell types suggesting that this effect is cell type-independent.
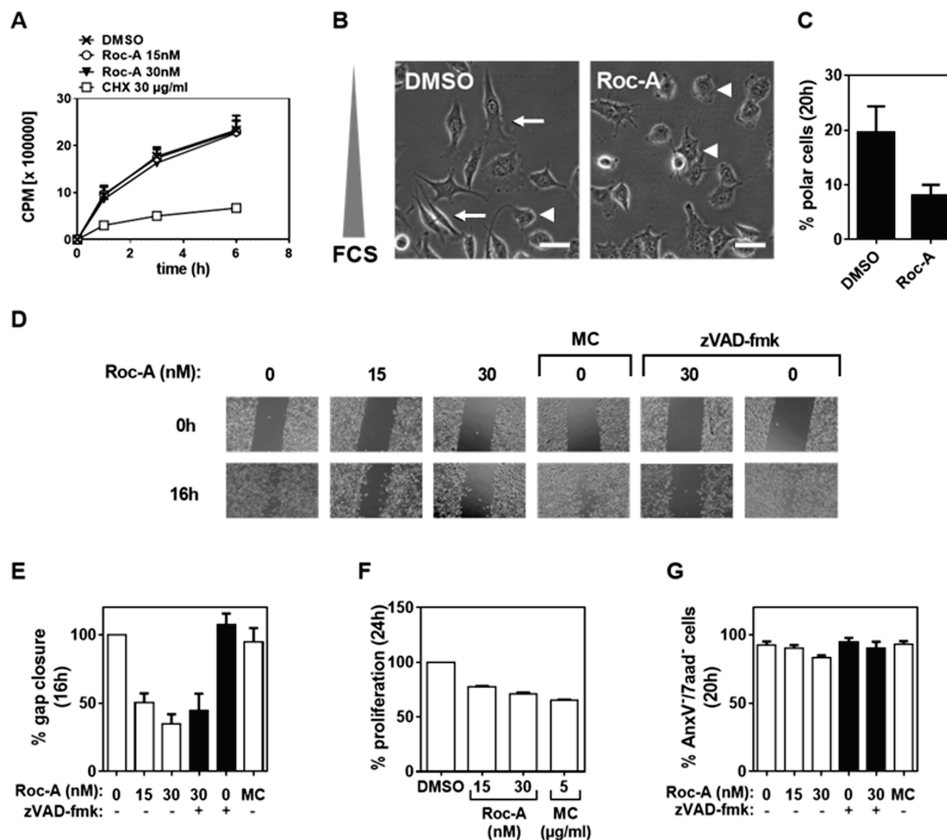
Figure 1: Roc-A inhibits PC-3 cell migration independent of its cytotoxic and anti-proliferative effects. A. Effect of Roc-A on protein translation. PC3 cells were treated with different doses of Roc-A as indicated. The activities of protein synthesis were monitored by incorporation of ^{35}S-methionine. **B**. Roc-A decreases cell polarity in PC-3 cells. PC-3 cells were exposed to a gradient of FCS (0-10%) in the presence of 15 nM Roc-A or solvent (DMSO) for 20 h. Examples of polarized (arrow) and unpolarized (arrowhead) cells are indicated. Scale bare = 50 μm. Representative images are shown. **C.** Quantification of B. At least 230 cells per treatment were analyzed. Results are an average of three independent experiments. Error bars (S.D.) are shown. **D.** Wound assay. A gap was created in confluent PC-3 cell monolayers and then cells were treated with different concentrations of Roc-A in the absence or presence of zVAD (25 μM for 20 min prior to treatment) for 16 h or treated with 5 μg/ml Mitomycin C (MC) for 1h as described in Material and Methods and then further cultured for 16 h. The gaps before (0 h) and after (16 h) treatment are shown. **E**. Quantification of the gap closure. The effects of different drugs on cell migration were quantified as percentage of gap closure. Results are an average of three independent experiments. Error bars (S.D.) are shown. **F.** Analysis of the effects of different drugs on proliferation. PC-3 cells were stained with CFSE as described in Materials and Methods and then seeded and treated as in C. The percentage of proliferative cells was determined and normalized to DMSO treatment. Results are an average of three independent experiments. Error bars (S.D.) are shown. **G.** Analysis of the effects of different drugs on cell viability. The percentage of viable cells was determined as AnxV-/7aad- cells 20 h after drug treatment. Results are an average of three independent experiments. Error bars (S.D.) are shown.

Roc-A inhibits cancer cell invasion and impairs directed cellular migration

In order to form metastasis cancer cells need to leave the primary tumor site *via* the blood stream or lymphatic system. To reach blood or lymphatic vessels, extracellular matrix (ECM) constituents have to be degraded in a process termed invasion [18]. Therefore, we asked whether Roc-A is able to block the invasive behavior of cancer cells. To investigate this question, we used a Boydon Chamber assay with matrigel as an ECM substituent. PC3 cells were seeded in FCS-free medium on top of matrigel-coated filters in the presence of 15 nM Roc-A or solvent (DMSO). A gradient of FCS and/or EGF was generated by adding 100 ng/ml of EGF and/or 5 % FCS (used as a chemoattractant) to the well below the

filter. The experiment showed that treatment of PC-3 cells with Roc-A for 24 h blocked FCS-attracted invasion to more than 70% (Figure 3A). Addition of EGF to FCS led to a twofold increase in cellular invasion, which could also be blocked by Roc-A (Figure 3A). These results indicate that Roc-A can inhibit cellular invasion.

Both, the wound (Figure 1D, 2A and 2B) assay and the invasion (Figure 3A) assay, however, measure cellular migration only indirectly. To directly analyze the effect of Roc-A on cellular migration we performed a live cell imaging experiment. In this experiment PC-3 cells were exposed to a gradient of FCS ranging from 0 to 10% and migration of individual cells were tracked over a time period of 20 h. In average, cells migrated towards the side of the chamber where FCS concentration was highest. In the presence of Roc-A, cellular migration was strongly
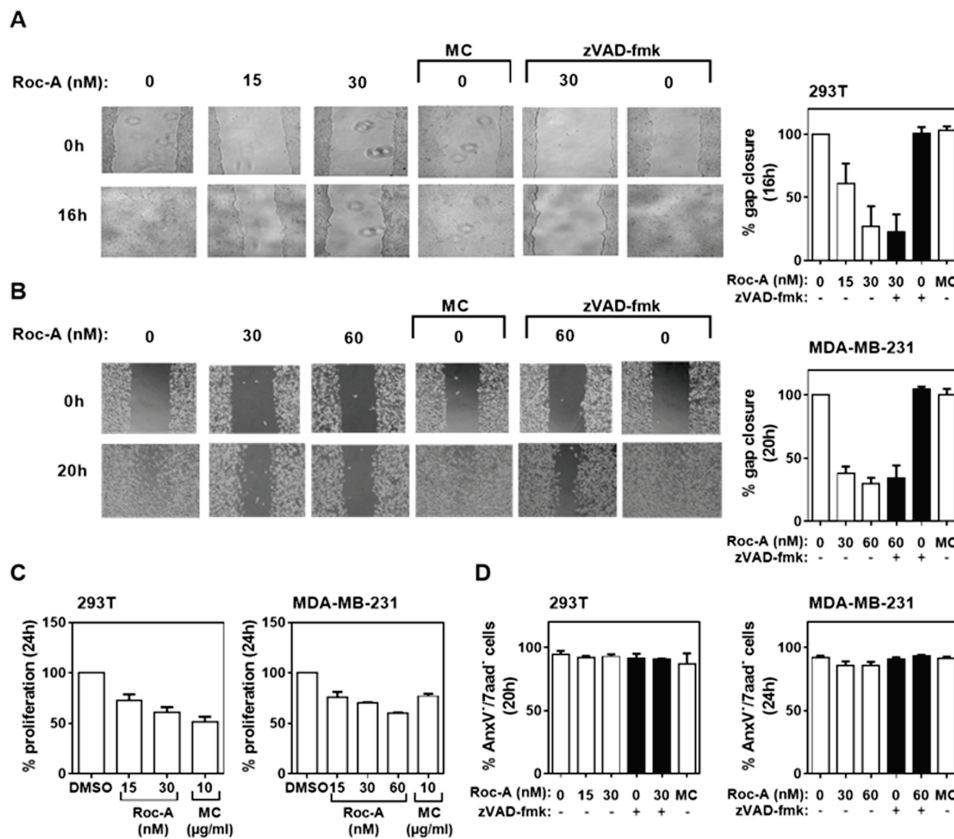
Figure 2: Roc-A inhibits migration of different types of cancer cells. A and **B.** Roc-A inhibits cell migration in 293T and MDA-MB-231 cells. 293T and MDA-MB-231 cells were subjected to treatment with different drugs and the percentage of gap closure was quantified as described in Figure 1C and 1D. Representative images are shown. **C.** Analysis of the effects of different drugs on proliferation in 293T and MDM-MB-231 cells. The percentage of proliferative cells was determined and normalized to DMSO treatment. Results are an average of three independent experiments. Error bars (S.D.) are shown. **D**. Analysis of the effects of different drugs on cell viability. The percentage of viable cells was determined as AnxV⁻/7aad⁻ cells 20 h (293T) and 24 h (MDA-MB-231) after drug treatment. Results are an average of three independent experiments. Error bars (S.D.) are shown.

inhibited (Figure 3B, upper panel). Notably, Roc-A impaired all parameters of cellular migration measured (Figure 3B, lower panel). The strongest impairment was seen for the center of mass and Euclidean distance (Figure 3B, lower panel). The former is a measure for average migration of the entire cell population in direction of FCS gradient and the latter describes the direct distance between the end and starting point of migration of each cell. In conclusion, this experiment indicates that directed migration is inhibited by Roc-A.

Roc-A alters the morphology of F-actin-based protrusions by an indirect effect on actin polymerization

One of the most crucial steps in cellular migration is reorganization of the actin cytoskeleton. During migration the monomeric form of actin polymerizes at the leading edge into a branched network of F-actin, while F-actin at the trailing edge is being degraded [19]. Due to the importance of actin reorganization in cellular migration, we further investigated the influence of Roc-A on actin reorganization. To do so, we performed confocal microscopy on F-actin stained cells. PC-3, 293T or MDA-MB-231 cells were treated for 24 h with Roc-A or solvent (DMSO) and cells were subsequently stained for F-actin (Alexa Fluor 488-Phalloidin) and nuclei (DAPI). The experiment showed that Roc-A induced marked changes in F-actin-rich protrusions (Figure 4A). In PC3 cells, while control (DMSO-treated) cells showed filopodia, Roc-A-treated cells largely lacked filopodia and showed increased membrane ruffling (Figure 4A, left panel). In 293T and MDA-MB-231 cells, Roc-A treatment caused a decrease in lamellipodia formation and rounding of cells (Figure 4A, middle and right panel). In summary, Roc-A treatment causes marked changes in cell morphology and F-actin-rich protrusions and the characteristics of these changes are different among different types of cancer cells.
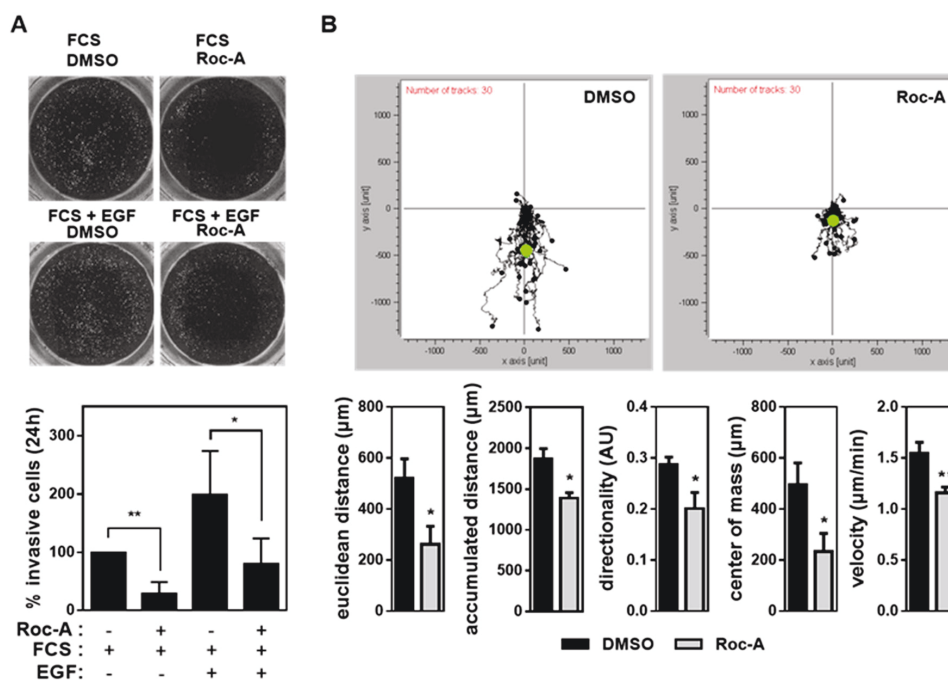
Figure 3: Roc-A inhibits cancer cell invasion and impairs directed cellular migration. A. Roc-A inhibits PC-3 cell invasion. PC-3 cells were seeded in FCS-free medium on matrigel-coated filters and treated with 15 nM Roc-A or solvent (DMSO). A gradient of FCS and/or EGF was applied by adding 100 ng/ml EGF and/or 5 % FCS to the well below the filter. The upper panel shows the representative image. The lower panel shows the number of invasive cells determined 24 h after treatment and normalized to DMSO-treated cells. Representative images of calcein-stained cells are shown. Results are an average of four independent experiments. Error bars (S.D.) are shown. Asterisks indicate statistical significance with * $p < 0.05$, **$p < 0.01$, calculated by unpaired Student's t-test with Welch's correction. **B**. Roc-A impairs directed cellular migration in PC-3 cells. PC-3 cells were exposed to a gradient of FCS (0-10%) and in parallel treated with 15 nM Roc-A or solvent (DMSO). The upper panel shows the movement of 30 cells per treatment tracked over a period of 24 h. Black dots show relative cell positions over 24 h and the green dot indicates the center of mass at the end of the observation period. The lower panel shows the parameters of cellular migration determined. Results are an average of three independent experiments. Error bars (S.D.) are shown. Asterisks indicate statistical significance with * $p < 0.05$, **$p < 0.01$, calculated by unpaired Student's t-test with Welch's correction.

To analyze whether the morphological changes in F-actin-based protrusions were caused by a direct effect of Roc-A on actin polymerization or depolymerization, we performed a cell-free *in vitro* polymerization or depolymerization assay. In the actin polymerization assay, pyrene-conjugated monomeric actin is polymerized, leading to an increase in fluorescence. The actin polymerization-inducer Jasplakinolide was used as a positive control. While Jasplakinolide accelerated the rate of actin polymerization, Roc-A treatment did not differ from the control treatment (Figure 4B). To further analyze whether Roc-A could influence the stability of preformed F-actin filaments directly, we performed a cell-free *in vitro* depolymerization assay. While the known F-actin stabilizing agent Phalloidin strongly delayed F-actin depolymerization, Roc-A did not alter the rate of

depolymerizaton (Figure 4C). These results suggest that Roc-A has no direct effect on F-actin stability, neither on actin polymerization nor on actin depolymerization of F-actin filaments.

Roc-A inhibits the activity of the Rho GTPases RhoA, Rac1 and Cdc42

As Roc-A did not influence F-actin polymerization directly (Figure 4B and 4C), we asked whether Roc-A affects activities of the upstream regulators of actin remodeling. The Rho GTPases RhoA, Rac1 and Cdc42 have been shown to be the main upstream regulators of actin remodeling [5, 6]. Therefore, we further investigated the role of Roc-A in regulation of the activities of Rho GTPases by transfection of 293T cells with Förster
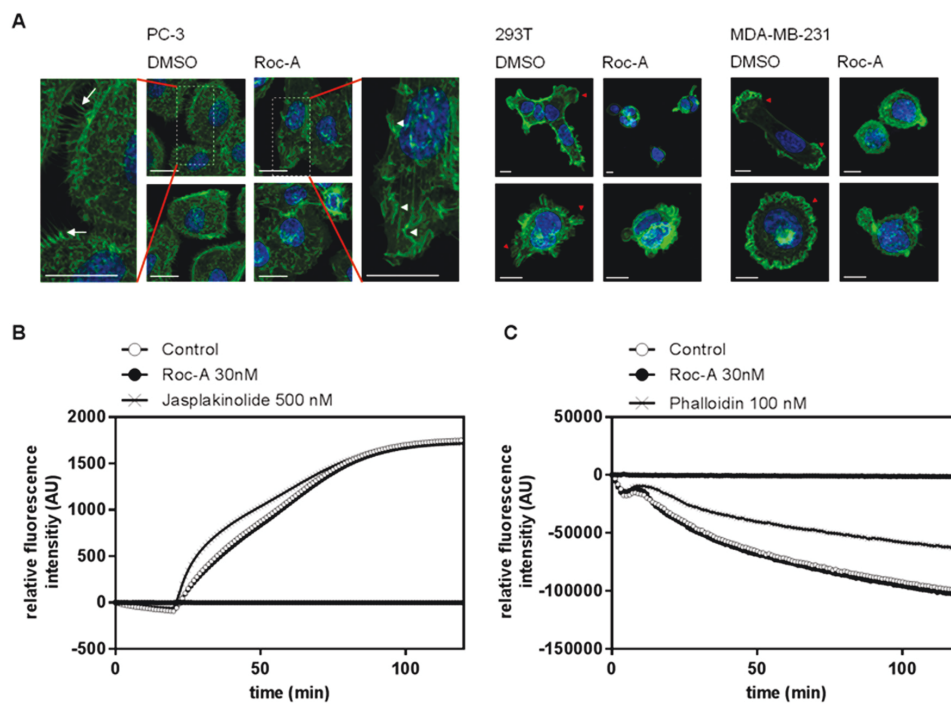
Figure 4: Roc-A alters the morphology of F-actin-based protrusions by an indirect effect on actin polymerization. A. Roc-A alters the morphology of F-actin-based protrusions. PC-3, MDA-MB-231 and 293T cells were treated with Roc-A (15 nM for PC3, 60 nM for MDA-MB-231 and 30 nM for 293T) or solvent (DMSO) for 24h followed by staining of F-actin (green) and nuclei (blue). Three independent experiments were carried out per cell line. Representative images (Z-stacks) per cell line are shown. Scale bar = 20 μm (PC-3) or 10 μm (293T and MDA-MB-231). **B.** Roc-A does not directly affect actin polymerization. The influence of Roc-A on polymerization of pyrene-conjugated actin monomers was monitored by measuring the increase in fluorescence that occurs upon polymerization of pyrene-conjugated actin. Roc-A, solvent control or the known actin polymerization promoting agent Jasplakinolide were added to pyrene-conjugated actin monomers and 20 min later actin polymerization was initiated. Results are representative of three independent experiments. **C.** Roc-A does not directly affect actin depolymerization. The influence of Roc-A on depolymerization of pyrene-conjugated actin monomers was monitored by measuring the decrease in fluorescence that occurs upon depolymeization of pyrene-conjugated actin. Roc-A, solvent control or the known F-actin stabilizer phalloidin were added to polymerized pyrene-conjugated actin for 20 min, after which depolymerization of actin was initiated. Results are representative of three independent experiments.

Resonance Energy Transfer (FRET)-based Rho GTPase sensors for RhoA, Rac1 or Cdc42 [20-22]. The transfected cells were treated with Roc-A or solvent DMSO as control. A decrease in Rho GTPase activity would result in reduction in FRET efficiency which can be monitored by fluorescence microscopy. We also cotransfected FRET-Rho GTPase sensors with excess RhoGDI, a physiologic regulator of Rho GTPase activity that is known to bind and stabilize Rho GTPases in their inactive state [20-23]. We thus created a situation with maximal physiological inhibition of the Rho GTPase activity and comparability between the three Rho GTPases used. As shown in Figure 5A and 5B, Roc-A inhibited the activity of RhoA, Rac1 and Cdc42 by approximately 15 to 22 %, with the strongest effect towards Cdc42 and RhoA. Similar results (approximately 15 to 31% inhibition) were also observed when the experiments were carried out in HeLa cells (Figure 5C). Thus, Roc-A can inhibit the activities of RhoA, Rac1 and Cdc42. To investigate whether the reduced Rho GTPase activity is due to reduction in protein expression, we examined the protein levels in PC3, MDA-MB-231 and 293T cells after Roc-A treatment for 24 h by immunoblot. The analysis showed that Roc-A treatment did not affect the expression levels of the Rho GTPases

(Supplementary Figure S6). This is in line with the fact that the concentrations of Roc-A used in this study had little effects on protein translation (Figure 1A and Supplementary Figure S1A).

Since the activity of Rho GTPases is positively regulated by guanine nucleotide exchange factors (GEFs) and negatively regulated by GTPase activating proteins (GAPs) [24, 25], we asked whether Roc-A could directly interfere with GEF-mediated activation or GAP-mediated inactivation of Rho proteins. To answer this question, we performed an *in vitro* GEF/GAP activity assay based on fluorescent mant-GDP/tamra-GTP bound Rho GTPases [26]. Roc-A was shown to neither affect the activation of Rho GTPases madiated by specific GEFs (LARG, Vav2 and ITSN; Figure 6A) nor the inactivation of Rho GTPases mediated by p50GAP (Figure 6B). These results clearly ruled out the possibility that Roc-A directly interferes with the activity of GEFs or GAPs in general.

Besides GAPs and GEFs, Rho GTPase activity can also be regulated by Rho-specific guanine nucleotide dissociation inhibitor (GDI). GDI binding to Rho GTPases blocks their activity and prevents them from translocating to the plasma membrane [20-22, 27]. To address this possibility, we performed a GDI knockdown
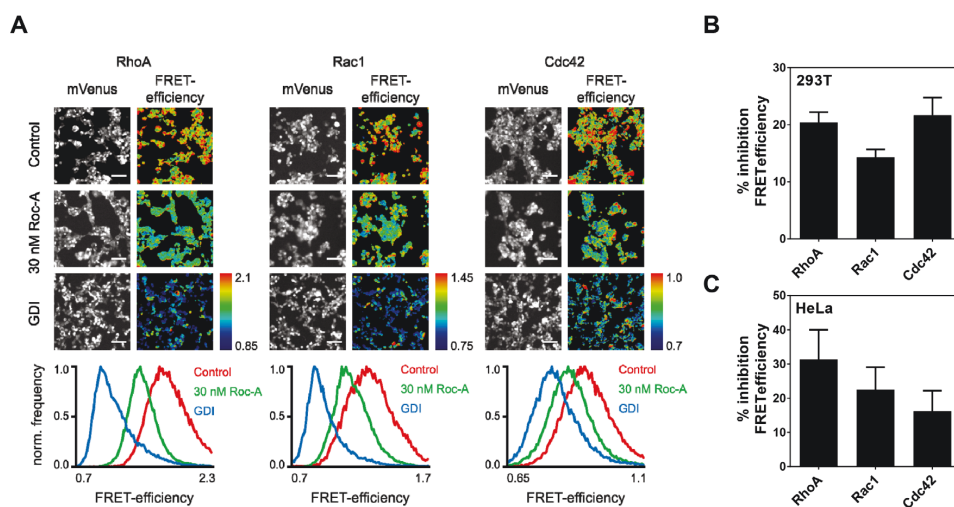
Figure 5: Roc-A inhibits the activity of the Rho GTPases RhoA, Rac1 and Cdc42. A. Roc-A inhibits the activity of the Rho GTPases RhoA, Rac1 and Cdc42. RhoA, Rac1 or Cdc42 FRET sensors were overexpressed in 293T cells either with a control plasmid (Control, 30 nM Roc-A) or together with GDI. Cells were treated with 30 nM Roc-A or vehicle (DMSO for Control and GDI) for 24h. Representative fluorescence micrographs show mVenus channel of 293T cells expressing the indicated FRET sensors. Scale bars: 100 μm. Pseudocolored FRET efficiency images of the same field of view were calculated as a ratio of FRET acceptor over FRET donor emission intensity reflecting the GTPase activity levels. The histograms show the pixel distribution of the FRET efficiency within the FRET emission ratio images. **B.** Quantification of A. FRET efficiency was normalized to GDI and DMSO values and % inhibition FRET efficiency was calculated. Results are an average of six independent experiments. Error bars (S.E.M.) are shown. **C.** Roc-A inhibits the activity of the Rho GTPases RhoA, Rac1 and Cdc42 in HeLa cells. RhoA, Rac1 or Cdc42 FRET sensors were overexpressed in HeLa cells either with a control plasmid (Control, 30 nM Roc-A) or together with GDI. Cells were treated with 30 nM Roc-A or vehicle (DMSO for Control and GDI) for 24h. FRET efficiency was normalized to GDI and DMSO values and % inhibition FRET efficiency was calculated. Results are an average of three independent experiments. Error bars (S.E.M.) are shown.

experiment. Cells were stably transfected with shRNAs directed against GDI or control. The sequence of shRNA was designed to target an untranslated region of GDI to only interfere with the endogenous GDI expression. The experiment showed that knockdown of GDI did not affect the inhibitory effect of Roc-A on the activity of RhoA (Supplementary Figure S7). Thus, this experiment also ruled out that Roc-A might inhibit Rho GTPase activity through stabilizing the binding of GDI to Rho GTPases.

Whereas RhoA is mainly found in the cytoplasm, Rac1 has been described to be additionally localized at the plasma membrane and Cdc42 only minimally localizes to the plasma membrane [28]. Certain molecules have been described to influence the localization of Rho GTPases [29, 30]. To analyze whether Roc-A may influence the intracellular localization of Cdc42, Rac1 or RhoA, we coexpressed the respective RhoGTPaes together with the plasma membrane marker tH and examined their membrane localization by confocal microscopy. As described in the literature, RhoA was mainly expressed in the cytoplasm, whereas Rac-1 was also localized at

the plasma membrane overlapping with tH expression (Supplementary Figure S8). Cdc42 was only partially found at the plasma membrane with clearly dominant cytoplasmic localization. We could not observe any changes in the intracellular localization of all three Rho GTPases upon Roc-A treatment, ruling out that Roc-A interferes with the intracellular localization of Rho GTPases.

In an attempt to find putative upstream pathways with which Roc-A might interfere to attenuate Rho GTPase activity, we looked for known intracellular interaction partners of Roc-A. Recently, we have identified prohibitin (PHB) as the direct target of rocaglamides [16]. Binding of rocaglamides to PHB prevents interaction between PHB and CRaf and, consequently, inhibits CRaf activation and CRaf-MEK-ERK signalling. This action leads to inhibition of protein synthesis [16]. Therefore, we examined the ERK activity at 15 nM Roc-A treatment. Consistent with the translation data (Figure 1A), Roc-A had no influence on ERK activity at the concentration of 15 nM (Supplementary Figure S9A). To further investigate
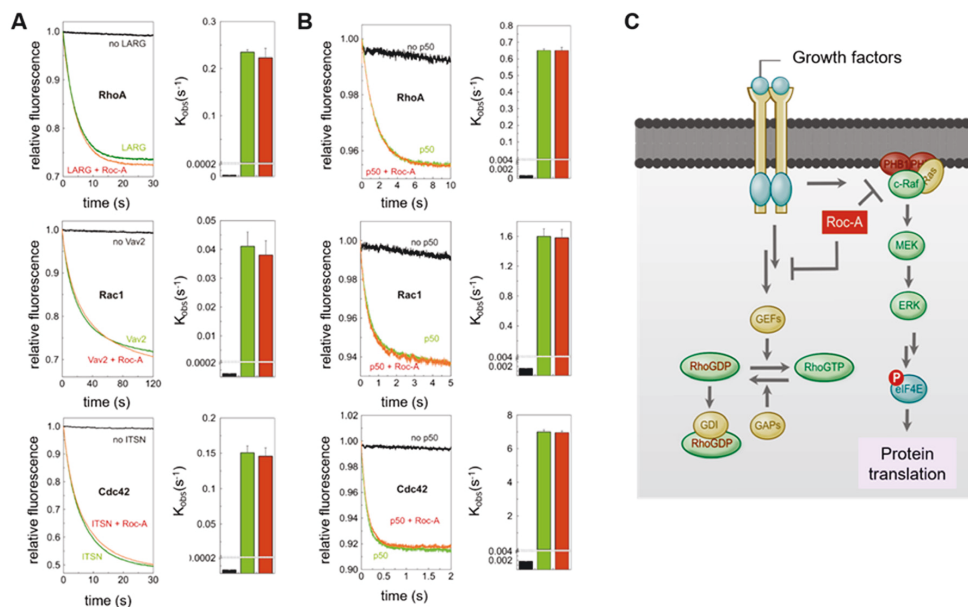
Figure 6: Roc-A does not directly interfere with the activity of GEFs or GAPs. A. No significant effect of Roc-A on the GEF-accelerated nucleotide exchange of Rho proteins. Dissociation of fluorescent mant-GDP from Rho proteins (RhoA, Rac1 and Cdc42, respectively), accelerated by the RhoGEFs (LARG, Vav2 and ITSN, respectively), was monitored in the absence (green) and in the presence (red) of Roc-A (10 μM). The reactions without RhoGEFs are shown in black. In the right panel, observed rate constants (k_{obs}) of the respective measurements are illustrated. **B.** No significant effect of Roc-A on the GAP-accelerated GTP hydrolysis of Rho proteins. GTP hydrolysis of fluorescent tamra-GTP by Rac1 and Cdc42, respectively, and cy3-GTP by RhoA, stimulated by p50GAP, was monitored in the absence (green) and in the presence (red) of Roc-A (10 μM). The reactions in absence of GAP are shown in black. In the right panel, observed rate constants (k_{obs}) of the respective measurements are illustrated. All data shown in A and B are an average of four to five different experiments. **C.** Schematic representation of the mechanism by which Roc-A inhibits cellular migration. We hypothesize that Roc-A blocks a signal upstream of Rho-GTPases leading to down-regulation of Rho-GTPase activities and, consequently, inhibition of cellular migration.

whether the CRaf-MEK-ERK signalling pathway is necessary for Roc-A-mediated inhibition of cell migration, we carried out a siRNA approach to knockdown PHB expression. The experiment showed that knockdown of PHB in PC3 cells had no influence on the effect of Roc-A on inhibition of cell migration (Supplementary Figure S9B and S9C).

In summary, Roc-A inhibits the activation of Rho GTPases Cdc42, Rac1 and RhoA by an indirect effect and independent from the previously described target protein prohibitin.

DISCUSSION

Metastasis formation is the major cause of death in cancer patients [18]. So far, most cancer treatments are not efficient in fighting metastases because tumors often develop chemo-resistance during therapy [18]. Several studies even show that chemotherapy may enhance metastasis formation [1, 2]. For instance, cisplatin or paclitaxel treatment has been reported to enhance metastasis formation in an *in vivo* lung metastasis model [2]. This side effect highlights a demand for new anticancer drugs that can efficiently kill tumor cells and also inhibit metastasis formation at the same time. In this study, we show that Roc-A may be a promising candidate for such a drug.

To firmly confirm the role of Roc-A in inhibition of cellular migration of cancer cells, we performed three different assays: wound-assay (Figures 1 and 2), invasion assay (Figure 3A) and live cell imaging of cellular migration at very low concentrations (15 to 30 nM) of Roc-A which have no or only minor influence on viability of tumor cells (Figure 3B). All three assays showed a 50 – 80% inhibition of tumor cell migration/invasion after treatment with Roc-A. Roc-A is known to have several other anticancer properties such as inhibition of cell proliferation and induction of apoptosis [10, 15, 16, 31]. Thus, we carried out the assays in the presence of the anti-proliferative drug Mitomycin-C (MC) or the pan-caspase inhibitor zVAD to exclude the possibility that the observed effect of Roc-A on cellular migration was due to its anti-proliferative or cytotoxic activities. We show that Roc-A inhibits tumor cell migration independently of its anti-proliferative or cytotoxic effects by three evidences: First, the anti-proliferative drug MC did not influence cellular migration, although it inhibited proliferation to a similar or even a higher extent than Roc-A (Figures 1D and 2E); second, the concentrations of Roc-A used in cell migration assays caused only 5% or less apoptotic cell death (Figures 1G and 2D); and third, the pan-caspase inhibitor zVAD could not prevent Roc-A-mediated inhibition of gap closure (Figure 1D, 1E and 2A, 2B, 2D). We found that Roc-A can also inhibit migration of non-tumor cells tested on the normal fibroblast NIH-3T3 cells. However, it is not uncommon that anti-metastatic

drugs can also block the migration of non-malignant cells. For instance, anti-metastatic Axl-kinase inhibitors are already in clinical trials [32], despite the fact that Axl-deficient primary fibroblasts show reduced migration [33]. In comparison to the more severe side effects observed for most chemotherapeutics (anemia, neutropenia etc.), wound-healing impairment would not be graded as severe. In this regard, we and others have shown that Roc-A is less toxic to many primary non-malignant cells than most chemotherapeutics [8]. Additionally, Roc-A and its derivatives have been tested in several *in vivo* models. Thus far, no adverse toxicities caused by impaired wound healing could be observed. Nevertheless, future *in vivo* studies should particularly monitor for wound healing-related side effects.

Recently, an *in vivo* study with a mouse pancreatic cancer model showed that Roc-A treatment resulted in a significant increase in the lifespan of tumor-bearing mice [34]. In consistence with our study, the study also observed a reduction in tumor metastasis in the lung [34]. However, in that study the concentrations of Roc-A used are quite high and were shown to kill the tumor cells by approximately 50% already. Therefore, it cannot be excluded that the observed effect of Roc-A on metastasis may be largely due to death of cells or inhibition of cell proliferation. In our study, we convincingly demonstrate that Roc-A can inhibit cancer cell migration and invasion independently of its cytotoxic and anti-proliferative activities. Furthermore, our data also show that the inhibitory effect of Roc-A on tumor cell migration is not limited to a specific cancer-type. We have investigated the effect of Roc-A on three different types of cancers: PC-3 (prostate cancer), MDA-MB-231 (breast cancer) and 293T (transformed embryonic kidney). All three cancer types showed a similar response to Roc-A treatment. Thus, Roc-A may be applicable to a wide variety of tumor cells.

In this study, we also further investigated the molecular mechanism by which Roc-A inhibits cellular migration. We found that Roc-A inhibited the activity of all three Rho GTPases (Rac1, RhoA and Cdc42) by approximately 15 to 22% (Figure 5). Rac1, RhoA and Cdc42 are the major regulators of actin remodeling, with their interplay determining the orientation, direction and speed of cellular migration [6, 35]. It has been shown that an increase in only 30% activity of RhoA could cause an increase in cellular migration by approximately 80% [36]. Therefore, we assume that reduction of about 20% of the activities of all three Rho GTPases may lead to a significant reduction of cellular migration. However, we cannot exclude that Roc-A may alter other signaling pathways next to Rho GTPase inhibition that contribute to a reduction in cellular migration. In addition, numerous loss-of-function studies have shown that loss of either of the three Rho GTPases causes a dramatic decrease in cellular migration in many cell types [35]. Coinciding with the inhibition of Rho GTPases by Roc-A, we found that

Roc-A treatment induced marked changes in morphology of F-actin-rich protrusions (Figure 4A). Roc-A treatment inhibited formation of filopodia (Figure 4, left panel) and lamellipodia (Figure 4, middle and right panel). Inhibition of Rac1 in MDA-MB-231 cells was shown to result in failure of lamellipodia formation and, subsequently, in cellular migration [37]. Hence, Roc-A-mediated inhibition of Rho GTPases may be one of the molecular mechanisms by which Roc-A causes changes in F-actin-based protrusions (Figure 4) and inhibition of cellular migration (Figures 1-3; Supplementary Figure S2 and S3). Furthermore, reorganization of actin was shown to be necessary for cellular migration [38]. For instance, drugs, such as Cytochalasin D or Jasplinakolide that interfere with actin polymerization directly, strongly inhibit cancer cell migration [39, 40]. Thus, alteration of F-actin morphology by Roc-A is in line with its anti-migratory effect.

In an attempt to unravel the underlying mechanism behind the inhibitory effect of Roc-A on Rho GTPases, we could show that Roc-A did neither influence the expression level nor intracellular localization of Rho GTPases, nor did it interfere with direct binding of GEFs, GAPs or GDIs to Rho GTPases. Consequently, the effect of Roc-A on Rho GTPase activity most likely is being located more upstream in the signaling pathway (Figure 6C). As we could exclude that the inhibitory effect of Roc-A on Rho GTPase activity is mediated by prohibitin or protein translation, another yet undiscovered target of Roc-A must show responsible for the observed inhibitory effect.

So far, the main mechanisms by which Roc-A inhibits cancer cell proliferation have been shown to be due to inhibition of protein synthesis initiation [8] and induction of Cdc25A degradation by activation of the ATM/ATR check point pathway [10]. As shown in our study (Figures 1F and 2C), Roc-A substantially inhibited cell proliferation although the doses used had no or little effect on translation inhibition. Rho GTPases have been described to be involved in regulation of cell cycle progression. Several studies show that inhibition of Rho GTPase activity causes inhibition of cell proliferation [5, 41]. Thus, inhibition of Rho GTPase activity by Roc-A may explain the anti-proliferative effect observed at low concentrations of Roc-A.

Taken together, we show that Roc-A does not only exert cytotoxic and cytostatic effects on cancer cells, but also inhibits tumor cell migration most likely *via* inhibition of activities of Rho GTPases (Figure 6C). Our study strongly suggests that Roc-A may be a lead compound for a new class of chemotherapeutic drugs that kill tumor cells and prevent metastasis at the same time.

EXPERIMENTAL PROCEDURES

Cell culture and reagents

The non-tumor fibroblast cell line NIH-3T3, the human cell lines PC-3 (prostate cancer), MDA-MB-231 (breast cancer), the human colon cancer cell line HCT116, the human cervical cancer cell line HeLa, and 293T (transformed embryonic kidney) were cultured at 37°C with 5% CO_2 in RPMI-1640 medium (Sigma-Aldrich, Munich, Germany) supplemented with 10 % FCS (PC-3 and MDA-MB-231) or in DMEM medium (Sigma-Aldrich) supplemented with 10 % FCS (293T) until otherwise stated in the text. Roc-A (>98 % pure) (Enzo Life Sciences, Lörrach, Germany), Mitomycin-C (Gerbu Biotechnik, Heidelberg, Germany), zVAD-fmk (Bachem, Bubendorf, Switzerland), recombinant human EGF (BioVision, Milpitas, USA), Jasplakinolide (VWR international, Darmstadt, Germany) and Phalloidin (Biotrend, Köln, Germany) were used as indicated in the respective figure legends.

Wound assay

Cells were seeded in wound assay cell culture inserts (Ibidi, Munich, Germany) and cultivated until 100 % confluence was reached. Subsequently, inserts were removed and cell layers were washed with phosphate buffered saline (PBS), followed by addition of fresh medium containing either Mitomycin-C, solvent (DMSO) as control or Roc-A. After 1 h Mitomycin-C was washed out and fresh medium was added. ZVAD-fmk was added to indicated samples 20 min prior to adding solvent (DMSO) or Roc-A. Pictures of the gap between the two cell layers were taken directly after addition of drugs and at the end of the indicated incubation time. The change in cell-free surface over time was quantified by use of TScratch [42] and normalized to DMSO-treated control samples.

Determination of cell viability

Cells that were previously analyzed in wound assays, were detached by trypsinization and washed once with Annexin-V binding buffer (0.01 M Hepes, 2.5 mM $CaCl_2$, 0.14 M NaCl). Subsequently, cells were stained with 7-amino-actinomycin D (7-aad; Sigma-Aldrich) and Annexin-V–FITC antibody (Immunotools, Friesoythe, Germany) at 4°C for 30 min, followed by a wash step and quantification of Annexin-V/7-aad double-negative cells by flow cytometry.

Determination of cell proliferation

Cells were labeled with carboxyfluorescein succinimidyl ester (CFSE; Molecular Probes/Thermo Fisher Scientific, Waltham, USA) by incubation of 2 x 10^6 cells with CFSE (2.5 μM) for 10 min at 37°C in the dark. Incorporation was stopped by addition of ice-cold FCS (10% in PBS). Subsequently, cells were washed three times and were employed in wound assays. 24 h after drug treatment, the amount of incorporated CFSE was quantified by flow cytometry. Proliferation data was normalized to DMSO-treated samples.

Invasion assay

Invasion assays were carried out according to the manufacturer´s instructions. Briefly, 8.5 x 10^{4} cells were plated on top of each rehydrated culture insert (BD BioCoat™ Matrigel™ Invasion Chamber; BD Biosciences, Heidelberg, Germany) in FCS-free medium. Following an incubation time of 24 h, remaining cells in the upper compartment were removed and cells that had migrated through Matrigel™ were stained with Calcein (4 μM; Sigma-Aldrich), followed by quantification as previously described [43].

Chemotaxis assay

For 2D chemotaxis assays "μ-Slide Chemotaxis"-chambers (Ibidi, Munich, Germany) were used. Chemotaxis assays were carried out according to the manufacturer´s instructions. Cells that divided or died during the observation period were excluded from analysis. Images were taken every 5 min for an observation period of 20 h. ImageJ [44] was used for tracking of cells and Chemotaxis and Migration Tool (Ibidi, Munich, Germany) was used for evaluating tracked cell data.

Confocal microscopy

0.4 x 10^{4} – 0.4 x 10^{5} cells were seeded in each well of a 8-well chamber glass slide (VWR International, Darmstadt, Germany), followed by starvation of cells for 24h in FCS-free medium. In parallel, cells were treated as indicated in the figure legends after which 10 % FCS (in medium) was added for 30 min to stimulate growth factor signaling. Subsequently, cells were washed with PBS twice, fixed with formaldehyde (3%, 15 min), washed three times again with PBS and permeabilized with Triton-X 100 (0.2 %, 10 min). Three PBS wash steps were followed by staining actin with acti-stain 488 phalloidin (Tebu, Offenbach, Germany) for 30 min at room temperature. DAPI mounting medium (Dianova, Hamburg, Germany) was used to stain nuclei.

Actin (De)polymerization assay

Actin (De)Polymerization Assays were carried out according to manufacturer´s instructions using Actin Polymerization Biochem Kit (Cytoskeleton Inc, Denver, USA). Fluorescence was measured for a total time of 120 min with 60 sec intervals. Baseline fluorescence values were established by measurement of unpolymerized pyrene actin or polymerized pyrene actin, respectively, for 5 min, after which drugs or solvent were added. For actin polymerization experiments, actin polymerization was initiated by addition of 10 x Actin Polymerization Buffer (500 mM KCl, 20 mM MgCl2, 10 mM ATP) 20 min after drugs were added.

Rho GTPase activity measurement – FRET imaging

To study the effect of Roc-A on Rho GTPase activity, 293T cells were transiently transfected with RhoA, Rac1 and Cdc42 FRET sensors [20-22, 45] for 40 h. Each Rho GTPase used in these measurements is labeled with a donor and an acceptor fluorophore. Upon activation of the Rho GTPase, the donor and acceptor fluorophores get into close proximity causing an increase in FRET efficiency. Imaging was performed on an inverted microscope (IX81, Olympus) equipped with a xenon arc burner epifluorescence illumination system (MT20, Olympus), a fluorescence emission filter wheel (Olympus) and an EM-CCD camera (ImagEM, Hamamatsu). Images were taken with a 10x/NA 0.4 Super Apochromat air objective (Olympus) enabling the simultaneous analysis of multiple cells. FRET images were taken with the following settings (excitation, dichroic mirror, emission): FRET-donor 430/25, zt442RDC, 483/32; FRET-acceptor 430/25, zt442RDC, 542/27. Images were analyzed using Image J software. Images were background corrected and regions of interest were defined by FRET-sensor Venus intensity. Average intensities of FRET-acceptor channel were divided by FRET-donor channel to calculate FRET efficiency. To study the effect of Roc-A on Rho GTPase activity in HeLa cells, 1.25 x 10^{4} cells were seeded into each well of a 96 well plate (μ-plate, ibidi). The next day, cells were transiently transfected with FRET sensors for RhoA, Rac1 and Cdc42, together with a control plasmid or GDI for 24h. Cells were then treated with 30 nM Roc-A or vehicle (DMSO for Control and GDI) for 24h. Images were taken using a 20x/NA 0.75 UV Apochromat objective (Olympus). FRET ratio was normalized to the DMSO control.

Translation assay

The rate of protein synthesis was determined by measuring the amount of incorporated ^{35}S-methionine. Briefly, cells were incubated for 3 h in methionine-free medium, followed by addition of 7 μCi of ^{35}S-methionine-labeling mix (PerkinElmer, Waltham, MA, USA) per well. An incubation of indicated times was followed by washing with PBS and lysis in ice-cold lysis buffer for 15 min on ice. After clearing of cell lysates 50 μl of each lysate was incubated in 1 ml of Liquid Scintillation Cocktail solution (Beckman coulter, Brea, CA, USA) and radioactivity was determined by Liquid Scintillation counting.

siRNA knockdown experiment

PC-3 cells were transiently transfected with siRNA directed against PHB (FlexiTube siRNA Hs_PHB_6 [Qiagen, Hilden, Germany]) by use of Lipofectamine 2000 according to the manufacturer´s instructions. Transfections

were performed in Opti-MEM-GlutaMAX Medium (Thermo Fisher, Waltham, MA, USA).

GEF and GAP activity measurements

Human RhoA (aa 1-181), Rac1 (aa 1-184), Cdc42 (aa 1-178), the catalytic DH-PH tandem domain of Vav2 (aa 168–543), ITSN (aa 1229–1580), LARG (aa 766–1138) and GAP domain of p50 (aa 198-439) were produced as glutathione S-transferase (GST) fusion proteins in *Escherichia coli* as described previously [26]. Rho protein preparation, including nucleotide-free and fluorescent methylanthraniloyl (mant) GDP/GTP-bound Rho proteins, were prepared as described before [46]. For kinetic measurement, Fluorescence measurements were performed at 25°C in a buffer, containing 30 mM Tris/HCl, pH 7.5, 10 mM K_2HPO_4/KH_2PO_4, pH 7.5, 5 mM $MgCl_2$, and 3 mM dithiothreitol. Changes in fluorescent intensity were monitored in real-time using a stopped-flow instrument (HiTech Scientific SF-61) with a mercury xenon light source and TgK Scientific Kinetic Studio software. For measurement of GEF activity, the dissociation of mant-GDP from Rho proteins (0.2 μM) in the absence and presence of the DH-PH domain (2 μM) of the respective GEFs and excess amounts of GDP (20 μM) was monitored (in absence and presence of Roc-A) [47]. An excitation wavelength of 366 nm was used and emission was detected using a cutoff filter of 408 nm. For measurement of GAP activity, fluorescent GTP-bound Rho proteins (pre-mixing 0.3 μM nucleotide-free Rho and 0.2 μM tamra-/cy3-GTP) and the catalytic domain of p50GAP (2 μM) were rapidly mixed by stopped-flow spectrophotometer (in absence and presence of Roc-A) [48]. Excitation wavelengths of 546 nm and 550 nm were used for tamra and cy3 fluorophores, respectively, and a 570 nm (tamra and cy3) cut-off-filter (Schott glass) was used to collect emitted light. The observed rate constants were calculated by fitting the data as single exponential decay using the GraFit program (Erithacus software).

Localization of Rho GTPases after RocA treatment

1.25 x 10^4 cells (HeLa) were seeded on each well of an 8 well slide (μ-slide, ibidi). The next day, cells were transiently transfected with mCitrine-RhoA, mCitrine-Rac1 or mCitrine-Cdc42 each together with mCerulean-tH which comprises only the C-terminal 10 amino acids of HRas and, thus, served as a plasma membrane marker [49, 50]. Cells were treated with 30 nM Roc-A or vehicle (DMSO for Control and GDI) for 24h. Images were taken using a SP8 inverted confocal microscope equipped with a HC PL APO 63x/NA 1.3 glycerol objective. Representative images (Z-slices) are shown.

GDI-knockdown by shRNA lentiviral vector

To generate cell lines with stable RNAi knockdown of GDI, lentiviral shRNA-mediated stable gene silencing cells was done in 293T as described [51]. CGTCTAACCATGATGCCTTAA was used as targeting sequence in the shRNA and the 1.9 kb stuffer sequence as control. 5.5 x 10^4 cells of each cell line were seeded on each well of a 96 well plate (μ-plate, ibidi). The next day, cells were transiently transfected with FRET sensors for RhoA, Rac1 and Cdc42, together with a control plasmid or GDI for 24h. Cells were then treated with 30 nM Roc-A or vehicle (DMSO for Control and GDI) for 24h. FRET ratio was normalized to DMSO control. Results are an average of four experiments.

ACKNOWLEDGMENTS

CONFLICTS OF INTEREST

The authors declare no conflicts of interest.

REFERENCES

1. Park SI, Liao J, Berry JE, Li X, Koh AJ, Michalski ME, Eber MR, Soki FN, Sadler D, Sud S, Tisdelle S, Daignault SD, Nemeth J a, et al., Cyclophosphamide creates a receptive microenvironment for prostate cancer skeletal metastasis. Cancer Res. 2012; 72: 2522–32.

2. Daenen LGM, Roodhart JML, van Amersfoort M, Dehnad M, Roessingh W, Ulfman LH, Derksen PWB, Voest EE, Chemotherapy enhances metastasis formation via VEGFR-1-expressing endothelial cells. Cancer Res. 2011; 71: 6976–85.

3. Gardel ML, Schneider IC, Aratyn-Schaus Y, Waterman CM, Mechanical integration of actin and adhesion dynamics in cell migration. Annu. Rev. Cell Dev. Biol. 2010; 26: 315–33.

4. Yamaguchi H, Condeelis J, Regulation of the actin cytoskeleton in cancer cell migration and invasion. Biochim. Biophys. Acta - Mol. Cell Res. 2007; 1773: 642–52.

5. Vega FM, Ridley AJ, Rho GTPases in cancer cell biology. FEBS Lett. 2008; 582: 2093–101.

6. Ridley a J, Rho GTPases and cell migration. J. Cell Sci. 2001; 114: 2713–22.

7. Ridley A, Rho GTPase signalling in cell migration. Curr. Opin. Cell Biol. 2015; 36: 103–12.

8. Li-Weber M, Molecular mechanisms and anti-cancer aspects of the medicinal phytochemicals rocaglamides (=flavaglines). Int. J. Cancer. 2015; 137: 1791–9.

9. Ebada SS, Lajkiewicz N, Porco JA, Li-Weber M, Proksch P, Chemistry and biology of rocaglamides (= flavaglines) and related derivatives from aglaia species (meliaceae). Prog. Chem. Org. Nat. Prod. 2011; 94: 1–58.

10. Neumann J, Boerries M, Köhler R, Giaisi M, Krammer PH, Busch H, Li-Weber M, The natural anticancer compound rocaglamide selectively inhibits the G1-S-phase transition in cancer cells through the ATM/ATR-mediated Chk1/2 cell cycle checkpoints. Int. J. Cancer. 2014; 134: 1991–2002.

11. Becker MS, Schmezer P, Breuer R, Haas SF, Essers MA, Krammer PH, The traditional Chinese medical compound Rocaglamide protects nonmalignant primary cells from DNA damage-induced toxicity by inhibition of p53 expression. Cell Death Dis. 2014; 5: e1000.

12. Cencic R, Carrier M, Galicia-Vázquez G, Bordeleau M-E, Sukarieh R, Bourdeau A, Brem B, Teodoro JG, Greger H, Tremblay ML, Porco JA, Pelletier J, Antitumor activity and mechanism of action of the cyclopenta[b]benzofuran, silvestrol. PLoS One. 2009; 4: e5223.

13. Santagata S, Mendillo ML, Tang Y, Subramanian A, Perley CC, Roche SP, Wong B, Narayan R, Kwon H, Koeva M, Amon A, Golub TR, Porco J a, et al., Tight coordination of protein translation and HSF1 activation supports the anabolic malignant state. Science. 2013; 341: 1238303.

14. Boussemart L, Malka-Mahieu H, Girault I, Allard D, Hemmingsson O, Tomasic G, Thomas M, Basmadjian C, Ribeiro N, Thuaud F, Mateus C, Routier E, Kamsu-Kom N, et al., eIF4F is a nexus of resistance to anti-BRAF and anti-MEK cancer therapies. Nature. 2014; 513: 105–9.

15. Sadlish H, Galicia-Vazquez G, Paris CG, Aust T, Bhullar B, Chang L, Helliwell SB, Hoepfner D, Knapp B, Riedl R, Roggo S, Schuierer S, Studer C, et al., Evidence for a Functionally Relevant Rocaglamide Binding Site on the eIF4A-RNA Complex. ACS Chem. Biol. 2013; 8: 1519–27.

16. Polier G, Neumann J, Thuaud F, Ribeiro N, Gelhaus C, Schmidt H, Giaisi M, Köhler R, Müller WW, Proksch P, Leippe M, Janssen O, Désaubry L, et al., The natural anticancer compounds rocaglamides inhibit the Raf-MEK-ERK pathway by targeting prohibitin 1 and 2. Chem. Biol. 2012; 19: 1093–104.

17. Bordeleau M, Robert F, Gerard B, Lindqvist L, Chen SMH, Wendel H, Brem B, Greger H, Lowe SW, Jr JAP, Pelletier J, Therapeutic suppression of translation initiation modulates chemosensitivity in a mouse lymphoma model. Cancer. 2008; 118: 1–10.

18. Valastyan S, Weinberg RA, Review Tumor Metastasis : Molecular Insights and Evolving Paradigms. Cell. 2011; 147: 275–92.

19. Wehrle-Haller B, Imhof B a, Actin, microtubules and focal adhesion dynamics during cell migration. Int. J. Biochem. Cell Biol. 2003; 35: 39–50.

20. Fritz RD, Letzelter M, Reimann A, Martin K, Fusco L, Ritsma L, Ponsioen B, Fluri E, Schulte-Merker S, van Rheenen J, Pertz O, A Versatile Toolkit to Produce Sensitive FRET Biosensors to Visualize Signaling in Time and Space. Sci. Signal. 2013; 6: rs12.

21. Hanna S, Miskolci V, Cox D, Hodgson L, A New Genetically Encoded Single-Chain Biosensor for Cdc42 Based on FRET, Useful for Live-Cell Imaging. PLoS One. 2014; 9: e96469.

22. Moshfegh Y, Bravo-Cordero JJ, Miskolci V, Condeelis J, Hodgson L, A Trio-Rac1-Pak1 signalling axis drives invadopodia disassembly. Nat. Cell Biol. 2014; 16: 571–85.

23. Pertz O, Hodgson L, Klemke R, Hahn K, Spatiotemporal dynamics of RhoA activity in migrating cells. Nature. 2006; 440: 1069–72.

24. Vigil D, Cherfils J, Rossman KL, Der CJ, Ras superfamily GEFs and GAPs: validated and tractable targets for cancer therapy? Nat. Rev. Cancer. 2010; 10: 842–57.

25. Dvorsky R, Ahmadian MR, Always look on the bright site of Rho: structural implications for a conserved intermolecular interface. EMBO Rep. 2004; 5: 1130–6.

26. Eberth A, Ahmadian MR, In vitro GEF and GAP assays. Curr. Protoc. Cell Biol. 2009; Chapter 14: Unit 14.9.

27. Pertz O, Spatio-temporal Rho GTPase signaling - where are we now? J. Cell Sci. 2010; 123: 1841–50.

28. Michaelson D, Silletti J, Murphy G, D'Eustachio P, Rush M, Philips MR, Differential localization of Rho GTPases in live cells: regulation by hypervariable regions and RhoGDI binding. J. Cell Biol. 2001; 152: 111–26.

29. Fibbi B, Morelli A, Marini M, Zhang X-H, Mancina R, Vignozzi L, Filippi S, Chavalmane A, Silvestrini E, Colli E, Adorini L, Vannelli GB, Maggi M, Atorvastatin but not elocalcitol increases sildenafil responsiveness in spontaneously hypertensive rats by regulating the RhoA/ROCK pathway. J. Androl. 29: 70–84.

30. Ruiz-Velasco R, Lanning CC, Williams CL, The activation of Rac1 by M3 muscarinic acetylcholine receptors involves the translocation of Rac1 and IQGAP1 to cell junctions and changes in the composition of protein complexes containing Rac1, IQGAP1, and actin. J. Biol. Chem. 2002; 277: 33081–91.

31. Li-Weber M, Targeting apoptosis pathways in cancer by Chinese medicine. Cancer Lett. 2013; 332: 304–12.

32. Myers SH, Brunton VG, Unciti-Broceta A, AXL Inhibitors in Cancer: A Medicinal Chemistry Perspective. J. Med. Chem. 2016; 59: 3593–608.

33. Linger RMA, Keating AK, Earp HS, Graham DK, TAM receptor tyrosine kinases: biologic functions, signaling, and potential therapeutic targeting in human cancer. Adv. Cancer Res. 2008; 100: 35–83.

34. Luan Z, He Y, Alattar M, Chen Z, He F, Targeting the prohibitin scaffold-CRAF kinase interaction in RAS-ERK-driven pancreatic ductal adenocarcinoma. Mol. Cancer. 2014; 13: 38.

35. Heasman SJ, Ridley AJ, Mammalian Rho GTPases: new insights into their functions from in vivo studies. Nat. Rev. Mol. Cell Biol. 2008; 9: 690–701.

36. Seo M, Lee W, Suk K, Identification of novel cell migration-promoting genes by a functional genetic screen. FASEB J. 2010; 24: 464–78.

37. Montalvo-Ortiz BL, Castillo-Pichardo L, Hernández E, Humphries-Bickley T, De la Mota-Peynado A, Cubano LA, Vlaar CP, Dharmawardhane S, Characterization of EHop-016, novel small molecule inhibitor of Rac GTPase. J. Biol. Chem. 2012; 287: 13228–38.

38. Insall RH, Machesky LM, Actin dynamics at the leading edge: from simple machinery to complex networks. Dev. Cell. 2009; 17: 310–22.

39. Fenteany G, Zhu S, Small-molecule inhibitors of actin dynamics and cell motility. Curr. Top. Med. Chem. 2003; 3: 593–616.

40. Yarrow JC, Totsukawa G, Charras GT, Mitchison TJ, Screening for cell migration inhibitors via automated microscopy reveals a Rho-kinase inhibitor. Chem. Biol. 2005; 12: 385–95.

41. Yoshida T, Zhang Y, Rivera Rosado L a, Chen J, Khan T, Moon SY, Zhang B, Blockade of Rac1 activity induces G1 cell cycle arrest or apoptosis in breast cancer cells through downregulation of cyclin D1, survivin, and X-linked inhibitor of apoptosis protein. Mol. Cancer Ther. 2010; 9: 1657–1668.

42. Gebäck T, Schulz, M.M.P., Koumoutsakos P, Detmar M, A novel and simple software tool for automated analysis of monolayer wound healing assays. Biotechniques. 2009; 46: 265–74.

43. Brockschmidt A, Trost D, Peterziel H, Zimmermann K, Ehrler M, Grassmann H, Pfenning PN, Waha A, Wohlleber D, Brockschmidt FF, Jugold M, Hoischen A, Kalla C, et al., KIAA1797/FOCAD encodes a novel focal adhesion protein with tumour suppressor function in gliomas. Brain. 2012; 135: 1027–41.

44. Schneider CA, Rasband WS, Eliceiri KW, NIH Image to ImageJ: 25 years of image analysis. Nat. Methods. 2012; 9: 671–75.

45. Zadran S, Standley S, Wong K, Otiniano E, Amighi A, Baudry M, Fluorescence resonance energy transfer (FRET)-based biosensors: visualizing cellular dynamics and bioenergetics. Appl. Microbiol. Biotechnol. 2012; 96: 895–902.

46. Jaiswal M, Dubey BN, Koessmeier KT, Gremer L, Ahmadian MR, Biochemical assays to characterize Rho GTPases. Methods Mol. Biol. 2012; 827: 37–58.

47. Jaiswal M, Gremer L, Dvorsky R, Haeusler LC, Cirstea IC, Uhlenbrock K, Ahmadian MR, Mechanistic insights into specificity, activity, and regulatory elements of the regulator of G-protein signaling (RGS)-containing Rho-specific guanine nucleotide exchange factors (GEFs) p115, PDZ-RhoGEF (PRG), and leukemia-associated RhoGEF (LARG). J. Biol. Chem. 2011; 286: 18202–12.

48. Jaiswal M, Dvorsky R, Amin E, Risse SL, Fansa EK, Zhang S-C, Taha MS, Gauhar AR, Nakhaei-Rad S, Kordes C, Koessmeier KT, Cirstea IC, Olayioye MA, et al., Functional cross-talk between ras and rho pathways: a Ras-specific GTPase-activating protein (p120RasGAP) competitively inhibits the RhoGAP activity of deleted in liver cancer (DLC) tumor suppressor by masking the catalytic arginine finger. J. Biol. Chem. 2014; 289: 6839–49.

49. Hancock JF, Cadwallader K, Paterson H, Marshall CJ, A CAAX or a CAAL motif and a second signal are sufficient for plasma membrane targeting of ras proteins. EMBO J. 1991; 10: 4033–9.

50. Choy E, Chiu VK, Silletti J, Feoktistov M, Morimoto T, Michaelson D, Ivanov IE, Philips MR, Endomembrane trafficking of ras: the CAAX motif targets proteins to the ER and Golgi. Cell. 1999; 98: 69–80.

51. Moffat J, Grueneberg DA, Yang X, Kim SY, Kloepfer AM, Hinkle G, Piqani B, Eisenhaure TM, Luo B, Grenier JK, Carpenter AE, Foo SY, Stewart SA, et al., A lentiviral RNAi library for human and mouse genes applied to an arrayed viral high-content screen. Cell. 2006; 124: 1283–98.

The anticancer phytochemical rocaglamide inhibits Rho GTPase activity and cancer cell migration

SUPPLEMENTARY MATERIALS
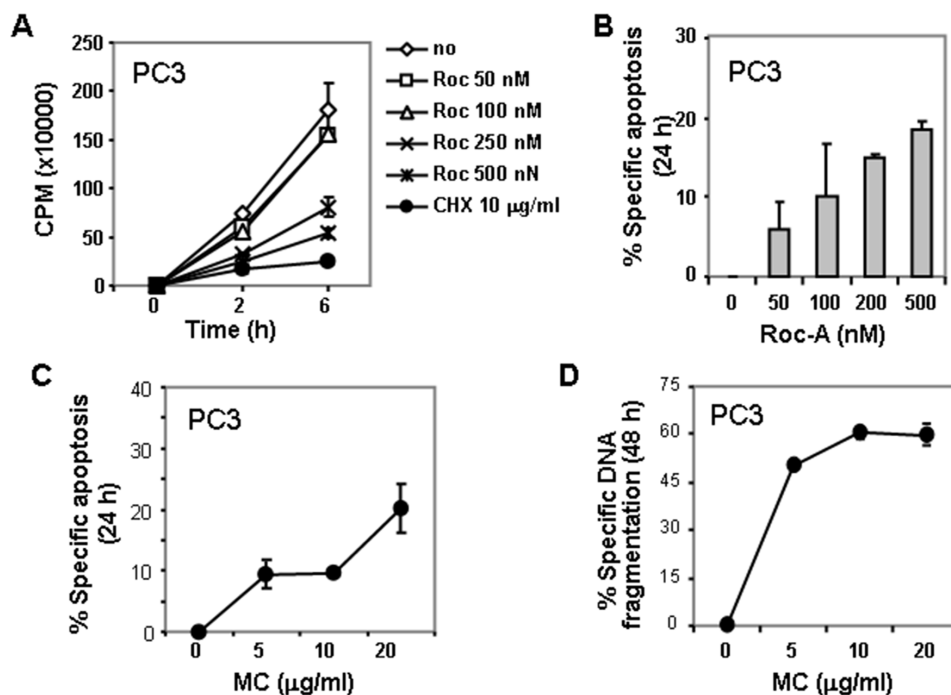
Supplementary Figure S1: Analysis of the effects of Roc-A and Mitomycin C (MC) on translation inhibition and apoptosis induction in PC3 cells. A. Effects of Roc-A and MC on translation inhibition in PC3 cells. **B**. Effects of Roc-A on apoptosis induction in PC3 cells. **C.** Effects of MC on apoptosis induction in PC3 cells at 24 h (AnxV/7aad staining). **D.** Effects of MC on apoptosis induction in PC3 cells at 48 h. (DNA fragmentation).
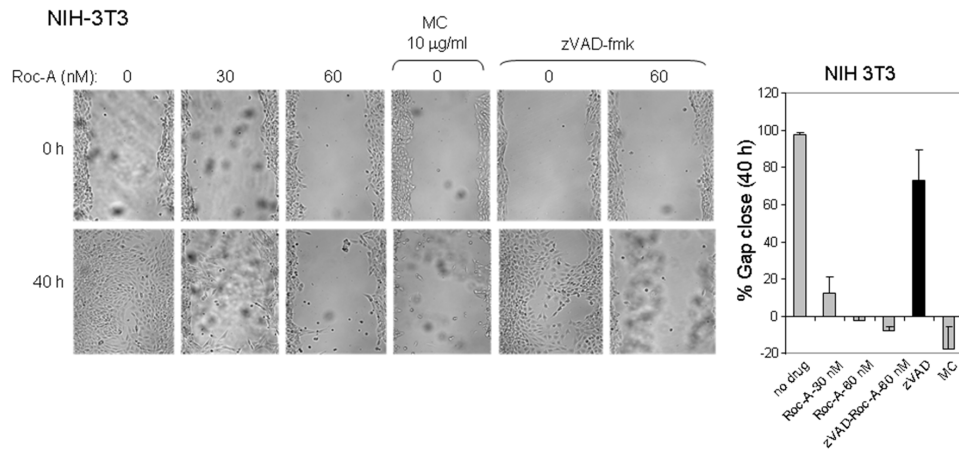
Supplementary Figure S2: Roc-A inhibits migration of the mouse non-tumor fibroblast cell line NIH-3T3. The experiment was carried out as described in Figure 1 and 2.
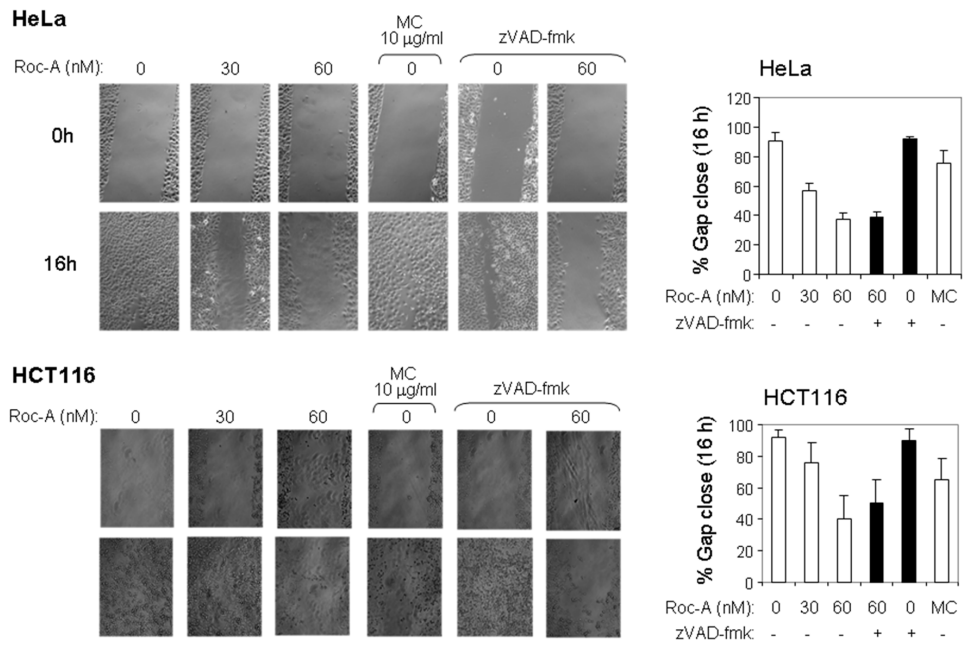
Supplementary Figure S3: Roc-A inhibits migration of the human cervical HeLa cancer cells and the human colon HCT116 cancer cells. The experiments were carried out as described in Figure 1 and 2.
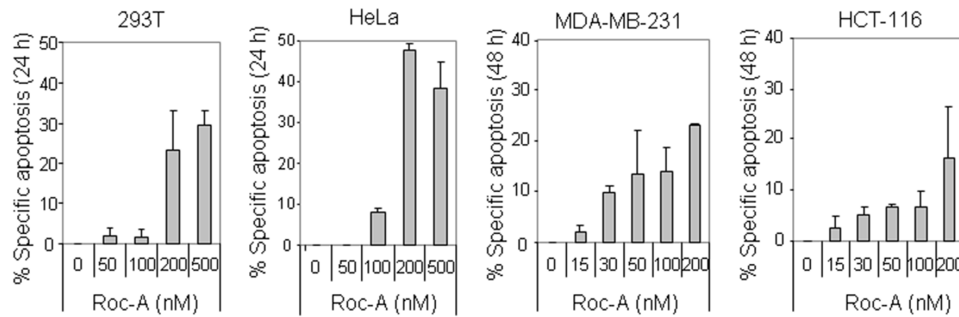
Supplementary Figure S4: Effects of Roc-A on cell viability in different cancer cell lines. Cancer cell lines used in the wound-assay analysis were treated with different doses of Roc-A (A) for the indicated times. Apoptotic cell death was examined by AnxV and 7aad staining.
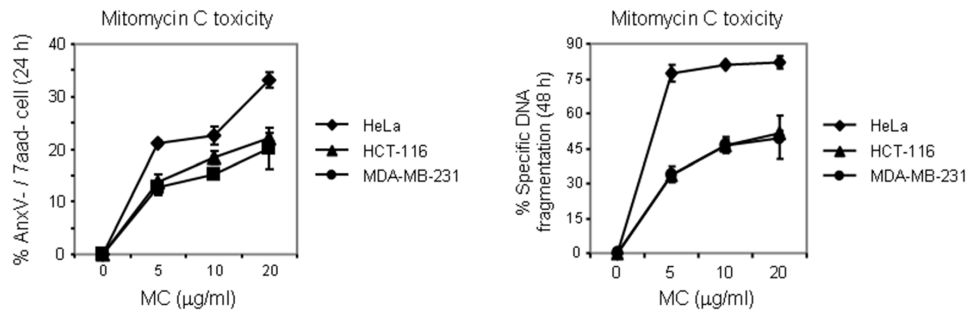
Supplementary Figure S5: Effects of Mitomycin C (MC) on cell viability in different cancer cell lines. Cancer cell lines used in the wound-assay analysis were treated with different doses of MC for 24 or 48 h as indicated. MC-induced apoptotic cell death was determined by either AnxV / 7aad staining (at 24 h) or DNA fragmentation (at 48 h).
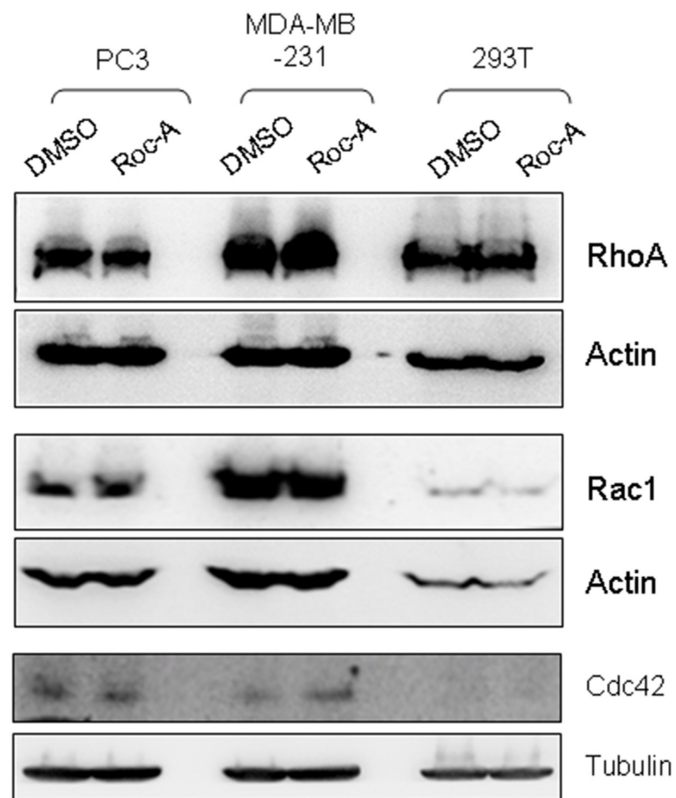
Supplementary Figure S6: The protein expression levels of Rho GTPases are not affected by Roc-A. PC3, MDA-MB-231 and 293T cells were treated with 50 nM of Roc-A for 24 h. Cell lysates were subjected to immunoblot analysis for the expression levels of RhoA, Rac1 and Cdc42. Data represent one of two independent experiments.
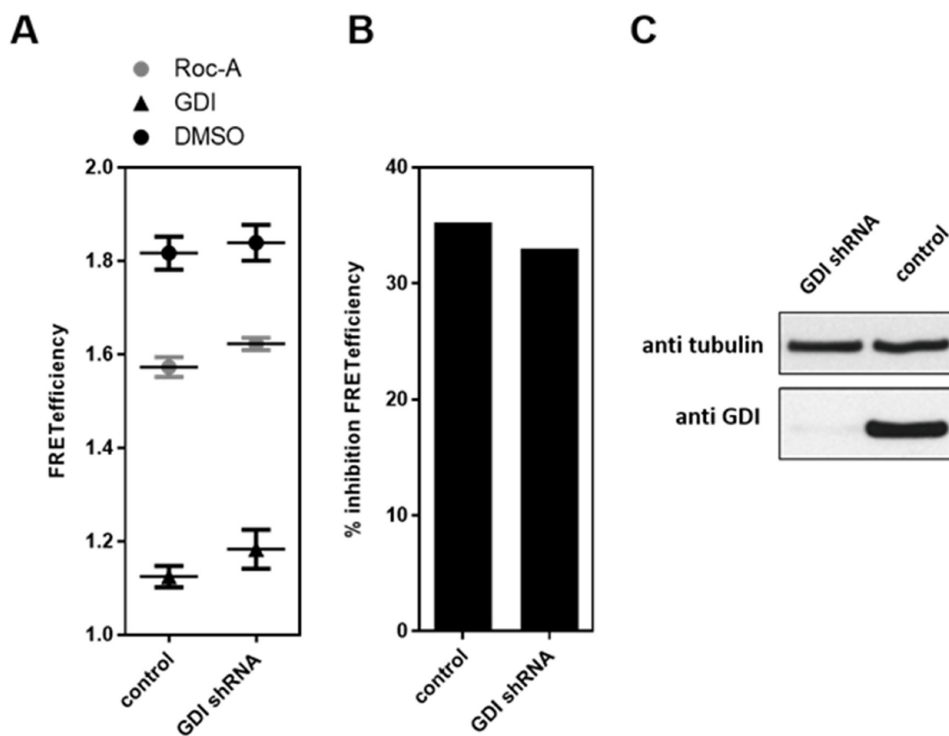
Supplementary Figure S7: Effect of GDI knockdown on Roc-A-mediated inhibition of RhoA activity. A. GDI was knocked down in 293T cells, followed by overexpression of RhoA FRET sensors either with a control plasmid (Control, 30 nM Roc-A) or together with GDI. Cells were treated with 30 nM Roc-A or vehicle (DMSO for Control and GDI) for 24h. Results are an average of three independent experiments. Error bars (S.E.M.) are shown. **B.** FRET efficiency from B was normalized to GDI and DMSO values and % inhibition FRET efficiency was calculated. **C.** Western blot showing the expression levels of GDI in GDI shRNA- and control-transfected cells.
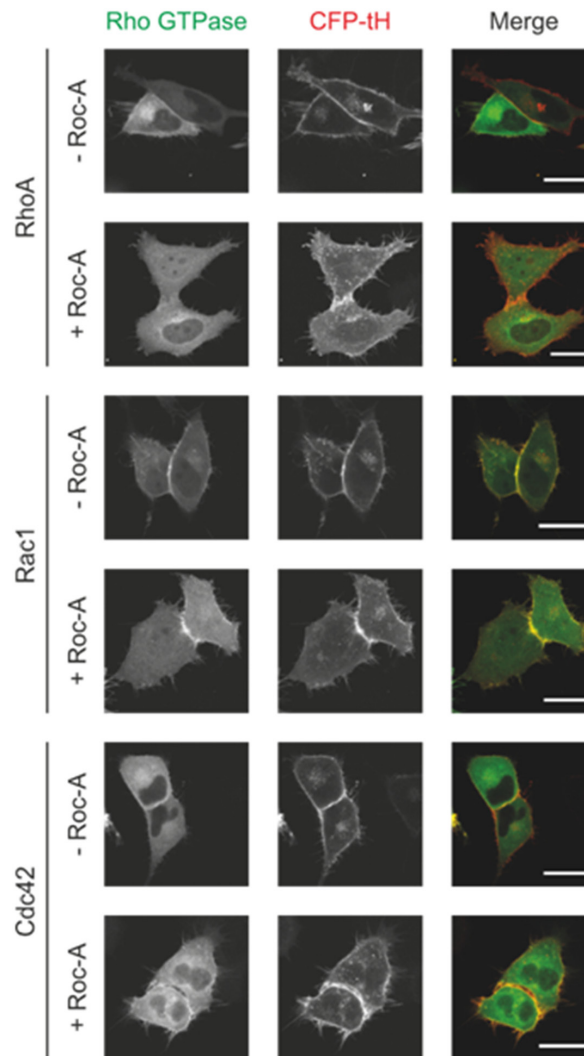
Supplementary Figure S8: Roc-A has no effect on cellular localization of Rho GTPases RhoA, Rac1 and Cdc42 in HeLa cells. mCitrine-RhoA, -Rac1 or -Cdc42 (green) were overexpressed in HeLa cells each together with the cell membrane marker mCerulean-tH (red). Cells were treated with 30 nM Roc-A or vehicle (DMSO) for 24h. Representative images (Z-slices) are shown. Scale bar = 20 μm.
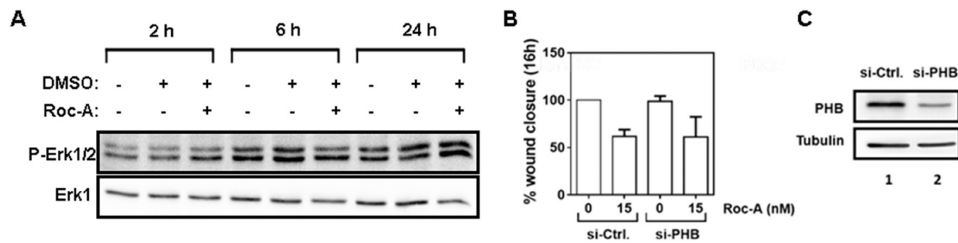
Supplementary Figure S9: Roc-A does not inhibit cell migration *via* PHB. A. Roc-A does not influence Erk phosphorylation at low concentrations. PC-3 cells were treated with solvent (DMSO) or Roc-A (15 nM) for the indicated time periods. The phosphorylation of Erk and total Erk expression levels were analyzed by Western blotting. Results are representative of two independent experiments. **B.** The level of PHB expression does not influence the anti-migratory effect of Roc-A. PC-3 cells were transiently transfected with siRNA against PHB and 24h later used in wound-assays. Control-transfected cells and PHB-si-RNA-transfected cells were treated with solvent (DMSO) or Roc-A as indicated and the percentage of gap closure was quantified 16h following treatment. Results are an average of three independent experiments. Error bars (S.D.) are shown. **C.** Western blot analysis of the efficiency of PHB knockdown. A representative blot is shown. Protein lysates were analyzed 48h post-transfection. Results correspond to B and are representative of three independent experiments.

Chapter 6

Kinetics of RHOA activation by p115

New evidence for a multistep mechanism of RHOA nucleotide exchange catalyzed by the diffuse B-cell lymphoma homology domain of p115

Ehsan Amin, Zhong Guo, Marcel Buchholzer, Radovan Dvorsky, Roger S. Goody, Mohammad Reza Ahmadian
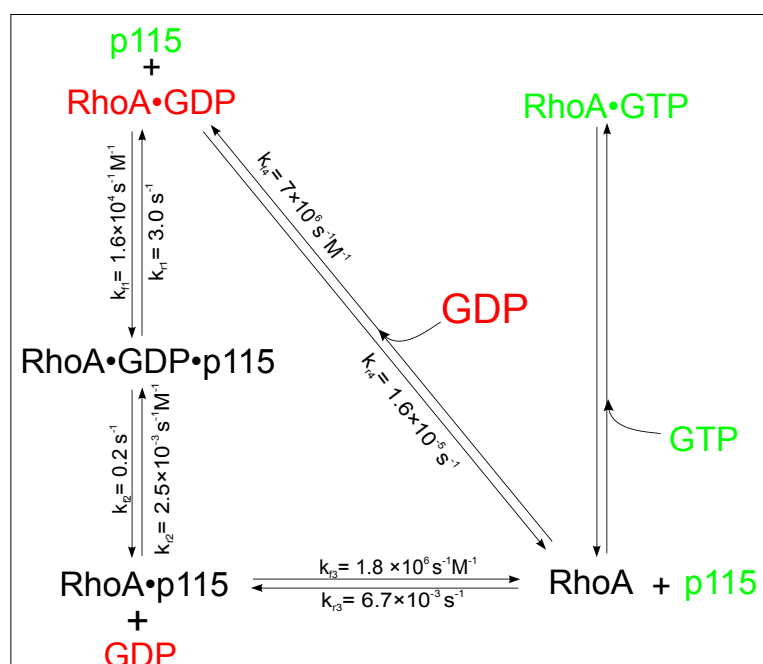
Status:	In preparation
Impact factor:	–
Own Proportion to this work:	50 %; design and perform the experiments, write manuscript

6.1   Background

Two unrelated human GEF families for RHO proteins have been described, a diffuse B-cell lymphoma (DBL) family and dedicator of cytokinesis (DOCK) family (Goicoechea et al., 2014; Namekata et al., 2014; Rittinger, 2009). A third RHO protein-specific GEF family is represented by the SopE/WxxxE-type exchange factors that are classified as type III effector proteins of pathogenic bacteria (Bulgin et al., 2010). In comparison to eleven human DOCK family proteins, there are 74 multimodular DBL domains in human proteome (Jaiswal et al., 2013). In response to diverse extracellular stimuli, DBL family proteins regulate numerous cellular responses such as proliferation, differentiation and movement (Rossman et al., 2005; Schiller, 2006) The DBL homology (DH) domain represents a common structural module in all GEFs of DBL family (Rossman et al., 2005). It is responsible for the GDP/GTP exchange by accelerating the very slow intrinsic GDP dissociation (Jaiswal et al., 2013), thereby initiating specific downstream signaling events. DH domain is the signature of all DBL family proteins and consists of around 200 residues. In the majority of DBL family proteins, the catalytic DH domain is followed by a pleckstrin homology (PH) domain indicating an essential and conserved function (Aittaleb et al., 2010; Jaiswal et al., 2011; Rossman et al., 2005; Viaud et al., 2012). Spatio-temporal regulation of the DBL proteins has been implicated to initiate activation of substrate RHO proteins and to control a broad spectrum of normal and pathological cellular functions (Cook et al., 2014; Droppelmann et al., 2014; Schiller, 2006). It is evident that members of the DBL protein family are attractive therapeutic targets for a variety of diseases (Bos et al., 2007; Lazer et al., 2011; Loirand et al., 2008; Vigil et al., 2010). Thus, understanding the mechanism of GEF-catalyzed nucleotide exchange reaction is of major importance. Evidence for a complex multistep mechanism of GEF-catalyzed nucleotide exchange has emerged from equilibrium and kinetic studies on RANGEF RCC 1 (Klebe et al., 1995), RASGEF CDC25Mm (Guo et al., 2005; Lenzen et al., 1998), RABGEFs VPS9, RABEX-5, DSS4, RABIN8 and GRAB (Esters et al., 2001; Guo et al., 2013; Itzen et al., 2007), SMGGDS, a GEF with a broad substrate specificity including RAS, RAP1A, RAC1, RHOA and CDC42 (Hutchinson et al., 2000), and RHOGEFs LBC and DBL. A sequential reaction scheme for DBL-catalyzed nucleotide exchange reaction of RHO GTPases has been proposed (Cherfils et al., 1999; Vetter et al., 2001). It begins with the formation of a low affinity RHO-GDP-Mg^{2+}-GEF complex that rapidly converts to a high affinity RHO-GEF complex concomitant with expulsion of GDP and Mg^{2+}. The binding of GTP-Mg^{2+} leads to an unstable complex of RHO-GTP-Mg^{2+}-GEF, which is followed by dissociation of the GEF from the GTP-bound, active RHO.

6.2   Results

Activation of RHOA by p115 contains several stages that kinetics of all steps have not been investigated yet. In this study by means of two different fluorescence labelling strategies on RHOA, we have measured rate constants of every step. One strategy is labelling of GDP itself with mant and another one is AEDANS labelling of RHOA in the interface with p115. Therefore, we were able to measure all kinetic parameters in the mechanism. To simulate kinetic activation of RHOA we needed the cell concentration of RHOA, p115, GDP and GTP. Firstly, we purified RHOA, RHOB, RHOC to confirm specificity of RHOA antibody. Then, calibration with different concentrations

of purified proteins enabled us to estimate the cellular concentration of RHOA and p115 in endothelial cells.
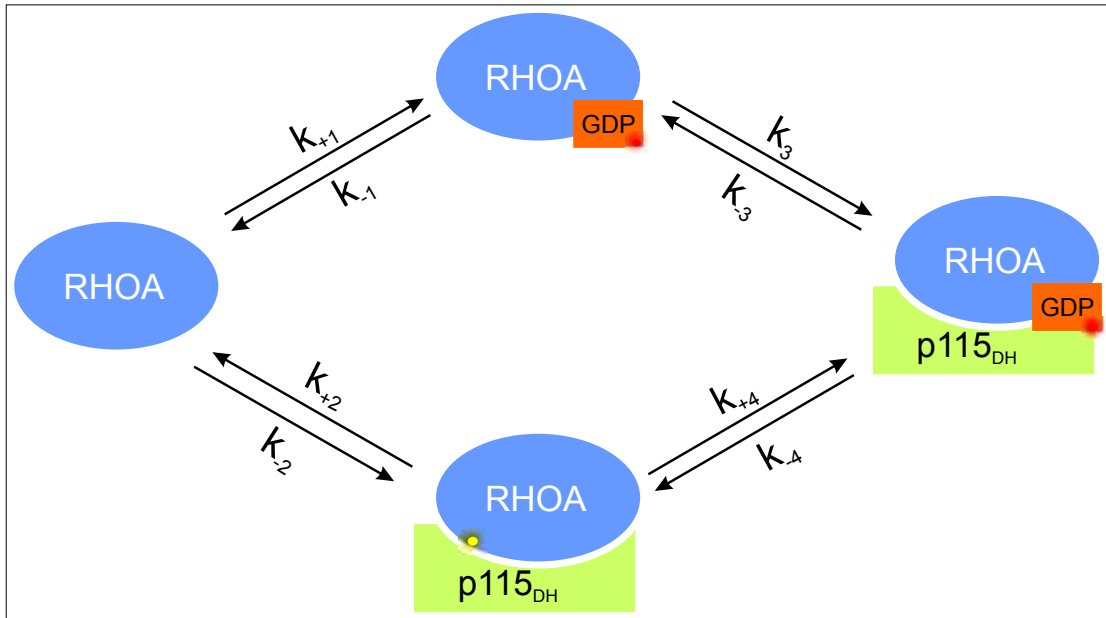
FIGURE 6.1: RHOA activation cycle by p115. Binding of p115 to RHOA decreases the affinity of GDP to RHOA and facilitates nucleotide exchange. To measure k_1 and k_3, GDP has been labeled with mant. Also to estimate rate constants k_2 and k_4, Cys-33 has been labeled with AEDANS.

By having all rate constants of reactions and initial concentration of proteins, we implemented differential equations in Openmodelica program and simulated timing of RHOA activation by p115RHOGEF.

6.3 Conclusion

GTPase activation switches on different cellular pathways. One of these critical pathways regulates endothelial barrier permeability. p115RHOGEF plays a main role in activation of RHOA and subsequently increases endothelial permeability. But still the timing of this activation is not well understood. By two different fluorescence labeling we have been measured rate constants of all steps. Concentration calibration by purified proteins provides us the possibility to estimate protein concentrations inside the endothelial cells. our study provide an detailed insights for future systems biology studies to model endothelial barrier permeability and understand the regulation effects of RHO GTPases.

Chapter 7

Molecular and Functional Basis of RHOGAP Family Proteins

Deciphering the molecular and functional basis of the RHOGAP family proteins: A systematic approach towards selective inactivation of the Rho family proteins
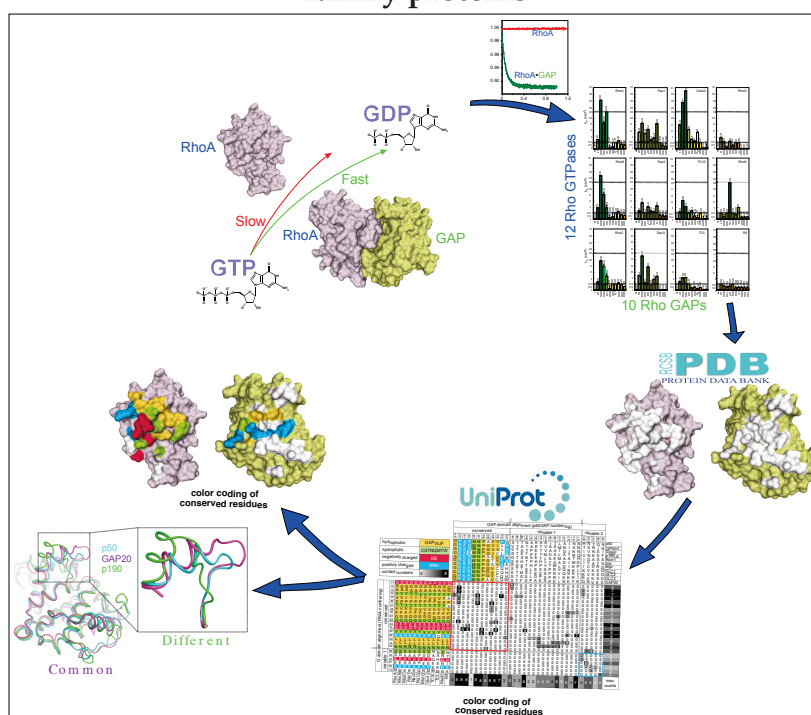
Deciphering the Molecular and Functional Basis of RHOGAP Family Proteins
A SYSTEMATIC APPROACH TOWARD SELECTIVE INACTIVATION OF RHO FAMILY PROTEINS[*][S]

Ehsan Amin[‡], **Mamta Jaiswal**[‡1], **Urszula Derewenda**[§], **Katarina Reis**[¶], **Kazem Nouri**[‡], **Katja T. Koessmeier**[‡],
Pontus Aspenström[¶], **Avril V. Somlyo**[§], **Radovan Dvorsky**[‡2], and **Mohammad R. Ahmadian**[‡3]

From the ‡Institute of Biochemistry and Molecular Biology II, Medical Faculty, Heinrich-Heine-University, 40225 Düsseldorf, Germany, the §Department of Molecular Physiology and Biological Physics, University of Virginia, Charlottesville, Virginia 22908, and the ¶Department of Microbiology, Tumor and Cell Biology, Karolinska Institutet, SE-171 77 Stockholm, Sweden

RHO GTPase-activating proteins (RHOGAPs) are one of the major classes of regulators of the RHO-related protein family that are crucial in many cellular processes, motility, contractility, growth, differentiation, and development. Using database searches, we extracted 66 distinct human RHOGAPs, from which 57 have a common catalytic domain capable of terminating RHO protein signaling by stimulating the slow intrinsic GTP hydrolysis (GTPase) reaction. The specificity of the majority of the members of RHOGAP family is largely uncharacterized. Here, we comprehensively investigated the sequence-structure-function relationship between RHOGAPs and RHO proteins by combining our *in vitro* data with *in silico* data. The activity of 14 representatives of the RHOGAP family toward 12 RHO family proteins was determined in real time. We identified and structurally verified hot spots in the interface between RHOGAPs and RHO proteins as critical determinants for binding and catalysis. We have found that the RHOGAP domain itself is nonselective and in some cases rather inefficient under cell-free conditions. Thus, we propose that other domains of RHOGAPs confer substrate specificity and fine-tune their catalytic efficiency in cells.

Hydrolysis of the bound GTP to GDP and inorganic phosphate is the timing mechanism that terminates signal transduction of the majority of RHO family proteins returning them to their inactive GDP-bound state (1, 2). The intrinsic GTP hydrolysis (GTPase) reaction is usually very slow (2) but can be stimulated by several orders of magnitude through the interaction of the RHO proteins with RHO GTPase-activating proteins (RHOGAPs)[4] (3–8). RHOGAPs are defined by the presence of a conserved catalytic domain of ~190 amino acids, which supplies a conserved arginine residue termed the "arginine finger." This complements an inefficient active site by stabilizing the transition state of the GTPase reaction of the RHO proteins (4, 9–14). Most remarkably, the same mechanistic strategy has been shown for bacterial GAPs, such as the *Salmonella typhimurium* virulence factor SptP, the *Pseudomonas aeruginosa* cytotoxin ExoS, and the *Yersinia pestis* YopE, even though they do not share any sequence or structural similarities with eukaryotic RHOGAP domains (15–17).

Mining in the UniProt database led to the identification of 66 distinct human proteins containing a common RHOGAP domain (Fig. 1; Table 1), a number that is slightly different from previous reports (18–25). Among them p50RHOGAP (26), also known as CDC42GAP (27), p190 (28), and BCR (29) were the first identified and also the best characterized family members. Apart from conserved RHOGAP domains, RHOGAP family proteins possess several sequence motifs and structural domains, which play a role in autoregulation (30), lipid membrane association, subcellular localization, and connection to upstream signals (8, 18, 21, 31, 32). The majority of RHOGAP family members are largely uncharacterized. To date, the selectivity of about one-third of RHOGAPs has been experimentally determined, mainly for their activities toward CDC42, RAC1, and RHOA using diverse methods (Table 1) (8, 18, 21, 25, 31, 33, 34). Despite their significance, the data reported so far do not allow general conclusions about their selectivity (bimolecular recognition and interaction), efficiency (the capability of GAPs to accelerate GTP hydrolysis), and specificity (multimodal

Molecular Basis of the RHOGAP Family Proteins

interaction at a specific subcellular site influenced by additional domains, motifs and scaffold/adapter proteins) toward RHO proteins. This is mainly due to a large variation of methods and experimental designs.

To revise this status quo, we performed a meta-analysis aiming to evaluate the sequence-structure-function relationship of a variety of RHOGAPs and RHO proteins under cell-free conditions. Therefore, we first measured the GAP activities of 14 RHOGAPs toward 12 GAP-competent RHO proteins, related them to the intrinsic GTP hydrolysis properties of RHO proteins (35, 36) and calculated the fold activation by RHOGAP domain. Second, we combined obtained data with sequence alignments, evolutionary analysis, and accessible structural and functional data from previous studies. All information was then systematically assessed in an ensemble approach focusing on various biochemical aspects of the RHO-RHOGAP interactions. Extracted data at the final stage enabled us to predict activity and selectivity of 66 RHOGAPs and to conclude that the specificity of the non-selective GAP domain in cells is most likely determined by other functional motif(s) and domain(s) in the respective polypeptide chain.

Results

RHO and RHOGAPs, a Wide and Complex Network—Our original intention was to inspect the GAP activity of 14 representative RHOGAPs (Table 1; supplemental Fig. S1) toward 14 RHO proteins with GTPase activity (supplemental Fig. S2) (35, 36). GTPase-deficient and GAP-insensitive RHO family members, such as RND proteins and RHOH/TTF (35), were excluded. As purified WRCH1 and CHP/WRCH2 proteins were not stable in our hands, the following 12 RHO proteins were included in our study: RHOA, RHOB, RHOC, RAC1, RAC2, RAC3, RHOG, CDC42, TC10, TCL, RHOD, and RIF.

Stimulated GTP hydrolysis reaction was measured by real time fluorescence spectroscopic methods using purified recombinant proteins. In this method, rapid hydrolysis of tamraGTP by the respective RHO proteins was monitored in the presence of an excess amount of the respective RHOGAPs using a stopped-flow instrument (Fig. 2). Fluorescent tamraGTP has been previously described as a GTP hydrolysis sensor for most RHO proteins (6). To be able to detect activity of RHOGAPs with even very low efficiency, we used a 50-fold higher molar concentration of the RHOGAP domains above the respective RHO protein, in all GAP-stimulated reactions. However, even such excess did not lead to a measurable GAP activity of some proteins, such as OCRL1 and p85α (data not shown), which were therefore excluded. Ultimately, p50GAP (hereafter called p50), oligophrenin 1 (hereafter called OPHN1), GRAF1, RICH1 (also called Nadrin), p190A (hereafter called p190), ABR, MGCRAC-GAP (also called RACGAP1; hereafter MGC), DLC1, DLC2, and DLC3 were used in this study.

Molecular Basis of the RHOGAP Family Proteins

GAP-stimulated cy3GTP Hydrolysis by RHO Proteins—The measurement of the GAP-stimulated tamraGTP hydrolysis was suboptimal for RHOA, RHOB, and RHOC (Fig. 2). Therefore, we turned to other fluorescent nucleotides that enable reliable monitoring of real time kinetics of the hydrolysis reaction by RHO isoforms. We examined the following GTP analogs: $ATTO_{550}$-GTP, $ATTO_{495}$-GTP, $ATTO_{488}$-GTP, FAM5-GTP, and cy3GTP. As the p50-stimulated cy3GTP hydrolysis by RHOA provided a substantially distinct decrease in fluorescence (Fig. 2), we measured and evaluated the RHOGAP activities toward RHOA, RHOB, and RHOC using cy3GTP.

In total, we have measured hydrolysis of fluorescently labeled GTP by 12 RHO proteins in all mutual combinations with 10 RHOGAPs. Evaluated observed rate constants (k_{obs}) are shown in Fig. 3 as a *bar diagram* and summarized in Table 2 in fold activation. Intrinsic GTP hydrolysis was used as control experiments.

RHOGAPs Lack Selectivity—In general, the investigated GAPs do not show any selectivity toward particular RHO proteins or their isoforms. p50 appears to be the most universal GAP as it stimulated the GTP hydrolysis of all RHO proteins more than 200-fold as compared with the intrinsic GTPase reaction (Fig. 3). However, there is a large difference between the highest activity toward CDC42 with a k_{obs} value of 14 s^{-1} and the lowest activity toward RHOD with k_{obs} value of 0.12 s^{-1} (Fig. 3). p190 was also highly active on all RHO proteins with a relatively low stimulation of the RIF GTPase reaction. Noteworthy, p190 revealed a high activity toward RHOD that was as efficient as p190 activity toward RHOA. OPHN1, a Bin/Amphiphysin/Rvs (BAR) domain-containing protein (see Fig. 1), exhibited overall the highest activities reaching a stimulation of 5 orders of magnitude in the case of RHOA and RHOB. GRAF1, an OPHN1-homologous protein, was found with an absolute k_{obs} value of 90 s^{-1} for CDC42 as a fastest stimulated GTP hydrolysis reaction among the GAPs investigated in this study. Differences between the fastest and slowest stimulation for OPHN1 or GRAF1 remarkably exceed 3 orders of magnitude, pointing to an extreme span of measured activities for a single GAP.

Intermediate activities were measured for MGC, RICH1, and ABR, which are still able to stimulate the GTP hydrolysis of measured RHO proteins but to a significantly lower extent than the previously mentioned RHOGAPs, especially for TCL and RHO isoforms. Accordingly, all three proteins can be classified as preferential to CDC42 and RAC isoforms, with an addition of MGC acting on RHOD and RICH1 acting on TC10. Rather inefficient GAP activities were detected for the DLC isoforms, except for the DLC1 activity toward the RHO isoforms and marginally toward CDC42, RAC1, and TC10. Overall disability of DLC2 and DLC3 proteins to operate on analyzed RHO pro-

FIGURE 1. **Evolutionary conservation of domains of the RHOGAP family.** Domain composition of 66 RHOGAPs is presented according to their phylogenetic categorization based on GAP domain alignment. In addition to a catalytic GAP domain (*red*), most RHOGAPs have multiple other functional domains, which are probably involved in lipid and membrane binding (*blue*), protein interaction (*green*), or enzymatic activities (*red* and *orange*). A scale of amino acid numbers in increments of 200 is shown at the *bottom*; the total number of the amino acids of the respective RHOGAPs is listed in Table 1. Domain properties and statistics are compiled in supplemental Tables S4 and S5.

Molecular Basis of the RHOGAP Family Proteins

TABLE 1

Human RhoGAP family proteins

All proteins investigated in this study are shown in boldface type. RHOGAPs analyzed in other studies mostly towards RHOA, RAC1, and/or CDC42 are underlined. Last eight proteins are GAP-like proteins.

No.	Entry name	Accession no.	Gene names or aliases	Amino acid no.
1	3BP1	Q9Y3L3	SH3BP1, ARHGAP43	701
2	**ABR**	Q12979	ABR, MDB	859
3	ARHGAP6	O43182	ARHGAP6, RHOGAP6	974
4	ARHGAP8	P85298	ARHGAP8, BPGAP1	464
5	ARHGAP9	Q9BRR9	ARHGAP9, RGL1	750
6	ARHGAP11A	Q6P4F7	ARHGAP11A, KIAA0013, FAM7B1	1023
7	ARHGAP11B	Q3KRB8	ARHGAP11B	267
8	ARHGAP12	Q8IWW6	ARHGAP12	846
9	ARHGAP15	Q53QZ3	ARHGAP15, BM-024, BM-030, BM-046	475
10	ARHGAP19	Q14CB8	ARHGAP19	494
11	ARHGAP20	Q9P2F6	ARHGAP20, KIAA1391, RA-RhoGAP	1191
12	ARHGAP21	Q5T5U3	ARHGAP21, KIAA1424	1957
13	ARHGAP22	Q7Z5H3	ARHGAP22, RHOGAP2	698
14	ARHGAP23	Q9P227	ARHGAP23, KIAA1501	1491
15	ARHGAP25	P42331	ARHGAP25, KIAA0053	645
16	ARHGAP28	Q9P2N2	ARHGAP28, KIAA1314	729
17	ARHGAP30	Q7Z6I6	ARHGAP30	1101
18	ARHGAP39	Q9C0H5	ARHGAP39, KIAA1688, Vilse, CrGAP	1083
19	ARHGAP40	Q5TG30	ARHGAP40, C20orf95	622
20	ARHGAP42	A6NI28	ARHGAP42, GRAF3	874
21	BCR	P11274	BCR, BCR1, D22S11	1271
22	β-Chimaerin	P52757	CHN2, ARHGAP3, BCH	468
23	CAMGAP1	Q6ZUM4	ARHGAP27, CAMGAP1, SH3D20, PP905	889
24	CDGAP	Q2M1Z3	ARHGAP31, CDGAP, KIAA1204	1444
25	CNT-D2	Q96P48	ARAP1, CENTD2, KIAA0782	1450
26	CNT-D3	Q8WWN8	ARAP3, CENTD3	1544
27	**DLC1**	Q96QB1	DLC1, ARHGAP7, KIAA1723, STARD12	1528
28	**DLC2**	Q9Y3M8	STARD13, DLC2, GT650	1113
29	**DLC3**	Q92502	STARD8, DLC3, KIAA0189	1023
30	FAM13A	O94988	FAM13A, FAM13A1, KIAA0914	1023
31	GMIP	Q9P107	ARHGAP46, GMIP	970
32	**GRAF**	Q9UNA1	ARHGAP26, GRAF, KIAA0621, OPHN1L	814
33	GRAF2	A1A4S6	ARHGAP10, GRAF2, PSGAP	786
34	HMHA1	Q92619	HMHA1, KIAA0223	1136
35	MacGAP	Q8N392	ARHGAP18	663
36	**MgcRacGAP**	Q9H0H5	RACGAP1, KIAA1478, MgcRACGAP, CYK4	632
37	MYO9A	B2RTY4	MYO9A, MYR7	2548
38	MYO9B	Q13459	MYO9B, MYR5	2157
39	N-Chimaerin	P15882	CHN1, ARHGAP2, CHN	459
40	**OPHN1**	O60890	OPHN1, ARHGAP41	802
41	PARG1	Q52LW3	ARHGAP29	1261
42	p115	P98171	ARHGAP4, KIAA0131, RGC1, RHOGAP4	946
43	**p190A**	Q9NRY4	ARHGAP35, GRF1, GRLF1, KIAA1722	1499
44	p190B	Q13017	ARHGAP5, RHOGAP5	1502
45	p200	A7KAX9	ARHGAP32, GRIT, KIAA0712, RICS	2087
46	**p50**	Q07960	ARHGAP1, CDC42GAP, RHOGAP1	439
47	p73	Q8N264	ARHGAP24, FILGAP	748
48	RALBP1	Q15311	RALBP1, RLIP1, RLIP76	655
49	**RICH1**	Q68EM7	ARHGAP17, RICH1, MSTP066, MSTP110	881
50	RICH2	Q17R89	ARHGAP44, KIAA0672, RICH2	818
51	SRGAP1	Q7Z6B7	SRGAP1, ARHGAP13, KIAA1304	1085
52	SRGAP2	O75044	SRGAP2, ARHGAP34, FNBP2, KIAA0456	1071
53	SRGAP3	O43295	SRGAP3, ARHGAP14, KIAA0411, MEGAP	1099
54	SYDE1	Q6ZW31	SYDE1	735
55	SYDE2	Q5VT97	SYDE2	1194
56	TAGAP	Q8N103	TAGAP, TAGAP1, FKSG15, ARHGAP7	731
57	TCGAP	O14559	ARHGAP33, SNX26, TCGAP	1287
58	ARHGAP36	Q6ZRI8	ARHGAP36	547
59	CNTd1	Q8WZ64	ARAP2, CENTD1, KIAA0580	1704
60	DEP1A	Q5TB30	DEPDC1, DEPDC1A	811
61	DEP1B	Q8WUY9	DEPDC1B, XTP8	529
62	FAM13B	Q9NYF5	FAM13B, C5orf5, FAM13B1	915
63	**INPP5B**	P32019	INPP5B, OCRL2	993
64	**OCRL1**	Q01968	OCRL, INPP5F, OCRL1	901
65	**P85A**	P27986	PIK3R1, GRB1	724
66	**P85B**	O00459	PIK3R2	728

teins raises a question about proper conditions under which these proteins may exert their GAP functions.

New Insights from Differential Catalytic Efficiencies—A remarkable finding of our analysis is a broad spectrum of catalytic efficiencies and substrate-selective properties of investigated proteins ranging from a 1-fold to a 120,000-fold stimulation of the intrinsic GTP hydrolysis (Table 2). To illustrate this

explicitly, we plotted all 120 pairs of RHOGAP and RHO proteins (*x* axis) against fold activation (*y* axis) in numeric order starting with OPHN1-RHOB with the highest efficiency and ending with DLC2-RHOG with no activity (Fig. 4; Table 2). Overall, the RHOGAP-RHO protein pairs were subdivided into six groups based on their catalytic efficiency to stimulate the intrinsic GTP hydrolysis of the RHO proteins (Fig. 4). OPHN1

Molecular Basis of the RHOGAP Family Proteins
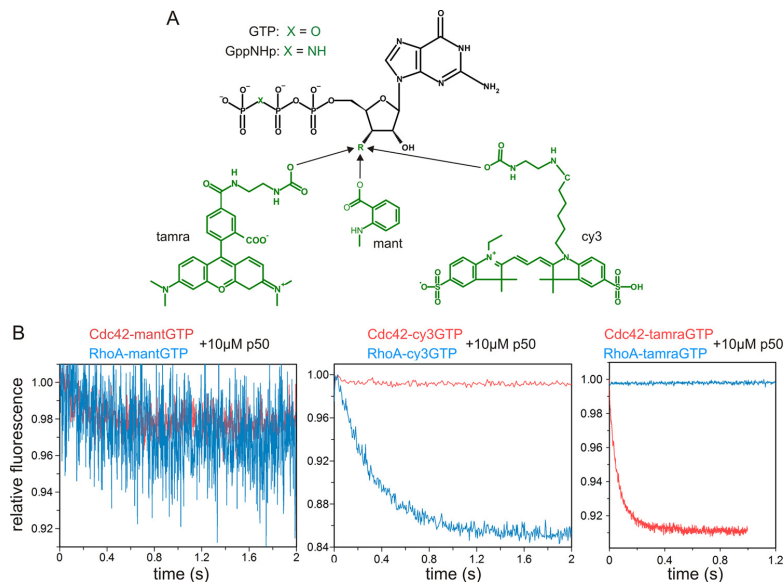
FIGURE 2. **tamraGTP and cy3GTP but not mant-GTP as fluorescent sensors for monitoring GAP-stimulated GTP hydrolysis of RHO proteins in real time.** *A*, chemical structure of fluorescent reporter groups (mant, TAMRA-ethylenediamine, and cy3-ethylenediamine) coupled to GTP and its non-hydrolyzable analog GppNHp. *B*, stimulated GTP hydrolysis of CDC42 and RHOA (0.2 μM) was measured using fluorescent GTP and p50GAP (10 μM) in a Hi-Tech Scientific (SF-61) stopped-flow instrument and a buffer containing 30 mM Tris, pH 7.5, 10 mM potassium phosphate, 10 mM MgCl$_2$, and 3 mM dithiothreitol at 25 °C as described (2). In contrast to mantGTP, which did not provide any significant change in fluorescence, cy3GTP turned out to be most suitable for the RHO isoforms and tamraGTP the most suitable for CDC42-and-RAC-like proteins (CDC42 is shown as a representative) as well as for RHOD and RIF. Observed rate constants (k_{obs}) for GAP-catalyzed GTPase reactions can be obtained by single exponential fitting of the fluorescence decay using GraFit program.

and its homolog GRAF1 form the first group as they have emerged as highly efficient GAPs not only for the RHO isoforms but also for CDC42 and TC10 (Fig. 4). p50 and p190 also belong to this group of GAPs with the highest catalytic efficiency particularly for their selectivity toward RHOB and RHOD, respectively. MGC and RICH1 rank as the second highest efficiency group because of their activities toward RAC1, RHOD, and TC10. We also indexed p190 to this group as it clearly revealed significantly higher activities toward RAC1 and RAC3. The third group with intermediate efficiency is interestingly populated by RHO isoform-specific DLC1 and RAC-specific ABR. The p50-RIF pair is the most active in the fourth group, which overall displays low efficiency. However, as p50 showed a poor selectivity (Table 2), it is rather doubtful that p50 may be a physiological RIFGAP. Caution should be applied when looking at the data of group five (with 45 pairs in the largest group) in Fig. 4 (pairs between 10- and 150-fold activations). To this group belong protein pairs with the lowest activity, for instance the DLC isoforms on the one hand and RIF and RHOD on the other hand. We scored this group despite their obvious but low GAP activities as inefficient pairs. A very small group of only four pairs with an output of less than 10-fold activation was categorized as the sixth group and graded as "inactive" due to their extremely low catalytic efficiency.

Two Critical Steps in Stimulating GTP Hydrolysis—Two critical steps that may control the catalytic efficiency of the GAPs under the conditions used in this study are as follows: (i) association of the RHOGAP with the GTP-bound RHO protein and (ii) the stimulation of the GTP hydrolysis reaction itself. To

examine whether an association-controlled mechanism is a reason for the extreme differences in the catalytic efficiency, we loaded CDC42 with tamraGppNHp, a non-hydrolysable fluorescent GTP analog (6), and measured in real time its association with the RHOGAPs. As shown in Fig. 5, there is a clear correlation between the reaction rates of association and GTP hydrolysis. Correspondingly, DLC isoforms, for example, revealed a 1500-fold lower association rate when compared with OPHN1 (Fig. 5, *left panel*). These data strongly suggest that the catalytic efficiency of the RHOGAPs is directly proportional to the rate of their association with the RHO proteins.

Identification of Hot Spots within Protein Interfaces—To inspect molecular details of interaction between RHO proteins and RHOGAPs, we have analyzed 42 structures of RHOGAP alone and in the complex with RHO proteins available in the PDB (supplemental Table S1). Residues involved in intermolecular interaction were defined to have at least one inter-atomic distance shorter than 4.0 Å. They constitute interacting interface highlighted on the crystal structure of RHOA-p50GAP (Fig. 6A). We have extracted information about interacting amino acids from different complex structures and combined them with sequence alignments of all investigated proteins in the form of an interaction matrix (Fig. 6B). Each element of the matrix, which we call "hot spot," relates one homologous residue from RHO proteins to one homologous residue from RHOGAPs (see also supplemental Figs. S1 and S2). The number value of this element represents the number of complex structures in which these residues interact. Thus, a zero value of the element means that these two residues do not face each

Molecular Basis of the RHOGAP Family Proteins
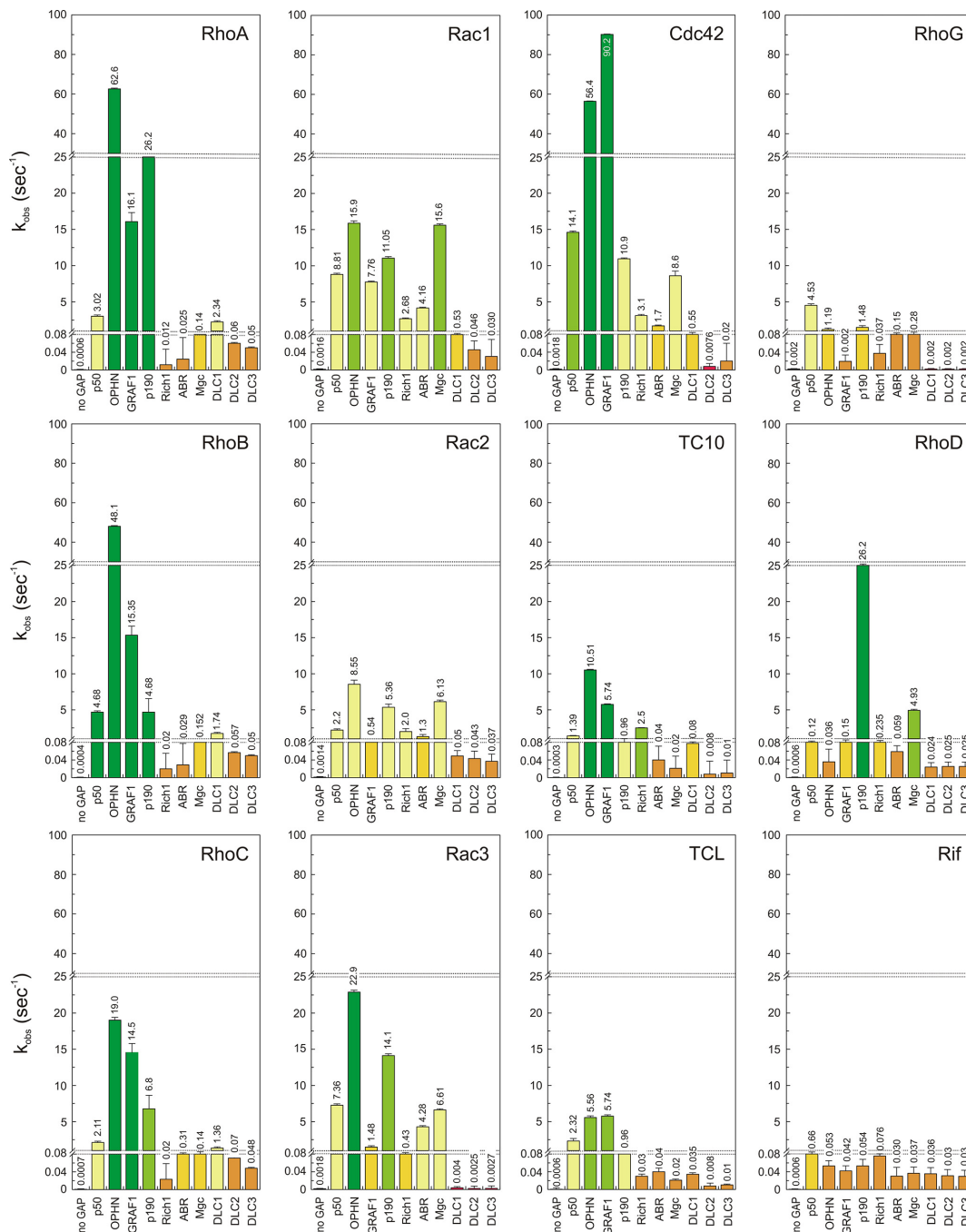
FIGURE 3. **Varying activity and broad selectivity of the RHOGAP family proteins.** Individual GTP hydrolysis reaction rates (k_{obs}; values on the *bar charts*) of 12 RHO proteins (0.2 μM, respectively) in the absence (no GAP) and in the presence of 10 RHOGAPs (10 μM, respectively) are plotted as *bar charts*. All data shown are an average of 4–5 different experiments. Color coding is the same as in Table 2 and changes from *green* for very high to *yellow* for middle and to *red* for no GAP activity.

Molecular Basis of the RHOGAP Family Proteins

TABLE 2

Catalytic efficiency of RHOGAPs represented as fold activation

The catalytic hydrolysis activities, calculated as fold activation, are divided into six groups according to Fig. 4. Fold activation was obtained by dividing the k_{obs} values of GTP hydrolysis reactions by the k_{obs} values of the intrinsic reactions (Fig. 3). Color codes are the same as used in Fig. 3 and correlate in a gradient fashion with green for very high, yellow for middle, and red for no GAP activity.

	RhoA	RhoB	RhoC	Rac1	Rac2	Rac3	RhoG	Cdc42	TC10	TCL	RhoD	Rif
p50	5037	11713	3028	5506	1571	4033	2264	8116	4637	3872	206	1093
OPNH1	104389	120103	27163	9925	6106	12713	594	31318	35036	9278	60	89
GRAF1	26790	38367	20771	4849	383	825	10	50108	19136	9568	255	70
p190	43671	11713	9686	6908	3826	7840	743	6081	3217	1609	43663	89
Rich1	20	50	33	1676	1424	240	19	1732	8333	50	392	126
Abr	41	72	446	2602	930	2380	75	940	133	67	98	51
Mgc	234	380	197	9756	4379	3674	139	4780	71	35	8217	61
DLC1	3731	4347	1946	333	35	2	1	306	258	58	40	59
DLC2	100	142	102	29	31	1	1	4	27	13	42	52
DLC3	83	125	69	19	26	2	1	11	35	17	42	50
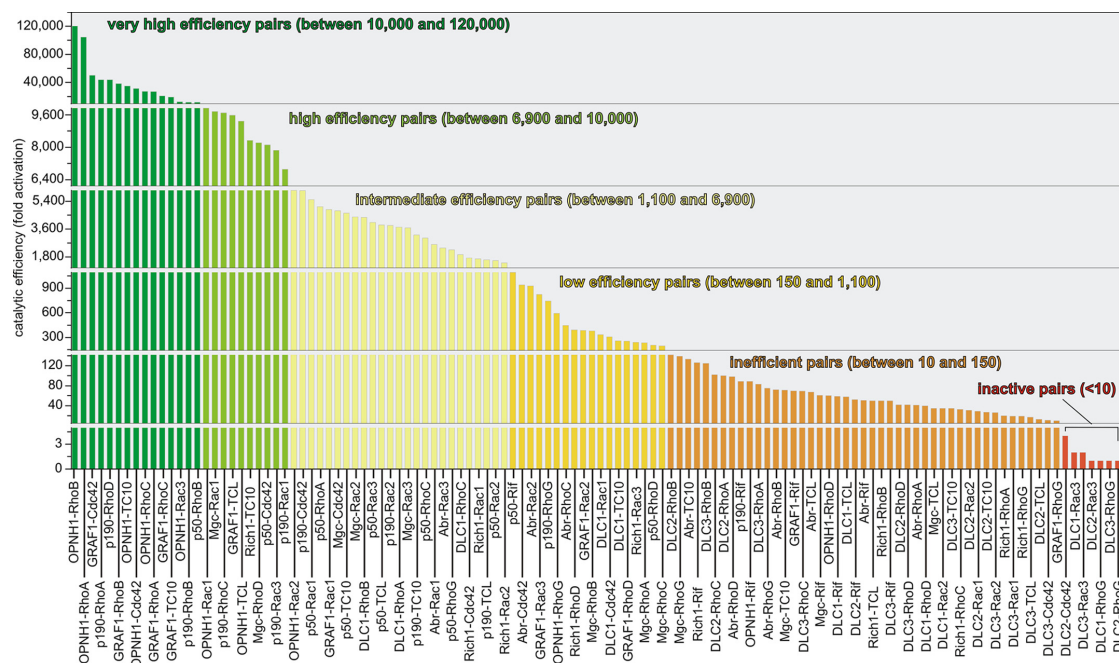
FIGURE 4. **Statistical diagram of the catalytic efficiency of the RHOGAPs.** Values of fold activation are plotted against respective RHOGAP-RHO protein pairs in numeric order. This diagram illustrates the broad spectrum of catalytic efficiencies and substrate-specific properties of various RHOGAPs for the different RHO proteins, which are divided into six efficiency groups as indicated. Color codes are the same as used in Fig. 3 and Table 2.

other in any structure, whereas value 8 means that this particular interaction is to be found in all known structures. We have sorted the residues at both sides of the matrix according to the conservation *versus* variability. As can be seen (Fig. 6B), more than a half of the residues (17 out of 24) on the side of RHO proteins are identical or highly conserved (Gly/Ala-15, Ser/

Thr-37, Asp/Glu-64, and Asp/Glu-65). These residues comprise mostly switch I and switch II and create a continuous patch on the surface (Fig. 6A, *left panel*). On the other side, only six amino acids are identical in RHOGAPs; five are homologous, and the majority of the GTPase interacting residues are variable (Fig. 6A, *right panel*). Strikingly, identical and con-

Molecular Basis of the RHOGAP Family Proteins
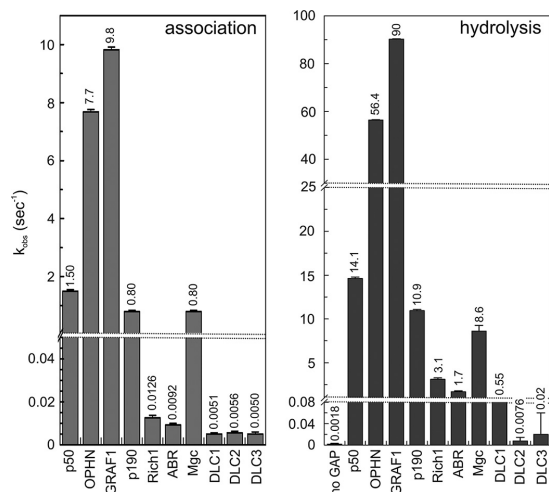
FIGURE 5. **Binding affinity of RHOGAPs to CDC42.** Real time monitoring of the association reaction rates of GAPs (10 μM) with mantGppNHp-bound CDC42 (0.2 μM) has been measured and represented as *bar diagram* (*left panel*) in direct comparison with the reaction rates obtained for the respective GAP-stimulated GTP hydrolysis of CDC42 (*right panel*).

served residues form a patch on the GAP domain. We postulate that the interaction between conserved patches of RHO proteins and RHOGAPs is responsible for both the recognition of the two proteins and the catalysis of GTP hydrolysis. This hypothesis is supported by the fact that an identical arginine 282 (p50 numbering), known as the arginine finger, essential for the catalysis (12, 13, 37), is a central residue of the conserved patch on GAP and contacts only identical residues on RHO proteins (Fig. 6). Interactions on this region are not expected to contribute to the differences in activities (or selectivities) and therefore were excluded from further analysis. However, the number of remaining variable pairs is still high and indicates that the relationship between observed diversity of stimulation and molecular interactions is not simple but is quite complex and multifaceted.

The four most effective GAPs, including OPHN1, GRAF1, p190, and p50, share an asparagine (glutamine in p190) at position 417 (p50 numbering), which is not present in other investigated GAP domains (Fig. 6B). Their predominant counterpart residue in RHO proteins is Tyr-66. Its particular interaction with the amide group may contribute to higher activity. Moreover, OPHN1, the most efficient RHOGAP (Fig. 4; Table 2), has in this region two unique residues containing the hydroxyl group, Thr-283 and Ser-286 (supplemental Fig. S1). Thr-283 undergoes a favorable contact with serine and asparagine at position 88 as well as variable residues at position 90 of RHO proteins (Fig. 6B). RAC isoforms have at the latter position hydrophobic residues that are disfavored by Thr-283 in OPHN1, which contributes to the lower OPNH1-stimulated GTP hydrolysis by RAC isoforms. Going beyond the variable regions of interacting interface, three of four most active GAPs have unique leucine at the position 386, which is otherwise replaced by a lysine or a glutamine (Fig. 6B). Its counterpart residue on the side of RHO proteins is the invariant Tyr-34. The nature of the interactions, in which they are involved, is con-

tributing to observed differences. Tyrosine can be involved either in hydrophobic interactions with leucines by utilizing its phenyl moiety or in electrostatic interactions with lysines employing its hydroxyl group.

Similarly, DLC isoforms that were found to be least efficient in stimulating the GTP hydrolysis of RHO proteins contain within the interacting interface unique positively charged residues, arginine and lysine at positions 409 and 413, respectively (Fig. 6B). Such amino acids at these positions are rather unfavorable because the presence of prevailingly hydrophobic residues is required in this region of the GAP surface as it contacts the hydrophobic patch on RHO proteins formed by invariant Val-36, Phe-37, Leu-67, and Leu-70 (RHOA numbering; Fig. 6). However, considering only DLC GAPs, there are no differences in their interacting residues that could explain partial selectivity of DLC1 for the RHO isoforms. Although it is also not directly possible to interpret an overall low activity of RHOGAPs on RHOG, RHOD, and especially RIF, the interaction matrix enables us to determine the regions that are very likely responsible for these low activities. They include variable positions on RHO proteins, e.g. 90, 97, and 134, and on RHOGAPs, e.g. 283, 286, 287, 288, and 309 (Fig. 6B). A similar situation exists for a considerable effect of p190 on RHOD. RHOD has a unique threonine at position 35, but it interacts with identical residues of GAPs (Fig. 6B). On the other side, p190 also has unique amino acids at positions 323, 390, 408, and 413, but they interact reciprocally with identical residues of RHO proteins. Both proteins interact further through variable regions; thus, a full elucidation of a broad spectrum of GAP catalytic activities on RHO proteins would require global evaluation of synergic effect of multifaceted interaction between varying amino acids.

RHOA-p190 Complex, Crystal Structure Verified a Matrix-based Predicted Interaction—Taking into account that RHO proteins and RHOGAPs are highly homologous, it is legitimate to assume that yet unknown complex structures will share the same structural architecture. Consequently, corresponding residues according to sequence alignments are expected to interact in the manner of known complex structures. Thus, in the absence of structural information for some RHO-RHOGAP complexes, the interaction matrix enables us to deduce which amino acids could be involved in the interaction between these two proteins.

To prove the validity of such an hypothesis, we solved the crystal structure of RHOA in complex with the GAP domain of p190 at high resolution (supplemental Table S3; Fig. 7A), and we used this structure as a benchmark for the verification of our assumptions.

As expected, the overall structure arrangement of the RHOA-p190-GAP complex is similar to complexes of RHO proteins with other GAPs (similarity of p190 to p50 and GAP20 is 25.1 and 17.9%, respectively; supplemental Table S2). The RHOA structure corresponds to an active GTP-bound conformation and clearly differs from its GDP-bound form (Fig. 7A). Conformation of p190 differs in some regions from the structures of p50 and ARHGAP20 (Fig. 7B). However, most relevant for our study were both its high structural similarity in the conserved region of the interacting interface and its conformational variability within the loop between residues 1406 and 1419 (Fig. 7C). Position and orientation of catalytic Arg-1284 are very similar to those found for the arginine fingers in other
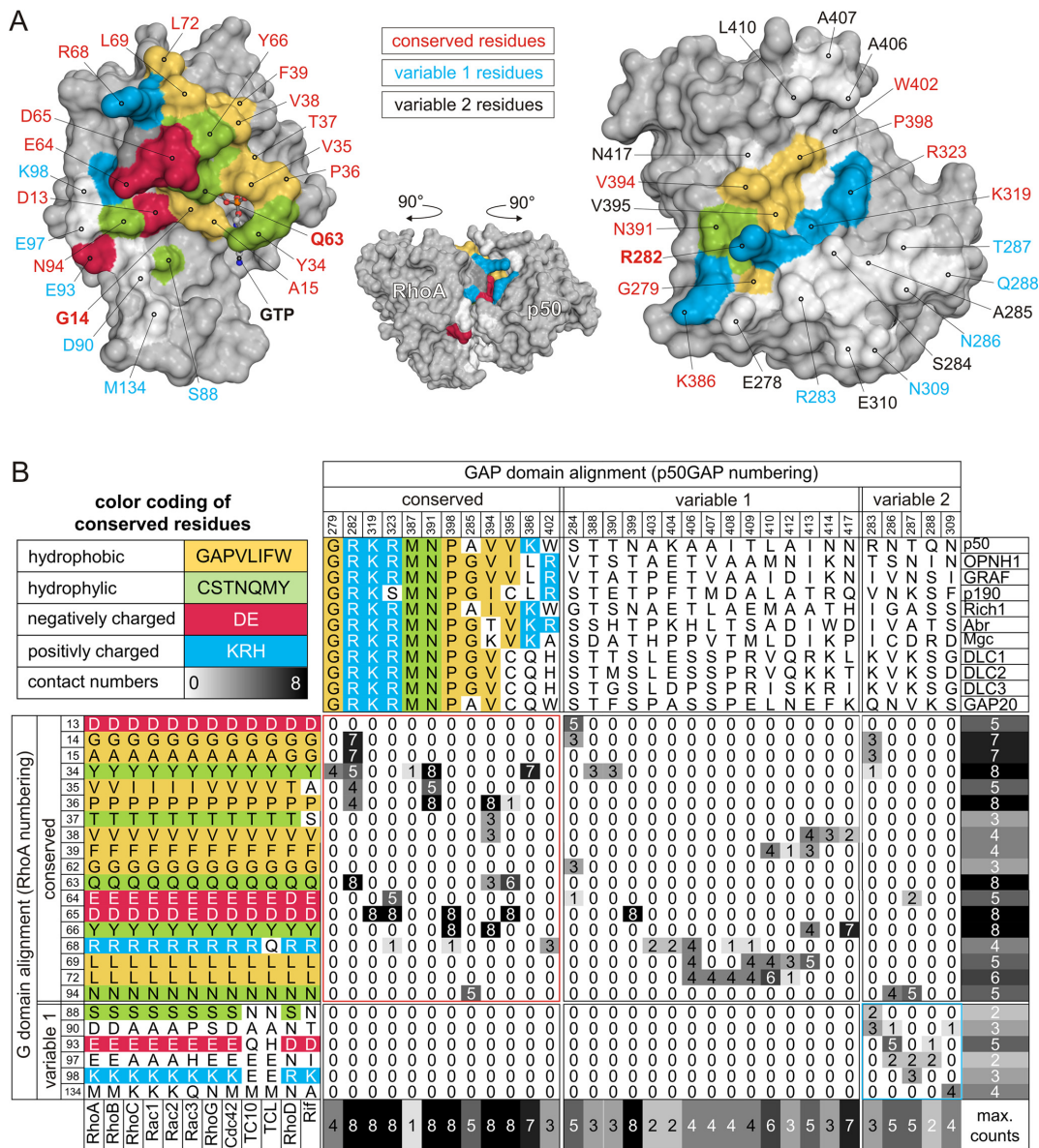
FIGURE 6. **Interaction interface between RHO and RHOGAP proteins.** *A,* interacting residues (<4 Å in distance; color-coded) of the RHO-RHOGAP complex are indicated using an open book representation (rotated 90° along a horizontal axis) of the crystal structure of the RHOA-p50 complex (PDB code 1TX4; RHOA, aa 1–181; p50, aa 236–431). Conserved and variable residues are shown in *red, blue,* and *black,* respectively. Coloring criteria were taken from the interaction matrix in *B. B,* interaction matrix of RHO and RHOGAP proteins. The interacting residues (<4 Å in distance) were determined using the six available crystal structures of RHO-RHOGAP proteins complexes counting eight distinct RHO-GAP pairs (supplemental Table S1). They are shown with corresponding residues from the alignment of the GAP and G domains of RHOGAPs and RHO proteins (supplemental Figs. S1 and S2) used in this study, respectively. Orientation numbers for interacting residues correspond to the numbering of p50 and RHOA, respectively. Residues sharing more than 60% sequence similarity in alignments (supplemental Figs. S1 and S2) are colored as follows: *yellow,* hydrophobic residues; *green,* hydrophilic residues; *blue,* positively charged residues; *red,* negatively charged residues. Numbers (*0–8*) in the *black-gray-white gradient-colored boxes* illustrate the respective contacts found in eight RHO-GAP pairs. *Red* and *blue boxes* represent contacts between conserved and variable regions, respectively.

complexes (supplemental Table S1). We note that the weak electron density around the residues 26–31 of RHOA did not allow us to fully build its switch I region.

Relating the complex structure to interaction matrix, non-zero matrix elements can predict possible interactions in the RHOA-p190 complex. A higher number of the element indi-

Molecular Basis of the RHOGAP Family Proteins
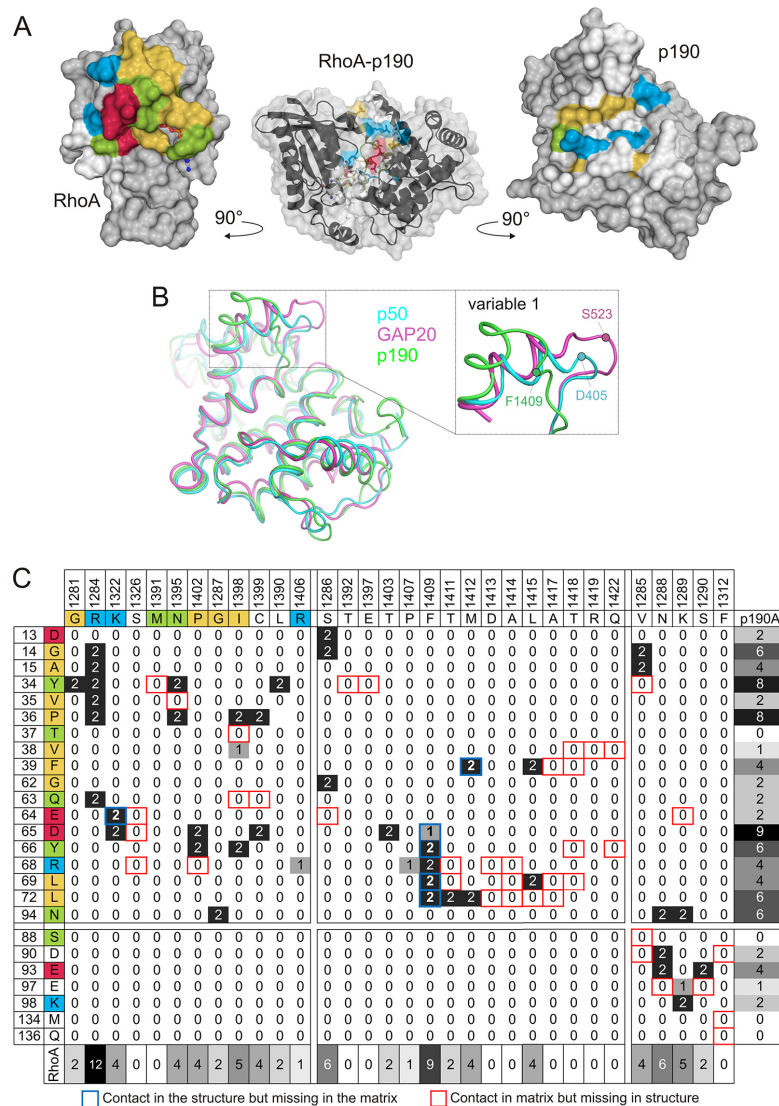
FIGURE 7. Interaction matrix adapted for the crystal structure of p190 in complex with RHOA. *A,* crystal structure of the RHOA-p190 complex (PDB code 5IRC) is illustrated in close representation as surface and ribbon (*middle panel*) and as open book representation rotated 90° along a horizontal axis. The interacting residues (<4 Å in distance) are color-coded as in Fig. 6. *B,* overlay of p190, p50, and ARHGAP20 structures. Overlay of p190 (PDB code 5IRC), p50 (PDB code 1TX4), and GAP20 (PDB code 3MSX) reveals high structural conservation except for the zoomed variable 1 region. *C,* interaction matrix calculated solely for the RHOA-p190 structure. Corresponding residues from p50 GAP are left as reference. Hot spots are *highlighted* in agreement with general interaction matrix in Fig. 6. Contacts missing or excessive in the RHOA-p190 structure are shown as *red* or *blue*, respectively.

cates higher probability of contact occurrence in complex (Fig. 6*B*). We have thus calculated interaction matrix only for RHOA-p190 complex structure and compared it with the original interaction matrix. The vast majority of conserved residues, which were predicted to be in the contacts, are indeed presented in the structure (Fig. 7). One exception is a conserved arginine at position 323 (Fig. 6*B, p50 numbering*), which is exclusively a serine in p190A (Ser-1326). These residues are supposed to interact with Glu-65 of RHOA. Structure of the

RHOA-p190 complex revealed that Ser-1326 at this site is in the vicinity of Glu-65 but is simply not long enough to form the contact with it (data not shown). Largest discrepancies between predicted and observed contacts comprise the interaction of "conserved" patches of RHO proteins and "variable 1" of RHOGAPs. The reason is that sequence alignment of all RHOGAPs (supplemental Fig. S1) contains in this region many gaps and shifts that preclude reliable prediction of its structure and proper assignment of similar residues. However, it has to be
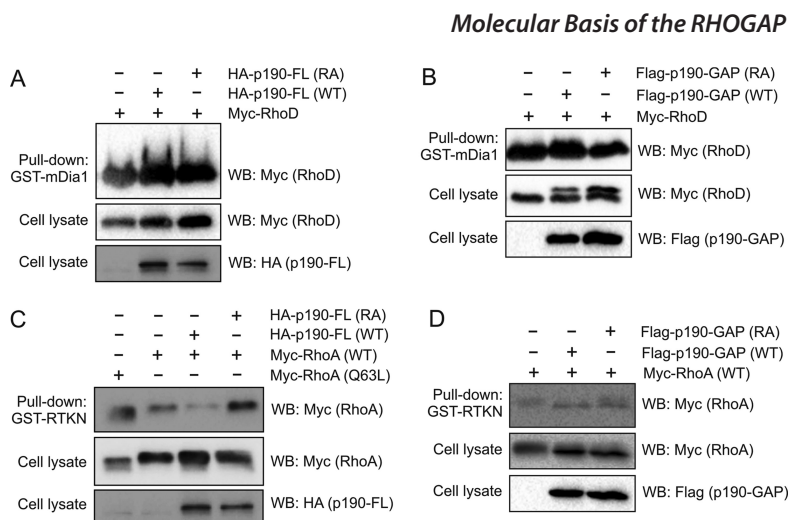
FIGURE 8. **p190-FL acts on RHOA in cells but not on RHOD.** Transiently expressed Myc-tagged RHOD (*A* and *B*) and RHOA (*C* and *D*) were pulled down from HEK293T cell lysates with RHO-binding domains of DIA1 and RTKN, respectively, as GST-fused proteins in the presence of either HA-tagged p190-FL (*A* and *C*) or FLAG-tagged p190GAP domain (*B* and *D*). R1284A and Q63L variants of p190 and RHOA were used in addition to wild type (*WT*). Immunoblots of pulled down samples and the cell lysates were performed using antibodies against the respective tags. *WB*, Western blot.

borne in mind that the interaction matrix was constructed on the basis of only four crystal structures. Including more structures for its calculation would certainly increase its reliability and enable more precise prediction of unknown complexes between RHO proteins and RHOGAPs.

p190 Acts on RHOA but Not on RHOD in Cells—An obviously demanding question is as follows. To what extent does the substrate selectivity of the RHOGAP domain determined in this study under cell-free conditions reflect the cell-based specificity of RHOGAPs and how relevant is that to multicomponent and multidomain cellular machineries? Addressing this question is of ultimate importance due to the fact that RHOGAPs did not in general reveal strong selectivity for some particular RHO proteins (Fig. 3; Table 2). An interesting observation in this regard is the high activity of p190 toward RHOD that is comparable with its activity toward RHOA (Fig. 4; Table 2). To answer the question of whether the p190 is also a GAP for RHOD in cells, we used GST fusion of DIA-RBD and RTKN-RBD to pull down GTP-bound RHOD and RHOA, respectively (38). Strikingly, the obtained data revealed that the amount of pulled down RHOD-GTP remained unchanged in cells overexpressing either full-length (FL) or the GAP domain of p190 (Fig. 8, *A* and *B*). Control experiments showed that p190-FL indeed acts as a GAP for RHOA, but overexpression of only the GAP domain failed to stimulate GTPase activity of RHOA (Fig. 8, *C* and *D*). These results provide a clear indication that other domains and motifs of p190-FL determine its specificity for RHOA in cells and not, for example, for RHOD. Extrapolating it on the activities of the GAP domains measured under cell-free conditions for members of the RHO family, we postulate that they are not directly proportional to specificities of GAP proteins within the cell.

Role of Other Domains as the Determinants of GAP Specificity—Results described above brought us the question about the activity of GAP domains in the context of the full-

length proteins and their niche within the cell. Another question in the same context is whether and to what extent GAPs can regulate multiple signaling pathways, which in turn seem to be dominated by the composition of their domains as illustrated with our data. Therefore, we conducted a phylogenetic analysis of 66 human RHOGAP proteins (Table 1) based only on the sequence of respective domains of the RHOGAP family members. The phylogenetic order correlated with the arrangement of proteins according to their domain and motif compositions (Fig. 1). We assigned so far 33 different domains with different properties (supplemental Table S4). The majority of them can be classified into the following three major groups: (i) lipid and membrane binding domains; (ii) peptide and protein interacting domains; and (iii) catalytic domains with enzyme activities (Fig. 1). Most widespread domains are pleckstrin homology (30), CC (25), P (16), Src homology 3 (15), and BAR/F-BAR (14). Most RHOGAPs have 3–4 additional domains, whereas CNT-D1 has another 10 and MYO9B even 11 domains (Fig. 1; supplemental Tables S4 and S5). Thirteen GAPs lack any additional putative domains but contain highly variable regions at their N and C termini. It is possible that these regions consist of not yet identified motifs, which may contribute to their specific function in the cell. ARHGAP11B is the smallest RHOGAP protein belonging to this group (Fig. 1; Table 1). A blast search of the terminal 63 and 17 amino acids of ARHGAP11B revealed a consensus motif, KLL(X_5)RED, at its C-terminal region, which exist in many proteins (data not shown). Both KLL and RED motifs have been reported to be involved in protein-protein interactions (39–41).

Discussion

General Profile, RHO Protein Selectivity of the GAP Domain—The most efficient activator of the GTPase reaction among investigated GAP domains is OPHN1 that stimulated GTP hydrolysis of RHOA and RHOB up to 5 orders of magnitude as compared with the other investigated RHOGAPs. Its

Molecular Basis of the RHOGAP Family Proteins

second striking feature is that it can efficiently deactivate a broad spectrum of investigated RHO proteins, including the RHO and RAC isoforms, CDC42, TC10, and TCL (Table 2). The ability to stimulate efficiently GTP hydrolysis of various RHO proteins was also observed for GRAF1, p190, and p50. These four GAPs are in general active on the same RHO proteins. Least susceptible are RHOG and RIF that could be in fact deactivated only by p50.

Although the GTP hydrolysis of RHOG was to a limited extent stimulated by OPHN1 and p190, there is no GAP in our set that could actually act on RIF. Remarkably, GTP hydrolysis of RHOD was only markedly stimulated by p190 and MGC. The spectrum of activity for MGC on the different RHO proteins is not as broad as the spectrum of above mentioned GAPs. Its activity on RHO isoforms is about 10-fold lower compared with RHOD, CDC42, and RAC isoforms, and it is practically inactive on TC10 and TCL. RICH1 was found to be even less effective, as it significantly stimulated GTP hydrolysis reaction of only TC10 and to a lesser extent of CDC42, RAC1, and RAC2. Interestingly, TCL, RHOG, and RHO isoforms are less sensitive to hydrolysis by RICH1, but in contrast, RHO isoforms appeared to be an exclusive substrate for DLC1. In fact, a unique selectivity was observed for the DLC1 GAP domain, which acts specifically on RHOB, RHOA, and RHOC (Table 2). ABR was the least effective, but it effectively deactivated RAC1 and RAC3. However, we do not designate it as selective for these RAC isoforms because its hydrolytic activity toward other GTPases was not so distinct as the activity of DLC1 for RHO proteins. DLC2 and DLC3 did not show any considerable GAP activity, an observation that raises the question whether these proteins still can be considered as RHOGAPs.

Taken together, there is no certain selectivity between investigated RHOGAP domains and particular RHO proteins or their isoforms. Our observation regarding the selectivity of GAP domains is in contrast to the guanine exchange factors (GEFs) of diffuse B-cell lymphoma (DBL) family that activate RHO proteins by accelerating the GDP/GTP exchange reaction. We showed in previous study that their isolated DBL homology (DH) domain, which is actually responsible for nucleotide exchange, showed both selectivity and specificity for their substrate RHO proteins (36). This finding challenges the fundamental principles of cell signaling exemplifying that there are two principally different manners of interplay between the RHO proteins and their regulatory proteins. In the first case of DBL family GEFs, the catalytic DH domain directly interacting with the substrate RHO protein is itself able to selectively discriminate among the RHO proteins, and other additional domains and motifs of the full-length RHOGEF protein provide an additional degree of regulation in the cell. In the second case, when the catalytic domains directly interacting with the substrate RHO proteins do not show any distinct selectivity, as we have found for the RHOGAP domains, secondary domains and motifs of the full-length RHOGAP inevitably determine, beyond other features, the specificity for the substrate RHO proteins. This is nicely demonstrated in this study by an example of p190 protein. Its GAP domain was equally and highly active on RHOA and RHOD under cell-free conditions, but its full-length version in the cells was able to specifically inactivate

only RHOA and not RHOD. The existence of multiple determinants in full-length RHOGAPs, which dictate their localized recruitment, activation, "specific" function in cells by including distinct protein and lipid interaction domains and motifs, as well as post-translational modification, has been suggested by several previous articles (18, 42–47). It has been shown that the spatial distribution of RHOGAPs and their specificity toward individual RHO proteins are controlled by their interactions with various proteins within signaling complexes (48, 49). Our results thus elegantly complement the scenario for the function of GAP proteins in which a concerted action of the whole protein is required. Accordingly, we conclude that p190 cannot be recruited to RHOD because it is RHOA-specific or that p190 and RHOD do not find each other under the used experimental conditions. We can, however, not exclude the possibility that p190 might specifically operate on RHOD in a specific cell type.

Pair Interaction and Interaction Matrix—To shed light on the molecular interactions of RHOGAPs with RHO proteins, we have analyzed available crystal structures of their complexes and combined the data about interacting residues with two multiple sequence alignments of investigated RHOGAPs and RHO proteins in the form of a structure-based interaction matrix (Fig. 6A). Such interaction matrix allows us to predict which residues of two sets of homologous proteins are likely to interact in their binary complexes. In addition, it provides a complete overview of the occurrence of particular contacts in analyzed structures as well as the conservation or variability of respective amino acids utilized by both GAP domain of RHOGAP proteins and G domain of RHO proteins upon interaction.

In terms of conservation, GAP side residues are largely variable (supplemental Fig. S2) in contrast to the RHO side residues, which are mostly identical. The variability of the latter originates almost exclusively from the helix 3 and the insert helix (Figs. 6 and supplemental Fig. S2). Reordering of residues in the matrix according to their conservation enabled us to divide hot spots into three distinct regions that also correspond to three exclusive regions on the interacting interface. Each of these regions also includes distinctive interacting pairs of amino acids (Fig. 6; supplemental Fig. S1–S3, *color-coded regions*). They can be classified into three different groups as follows: interaction pairs of conserved residues, pairs of variable residues on both sides, and the interactions of conserved residues on RHO side and variable residues on GAP side.

We have hoped that our analysis would reveal special distinctiveness in the interactions between RHO and RHOGAP proteins that could at least semi-quantitatively explain differences in observed activities. What we have found instead was an abundance of combinatorial possibilities and the complexity incorporated in the formation of binary protein complexes. To relate observed stimulations of GTP hydrolysis with sequence differences among investigated proteins and to describe them quantitatively, the contributions from all matrix points have to be considered. Each element in the matrix represents in principle the combination of 12 RHO protein and 10 RHOGAPs, *e.g.* 120 possibilities. To assess the contributions of all such combinations requires the evaluation of the impact of all different amino acids at each particular spot. For example, in the case of

invariant Tyr-34 of RHO proteins, all types of its interactions with leucine, lysine, or glutamine of GAPs at position 386 have to be considered (Figs. 6*B* and supplemental Fig. S3). The interaction properties of these amino acids are as diverse as their chemical properties. The situation is even more complex for the second discussed invariant Tyr-66 in RHO proteins because it contacts nine different amino acids of RHOGAPs (Fig. 6*B*). Spots that have variable residues on both sides of the matrix would require an even more thorough evaluation. Finally, an overall contribution of all individual elements from the interaction matrix would have to be correlated with observed differences in activities to obtain fully qualitative description.

Predicted RHOA-p190 Interacting Interface Verified by the Crystal Structure—Interaction matrix also allows to predict which residues of one RHO protein would interact with one of RHOGAPs. To validate this approach, we have solved the structure of RHOA-p190GAP complex (Fig. 7*A*), calculated the interaction matrix exclusively for this structure, and compared it with the original interaction matrix (Fig. 7*C*). As can be seen, a majority of residues interacting between conserved patches could be successfully anticipated. Most of deviated contacts pertain to the interactions between conserved RHO residues and variable 1 of RHOGAPs. The reason is the gaps in sequence alignment of GAP domains, namely in hypervariable regions (supplemental Fig. S1). They enable shifts of corresponding amino acids so their space positions in the presumed complex structures might differ from positions found in known structures. A comparison of three distinct RHOGAPs from complex structures (supplemental Table S1), *i.e.* p50, RAGAP20, and p190, nicely demonstrates that the conformation of this variable region is indeed very diverse. The whole loop in p190 comprising residues 1406–1419 is folded completely differently when compared with the corresponding loop of p50 (Fig. 7*B*). Interaction of this region of RHOGAPs with conserved residues of RHO proteins seems to be responsible for observed differences in their activities. However, interaction of conserved patches on both sides of complexes is preserved and exclusively determines the formation of the complex between RHO proteins and RHOGAPs.

Cellular Context, How the RHOGAPs Determine and Regulate Specificity—Several cell-based studies have shown that there is specificity between RHOGAP and RHO proteins as follows: ARHGAP15, BCR, β-chimaerin, 3BP1, p68RACGAP, and FILGAP are specific for RAC1 (29, 50–54); RALBP1 and MGCRACGAP1 are specific for both CDC42 and RAC1 (55–57); RICH1 and CDGAP are specific for CDC42 (58, 59); ARHGAP6, DLC1, DLC3, myosin IXb, OPHN1, p190A, and RA-RHOGAP are specific for RHOA (34, 47, 60–68); ARHGAP18, ARHGAP21, and DLC1 are specific for RHOC (64, 66, 69); TCGAP is specific for TC10 (70); PARG1 is specific for RHOA (71), and ARHGAP30 is specific for WRCH1 (72).

Our observations, however, show that RHOGAP domains are not able to selectively deactivate particular RHO protein or its isoforms. Such discrepancy raises the question of what other factors, processes, or circumstances may determine the specificity between RHOGAPs and RHO proteins. Cellular context is certainly crucial as, for example, studies on p190 (73, 74) and myosin IXb (75) showed that these proteins have different spec-

Molecular Basis of the RHOGAP Family Proteins

ificity *in vitro* and *in vivo*. There are several possibilities for the regulation of the GAP activity in cells ranging from intermolecular autoinhibition (β-chimerin, p50, OPHN1, and DLC1) (8, 30, 76, 77) to post-translational modifications (78). For instance, "activating" phosphorylation generates in p190 a new contact site for p120RASGAP (79), releases DLC1 from its autoinhibited state (76), or converts MGCGAP to a RHO-specific GAP (80). Furthermore, SUMOylation of ARHGAP21 may represent a way of guiding its function (81), and non-proteolytic ubiquitination of p250GAP controls axon growth (82).

The fact that almost all GAP proteins consist of several diverse domains and motifs strongly indicates that the regions accompanying the GAP domain are crucial for their function. Sixty-six GAPs identified in the human genome contain 33 different domains (Fig. 1; supplemental Tables S4 and S5). Some of them possess up to five different domains, and there are some proteins that contain four or even five copies of the same domain (Fig. 1; supplemental Table S5). Domain composition of GAPs together with the nature of individual domains demarcates on a higher level their subcellular localization and function. For example, the BAR domain of OPHN1 and GRAF1 is simultaneously involved in membrane tubulation and GAP inhibitory functions (8). The SEC14-like domain of p50 homology appears not only to regulate the GAP activity (77) but also to localize p50 in the endosomal membrane as a link between RHO and RAB proteins (83). Similarly, phospholipid binding to the C1 domain both recruits β-chimerin to the plasma membrane and activates its RACGAP activity (30). The RHOGAP activity of DLC1 has been proposed to be inhibited by an intramolecular interaction between the SAM and RHOGAP domains (84). Phosphorylation by CDK5 and association with both phospholipids and the scaffold proteins tensin and talin has been shown to release DLC1 from its inhibited state and to significantly promote its RHOGAP activity (67, 76, 84, 85). C2 or pleckstrin homology domains of GRAF, ABR, OPHN1, and MGC are the modules mediating association with the membrane according to the calcium-dependent phospholipid binding or phosphatidylinositol concentration (8, 31, 80, 86–90).

Being the smallest human RHOGAP, ARHGAP11B is not decorated with any known domain or motif (Fig. 1). The involvement of ARHGAP11B in neuronal development by promoting basal progenitor amplification and neocortex expansion has been reported recently (91). This study has shown that ARHGAP11B does not exhibit RHOGAP activity as compared with AHRGAP11A and its variants. However, its GAP activity was measured indirectly by monitoring more downstream RHOA/ROCK activity. ARHGAP11A and -11B share 90% identical sequences in their RHOGAP domain and mainly differ at the very C-terminal end (91), which is highly variable in all RHOGAPs (supplemental Fig. S1). Other residues that are essential for the RHOGAP activity are highly conserved in ARHGAP11B indicating that this GAP, although very small, may act as GAP for RHO proteins. In this context, the C-terminal KLL and RED motifs that were detected in a blast search in this study (see above) may play a role in protein-protein interactions (39–41).

Molecular Basis of the RHOGAP Family Proteins

Functionalization of the RHOGAPs with various modular building blocks, especially the membrane-associating domains, is a prerequisite for successful orchestration of a series of spatiotemporal events, including recruitment, subcellular localization, assembly of proactive protein complexes, and ultimately association with and inactivation of the substrate RHO protein. Reduced dimensionality on distinct regions of the cell membrane does not only achieve high specificity of the RHOGAPs but also tremendously enhances their overall catalytic activity.

Enhancing an Inefficient GAP or Using It for Very Slow Processes—The efficiency of a RHOGAP depends largely on the cellular processes, in which they are involved. There are very fast processes, *e.g.* calcium fluxes, exocytosis, or muscle contraction, and very slow processes, *e.g.* differentiation, apoptosis, or metabolism, which are also very much dependent on cell types. The GAP protein that is inefficient under cell-free conditions may efficiently operate through the function of its other domains in an appropriate cellular niche. An example is provided by DLC proteins that were mostly found as inefficient or even inactive in this study (Fig. 4). DLC1 has been thought to play a major role as a tumor suppressor probably in a GAP domain-independent manner (92). However, the DLC1 activity is, as compared with DLC2 and DLC3 activities, relatively high toward the RHO isoforms, RAC1, CDC42, and TC10 (Fig. 4). Thus, it is conceivable that additional mechanisms contribute to further enhancement of its GAP activity, comprising CDK5 phosphorylation, association with scaffold proteins, such as tensin and talin, and/or association with lipid membranes (67, 76, 84, 85). However, there are also mechanisms to inhibit the DLC1 RHOGAP activity, including phosphorylation by protein kinases C and D, and subsequent association with 14-3-3 proteins (62) or direct association of the Src homology 3 domain of p120RASGAP with its RHOGAP domain (32, 93). Similar regulatory mechanisms have been proposed for DLC2 and DLC3 (67) suggesting that inefficient RHOGAPs under cell-free conditions can be highly efficient in proper cellular context and appropriate protein network.

An inefficient GAP can otherwise be employed in the control of a slow cellular process, including actin dynamics. A group of nonconventional RHO proteins, such as RHOD, RIF, and RAC1b, mainly persists in their active state under resting conditions (35, 94). They accumulate in their GTP-bound state and thus are essentially dependent on a specific GAP to be switched off (35). Both RHOD and RIF are involved in the integration of cytoskeletal reorganization and membrane trafficking (95, 96); however, specific RHOGAPs for these atypical members of the RHO family remain to be discovered.

Not all RHOGAP Domain-containing Proteins Are GAPs—According to the mechanism of the GAP-stimulated GTPase reactions, the RHOGAP domain supplies an arginine finger directly into the active site of the substrate RHO proteins to stabilize the transition state (13, 97). A first inspection of the sequence alignment of the 66 RHOGAP domains revealed that ARHGAP36, CNT-D1, DEP1, DEP2, FAM13B, INPP5P, and OCRL1 lack an arginine finger at the corresponding position (supplemental Fig. S1). These proteins have serine, threonine, or glutamine instead and thus cannot substitute for the arginine

function. ARHGAP36 is poorly investigated. It has been shown to be involved in Gli transcription factor activation but independent on its GAP domain (98). The ARFGAP and RHOGAP domain-containing CNT-D1 (also called ARAP2; Table 1) lacks RHOGAP activity and acts as an ARF6 GAP (99). DEP1 and DEP2 coordinate cell cycle progression and interfere with RHOA and signaling despite lacking RHOGAP activity (100). OCRL1 has been shown to interact with GTP-bound RAC1 without the stimulation of its hydrolysis (101). p85α and p85β (85-kDa regulatory subunits of the phosphoinositide 3-kinases) can also be included on the list of RHOGAP-like proteins (Table 1; supplemental Fig. S1), as they do not show any detectable GAP activity toward different RHO proteins (102). An essential prerequisite of the GAP function is that the GAP domain, in order to position its catalytic residue Arg-282 (p50 numbering), must employ a number of amino acids that are responsible for binding and stabilizing the protein complex (Fig. 6A). Both p85 isoforms lack most of these binding determinants, *e.g.* Arg-323, Asn-391, Val-394, and Pro-398, along with the conserved amino acids around the arginine finger (p50 numbering; supplemental Fig. S3) (4).

Concluding Remarks—Unlike the RHOGEF domains (so-called DBL homology or DH domains), which exhibit high selectivity for the RHO-, CDC42-, and RAC-like proteins (36), we have found that the RHOGAP domain itself is nonselective and in some cases rather inefficient under cell-free conditions. Thus, we propose that other domains of RHOGAPs confer substrate specificity and fine-tune their catalytic efficiency in cells. They dictate the specificity of the respective RHOGAPs most likely through different successive steps as follows: (i) recruitment to a specific subcellular structure at a given time; (ii) release of its (auto)inhibited and most likely membrane-associated state; (iii) recognition and association with the substrate RHO protein; (iv) complementation of an inefficient active site with a catalytic arginine; (v) stimulation of GTPases reaction by orders of magnitudes; and (vi) finally dissociation from the inactivated GDP-bound RHO proteins. One approach of verifying this hypothesis is conducting RHOGAP domain-swapping experiments in cells using two RHOGAPs with verified specificities. Results may show that the specificity of these RHOGAPs remains unchanged irrespective of recombined RHOGAP domain.

Formation of binary complexes between two classes of proteins, such as RHO proteins and RHOGAPs, is a straightforward biochemical process. However, we have shown that its detailed description requires a sophisticated approach capable of covering a huge number of combinatorial possibilities incorporated in such molecular system. Our structural analysis based on the interaction matrix aspires to be such an approach. Its application led to the division of interacting interface into two parts. The first part determines the formation of complexes and supports the catalytic mechanism, and the second part is responsible for the diversity in catalytic activities. Although it remains to be proven whether such an approach is also applicable to other protein systems, we believe that its further elaboration will enable a precise prediction of interacting residues in the unknown structure of complexes between RHO proteins and RHOGAPs.

A critical issue regarding experimental determination of the specificity of RHOGAPs in cells is that arginine finger mutants, mostly to alanine (RA mutant), are often used to compromise the RHOGAP function. This approach is in principle very useful under cell-free conditions but is not really optimal in the cells because an RA mutant may provide a similar readout as the wild type; it interferes with downstream signaling by competing with the effector(s) for binding to the RHO proteins. RHOGAP mutants at this site are able to persistently bind to and sequester the target RHO protein. This most likely displays a similar readout as the activity of wild type RHOGAP. Instead of the catalytic arginine, we recommend mutating critical "binding determinants," particularly Lys-319 and Arg-323 (p50 numbering; Figs. 6 and 7*B*). Charge reversal of these residues most likely leads to loss of RHOGAP association with its substrate RHO proteins and consequently the activity of the GAP domain. This is not only a tool for determining the specificity of RHOGAPs but also for investigating GAP domain-independent function(s) of the RHOGAPs.

Experimental Procedures

Constructs—Constructs containing the GAP domain of human p50 (amino acids or aa 198–439), GRAF1 (aa 383–583), RICH1 (aa 245–499), p190A (aa 1250–1531), OPHN1 (aa 375–583), ABR (aa 559–822), MGCRACGAP (aa 343–620), DLC1 (aa 609–878), DLC2 (aa 644–916), and DLC3 (aa 620–890) were amplified by standard PCR and cloned in either pGEX-4T1 or pGEX-4T1-Ntev vector. All RHO protein constructs have been reported before (35). Human RHOA, its Gln-63 variant to leucine (Q63L mutant), and RHOD were cloned in pRK5-Myc. Human p190-FL and its GAP domain and their Arg-1284 variant to alanine (RA mutant) were cloned in HA-pKH3 and pRK5, respectively. Rat p190 GAP domain (1242–1439) was cloned into pGST-parallel vector (103).

Proteins—All RHO proteins and GAP domains of RHOGAPs were purified as glutathione *S*-transferase (GST) fusion proteins from *Escherichia coli* BL21(DE3) pLysS or CodonPlusRIL as described previously (2, 104). All RHO proteins and their nucleotide-free forms were prepared as described (2, 105).

Fluorescent Nucleotides—Various fluorescence reporter groups, including mant, tamra, and cy3, have been coupled to 2′(3′)-hydroxyl group of the ribose moiety of the guanine nucleotide GTP via ethylenediamine to obtain fluorescent GTP variants (Jena Bioscience, Germany) for the analysis of the GAP-stimulated GTP hydrolysis reactions of the RHO proteins.

Kinetics Measurements—All GAP-stimulated GTP hydrolysis fluorescence measurements of RHO proteins were performed at 25 °C. Fluorescent GTP-bound RHO proteins (pre-mixing 0.3 μM nucleotide-free RHO and 0.2 μM tamra-/cy3-labeled GTP) and the catalytic domain of RHOGAPs (10 μM) were rapidly mixed in a buffer containing 30 mM Tris-HCl, pH 7.5, 10 mM $KH_2PO_4 \cdot K_2HPO_4$, 10 mM $MgCl_2$, and 3 mM dithiothreitol using a Hi-Tech Scientific (SF-61) stopped-flow spectrophotometer instrument with mercury xenon light source as described (32). For excitation, wavelengths of 546 and 550 nm were used for tamra and cy3 fluorophores, respectively,

and a 570 nm (tamra and cy3) cutoff filter (Schott glass) was used to collect emitted light.

Sequence and Structural Analysis—Sequence alignments were performed with BioEdit program using ClustalW algorithm (106). The intermolecular contacts were determined ($\leq$4.0 Å) between RHOGAP and RHO proteins using available RHO-RHOGAP complex structures in the Protein Data Bank (supplemental Table S1). A python code has been written including BioPython modules (pairwise2 and SubsMat.Matrix-Info) (107) to get PDB and alignment files and returns corresponding interaction pairs in a matrix form. RHOGAP domains discussed in the matrix have sequence similarities between 20 and 80% (supplemental Table S2) (108) and are assumed to have identical fold and form molecular complexes with similar arrangement. All structural representations were generated using PyMOL viewer (109).

Structure Determination—A mixture of RHOA-GDP and p190-GAP with a small molar excess of RHOA was dialyzed overnight in a buffer, containing 20 mM Hepes, 100 mM NaCl, 5 mM NaF, 5 mM $MgCl_2$, 5 mM β-mercaptoethanol. The sample was loaded on a Superdex 200 gel filtration column. Fractions containing RHOA-GDP-MgF$_3^-$-p190-GAP complex were pooled and concentrated to 8 mg/ml for crystallization trials. The vapor diffusion method was used for crystallization with sitting drops of 1:1 ratio of protein and crystallization reagent. Best crystals grew from JSCG+ screen (Molecular Dimensions) reagent 82. The crystallization conditions were further optimized, and a buffer, containing 30% PEG2000 MME, 0.15 M KCSN in 0.1 M MES, pH 6.5, produced crystals of diffraction quality. For data collection the crystals were frozen in a cryosolution containing mother liquor with an addition of 0.2 M ascorbic acid and 12.5% glycerol. X-ray data were collected at Argonne National Laboratory, South-Eastern Region Collaborative Access Team (SER-CAT) beamline of Advanced Photon Source (supplemental Table S3). The structure was solved by molecular replacement method using program Balbes (110) and refined using Phenix (111). Manual rebuilding of the model during refinement was performed using Coot (112). Final refinement statistics can be found in Table S3. Structure was deposited with PDB accession number 5IRC.

Pulldown Assay—RHOD and RHOA were pulled down in their activated states as described previously (38), and HEK293T cells were seeded in 6-cm dishes. Next day, cells were transfected with 2 μg of DNA of pRK5-Myc-RHOA or pRK5-Myc-RHOD together with 1 μg of DNA of HA-pKH3-p190-FL (WT) or pRK5-FLAG-p190-GAP domain using the PolyPlus JetPEI transfection reagent. Cells were incubated 24 h post-transfection, followed by lysis in ice-cold buffer, including 50 mM Tris-HCl, pH 7.5, 1% Triton X-100, 150 mM NaCl, 10 mM $MgCl_2$, and protease inhibitor mixture (cOmplete™, EDTA-free, Roche Applied Science). Cell lysates were transferred to pre-chilled tubes and centrifuged at 13,000 rpm for 5 min at 4 °C. 1/25th of each cell lysate was transferred to a new tube, and 3× SDS-PAGE sample buffer was added. The rest of the sample lysates were transferred to new tubes, and GST fusion proteins on glutathione beads were added. GST-RTKN was added to the pRK5-Myc-RHOA samples and GST-DIA1 to the pRK5-Myc-RHOD samples. GST-RTKN and GST-DIA1 were

Molecular Basis of the RHOGAP Family Proteins

overexpressed in *E. coli* and isolated from the lysate using glutathione beads as described previously (38). Samples were carefully rotated at 4 °C for 10 min and then centrifuged and washed four times with 0.5 ml of ice-cold buffer, including 50 mM Tris-HCl, pH 7.5, 1% Triton X-100, 150 mM NaCl, 10 mM MgCl$_2$. SDS-PAGE sample buffer (3×) was added to each sample. Samples were separated on 10% SDS-polyacrylamide gels followed by transfer to nitrocellulose membrane. Proteins were detected with 9E10 mouse monoclonal anti-c-Myc antibody (Covance), 12CA5 mouse monoclonal anti-HA antibody (Roche Applied Science), and M2 mouse monoclonal anti-FLAG antibody (Sigma).

References

1. Dvorsky, R., and Ahmadian, M. R. (2004) Always look on the bright site of Rho: structural implications for a conserved intermolecular interface. *EMBO Rep.* **5,** 1130–1136
2. Jaiswal, M., Dubey, B. N., Koessmeier, K. T., Gremer, L., and Ahmadian, M. R. (2012) in *Rho GTPases Methods and Protocols* (Rivero, F., ed) pp. 37–58, Springer, Germany
3. Zhang, B., and Zheng, Y. (1998) Regulation of RhoA GTP hydrolysis by the GTPase-activating proteins p190, p50RhoGAP, Bcr, and 3BP-1. *Biochemistry* **37,** 5249–5257
4. Fidyk, N. J., and Cerione, R. A. (2002) Understanding the catalytic mechanism of GTPase-activating proteins: demonstration of the importance of switch domain stabilization in the stimulation of GTP hydrolysis. *Biochemistry* **41,** 15644–15653
5. Haeusler, L. C., Blumenstein, L., Stege, P., Dvorsky, R., and Ahmadian, M. R. (2003) Comparative functional analysis of the RAC GTPases. *FEBS Lett.* **555,** 556–560
6. Eberth, A., Dvorsky, R., Becker, C. F., Beste, A., Goody, R. S., and Ahmadian, M. R. (2005) Monitoring the real time kinetics of the hydrolysis reaction of guanine nucleotide-binding proteins. *Biol. Chem.* **386,** 1105–1114
7. Kötting, C., and Gerwert, K. (2013) The dynamics of the catalytic site in small GTPases, variations on a common motif. *FEBS Lett.* **587,** 2025–2027
8. Eberth, A., Lundmark, R., Gremer, L., Dvorsky, R., Koessmeier, K. T., McMahon, H. T., and Ahmadian, M. R. (2009) A BAR domain-mediated autoinhibitory mechanism for RhoGAPs of the GRAF family. *Biochem. J.* **417,** 371–377
9. Graham, D. L., Eccleston, J. F., and Lowe, P. N. (1999) The conserved arginine in rho-GTPase-activating protein is essential for efficient catalysis but not for complex formation with Rho·GDP and aluminum fluoride. *Biochemistry* **38,** 985–991
10. Nassar, N., Hoffman, G. R., Manor, D., Clardy, J. C., and Cerione, R. A. (1998) Structures of CDC42 bound to the active and catalytically compromised forms of CDC42GAP. *Nat. Struct. Biol.* **5,** 1047–1052
11. Barrett, T., Xiao, B., Dodson, E. J., Dodson, G., Ludbrook, S. B., Nurmahomed, K., Gamblin, S. J., Musacchio, A., Smerdon, S. J., and Eccleston, J. F. (1997) The structure of the GTPase-activating domain from p50rhoGAP. *Nature* **385,** 458–461
12. Rittinger, K., Walker, P. A., Eccleston, J. F., Nurmahomed, K., Owen, D., Laue, E., Gamblin, S. J., and Smerdon, S. J. (1997) Crystal structure of a small G protein in complex with the GTPase-activating protein rhoGAP. *Nature* **388,** 693–697
13. Scheffzek, K., Ahmadian, M. R., and Wittinghofer, A. (1998) GTPase-activating proteins: helping hands to complement an active site. *Trends Biochem. Sci.* **23,** 257–262
14. Ahmadian, M. R., Mittal, R., Hall, A., and Wittinghofer, A. (1997) Aluminum fluoride associates with the small guanine nucleotide binding proteins. *FEBS Lett.* **408,** 315–318
15. Stebbins, C. E., and Galán, J. E. (2000) Modulation of host signaling by a bacterial mimic: structure of the *Salmonella* effector SptP bound to RAC1. *Mol. Cell* **6,** 1449–1460
16. Würtele, M., Wolf, E., Pederson, K. J., Buchwald, G., Ahmadian, M. R., Barbieri, J. T., and Wittinghofer, A. (2001) How the *Pseudomonas aeruginosa* ExoS toxin downregulates RAC. *Nat. Struct. Biol.* **8,** 23–26
17. Evdokimov, A. G., Tropea, J. E., Routzahn, K. M., and Waugh, D. S. (2002) Crystal structure of the *Yersinia pestis* GTPase activator YopE. *Protein Sci.* **11,** 401–408
18. Tcherkezian, J., and Lamarche-Vane, N. (2007) Current knowledge of the large RhoGAP family of proteins. *Biol. Cell* **99,** 67–86
19. Brandão, M. M., Silva-Brandão, K. L., Costa, F. F., and Saad, S. T. (2006) Phylogenetic analysis of RhoGAP domain-containing proteins. *Genomics Proteomics Bioinformatics* **4,** 182–188
20. Peck, J., Douglas, G., 4th, Wu, C. H., and Burbelo, P. D. (2002) Human RhoGAP domain-containing proteins: structure, function and evolutionary relationships. *FEBS Lett.* **528,** 27–34
21. Moon, S. Y., and Zheng, Y. (2003) Rho GTPase-activating proteins in cell regulation. *Trends Cell Biol.* **13,** 13–22
22. Csépányi-Kömi, R., Sáfár, D., Grósz, V., Tarján, Z. L., and Ligeti, E. (2013) *In silico* tissue-distribution of human Rho family GTPase activating proteins. *Small GTPases* **4,** 90–101
23. Lamarche, N., and Hall, A. (1994) GAPs for rho-related GTPases. *Trends Genet.* **10,** 436–440
24. Kandpal, R. P. (2006) Rho GTPase activating proteins in cancer phenotypes. *Curr. Protein Pept. Sci.* **7,** 355–365
25. Bernards, A., and Settleman, J. (2005) GAPs in growth factor signalling. *Growth Factors* **23,** 143–149
26. Garrett, M. D., Self, A. J., van Oers, C., and Hall, A. (1989) Identification of distinct cytoplasmic targets for ras/R-ras and rho regulatory proteins. *J. Biol. Chem.* **264,** 10–13
27. Hart, M. J., Shinjo, K., Hall, A., Evans, T., and Cerione, R. A. (1991) Identification of the human platelet GTPase activating protein for the CDC42Hs protein. *J. Biol. Chem.* **266,** 20840–20848
28. Settleman, J., Albright, C. F., Foster, L. C., and Weinberg, R. A. (1992) Association between GTPase activators for Rho and Ras families. *Nature* **359,** 153–154
29. Diekmann, D., Brill, S., Garrett, M. D., Totty, N., Hsuan, J., Monfries, C., Hall, C., Lim, L., and Hall, A. (1991) Bcr encodes a GTPase-activating protein for p21rac. *Nature* **351,** 400–402
30. Canagarajah, B., Leskow, F. C., Ho, J. Y., Mischak, H., Saidi, L. F., Kazanietz, M. G., and Hurley, J. H. (2004) Structural mechanism for lipid activation of the RAC-specific GAP, β2-chimaerin. *Cell* **119,** 407–418
31. Bernards, A., and Settleman, J. (2004) GAP control: regulating the regulators of small GTPases. *Trends Cell Biol.* **14,** 377–385
32. Jaiswal, M., Dvorsky, R., Amin, E., Risse, S. L., Fansa, E. K., Zhang, S. C., Taha, M. S., Gauhar, A. R., Nakhaei-Rad, S., Kordes, C., Koessmeier, K. T., Cirstea, I. C., Olayioye, M. A., Häussinger, D., and Ahmadian, M. R.

Molecular Basis of the RHOGAP Family Proteins

(2014) Functional crosstalk between Ras and Rho pathways: p120RasGAP competitively inhibits the RhoGAP activity of Deleted in Liver Cancer (DLC) tumor suppressors by masking its catalytic arginine finger. *J. Biol. Chem.* **289,** 6839–6849

33. Ohta, Y., Hartwig, J. H., and Stossel, T. P. (2006) FilGAP, a Rho- and ROCK-regulated GAP for RAC binds filamin A to control actin remodelling. *Nat. Cell Biol.* **8,** 803–814

34. Fauchereau, F., Herbrand, U., Chafey, P., Eberth, A., Koulakoff, A., Vinet, M. C., Ahmadian, M. R., Chelly, J., and Billuart, P. (2003) The RhoGAP activity of OPHN1, a new F-actin-binding protein, is negatively controlled by its amino-terminal domain. *Mol. Cell. Neurosci.* **23,** 574–586

35. Jaiswal, M., Fansa, E. K., Dvorsky, R., and Ahmadian, M. R. (2013) New insight into the molecular switch mechanism of human Rho family proteins: shifting a paradigm. *Biol. Chem.* **394,** 89–95

36. Jaiswal, M., Dvorsky, R., and Ahmadian, M. R. (2013) Deciphering the molecular and functional basis of Dbl family proteins: a novel systematic approach toward classification of selective activation of the Rho family proteins. *J. Biol. Chem.* **288,** 4486–4500

37. Ahmadian, M. R., Stege, P., Scheffzek, K., and Wittinghofer, A. (1997) Confirmation of the arginine-finger hypothesis for the GAP-stimulated GTP-hydrolysis reaction of Ras. *Nat. Struct. Biol.* **4,** 686–689

38. Edlund, S., Landström, M., Heldin, C. H., and Aspenström, P. (2002) Transforming growth factor-β-induced mobilization of actin cytoskeleton requires signaling by small GTPases CDC42 and RhoA. *Mol. Biol. Cell* **13,** 902–914

39. Guo, X., Engel, J. L., Xiao, J., Tagliabracci, V. S., Wang, X., Huang, L., and Dixon, J. E. (2011) UBLCP1 is a 26S proteasome phosphatase that regulates nuclear proteasome activity. *Proc. Natl. Acad. Sci. U.S.A.* **108,** 18649–18654

40. Fan, L., Arvai, A. S., Cooper, P. K., Iwai, S., Hanaoka, F., and Tainer, J. A. (2006) Conserved XPB core structure and motifs for DNA unwinding: implications for pathway selection of transcription or excision repair. *Mol. Cell* **22,** 27–37

41. Chen, B., Liu, H., Sun, X., and Yang, C. G. (2010) Mechanistic insight into the recognition of single-stranded and double-stranded DNA substrates by ABH2 and ABH3. *Mol. Biosyst.* **6,** 2143–2149

42. Boulter, E., Estrach, S., Garcia-Mata, R., and Féral, C. C. (2012) Off the beaten paths: alternative and crosstalk regulation of Rho GTPases. *FASEB J.* **26,** 469–479

43. Nakamura, F. (2013) FilGAP and its close relatives: a mediator of Rho-RAC antagonism that regulates cell morphology and migration. *Biochem. J.* **453,** 17–25

44. Moon, S. Y., Zang, H., and Zheng, Y. (2003) Characterization of a brain-specific Rho GTPase-activating protein, p200RhoGAP. *J. Biol. Chem.* **278,** 4151–4159

45. Csépányi-Kömi, R., Lévay, M., and Ligeti, E. (2012) Rho/RACGAPs: embarras de richesse? *Small GTPases* **3,** 178–182

46. Lua, B. L., and Low, B. C. (2004) BPGAP1 interacts with cortactin and facilitates its translocation to cell periphery for enhanced cell migration. *Mol. Biol. Cell* **15,** 2873–2883

47. Wennerberg, K., Forget, M. A., Ellerbroek, S. M., Arthur, W. T., Burridge, K., Settleman, J., Der, C. J., and Hansen, S. H. (2003) Rnd proteins function as RhoA antagonists by activating p190 RhoGAP. *Curr. Biol.* **13,** 1106–1115

48. Shang, X., Zhou, Y. T., and Low, B. C. (2003) Concerted regulation of cell dynamics by BNIP-2 and CDC42GAP homology/Sec14p-like, proline-rich, and GTPase-activating protein domains of a novel Rho GTPase-activating protein, BPGAP1. *J. Biol. Chem.* **278,** 45903–45914

49. Okada, H., Uezu, A., Mason, F. M., Soderblom, E. J., Moseley, M. A., 3rd, and Soderling, S. H. (2011) SH3 domain-based phototrapping in living cells reveals Rho family GAP signaling complexes. *Sci. Signal.* **4,** 1–17

50. Cicchetti, P., Ridley, A. J., Zheng, Y., Cerione, R. A., and Baltimore, D. (1995) 3BP-1, an SH3 domain binding protein, has GAP activity for RAC and inhibits growth factor-induced membrane ruffling in fibroblasts. *EMBO J.* **14,** 3127–3135

51. Caloca, M. J., Wang, H., and Kazanietz, M. G. (2003) Characterization of the RAC-GAP (RAC-GTPase-activating protein) activity of β2-chima-

erin, a 'non-protein kinase C' phorbol ester receptor. *Biochem. J.* **375,** 313–321

52. Aitsebaomo, J., Wennerberg, K., Der, C. J., Zhang, C., Kedar, V., Moser, M., Kingsley-Kallesen, M. L., Zeng, G. Q., and Patterson, C. (2004) p68RACGAP is a novel GTPase-activating protein that interacts with vascular endothelial zinc finger-1 and modulates endothelial cell capillary formation. *J. Biol. Chem.* **279,** 17963–17972

53. Radu, M., Rawat, S. J., Beeser, A., Iliuk, A., Tao, W. A., and Chernoff, J. (2013) ArhGAP15, a RAC-specific GTPase-activating protein, plays a dual role in inhibiting small GTPase signaling. *J. Biol. Chem.* **288,** 21117–21125

54. Nakahara, S., Tsutsumi, K., Zuinen, T., and Ohta, Y. (2015) FilGAP, a Rho-ROCK-regulated GAP for RAC, controls adherens junctions in MDCK cells. *J. Cell Sci.* **128,** 2047–2056

55. Richnau, N., and Aspenström, P. (2001) Rich, a rho GTPase-activating protein domain-containing protein involved in signaling by CDC42 and RAC1. *J. Biol. Chem.* **276,** 35060–35070

56. Jullien-Flores, V., Dorseuil, O., Romero, F., Letourneur, F., Saragosti, S., Berger, R., Tavitian, A., Gacon, G., and Camonis, J. H. (1995) Bridging Ral GTPase to Rho pathways. RLIP76, a Ral effector with CDC42/RAC
GTPase-activating protein activity. *J. Biol. Chem.* **270,** 22473–22477

57. Touré, A., Dorseuil, O., Morin, L., Timmons, P., Jégou, B., Reibel, L., and Gacon, G. (1998) MGCRACGAP, a new human GTPase-activating protein for RAC and CDC42 similar to *Drosophila* rotundRAC-GAP gene product, is expressed in male germ cells. *J. Biol. Chem.* **273,** 6019–6023

58. Karimzadeh, F., Primeau, M., Mountassif, D., Rouiller, I., and Lamarche-Vane, N. (2012) A stretch of polybasic residues mediates CDC42 GTPase-activating protein (CdGAP) binding to phosphatidylinositol 3,4,5-trisphosphate and regulates its GAP activity. *J. Biol. Chem.* **287,** 19610–19621

59. Wells, C. D., Fawcett, J. P., Traweger, A., Yamanaka, Y., Goudreault, M., Elder, K., Kulkarni, S., Gish, G., Virag, C., Lim, C., Colwill, K., Starostine, A., Metalnikov, P., and Pawson, T. (2006) A RICH1/Amot complex regulates the CDC42 GTPase and apical-polarity proteins in epithelial cells. *Cell* **125,** 535–548

60. Prakash, S. K., Paylor, R., Jenna, S., Lamarche-Vane, N., Armstrong, D. L., Xu, B., Mancini, M. A., and Zoghbi, H. Y. (2000) Functional analysis of ARHGAP6, a novel GTPase-activating protein for RhoA. *Hum. Mol. Genet.* **9,** 477–488

61. Yamada, T., Sakisaka, T., Hisata, S., Baba, T., and Takai, Y. (2005) RA-RhoGAP, Rap-activated Rho GTPase-activating protein implicated in neurite outgrowth through Rho. *J. Biol. Chem.* **280,** 33026–33034

62. Scholz, R. P., Regner, J., Theil, A., Erlmann, P., Holeiter, G., Jähne, R., Schmid, S., Hausser, A., and Olayioye, M. A. (2009) DLC1 interacts with 14-3-3 proteins to inhibit RhoGAP activity and block nucleocytoplasmic shuttling. *J. Cell Sci.* **122,** 92–102

63. Asnaghi, L., Vass, W. C., Quadri, R., Day, P. M., Qian, X., Braverman, R., Papageorge, A. G., and Lowy, D. R. (2010) E-cadherin negatively regulates neoplastic growth in non-small cell lung cancer: role of Rho GTPases. *Oncogene* **29,** 2760–2771

64. Lazarini, M., Traina, F., Machado-Neto, J. A., Barcellos, K. S., Moreira, Y. B., Brandão, M. M., Verjovski-Almeida, S., Ridley, A. J., and Saad, S. T. (2013) ARHGAP21 is a RhoGAP for RhoA and RhoC with a role in proliferation and migration of prostate adenocarcinoma cells. *Biochim. Biophys. Acta* **1832,** 365–374

65. Xu, Y., Pektor, S., Balkow, S., Hemkemeyer, S. A., Liu, Z., Grobe, K., Hanley, P. J., Shen, L., Bros, M., Schmidt, T., Bähler, M., and Grabbe, S. (2014) Dendritic cell motility and T cell activation requires regulation of Rho-cofilin signaling by the Rho-GTPase activating protein myosin IXb. *J. Immunol.* **192,** 3559–3568

66. Tripathi, V., Popescu, N. C., and Zimonjic, D. B. (2014) DLC1 induces expression of E-cadherin in prostate cancer cells through Rho pathway and suppresses invasion. *Oncogene* **33,** 724–733

67. Braun, A. C., Hendrick, J., Eisler, S. A., Schmid, S., Hausser, A., and Olayioye, M. A. (2015) The Rho-specific GAP protein DLC3 coordinates endocytic membrane trafficking. *J. Cell Sci.* **128,** 1386–1399

Molecular Basis of the RHOGAP Family Proteins

68. Fotinos, A., Klier, M., Gowert, N. S., Münzer, P., Klatt, C., Beck, S., Borst, O., Billuart, P., Schaller, M., Lang, F., Gawaz, M., and Elvers, M. (2015) Loss of oligophrenin1 leads to uncontrolled Rho activation and increased thrombus formation in mice. *J. Thromb. Haemost.* **13,** 619–630

69. Chang, G. H., Lay, A. J., Ting, K. K., Zhao, Y., Coleman, P. R., Powter, E. E., Formaz-Preston, A., Jolly, C. J., Bower, N. I., Hogan, B. M., Rinkwitz, S., Becker, T. S., Vadas, M. A., and Gamble, J. R. (2014) ARHGAP18: an endogenous inhibitor of angiogenesis, limiting tip formation and stabilizing junctions. *Small GTPases* **5,** 1–15

70. Chiang, S. H., Hwang, J., Legendre, M., Zhang, M., Kimura, A., and Saltiel, A. R. (2003) TCGAP, a multidomain Rho GTPase-activating protein involved in insulin-stimulated glucose transport. *EMBO J.* **22,** 2679–2691

71. Saras, J., Franzén, P., Aspenström, P., Hellman, U., Gonez, L. J., and Heldin, C. H. (1997) A novel GTPase-activating protein for Rho interacts with a PDZ domain of the protein-tyrosine phosphatase PTPL1. *J. Biol. Chem.* **272,** 24333–24338

72. Naji, L., Pacholsky, D., and Aspenström, P. (2011) ARHGAP30 is a WRCH-1-interacting protein involved in actin dynamics and cell adhesion. *Biochem. Biophys. Res. Commun.* **409,** 96–102

73. Settleman, J., Narasimhan, V., Foster, L. C., and Weinberg, R. A. (1992) Molecular cloning of cDNAs encoding the GAP-associated protein p190: implications for a signaling pathway from ras to the nucleus. *Cell* **69,** 539–549

74. Ridley, A. J., Self, A. J., Kasmi, F., Paterson, H. F., Hall, A., Marshall, C. J., and Ellis, C. (1993) Rho family GTPase activating proteins p190, bcr and rhoGAP show distinct specificities *in vitro* and *in vivo*. *EMBO J.* **12,** 5151–5160

75. Wirth, J. A., Jensen, K. A., Post, P. L., Bement, W. M., and Mooseker, M. S. (1996) Human myosin-IXb, an unconventional myosin with a chimerin-like rho/rac GTPase-activating protein domain in its tail. *J. Cell Sci.* **109,** 653–661

76. Tripathi, B. K., Qian, X., Mertins, P., Wang, D., Papageorge, A. G., Carr, S. A., and Lowy, D. R. (2014) CDK5 is a major regulator of the tumor suppressor DLC1. *J. Cell Biol.* **207,** 627–642

77. Moskwa, P., Paclet, M. H., Dagher, M. C., and Ligeti, E. (2005) Autoinhibition of p50 Rho GTPase-activating protein (GAP) is released by prenylated small GTPases. *J. Biol. Chem.* **280,** 6716–6720

78. Csépányi-Kömi, R., Lévay, M., and Ligeti, E. (2012) Small G proteins and their regulators in cellular signalling. *Mol. Cell. Endocrinol.* **353,** 10–20

79. Chang, J. H., Gill, S., Settleman, J., and Parsons, S. J. (1995) c-Src regulates the simultaneous rearrangement of actin cytoskeleton, p190RhoGAP, and p120RasGAP following epidermal growth factor stimulation. *J. Cell Biol.* **130,** 355–368

80. Minoshima, Y., Kawashima, T., Hirose, K., Tonozuka, Y., Kawajiri, A., Bao, Y. C., Deng, X., Tatsuka, M., Narumiya, S., May, W. S., Jr, Nosaka, T., Semba, K., Inoue, T., Satoh, T., Inagaki, M., and Kitamura, T. (2003) Phosphorylation by aurora B converts MgcRacGAP to a RhoGAP during cytokinesis. *Dev. Cell* **4,** 549–560

81. Bigarella, C. L., Ferro, K. P., Barcellos, K. S., Martins-de-Souza, D., Traina, F., Novello, J. C., Saad, S. T., and Archangelo, L. F. (2012) Posttranslational modification of the RhoGTPase activating protein 21, ARHGAP21, by SUMO2/3. *FEBS Lett.* **586,** 3522–3528

82. Kannan, M., Lee, S. J., Schwedhelm-Domeyer, N., Nakazawa, T., and Stegmüller, J. (2012) p250GAP is a novel player in the Cdh1-APC/Smurf1 pathway of axon growth regulation. *PLoS ONE* **7,** e50735

83. Sirokmány, G., Szidonya, L., Káldi, K., Gáborik, Z., Ligeti, E., and Geiszt, M. (2006) Sec14 homology domain targets p50RhoGAP to endosomes and provides a link between Rab and Rho GTPases. *J. Biol. Chem.* **281,** 6096–6105

84. Cao, X., Voss, C., Zhao, B., Kaneko, T., and Li, S. S. (2012) Differential regulation of the activity of deleted in liver cancer 1 (DLC1) by tensins controls cell migration and transformation. *Proc. Natl. Acad. Sci. U.S.A.* **109,** 1455–1460

85. Erlmann, P., Schmid, S., Horenkamp, F. A., Geyer, M., Pomorski, T. G., and Olayioye, M. A. (2009) DLC1 activation requires lipid interaction through a polybasic region preceding the RhoGAP domain. *Mol. Cell. Biol.* **20,** 4400–4411

86. Hu, K. Q., and Settleman, J. (1997) Tandem SH2 binding sites mediate the RasGAP-RhoGAP interaction: a conformational mechanism for SH3 domain regulation. *EMBO J.* **16,** 473–483

87. Ahmed, S., Lee, J., Kozma, R., Best, A., Monfries, C., and Lim, L. (1993) A novel functional target for tumor-promoting phorbol esters and lysophosphatidic acid. The p21rac-GTPase activating protein n-chimaerin. *J. Biol. Chem.* **268,** 10709–10712

88. Jenna, S., Hussain, N. K., Danek, E. I., Triki, I., Wasiak, S., McPherson, P. S., and Lamarche-Vane, N. (2002) The activity of the GTPase-activating protein CdGAP is regulated by the endocytic protein intersectin. *J. Biol. Chem.* **277,** 6366–6373

89. Roof, R. W., Haskell, M. D., Dukes, B. D., Sherman, N., Kinter, M., and Parsons, S. J. (1998) Phosphotyrosine (p-Tyr)-dependent and -independent mechanisms of p190 RhoGAP-p120 RasGAP interaction: Tyr 1105 of p190, a substrate for c-Src, is the sole p-Tyr mediator of complex formation. *Mol. Cell. Biol.* **18,** 7052–7063

90. Schlam, D., Bagshaw, R. D., Freeman, S. A., Collins, R. F., Pawson, T., Fairn, G. D., and Grinstein, S. (2015) Phosphoinoside 3-kinase enables phagocytosis of large particles by terminating actin assembly through RAC/CDC42 GTPase-activating proteins. *Nat. Commun.* **6,** 1–12

91. Florio, M., Albert, M., Taverna, E., Namba, T., Brandl, H., Lewitus, E., Haffner, C., Sykes, A., Wong, F. K., Peters, J., Guhr, E., Klemroth, S., Prüfer, K., Kelso, J., Naumann, R., *et al.* (2015) Human-specific gene ARHGAP11B promotes basal progenitor amplification and neocortex expansion. *Science* **347,** 1465–1470

92. Barras, D., and Widmann, C. (2014) GAP-independent functions of DLC1 in metastasis. *Cancer Metastasis Rev.* **33,** 87–100

93. Yang, X. Y., Guan, M., Vigil, D., Der, C. J., Lowy, D. R., and Popescu, N. C. (2009) p120Ras-GAP binds the DLC1 Rho-GAP tumor suppressor protein and inhibits its RhoA GTPase and growth-suppressing activities. *Oncogene* **28,** 1401–1409

94. Fiegen, D., Haeusler, L. C., Blumenstein, L., Herbrand, U., Dvorsky, R., Vetter, I. R., and Ahmadian, M. R. (2004) Alternative splicing of RAC1 generates RAC1b, a self-activating GTPase. *J. Biol. Chem.* **279,** 4743–4749

95. Fan, L., and Mellor, H. (2012) The small Rho GTPase RIF and actin cytoskeletal remodelling. *Biochem. Soc. Trans.* **40,** 268–272

96. Aspenström, P. (2014) Atypical Rho GTPases RhoD and RIF integrate cytoskeletal dynamics and membrane trafficking. *Biol. Chem.* **395,** 477–484

97. Scheffzek, K., and Ahmadian, M. R. (2005) GTPase activating proteins: structural and functional insights 18 years after discovery. *Cell. Mol. Life Sci.* **62,** 3014–3038

98. Rack, P. G., Ni, J., Payumo, A. Y., Nguyen, V., Crapster, J. A., Hovestadt, V., Kool, M., Jones, D. T., Mich, J. K., Firestone, A. J., Pfister, S. M., Cho, Y.-J., and Chen, J. K. (2014) Arhgap36-dependent activation of Gli transcription factors. *Proc. Natl. Acad. Sci. U.S.A.* **111,** 11061–11066

99. Yoon, H. Y., Miura, K., Cuthbert, E. J., Davis, K. K., Ahvazi, B., Casanova, J. E., and Randazzo, P. A. (2006) ARAP2 effects on the actin cytoskeleton are dependent on ARF6-specific GTPase-activating-protein activity and binding to RhoA-GTP. *J. Cell Sci.* **119,** 4650–4666

100. Marchesi, S., Montani, F., Deflorian, G., D'Antuono, R., Cuomo, A., Bologna, S., Mazzoccoli, C., Bonaldi, T., Di Fiore, P. P., and Nicassio, F. (2014) DEPDC1B coordinates de-adhesion events and cell-cycle progression at mitosis. *Dev. Cell* **31,** 420–433

101. Faucherre, A., Desbois, P., Satre, V., Lunardi, J., Dorseuil, O., and Gacon, G. (2003) Lowe syndrome protein OCRL1 interacts with RAC GTPase in the trans-Golgi network. *Hum. Mol. Genet.* **12,** 2449–2456

102. Zheng, Y., Bagrodia, S., and Cerione, R. A. (1994) Activation of phosphoinositide 3-kinase activity by CDC42Hs binding to p85. *J. Biol. Chem.* **269,** 18727–18730

103. Sheffield, P., Garrard, S., and Derewenda, Z. (1999) Overcoming expression and purification problems of RhoGDI using a family of "parallel" expression vectors. *Protein Expr. Purif.* **15,** 34–39

104. Hemsath, L., and Ahmadian, M. R. (2005) Fluorescence approaches for monitoring interactions of Rho GTPases with nucleotides, regulators, and effectors. *Methods* **37,** 173–182

105. Ahmadian, M. R., Wittinghofer, A., and Herrmann, C. (2002) Fluorescence methods in the study of small GTP-binding proteins. *Methods Mol. Biol.* **189,** 45–63

106. Hall, T. A. (1999) BioEdit: a user-friendly biological sequence alignment editor and analysis program for Windows 95/98/NT. *Nucleic Acids Symp. Ser.* **41,** 95–98

107. Cock, P. J., Antao, T., Chang, J. T., Chapman, B. A., Cox, C. J., Dalke, A., Friedberg, I., Hamelryck, T., Kauff, F., Wilczynski, B., and de Hoon, M. J. (2009) Biopython: freely available Python tools for computational molecular biology and bioinformatics. *Bioinformatics* **25,** 1422–1423

108. Stothard, P. (2000) The Sequence Manipulation Suite: JavaScript programs for analyzing and formatting protein and DNA sequences. *BioTechniques* **28,** 1102–1104

109. DeLano, W. L. (2002) *The PyMOL Molecular Graphics System,* Version 1.8.2.3. DeLano Scientific LLC, San Carlos, CA

110. Long, F., Vagin, A. A., Young, P., and Murshudov, G. N. (2008) BALBES: a molecular-replacement pipeline. *Acta Crystallogr. D Biol. Crystallogr.* **64,** 125–132

111. Afonine, P. V., Grosse-Kunstleve, R. W., Echols, N., Headd, J. J., Moriarty, N. W., Mustyakimov, M., Terwilliger, T. C., Urzhumtsev, A., Zwart, P. H., and Adams, P. D. (2012) Toward automated crystallographic structure refinement with phenix.refine. *Acta Crystallogr. D Biol. Crystallogr.* **68,** 352–367

112. Emsley, P., and Cowtan, K. (2004) Coot: model-building tools for molecular graphics. *Acta Crystallogr. D Biol. Crystallogr.* **60,** 2126–2132

Supplemental Information

Deciphering the molecular and functional basis of RHOGAP family proteins: A systematic approach towards selective inactivation of RHO family proteins*

Ehsan Amin, Mamta Jaiswal, Urszula Derewenda, Katarina Reis, Kazem Nouri, Katja T. Kossemeier, Pontus Aspenström, Avril V. Somlyo, Radovan Dvorsky, and Mohammad R. Ahmadian

Institute of Biochemistry and Molecular Biology II, Medical Faculty, Heinrich-Heine-University Düsseldorf, Germany

TABLE S1
Published structures of RHO and RHOGAP proteins, and their complexes

RHO protein structures			
Protein	**PDB ID**	**Resolution (Å)**	**Reference**
CDC42	1AN0	2.80	(1)
CDC42	1AJE	NMR	(2)
CDC42 (F28L)	2ASE	NMR	(3)
CDC42(G12V)	1A4R	2.50	(4)
CDC42(T35A)	2KB0	NMR	to be published
RAC1	2P2L	1.90	(5)
RAC1b	1RYH, 1RYF	1.75, 1.75	(6)
RAC2(G12V)	2W2T, 2W2V	1.95, 2.00	(7)
RAC3	2IC5, 2G0N, 2C2H	1.90, 1.90, 1.85	to be published
RHOA	1A2B	2.40	(8)
RHOA	1DPF	2.00	(9)
RHOA(F25N)	1FTN	2.10	(10)
RHOA(Q63L/F25N)	1KMQ	1.55	(11)
RHOB	2FV8	1.90	(12)
RHOC	2GCN, 2GCO,2GCP	1.85, 1.40, 2.15	(13)
RHOD	2J1L	2.50	to be published
Rnd1	2CLS	2.31	to be published
Rnd3	1M7B	2.00	(6)
Rnd3	1GWN	2.10	(14)
TC10	2ATX	2.65	(15)
Wrch1	2Q3H	1.73	to be published
RHOGAP protein structures			
Protein	**PDB ID**	**Resolution (Å)**	**Reference**
DLC1	3KUQ	2.3	to be published
GRAF	1F7C	2.4	(16)
GRB1	1PBW	2.0	(17)
MGCRACGAP	2OVJ	1.49	to be published
MGCRACGAP	3W6R	1.9	(18)
N-chimaerin	2OSA, 3CXL	1.8, 2.6	to be published
OCRL1	2QV2	2.4	(19)
OCRL1	3QIS	2.3	(20)
p190A	3FK2	2.8	to be published
p190B	2EE4, 2EE5	NMR	to be published
p50	1RGP	2.0	(21)
RALBP1	2MBG	NMR	(22)
RHOGAP11A	3EAP	2.3	to be published
RHOGAP15	3BYI	2.25	to be published
RICS (p250GAP)	3IUG	1.77	to be published
β-chimaerin	1XA6	3.2	(23)
RHOGAP-RHO protein complexes			
Protein	**PDB ID**	**Resolution (Å)**	**Reference**
CDC42-GDP-AlF$_3$-p50	1GRN, 2NGR	2.1, 1.9	(24)
CDC42-GppNHp-p50	1AM4	2.7	(25)
RHOAGDP-AlF$_4^-$-p50	1TX4	1.65	(26)
RHOA-GDP-MgF$_3^-$-p50	1OW3	1.8	(27)
RHOA-GDP-MgF$_3^-$-ARHGAP20	3MSX	1.65	(28)
RHOA-GDP-MgF$_3^-$-p190-GAP	5IRC	1.72	this study

TABLE S2
The sequence similarities (%) of the RHOGAP domains
Sequence similarities of RHOGAPs presented in interaction matrix has been calculated *via* the Sequence Manipulation Suite (SMS) (29) by providing their multiple sequence alignment.

	OPHN1	GARF	p190	RICH1	ABR	MGC	DLC1	DLC2	DLC3	GAP20
p50	23.1	21.5	25.1	26.4	23.4	25.5	23.4	21.6	21.5	27.1
OPHN1		54.3	26.0	24.5	24.3	29.4	20.8	16.6	16.6	22.3
GARF			25.0	24.5	27.7	31.5	20.3	18.0	18.0	20.7
p190				27.6	24.1	21.1	21.6	22.2	20.8	17.9
RICH1					28.5	24.5	23.7	21.8	21.3	23.6
ABR						35.2	23.9	22.1	22.5	20.5
MGC							18.2	17.3	19.1	21.9
DLC1								80.2	70.5	17.9
DLC2									68.1	20.4
DLC3										21.8
GAP20										

min   max

TABLE S3
Crystallographic data of the RHOA-p190-GAP structure

Data collection	
Wavelength	*1.0*
Space group	*P212121*
Unit cell (Å,°)	*a=47.03, b=112.32, c=147.61*
Resolution (Å)*	*1.72(1.75-1.72)*
No. of total reflections	459,261
Redundancy	5.6(2.6)
Completeness (%)	97.0(70.0)
R_{merge} (%) **	5.9(36.7)
I/σ(I)	26.2(2.5)
Refinement statistics	
Resolution limits(Å)	32.5-1.72
Unique reflections	81,424
Reflections in R_{free} set	1,620
R§ (%)	17.1
R_{free} § (%)	21.3
R.m.s.d., bond length(Å)	0.007
R.m.s.d., bond angles(°)	1.15
No. of atoms	
Protein atoms	5854
O atoms of water	1019
Ligand/ion atoms	66
Clashscore	1.97
Rotamer outliers (%)	3/0.47%
Ramachandran outliers	0/0.00%
Ramachandran favored	715/98.35%

* The numbers in parentheses describe the relevant value for the last resolution shell.
** $R_{merge} = \sum_{hkl} \sum_i |I_i(hkl) - <I(hkl)>| / \sum_{hkl}\sum_i I_i(hkl)$, where $<I_i(hkl)>$ is the mean of i observations $I_i(hkl)$ of reflection hkl.
§ R factor and $R_{free} = \sum_{hkl} ||F_{obs}| - |F_{calc}|| / \sum_{hkl}|F_{obs}|$, | where F_{obs} and F_{calc} are the observed and calculated structure factors, respectively, calculated for recorded data (R factor) and for a test set of randomly selected data which were omitted from refinement (R_{free}).

3

TABLE S4
Domain properties of RHOGAP family proteins
Domain color codes: Blue, lipid and membrane binding; green, protein interaction; red and orange enzyme activities.

No.	Domain	Description
1	ANK	Ankyrin repeats involved in protein interactions
2	ArfGAP	Arf-specific GTPase activating proteins with putative zinc finger motif
3	ASH	ASPM/SPD-2/Hydin involved in microtubule association
4	BAR	Bin/amphiphysin/Rvs involved in membrane binding and bending
5	C1	Cysteine-rich diacylglycerol binding
6	C2	Calcium-dependent phospholipid binding
7	CC	Putative coiled-coil involved in oligomerization and/or protein interaction
8	DEP	Dishevelled/Egl-10/Pleckstrin involved in protein interaction
9	DH	Catalytic Dbl homology involved in RHO protein activation
10	FAT	Focal adhesion targeting involved in localization to focal adhesions
11	F-BAR	Fes/CIP4 homology BAR involved in membrane binding and bending
12	FF	a domain with two conserved phenylalanines involved in protein interaction
13	GTPase	a putative GTP binding domain
14	IPP5	Inositol polyphosphate 5-phosphatase
15	IQ	an isoleucine/glutamine-containing calmodulin binding motif
16	Kinase	a serine/threonine kinase domain
17	MYSc	Myosin motor, an actin-activated Mg^{2+}-ATPases
30	MyTH4	Myosin tail homology 4 provides a link between an actin-based motor protein and microtubules
18	P	Proline-rich motifs as putative binding sites for SH3 domains
19	PBR	Polybasic region involved in PIP2 binding(30)[30]
20	PDZ	PSD-95/discs large/ZO-1 involved in anchoring signaling complexes at cellular membranes
21	PEST	Proline/glutamic acid/serine/threonine-rich motif involved in signal peptide processing
22	PH	Pleckstrin homology involved in phospholipid binding and protein interaction
24	PX	Phox homology involved in phospholipid binding
23	RA	Putative Ras association
25	RalBD	Ral (a Ras-like protein) binding
26	RHOGAP	Catalytic RHO-specific GAP domain
27	SAM	Sterile α motif is involved in homo-/hetero-oligomerization and lipid binding
28	SEC14	Sec14p homology to yeast PI-transfer protein involved in membrane interaction
29	SH2	Src homology 2 involved in interaction with phosphotyrosine-containing polypeptides
31	SH3	Src homology 3 involved in interaction with proline-rich motifs
32	StART	Steroidogenic acute regulatory-related lipid transfer as putative lipid-binding domain
33	WW	Tryptophan-containing proline-rich binding

TABLE S5

Domain composition of RHOGAP family proteins

Digits gives the number of each domain in RHOGAPs (33 distinct domain domains to date and 258 in total), ranging from 0 (white) to 5 (black). Last column gives the total domain number per protein and last row the domain number for 66 RHOGAPs, including RHOGAP-like proteins (red). Domain color codes: Blue, lipid and membrane binding; green, protein interaction; red and orange enzyme activities.

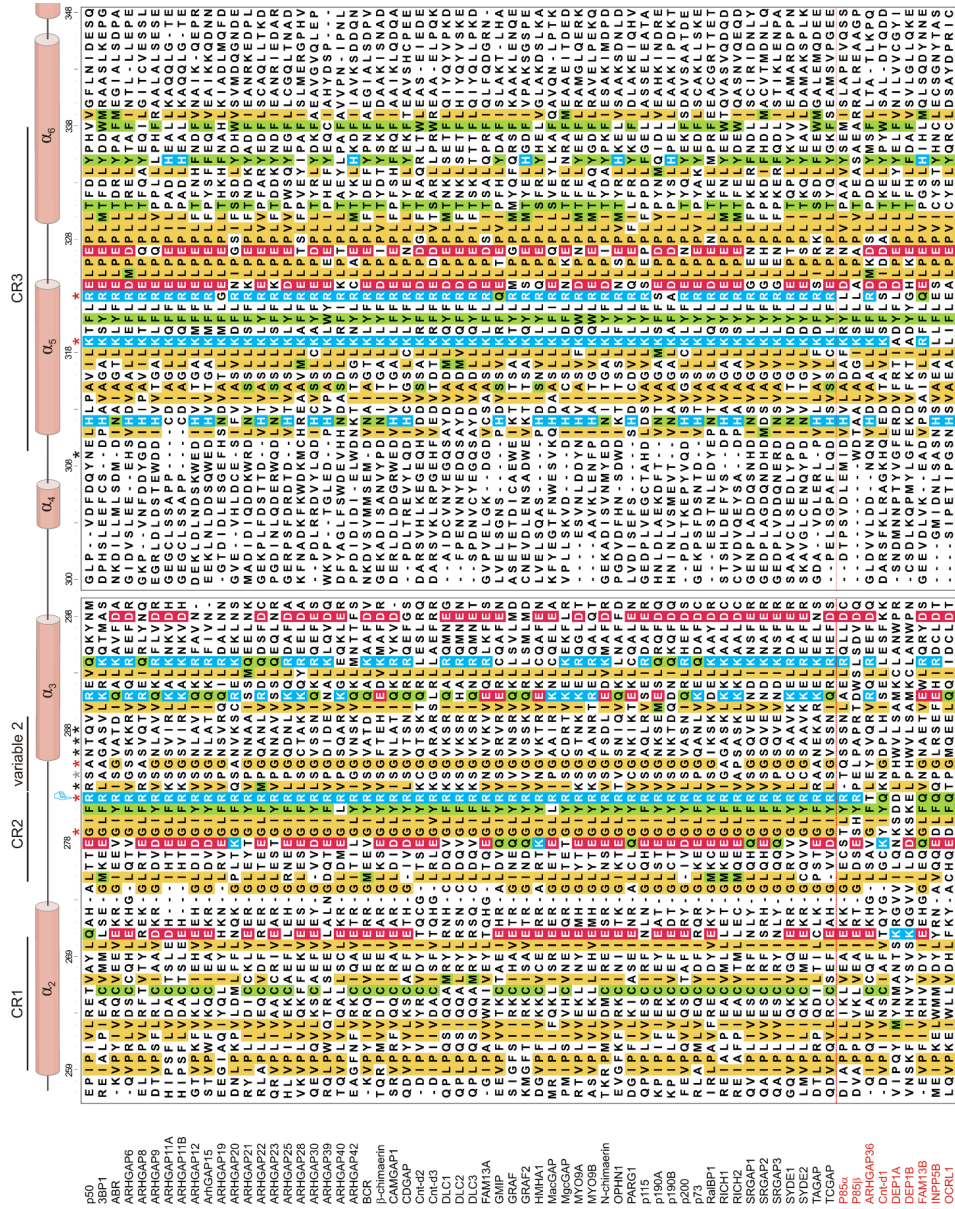| Proteins	aa no.	RHOGAP	ArfGAP	DH	GTPase	IPP5	Kinase	BAR	F-BAR	C1	C2	PBR	PH	PX	SAM	Sec14	StART	ANK	ASH	CC	DEP	FAT	FF	IQ	MYSc	MyTH4	P	PDZ	PEST	RA	RalBD	SH2	SH3	WW	Total
DEP1A	811	1	0	0	0	0	0	0	0	0	0	0	0	0	0	0	0	0	0	0	1	0	0	0	0	0	0	0	0	0	0	0	0	0	2
DEP1B	529	1	0	0	0	0	0	0	0	0	0	0	0	0	0	0	0	0	0	0	1	0	0	0	0	0	0	0	0	0	0	0	0	0	2
p50	439	1	0	0	0	0	0	0	0	0	0	0	1	0	0	1	0	0	0	0	0	0	0	0	0	0	0	0	0	0	0	0	0	0	3
ARHGAP8	464	1	0	0	0	0	0	0	0	0	0	0	0	0	0	1	0	0	0	0	0	0	0	0	0	0	0	0	0	0	0	0	0	0	2
ARHGAP20	1191	1	0	0	0	0	0	0	0	0	0	0	1	0	0	0	0	0	0	0	0	0	0	0	0	0	0	0	0	1	0	0	0	0	3
TAGAP	731	1	0	0	0	0	0	0	0	0	0	0	0	0	0	0	0	0	0	0	0	0	0	0	0	0	0	0	0	0	0	0	0	0	1
3BP1	701	1	0	0	0	0	0	1	0	0	0	0	0	0	0	0	0	0	0	0	0	0	0	0	0	0	0	0	0	0	0	0	0	0	2
RICH-1	881	1	0	0	0	0	0	0	1	0	0	0	0	0	0	0	0	0	0	1	0	0	0	0	0	0	0	1	1	0	0	0	0	0	5
RICH-2	818	1	0	0	0	0	0	1	0	0	0	0	0	0	0	0	0	0	0	0	0	0	0	0	0	0	0	0	0	0	0	0	1	0	3
ARHGAP22	698	1	0	0	0	0	0	0	0	0	0	0	1	0	0	0	0	0	0	1	0	0	0	0	0	0	0	0	0	0	0	0	0	0	3
p73	748	1	0	0	0	0	0	0	0	0	0	0	1	0	0	0	0	0	0	1	0	0	0	0	0	0	0	0	0	0	0	0	0	0	3
ARHGAP25	645	1	0	0	0	0	0	0	0	0	0	0	1	0	0	0	0	0	0	1	0	0	0	0	0	0	0	0	0	0	0	0	0	0	3
p115	946	1	0	0	0	0	0	1	0	0	0	0	0	0	0	0	0	0	0	2	0	0	0	0	0	0	0	0	0	0	0	0	1	0	5
SRGAP1	1085	1	0	0	0	0	0	0	1	0	0	0	0	0	0	0	0	0	0	2	0	0	0	0	0	0	0	0	0	0	0	0	1	0	5
SRGAP2	1071	1	0	0	0	0	0	0	1	0	0	0	0	0	0	0	0	0	0	2	0	0	0	0	0	0	0	0	0	0	0	0	1	0	5
SRGAP3	1099	1	0	0	0	0	0	0	1	0	0	0	0	0	0	0	0	0	0	2	0	0	0	0	0	0	0	0	0	0	0	0	1	0	5
ARHGAP11A	1023	1	0	0	0	0	0	0	0	0	0	0	0	0	0	0	0	0	0	0	0	0	0	0	0	0	0	0	0	0	0	0	0	0	1
ARHGAP11B	267	1	0	0	0	0	0	0	0	0	0	0	0	0	0	0	0	0	0	0	0	0	0	0	0	0	0	0	0	0	0	0	0	0	1
ABR	859	1	0	1	0	0	0	0	0	1	0	0	1	0	0	0	0	0	0	0	0	0	0	0	0	0	1	0	0	0	0	0	0	0	5
BCR	1271	1	0	1	0	0	1	0	0	1	0	0	1	0	0	0	0	0	0	0	0	0	0	0	0	0	1	0	0	0	0	0	0	0	6
SYDE1	735	1	0	0	0	0	0	0	0	0	0	0	0	0	0	0	0	0	0	0	0	0	0	0	0	0	1	0	0	0	0	0	0	0	2
SYDE2	1194	1	0	0	0	0	0	0	0	0	0	0	1	0	0	0	0	0	0	1	0	0	0	0	0	0	0	0	0	0	0	0	0	0	3
ARHGAP9	750	1	0	0	0	0	0	0	0	0	0	0	1	0	0	0	0	0	0	0	0	0	0	0	0	0	0	0	0	0	0	0	1	1	4
ARHGAP12	846	1	0	0	0	0	0	0	0	0	0	0	1	0	0	0	0	0	0	0	0	0	0	0	0	0	0	0	0	0	0	0	1	2	5
ArhGAP15	475	1	0	0	0	0	0	0	0	0	0	0	1	0	0	0	0	0	0	0	0	0	0	0	0	0	0	0	0	0	0	0	0	0	2
CAMGAP1	889	1	0	0	0	0	0	0	0	0	0	1	1	0	0	0	0	0	0	0	0	0	0	0	0	0	0	0	0	0	0	0	3	0	6
ARHGAP21	1957	1	0	0	0	0	0	0	0	0	0	0	1	0	0	0	0	0	0	0	0	0	0	0	0	0	1	0	0	0	0	0	0	0	3
ARHGAP23	1491	1	0	0	0	0	0	0	0	0	0	1	1	0	0	0	0	0	0	0	0	0	0	1	0	0	1	0	0	0	0	0	0	0	5
β-CHIMAERIN	468	1	0	0	0	0	0	0	0	1	0	0	0	0	0	0	0	0	0	0	0	0	0	0	0	0	0	0	0	0	0	1	0	0	3
N-CHIMAERIN	459	1	0	0	0	0	0	0	0	1	0	0	0	0	0	0	0	0	0	0	0	0	0	0	0	0	0	0	0	0	0	1	0	0	3
p190-A	1499	1	0	0	1	0	0	0	0	0	0	0	0	0	0	0	0	0	0	0	0	0	4	0	0	0	1	0	0	0	0	0	0	0	7
p190-B	1502	1	0	0	1	0	0	0	0	0	0	0	0	0	0	0	0	0	0	0	0	0	4	0	0	0	1	0	0	0	0	0	0	0	7
ARHGAP42	874	1	0	0	0	0	0	1	0	0	0	0	1	0	0	0	0	0	0	0	0	0	0	0	0	0	0	0	0	0	0	0	1	0	4
GRAF	814	1	0	0	0	0	0	1	0	0	0	0	1	0	0	0	0	0	0	0	0	0	0	0	0	0	0	0	0	0	0	0	1	0	4
GRAF2	786	1	0	0	0	0	0	1	0	0	0	0	1	0	0	0	0	0	0	0	0	0	0	0	0	0	0	0	0	0	0	0	1	0	4
OPHN1	802	1	0	0	0	0	0	1	0	0	0	0	1	0	0	0	0	0	0	0	0	0	0	0	0	0	3	0	0	0	0	0	0	0	6
MGCRACGAP	632	1	0	0	0	0	0	0	0	1	0	0	0	0	0	0	0	0	0	1	0	0	0	0	0	0	0	0	0	0	0	0	0	0	3
ARHGAP30	1101	1	0	0	0	0	0	0	0	0	0	0	0	0	0	0	0	0	0	0	0	0	0	0	0	0	0	0	0	0	0	0	0	0	1
p200	2087	1	0	0	0	0	0	0	0	0	0	0	1	1	0	0	0	0	0	0	0	0	0	0	0	0	0	0	0	0	0	0	1	0	3
TCGAP	1287	1	0	0	0	0	0	0	0	0	0	0	1	1	0	0	0	0	0	0	0	0	0	0	0	0	0	0	0	0	0	0	1	0	3
CDGAP	1444	1	0	0	0	0	0	0	0	1	0	0	0	0	0	0	0	0	0	0	0	0	0	0	0	0	0	0	0	0	0	0	0	0	2
MYO9A	2548	1	0	0	0	0	0	0	0	0	2	0	0	0	0	0	0	0	0	3	0	0	0	4	1	0	0	0	0	0	0	0	0	0	11
MYO9B	2157	1	0	0	0	0	0	0	0	0	1	0	0	0	0	0	0	0	0	3	0	0	0	4	1	1	0	0	0	0	0	0	0	0	11
RALBP1	655	1	0	0	0	0	0	0	0	0	0	0	1	0	0	0	0	0	0	0	0	0	0	0	0	0	0	0	0	0	1	0	0	0	3
ARHGAP19	494	1	0	0	0	0	0	0	0	0	0	0	0	0	0	0	0	0	0	0	0	0	0	0	0	0	0	0	0	0	0	0	0	0	1
ARHGAP28	729	1	0	0	0	0	0	0	0	0	0	0	0	0	0	0	0	0	0	0	0	0	0	0	0	0	0	0	0	0	0	0	0	0	1
ARHGAP40	622	1	0	0	0	0	0	0	0	0	0	0	0	0	0	0	0	0	0	0	0	0	0	0	0	0	0	0	0	0	0	0	0	0	1
MACGAP	663	1	0	0	0	0	0	0	0	0	0	0	0	0	0	0	0	0	0	0	0	0	0	0	0	0	0	0	0	0	0	0	0	0	1
DLC-1	1528	1	0	0	0	0	0	0	0	0	0	1	0	0	1	0	1	0	0	1	0	0	0	0	0	0	0	0	0	0	0	0	0	0	5
DLC-2	1113	1	0	0	0	0	0	0	0	0	0	0	0	0	1	0	1	0	0	0	0	0	0	0	0	0	0	0	0	0	0	0	0	0	3
DLC-3	1023	1	0	0	0	0	0	0	0	0	0	0	0	0	0	0	1	0	0	0	0	0	0	0	0	0	0	0	0	0	0	0	0	0	2
ARHGAP6	974	1	0	0	0	0	0	0	0	0	0	0	0	0	0	0	0	0	0	0	0	0	0	0	0	0	1	0	0	0	0	0	0	0	2
ARHGAP36	547	1	0	0	0	0	0	0	0	1	0	0	0	0	0	0	0	0	0	0	0	0	0	0	0	0	0	0	0	0	0	0	0	0	2
CNT-D1	1704	1	1	0	0	0	0	0	0	0	0	0	5	0	1	0	0	1	0	0	0	0	0	0	0	0	0	0	0	1	0	0	0	0	10
CNT-D2	1450	1	1	0	0	0	0	0	0	0	0	0	4	0	1	0	0	1	0	0	0	0	0	0	0	0	0	0	0	1	0	0	0	0	9
CNT-D3	1544	1	1	0	0	0	0	0	0	0	0	0	3	0	1	0	0	1	0	0	0	0	0	0	0	0	2	0	0	1	0	0	0	0	10
FAM13A	1023	1	0	0	0	0	0	0	0	0	0	0	0	0	0	0	0	0	0	2	0	0	0	0	0	0	0	0	0	0	0	0	0	0	3
FAM13B	915	1	0	0	0	0	0	0	0	0	0	0	0	0	0	0	0	0	0	0	0	0	0	0	0	0	0	0	0	0	0	0	0	0	1
PARG1	1261	1	0	0	0	0	0	0	1	1	0	0	0	0	0	0	0	0	0	1	0	0	0	0	0	0	0	0	0	0	0	0	0	0	4
HMHA1	1136	1	0	0	0	0	0	0	1	1	0	0	0	0	0	0	0	0	0	2	0	0	0	0	0	0	0	0	0	0	0	0	0	0	5
GMIP	970	1	0	0	0	0	0	0	1	1	0	0	0	0	0	0	0	0	0	0	0	0	0	0	0	0	2	0	0	0	0	0	0	0	5
ARHGAP39	1083	1	0	0	0	0	0	0	0	0	0	0	0	0	0	0	0	0	0	0	0	0	0	1	1	0	0	0	0	0	0	0	0	2	5
p85A	724	1	0	0	0	0	0	0	0	0	0	0	0	0	0	0	0	0	0	0	0	0	0	0	0	0	0	0	0	0	0	2	1	0	4
p85B	728	1	0	0	0	0	0	0	0	0	0	0	0	0	0	0	0	0	0	0	0	0	0	0	0	0	0	0	0	0	0	2	1	0	4
INPP5B	993	1	0	0	0	1	0	0	0	0	0	0	1	0	0	0	0	0	1	0	0	0	0	0	0	0	0	0	0	0	0	0	0	0	4
OCRL1	901	1	0	0	0	1	0	0	0	0	0	0	1	0	0	0	0	0	1	0	0	0	0	0	0	0	0	0	0	0	0	0	0	0	4
		66	3	2	2	2	1	7	7	9	3	6	30	2	5	2	3	3	2	25	2	1	8	9	2	1	16	2	1	6	1	6	15	8	258

5

FIGURE S1. **Sequence alignment of the catalytic domains of all human RHOGAP proteins (continued on next page).** Amino acid sequences of GAP domains of 66 RHOGAP family proteins is aligned by using ClustalW implemented in Bioedit with default multiple alignment parameters. Comprehensive analysis of the amino acid sequences of all human RHOGAP proteins along with all biochemical and structural data of this and other studies resulted in the determination of regions and residues essential for both binding to RHO proteins and stimulating their GTP hydrolysis (symbol 🖑 denotes essential catalytic arginine).
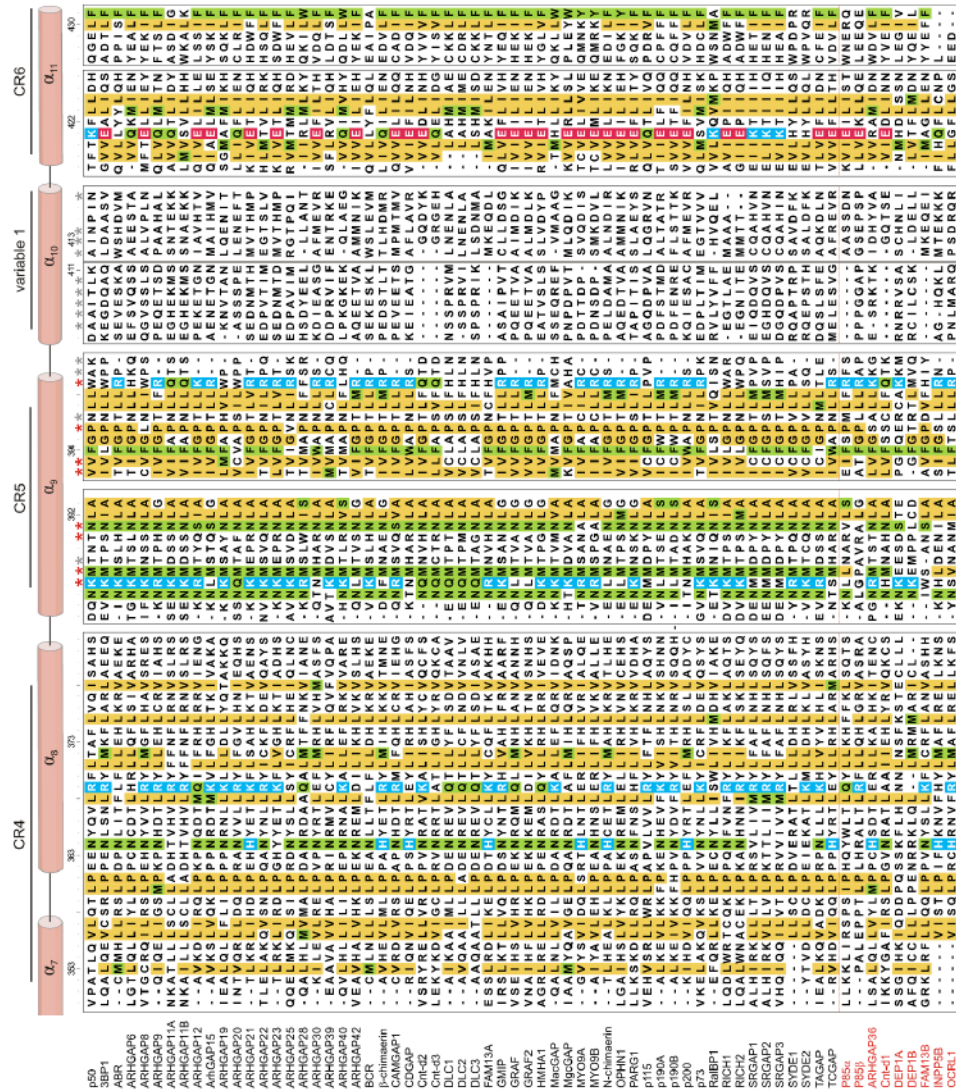
FIGURE S1 (Continued from previous page). Asterisks highlight all amino acids that have been selected for the interaction matrix (Fig. 6A): red, conserved; grey, variable 1; black, variable 2. Secondary structural elements are presented on the top of the alignment; the RHOGAP domain has an all-helical domain (21)(Helices are shown as cylinder). Proteins below the dashed line were excluded from the RHOGAP family and can be considered as RHOGAP-like proteins (red). Due to space limits only the most critical regions of the RHOGAP domain is shown. CR1-6 stands for conserved regions 1-6. HVR stands for hypervariable region. Background color codes are the same as Fig 6A.
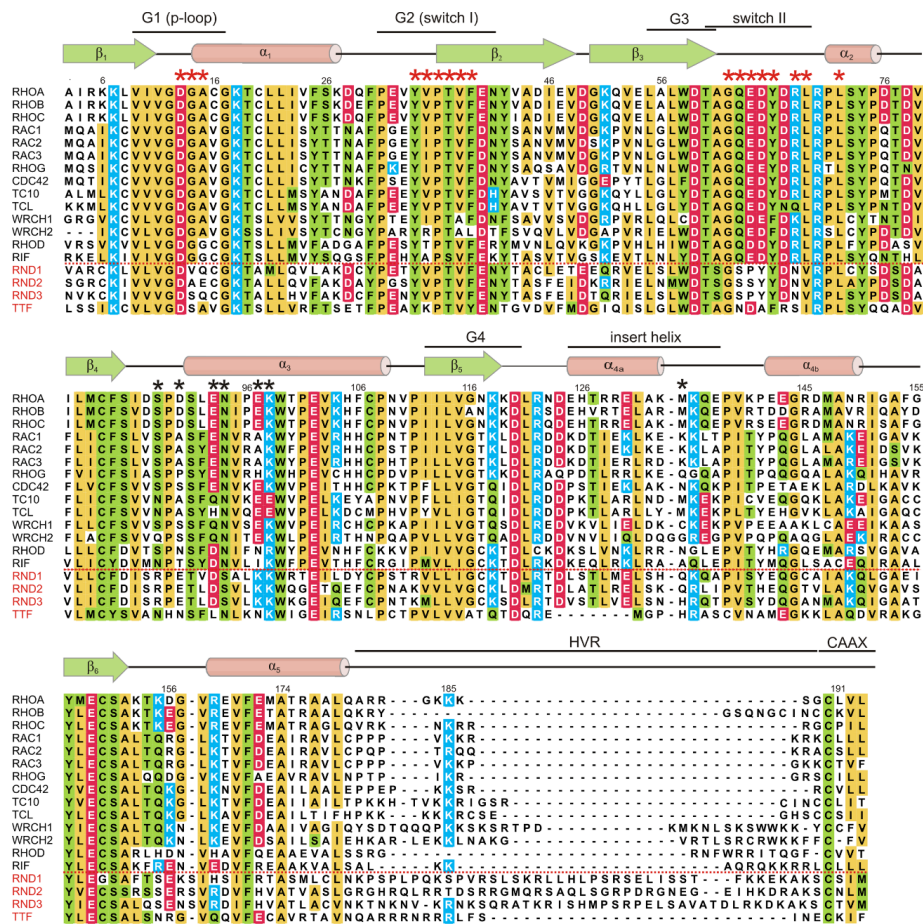
FIGURE S2. **Multiple sequence alignment of RHO protein family.** The Amino acid sequences of 18 RHO family proteins were aligned using ClustalW utility in Bioedit. Conserved signatures of the RHO proteins critical for GDP/GTP binding, GTP hydrolysis and proteins interactions are represented as G1 (or P loop for phosphate binding and magnesium ion coordination), G2 (or switch I for magnesium ion coordination and γ-phosphate binding), G3 (or switch II for γ-phosphate binding containing the catalytic glutamine), G4 (major determinant of guanine base binding specificity) and G5 box (for guanine base binding). HVR (hypervariable region) and CAAX (C is cysteine, A is any aliphatic amino acid, and X is any amino acid) are itical motifs for association with cell membrane. Secondary structural elements are presented on the top of an alignment, helices as cylinder and beta sheets by an arrow. Asterisks highlight all amino acids that have been selected for the interaction matrix (Fig. 6A): red, conserved; black, variable. Proteins below the dashed line were excluded from the RHO family as they can be considered as GTPase-deficient, RHO-related GTP-binding proteins. Background color codes are the same as in Fig 6A.
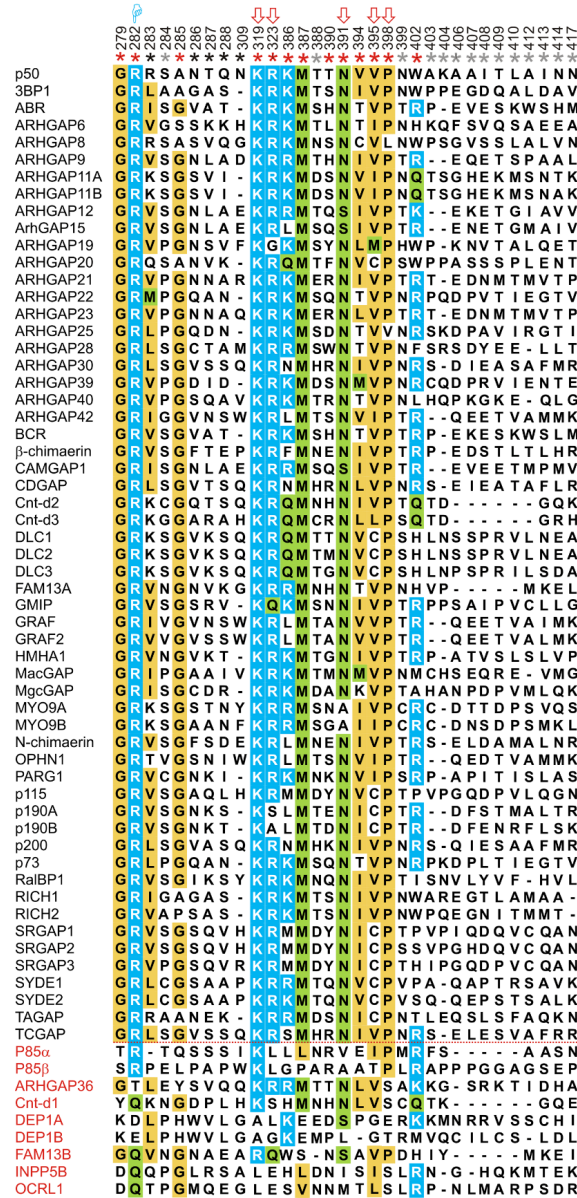
FIGURE S3. **Alignment of GAP residues involved in the interaction with RHO proteins.** Amino acids presented in interaction matrix for investigated RHOGAPs in this study (Fig. 6A) are extracted from the global alignment of GAP domains of all RHOGAPs, including the RHOGAP-like proteins (red) below the dashed line. Background color codes are the same as in Fig 6A. Arginine finger is marked by 🔹 and RHO protein binding determinants by ⬇.

Supplemental References

1. Kongsaeree, P., Cerione, R.A., Clardy, J.C. (1999) The Structure Determination of Cdc42Hs and Gdp Complex. **To be published**

2. Feltham, J. L., Dotsch, V., Raza, S., Manor, D., Cerione, R. A., Sutcliffe, M. J., Wagner, G., and Oswald, R. E. (1997) Definition of the switch surface in the solution structure of Cdc42Hs. *Biochemistry* **36**, 8755-8766

3. Adams, P. D., and Oswald, R. E. (2006) Solution structure of an oncogenic mutant of Cdc42Hs. *Biochemistry* **45**, 2577-2583

4. Rudolph, M. G., Wittinghofer, A., and Vetter, I. R. (1999) Nucleotide binding to the G12V-mutant of Cdc42 investigated by X-ray diffraction and fluorescence spectroscopy: two different nucleotide states in one crystal. *Protein Sci.* **8**, 778-787

5. Prehna, G., and Stebbins, C. E. (2007) A Rac1-GDP trimer complex binds zinc with tetrahedral and octahedral coordination, displacing magnesium. *Acta Crystallogr. Sect. D-Biol. Crystallogr.* **63**, 628-635

6. Fiegen, D., Haeusler, L. C., Blumenstein, L., Herbrand, U., Dvorsky, R., Vetter, I. R., and Ahmadian, M. R. (2004) Alternative splicing of Rac1 generates Rac1b, a self-activating GTPase. *J. Biol. Chem.* **279**, 4743-4749

7. Bunney, T. D., Opaleye, O., Roe, S. M., Vatter, P., Baxendale, R. W., Walliser, C., Everett, K. L., Josephs, M. B., Christow, C., Rodrigues-Lima, F., Gierschik, P., Pearl, L. H., and Katan, M. (2009) Structural insights into formation of an active signaling complex between Rac and phospholipase C gamma 2. *Mol. Cell* **34**, 223-233

8. Ihara, K., Muraguchi, S., Kato, M., Shimizu, T., Shirakawa, M., Kuroda, S., Kaibuchi, K., and Hakoshima, T. (1998) Crystal structure of human RhoA in a dominantly active form complexed with a GTP analogue. *J. Biol. Chem.* **273**, 9656-9666

9. Shimizu, T., Ihara, K., Maesaki, R., Kuroda, S., Kaibuchi, K., and Hakoshima, T. (2000) An open conformation of switch I revealed by the crystal structure of a Mg2+-free form of RHOA complexed with GDP. Implications for the GDP/GTP exchange mechanism. *J. Biol. Chem.* **275**, 18311-18317

10. Wei, Y., Zhang, Y., Derewenda, U., Liu, X., Minor, W., Nakamoto, R. K., Somlyo, A. V., Somlyo, A. P., and Derewenda, Z. S. (1997) Crystal structure of RhoA-GDP and its functional implications. *Nat. Struct. Biol.* **4**, 699-703

11. Longenecker, K., Read, P., Lin, S. K., Somlyo, A. P., Nakamoto, R. K., and Derewenda, Z. S. (2003) Structure of a constitutively activated RhoA mutant (Q63L) at 1.55 A resolution. *Acta Crystallogr. Sect. D-Biol. Crystallogr.* **59**, 876-880

12. Turnbull A.P., S. M., Smee C., Johansson C., Schoch G., Gorrec F., Bray J., Papagrigoriou E., von Delft F., Weigelt J., Edwards A., Arrowsmith C., Sundstrom M., Doyle D. (2006) The crystal structure of RhoB in the GDP-bound state. **To be published**

13. Dias, S. M., and Cerione, R. A. (2007) X-ray crystal structures reveal two activated states for RhoC. *Biochemistry* **46**, 6547-6558

14. Garavini, H., Riento, K., Phelan, J. P., McAlister, M. S., Ridley, A. J., and Keep, N. H. (2002) Crystal structure of the core domain of RhoE/Rnd3: a constitutively activated small G protein. *Biochemistry* **41**, 6303-6310

15. Hemsath, L., Dvorsky, R., Fiegen, D., Carlier, M. F., and Ahmadian, M. R. (2005) An electrostatic steering mechanism of Cdc42 recognition by Wiskott-Aldrich syndrome proteins. *Mol. Cell* **20**, 313-324

16. Longenecker, K. L., Zhang, B., Derewenda, U., Sheffield, P. J., Dauter, Z., Parsons, J. T., Zheng, Y., and Derewenda, Z. S. (2000) Structure of the BH domain from graf and its implications for Rho GTPase recognition. *J. Biol. Chem.* **275**, 38605-38610

17. Musacchio, A., Cantley, L. C., and Harrison, S. C. (1996) Crystal structure of the breakpoint cluster region-homology domain from phosphoinositide 3-kinase p85 alpha subunit. *Proc. Natl. Acad. Sci. U. S. A.* **93**, 14373-14378

18. Matsuura, A., and Lee, H. H. (2013) Crystal structure of GTPase-activating domain from human MgcRacGAP. *Biochem. Biophys. Res. Commun.* **435**, 367-372

19. Erdmann, K. S., Mao, Y., McCrea, H. J., Zoncu, R., Lee, S., Paradise, S., Modregger, J., Biemesderfer, D., Toomre, D., and De Camilli, P. (2007) A role of the Lowe syndrome protein OCRL in early steps of the endocytic pathway. *Dev. Cell* **13**, 377-390

20. Pirruccello, M., Swan, L. E., Folta-Stogniew, E., and De Camilli, P. (2011) Recognition of the F&H motif by the Lowe syndrome protein OCRL. *Nat. Struct. Mol. Biol.* **18**, 789-795

21. Barrett, T., Xiao, B., Dodson, E. J., Dodson, G., Ludbrook, S. B., Nurmahomed, K., Gamblin, S. J., Musacchio, A., Smerdon, S. J., and Eccleston, J. F. (1997) The structure of the GTPase-activating domain from p50rhoGAP. *Nature* **385**, 458-461

22. Rajasekar, K. V., Campbell, L. J., Nietlispach, D., Owen, D., and Mott, H. R. (2013) The structure of the RLIP76 RhoGAP-Ral binding domain dyad: fixed position of the domains leads to dual engagement of small G proteins at the membrane. *Structure* **21**, 2131-2142

23. Canagarajah, B., Leskow, F. C., Ho, J. Y., Mischak, H., Saidi, L. F., Kazanietz, M. G., and Hurley, J. H. (2004) Structural mechanism for lipid activation of the Rac-specific GAP, beta2-chimaerin. *Cell* **119**, 407-418

24. Nassar, N., Hoffman, G. R., Manor, D., Clardy, J. C., and Cerione, R. A. (1998) Structures of Cdc42 bound to the active and catalytically compromised forms of Cdc42GAP. *Nat. Struct. Biol.* **5**, 1047-1052

25. Rittinger, K., Walker, P. A., Eccleston, J. F., Nurmahomed, K., Owen, D., Laue, E., Gamblin, S. J., and Smerdon, S. J. (1997) Crystal structure of a small G protein in complex with the GTPase-activating protein rhoGAP. *Nature* **388**, 693-697

26. Rittinger, K., Walker, P. A., Eccleston, J. F., Smerdon, S. J., and Gamblin, S. J. (1997) Structure at 1.65 A of RhoA and its GTPase-activating protein in complex with a transition-state analogue. *Nature* **389**, 758-762

27. Graham, D. L., Lowe, P. N., Grime, G. W., Marsh, M., Rittinger, K., Smerdon, S. J., Gamblin, S. J., and Eccleston, J. F. (2002) MgF(3)(-) as a transition state analog of phosphoryl transfer. *Chem. Biol.* **9**, 375-381

28. Utepbergenov D., C. D. R., Derewenda U., Somlyo A.V., Derewenda Z.S. Mechanism of molecular specificity of RhoGAP domains towards small GTPases of RhoA family. **to be published**

29. Stothard, P. (2000) The Sequence Manipulation Suite: JavaScript programs for analyzing and formatting protein and DNA sequences. *Biotechniques* **28**, 1102-1104

30. Karimzadeh, F., Primeau, M., Mountassif, D., Rouiller, I., and Lamarche-Vane, N. (2012) A stretch of polybasic residues mediates Cdc42 GTPase-activating protein (CdGAP) binding to phosphatidylinositol 3,4,5-trisphosphate and regulates its GAP activity. *J. Biol. Chem.* **287**, 19610-19621

Chapter 8

Structure-function relationship of ROCK1

Structural and functional insights into the p160 RHO-associated coiled-coil-containing protein kinase

Badri Nath Dubey, Ehsan Amin, Radovan Dvorsky, Lothar Gremer, Jens M. Moll1, Martin Wolff, Yan Nie, Melissa Graewert, Britta Tschapek, Ingrid R. Vetter, Lutz Schmitt, Dmitri Svergun, Stefan Raunser, Georg Groth, Luitgard Nagel-Steger, and Mohammad R. Ahmadian
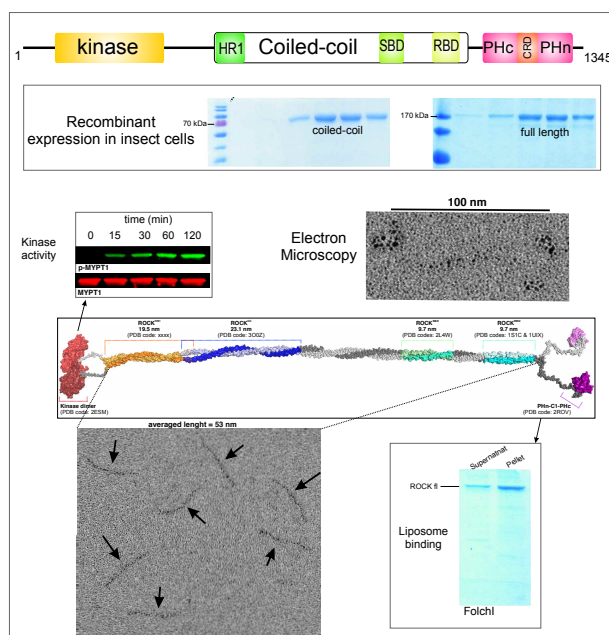
Status:	In preparation
Impact factor:	–
Own Proportion to this work:	75 %; design and perform the experiments, analyse data and writing manuscript

8.1 Background

The serine/threonine Rho-associated protein kinases (ROCKI/II), which are key determinants in many fundamental cellular functions, serve as distinguished therapeutic targets in the treatment of a wide variety of diseases, particularly cardiovascular diseases. In contrast to the terminal globular kinase domain and the PH-CRD tandem, little is known about the structure-function relationship of the central amphipathic α-helical segment of the ROCK proteins. Thus, a major aim of this study was to elucidate the structural basis of the entire segment of ROCKI and also ROCK full length by using multiple biophysical platforms, including multi-angle light scattering (MALS), analytical ultracentrifugation (AUC), small angle X-ray scattering (SAXS), electron microscopy (EM) and X-ray crystallography.

8.2 Results

The crystal structure of the homology region 1 (HR1) at the N-terminus of the amphipathic segment, determined to a resolution of 2.2 Å, provided the first experimental evidence for the existence of a canonical parallel coiled-coil dimer and revealed major differences to the antiparallel coiled-coil HR1 module of protein kinase N1 (PKN1), another Rho-associated kinase.
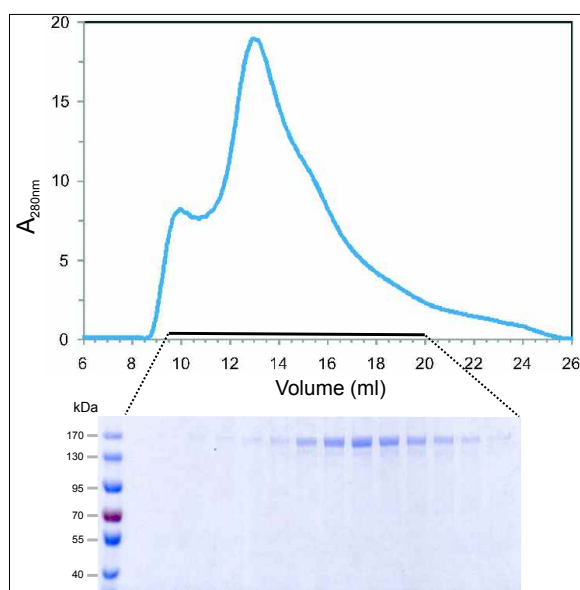
FIGURE 8.1: ROCK1 size exclusion chromatography. ROCK1 full length, purified by affinity chromatography, was loaded on size exclusion chromatography (Superdex 6 10/300) and eluted fractions have been analysed by SDS-PAGE.

ROCK1 full coiled coil (ROCK-FCC) segment and ROCK full length containing 1354 amino acids have been cloned and expressed in recently designed insect cells (tnao38) (Wilde et al., 2014). These proteins have been purified with high purity via affinity and size exclusion chromatography methods (Figure 8.1).
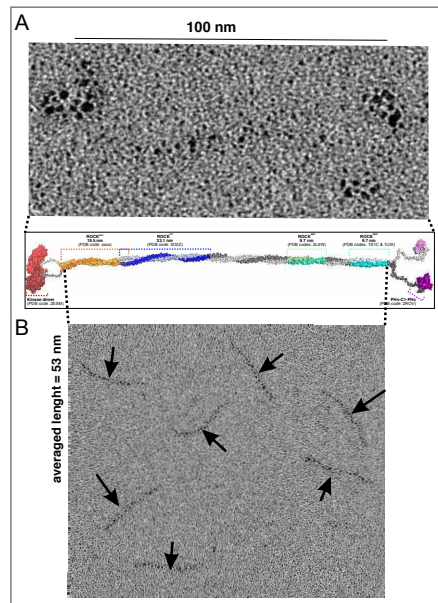
FIGURE 8.2: Electron microscopy imaging of ROCK FL and FCC. Purified proteins were sprayed on microscopy grids and were shot by heavy atoms in very low angles, the method called shadowing staining. Then the conformations of ROCK FL (A) and ROCK FCC (B) have been recorded by electron microscopy.

Purified ROCK FL and FCC segment were subjected to electron microscopy after shadowing staining (Figure 8.2). ROCK1 FL showed an elongated structure with the length of about 100 nm. But interestingly ROCK FCC segments presents fragments of about 50 nm which propose bended conformation. Enzymatic assays of ROCK has been established and results show slight effect in presence of RHOA and/or liposome on kinase activity (Figure 8.3). The obtained results led to new and important insights into the structural organization of the ROCK proteins.

8.3 Conclusion

We have observed elongated dimer structure of ROCK full length in vitro. This will make the hypothesis of kinase inhibition by PH domain controversial. this is possible that in the context of cell, other unknown or even known binding partners lead to conformational changes of ROCK1 and induce bended structure in which PH domain binds and inhibits kinase domain. Future identification of these partners can introduce new specific drug targets to treat various diseases.
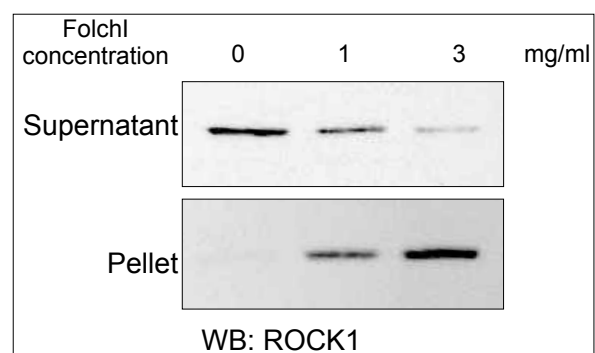
FIGURE 8.3: Binding of ROCK1 to liposomes. Different concentration of FolchI has been used to examine liposome binding ability of ROCK1 full length. Sedimentation assay separate liposome binded fraction (pellet) from not-binded portion (supernatant).

Chapter 9

Protection Against Hypertension by CNTF Deficiency

Ciliary Neurtrophic Factor (CNTF) Deficiency Protects Against Angiotensin II-dependent Hypertension

Johannes Stegbauer[1], Yuriko Mori[2], Sebastian Alexander Potthoff[1], Ehsan Amin[3], Esra Sahin[1], Magdalena Woznowski[1], Eva Koenigshausen[1], Lorenz Sellin[1], Mohammad R Ahmadian[3], Lars C. Rump[1] and Ivo Quack[1]

[1]Nephrology, University Hospital Duesseldorf, Duesseldorf, Germany, [3]Nuclear Medicine, University Hospital Duesseldorf, Duesseldorf, Germany and 3Institute of Biochemistry and Molecular Biology II, Heinrich-Heine University Medical Center, Düsseldorf, Germany
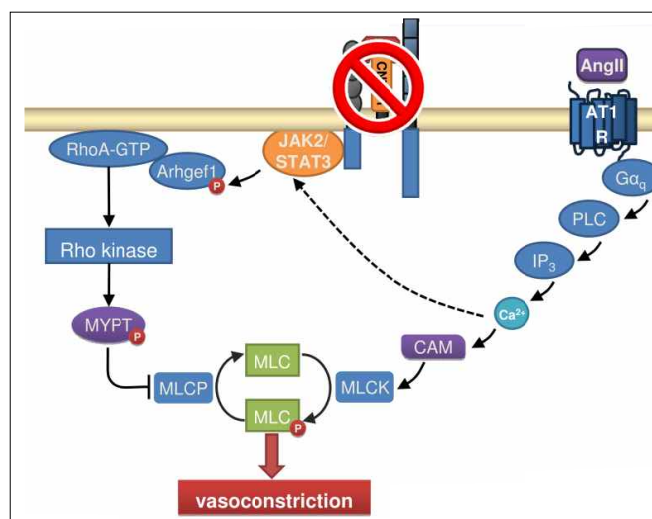
Status:	In preparation
Impact factor:	–
Own Proportion to this work:	10 %; investing of MYPT1 phosphorylation regulation in mouse aorta

9.1 background

Recently, it has been shown that the JAK 2 / STAT3 signaling cascade modulates Ang II (Ang II)-dependent hypertension. The ciliary neutrophic factor (CNTF) is an interleukin-6-like cytokine which plays a distinct role in survival and differentiation of neuronal cells by activating the JAK2 / STAT3 signaling cascade. Despite the well examined role of CNTF in the central nervous system and its ubiquitary abundance, the function of CNTF in other tissues is poorly understood. This study focuses on the role of CNTF in Ang II-dependent hypertension in a model of uninephrectomized mice.

9.2 Results

Two weeks after uninephrectomy, Ang II osmotic minipumps (1000 ng/min/kg BW) were implanted in CNTF-KO and age-matched C57/Bl6J male mice (WT). Blood pressures (BP) were measured for 3 weeks by radiotelemetry, starting one week before implantation. Histological and mRNA analysis were performed at the end of the observation period. Renal vascular function was evaluated in the isolated perfused kidney. Under baseline conditions, systolic BPs were similar in CNTF-KO and WT mice (119± 2 vs.124±1 mmHg). Interestingly, chronic Ang II infusion attenuated the increase of BP in CNTF-KO mice compared to WT mice (week 1: 139±3 vs. 153±3 mmHg; week 2: 151±5 vs. 168±4 mmHg; n=19; P<0.01). Likewise, heart hypertrophy (6.5±0.4 vs. 8.2±0.6 mg/g BW; P<0.01) and cardiac fibrosis was significantly less in the CNTF-KO compared to the WT-group. In accordance, histological and mRNA analysis revealed significantly attenuated renal vascular fibrosis, tubulo-interstitial damage and CD4/CD8 positive cell infiltration as well as reduced NGAL and fibronectin expression in kidneys of Ang II treated CNTF-KO mice compared to WT mice.

   In the isolated perfused kidney, pressor response to Ang II was significantly attenuated in CNTF-KO mice. Administration of CNTF (0.5nM) increased the Ang II dependent pressor response significantly. This effect was mediated through a JAK2/STAT3 pathway as static, a selective STAT3 inhibitor abolished the CNTF induced increase in pressor response in kidneys of CNTF-KO. Additional, CNTF induced STAT3 phosphorylation in a concentration dependent manner in VSMCs. Moreover, phosphorylation of MYPT, a downstream target of JAK2/STAT3 and regulator of the myosin light chain kinase was significantly reduced in angiotensin II infused CNTF-KO mice compared to angiotensin II infused WT mice (Figure 9.1).

9.3 Conclusion

In conclusion, these results suggest that CNTF has a major impact on blood pressure regulation in Ang II-dependent hypertension. CNTF seems to modulate the Ang II induced renal pressor response via a JAK2 / STAT3 dependent mechanism. Thus, CNTF could be an important regulatory cytokine in the pathogenesis of Ang II-dependent hypertension.
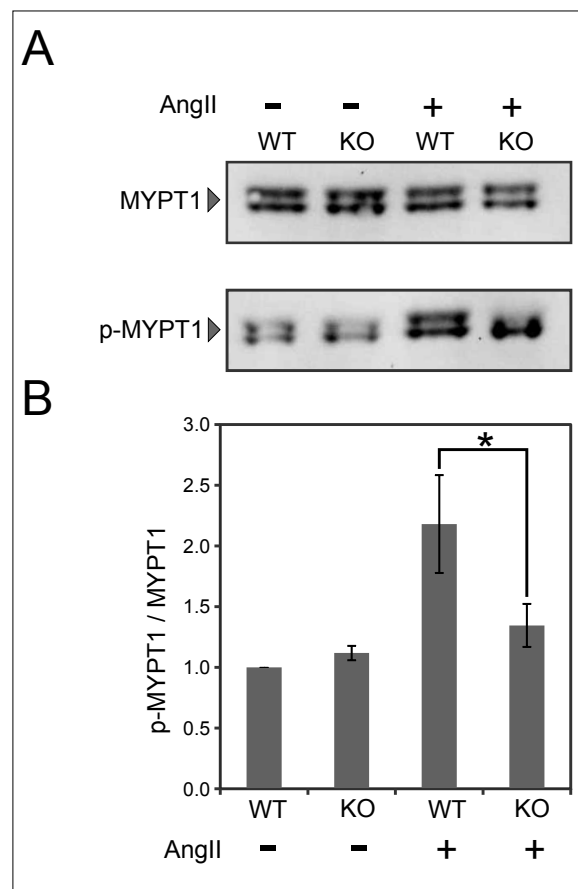
FIGURE 9.1: MYPT1 phosphorylation of WT and CNTF knockout aorta samples. A) total and phospho-MYPT1 of WT and CNTF knockout in the unstimulated and stimulated with Ang II. B) quantification of corresponding western blots.

Chapter 10

IQGAP1 interaction mechanism with RAC1 and CDC42

IQGAP1 interaction with RHO family proteins revisited: kinetic and equilibrium evidence for two distinct binding sites
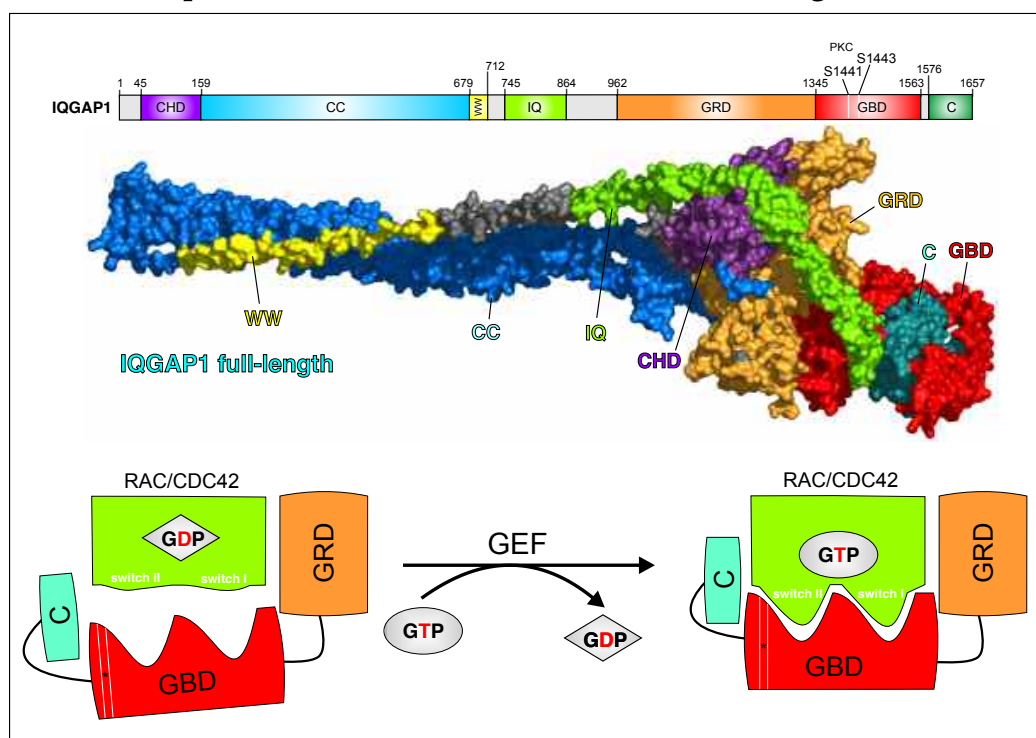
Status:	Under revision in Journal of biological chemistry
Impact factor:	4.57
Own Proportion to this work:	20 %; design and perform experiments and discussion

IQGAP1 interaction with RHO family proteins revisited: Kinetic and equilibrium evidence for multiple distinct binding sites*

Kazem Nouri[1], Eyad K. Fansa[1§], Ehsan Amin[1], Radovan Dvorsky[1], Lothar Gremer[2, 3], Dieter Willbold[2,3], Lutz Schmitt[4], David J. Timson[5], and Mohammad R. Ahmadian[1@]

[1]Institute of Biochemistry and Molecular Biology II, Medical Faculty of the Heinrich-Heine University, 40225 Düsseldorf, Germany; [2]Institute of Physical Biology, Heinrich-Heine University, Düsseldorf, Germany; [3]Forschungszentrum Jülich, ICS-6, 52428 Jülich, Germany
; [4]Institute of Biochemistry, Heinrich-Heine University, Düsseldorf, Germany; [5]School of Pharmacy and Biomolecular Sciences, University of Brighton, Huxley Building, Lewes Road, Brighton BN2 4GJ, United Kingdom.

*Running title: New IQGAP binding mode for CDC42 and RAC1

§Current Address: Structural Biology Group, Max Planck Institute of Molecular Physiology, 44227, Dortmund, Germany

@To whom correspondence should be addressed: Prof. Dr. Mohammad Reza Ahmadian, Institut für Biochemie und Molekularbiologie II, Medizinische Fakultät der Heinrich-Heine-Universität, Universitätsstr. 1, Gebäude 22.03, 40255 Düsseldorf, Germany, Tel.: #49-211-811 2384, #Fax: 49-211-811 2726, e-mail: reza.ahmadian@uni-duesseldorf.de

SUMMARY
IQ motif-containing GTPase activating protein 1 (IQGAP1) plays a central role in the physical assembly of relevant signaling networks that are responsible for various cellular processes, including cell adhesion, polarity and transmigration. The RHO family proteins CDC42 and RAC1, have been proposed to interact with the GAP-related domain (GRD) of IQGAP1. However, the exact nature of this interaction has remained obscure. Here, we demonstrate that the interaction of CDC42 with the C-terminal half of IQGAP1, consisting of at least three different domains, underlies a multiple-step binding mechanism: (i) a high-affinity, GTP-dependent binding of the CDC42/RAC1 association domain (CRAD) to the switch regions of CDC42 or RAC1, and (ii) a very low-affinity, nucleotide-independent binding of GRD and the extreme C-terminal domain of IQGAP1 (CT) outside the switch regions. These data were confirmed by phosphomimetic mutations of Serine 1443 to Glutamate within CRAD, which resulted in lower affinity of the IQGAP1 interaction with CDC42 and RAC1, clearly disclosing the critical role of CRAD for these interactions. Unlike CDC42, a RAC1-GRD interaction was not observed, suggesting that the molecular nature of IQGAP1 interaction with CDC42 partially differs from that of RAC1. Our study provides new insights into the interactions characteristics of IQGAP1 with RHO family proteins and highlight the complementary importance of kinetic and equilibrium analyses. We propose that the ability of IQGAP1 to interact with RHO proteins is based on a multiple-step binding process, which is a prerequisite for the dynamic functions of IQGAP1 as a scaffolding protein and a critical mechanism in temporal regulation and integration of IQGAP1-mediated cellular responses.

INTRODUCTION

The RHO family proteins are critical regulators of many diverse cellular functions (1). They share two common functional characteristics, potential membrane anchorage and an on/off switch cycle (2). RHO protein function is dependent on the guanine nucleotide-binding (G) domain that contains the principal GDP/GTP binding pocket and presents, depending on its nucleotide-bound state, various contact sites for regulators and effectors (2). Membrane-associated RHO proteins act, with some exceptions (3), as molecular switches by cycling between an inactive GDP-bound state and an active GTP-bound state. This cycle underlies two critical intrinsic functions, the GDP/GTP exchange and GTP hydrolysis (3) and is controlled by three main classes of regulatory proteins, guanine nucleotide dissociation inhibitors (GDIs), guanine nucleotide exchange factors (GEFs) and GTPase activating proteins (GAPs) (2). The formation of the active, GTP-bound state of RHO proteins is accompanied by a conformational change in two regions known as switch I and II (2). These regions provide a platform for the selective interaction with structurally and functionally diverse effectors (4), *e.g.*, p21-activated kinase 1 (PAK1) (5), Wiskott-Aldrich syndrome proteins (WASP) (6), p67[phox], a member of the NADPH oxidase family (7), semaphorin receptor Plexin B1 (8,9) as well as the IQ motif-containing GTPase activating proteins (IQGAPs) (10,11).

IQGAP1 is an ubiquitously expressed scaffold protein involved in a variety of cellular processes such as cytoskeleton regulation, regulating cell motility, cell–cell adhesion, protein trafficking, neoplasia, and microbial pathogenesis (10-13). A prerequisite to achieve these functions is association of a multitude of signaling molecules, *e.g.*, calmodulin, kinases and GTPases such as CDC42 and RAC1 (14-17). Distinct domains of IQGAP1, include an N-terminal calponin homology domain (CHD), a coiled-coil repeat region (CC), a tryptophan-containing proline-rich motif-binding region (WW), four isoleucine/glutamine-containing motifs (IQ), a RAS GAP-related domain (GRD), an originally called RASGAP C-terminal domain (RGCT) (14) which is called CDC42/RAC1 associating domain (CRAD) in

this study, and an extreme C-terminal domain (CT). Work from several laboratories has shown that the C-terminal half of IQGAP1, encompassing a GRD and CRAD, binds preferentially to active, GTP-bound form of CDC42 (18-21) (see also Table 1). IQGAP1 GRD, which is structurally a RASGAP homologue but functionally an inactive RASGAP (22), has been demonstrated to undergo interaction with CDC42, although with a substantially lower affinity than the larger protein fragment, containing GRD and CRAD (21,22). These works, together with homology modeling using RHOA-RHOGAP (23) and CDC42-RHOGAP (24) and HRAS-RASGAP (25) complex structures, provided structural models of IQGAP1 GRD that contacts the switch regions of active CDC42 (21,22,26). Interestingly, CRAD contains two serines, 1441 and 1443, which have been shown to be phosphorylation sites by protein kinase C epsilon (PKCε) (27). Phosphomimetic mutations at these sites has been shown to significantly impair IQGAP1 interaction with CDC42 (20). This strongly indicates that regions or domains adjacent to the GRD may be critical for the interaction with the RHO family proteins. In order to shed more light on a structure-function relationship of IQGAP1 interaction with CDC42 and RAC1, we purified different IQGAP1 regions (Fig. 1) and comprehensively investigated these interactions using both a time-resolved fluorescence stopped-flow spectrometry and fluorescence polarization under equilibrium condition. The data provide unprecedented and novel mechanistic insights into the binding mode of IQGAP1 to RHO proteins and suggest that IQGAP1 binds CDC42 and RAC1 while utilizing the CRAD domain rather than the GRD domain to contact their switch regions.

RESULTS

Kinetics of the IQGAP1 interaction with CDC42 and RAC1—Previous work has established that RHO proteins in complex with mGppNHp, a fluorescent and non-hydrolysable GTP analog (Fig. 2A), shows a change in fluorescence upon association with

their downstream effectors using stopped-flow fluorimetry (6). This signal can be used to monitor kinetics of the effector interactions with RHO proteins. Thus we examined whether such a signal can be generated upon the interaction between IQGAP1 and RHO proteins. Equal volumes of two different solutions containing IQGAP1 or RHO protein were rapidly shot into a mixing chamber and the fluorescence was directly detected after a dead time of < 4 ms (Fig. 2B). We observed a rapid change in fluorescence after mixing the GRD1-CT (comprising the C-terminal half of IQGAP1; Fig. 1) with mGppNHp-bound RAC1 (Fig. 2C) or CDC42 (Fig. 2D), which is directly related to the association reaction (see below). There was no change in fluorescence when RHOA-mGppNHp was mixed with GRD1-CT (Fig. 2C), clearly showing that RHOA, in contrast to CDC42 and RAC1, does not associate directly with IQGAP1 under these experimental conditions.

Interestingly, IQGAP1GRD1-CT binding to RAC1-mGppNHp results in an increase in fluorescence (Fig. 2C) whereas association with CDC42-mGppNHp led to a fluorescence decay (Fig. 2D). This indicates that CDC42 and RAC1, in spite of their high sequence identity (71%), obviously differ in regard to their binding modes with IQGAP1. Consistent with our results Owen *et al.* have studied GRD1-CT interaction with a large panel of CDC42 and RAC1 mutants and have suggested that CDC42 and RAC1 appear to have only partially overlapping binding sites for IQGAP1 and may use different structural determinants to achieve high affinity binding (21). To examine this issue we performed competition experiments by mixing GRD1-CT with fluorescent RAC1-mGppNHp and an excess of non-fluorescent CDC42-GppNHp under otherwise the same conditions as above. Figure 2E shows that the presence of CDC42-GppNHp completely blocked GRD1-CT association with RAC1-mGppNHp. A reverse experiment, mixing GRD1-CT with fluorescent CDC42-mGppNHp and an excess of non-fluorescent RAC1-GppNHp, led to the same results (Fig. 2F). These data indicated that CDC42 and RAC1, in spite of obvious differences, share an overlapping binding region for GRD1-CT.

Control experiments using mGDP-bound, inactive CDC42 and RAC1 proteins showed no change in fluorescence when they were mixed with GRD1-CT (Figs. 2C and 2D). This result

supports previous observations (26,28,29), and indicate that IQGAP1 primarily recognizes the switch regions of CDC42 and RAC1, preferentially binding to their GTP-bound active state. To investigate IQGAP1 interaction with RHO proteins in more details, we purified two different GRD fragments designated as GRD1 and GRD2 (Fig. 1) and analyzed their association with mGppNHp-bound RAC1 or CDC42. In contrast to the GRD1-CT, none of these fragments show any change in the fluorescence signal (Figs. 2C and 2D), even at very high concentrations of GRD1 and GRD2 (data not shown). This result was unexpected because GRD has been generally demonstrated as the RAC1- and CDC42-binding domain of IQGAP1 to date (20-22,26). These data suggest that GRD either does not directly interact with CDC42 and RAC1 or it associates outside the switch regions in a distant site from the fluorescent mant moiety of the nucleotide thereby generating no change in the fluorescence signal.

IQGAP1 possesses at least two CDC42-binding domains—The next question addressed was whether IQGAP1 GRD can physically associate with parts of CDC42 and RAC1 other than their switch regions. We applied fluorescence polarization, a different approach to determine the binding affinity of the two proteins at equilibrium (Fig. 3A), and measured the dissociation constant (K_d) of their interaction (30). Figures 3B and 3C show that titration of mGppNHp-bound CDC42 and RAC1 with increasing amounts of not only GRD1-CT but remarkably also GRD2 led to an increase of polarization. These IQGAP1 domains, however, did not exhibit any association with RHOA-mGppNHp (Figs. 3B and 3C). K_d values obtained from these measurements showed that GRD1-CT is a high affinity binder as compared to GRD2 which shows 9- and 15-fold lower affinity for mGppNHp-bound CDC42 and RAC1, respectively (Fig. 3C; Table 1).

The explanation for our observations regarding interaction of GRD with active form of RAC1 is simple; in direct mode only a change in fluorescence can be observed when the associating protein (*e.g.*, GRD1-CT) binds in close vicinity of the fluorophore (mant group of the bound mGppNHp) on the surface of CDC42 and RAC1 (Fig. 2). This surface covers the switch regions that change their conformation upon a GDP/GTP exchange (2). This is of fundamental importance because the

effectors (such as IQGAP1) binding to the switch regions determine the specificity of the signal transduction in cells (2,6,31). So far our data suggest that the binding of the GRD domain to RHO proteins seems to happen outside the switch regions and thus would be expected to be independent of the nucleotide status of the RHO protein. To prove this idea, we repeated the measurements by using mGDP-bound, inactive RHO proteins. Both GRD1-CT and GRD2 were able to interact with mGDP-bound CDC42 although with very low affinities but surprisingly not with RAC1 (Figs. 3D and 3E; Table 1); the latter was also the case for RHOA. This strongly suggests that the molecular nature of IQGAP1 interaction with CDC42 partially differs from that with RAC1 particularly with regard to the role of GRD. We propose that IQGAP1 harbors at least two distinct binding domains. CRAD contributes to a high affinity binding to the switch regions of the GTP-bound, active CDC42 and RAC1. GRD more selectively recognizes active forms of CDC42 and RAC1 but also binds to other regions outside of the switch regions of CDC42 in a nucleotide-independent manner.

CRAD is primarily critical for the IQGAP1 association with CDC42 and RAC1—To further prove the critical role of the C-terminal domains of IQGAP1 beyond GRD we generated various deletion and point mutations of IQGAP1 (Fig. 1). We measured the effect of the last 99 amino acids of IQGAP1 on CDC42 and RAC1 binding by using purified CT and GRD1-CRAD (IQGAP1$^{877-1558}$), which lacks this region (Fig. 1). In contrast to GRD1-CRAD, isolated CT itself did not show, similarly to GRD1 and GRD2, any change in fluorescence upon mixing it with CDC42 and RAC1, respectively (Figs. 2C, 2D and 4A). For comparison, the k_{obs} values were obtained by fitting all data as single exponential and plotted as bar charts, which illustrates that GRD1-CRAD associated slightly faster with CDC42 and RAC1 than GRD1-CT (Fig. 4C). These data emphasize the essential role of a region between GRD and CT, encompassing the residues 1345 to 1575, for direct association of IQGAP1 with the switch regions of CDC42 and RAC1. We were able to purify this region, designated as CRAD in this study (aa 1276-1575), and also CRAD-CT (aa 1276-1657) as GST fusion protein (Fig. 1). Both proteins tend to strongly aggregate and were, thus, disabled

from associating with CDC42 and RAC1 (data not shown).

Interestingly, CRAD contains two PKCε phosphorylation sites (S1441 and S1443; Fig. 1) (20,27), which differently affect GRD1-CRAD association with RAC1-mGppNHp upon their phosphomimetic mutations. To investigate the effect of IQGAP1 phosphorylation on the interaction with RAC1 and CDC42 in more details, we generated and purified phosphomemetic mutants of the GRD1-CRAD^{WT} domain (GRD1-CRAD^{S1441E} and GRD1-CRAD^{S1443E}). In spite of having the same overall secondary structure based on circular dichroism (CD) measurements (data not shown), in contrast to GRD1-CRAD^{S1441E}, with Ser-1441 substituted by Glu, GRD1-CRAD^{S1443E} strongly impaired the observed association of GRD1-CRAD with active CDC42 and RAC1 (Figs. 4A-C). GRD1-CRAD^{S1443E} association with RAC1-mGppNHp is significantly slower as compared to wild type (WT) or S1441E mutant (Figs. 4A and 4B). Determination of the K_d values for the RAC1 and CDC42-binding GRD1-CRAD variants using fluorescence polarization showed that GRD1-CRAD and GRD1-CRAD^{S1441E} exhibited binding affinities for RAC1 and CDC42 in a similar range, which significantly differs from GRD1-CRAD^{S1443E} (Figs. 4D-F; Table 1). These data strongly suggest that CRAD is a critical domain in IQGAP1 primarily responsible for the recognition of and association with the GTP-bound CDC42 and RAC1, and that Ser-1443 phosphorylation may serve as a regulatory switch for these interactions. Our data thus support the previous study by *Li et al.*, which highlighted the importance of this phosphorylation event in IQGAP1-mediated cellular signaling (27).

Modulatory effects of CT on IQGAP1 interaction with CDC42 and RAC1—In order to understand the IQGAP1 interaction with CDC42 and RAC1 in more details, kinetic measurements were performed. This allowed us to obtain individual rate constants k_{on} and k_{off}, for the rate of association and dissociation, respectively as well as the dissociation constant (K_d) calculated from the ratio of k_{off}/k_{on}. To calculate the k_{on} value, association of mGppNHp-bound RAC1 and CDC42 with increasing concentrations of GRD1-CT was measured, leading to changes in fluorescence curves characterized by individual k_{obs} values (Figs. 5A and B, left panels). Obtained k_{obs}

values were fitted in a linear fashion as a function of GRD1-CT concentrations and the slope of fitted line provided the k_{on} (Figs. 5A and B, middle panels). Displacement of GRD1-CT from fluorescently labeled RAC1 and CDC42 was measured by mixing the RAC1/CDC42-mGppNHp-GRD1-CT complex with an excess amount of non-fluorescent RAC1/CDC42-GppNHp. Figures 5A and B (right panels) shows a monoexponential fluorescence decay for RAC1 and increase for CDC42 yielding the k_{off} value for RAC1 and CDC42, respectively. From the ratio of k_{off}/k_{on} we calculated the dissociation constant (K_d) of 0.94 and 0.30 µM for RAC1 and CDC42, respectively which is comparable to the values obtained by fluorescence polarization in this study and other methods in other laboratories (Table 1; Fig. 5C); (19,21,22).

CDC42 as compared to RAC1 exhibited a faster k_{on}, a slower k_{off} and therefore, a three-fold higher binding affinity for GRD1-CT (Figs. 5B and 5C). GRD1-CRAD, lacking the C-terminal CT domain, strikingly revealed a six-fold faster k_{off} in comparison to GRD1-CT, while the k_{on} values remained largely the same (Fig. 5C, Supplemental Figs. S1 and S2). Thus, C-terminal truncation of IQGAP1 reduced its overall affinity for CDC42 and RAC1, indicating that CT either acts directly as a secondary CDC42- and RAC1-binding domain or may indirectly stabilize CRAD and/or GRD binding to CDC42 and RAC1.

To examine a direct interaction of IQGAP1 CT, encompassing the C-terminal 99 amino acids (Fig. 1), we used the RHO proteins and isolated CT domain as a GST fusion protein and measured their interaction ability by the fluorescence polarization. The data revealed CT to have a binding capacity of its own for CDC42, RAC1 and RHOA that is rather very low (Supplemental Fig. S3). In addition to CRAD and GRD, CT may play, as a very low-affinity binder, a direct role in the CDC42 and RAC1 interaction. CT also seems to bind RHOA, which means that its binding region on the surface of these prominent members of the RHO family must be conserved (see discussion).

From the two reported phosphorylation sites (27), Ser-1443 turned out to be critical for the IQGAP1 interaction with CDC42 and RAC1 but not Ser-1441 (Fig. 4). Kinetic data shown in Figures 5C, S1 and S2 clearly revealed that Ser-1443 substitution for Glu more strongly affected the GRD1-CRAD association with

CDC42 and also RAC1 as compared to the dissociation reaction. The rate constants obtained for GRD1-CRAD^{S1441E} were as the wild-type (WT) (Fig. 5C). Thus, we propose that CRAD is critical for IQGAP1 association with CDC42 and RAC1, which is modulated by Ser-1443 phosphorylation, while GRD and probably CT control the resident time and the off rate of the protein complex.

DISCUSSION

Association of downstream effectors with their specific small GTPases has been generally accepted to release them from an autoinhibited state resulting in their activation. The switch regions of small GTPases have been previously proposed as the first binding site for the downstream effectors. When this first contact is achieved then additional contacts outside the switch regions are required to fulfill effector activation (2). The molecular mechanism of this process which is critical for signal transduction is unclear for most effectors, especially for scaffolding proteins. A straight-forward example is WASP, which is able to activate the actin-related proteins ARP2/3, if its C-terminal ARP2/3-binding domains are unmasked upon association with CDC42 (6). This process controls assembly of actin filaments (32). In contrast, IQGAP1 is a multifaceted protein that employs a variety of domains in an assembly of multitude protein complexes which coordinates different processes in a variety of cell types (10-13).

A key role has been previously assigned to the IQGAP1 GRD association with the switch regions of CDC42 and RAC1 (21,22) and this has been generally accepted as an interaction model for these proteins, albeit with suggestions that critical determinants for RAC1 binding to IQGAP1 lie outside this region (21). However, data obtained from different deletion and point mutations of IQGAP1 in this study clearly exclude a central role for GRD in the recognition of RHO proteins as it binds adjacent to the switch regions of CDC42 and, to a certain extent, also RAC1. Instead, a region next to GRD appeared as the central domain for the association of IQGAP1 with the switch regions of both CDC42 and RAC1. Mimetic mutations of the PKCε phosphorylation site Ser-1443 in this domain significantly affected IQGAP1 association with CDC42 and RAC1. For this reason, we renamed the original name of this region, RGCT (RASGAP C-terminal), to CRAD (CDC42/RAC associating domain),

particularly because it does not bind RHOA. In contrast to CDC42 and RAC1 and unlike previous cell-based studies (33,34), but very much in line with early studies (28,35-40), no physical interaction of neither GRD2 or GRD1-CT was observed with RHOA using both kinetic and equilibrium measurements (Figs. 2C, 3B and 3C). This clearly indicates that observed IQGAP1 association with RHOA are indirectly mediated by other proteins in co-immunoprecipitates. Interaction of GRD1-CT with CDC42 and RAC1 is strong and GTP dependent. GRD makes a considerable contribution to an overall binding affinity of IQGAP1 to CDC42 and RAC1, although its role in these interactions turned out to be rather different (Fig. 3). GRD undergoes a weak interaction with mGDP-bound, inactive CDC42 but not with RAC1-mGDP. This rather suggests that GRD binds to a surface outside the switch regions of CDC42, which is obviously not conserved in RAC1. Furthermore, our data also demonstrate that the extreme C-terminal region of IQGAP1, CT (99 aa), may also bind, although with a very low affinity, to a common site of CDC42 and RAC1 that is also shared by RHOA (Supplemental Fig. S3).

Previous studies by other groups have shown that shorter IQGAP1 fragments, encompassing the GRD domain, are responsible for the CDC42 and RAC1 interactions. *Zhang and coworkers* showed that an activated form of CDC42 is able to bind IQGAP1 GRD1-CT (aa 864-1657) (41). One year later the same group reported that not only CDC42 but also RAC1, although with lower affinity, could interact to GRD1-CT (19). Afterwards, *Nomanbhoy and Cerione*, have shown that GRD1-CT interacts tightly with CDC42-mGTP using a fluorescence assay (42). *Owen et al.* have also reported that a GRD protein (aa 950-1407) was able to tightly bind CDC42(Q61L) with a K_d value of 140 nM but failed to bind RAC1(Q61L) using a scintillation proximity assay (21). In contrast, GRD1-CT has shown a much higher affinity for the Q61L mutant of not only CDC42 but also of RAC1, and yet the GRD was proposed to be the binding domain of IQGAP1 that associates with the switch regions of CDC42. Correspondingly, *Kurella et al.* have reported that GRD2 (aa 962-1345) binds CDC42 in a GTP-dependent manner with an affinity of 1.3 μM using isothermal titration calorimetry (22). These biochemical data (summarized in Table 1) along with the

homology modeling based on the RAS-RASGAP structure (25), provided up to date a structural model of IQGAP1 GRD contacting the switch regions of the CDC42, which is generally accepted in the community (20-22,26,43). Contrary to the existing model, we observed different properties of GRD1-CT and GRD2 in their interactions with CDC42 and RAC1. This was evidenced by kinetic measurements of GRD1-CT and GRD1-CRAD association, but not GRD, with CDC42 and RAC1 proteins (Figs. 2 and 4; no changes in fluorescence were observed with GRD). Equilibrium measurements using fluorescence polarization not only substantiated the essential role of IQGAP1 CRAD in a GTP-dependent interaction with CDC42 and RAC1 in agreement with our kinetic analysis but also provided striking insights into the main feature of IQGAP1 GRD. Our quantitative analysis under equilibrium conditions clearly revealed that GRD undergoes a low-affinity interaction with CDC42 but its binding in contrast to CRAD is largely nucleotide independent and the binding site most likely resides outside the critical switch regions. mGDP-bound RHOA and particularly RAC1 did, however, not reveal any interaction with IQGAP1 GRD. A faster k_{on}, a slower k_{off} and a lower K_d of GRD1-CT for CDC42, in direct comparison to RAC1, strongly suppport our data from fluorescence polarization demonstrating that not only CRAD but also GRD bind mGppNHp-bound CDC42 and RAC1 (Fig. 3). The significance of CRAD (previously called RGTC) as a GTP-dependent interacting domain for CDC42 and RAC1 was proved using a single point mutant of GRD1-CRAD (Ser-1443 substituted by Glu) which led to the abolition of a GTP-dependent interaction of GRD1-CRAD while nucleotide-independent association with CDC42 through GRD was unchanged. Ser-1443 was identified as the major site phosphorylated on IQGAP1 in intact cells treated with PMA (phorbol 12-myristate 13-acetate) (27). Phosphomimetic mutation of Ser-1441, a second phosphorylation site, that was shown to be phosphorylated to a lesser extent as compared to Ser-1443 (27), did not affect the interaction with either CDC42 or RAC1. *Grohmanova* and coworkers previuosly have shown *via* GST pull down experiments and using MCF10A cell lysate, that in the presence of phosphatase inhibitor there is a significant reduction in the interaction between IQGAP1 and CDC42-GTP in contrast to

nucleotide depleted CDC42 which binds to phosphorylated IQGAP1 much more strongly (28). In addition, our data have clearly demonstrated that the region upstream of GRD2 (aa 863-961) is dispensable for the CDC42 and RAC1 interaction.

Another interesting issue was a significantly faster dissociation of GRD1-CRAD (lacking the CT domain) from CDC42 and RAC1 as compared to GRD1-CT. This clearly indicates an involvment of the very C-terminal 99 amino acids (CT) in the overall binding affinity of GRD1-CT for CDC42 and RAC1 (Fig. 5C). Our fluorescence polarization measurements showed that isolated CT has the tendency to associate with CDC42, RAC1 and also RHOA, although with low affinity (Fig. Supplemental S3).

A multiple-step binding mechanism—Our kinetic and equilibrium measurements challenge the paradigm that the ability of IQGAP1 to interact with RAC/CDC42 proteins is mainly attributed to its GAP-related domain (GRD). We propose that GRD1-CT, the C-terminal 795 amino acids of IQGAP1, encompasses at least three distinct domains, which may differently interact with CDC42 and RAC1 at different contact sites in a multistep, cooperative manner. The switch regions of the RHO family proteins are the first binding site for the downstream effectors. Once it is occupied, additional contacts outside the switch regions are required to guarantee effector activation (2,6). Accordingly, CRAD appears as a central domain that rapidly associates with the switch regions of GTP-bound CDC42 and RAC1 but not RHOA. CT may additionally bind to a different site conserved in RAC1 and CDC42, and extend the residence time of the respective complexes. A possible interaction of CT with RHOA seems to be physiologically irrelevant simply because CRAD and GRD do not recognize RHOA. These interactions may induce a local conformational change enabling GRD to bind selectively to GTP-bound CDC42 and RAC1 but not RHOA. Such sequential but differential association of IQGAP1 with CDC42 *vs*. RAC1 can be envisaged as conformational changes within IQGAP1 enabling a set of interactions at structurally accessible and available regions with its downstream targets depending on the upstream signals and the cell fate. The fact that GDP-bound CDC42, but not RAC1, is able to interact with GRD suggests that GRD may undergo a low-affinity complex with GDP-

bound, inactive CDC42 proteins outside its switch regions in a way that is independent of the upstream signals, providing GRD is structurally accessible and available for interactions. This may also be a model for the IQGAP1-mediated scaffolding of the CDC42-GTP-WASP complex regulating actin assembly, extension of lamellipodia and promotion of dendritic spine head formation (11,44,45).

CONCLUDING REMARKS

Protein-protein interaction studies on the active, GTP-bound form of CDC42 and RAC1 has identified IQGAP1 as a putative downstream effector (18-22,26,29,46-49). Accumulating evidence supports diverse roles for the IQGAP1 interaction with CDC42 and RAC1 in vertebrates, which has significance for a variety of biological functions. However, the nature of such protein-protein recognition processes has remained obscure. Initially it was thought that modulation of the cytoskeletal architecture is the primary function of the interaction of IQGAP1 with RHO proteins, but it is now clear that it has many critical physiological roles beyond the cytoskeleton. CDC42 promotes the interaction of PTPμ with IQGAP1 to stimulate actin remodeling and, eventually, neurite outgrowth (27,50), and also the complex of active CDC42, Lis1, and CLIP-170 with IQGAP1 seems to be crucial for cerebellar neuronal motility (48). Another example is in pancreatic β-cells where IQGAP1 scaffolds CDC42, RAB27A, and coronin-3 in the insulin secretory pathway and this complex controls endocytosis of insulin secretory vesicles (38). However, a major question remaining to be addressed is what are the consequences of different interaction of IQGAP1 with CDC42 *vs*. RAC1. Lack of GRD interaction with RAC1 may be compensated by calmodulin as an accessory protein, which has been reported as binding partner of RAC1 and IQGAP1 (51-53). The ability of GRD in binding outside the switch regions of CDC42 may facilitate the scaffolding function of IQGAP1 in localizing CDC42 and WASP at specific sites.

It is also of major interest to address the question whether the C-terminal domains CRAD and CT compete in binding to CDC42 and RAC1 with other proteins, including CLIP-170, E-cadherin, β-catenin, Adenomatous polyposis coli (APC), mDIA, CLASP2, TSG101, SEC3/8, and SMG9. These

proteins have also been reported to associate with CRAD and CT(11,36,54-59). APC has been shown to activate ASEF, a CDC42-specific Dbl protein (60), at the leading edge of a migrating cell, which may thereby initiate CDC42-IQGAP1 signaling. In addition, it remains to be addressed whether IQGAP1 interaction with CDC42 or RAC1 is initiated by association of IQGAP1 with membrane lipids, such as PIP2 or PIP3 (61).

There is one obvious consequence of IQGAP1 as a RAC1/CDC42 effector: IQGAP1 not only has direct interactions with the small GTPases, but also has been detected in a complex with an effector (PAK6) and a regulator (TIAM1) of small G proteins (62). Immunoprecipitation of IQGAP1 from human pulmonary artery endothelial cells isolated a complex containing TIAM1, RAC1, Src, cortactin, p47phox and phospholipase D2 (62), but the direct interaction of TIAM1 and IQGAP1 has not been reported yet, and the possible biological relevance of the interaction remains unknown.

IQGAP1 also bind RhoGDI (16), which is known to dislodge RHO proteins from the plasma membrane. It would be interesting to know whether IQGAP1 is a displacement factor for the RHOGDI complex with RAC1 or CDC42.

Another significant question to be answered is the possible role of these interactions in carcinogenesis. Dysregulation and in some cases, mutation of RAC1 and CDC42 leads to carcinogenesis (63,64). IQGAP1 is overexpressed in a variety of cancers and its overexpression enhances the active GTP-bound form of CDC42 and RAC1 in the cells, while knockdown of endogenous IQGAP1 considerably reduces the amount of active CDC42 and RAC1 (65-67). In addition, a dominant-negative IQGAP1 construct, which decreases the amount of active CDC42 in the cell (66) leads to reduction in neoplastic transformation of malignant MCF-7 human breast epithelial cells (65). These results suggest that blocking IQGAP1–CDC42 and IQGAP1–RAC1 complex formation will decrease the amount of active forms of CDC42 and RAC1 in carcinoma cells and thus reduce tumorigenesis. Therefore, antagonists which disrupt the binding of IQGAP1 to RAC1 and/or CDC42 could prevent tumor invasion, proliferation, and migration and could act as specific chemotherapeutic agents. However, the design of such antagonists absolutely and critically requires knowledge of the key protein-protein interfaces between IQGAP1 and these small GTPases. The data reported here provide an important step in defining these sites.

EXPERIMANTAL PROCEDURES
Constructs—Different constructs of pGEX vectors encoding an N-terminal glutathione S-transferase (GST) fusion protein were used for the overexpression of various human genes: Different IQGAP1 (acc. no. P46940) regions (aa 863-1345, 863-1657, 877-1558, 1276-1657, 1276-1575, 1576-1657), and also RAC1, CDC42, and RHOA, as reported before (8). pMCSG7 vector was used for overexpression of IQGAP1 aa 962-1345 and pET46 EkLIC vector (Merck, Nottingham, United Kingdom) for the overexpression of IGQAP1 S1441E and S1143E mutants (aa 877-1558) as His-tagged proteins. The Kazusa cDNA clone KIAA0051 (68) was used as a template for site directed mutagenesis.

Proteins—All proteins were purified according to the protocols described (3,69,70). Nucleotide-free RHO proteins were prepared using alkaline phosphatase (Roche) and phosphodiesterase (Sigma Aldrich) at 4°C as described (71). Fluorescent methylanthraniloyl (mant or m) bound to nucleotides was used to generate mGDP and mGppNHp loaded RHO proteins. GppNHp is a nonhydrolayzable analog of GTP. The quality and concentrations of labeled proteins were determined as described (71).

Stopped-flow fluorescence measurements—Kinetics measurements were monitored by stopped-flow apparatus (Hi-Tech Scientific SF-61 with a mercury xenon light source and TgK Scientific Kinetic Studio software), and performed as described (70). To obtain high accuracy data, four to six measurements were performed and averaged. The observed rate constants (k_{obs}) were fitted single exponentially using the GraFit program (Erithacus software).

Fluorescence polarization—Experiments were performed in a Fluoromax 4 fluorimeter in polarization mode as described (72). To increase the overall molecular mass of some IQGAP1 domains we used GST fusion proteins to get larger increase in the polarization signal upon binding. The dissociation constant (K_d) were calculated by fitting the concentration dependent binding curve using a quadratic ligand binding equation.

CONFLICT OF INTEREST
The authors declare no conflict of interest.

AUTHOR CONTRIBUTIONS
M.-R.A., conceived and coordinated the study; K.N., E.K.F., E.A., R.D., and L.G., designed, performed and analyzed the experiments; K.N., E.K.F., E.A., D.J.T., D.W., L.S., and M.-R.A. directed experiments, analyzed data and co-wrote the paper; all authors reviewed the results and approved the final version of the manuscript.

REFERENCES

1. Hall, A. (2012) Rho family GTPases. *Biochem Soc Trans* **40**, 1378-1382
2. Dvorsky, R., and Ahmadian, M. R. (2004) Always look on the bright site of Rho: structural implications for a conserved intermolecular interface. *EMBO Rep* **5**, 1130-1136
3. Jaiswal, M., Fansa, E. K., Dvorsky, R., and Ahmadian, M. R. (2013) New insight into the molecular switch mechanism of human Rho family proteins: shifting a paradigm. *Biol Chem* **394**, 89-95
4. Bishop, A. L., and Hall, A. (2000) Rho GTPases and their effector proteins. *Biochem J* **2**, 241-255
5. Lei, M., Lu, W., Meng, W., Parrini, M. C., Eck, M. J., Mayer, B. J., and Harrison, S. C. (2000) Structure of PAK1 in an autoinhibited conformation reveals a multistage activation switch. *Cell* **102**, 387-397
6. Hemsath, L., Dvorsky, R., Fiegen, D., Carlier, M. F., and Ahmadian, M. R. (2005) An electrostatic steering mechanism of Cdc42 recognition by Wiskott-Aldrich syndrome proteins. *Mol Cell* **20**, 313-324
7. Lapouge, K., Smith, S. J., Walker, P. A., Gamblin, S. J., Smerdon, S. J., and Rittinger, K. (2000) Structure of the TPR domain of p67phox in complex with Rac.GTP. *Mol Cell* **6**, 899-907
8. Fansa, E. K., Dvorsky, R., Zhang, S. C., Fiegen, D., and Ahmadian, M. R. (2013) Interaction characteristics of Plexin-B1 with Rho family proteins. *Biochem Biophys Res Commun* **434**, 785-790
9. Hota, P. K., and Buck, M. (2012) Plexin structures are coming: opportunities for multilevel investigations of semaphorin guidance receptors, their cell signaling mechanisms, and functions. *Cell Mol Life Sci* **69**, 3765-3805
10. Watanabe, T., Wang, S., and Kaibuchi, K. (2015) IQGAPs as Key Regulators of Actin-cytoskeleton Dynamics. *Cell Struct Funct* **40**, 69-77
11. Hedman, A. C., Smith, J. M., and Sacks, D. B. (2015) The biology of IQGAP proteins: beyond the cytoskeleton. *EMBO reports* **16**, 427-446
12. Choi, S., and Anderson, R. A. (2016) IQGAP1 is a phosphoinositide effector and kinase scaffold. *Advances in biological regulation* **60**, 29-35
13. Abel, A. M., Schuldt, K. M., Rajasekaran, K., Hwang, D., Riese, M. J., Rao, S., Thakar, M. S., and Malarkannan, S. (2015) IQGAP1: insights into the function of a molecular puppeteer. *Mol Immunol* **65**, 336-349
14. White, C. D., Erdemir, H. H., and Sacks, D. B. (2012) IQGAP1 and its binding proteins control diverse biological functions. *Cell Signal* **24**, 826-834
15. Malarkannan, S., Awasthi, A., Rajasekaran, K., Kumar, P., Schuldt, K. M., Bartoszek, A., Manoharan, N., Goldner, N. K., Umhoefer, C. M., and Thakar, M. S. (2012) IQGAP1: a regulator of intracellular spacetime relativity. *J Immunol* **188**, 2057-2063
16. Liu, J., Guidry, J. J., and Worthylake, D. K. (2014) Conserved sequence repeats of IQGAP1 mediate binding to Ezrin. *J Proteome Res* **13**, 1156-1166
17. Pathmanathan, S., Hamilton, E., Atcheson, E., and Timson, D. J. (2011) The interaction of IQGAPs with calmodulin-like proteins. *Biochem Soc Trans* **39**, 694-699
18. McCallum, S. J., Wu, W. J., and Cerione, R. A. (1996) Identification of a putative effector for Cdc42Hs with high sequence similarity to the RasGAP-related protein IQGAP1 and a Cdc42Hs binding partner with similarity to IQGAP2. *J Biol Chem* **271**, 21732-21737
19. Zhang, B., Chernoff, J., and Zheng, Y. (1998) Interaction of Rac1 with GTPase-activating proteins and putative effectors. A comparison with Cdc42 and RhoA. *J Biol Chem* **273**, 8776-8782
20. Elliott, S. F., Allen, G., and Timson, D. J. (2012) Biochemical analysis of the interactions of IQGAP1 C-terminal domain with CDC42. *World J Biol Chem* **3**, 53-60
21. Owen, D., Campbell, L. J., Littlefield, K., Evetts, K. A., Li, Z., Sacks, D. B., Lowe, P. N., and Mott, H. R. (2008) The IQGAP1-Rac1 and IQGAP1-Cdc42 interactions: interfaces differ between the complexes. *J Biol Chem* **283**, 1692-1704

22. Kurella, V. B., Richard, J. M., Parke, C. L., Lecour, L. F., Jr., Bellamy, H. D., and Worthylake, D. K. (2009) Crystal structure of the GTPase-activating protein-related domain from IQGAP1. *J Biol Chem* **284**, 14857-14865

23. Rittinger, K., Walker, P. A., Eccleston, J. F., Nurmahomed, K., Owen, D., Laue, E., Gamblin, S. J., and Smerdon, S. J. (1997) Crystal structure of a small G protein in complex with the GTPase-activating protein rhoGAP. *Nature* **388**, 693-697

24. Nassar, N., Hoffman, G. R., Manor, D., Clardy, J. C., and Cerione, R. A. (1998) Structures of Cdc42 bound to the active and catalytically compromised forms of Cdc42GAP. *Nat Struct Biol* **5**, 1047-1052

25. Scheffzek, K., Ahmadian, M. R., Kabsch, W., Wiesmuller, L., Lautwein, A., Schmitz, F., and Wittinghofer, A. (1997) The Ras-RasGAP complex: structural basis for GTPase activation and its loss in oncogenic Ras mutants. *Science* **277**, 333-338

26. Mataraza, J. M., Briggs, M. W., Li, Z., Frank, R., and Sacks, D. B. (2003) Identification and characterization of the Cdc42-binding site of IQGAP1. *Biochem Biophys Res Commun* **305**, 315-321

27. Li, Z., McNulty, D. E., Marler, K. J., Lim, L., Hall, C., Annan, R. S., and Sacks, D. B. (2005) IQGAP1 promotes neurite outgrowth in a phosphorylation-dependent manner. *J Biol Chem* **280**, 13871-13878

28. Grohmanova, K., Schlaepfer, D., Hess, D., Gutierrez, P., Beck, M., and Kroschewski, R. (2004) Phosphorylation of IQGAP1 modulates its binding to Cdc42, revealing a new type of rho-GTPase regulator. *J Biol Chem* **279**, 48495-48504

29. Noritake, J., Watanabe, T., Sato, K., Wang, S., and Kaibuchi, K. (2005) IQGAP1: a key regulator of adhesion and migration. *J Cell Sci* **118**, 2085-2092

30. Raines, R. T. (2015) Fluorescence polarization assay to quantify protein-protein interactions: an update. *Methods Mol Biol* **1278**, 323-327

31. Li, R., Debreceni, B., Jia, B., Gao, Y., Tigyi, G., and Zheng, Y. (1999) Localization of the PAK1-, WASP-, and IQGAP1-specifying regions of Cdc42. *J Biol Chem* **274**, 29648-29654

32. Carlier, M. F., Pernier, J., Montaville, P., Shekhar, S., and Kuhn, S. (2015) Control of polarized assembly of actin filaments in cell motility. *Cell Mol Life Sci* **72**, 3051-3067

33. Casteel, D. E., Turner, S., Schwappacher, R., Rangaswami, H., Su-Yuo, J., Zhuang, S., Boss, G. R., and Pilz, R. B. (2012) Rho isoform-specific interaction with IQGAP1 promotes breast cancer cell proliferation and migration. *J Biol Chem* **287**, 38367-38378

34. Bhattacharya, M., Sundaram, A., Kudo, M., Farmer, J., Ganesan, P., Khalifeh-Soltani, A., Arjomandi, M., Atabai, K., Huang, X., and Sheppard, D. (2014) IQGAP1-dependent scaffold suppresses RhoA and inhibits airway smooth muscle contraction. *J Clin Invest* **124**, 4895-4898

35. Brill, S., Li, S., Lyman, C. W., Church, D. M., Wasmuth, J. J., Weissbach, L., Bernards, A., and Snijders, A. J. (1996) The Ras GTPase-activating-protein-related human protein IQGAP2 harbors a potential actin binding domain and interacts with calmodulin and Rho family GTPases. *Mol Cell Biol* **16**, 4869-4878

36. Watanabe, T., Wang, S., Noritake, J., Sato, K., Fukata, M., Takefuji, M., Nakagawa, M., Izumi, N., Akiyama, T., and Kaibuchi, K. (2004) Interaction with IQGAP1 links APC to Rac1, Cdc42, and actin filaments during cell polarization and migration. *Dev Cell* **7**, 871-883

37. Wang, S., Watanabe, T., Noritake, J., Fukata, M., Yoshimura, T., Itoh, N., Harada, T., Nakagawa, M., Matsuura, Y., Arimura, N., and Kaibuchi, K. (2007) IQGAP3, a novel effector of Rac1 and Cdc42, regulates neurite outgrowth. *J Cell Sci* **120**, 567-577

38. Kimura, T., Yamaoka, M., Taniguchi, S., Okamoto, M., Takei, M., Ando, T., Iwamatsu, A., Watanabe, T., Kaibuchi, K., Ishizaki, T., and Niki, I. (2013) Activated Cdc42-bound IQGAP1 determines the cellular endocytic site. *Mol Cell Biol* **33**, 4834-4843

39. Kuroda, S., Fukata, M., Kobayashi, K., Nakafuku, M., Nomura, N., Iwamatsu, A., and Kaibuchi, K. (1996) Identification of IQGAP as a putative target for the small GTPases, Cdc42 and Rac1. *J Biol Chem* **271**, 23363-23367

40. Hart, M. J., Callow, M. G., Souza, B., and Polakis, P. (1996) IQGAP1, a calmodulin-binding protein with a rasGAP-related domain, is a potential effector for cdc42Hs. *Embo J* **15**, 2997-3005

41. Zhang, B., Wang, Z. X., and Zheng, Y. (1997) Characterization of the interactions between the small GTPase Cdc42 and its GTPase-activating proteins and putative effectors. Comparison of kinetic properties of Cdc42 binding to the Cdc42-interactive domains. *J Biol Chem* **272**, 21999-22007

42. Nomanbhoy, T., and Cerione, R. A. (1999) Fluorescence assays of Cdc42 interactions with target/effector proteins. *Biochemistry* **38**, 15878-15884

43. Kuroda, S., Fukata, M., Nakagawa, M., Fujii, K., Nakamura, T., Ookubo, T., Izawa, I., Nagase, T., Nomura, N., Tani, H., Shoji, I., Matsuura, Y., Yonehara, S., and Kaibuchi, K. (1998) Role of IQGAP1, a target of the small GTPases Cdc42 and Rac1, in regulation of E-cadherin- mediated cell-cell adhesion. *Science* **281**, 832-835

44. Le Clainche, C., Schlaepfer, D., Ferrari, A., Klingauf, M., Grohmanova, K., Veligodskiy, A., Didry, D., Le, D., Egile, C., Carlier, M. F., and Kroschewski, R. (2007) IQGAP1 stimulates actin assembly through the N-WASP-Arp2/3 pathway. *J Biol Chem* **282**, 426-435

45. Jausoro, I., Mestres, I., Quassollo, G., Masseroni, L., Heredia, F., and Caceres, A. (2013) Regulation of spine density and morphology by IQGAP1 protein domains. *PLoS One* **8**, e56574

46. Kuroda, S., Fukata, M., Nakagawa, M., and Kaibuchi, K. (1999) Cdc42, Rac1, and their effector IQGAP1 as molecular switches for cadherin-mediated cell-cell adhesion. *Biochem Biophys Res Commun* **262**, 1-6

47. Izumi, G., Sakisaka, T., Baba, T., Tanaka, S., Morimoto, K., and Takai, Y. (2004) Endocytosis of E-cadherin regulated by Rac and Cdc42 small G proteins through IQGAP1 and actin filaments. *J Cell Biol* **166**, 237-248

48. Kholmanskikh, S. S., Koeller, H. B., Wynshaw-Boris, A., Gomez, T., Letourneau, P. C., and Ross, M. E. (2006) Calcium-dependent interaction of Lis1 with IQGAP1 and Cdc42 promotes neuronal motility. *Nat Neurosci* **9**, 50-57

49. Brown, M. D., Bry, L., Li, Z., and Sacks, D. B. (2007) IQGAP1 regulates Salmonella invasion through interactions with actin, Rac1, and Cdc42. *J Biol Chem* **282**, 30265-30272

50. Phillips-Mason, P. J., Gates, T. J., Major, D. L., Sacks, D. B., and Brady-Kalnay, S. M. (2006) The receptor protein-tyrosine phosphatase PTPmu interacts with IQGAP1. *J Biol Chem* **281**, 4903-4910

51. Ruiz-Velasco, R., Lanning, C. C., and Williams, C. L. (2002) The activation of Rac1 by M3 muscarinic acetylcholine receptors involves the translocation of Rac1 and IQGAP1 to cell junctions and changes in the composition of protein complexes containing Rac1, IQGAP1, and actin. *J Biol Chem* **277**, 33081-33091

52. Vidal-Quadras, M., Gelabert-Baldrich, M., Soriano-Castell, D., Llado, A., Rentero, C., Calvo, M., Pol, A., Enrich, C., and Tebar, F. (2011) Rac1 and calmodulin interactions modulate dynamics of ARF6-dependent endocytosis. *Traffic* **12**, 1879-1896

53. Ho, Y. D., Joyal, J. L., Li, Z., and Sacks, D. B. (1999) IQGAP1 integrates Ca2+/calmodulin and Cdc42 signaling. *J Biol Chem* **274**, 464-470

54. Fukata, M., Kuroda, S., Nakagawa, M., Kawajiri, A., Itoh, N., Shoji, I., Matsuura, Y., Yonehara, S., Fujisawa, H., Kikuchi, A., and Kaibuchi, K. (1999) Cdc42 and Rac1 regulate the interaction of IQGAP1 with beta-catenin. *J Biol Chem* **274**, 26044-26050

55. Brandt, D. T., Marion, S., Griffiths, G., Watanabe, T., Kaibuchi, K., and Grosse, R. (2007) Dia1 and IQGAP1 interact in cell migration and phagocytic cup formation. *J Cell Biol* **178**, 193-200

56. Watanabe, T., Noritake, J., Kakeno, M., Matsui, T., Harada, T., Wang, S., Itoh, N., Sato, K., Matsuzawa, K., Iwamatsu, A., Galjart, N., and Kaibuchi, K. (2009) Phosphorylation of CLASP2 by GSK-3beta regulates its interaction with IQGAP1, EB1 and microtubules. *J Cell Sci* **122**, 2969-2979

57.   Dolnik, O., Kolesnikova, L., Welsch, S., Strecker, T., Schudt, G., and Becker, S. (2014) Interaction with Tsg101 is necessary for the efficient transport and release of nucleocapsids in marburg virus-infected cells. *PLoS Pathog* **10**, e1004463

58.   Sakurai-Yageta, M., Recchi, C., Le Dez, G., Sibarita, J. B., Daviet, L., Camonis, J., D'Souza-Schorey, C., and Chavrier, P. (2008) The interaction of IQGAP1 with the exocyst complex is required for tumor cell invasion downstream of Cdc42 and RhoA. *J Cell Biol* **181**, 985-998

59.   Takeda, S., Fujimoto, A., Yamauchi, E., Hiyoshi, M., Kido, H., Watanabe, T., Kaibuchi, K., Ohta, T., and Konishi, H. (2011) Role of a tyrosine phosphorylation of SMG-9 in binding of SMG-9 to IQGAP and the NMD complex. *Biochem Biophys Res Commun* **410**, 29-33

60.   Gotthardt, K., and Ahmadian, M. R. (2007) Asef is a Cdc42-specific guanine nucleotide exchange factor. *Biol Chem* **388**, 67-71

61.   Choi, S., Thapa, N., Hedman, A. C., Li, Z., Sacks, D. B., and Anderson, R. A. (2013) IQGAP1 is a novel phosphatidylinositol 4,5 bisphosphate effector in regulation of directional cell migration. *Embo j* **32**, 2617-2630

62.   Usatyuk, P. V., Gorshkova, I. A., He, D., Zhao, Y., Kalari, S. K., Garcia, J. G., and Natarajan, V. (2009) Phospholipase D-mediated activation of IQGAP1 through Rac1 regulates hyperoxia-induced p47phox translocation and reactive oxygen species generation in lung endothelial cells. *J Biol Chem* **284**, 15339-15352

63.   Davis, M. J., Ha, B. H., Holman, E. C., Halaban, R., Schlessinger, J., and Boggon, T. J. (2013) RAC1P29S is a spontaneously activating cancer-associated GTPase. *Proc Natl Acad Sci U S A* **110**, 912-917

64.   Sahai, E., and Marshall, C. J. (2002) RHO-GTPases and cancer. *Nat Rev Cancer* **2**, 133-142

65.   Jadeski, L., Mataraza, J. M., Jeong, H. W., Li, Z., and Sacks, D. B. (2008) IQGAP1 stimulates proliferation and enhances tumorigenesis of human breast epithelial cells. *J Biol Chem* **283**, 1008-1017

66.   Swart-Mataraza, J. M., Li, Z., and Sacks, D. B. (2002) IQGAP1 is a component of Cdc42 signaling to the cytoskeleton. *J Biol Chem* **277**, 24753-24763

67.   White, C. D., Brown, M. D., and Sacks, D. B. (2009) IQGAPs in cancer: a family of scaffold proteins underlying tumorigenesis. *FEBS Lett* **583**, 1817-1824

68.   Suyama, M., Nagase, T., and Ohara, O. (1999) HUGE: a database for human large proteins identified by Kazusa cDNA sequencing project. *Nucleic Acids Res* **27**, 338-339

69.   Fiegen, D., Blumenstein, L., Stege, P., Vetter, I. R., and Ahmadian, M. R. (2002) Crystal structure of Rnd3/RhoE: functional implications. *FEBS Lett* **525**, 100-104

70.   Hemsath, L., and Ahmadian, M. R. (2005) Fluorescence approaches for monitoring interactions of Rho GTPases with nucleotides, regulators, and effectors. *Methods* **37**, 173-182

71.   Jaiswal, M., Dubey, B. N., Koessmeier, K. T., Gremer, L., and Ahmadian, M. R. (2012) Biochemical assays to characterize Rho GTPases. *Methods Mol Biol* **827**, 37-58

72.   Nouri, K., J., M. M., Milroy LG, Hain, A., Dvorsky, R., Amin, E., Lenders, M., Nagel-Steger, L., Howe, S., Smits, S. H. J., Hengel, H., Schmitt, L., Münk, C., Brunsveld, L., and Ahmadian, M. R. (2015) Biophysical Characterization of Nucleophosmin Interactions with Human Immunodeficiency Virus Rev and Herpes Simplex Virus US11. *PLoS ONE*

FIGURE LEGENDS

FIGURE 1. **Schematic representation of domain organization, various constructs and proteins of IQGAP1.** IQGAP1 Domain organization along with the PKCε phosphorylation sites S1441 and S1443, constructs and proteins relevant to this study. Coomassie brilliant blue (CBB) stained SDS-PAGE (12.5 %) of purified IQGAP1 proteins used in this study. Abbreviations: CHD, calponin homology domain; CC, coiled-coil repeat region; WW, tryptophan-containing proline-rich motif-binding region; IQ, four isoleucine/glutamine-containing motifs, GRD, GAP-related domain; CRAD, CDC42/RAC1 associating domain; CT, C-terminal domain.

FIGURE 2. **GRD-CT but not GRD selectively associates only with mGppNHp-bound, active RAC1 and CDC42.** **(A)** Chemical structure of mGppNHp, a fluorescently labelled, non-hydrolyzable GTP analog, used in this study. **(B)** The stopped-flow device. The stopped-flow device consists, among others, of two motorized, thermostated syringes, a mixing chamber and a fluorescence detector. Two different protein solutions indicated in brackets are rapidly mixed and transferred to fluorescence detection cell within less than 4 ms. mGppNHp- or mGDP-bound RHO proteins were used in this study as the fluorescent reporter groups. **(C-D)** Association of GRD1-CT with active, mGppNHp-bound CDC42 and RAC1. Kinetics of association were followed by rapidly mixing 2 μM GRD1-CT, GRD1 or GRD2 with 0.2 μM mGppNHp- or mGDP-bound RAC1 (C) or CDC42 (D). Obtained data are the average of four to six independent measurements. The k_{obs} values obtained for the association of GRD1-CT with mGppNHp-bound CDC42 and RAC1 are 1.68 and 1.80 s^{-1}, respectively. No change in fluorescence was observed for GRD1-CT and mGDP-bound RAC1 or CDC42 (black), GRD1 or GRD2 with mGppNHp-bound RAC1 or CDC42 (red), and GRD1-CT with RHOA-mGppNHp (blue). **(E-F)** Overlapping binding sites of CDC42 and RAC1 for GRD1-CT. Association of RAC1-mGppNHp (0.2 μM) with GRD1-CT (2 μM) was blocked in the presence of excess amount of non-fluorescent CDC42-GppNHp (10 μM) **(E)**. Association of CDC42-mGppNHp (0.2 μM) with GRD1-CT (2 μM) was blocked in the presence of excess amount of non-fluorescent RAC1-GppNHp (10 μM) **(F)**.

FIGURE 3. **IQGAP1 GRD binds CDC42 but not RAC1 in a nucleotide-independent manner.** **(A)** Fluorescence polarization assay. Fluorescence polarization signal of a fast tumbling fluorescent molecule, *e.g.*, RAC1-mGppNHp in its unbound state, increases if a larger protein, *e.g.*, IQGAP1, binds to it and forms a slow tumbling complex. **(B)** Fluorescence polarization experiments were conducted titrating mGppNHp-bound, active forms of CDC42, RAC1, and RHOA (1 μM, respectively) with increasing concentrations of GRD1-CT (0 to 20 μM) or GRD2 (0 to 120 μM), respectively. **(C)** Evaluated dissociation constant (K_d) shown as bars illustrates a significant difference in the binding properties of these two IQGAP1 proteins measured in B. **(D)** Fluorescence polarization experiments were conducted under the same conditions as in B, using mGDP-bound, inactive forms of CDC42, RAC1, and RHOA. **(E)** Calculated K_d values shown as bars clearly indicated interaction of GRD1-CT and GRD2 with CDC42-mGDP but not with RAC1 and RHOA.

FIGURE 4. **IQGAP1 variants significantly differ in their interaction properties with CDC42 and RAC1.** **(A-B)** Association of different GRD1-CRAD variants and CT (2 μM, respectively) with mGppNHp-RAC1/CDC42 (0.2 μM) was measured. **(A)** Association of GRD1-CRAD^{WT} (black), GRD1-CRAD^{S1441E} (green), but not with CT (blue), with RAC1-mGppNHp. **(B)** Association of GRD1-CRAD^{S1443E} with mGppNHp-RAC1 is much slower in comparison to GRD1-CRAD^{WT} and GRD1-CRAD^{S1441E}. **(C)** The k_{obs} values, shown as bars, comparatively illustrate association rates of GRD1-CT, GRD1-CRAD^{WT} and GRD1-CRAD^{S1441E} with mGppNHp-bound forms of CDC42 and RAC1, which is significantly reduced in the case of GRD1-CRAD^{S1443E}, and completely absent in the case of GRD1, GRD2 and CT under these experimental conditions. **(D-F)** Fluorescence polarization experiments were conducted to measure the interaction of mGppNHp-bound forms of RAC1 **(D)** and CDC42 **(E)** with increasing concentrations of GRD1-CRAD variants (WT, S1441E, and S1443E; 0 to 36 μM, respectively). **(F)** Calculated K_d values, shown as bars, reveal a significant decrease in the binding affinities of GRD1-CRAD^{S1443E} as compared to GRD1-CRAD^{WT} and GRD1-CRAD^{S1441E}.

FIGURE 5. **Kinetics of interaction of the IQGAP1 variants with RAC1 and CDC42. (A, B)** Individual rate constants for the GRD1-CT interaction with RAC1 and CDC42 are represented in **A** and **B**. Left panel: Association of mGppNHp-bound RAC1 or CDC42 (0.2 μM, respectively) with increasing concentrations of GRD1-CT (2 to 12 μM). Middle panel: Evaluated association rate constant (k_{on}) from the plot of the k_{obs} values, obtained from the exponential fits to the association data in the left panel, against the corresponding concentrations of the GRD1-CT. Right panel: Evaluated dissociation rate constant (k_{off}) measured by the displacement of the GRD1-CT (2μM) from its complex with mGppNHp-bound RAC1 or CDC42 (0.2 μM, respectively) in the presence of excess amounts of non-fluorescent RAC1-GppNHp (10μM). Other kinetics are given in supplemental Figures S1 and S2. **(C)** Calculated individual rate constants for the interaction of the IQGAP1 variants with RAC1 and CDC42, respectively, plotted as bar charts. Dissociation constants (K_d) were obtained from the ratio k_{off} / k_{on}.

Table 1. Data summary for the interaction of RHO proteins with IQGAP1 variants

Proteins[a]	K_d (µM)[b1]	Method[c]	Reference
GRD1/RAC1-mGppNHp	n. s. o.	SFF	this study
GRD1/CDC42-mGppNHp	n. s. o.	SFF	this study
GRD2/RAC1-mGppNHp	n. s. o.	SFF	this study
GRD2/CDC42-mGppNHp	n. s. o.	SFF	this study
GRD1-CT/RAC1-mGppNHp	0.94	SFF	this study
GRD1-CT/RAC1-mGDP	n. s. o	SFF	this study
GRD1-CT/CDC42-mGppNHp	0.30	SFF	this study
GRD1-CT/CDC42-mGDP	n. s. o.	SFF	this study
GRD1-CT/RHOA-mGppNHp	n. s. o.	SFF	this study
GRD1-CRAD/RAC1-mGppNHp	3.47	SFF	this study
GRD1-CRAD/CDC42-mGppNHp	2.72	SFF	this study
GRD1-CRAD^{S1441E}/RAC1-mGppNHp	4.72	SFF	this study
GRD1-CRAD^{S1441E}/CDC42-mGppNHp	2.05	SFF	this study
GRD1-CRAD^{S1443E}/RAC1-mGppNHp	12.28	SFF	this study
GRD1-CRAD^{S1443E}/CDC42-mGppNHp	15.48	SFF	this study
CT/RAC1-mGppNHp	n. s. o.	SFF	this study
CT/CDC42-mGppNHp	n. s. o.	SFF	this study
GRD1-CRAD/CDC42-GDP	1.30	SPR	(20)
GRD1-CRAD^{S1443D}/CDC42-GDP	0.81	SPR	(20)
GRD1-CRAD^{S1441E}/CDC42-GDP	220.0	SPR	(20)
Proteins[a]	eK_d (µM)[b2]	Method[c]	Reference
GRD2/RAC1-mGppNHp	81.45	FP	this study
GRD2/RAC1-mGDP	n.b.o	FP	this study
GRD2/CDC42-mGDP	184.7	FP	this study
GRD1-CT/RAC1-mGppNHp	5.53	FP	this study
GRD1-CT/CDC42-mGDP	95.10	FP	this study
GRD2/CDC42-mGppNHp	30.20	FP	this study
GRD1-CT/CDC42-mGppNHp	3.40	FP	this study
GRD2/RHOA-mGppNHp	n. b. o.	FP	this study
GRD1-CT/RHOA-mGppNHp	n. b. o.	FP	this study
GRD1-CRAD/RAC1-mGppNHp	4.57	FP	this study
GRD1-CRAD^{S1441E}/RAC1-mGppNHp	6.68	FP	this study
GRD1-CRAD^{S1443E}/RAC1-mGppNHp	31.65	FP	this study
GRD1-CRAD/CDC42-mGppNHp	4.69	FP	this study
GRD1-CRAD^{S1441E}/CDC42-mGppNHp	3.61	FP	this study
GRD1-CRAD^{S1443E}/CDC42-mGppNHp	14.58	FP	this study
GRD1/CDC42-mdGTP	0.028	FA	(42)
GRD1-CT/RAC1^{Q61L}-[^{3}H]GTP	0.018	SPA	(21)
GRD2*/RAC1^{Q61L}-[^{3}H]GTP	n. b. o.	SPA	(21)
GRD1-CT/CDC42^{Q61L}-[^{3}H]GTP	0.024	SPA	(21)
GRD2*/CDC42^{Q61L}-[^{3}H]GTP	0. 14	SPA	(21)
GRD2/CDC42^{Q61L}-GTP	1.30	ITC	(22)
GRD2/CDC42-GDP	n. b. o.	ITC	(22)
Proteins[a]	K_i (µM)[b3]	Method[c]	Reference
GRD1-CT/CDC42^{Q61L}-GTP	0.082	PRA	(41)
GRD1-CT/CDC42-GTP	0.39	PRA	(19)
GRD1-CT/RAC1-GTP	2.13	PRA	(19)

[a]IQGAP1 proteins. GRD2* encompasses amino acids 950-1407; [b]the binding affinity of the IQGAP proteins for various RHO proteins has been analyzed in different ways: [b1]under kinetic condition that provides the individual association and dissociation rate constant (k_{on} and k_{off}) and determines the dissociation constants (K_d) or [b2]under equilibrium conditions by determining the equilibrium dissociation constants (eK_d) or [b3]under competitive reaction conditions, for example inhibition the intrinsic GTP-hydrolysis reaction the RHO proteins that determines the equilibrium inhibition constant (K_i). n. s. o. means no (fluorescence) signal observed; n. b. o. means no binding observed; [c] SFF, stopped-flow fluorimetry; FA, fluorescence assay; FP, fluorescence polarization; ITC, isothermal titration calorimetry; PRA, phosphate-release assay; SPA, scintillation proximity assay; SPR, surface plasmon resonance.

Nouri *et al*., Figure 1
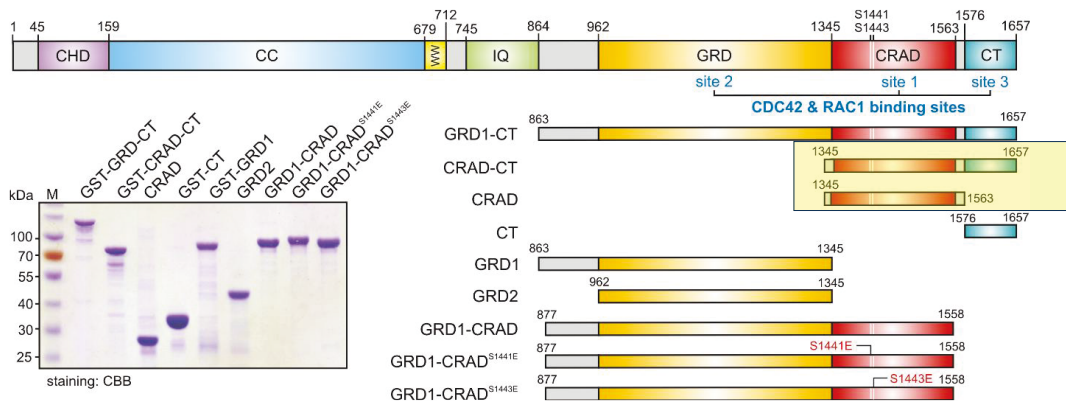
Nouri *et al*., Figure 2
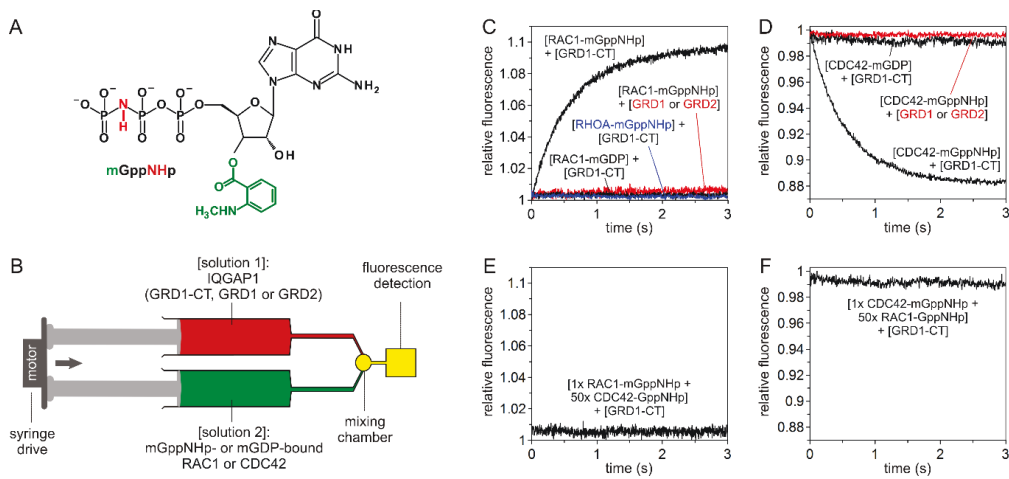
Nouri *et al*., Figure 3
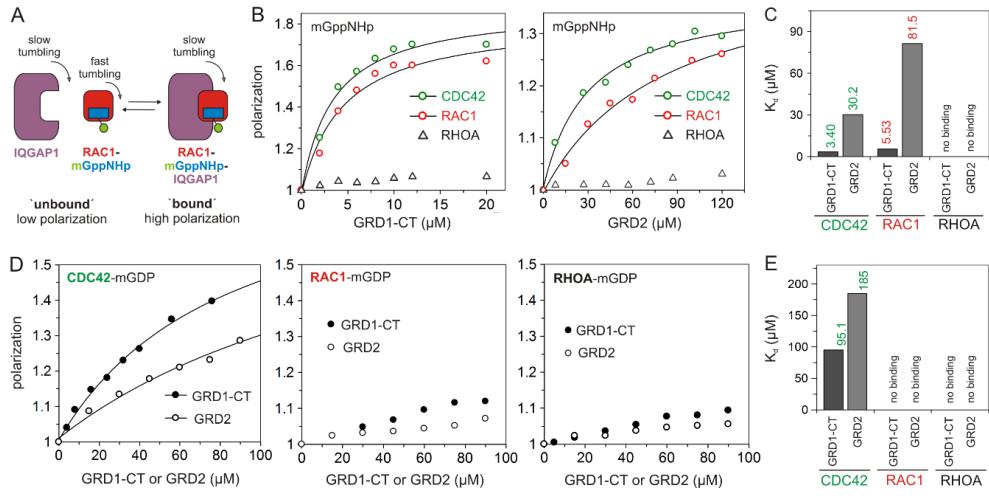
Nouri *et al*., Figure 4
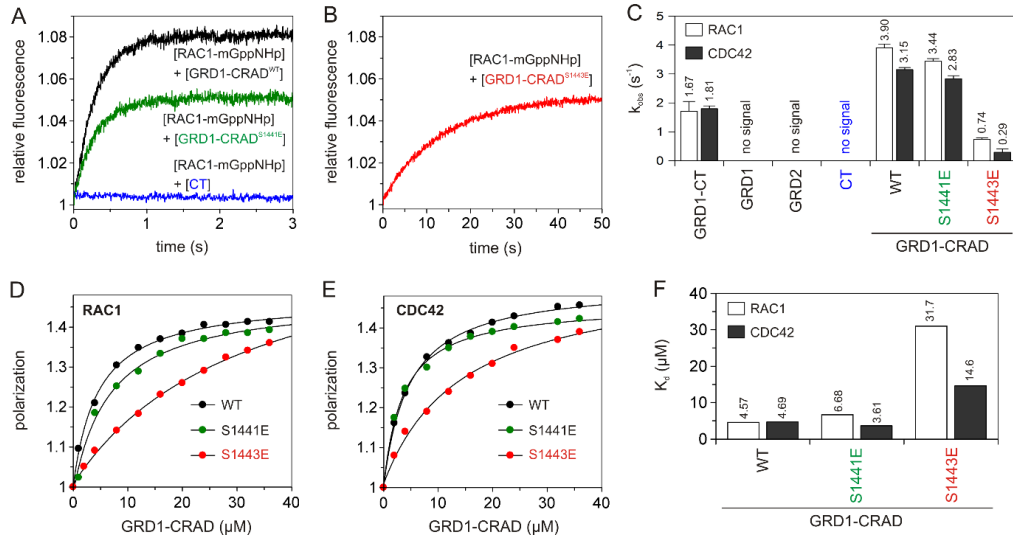
Nouri *et al*., Figure 5
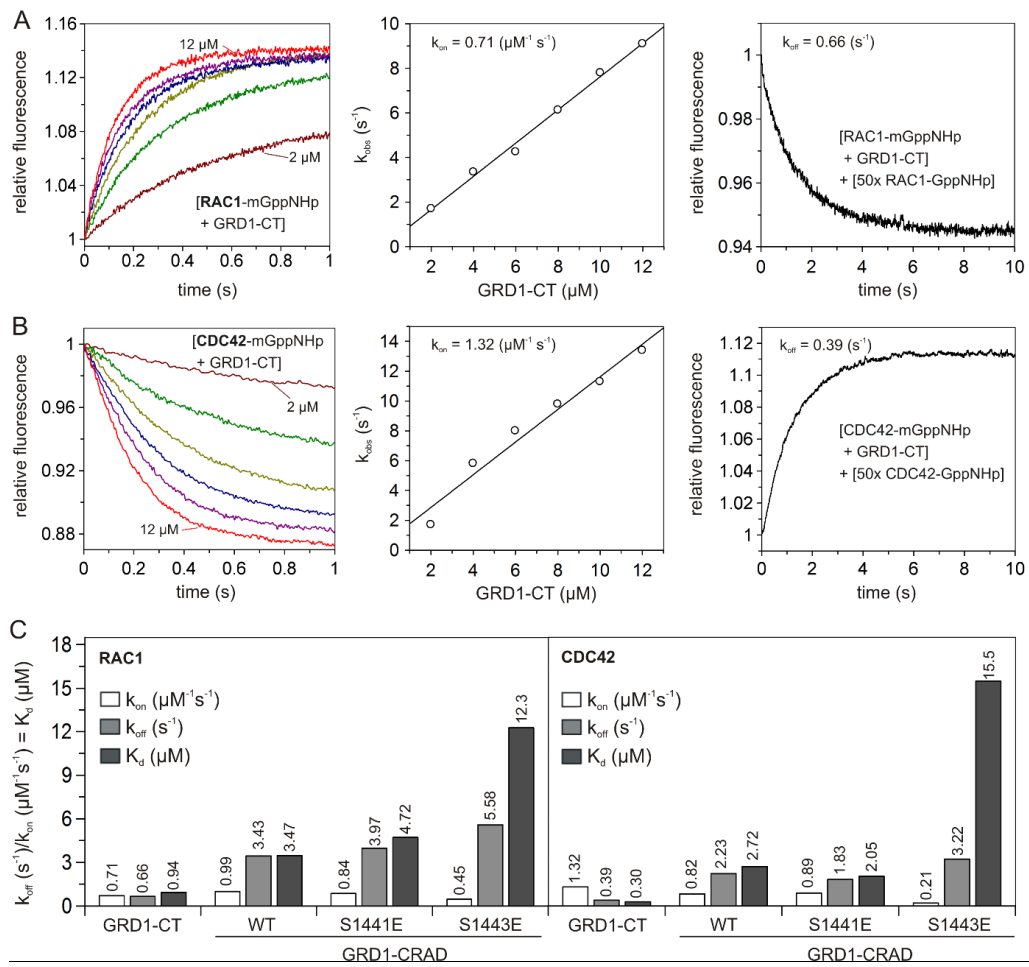
SUPPLEMENTAL INFORMATION

IQGAP1 interaction with RHO family proteins revisited: Kinetic and equilibrium evidence for multiple distinct binding sites

Kazem Nouri, Eyad K. Fansa, Ehsan Amin, Radovan Dvorsky, Lothar Gremer, Dieter Willbold, Lutz Schmitt, David J. Timson, and Mohammad R. Ahmadian

Institute of Biochemistry and Molecular Biology II, Medical Faculty of the Heinrich-Heine University, 40225 Düsseldorf, Germany.
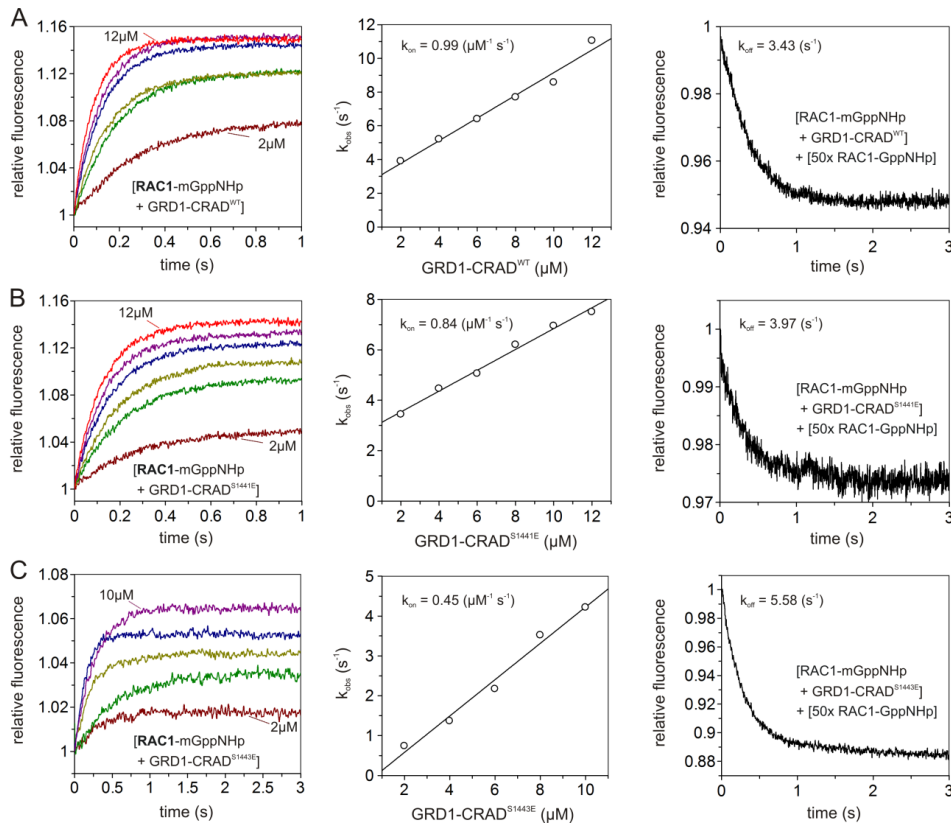
FIGURE S1. **Kinetics of interaction between Rac1-mGppNHp and the GRD1-CRAD variants, WT (A), S1441E (B) and S1443E (C).** Left panel: Association of Rac1-mGppNHp (0.2 μM) with increasing concentrations of GRD1-CRAD variants (2 to 12 μM). Middle panel: Evaluated association rate constant (k_{on}) from the plot of the k_{obs} values, obtained from the exponential fits to the association data in the left panel, against the corresponding concentrations of the GRD1-CRAD variants. Right panel: Dissociation of the GRD1-CRAD variants (2μM, respectively) from their complex with RAC1-mGppNHp (0.2 μM) in the presence of excess amounts of non-fluorescent RAC1-GppNHp (10μM). Calculated dissociation constants (K_d) are summarized in Figure 5C and Table 1.
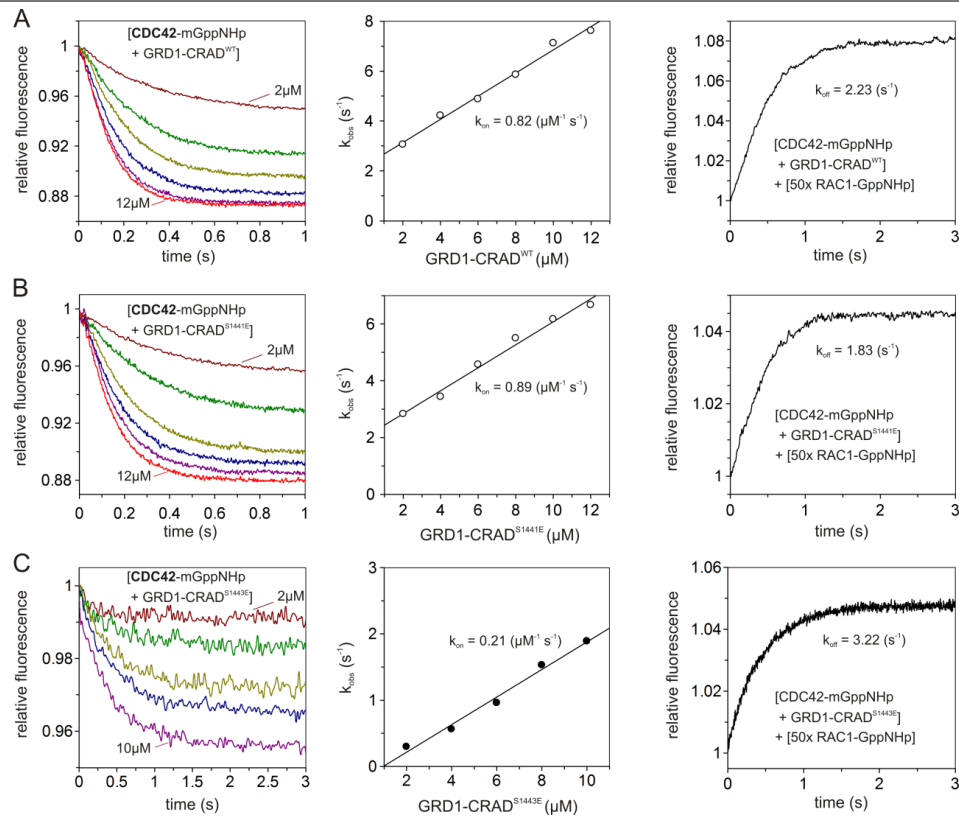
FIGURE S2. **Kinetics of interaction between CDC42-mGppNHp and the GRD1-CRAD variants, WT (A), S1441E (B) and S1443E (C).** Left panel: Association of CDC42-mGppNHp (0.2 μM) with increasing concentrations of GRD1-CRAD variants (2 to 12 μM). Middle panel: Evaluated association rate constant (k_{on}) from the plot of the k_{obs} values, obtained from the exponential fits to the association data in the left panel, against the corresponding concentrations of the GRD1-CRAD variants. Right panel: Dissociation of the GRD1-CRAD variants (2μM, respectively) from their complex with CDC42-mGppNHp (0.2 μM) in the presence of excess amounts of non-fluorescent CDC42-GppNHp (10μM). Calculated dissociation constants (K_d) are summarized in Figure 5C and Table 1.
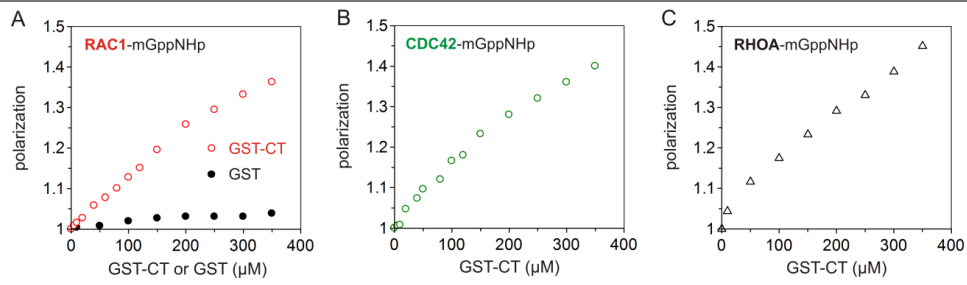
FIGURE S3. **IQGAP1 CT binds very weakly to RAC1, CDC42, and RHOA proteins**. **(A-C)** Fluorescence polarization experiments were performed using 1 µM mGppNHp-bound RAC1 (A), CDC42 (B), and RHOA (C), respectively, and increasing concentrations of GST-CT (1 to 350 µM). Increased in polarization strongly suggest is a very weak interaction between GST-CT with RHO proteins, which was not observed with GST alone (A).

Chapter 11

Inhibition of platelet activation by RAC1 inhibitors

Critical off-target effects of the widely used RAC1 inhibitors NSC23766 and EHT1864 in mouse platelets
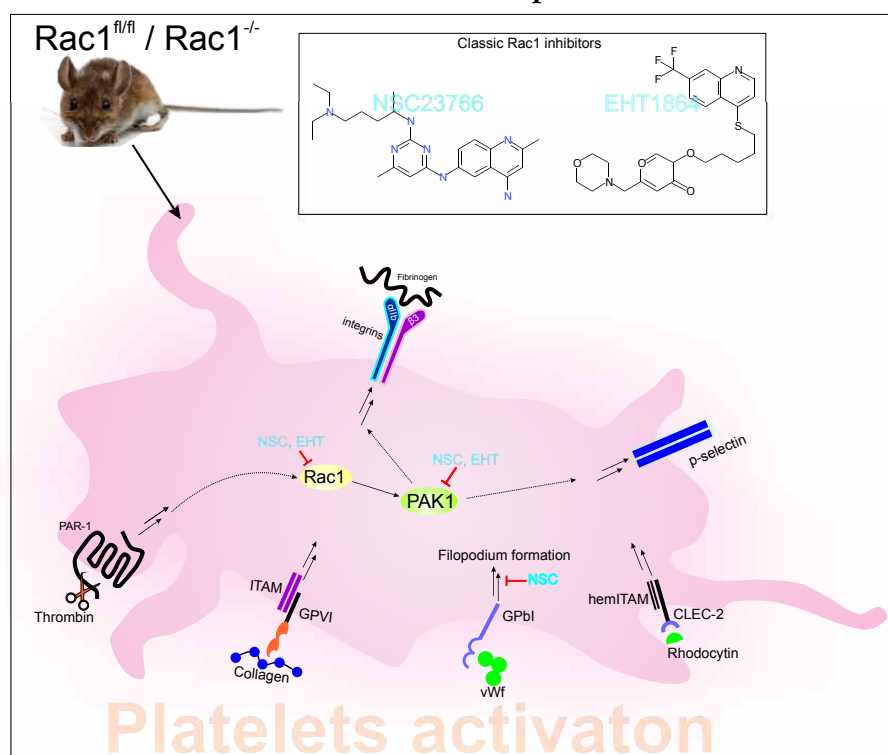
Status:	Published in Journal of Thrombosis and Haemostasis (2015), 13: 1–12
Impact factor:	5.72
Own Proportion to this work:	10 %; investigating the inhibitory effects of inhibitors on PAK1 activity in vitro (Figure 7)

ORIGINAL ARTICLE

Critical off-target effects of the widely used Rac1 inhibitors NSC23766 and EHT1864 in mouse platelets

S. DÜTTING,* J. HEIDENREICH,* D. CHERPOKOVA,* E. AMIN,† S.-C. ZHANG,†[1,2]
M. R. AHMADIAN,† C. BRAKEBUSCH‡ and B. NIESWANDT*

*Department of Experimental Biomedicine, University Hospital and Rudolf Virchow Center for Experimental Biomedicine, University of Würzburg, Würzburg; †Institute of Biochemistry and Molecular Biology II, Medical Faculty, Heinrich-Heine-University, Düsseldorf, Germany; and ‡BRIC, Biomedical Institute, University of Copenhagen, Copenhagen, Denmark

Summary. *Background:* Platelet aggregation at sites of vascular injury is essential for normal hemostasis, but may also cause pathologic vessel occlusion. Rho GTPases are molecular switches that regulate essential cellular processes, and they have pivotal functions in the cardiovascular system. Rac1 is an important regulator of platelet cytoskeletal reorganization, and contributes to platelet activation. Rac1 inhibitors are thought to be beneficial in a wide range of therapeutic settings, and have therefore been tested *in vivo* for a variety of disorders. Two small-molecule inhibitors, NSC23766 and EHT1864, have been characterized in different cell types, demonstrating high specificity for Rac1 and Rac, respectively. *Objectives:* To analyze the specificity of NSC23766 and EHT1864. *Methods:* Platelet function was assessed in mouse wild-type and Rac1-deficient platelets by the use of flow cytometric analysis of cellular activation and aggregometry. Platelet spreading was analyzed with differential interference contrast microscopy, and activation of effector molecules was analyzed with biochemical approaches. *Results:* NSC23766 and EHT1864 showed strong and distinct Rac1-independent effects at 100 μM in platelet function tests. Both inhibitors induced Rac1-specific inhibition of platelet spreading, but also markedly impaired agonist-induced activation of $Rac1^{-/-}$ platelets. Furthermore, glycoprotein Ib-mediated signaling was dramatically inhibited by NSC23766 in both wild-type and Rac1-deficient platelets. Importantly, these inhibitors directly affected the activation of the Rac1 effectors p21-activated kinase (PAK)1 and PAK2. *Conclusions:* Our results reveal critical off-target effects of NSC23766 and EHT1864 at 100 μM in mammalian cells, raising questions about their utility as specific Rac1/Rac inhibitors in biochemical studies at these concentrations and possibly as therapeutic agents.

Keywords: blood platelets; enzyme inhibitors; Rac1 GTP-binding protein; signal transduction; thrombosis.

Correspondence: Sebastian Dütting, Department of Experimental Biomedicine – Vascular Medicine, University Hospital and Rudolf Virchow Center for Experimental Biomedicine, University of Würzburg, Josef-Schneider-Str. 2, 97080 Würzburg, Germany.
Tel.: +49 931 31 80405; fax: +49 931 31 804050.
E-mail: sebastian.duetting@virchow.uni-wuerzburg.de

Current address: [1]Department of Microbiology and Immunobiology, Harvard Medical School, Boston, MA, USA.
[2]Division of Neuroscience, New England Primate Research Center, Southborough, MA, USA.

Introduction

Platelets are essential for the formation of a hemostatic plug, which seals the wound and prevents excessive blood loss, but may also lead to occlusion of vessels and the occurrence of acute ischemic events [1–3]. Regulation of the platelet actin cytoskeleton is essential for proper maintenance of platelet function and hemostasis, thereby implying that cytoskeletal regulators might serve as targets for antithrombotic therapy.

Rho GTPases belong to the superfamily of Ras-related proteins that act as molecular switches by cycling between an active GTP-bound state and an inactive GDP-bound state. Rho GTPases are best known for regulating actin dynamics in almost all cell types, but also for their involvement in the regulation of microtubule dynamics [4]. The best-characterized Rho GTPases are Rac1, RhoA, and Cdc42, whose activation is associated with the control of lamellipodium, stress fiber and filopodium formation, respectively [5–9]. The Rac subfamily consists of three isoforms – Rac1, Rac2, and Rac3 – but platelets only express Rac1 at the protein level [5]. In platelets, Rac1 is essential

2 *S. Dütting* et al

for lamellipodium formation during integrin $\alpha_{IIb}\beta_3$-mediated spreading and for signal transduction downstream of the immunoreceptor tyrosine-based activation motif (ITAM)-coupled receptor glycoprotein (GP) VI and the hemITAM-bearing receptor C-type lectin-like receptor 2. In contrast, a role for Rac1 in signaling pathways of G-protein-coupled receptors (GPCRs) has been shown by some, but not all, investigators [5,8,10]. As Rac proteins have pivotal functions in the cardiovascular system [11] and platelet-specific Rac1-deficient mice are protected from arterial thrombosis [8], the modulation of their activity by small-molecule inhibitors could represent a suitable pharmacologic approach for antithrombotic therapy.

The chemical compounds NSC23766 and EHT1864 have been used as Rac1 inhibitors in a variety of experimental settings. Both agents are supposed to inhibit Rac1 activity with high specificity, and are therefore considered to be potential lead structures for drug development [12,13]. NSC23766 was shown to specifically prevent conversion of Rac1-GDP to Rac1-GTP by competitively blocking the binding loop of Rac1-specific guanine nucleotide exchange factors [12], whereas EHT1864 was characterized as a specific inhibitor of the Rac family, binding Rac1, Rac2 and Rac3 in an allosteric manner, resulting in dissociation of nucleotides [13]. Although both inhibitors have been characterized in different cell types [14,15], they have never been tested for potential off-target effects in Rac1-deficient cells. Furthermore, they have been applied in a wide range of concentrations, from 10 μM up to 300 μM. Notably, it was shown that NSC23766 in this concentration range acts as a competitive antagonist of muscarinic acetylcholine receptors, thus questioning its potential as a therapeutic agent [16].

In the present study, we aimed to investigate the specificity of NSC23766 and EHT1864 by the use of mouse wild-type and Rac1-deficient platelets. We show that both compounds cause pronounced inhibition of different platelet activation pathways independently of Rac1. This reveals, for the first time, that NSC23766 and EHT1864 have profound off-target effects in mammalian cells.

Materials and methods

Generation of mice

To generate mice lacking Rac1 in megakaryocytes (MKs)/platelets, mice containing the *Rac1* gene flanked by loxP sites (*Rac1^{fl}*) were crossed with mice carrying the PF4-Cre transgene [17,18].

Rac1$^{fl/fl}$ $^{Pf4-cre+}$ mice were used for experiments, and littermates (*Rac1$^{fl/fl}$*) served as controls.

Rac1/Cdc42$^{-/-}$ mice were described previously [6], and *Rac1/RhoA$^{-/-}$* mice were generated accordingly (S. Dütting & B. Nieswandt, unpublished). Efficient deletion of the respective proteins was shown by western blot analysis (Fig. S1). Mice were maintained on a mixed SV/129/C57/

Bl-6 background. Animal studies were approved by the district government of Lower Franconia (Bezirksregierung Unterfranken).

Chemicals and reagents

EHT1864, NSC23766 (Tocris Bioscience, Bristol, UK), collagen (Kollagenreagent Horm; Nycomed, Munich, Germany), ADP, human fibrinogen, apyrase type III, protease inhibitor cocktail (Sigma-Aldrich, Steinheim, Germany), α-thrombin (Roche Diagnostics, Mannheim, Germany), high molecular weight heparin (Ratiopharm, Ulm, Germany), U46619, DiOC$_6$(3) (Enzo Life Sciences, Lörrach, Germany), electrochemiluminescence solution (Perkin-Elmer, Waltham, MA, USA), G-LISA (Cytoskeleton, Denver, CO, USA), integrilin (eptifibatide; Millennium Pharmaceuticals, Cambridge, MA, USA) and botrocetin (Pentapharm Ltd., Basel, Switzerland) were purchased. Collagen-related peptide (CRP) was generated as described previously [19]. Antibodies against Rac1 (Millipore, Darmstadt, Germany), p21-activated kinase (PAK)1, PAK2, PAK3, phospho-PAK1, phospho-PAK2 (Thr423/Thr402) and goat anti-rabbit IgG–horseradish peroxidase (Cell Signaling, Danvers, MA, USA) were purchased. The antibody against the activated form of $\alpha_{IIb}\beta_3$ (JON/A-PE) was from Emfret Analytics (Eibelstadt, Germany). All other antibodies were generated and modified in our laboratory as previously described [20].

Platelet preparation

Mice were bled from the retro-orbital plexus under isoflurane anesthesia. Blood was collected into heparin (20 U mL^{-1}), and platelet-rich plasma (PRP) was obtained by centrifugation at 300 ×g for 6 min at room temperature. For preparation of washed platelets, PRP was washed twice at 800 ×g for 5 min at room temperature, and the pellet was resuspended in Tyrodes–HEPES in the presence of prostacyclin (0.1 μg mL^{-1}) and apyrase (0.02 U mL^{-1}). Platelets were resuspended in Tyrodes–HEPES containing 2 mM CaCl$_2$ and 0.02 U mL^{-1} apyrase. For Rac1 inhibition, the platelet suspension was incubated in the presence of NSC23766 or EHT1864, respectively, for 5 min at 37 °C.

Platelet spreading

Coverslips were coated with 100 μg mL^{-1} human fibrinogen and blocked with 1% bovine serum albumin (BSA)/phosphate-buffered saline (PBS). Washed platelets (100 μL at 0.3 × 10^5 μL^{-1}) were activated with 0.01 U mL^{-1} thrombin and allowed to spread. Platelets were visualized with a Zeiss Axiovert 200 inverted microscope (× 100/1.4 oil objective) (Zeiss, Oberkochen, Germany). Digital images were recorded with a CoolSNAP-EZ camera (Visitron Systems GmbH, Puchheim, Germany), and analyzed

offline with METAVUE software (Molecular Devices, Sunnyvale, CA, USA).

For platelet spreading on von Willebrand factor (VWF), coverslips were coated with anti-human VWF antibody (0.25 mg mL^{-1}, A0082; Dako, Hamburg, Germany), and this was followed by incubation with mouse plasma to allow VWF binding and blocking with 1% BSA/PBS. Washed platelets were incubated with integrilin (40 μg mL^{-1}) and botrocetin (2 μg mL^{-1}), and allowed to adhere for 20 min. Platelets were visualized as described above.

Clot retraction

Mice were bled from the retro-orbital plexus with heparin-free capillaries into 70 μL of citrate. Clot retraction studies were performed at 37 °C in an aggregometer tube containing 250 μL of washed platelets (3 × 10^5 μL^{-1} in platelet-poor plasma), thrombin (3 U mL^{-1}; Sigma-Aldrich), and CaCl$_2$ (20 mmol L^{-1}). Clot retraction was recorded with a digital camera for 4.5 h after activation.

Aggregometry

Light transmission was measured on a Fibrintimer 4 channel aggregometer (APACT Laborgeräte und Analysensysteme, Hamburg, Germany) with washed platelets (160 μL with 5 × 10^5 μL^{-1}). Measurements in washed platelets were performed in the presence of 70 μg mL^{-1} fibrinogen, except for thrombin.

Flow cytometry

Washed platelets (0.5 × 10^5 μL^{-1}) were activated with agonists at the indicated concentrations, and stained with fluorophore-conjugated mAbs at saturating concentrations for 15 min at 37 °C as previously described [21]. For determination of phosphatidylserine (PS) exposure, washed platelets were incubated in the presence of annexin-V–DyLight 488 for 15 min at 37 °C. The reaction was stopped by addition of 500 μL of Tyrodes–HEPES containing 3 mM Ca^{2+}. For determination of mitochondrial membrane depolarization, washed platelets were incubated with 100 nM DiOC$_6$(3) for 20 min at room temperature. The reaction was stopped by addition of 500 μL PBS. All samples were directly analyzed on a FACSCalibur (BD Biosciences, Heidelberg, Germany).

Determination of GTPase activity by G-LISA

Washed platelets (7 × 10^5 μL^{-1}) were stimulated with 0.1 U mL^{-1} thrombin or 1 μg mL^{-1} CRP under constant stirring conditions at 37 °C in the presence of apyrase (2 U mL^{-1}) and indomethacin (10 μM). Stimulation was stopped by addition of 1 : 1 ice-cold G-LISA lysis buffer supplemented with protease inhibitor cocktail. After clearing,

samples were snap-frozen in liquid nitrogen. The protein concentration was adjusted to 0.25 mg mL^{-1}, and G-LISA was performed in duplicate as described by the supplier.

Protein phosphorylation studies

Washed platelets (5 × 10^5 μL^{-1}) were stimulated with 0.1 U mL^{-1} thrombin under constant stirring conditions at 37 °C in the presence of apyrase (2 U mL^{-1}) and indomethacin (10 μM). Stimulation was stopped by addition of 1 : 1 ice-cold lysis buffer (300 mM NaCl, 20 mM Tris, 2 mM EGTA, 2 mM EDTA, 2 mM Na$_3$VO$_4$, 10 mM NaF, pH 7.5, supplemented with protease inhibitor cocktail containing 2% Igepal CA-630). Samples were lyzed for 20 min at 4 °C, and centrifuged at 18 400 × *g* for 10 min; the supernatants were then collected. Samples were separated by SDS-PAGE under reducing conditions, blotted onto a poly (vinylidene difluoride) membrane, and stained with antibodies.

Cell-free kinase activity

Full-length human PAK1 and C-terminally truncated Cdc42 (1–178 amino acids) were expressed in *Escherichia coli* BL21(DE3) and purified as previously described [22,23]. Kinase activity was measured in buffer (30 mM HEPES, pH 7.4, 5 mM MgCl$_2$, 3 mM dithiothreitol) with 4 μM PAK1 and 15 μM Cdc42-GppNHp (non-hydrolyzable GTP analog). The reactions were started by addition of 100 μM ATP, incubated for 30 min at room temperature, and stopped by addition of 20 μL of 5 × SDS-loading buffer and incubation at 95 °C for 5 min. All samples were analyzed by SDS-PAGE and subsequent staining with both Pro-Q Diamond (Molecular Probes, Invitrogen, Darmstadt, Germany) and colloidal Coomassie, as previously described [24,25].

Data analysis

Results from at least three independent experiments per group are presented as mean ± standard deviation. Differences between two groups were assessed by ANOVA with Dunnett's T3 as the *post hoc* test. *P*-values of < 0.05 were considered to be statistically significant.

Results

At a high concentration, NSC23766 induces platelet receptor downregulation and EHT1864 triggers platelet apoptosis

NSC23766 and EHT1864 are widely used Rac1/Rac inhibitors in different cell systems [14,15], but they have never been tested for potential off-target effects in Rac1-deficient cells. We aimed to functionally evaluate both inhibitors by the use of mouse wild-type and Rac1-deficient platelets. On the basis of the reported IC50 values
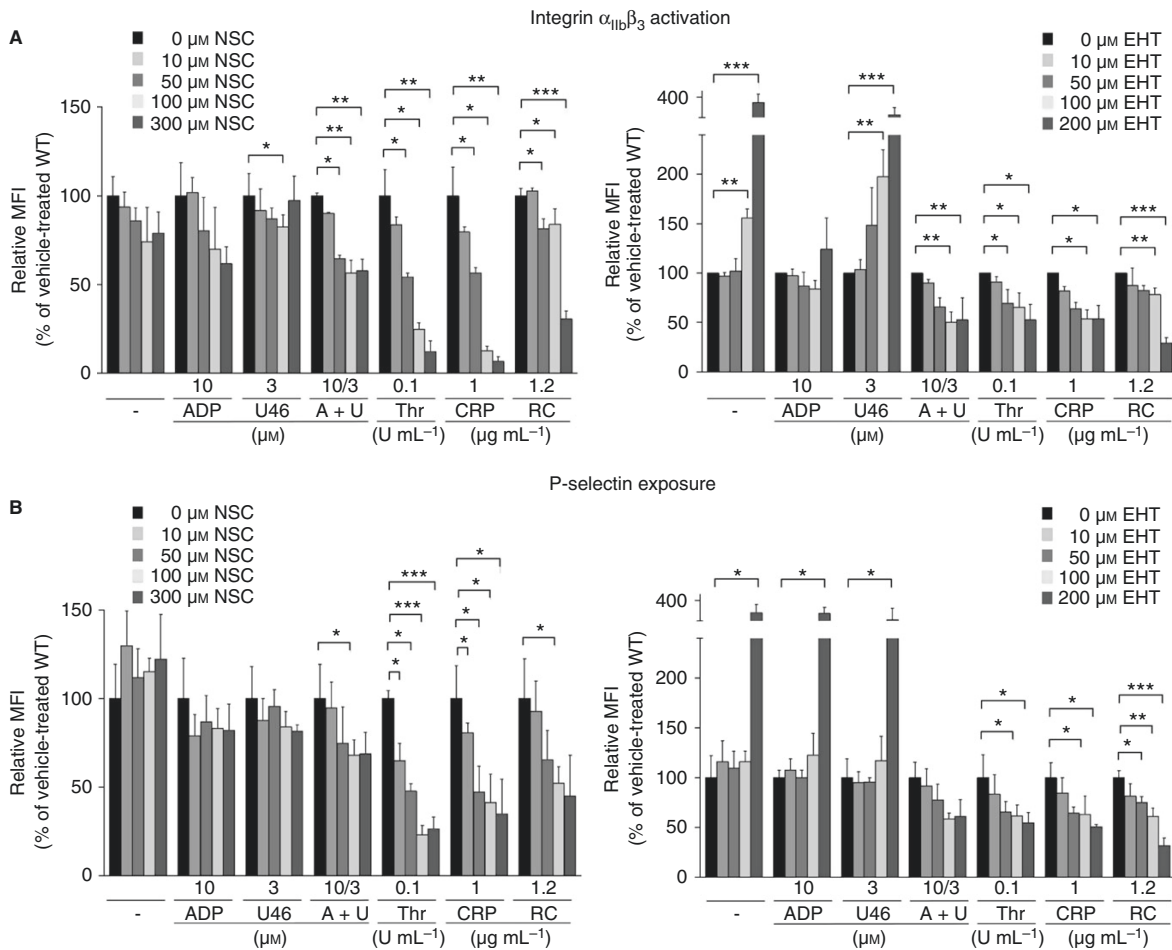
Fig. 1. Dose-dependent inhibition of $\alpha_{IIb}\beta_3$ activation and granule release by NSC23766 (NSC) and EHT1864 (EHT) in *Rac1*$^{+/+}$ platelets. (A, B) Flow cytometric analysis of $\alpha_{IIb}\beta_3$ activation (A) and degranulation-dependent P-selectin exposure (B) in response to the indicated agonists in washed *Rac1*$^{+/+}$ platelets after treatment with different concentrations of NSC23766, EHT1864 or vehicle for 5 min. Results are relative mean fluorescence intensities (MFIs) normalized to vehicle-treated wild-type (WT) control ± standard deviation of four mice per group, and are representative of three individual experiments. CRP: collagen-related peptide; RC, rhodocytin. *Significant difference ($P < 0.05$) as compared with vehicle-treated control. **Significant difference ($P < 0.01$) as compared with vehicle-treated control. ***Significant difference ($P < 0.001$) as compared with vehicle-treated control.

for NSC23766 [26,27], we set out to find the most suitable concentration for each inhibitor in platelets. Therefore, wild-type platelets were treated with NSC23766, EHT1864, or vehicle (ddH$_2$O), and $\alpha_{IIb}\beta_3$ activation and degranulation-dependent P-selectin surface exposure were analyzed (Fig. 1). In NSC23766-treated wild-type platelets, $\alpha_{IIb}\beta_3$ activation and α-granule secretion were dose-dependently decreased after stimulation of GPCRs and (hem)ITAM receptors. Importantly, expression levels of surface GPs were slightly, but significantly, decreased after NSC23766 treatment in a dose-dependent manner (Table 1). EHT1864-treated platelets showed diminished $\alpha_{IIb}\beta_3$ activation and α-granule secretion after stimulation of GPCRs, and (hem)ITAM signaling was inhibited with

less potency than with NSC23766. Administration of a low EHT1864 concentration (10 µM) had no significant effect on platelet activation, whereas treatment with a high dose (200 µM) caused platelet apoptosis, as demonstrated by altered forward/sideward scatter characteristics (increased cell debris) in flow cytometric analysis (data not shown), dramatically increased PS exposure, and depolarization of the mitochondrial membrane (Fig. 2).

Next, we repeated these dose–response experiments with platelets from conditional Rac1-deficient mice carrying the Cre recombinase under the control of the MK/platelet-specific platelet factor 4 (PF4) promoter [18], leading to conditional knockout of *Rac1* in MKs and platelets (subsequently referred to as *Rac1*$^{-/-}$). After

Table 1 Dose-dependent reduction in platelet glycoprotein (GP) expression of $Rac1^{+/+}$ platelets by NSC23766 (NSC)

–	0 μM NSC	50 μM NSC	100 μM NSC	300 μM NSC
GPVI	56 ± 3	51 ± 3	51 ± 1	44 ± 2**
α_2	73 ± 5	74 ± 2	71 ± 1	68 ± 2
β_1	120 ± 4	103 ± 3**	100 ± 3**	83 ± 4***
CD9	1075 ± 22	1028 ± 30	985 ± 28	820 ± 17***
GPIb	305 ± 5	297 ± 9	290 ± 5	271 ± 6**
GPIX	362 ± 14	343 ± 6	328 ± 4	294 ± 4**
$\alpha_{IIb}\beta_3$	533 ± 25	504 ± 19	478 ± 20	416 ± 18**
GPV	266 ± 13	242 ± 8	226 ± 1*	199 ± 4**

Expression of GPs on the platelet surface was determined by flow cytometry. Washed platelets were incubated with vehicle or different concentrations of NSC23766, and then incubated with fluorescein isothiocyanate-labeled antibodies under saturating conditions for 15 min at room temperature. Data are expressed as mean fluorescence intensity ± standard deviation ($n = 4$), and are representative of three individual experiments. *Significant difference ($P < 0.05$) as compared with vehicle-treated control. **Significant difference ($P < 0.01$) as compared with vehicle-treated control. ***Significant difference ($P < 0.001$) as compared with vehicle-treated control.

administration of NSC23766 or EHT1864 to $Rac1^{-/-}$ platelets, we did not observe any further inhibition of $\alpha_{IIb}\beta_3$ activation and α-granule secretion upon stimulation of (hem)ITAM receptors (Fig. S2). In contrast, both inhibitors impaired activation of $Rac1^{-/-}$ platelets after stimulation with GPCR agonists (Fig. S2). In addition, EHT1864-treated Rac1-deficient platelets showed a similar increase in PS exposure as compared with EHT1864-treated wild-type platelets, indicating that high doses of EHT1864 cause apoptosis independently of Rac1 (data not shown), and thereby also explaining the increased mean fluorescence intensity of P-selectin in the absence of activation (Fig. S2B).

These results clearly demonstrate that both inhibitors have Rac1-independent functions in mouse platelets, even at an intermediate concentration of 100 μM. At high concentrations, NSC23766 induces downregulation of several surface GPs, whereas high doses of EHT1864 result in severely decreased platelet viability. Therefore, we used a concentration of 100 μM for both inhibitors in all further experiments.

NSC23766 and EHT1864 cause Rac1-independent inhibition of GPCR-induced and ITAM-induced platelet activation

To analyze the effects of NSC23766 and EHT1864 on agonist-induced integrin activation and degranulation, washed platelets from $Rac1^{+/+}$ and $Rac1^{-/-}$ mice were incubated with either NSC23766, EHT1864, or vehicle, and both $\alpha_{IIb}\beta_3$ activation and P-selectin surface exposure in response to agonist stimulation were determined (Fig. 3A). The role of Rac1 in GPCR signaling of murine platelets is controversial [5,8,10]; however, our results obtained with platelet-specific PF4-Cre-induced Rac1 deletion revealed a crucial role of Rac1 in mediating
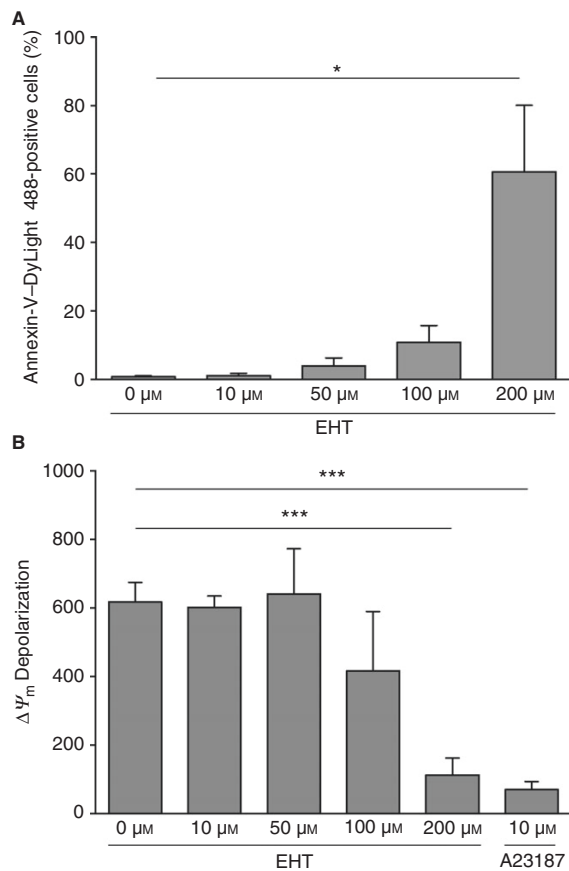
Fig. 2. Dose-dependent increase in platelet apoptosis of $Rac1^{+/+}$ platelets by EHT1864 (ETH). (A, B) Flow cytometric analysis of phosphatidylserine exposure (A) and mitochondrial membrane depolarization ($\Delta\Psi_m$) (B) in response to EHT1864 in $Rac1^{+/+}$ platelets. *Significant difference ($P < 0.05$) as compared with vehicle-treated control. ***Significant difference ($P < 0.001$) as compared with vehicle-treated control.

GPCR signaling (Fig. 3A). In line with this, in wild-type platelets, both inhibitors blocked integrin activation and degranulation after stimulation of both (hem)ITAM-bearing receptors and GPCRs almost to the levels seen in vehicle-treated $Rac1^{-/-}$ platelets, with NSC23766 showing stronger inhibition than EHT1864 (Fig. 3A). Notably, NSC23766 and EHT1864 showed significant additional inhibitory effects on thrombin-induced activation of $Rac1^{-/-}$ platelets (Fig. 3A). This defect in platelet activation and the lack of specificity of NSC23766 and EHT1864 were confirmed by *ex vivo* aggregation studies, which clearly showed Rac1-independent effects of the two inhibitors on platelet activation/aggregation (Fig. 3B). These results reveal that both compounds have strong, non-specific inhibitory effects on platelet activation.

6 *S. Dütting* et al
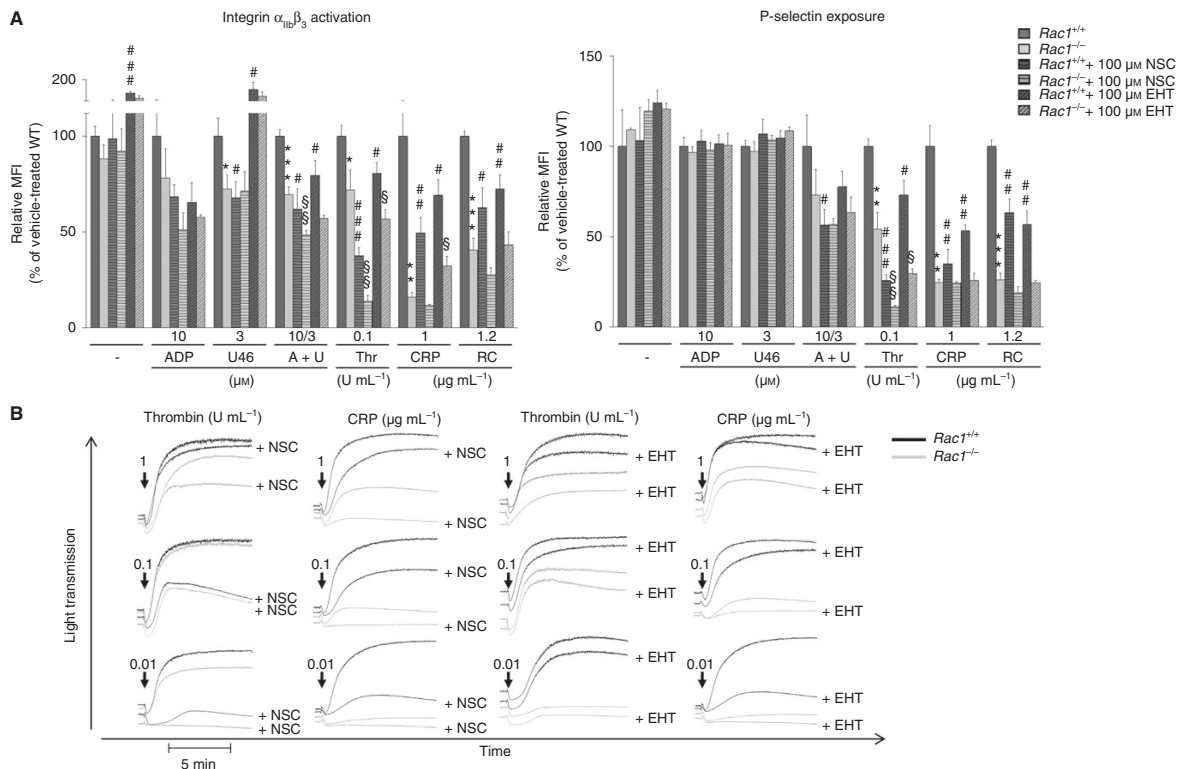
Fig. 3. Rac1-independent effects of NSC23766 (NSC) and EHT1864 (EHT) on integrin inside-out signaling and platelet aggregation after platelet activation. (A) Flow cytometric analysis of $\alpha_{IIb}\beta_3$ activation and degranulation-dependent P-selectin exposure in response to the indicated agonists in washed $Rac1^{+/+}$ and $Rac1^{-/-}$ platelets after treatment with 100 μM NSC23766, EHT1864 or vehicle for 5 min. Results are relative mean fluorescence intensities (MFIs) normalized to vehicle-treated wild-type (WT) control ± standard deviation of four mice per group, and are representative of three individual experiments. (B) Washed platelets from $Rac1^{+/+}$ (black line) and $Rac1^{-/-}$ (gray line) mice were incubated for 5 min prior to the experiment with NSC23766 or EHT1864, and then activated with the indicated concentrations of thrombin or CRP; light transmission was recorded on a Fibrintimer four-channel aggregometer. Representative aggregation traces of at least three individual experiments are depicted. *Significant difference ($P < 0.05$) between knockout and vehicle-treated WT control. #Significant difference ($P < 0.05$) between inhibitor-treated WT and vehicle-treated WT control. §Significant difference ($P < 0.05$) between inhibitor-treated knockout and vehicle-treated knockout control. CRP: collagen-related peptide; RC, rhodocytin.

NSC23766 and EHT1864 have minimal and distinct Rac1-independent effects on integrin outside-in signaling

Ligand-occupied $\alpha_{IIb}\beta_3$ mediates outside-in signaling leading to cytoskeletal reorganization and platelet spreading [28]. As shown previously, $Rac1^{-/-}$ platelets are unable to form lamellipodia on fibrinogen [5,8], and apparently in line with the central role of Rac1 in this process, EHT1864 [29,30] and NSC23766 [29] have been shown to impair spreading of wild-type platelets. To characterize the effects of NSC23766 and EHT1864 on $\alpha_{IIb}\beta_3$-mediated outside-in signaling in more detail, $Rac1^{+/+}$ and $Rac1^{-/-}$ platelets, treated with inhibitor or vehicle, were allowed to spread on a fibrinogen-coated surface in the presence of low concentrations of thrombin. $Rac1^{+/+}$ platelets treated with NSC23766 or EHT1864 retained the ability to adhere to the fibrinogen matrix, and lamellipodium formation could be observed; however, this was

clearly diminished as compared with vehicle-treated platelets (Fig. 4A). In contrast, the development of long, thin filopodia was slightly impaired (Fig. 4B). In $Rac1^{-/-}$ platelets, lamellipodium formation was absent both in the presence and in the absence of the inhibitors, whereas filopodium formation was slightly reduced after inhibitor treatment (Fig. 4A,B).

Integrin $\alpha_{IIb}\beta_3$ outside-in signaling also regulates clot retraction [31], and previous studies have indicated that Rac1 may be involved in this process [30,32]. To analyze the effects of NSC23766 and EHT1864 on clot retraction, we induced clot formation and monitored retraction over time. In marked contrast to previous findings [30,32], no differences between $Rac1^{+/+}$ and $Rac1^{-/-}$ platelets were observed, clearly demonstrating that Rac1 is not required for this $\alpha_{IIb}\beta_3$-controlled process (Fig. 4C,D). Interestingly, application of EHT1864 reduced retraction volume minimally, whereas NSC23766 showed no influence in
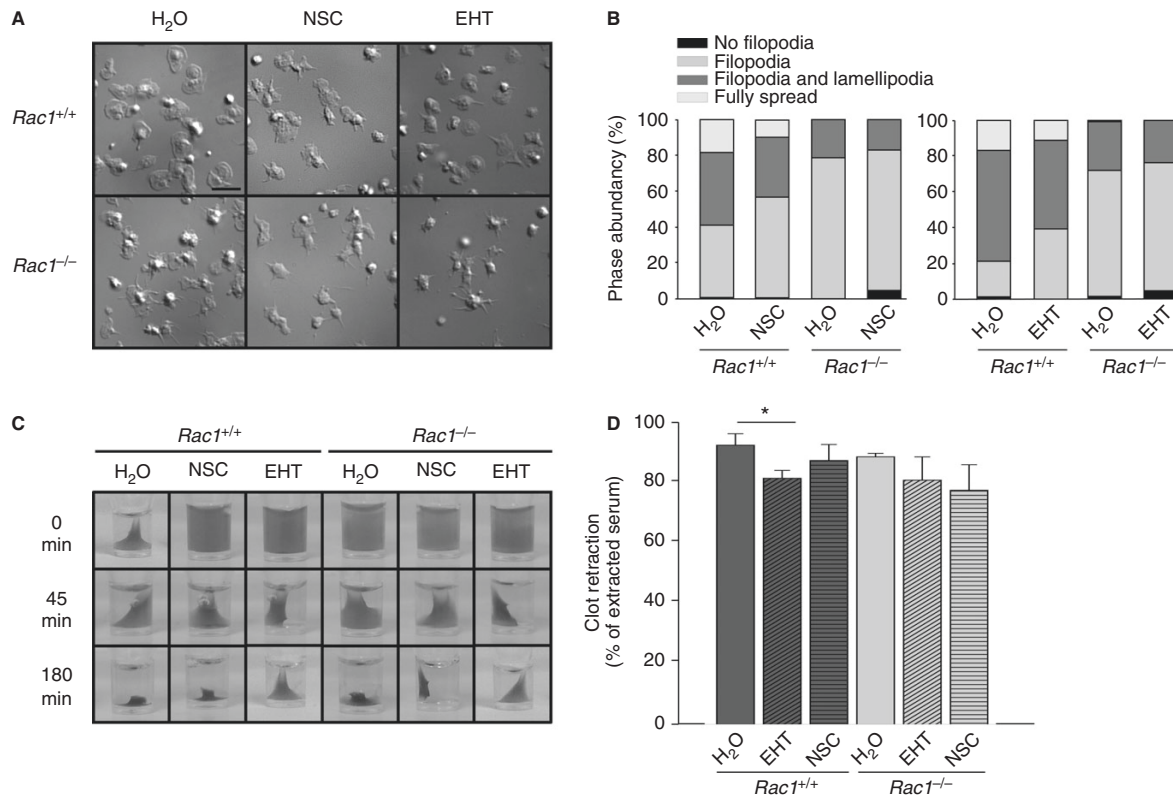
Fig. 4. Specific inhibition of $\alpha_{IIb}\beta_3$-mediated spreading and minor off-target effects of EHT1864 (EHT) during clot retraction. (A, B) Washed platelets from $Rac1^{+/+}$ and $Rac1^{-/-}$ mice were allowed to spread on fibrinogen (100 μg mL^{-1}) for 30 min after stimulation with 0.01 U mL^{-1} thrombin. Prior to the experiment, platelets were incubated for 5 min with 100 μM NSC23766, 100 μM EHT1864 (EHT), or vehicle. Representative differential interference contrast images of two individual experiments (A) and statistical evaluation of the percentages of spread platelets at different spreading stages (B) are shown. 1, roundish; 2, only filopodia; 3, filopodia and lamellipodia; 4, fully spread. (C, D) Clot retraction of platelet-rich plasma upon activation with 3 U mL^{-1} thrombin in the presence of 20 mmol L^{-1} CaCl$_2$ at the indicated time points. Representative images of three individual experiments (C) and statistical evaluation of clot retraction (D) are shown. *Significant difference ($P < 0.05$) as compared with vehicle control.

wild-type platelets (Fig. 4C,D). Together, these results suggest that NSC23766 and EHT1864 have no specific or only minor non-specific effects on $\alpha_{IIb}\beta_3$ outside-in signaling.

NSC23766 inhibits GPIb-mediated signaling independently of Rac1

We next evaluated the platelet response upon adhesion to a VWF-coated surface under conditions of $\alpha_{IIb}\beta_3$ blockade. Under these conditions, signaling via GPIb induces a shape change that is limited to contraction of the cell body and filopodia formation [33]. In line with previous reports [34,35], $Rac1^{-/-}$ platelets showed impaired filopodium formation on VWF. Interestingly, however, NSC23766 caused a dramatic decrease in filopodium formation in both wild-type and Rac1-deficient platelets, whereas application of EHT1864 had a milder effect (Fig. 5). These data demonstrate that NSC23766 has

additional off-target effects on GPIb-mediated signaling in mouse platelets.

NSC23766 and EHT2864 do not target Cdc42 or RhoA, but inhibit PAK1/PAK2 phosphorylation independently of Rac1

As Rac1 is the only Rac isoform expressed in (mouse) platelets, and Rac1 and Cdc42 (70.83% amino acid identity), and, to a lesser extent, Rac1 and RhoA (56.19% identity) are highly homologous, we hypothesized that these two GTPases may be targeted by NSC23766 and EHT1864 in the absence of Rac1, thereby causing the described off-target effects. It has been shown, by *in vitro* complex formation and *in vivo* pulldown assays, that NSC23766 and EHT1864 have no effects on the nucleotide exchange of RhoA and Cdc42 [12]. In line with this, we found that neither Cdc42 activity nor RhoA activity was affected by NSC23766 or EHT1864 in wild-type and Rac1-deficient platelets under resting conditions or after
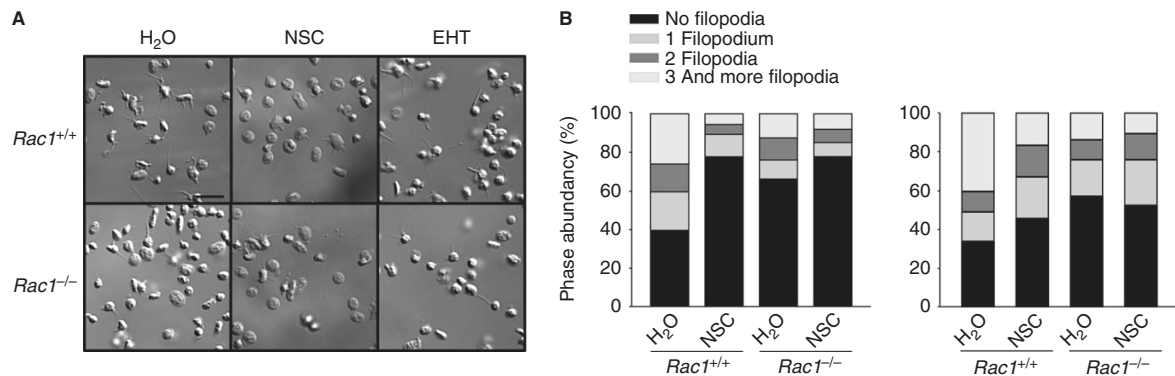
Fig. 5. NSC23766 (NSC) inhibits glycoprotein Ib-mediated filopodium formation independently of Rac1. (A, B) Washed platelets of $Rac1^{+/+}$ and $Rac1^{-/-}$ mice were allowed to adhere and spread on von Willebrand factor for 20 min after incubation with 100 μM NSC23766, EHT1864 (EHT) or vehicle. Representative images of three individual experiments (A) and statistical evaluation of the percentage of filopodia forming platelets (B) are shown.

activation (Fig. 6A and data not shown). To test whether NSC23766 and EHT1864 have potential effects on Cdc42 and/or RhoA independently of nucleotide exchange, we applied both inhibitors to platelets lacking Rac1 and Cdc42 ($Rac1/Cdc42^{-/-}$ [6]) as well as Rac1 and RhoA ($Rac1/RhoA^{-/-}$) (Dütting, Nieswandt, unpublished), and analyzed platelet activation responses to different agonists. Similarly to what was found for $Rac1^{-/-}$ platelets, application of NSC23766 or EHT1864 to $Rac1/RhoA^{-/-}$ platelets resulted in a further decrease in integrin activation as compared with vehicle-treated $Rac1/RhoA^{-/-}$ platelets (data not shown). Additionally, we observed similar side effects of NSC23766 and EHT1864 in $Rac1/Cdc42^{-/-}$ platelets, as demonstrated by further reduced platelet activation as compared with vehicle-treated $Rac1/Cdc42^{-/-}$ platelets (Fig. 6B,C). It is of note that double-deficient platelets showed marked hyperreactivity to agonist stimulation after application of EHT1864. These results strongly suggest that NSC23766 and EHT1864 do not block Cdc42 or RhoA in addition to Rac1.

By the use of NSC23766, it has been shown that Rac1 mediates cofilin dephosphorylation and inhibits PAK4/PAK5/PAK6 but not PAK1/PAK2 phosphorylation after thrombin stimulation of human platelets [14]. Cofilin is a small actin-dynamizing protein downstream of LIM domain kinase 1 (LIMK1) that takes part in platelet degranulation and lamellipodium assembly when dephosphorylated. LIMK1, in turn, is activated after phosphorylation by the RhoA effector Rho-associated protein kinase, but importantly also by PAK1, which is a direct effector molecule of Rac1 and Cdc42 [36]. Here, we showed that phosphorylation of PAK1/PAK2 (Thr423/Thr402) is reduced in thrombin-stimulated $Rac1^{-/-}$ platelets as compared with $Rac1^{+/+}$ platelets (Fig. 7A; Fig. S3). Furthermore, PAK1/PAK2 phosphorylation was more pronouncedly reduced in NSC23766-treated or EHT1864-treated $Rac1^{+/+}$ platelets than in vehicle-trea-

ted $Rac1^{+/+}$ platelets. Notably, we observed impaired PAK1/PAK2 phosphorylation in $Rac1^{-/-}$ platelets treated with NSC23766 or EHT1864 as compared with vehicle-treated $Rac1^{-/-}$ platelets (Fig. 7A; Fig. S3). Finally, the direct inhibitory effect on PAK activation was confirmed in a cell-free kinase activity assay (Fig. 7B). These results demonstrate that NSC23766 and EHT1864 directly inhibit phosphorylation/activation of the Rac1 effector molecules PAK1 and PAK2 independently of Rac1.

Discussion

In this study, we used Rac1-deficient mouse platelets to demonstrate that the Rac1/Rac inhibitors NSC23766 and ETH1864: (i) at high concentrations alter platelet surface GP levels and platelet viability, respectively; and importantly, (ii) have significant distinct off-target effects, at least in part because of Rac1-independent inhibition of PAK1/PAK2 activation. In addition, our data demonstrate that Rac1 is involved in (hem)ITAM-mediated and GPCR-mediated platelet activation and GPIb-induced signaling in platelets, whereas $\alpha_{IIb}\beta_3$-mediated clot retraction is unaffected by the absence of Rac1.
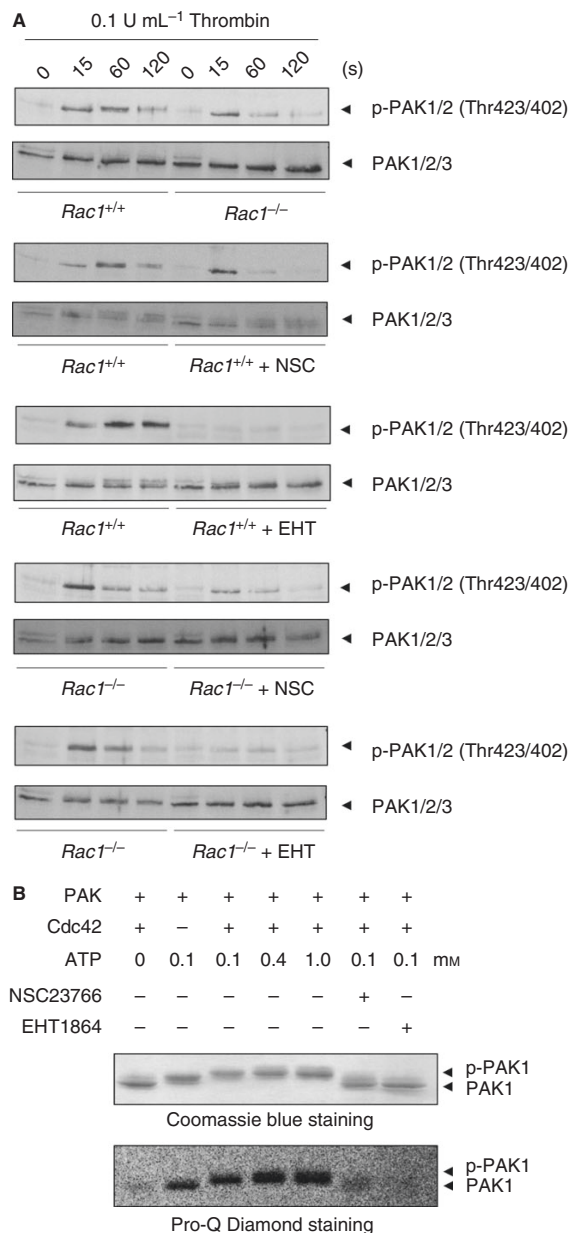
Rho GTPases are molecular switches that regulate essential cellular processes and have pivotal functions in the cardiovascular system [11]. As the classic Rho GTPases Rac1, Cdc42 and RhoA are key regulators of the platelet cytoskeleton and contribute to normal hemostasis, but also control pathologic thrombus formation [6–9], modulating Rho GTPase activity by small-molecule inhibitors may represent a suitable pharmacologic approach for antithrombotic therapy. Rac1 inhibitors are thought to be beneficial in a wide range of therapeutic settings, and have therefore been tested *in vivo* for a variety of disorders, including acute myeloid leukemia, proteinuric kidney disease, and diabetes [37–39]. To date, two different small-molecule inhibitors, NSC23766 and EHT1864, and
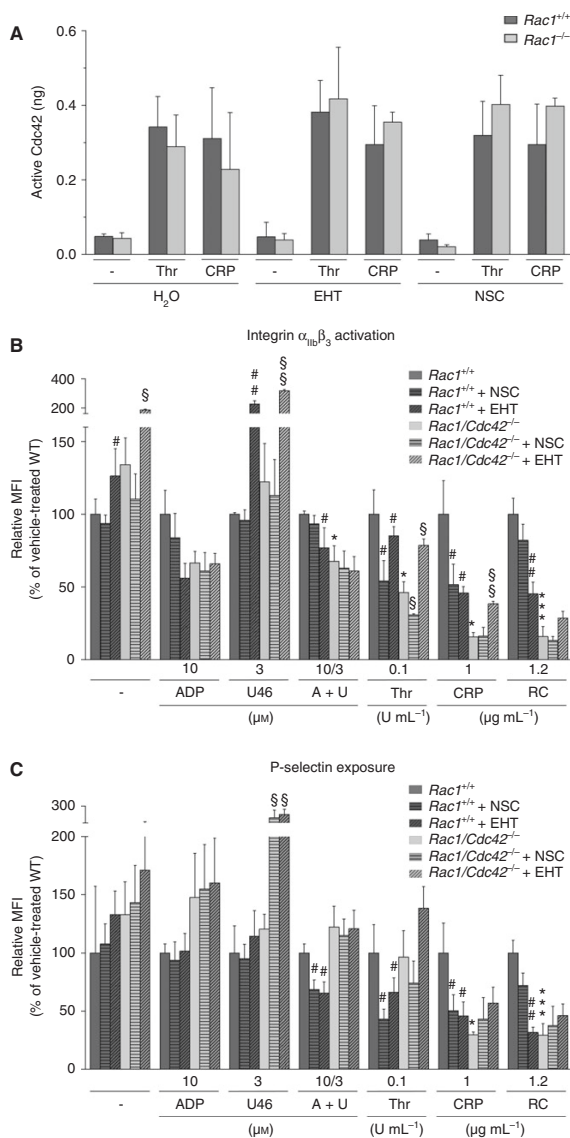
Fig. 6. NSC23766 (NSC) and EHT1864 (EHT) do not act on Cdc42. (A) Analysis of Cdc42 activity in resting $Rac1^{+/+}$ and $Rac1^{-/-}$ platelets and after stimulation with either 0.1 U mL^{-1} thrombin or 1 µg mL^{-1} collagen-related peptide (CRP). (B) Flow cytometric analysis of $\alpha_{IIb}\beta_3$ activation and degranulation-dependent P-selectin exposure in response to the indicated agonists in washed $Rac1/Cdc42^{+/+}$ and $Rac1/Cdc42^{-/-}$ platelets after treatment with 100 µM NSC23766, 100 µM EHT1864 or vehicle for 5 min. Results are relative mean fluorescence intensities (MFIs) normalized to vehicle-treated wild-type (WT) control ± standard deviation of four mice per group, and are representative of three individual experiments. *Significant difference ($P < 0.05$) between knockout and vehicle-treated WT control. #Significant difference ($P < 0.05$) between inhibitor-treated WT and vehicle-treated WT control. §Significant difference ($P < 0.05$) between inhibitor-treated knockout and vehicle-treated knockout control. RC, rhodocytin.

their derivatives have been characterized in different cell types, and have shown high specificity for Rac1 and Rac, respectively. Importantly, NSC23766 is applied *in vivo* in mouse models through injections, intrathecal catheters, or implanted Alzet osmotic pumps [37,38,40,41]. In different studies using NSC23766 to inhibit Rac1-dependent responses, IC50 values of 50–100 µM were reported [26, 27], but both inhibitors have also been applied at concentrations ranging from 10 µM to 300 µM. We observed dose-dependent inhibitory effects of NSC23766 and EHT1864 on platelet activation, as demonstrated by reduced integrin activation and P-selectin exposure after stimulation of GPCRs and (hem)ITAM receptors in wild-type platelets (Fig. 1), but, importantly, also in Rac1-deficient platelets downstream of GPCRs (Fig. S2). These data indicate that NSC23766 and EHT1864 have inhibitory effects on platelet activation that are, at least in part, independent of Rac1. Interestingly, we found that a high concentration of NSC23766 (300 µM) reduced the expression of prominent surface receptors on platelets, including $\alpha_{IIb}\beta_3$, GPVI, and GPV (Table 1), and that this was associated with an overall reduced signaling capacity independently of the inhibitory effect on Rac1. Furthermore, a high concentration of EHT1864 (200 µM) induced pronounced apoptosis (Fig. 2), questioning the use of this inhibitor concentration, at least for the analysis of platelet function. On the basis of these results, we concluded that the most tolerable concentration for our studies was 100 µM.

Importantly, our study compared both inhibitors in a Rac-deficient cell system for the first time, as Rac1 is the only expressed Rac isoform in platelets. Notably, NSC23766 and EHT1864 caused a strong reduction in platelet activation in the absence of Rac1 (Fig. 3), with significant off-target effects being found for both compounds in mammalian cells. Similar effects were observed in platelets that were double-deficient for Rac1 and Cdc42 (Fig. 6B,C), as well as for Rac1 and RhoA (data not shown), indicating that NSC27366 and EHT1864 do not act on Cdc42 or RhoA, which is in line with previous studies [14,15]. Interestingly, we found that NSC23766 and EHT1864 had minimal and distinct Rac1-independent effects on integrin outside-in signaling (Fig. 4). Whereas neither compound showed an effect on platelet spreading (Fig. 4A,B), EHT1864 slightly inhibited clot retraction in wild-type platelets, although this process was unaltered in vehicle-treated Rac1-deficient platelets (Fig. 4C,D). These data additionally demonstrate that Rac1 is dispensable for clot retraction, which is in contrast to the findings of previous studies using NSC23766, EHT1864, and/or a Rac1-deficient mouse model [30,32]. Stefanini *et al.* [30] showed that clot retraction was more markedly reduced in EHT1864-treated wild-type platelets than in controls, which might be explained by the relatively high concentration of 150 µM used in that study, at

10 *S. Dütting* et al

A   0.1 U mL^{-1} Thrombin

Fig. 7. Rac1-independent inhibition of p21-activated kinase (PAK)1/PAK2 activation. (A) Washed platelets (7×10^5 µL^{-1}) from *Rac1$^{+/+}$* and *Rac1$^{-/-}$* mice were incubated with NSC23766 (NSC), EHT1864 (EHT) or vehicle, and then stimulated with 0.1 U mL^{-1} thrombin under stirring at 37 °C. Aliquots were taken at the indicated time points, and subsequently lysed with NP-40 detergent. Proteins were separated by reducing SDS-PAGE (10%), blotted on a poly(vinylidene difluoride) membrane, and stained with the phospho-specific PAK1/PAK2 (Thr423/Thr402) antibody. Staining of the respective non-phosphorylated proteins (PAK1/PAK2/PAK3) served as a loading control. The results shown are representative of three individual experiments. (B) Kinase activity was measured in HEPES buffer with full-length PAK1 (4 µm) and the non-hydrolyzable GTP analog Cdc42-GppNHp (15 µm) in the presence or absence of NSC23766 and EHT1864, respectively. The reactions were started by addition of 100 µm ATP, incubated for 30 min at room temperature, and stopped by addition of 20 µL of 5 × SDS-loading buffer and incubation at 95 °C for 5 min. All samples were analyzed by SDS-PAGE and subsequent staining with both Pro-Q Diamond and colloidal Coomassie as described.

PF4-Cre) might influence the results, as previous studies by our group and others demonstrated no effect of Rac1 deficiency on GPCR signaling with the use of Mx-Cre-mediated hematopoietic deletion of Rac1 [7,10]. In contrast, we found a profound defect in GPCR-mediated platelet activation in mice with an MK/platelet-specific PF4-Cre-mediated Rac1 deficiency (Fig. 3). Furthermore, GPIb-mediated filopodia formation on VWF was dramatically inhibited in NSC23766-treated platelets and mildly inhibited in EHT1864-treated wild-type platelets, and NSC23766 also reduced filopodium formation of Rac1-deficient platelets, demonstrating that NSC23766 interferes with this process independently of Rac1 (Fig. 5).

PAKs are direct downstream effectors of Rac1 and Cdc42 in almost all cell types. Binding of PAK1 and PAK2 to Rac1-GTP and Cdc42-GTP results in the autophosphorylation of PAK1 (Thr423) and PAK2 (Thr402) that is necessary for their activation and subsequent signal propagation [42]. Our data demonstrate that thrombin-induced activation of PAK1/PAK2 was significantly impaired in Rac1-deficient platelets, but almost completely abolished in NSC23766-treated or EHT1864-treated wild-type platelets, indicating that the inhibitors exert other effects in addition to Rac1 inhibition in this assay. This was confirmed by the marked inhibition of PAK1/PAK2 phosphorylation by the two inhibitors in thrombin-stimulated Rac1-deficient platelets (Fig. 7A; Fig. S3) and in a cell-free PAK activity assay (Fig. 7B), demonstrating that both compounds affect PAK1/PAK2 activity independently of Rac1. This may explain the observed Rac1-independent defects in platelet activation induced by thrombin signaling. Interestingly, Levay et al. [16] demonstrated that NSC23766 is also a non-selective, competitive antagonist of muscarinic acetylcholine receptors [16]. Binding modeling revealed that NSC23766 could be docked well to the orthosteric binding pocket of the M2 and M3 muscarinic acetylcholine receptors. It is tempting to speculate that

which a significant percentage of mouse platelets were already apoptotic in our hands (Fig. 2). In contrast, Flevaris *et al.* [32] showed reduced clot retraction of wild-type platelets treated with 20 µm NSC23766. The discrepancy between these results and our data is more difficult to explain, but may possibly be attributable to prolonged incubation times with the inhibitor in their experimental settings. Furthermore, Flevaris *et al.* [32] showed defective clot retraction of Rac1-deficient platelets generated by Mx-Cre-mediated gene deletion. Our results indicate that the Cre-mouse line used to delete Rac1 (Mx-Cre vs.

NSC23766 might also directly bind to PAK1 and PAK2, thereby inhibiting their activatory auto phosphorylation and causing the non-specific effects.

In summary, our data demonstrate profound off-target effects of the widely used Rac1 inhibitors NSC23766 and EHT1864 in mouse platelets that are in part based on Rac1-independent inhibition of PAK1/PAK2 activation. Besides the limitation of these compounds resulting from probably undesired on-target effects on other cell types, this previously unrecognized lack of specificity may confine the potential of NSC23766 and EHT1864 as novel therapeutic agents or at least warrant further detailed studies.

Addendum

Acknowledgements

Disclosure of Conflict of Interests

The authors state that they have no conflict of interest.

Supporting Information

Additional Supporting Information may be found in the online version of this article:

Fig. S1. Analysis of Rac1 and Cdc42 expression.
Fig. S2. Dose-dependent inhibition of $\alpha_{IIb}\beta_3$ activation and granule release by NSC23766 (NSC) and EHT1864 (EHT) in $Rac1^{-/-}$ platelets.
Fig. S3. Quantification of Rac1-independent inhibition of PAK1/PAK2 activation after thrombin stimulation.

References

1 Jackson SP. Arterial thrombosis – insidious, unpredictable and deadly. *Nat Med* 2011; **17**: 1423–36.

2 Nieswandt B, Pleines I, Bender M. Platelet adhesion and activation mechanisms in arterial thrombosis and ischaemic stroke. *J Thromb Haemost* 2011; **9**(Suppl. 1): 92–104.

3 Nieswandt B, Aktas B, Moers A, Sachs UJ. Platelets in athero-thrombosis: lessons from mouse models. *J Thromb Haemost* 2005; **3**: 1725–36.

4 Etienne-Manneville S, Hall A. Rho GTPases in cell biology. *Nature* 2002; **420**: 629–35.

5 McCarty OJ, Larson MK, Auger JM, Kalia N, Atkinson BT, Pearce AC, Ruf S, Henderson RB, Tybulewicz VL, Machesky LM, Watson SP. Rac1 is essential for platelet lamellipodia formation and aggregate stability under flow. *J Biol Chem* 2005; **280**: 39474–84.

6 Pleines I, Dutting S, Cherpokova D, Eckly A, Meyer I, Morowski M, Krohne G, Schulze H, Gachet C, Debili N, Brakebusch C, Nieswandt B. Defective tubulin organization and proplatelet formation in murine megakaryocytes lacking Rac1 and Cdc42. *Blood* 2013; **122**: 3178–87.

7 Pleines I, Eckly A, Elvers M, Hagedorn I, Eliautou S, Bender M, Wu X, Lanza F, Gachet C, Brakebusch C, Nieswandt B. Multiple alterations of platelet functions dominated by increased secretion in mice lacking Cdc42 in platelets. *Blood* 2010; **115**: 3364–73.

8 Pleines I, Elvers M, Strehl A, Pozgajova M, Varga-Szabo D, May F, Chrostek-Grashoff A, Brakebusch C, Nieswandt B. Rac1 is essential for phospholipase C-gamma2 activation in platelets. *Pflugers Arch* 2009; **457**: 1173–85.

9 Pleines I, Hagedorn I, Gupta S, May F, Chakarova L, van Hengel J, Offermanns S, Krohne G, Kleinschnitz C, Brakebusch C, Nieswandt B. Megakaryocyte-specific RhoA deficiency causes macrothrombocytopenia and defective platelet activation in hemostasis and thrombosis. *Blood* 2012; **119**: 1054–63.

10 Akbar H, Kim J, Funk K, Cancelas JA, Shang X, Chen L, Johnson JF, Williams DA, Zheng Y. Genetic and pharmacologic evidence that Rac1 GTPase is involved in regulation of platelet secretion and aggregation. *J Thromb Haemost* 2007; **5**: 1747–55.

11 Brown JH, Del Re DP, Sussman MA. The Rac and Rho hall of fame: a decade of hypertrophic signaling hits. *Circ Res* 2006; **98**: 730–42.

12 Gao Y, Dickerson JB, Guo F, Zheng J, Zheng Y. Rational design and characterization of a Rac GTPase-specific small molecule inhibitor. *Proc Natl Acad Sci USA* 2004; **101**: 7618–23.

13 Shutes A, Onesto C, Picard V, Leblond B, Schweighoffer F, Der CJ. Specificity and mechanism of action of EHT 1864, a novel small molecule inhibitor of Rac family small GTPases. *J Biol Chem* 2007; **282**: 35666–78.

14 Pandey D, Goyal P, Dwivedi S, Siess W. Unraveling a novel Rac1-mediated signaling pathway that regulates cofilin dephosphorylation and secretion in thrombin-stimulated platelets. *Blood* 2009; **114**: 415–24.

15 Rahman A, Davis B, Lovdahl C, Hanumaiah VT, Feil R, Brakebusch C, Arner A. The small GTPase Rac1 is required for smooth muscle contraction. *J Physiol* 2014; **592**: 915–26.

16 Levay M, Krobert KA, Wittig K, Voigt N, Bermudez M, Wolber G, Dobrev D, Levy FO, Wieland T. NSC23766, a widely used inhibitor of Rac1 activation, additionally acts as a competitive antagonist at muscarinic acetylcholine receptors. *J Pharmacol Exp Ther* 2013; **347**: 69–79.

17 Chrostek A, Wu X, Quondamatteo F, Hu R, Sanecka A, Niemann C, Langbein L, Haase I, Brakebusch C. Rac1 is crucial for hair follicle integrity but is not essential for maintenance of the epidermis. *Mol Cell Biol* 2006; **26**: 6957–70.

18 Tiedt R, Schomber T, Hao-Shen H, Skoda RC. Pf4-Cre transgenic mice allow the generation of lineage-restricted gene knockouts for studying megakaryocyte and platelet function in vivo. *Blood* 2007; **109**: 1503–6.

19 Knight CG, Morton LF, Onley DJ, Peachey AR, Ichinohe T, Okuma M, Farndale RW, Barnes MJ. Collagen–platelet interac-

tion: Gly-Pro-Hyp is uniquely specific for platelet Gp VI and mediates platelet activation by collagen. *Cardiovasc Res* 1999; **41**: 450–7.

20 Nieswandt B, Bergmeier W, Rackebrandt K, Gessner JE, Zirngibl H. Identification of critical antigen-specific mechanisms in the development of immune thrombocytopenic purpura in mice. *Blood* 2000; **96**: 2520–7.

21 Gruner S, Prostredna M, Aktas B, Moers A, Schulte V, Krieg T, Offermanns S, Eckes B, Nieswandt B. Anti-glycoprotein VI treatment severely compromises hemostasis in mice with reduced alpha2beta1 levels or concomitant aspirin therapy. *Circulation* 2004; **110**: 2946–51.

22 Jaiswal M, Dubey BN, Koessmeier KT, Gremer L, Ahmadian MR. Biochemical assays to characterize Rho GTPases. *Methods Mol Biol* 2012; **827**: 37–58.

23 Zhang SC, Gremer L, Heise H, Janning P, Shymanets A, Cirstea IC, Krause E, Nurnberg B, Ahmadian MR. Liposome reconstitution and modulation of recombinant prenylated human Rac1 by GEFs, GDI1 and Pak1. *PLoS One* 2014; **9**: e102425.

24 Thakur HC, Singh M, Nagel-Steger L, Kremer J, Prumbaum D, Fansa EK, Ezzahoini H, Nouri K, Gremer L, Abts A, Schmitt L, Raunser S, Ahmadian MR, Piekorz RP. The centrosomal adaptor TACC3 and the microtubule polymerase chTOG interact via defined C-terminal subdomains in an Aurora-A kinase-independent manner. *J Biol Chem* 2014; **289**: 74–88.

25 Marondedze C, Lilley K, Thomas L. Comparative gel-based phosphoproteomics in response to signaling molecules. *Methods Mol Biol* 2013; **1016**: 139–54.

26 Haga K, Kruse AC, Asada H, Yurugi-Kobayashi T, Shiroishi M, Zhang C, Weis WI, Okada T, Kobilka BK, Haga T, Kobayashi T. Structure of the human M2 muscarinic acetylcholine receptor bound to an antagonist. *Nature* 2012; **482**: 547–51.

27 Montalvo-Ortiz BL, Castillo-Pichardo L, Hernandez E, Humphries-Bickley T, De la Mota-Peynado A, Cubano LA, Vlaar CP, Dharmawardhane S. Characterization of EHop-016, novel small molecule inhibitor of Rac GTPase. *J Biol Chem* 2012; **287**: 13228–38.

28 Shattil SJ, Kim C, Ginsberg MH. The final steps of integrin activation: the end game. *Nat Rev Mol Cell Biol* 2010; **11**: 288–300.

29 Aslan JE, Tormoen GW, Loren CP, Pang J, McCarty OJ. S6K1 and mTOR regulate Rac1-driven platelet activation and aggregation. *Blood* 2011; **118**: 3129–36.

30 Stefanini L, Boulaftali Y, Ouellette TD, Holinstat M, Desire L, Leblond B, Andre P, Conley PB, Bergmeier W. Rap1–Rac1 circuits potentiate platelet activation. *Arterioscler Thromb Vasc Biol* 2012; **32**: 434–41.

31 Cohen I. The contractile system of blood platelets and its function. *Methods Achiev Exp Pathol* 1979; **9**: 40–86.

32 Flevaris P, Li Z, Zhang G, Zheng Y, Liu J, Du X. Two distinct roles of mitogen-activated protein kinases in platelets and a novel Rac1–MAPK-dependent integrin outside-in retractile signaling pathway. *Blood* 2009; **113**: 893–901.

33 Yuan Y, Kulkarni S, Ulsemer P, Cranmer SL, Yap CL, Nesbitt WS, Harper I, Mistry N, Dopheide SM, Hughan SC, Williamson D, de la Salle C, Salem HH, Lanza F, Jackson SP. The von Willebrand factor–glycoprotein Ib/V/IX interaction induces actin polymerization and cytoskeletal reorganization in rolling platelets and glycoprotein Ib/V/IX-transfected cells. *J Biol Chem* 1999; **274**: 36241–51.

34 McCarty OJ, Calaminus SD, Berndt MC, Machesky LM, Watson SP. von Willebrand factor mediates platelet spreading through glycoprotein Ib and alpha(IIb)beta3 in the presence of botrocetin and ristocetin, respectively. *J Thromb Haemost* 2006; **4**: 1367–78.

35 Delaney MK, Liu J, Zheng Y, Berndt MC, Du X. The role of Rac1 in glycoprotein Ib–IX-mediated signal transduction and integrin activation. *Arterioscler Thromb Vasc Biol* 2012; **32**: 2761–8.

36 Heasman SJ, Ridley AJ. Mammalian Rho GTPases: new insights into their functions from in vivo studies. *Nat Rev Mol Cell Biol* 2008; **9**: 690–701.

37 Muller LU, Schore RJ, Zheng Y, Thomas EK, Kim MO, Cancelas JA, Gu Y, Williams DA. Rac guanosine triphosphatases represent a potential target in AML. *Leukemia* 2008; **22**: 1803–6.

38 Shibata S, Nagase M, Yoshida S, Kawarazaki W, Kurihara H, Tanaka H, Miyoshi J, Takai Y, Fujita T. Modification of mineralocorticoid receptor function by Rac1 GTPase: implication in proteinuric kidney disease. *Nat Med* 2008; **14**: 1370–6.

39 Tan AM, Samad OA, Fischer TZ, Zhao P, Persson AK, Waxman SG. Maladaptive dendritic spine remodeling contributes to diabetic neuropathic pain. *J Neurosci* 2012; **32**: 6795–807.

40 Binker MG, Binker-Cosen AA, Gaisano HY, Cosen-Binker LI. Inhibition of Rac1 decreases the severity of pancreatitis and pancreatitis-associated lung injury in mice. *Exp Physiol* 2008; **93**: 1091–103.

41 Colomba A, Giuriato S, Dejean E, Thornber K, Delsol G, Tronchere H, Meggetto F, Payrastre B, Gaits-Iacovoni F. Inhibition of Rac controls NPM-ALK-dependent lymphoma development and dissemination. *Blood Cancer J* 2011; **1**: e21.

42 Kumar R, Gururaj AE, Barnes CJ. p21-activated kinases in cancer. *Nat Rev Cancer* 2006; **6**: 459–71.

Chapter 12

The RAS-effector interface

The RAS-effector interface: Isoform-specific differences in the effector binding regions
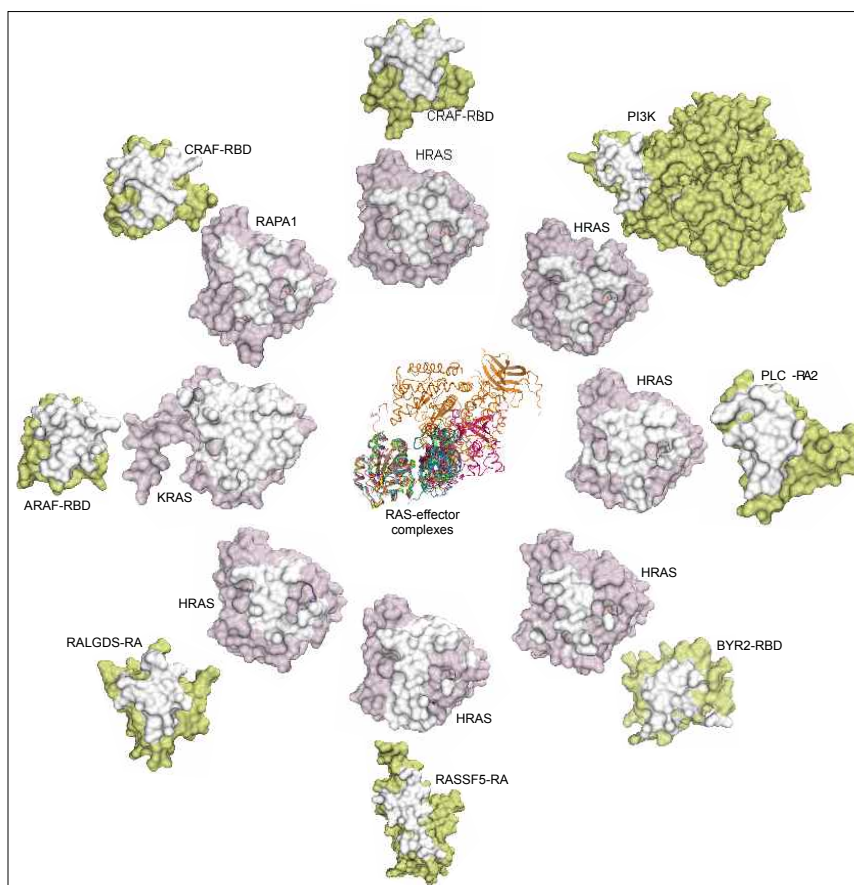
Status:	Submitted in PLOS ONE
Impact factor:	3.23
Own Proportion to this work:	25 %; design experiment, perform structural section analysis and writing manuscript

The RAS-effector interface: Isoform-specific differences in the effector binding regions

Hossein Nakhaeizadeh, Ehsan Amin, Saeideh Nakhaei-Rad, Radovan Dvorsky, Mohammad Reza Ahmadian

Institute of Biochemistry and Molecular Biology II, Medical Faculty of the Heinrich-Heine University, Düsseldorf, Germany

*Correspondences should be addressed to Prof. Dr. Reza Ahmadian, Institut für Biochemie und Molekularbiologie II, Medizinische Fakultät der Heinrich-Heine-Universität, Universitätsstr. 1, Gebäude 22.03, 40255 Düsseldorf, Germany, phone: #49-211-811 2384, Fax: #49-211-811 2726, e-mail: reza.ahmadian@uni-duesseldorf.de

Running title:
Effector selectivity of RAS proteins

Conflict of Interest statement:
The authors declare no conflict of interest.

Abstract
RAS effectors specifically interact with GTP-bound form of RAS in response to extracellular signals and link them to downstream signaling pathways. The molecular nature of effector interaction by RAS is well-studied but yet still incompletely understood in a comprehensive and systematic way. Here, structure-function relationships in the interaction between different RAS proteins and various effectors were investigated in detail by combining our *in vitro* data with *in silico* data. Equilibrium dissociation constants were determined for the binding of HRAS, KRAS, NRAS, RRAS1 and RRAS2 to both the RAS binding (RB) domain of CRAF and PI3Kα, and the RAS association (RA) domain of RASSF5, RALGDS and PLCε, respectively, using fluorescence polarization. An interaction matrix, constructed on the basis of available crystal structures, allowed identification of hotspots as critical determinants for RAS-effector interaction. New insights provided by this study are dissection of the identified hotspots in five distinct regions (R1 to R5) in spite of high sequence variability not only between but also within RB/RA domain-containing effectors proteins. Finally, we propose that intermolecular β-sheet interaction in R1 is a central recognition region while R3 may determine isoform specificity.

Key words: Binding affinity, Dissociation constant, Effector, hotspots, interaction, RAS, specificity, RAF kinase, PI3K

1

Introduction

RAS family proteins, including HRAS, KRAS, NRAS, RRAS1, RRAS2 (or TC21), RRAS3 (or MRAS) and ERAS, act as signaling nodes and regulate the function of various effectors with divergent biochemical functions in all eukaryotes [1-3]. Signal transduction implies physical association of these proteins with effectors and activation of a spectrum of functionally diverse downstream effectors, *e.g.*, CRAF, PI3Kα, RALGDS, PLCε and RASSF5 [1, 4-10]. CRAF, a serine/threonine kinase, activates the MEK-ERK axis and controls gene expression and cell proliferation [11]. PI3Kα generates phosphatidylinositol (3,4,5)-trisphosphate (PIP3) and regulates cell growth, cell survival, cytoskeleton reorganization, and metabolism [12]. RALGDS links RAS with RAL, a RAS-related protein, and regulates cellular processes, such as vesicular trafficking and migration [13]. PLCε generates two second messengers of diacylglycerol (DAG) and inositol trisphosphate (IP$_3$) leading to an intracellular increase of calcium levels, which controls endocytosis, exocytosis, and cytoskeletal reorganization [14]. RASSF5 undergoes a complex with heterodimer of MST1/2, human orthologues of Hippo, and WW45 and promotes apoptosis and cell cycle arrest [15].

Gain-of-function RAS mutations are frequently found in both human cancers, e.g., pancreatic cancer [16] and developmental disorders, including Noonan syndrome [17-19]. Whereas the latter is thought to commonly underlay dysregulation of mainly one pathway, the RAS-MAPK pathway [19]. RAS-mediated cancer progression involves activation of several pathways, *e.g.*, PI3K-AKT [3, 20], RALGDS-RAL [9, 13], PLCε-second messengers [14] or Hippo-YAP [21] as well as RAS-MAPK [22]. Understanding how effectors selectively recognize RAS-GTP is an attractive approach to functionalize peptides and peptidomimetics capable of inhibiting RAS interactions and signaling.

RAS effectors contain either a RAS binding (RB) or a RAS association (RA) domain [7, 23, 24]. RAS-effector interaction essentially requires RAS association with membranes and its activation by specific regulatory proteins (*e.g.*, guanine nucleotide exchange factors or GEFs), leading to the formation of GTP-bound, active RAS [25-27]. Notably, RAS proteins change their conformation mainly at two highly mobile regions, designated as switch I (residues 30-40) and switch II (residues 60-68) [28, 29]. Only in GTP-bound form, the switch regions of the RAS proteins provide a platform for the association of the effector proteins, especially through their RB or RA domains, respectively. This interaction appears to be a prerequisite for effector activation [24, 30-32]. RB/RA interactions with RAS proteins do not exhibit the same mode of interaction between different RAS effectors [24, 33-35]. However, CRAF-RB and RALGDS-RA domains share a similar ubiquitin-like fold and contact the switch I region *via* a similar binding mode, whereas PI3Kα-RB, RASSF5-RA and PLCε-RA domains do not share sequence and structural similarity but commonly associate with the switch regions, especially switch I [33-37]. Early cell-based studies have shown that distinct amino acids in switch I, *e.g.*, Thr-35, Glu-37, Asp-38 or Tyr-40) dictate effector specificity [38-41]. However, there is no clear explanation for such a differential selection of the switch I region by various effectors.

Up to date, various methods and different conditions for measuring the binding affinity for the interaction between different effectors and RAS proteins, especially HRAS, has been evaluated in many laboratories using various methods and different conditions (reviewed in [4, 24, 42]), as summarized in Table 1. In this study, the interactions of five different RAS proteins with both the RB domains of CRAF and PI3Kα, and the RA domains of RALGDS, PLCε and RASSF5 were reinvestigated under comparable conditions using fluorescence polarization. In addition, available complex structures and sequence alignments were utilized to systematically assess a matrix for the interaction of investigated effector domains with various RAS proteins. Obtained dissociation constants (K$_d$ values) were combined with the interaction matrix enabled us to determine common hotspots as critical specificity-determining residues and to predict selectivity of five RB- and RA-containing proteins.

Materials and Methods

Constructs

Fragments of human genes encoding both RBs of CRAF (accession number P04049; amino acids or aa 51–131), PI3Kα (P42336; aa 169-301), and RAs of RALGDS (Q12967; aa 777–872), PLCε (Q9P212; aa 2130–2240), RASSF5 (Q8WWW0; aa 200–358) were cloned in pMal-c5X-His vector.

Constructs for the expression of human HRAS, KRAS, NRAS, RRAS1 and RRAS2 isoforms are described previously [5].

Proteins
All RAS and the effector proteins were expressed in *Escherichia coli* using the pGEX and pMAL-His expression systems and prepared using glutathione and Ni-NTA based affinity chromatography as described previously [18]. RAS-mGppNHp was prepared as described [18].

Fluorescence polarization
RAS-effector interaction was performed in 50 mM Tris/HCl pH 7.5, 100 mM NaCl, 5 mM $MgCl_2$ and 3 mM dithiothreitol at 25 °C using a Fluoromax 4 fluorimeter in polarization mode as described [18]. Increasing amounts of MBP-tagged effector proteins (0.05 – 100 µM) titrated to 1 µM RAS-mGppNHp resulted in an increase of polarization. Equilibrium dissociation constants (K_d) were calculated by fitting the concentration dependent binding curve using a quadratic ligand binding equation.

Sequence and structural analysis
Sequence alignments were performed with Bioedit program using clustalW algorithm [43]. Chimera has been used to adjust sequence alignments with superimposed structures [44]. A python code has been written to get sequence alignments and PDB files of complex structures and return intermolecular contacts in frame of an interaction matrix. The intermolecular contacts were defined as pair residues with distance ≤4.0 Å between effectors and RAS proteins in available complex structures in the protein data bank (http://www.pdb.org). Biopython modules [45] were also used to elucidate corresponding residues in all available complex structures. All structural representations were generated using PyMol viewer [46].

Results
A general approach for quantitative study of RAS-effector interaction
As previous studies focused mainly on HRAS interaction with effectors, there is a lack of information for other RAS proteins (Table 1). Determined dissociation constants (K_d values) have been invaluable in providing insights into the particular RAS-effector interactions. However, they have been obtained under various conditions using diverse experimental techniques (see Table 1) and cannot be used as such for a comparative evaluation of the interaction of different RAS proteins with various effectors. For this reason, we set out to analyze the interaction of HRAS, KRAS, NRAS, RRAS1 and RRAS2, with five distinct RB- and RA-containing effectors under the same conditions. Since the kinetic analysis using stopped-flow spectrofluorometric method was not applicable to all isolated effector proteins, we utilized the advantage of fluorescence polarization approach [47].
Therefore, we have prepared both, the RAS proteins in complex with mant (m) GppNHp, a non-hydrolysable fluorescent GTP analog, and the effector proteins fused to maltose-binding protein (MBP, 42 kDa). We choose the MBP because it increases the molecular mass of small-sized RB or RA domains, leads to an amplified fluorescence signal (Fig. 2A) and ensures a homogeneous monomeric form of the fusion proteins. GST-fusion protein in contrast has yielded a mixture of dimeric and monomeric species (data not shown). Performed equilibrium titration experiments revealed a sufficient signal changes upon binding and guaranteed comparable experimental conditions for all measurements. By taking advantages of this method, complexes formed between these two types of proteins provided distinct polarized signals (Figs. 2A and S1) that enabled us to determine K_d values for RAS-effector interactions (Table 2).

Determined affinities for the interaction between RAS proteins and individual effector domains vary between 48 nM for the NRAS–CRAF interaction and 205 µM for an interaction between KRAS and PI3Kα (Fig. 2B; Table 2). In general, tested RAS proteins can be nicely divided according to their affinities into two distinctive groups, first comprising HRAS, KRAS, NRAS and the second RRAS proteins. Highest affinities were obtained for CRAF, which were roughly 3-8 folds higher as compared to that for RASSF5, followed by RALGDS and PLCε with K_d values in the lower micromolar ranges

3

(Fig. 2B; Table 2). In contrast, RRAS1 and RRAS2 have similar micromolar affinities for the effectors and, interestingly also for PI3Kα but not for PLCε. Our data clearly support previous findings (see Table 1) that isolated effector domains, such as RB or RA, represent functional units, capable of recognizing and tight binding RAS proteins. Exceptions are the low affinity of PLCε RA domain for the RRAS proteins and PI3Kα RB domain for HRAS, KRAS and NRAS.

Identification of hotspots within protein interfaces
Up to date eleven complex structures of RAS proteins and their effectors has been determined (Table S1). As some of them contain more than one complex in unit cell, there are altogether sixteen complex structures available for the analysis. In order to map atomic interactions responsible for observed variable affinities, we have extracted information about interacting interface from all these complex structures and combined them with their sequence alignments (Figs. S2 and S3). Interestingly, effectors show low sequence similarity (Fig. S2A), but their mode of interaction is well conserved as can be seen after a superposition of complex structures performed according to the RAS structure (Figs. 3 and S4). However, some amino acids aligned according to the sequence were quite distant in the space. Therefore, we edited the sequence alignment to synchronize it with structural alignment (Fig. S2A). Our python code finally took sequence alignments with PDB files of complex structures as inputs and calculated all interaction pairs in analyzed complex structures in the form of a matrix (Fig. 4A).

Interaction matrix and binding regions
Interaction matrix relates in a comprehensive manner interacting residues on both sides of complexes, RAS isoforms as rows and effector proteins as columns (Fig. 4A). All numbering in this study is based on HRAS and CRAF proteins. Each element of the matrix accounts for the number of contacts between corresponding residues in all analyzed structures. We identified five distinct regions (denoted from R1 to R5) in the matrix with the highest number of interactions, which are separately highlighted in Figure 4.
Most pronounced is R1 in the middle of matrix. Inspection of the particular interactions corresponding to this region clearly shows an arrangement of intermolecular β-sheet interactions in an anti-parallel fashion (Fig. 4B). As many of these contacts in R1 are mediated by main-chain/main-chain interactions, we divided each element of R1 in the matrix in four categories of interactions, including main-chain–main-chain, main-chain–side-chain, side-chain–main-chain and side-chain–side-chain (Fig. S5). Main-chain–main-chain interactions typically involve hydrogen bonds between the N-H group and the carbonyl oxygen. We found three interaction hotspots in all RAS-effector complexes, which seem to represent a central recognition site in R1. These amino acids are Glu-37, Asp-38 and Ser-39 from the RAS side and positions 66 to 69 from the effector side (Fig. 4A, red box). However, side-chain interactions are also highly populated in this region indicating that the nature of amino acids in this region also influences the RAS-effector association (Fig. S5).
R2 is another distinct region, which corresponds to the interactions between the residues 21 to 34 of RAS, including N-terminal half of switch I, and an elongated loop containing an α helix, in the case of PLCε and PI3Kα even two α helices, covering positions 83 to 90 (Fig. 4). However, an overall shape of this region as well as the spatial orientation of α-helical structures is very diverse (Fig. 4B). These structural diversities do not only cause widely dispersed interactions in R2 but are also responsible for the interactions in frames of regions R4. The capability of R2 in RB domains to interact also with the β-strand in switch I of RAS simultaneously involves the recognition region R1 and gives rise to the region R4 (Fig. 4B; upper panel). On the other hand, a spatial position of the N-terminal residues of RA domains in R1 is similar to the position of C-terminal residues RB domains in R2 leading to the interactions established in the region R5. Remarkably, the interaction matrix gives the hints for a region (Fig. 4; R3) that could not be defined as a general interaction patch from a direct pair-wise comparison of individual complex structures. This region comprises critical residues, including Ile-36, Glu-37 and Tyr-64 on the RAS side, and positions 57, 59 and 71 on effector side. R3 very likely determines the selectivity of RAS-effector interaction, especially because of both sequence deviations at this region (Arg-41 and Tyr-64) if comparing HRAS, KRAS and NRAS with RRAS1, RRAS2, RRAS3. Strikingly, the binding affinities between these two groups of RAS subfamilies are indeed different.

4

Discussion

Since the discovery of the first RAS effector [48-51], inhibition of RAS signaling by blocking RAS-effector interactions has been an ever-evolving and challenging venture [52-55]. Biochemical and biophysical studies providing insights into the interaction of the downstream effectors with RAS proteins and their mutants established the basic principles for drug design and development [30, 42, 52, 56, 57]. There is, however, a quite significant gap in our understanding of how RAS proteins specifically bind to and activate their diverse effectors. Rigorous understanding of the RAS-effector interplay would require an investigation of larger fragments or full-length effector protein that was so far accomplished only in a few studies [35, 58, 59]. For several reasons, isolated effector domains have been used in the vast majority of biochemical and structural studies for the investigation of their interactions with RAS proteins, predominantly with HRAS (Tables 1 and S1). However, interaction characteristics obtained for the same proteins differ considerably. For example, K_d values for the interaction of CRAF or RALGDS with HRAS-GTP vary from 5 to 330 nM and 80 nM to 39 μM (Tables 1). Another major difference of more than two orders of magnitude was observed for the interaction between RRAS1 and CRAF. Such a huge variation of K_d values (summarized in Table 1), which in addition have been determined by different groups using different methods and experimental conditions, made a comprehensive analysis of sequence-structure-function relationship practically impossible. That is why we have quantitatively analyzed the interaction between five effector domains and five RAS proteins, covering for the first time also RRAS2, under the same conditions (Table 2).

Our measurements reveal that the RAS isoforms (HRAS, KRAS and NRAS) behave similarly toward each effector but very differently as compared to RRAS isoforms (RRAS1 and RRAS2), in spite of their high sequence identity. A previous study has reported that RAS isoforms much stronger activate the MAPK pathway *via* the RAF kinase as compared to RRAS isoforms [59]. These data are consistent with K_d values determined in this study for RAS (ranging 0.048-0.142) and RRAS (2.29-4.09) isoforms. Notably, RRAS isoforms bind, except for PLCε, similarly to all tested effector domains with an up to 4-fold difference in binding affinities compare to RAS isoforms. Interestingly, they significantly interacted with PI3Kα but not with PLCε (Table 2), which is in agreement with the cell-based data reported previously [59].

In particular, the RAS isoforms, which exhibit high selectivity for CRAF followed by RASSF5, RALGDS and PLCε, seem not to retain its affinity for PI3Kα. It could be argued that isolated RB domain of PI3Kα, consisting of the amino acids 169-301, may lack additional binding determinants, in comparison to a 50-fold higher affinity obtained with isolated RB domain of PI3Kγ, consisting of the amino acids 144-1102 (Tables 1 and 2) [35]. A recent cell-based study has shown that RB domain of PI3Kα (aa 127–314) is sufficient to bind to ERAS, a new member of the RAS family, but obviously not to HRAS [5, 60]. However, the immunoprecipitation studies have revealed the endogenous PI3K isoforms α and δ interact with almost same affinity with both ERAS and HRAS [5]. These data suggest that RB domain of PI3K is sufficient for a tight interaction with ERAS but obviously requires additional capacity to properly associate with HRAS. Sequence deviations in effector binding regions may be critical for determining the minimal binding regions of RAS/effectors. It is, therefore, assumable that ERAS and RRAS isoforms but not RAS isoforms efficiently interact with RB domain of PI3Ks and RAS isoforms need a second binding region or alternatively a scaffold protein. Similar to the RAS isoforms, which have identical effector binding regions, the RRAS isoforms, also including RRAS3, revealed a very high sequence identity in these regions (Fig. S3). Among the amino acid deviations between the RAS and RRAS isoforms, there one critical residue (Arg-41 in RAS isoforms substituted by Thr/Leu in RRAS isoforms residues). It may determine effector selectivity between these isoforms, as confirmed for ERAS that has a tryptophan (Trp-79) at the corresponding position of Arg-41 in HRAS and has exhibited a higher selectivity for PI3K than CRAF [60].

The RB and RA domains share higher sequence homologies if they are aligned individually. However, there is no common consensus sequence for RAS binding if they are aligned together , particularly in the RAS binding regions R1 to R5 (Fig. S2; see arrowheads). Previous studies dealing with the interaction of small GTPases with their regulators have shown that there are patches of identical or highly homologous hotspots on both sides of protein surfaces that interact with each other [61-63].

Such interaction is evolutionary conserved and responsible for the recognition of counter proteins. Finding that there is no identical patch on RAS effector proteins (Figs. 4 and S2) seemed to break this rule. However, intermolecular β-sheet interactions between RAS proteins and their effectors are conserved and seem to supply the role of such critical patch, or in this special case a stretch, of homologous amino acid residues. The analysis of complex structures showed that these interactions, covered by the recognition region R1 in the interaction matrix, are prevailing and occur in almost all structures. Therefore, we have analyzed the proximity of effector binding residues in different RAS isoforms in the same way as of residues involved in β-sheet interactions and summarized the results as matrices (Figs. 4A and S5). Introduction of four different interaction types in the matrix with high scores of separated main-chain and side-chain RAS-effector interactions allowed a detailed inspection of central R1 region. Strikingly, there are three hotspots, which largely undergo main-chain/main-chain interactions (Glu-37 of RAS proteins with effector residues at position 68 and 69, respectively Asp-38 with residues at position 67; Fig. S5). These observations confirm the central role of R1 in the association of RAS proteins with their effectors and strongly suggest that the main-chain/main-chain interactions within this region are crucial for the recognition of these classes of proteins. Finally, we note that interactions in R1 also dependent, to certain extend, on side chains of accompanying amino acids. They indirectly support the formation of β-sheet on both sides of complexes. However, they also utilize their side chains in intramolecular interactions significantly contributing to the complex formation. In this way, Asp-38 interacts by its side chain exclusively with the effector residues at positions 68 and 69 within R1. Side chains of Glu-37 and Ile-37 undergo contacts with residues at positions 57 and 59 outside of the effector β-strand within the region R3. On the effector side of complexes, there are only two positions that contain identical or highly homologous amino acids, namely the position 59 and 84 (Fig. 4A). They are in both cases populated by positively charged residues, with exception of PLCε that has a Gln at position 59. These residues interact with negatively charged residues on RAS proteins (Glu-37 and Asp-33) and strongly contribute to the formation of complexes. However, no unique and/or particular residue of effectors can be attributed to overall differences observed for their association with RAS proteins. Effectors interacting residues are so variable at almost all interacting spots that only their concerted action is likely to explain measured diversity.

Previous studies have shown that RAS mutants (Thr-35, Glu-37, Asp-38 and Tyr-40) including also residues mentioned above, preferentially interact with some effectors but not others [38-41]. However, up to date there is no clear explanation for these variable selections of these mutants of RAS by specific effectors. The invariant Thr-35 of RAS was not gated in one of the three main regions in the matrix as it is mainly burden in RAS structure and does not directly interact with RAF1. However, Spoerner and colleagues have shown that T35S mutation drastically reduces HRAS affinity for effectors, including CRAF-RB (60-fold) and RALGDS-RA (>100-fold) [64]. They suggest that minor changes, such as truncating Thr-35 by a methyl group, strongly affect dynamic behavior of the switch 1 region and, in turn, its interaction with effectors. However, an early cell-based study has shown that HRAS T35S mutant interacts among RAS effectors only with CRAF but not PI3K, BYR2, RALGDS or RASSF5, and activates the MAPK pathway [38]. One explanation may be that galectin-1 scaffolds the HRAS[T35S]-CRAF [65]. On the other hand E37G mutation results in loss of PI3K and CRAF binding, but is able to interact with RA domain-containing effectors, such as RALGDS, RASSF5 and BYR2 [38]. Our interaction matrix shows contacts between E37G of HRAS and positively charged residues 61 and 69- and main-chain interactions with residue 69, and 70 of effectors. D38A mutation has been shown to retain CRAF binding but to lose interaction with PI3K, RALGDS and RASSF5 [41, 66]. Among different effector binding mutants, Y40C selectively activates PI3K but is unable to activate other effectors, such as RAF1, RALGDS, RASSF5 and BYR2 [67]. HRAS[G12V/Y40C] and HRAS[G12V/E37G] have been reported to cooperatively induce cell transformation *via* PI3K and RALGDS, respectively, but not *via* CRAF [39]. Vandal and colleagues have observed that KRAS[G12V/Y40C]-PI3K has shown the largest impact on an increase in tumor size whereas KRAS[G12V/E38G]-CRAF resulted in a decrease in tumor size but an increase of the number of tumors when combined with BRAF[V600E] [68]. Being central elements of R1, R3 and R4, our analysis not only confirms a prominent role of Glu-37, Asp-38 and Tyr-40 in effector binding but gives also hints for the mode of their interaction, which relies on the main-chain main-chain interaction. As this interaction is in the first rank independent on

accompanied side chains, it can be considered as conserved also in effectors. Consequently, it supplies thus the role of homologous residues found to be essential for the recognition of regulator proteins by Rho GTPases. Hence we state, that these RAS residues are responsible with their main-chain atoms for the recognition of effectors. On the other hand, side chains of these residues are still influential on the binding with effectors. Either indirectly affecting the structure of RAS switch I or directly interacting with effector residues within the regions R3 and R4 of our interaction matrix.

In conclusion, our data collectively support previous observations that the specificity in the signaling properties and biological functions of the various RAS proteins arises from the specific combination of effector pathways they regulate in each cell type. Considering the identity of interacting residues of different types of isoforms, a uniform association of RAS isoforms or rather RRAS isoforms can be expected with a particular effector. This raises the questions of how does the cell selects between respective RAS proteins and maintains respective effector activation. There are several review articles illustrating the current state of the art regarding the activation mechanism of various effectors [9, 11-13, 21, 69-71]. HRAS, KRAS and NRAS exhibit remarkable differences beyond their common interaction interfaces for regulators and effectors [72-74], especially at their C-terminal hypervariable region (Fig. S3), which has different features, including protein-protein interaction [75, 76]. An interesting issue, which is increasingly appreciated, is a RAS-membrane interface that appears to generate RAS isoform specificity with respect to effector interactions [77-79]. This is likely achieved by RAS-specific scaffold proteins, including CaM, GAL1, GAL3, IQGAPs, NPM1, NCL, SHOC2/SUR8 [76, 80], which may modulate isoform specificity at specific site of the cell. Another critical aspect is sorting/trafficking of the isoforms [81, 82] that has recently been shown to be highly specific for the respective RAS proteins and dependents on specific posttranslational modifications, including prenylation and acylation [83, 84] , phosphorylation [85, 86], ubiquitination [87-90] and acetylation [91-93]. Similar characteristics have been reported for the RRAS isoforms, including protein-protein interaction required for subcellular localization, e.g., at focal adhesion or recycling endosomes,[94, 95], and posttranslational modifications [96-98]. In addition, they contain extended N-termini (Fig. S3) that has been shown to be critical for RRAS1 in cell migration [99]. The N-terminus of ERAS, which undergoes multiple interaction with other proteins (Nakhaeizadeh *et al.*, unpublished), contains similar to RRAS1, putative SH3-binding motifs. These motifs may provide additional mechanisms for sorting and trafficking to specific subcellular sites.
An issue that remains to be elucidated in more details is the mechanism of effector activation. There are several review articles illustrating the current state of the art [9, 11-13, 21, 69-71]. Functional reconstitution of RAS interactions with full-length effector proteins eventually on liposomes

References

1.   Wittinghofer, A. and C. Herrmann, *Ras-effector interactions, the problem of specificity*. FEBS Lett, 1995. **369**(1): p. 52-6.

2.   Gutierrez-Erlandsson, S., et al., *R-RAS2 overexpression in tumors of the human central nervous system*. Mol Cancer, 2013. **12**(1): p. 127.

3.   Karnoub, A.E. and R.A. Weinberg, *Ras oncogenes: split personalities*. Nature reviews. Molecular cell biology, 2008. **9**(7): p. 517-31.

4.   Herrmann, C., *Ras-effector interactions: after one decade*. Curr Opin Struct Biol, 2003. **13**(1): p. 122-9.

5.   Nakhaei-Rad, S., et al., *The Role of Embryonic Stem Cell-expressed RAS (ERAS) in the Maintenance of Quiescent Hepatic Stellate Cells*. The Journal of biological chemistry, 2016. **291**(16): p. 8399-413.

6.   Castellano, E. and J. Downward, *Role of RAS in the regulation of PI 3-kinase*. Curr Top Microbiol Immunol, 2010. **346**: p. 143-69.

7.   Chan, J.J. and M. Katan, *PLCvarepsilon and the RASSF family in tumour suppression and other functions*. Advances in biological regulation, 2013. **53**(3): p. 258-79.

8.   Bunney, T.D. and M. Katan, *PLC regulation: emerging pictures for molecular mechanisms*. Trends Biochem Sci, 2011. **36**(2): p. 88-96.

9.   Ferro, E. and L. Trabalzini, *RalGDS family members couple Ras to Ral signalling and that's not all*. Cellular Signalling, 2010. **22**(12): p. 1804-10.

10.   Rajalingam, K., et al., *Ras oncogenes and their downstream targets*. Biochimica et biophysica acta, 2007. **1773**(8): p. 1177-95.

11.   Desideri, E., A.L. Cavallo, and M. Baccarini, *Alike but Different: RAF Paralogs and Their Signaling Outputs*. Cell, 2015. **161**(5): p. 967-70.

12.   Castellano, E. and J. Downward, *RAS Interaction with PI3K: More Than Just Another Effector Pathway*. Genes & cancer, 2011. **2**(3): p. 261-74.

13.   Gentry, L.R., et al., *Ral small GTPase signaling and oncogenesis: More than just 15minutes of fame*. Biochimica et biophysica acta, 2014. **1843**(12): p. 2976-2988.

14.   Bunney, T.D. and M. Katan, *Phospholipase C epsilon: linking second messengers and small GTPases*. Trends Cell Biol, 2006. **16**(12): p. 640-8.

15.   Feig, L.A. and R.J. Buchsbaum, *Cell signaling: life or death decisions of ras proteins*. Curr Biol, 2002. **12**(7): p. R259-61.

16.   Bryant, K.L., et al., *KRAS: feeding pancreatic cancer proliferation*. Trends Biochem Sci, 2014. **39**(2): p. 91-100.

17.   Cirstea, I.C., et al., *Diverging gain-of-function mechanisms of two novel KRAS mutations associated with Noonan and cardio-facio-cutaneous syndromes*. Human molecular genetics, 2013. **22**(2): p. 262-70.

18.   Gremer, L., et al., *Germline KRAS mutations cause aberrant biochemical and physical properties leading to developmental disorders*. Human mutation, 2011. **32**(1): p. 33-43.

19.   Lissewski, C., et al., *Copy number variants including RAS pathway genes-How much RASopathy is in the phenotype?* Am J Med Genet A, 2015. **167A**(11): p. 2685-90.

20.   McCormick, F., *KRAS as a Therapeutic Target*. Clin Cancer Res, 2015. **21**(8): p. 1797-801.

21.   Donninger, H., et al., *Ras signaling through RASSF proteins*. Seminars in cell & developmental biology, 2016.

22.   Dhillon, A.S., et al., *MAP kinase signalling pathways in cancer*. Oncogene, 2007. **26**(22): p. 3279-3290.

23.   Repasky, G.A., E.J. Chenette, and C.J. Der, *Renewing the conspiracy theory debate: does Raf function alone to mediate Ras oncogenesis?* Trends Cell Biol, 2004. **14**(11): p. 639-47.

9

24. Wohlgemuth, S., et al., *Recognizing and defining true Ras binding domains I: biochemical analysis*. Journal of molecular biology, 2005. **348**(3): p. 741-58.

25. Ahearn, I.M., et al., *Regulating the regulator: post-translational modification of RAS*. Nature reviews. Molecular cell biology, 2012. **13**(1): p. 39-51.

26. Hennig, A., et al., *Ras activation revisited: role of GEF and GAP systems*. Biol Chem, 2015. **396**(8): p. 831-48.

27. Fischer, A., et al., *B- and C-RAF display essential differences in their binding to Ras: the isotype-specific N terminus of B-RAF facilitates Ras binding*. The Journal of biological chemistry, 2007. **282**(36): p. 26503-16.

28. Mott, H.R. and D. Owen, *Structures of Ras superfamily effector complexes: What have we learnt in two decades?* Critical Reviews in Biochemistry and Molecular Biology, 2015. **50**(2): p. 85-133.

29. Vetter, I.R. and A. Wittinghofer, *The guanine nucleotide-binding switch in three dimensions*. Science, 2001. **294**(5545): p. 1299-304.

30. Athuluri-Divakar, S.K., et al., *A Small Molecule RAS-Mimetic Disrupts RAS Association with Effector Proteins to Block Signaling*. Cell, 2016. **165**(3): p. 643-55.

31. Thapar, R., J.G. Williams, and S.L. Campbell, *NMR characterization of full-length farnesylated and non-farnesylated H-Ras and its implications for Raf activation*. Journal of molecular biology, 2004. **343**(5): p. 1391-408.

32. Drugan, J.K., et al., *Ras interaction with two distinct binding domains in Raf-1 may be required for Ras transformation*. The Journal of biological chemistry, 1996. **271**(1): p. 233-7.

33. Bunney, T.D., et al., *Structural and mechanistic insights into ras association domains of phospholipase C epsilon*. Molecular cell, 2006. **21**(4): p. 495-507.

34. Stieglitz, B., et al., *Novel type of Ras effector interaction established between tumour suppressor NORE1A and Ras switch II*. EMBO J, 2008. **27**(14): p. 1995-2005.

35. Pacold, M.E., et al., *Crystal structure and functional analysis of Ras binding to its effector phosphoinositide 3-kinase gamma*. Cell, 2000. **103**(6): p. 931-43.

36. Huang, L., et al., *Structural basis for the interaction of Ras with RalGDS*. Nat Struct Biol, 1998. **5**(6): p. 422-6.

37. Nassar, N., et al., *The 2.2 A crystal structure of the Ras-binding domain of the serine/threonine kinase c-Raf1 in complex with Rap1A and a GTP analogue*. Nature, 1995. **375**(6532): p. 554-60.

38. White, M.A., et al., *Multiple Ras functions can contribute to mammalian cell transformation*. Cell, 1995. **80**(4): p. 533-41.

39. Khosravi-Far, R., et al., *Oncogenic Ras activation of Raf/mitogen-activated protein kinase-independent pathways is sufficient to cause tumorigenic transformation*. Mol Cell Biol, 1996. **16**(7): p. 3923-33.

40. Khwaja, A., et al., *Matrix adhesion and Ras transformation both activate a phosphoinositide 3-OH kinase and protein kinase B/Akt cellular survival pathway*. EMBO J, 1997. **16**(10): p. 2783-93.

41. Vavvas, D., et al., *Identification of Nore1 as a potential Ras effector*. J Biol Chem, 1998. **273**(10): p. 5439-42.

42. Erijman, A. and J.M. Shifman, *RAS/Effector Interactions from Structural and Biophysical Perspective*. Mini Rev Med Chem, 2016. **16**(5): p. 370-5.

43. Hall, T.A., *BioEdit: a user-friendly biological sequence alignment editor and analysis program for Windows 95/98/NT*. Nucleic Acids Symposium Series, 1999. **41**: p. 95-98.

44. Pettersen, E.F., et al., *UCSF Chimera—A visualization system for exploratory research and analysis*. Journal of Computational Chemistry, 2004. **25**(13): p. 1605-1612.

45.   Cock, P.J., et al., *Biopython: freely available Python tools for computational molecular biology and bioinformatics*. Bioinformatics, 2009. **25**(11): p. 1422-3.

46.   DeLano, W.L. *The PyMOL Molecular Graphics System*. 2002; Available from: http://www.pymol.org.

47.   Raines, R.T., *Fluorescence polarization assay to quantify protein-protein interactions: an update*. Methods Mol Biol, 2015. **1278**: p. 323-7.

48.   Kolch, W., et al., *Raf-1 protein kinase is required for growth of induced NIH/3T3 cells*. Nature, 1991. **349**(6308): p. 426-8.

49.   Warne, P.H., P.R. Viciana, and J. Downward, *Direct interaction of Ras and the amino-terminal region of Raf-1 in vitro*. Nature, 1993. **364**(6435): p. 352-5.

50.   Zhang, X.F., et al., *Normal and oncogenic p21ras proteins bind to the amino-terminal regulatory domain of c-Raf-1*. Nature, 1993. **364**(6435): p. 308-13.

51.   Moodie, S.A., et al., *Complexes of Ras.GTP with Raf-1 and mitogen-activated protein kinase kinase*. Science, 1993. **260**(5114): p. 1658-61.

52.   Lu, S., et al., *Drugging Ras GTPase: a comprehensive mechanistic and signaling structural view*. Chem Soc Rev, 2016.

53.   Shima, F., et al., *Discovery of small-molecule Ras inhibitors that display antitumor activity by interfering with Ras.GTP-effector interaction*. Enzymes, 2013. **34 Pt. B**: p. 1-23.

54.   Beeram, M., A. Patnaik, and E.K. Rowinsky, *Regulation of c-Raf-1: therapeutic implications*. Clin Adv Hematol Oncol, 2003. **1**(8): p. 476-81.

55.   Beeram, M., A. Patnaik, and E.K. Rowinsky, *Raf: a strategic target for therapeutic development against cancer*. J Clin Oncol, 2005. **23**(27): p. 6771-90.

56.   Ostrem, J.M. and K.M. Shokat, *Direct small-molecule inhibitors of KRAS: from structural insights to mechanism-based design*. Nat Rev Drug Discov, 2016.

57.   Cromm, P.M., et al., *Direct Modulation of Small GTPase Activity and Function*. Angew Chem Int Ed Engl, 2015. **54**(46): p. 13516-37.

58.   Kurig, B., et al., *Ras is an indispensable coregulator of the class IB phosphoinositide 3-kinase p87/p110gamma*. Proc Natl Acad Sci U S A, 2009. **106**(48): p. 20312-7.

59.   Rodriguez-Viciana, P., C. Sabatier, and F. McCormick, *Signaling specificity by Ras family GTPases is determined by the full spectrum of effectors they regulate*. Mol Cell Biol, 2004. **24**(11): p. 4943-54.

60.   Nakhaei-Rad, S., et al., *The Function of Embryonic Stem Cell-expressed RAS (E-RAS), a Unique RAS Family Member, Correlates with Its Additional Motifs and Its Structural Properties*. The Journal of biological chemistry, 2015. **290**(25): p. 15892-903.

61.   Dvorsky, R. and M.R. Ahmadian, *Always look on the bright site of Rho: structural implications for a conserved intermolecular interface*. EMBO Rep, 2004. **5**(12): p. 1130-6.

62.   Jaiswal, M., R. Dvorsky, and M.R. Ahmadian, *Deciphering the molecular and functional basis of Dbl family proteins: a novel systematic approach toward classification of selective activation of the Rho family proteins*. The Journal of biological chemistry, 2013. **288**(6): p. 4486-500.

63.   Amin, E., et al., *Deciphering the molecular and functional basis of RhoGAP family proteins: A systematic approach towards selective inactivation of Rho family proteins*. The Journal of biological chemistry, 2016.

64.   Spoerner, M., et al., *Dynamic properties of the Ras switch I region and its importance for binding to effectors*. Proc Natl Acad Sci U S A, 2001. **98**(9): p. 4944-9.

65.   Elad-Sfadia, G., et al., *Galectin-1 augments Ras activation and diverts Ras signals to Raf-1 at the expense of phosphoinositide 3-kinase*. J Biol Chem, 2002. **277**(40): p. 37169-75.

66. Katz, M.E. and F. McCormick, *Signal transduction from multiple Ras effectors*. Curr Opin Genet Dev, 1997. **7**(1): p. 75-9.

67. Rodriguez-Viciana, P., et al., *Role of phosphoinositide 3-OH kinase in cell transformation and control of the actin cytoskeleton by Ras*. Cell, 1997. **89**(3): p. 457-67.

68. Vandal, G., B. Geiling, and D. Dankort, *Ras effector mutant expression suggest a negative regulator inhibits lung tumor formation*. PLoS One, 2014. **9**(1): p. e84745.

69. Wing, M.R., D.M. Bourdon, and T.K. Harden, *PLC-epsilon: a shared effector protein in Ras-, Rho-, and G alpha beta gamma-mediated signaling*. Mol Interv, 2003. **3**(5): p. 273-80.

70. Wellbrock, C., M. Karasarides, and R. Marais, *The RAF proteins take centre stage*. Nature reviews. Molecular cell biology, 2004. **5**(11): p. 875-85.

71. Baljuls, A., B.N. Kholodenko, and W. Kolch, *It takes two to tango--signalling by dimeric Raf kinases*. Mol Biosyst, 2013. **9**(4): p. 551-8.

72. Ahmadian, M.R., et al., *Individual rate constants for the interaction of Ras proteins with GTPase-activating proteins determined by fluorescence spectroscopy*. Biochemistry, 1997. **36**(15): p. 4535-41.

73. Scheffzek, K., M.R. Ahmadian, and A. Wittinghofer, *GTPase-activating proteins: helping hands to complement an active site*. Trends Biochem Sci, 1998. **23**(7): p. 257-62.

74. Castellano, E. and E. Santos, *Functional specificity of ras isoforms: so similar but so different*. Genes & cancer, 2011. **2**(3): p. 216-31.

75. Chavan, T.S., et al., *High-Affinity Interaction of the K-Ras4B Hypervariable Region with the Ras Active Site*. Biophys J, 2015. **109**(12): p. 2602-13.

76. Abraham, S.J., et al., *The hypervariable region of K-Ras4B is responsible for its specific interactions with calmodulin*. Biochemistry, 2009. **48**(32): p. 7575-83.

77. Parker, J.A. and C. Mattos, *The Ras-Membrane Interface: Isoform-specific Differences in The Catalytic Domain*. Molecular cancer research : MCR, 2015. **13**(4): p. 595-603.

78. Abankwa, D., et al., *A novel switch region regulates H-ras membrane orientation and signal output*. EMBO J, 2008. **27**(5): p. 727-35.

79. Mazhab-Jafari, M.T., et al., *Oncogenic and RASopathy-associated K-RAS mutations relieve membrane-dependent occlusion of the effector-binding site*. Proc Natl Acad Sci U S A, 2015. **112**(21): p. 6625-30.

80. Rodriguez-Viciana, P., et al., *A phosphatase holoenzyme comprised of Shoc2/Sur8 and the catalytic subunit of PP1 functions as an M-Ras effector to modulate Raf activity*. Molecular Cell, 2006. **22**(2): p. 217-30.

81. Zhou, M., et al., *VPS35 binds farnesylated N-Ras in the cytosol to regulate N-Ras trafficking*. The Journal of cell biology, 2016. **214**(4): p. 445-58.

82. Zheng, Z.Y., et al., *CHMP6 and VPS4A mediate the recycling of Ras to the plasma membrane to promote growth factor signaling*. Oncogene, 2012. **31**(43): p. 4630-8.

83. Jang, H., et al., *Mechanisms of membrane binding of small GTPase K-Ras4B farnesylated hypervariable region*. The Journal of biological chemistry, 2015. **290**(15): p. 9465-77.

84. Lynch, S.J., et al., *The differential palmitoylation states of N-Ras and H-Ras determine their distinct Golgi subcompartment localizations*. J Cell Physiol, 2015. **230**(3): p. 610-9.

85. Bivona, T.G., et al., *PKC regulates a farnesyl-electrostatic switch on K-Ras that promotes its association with Bcl-XL on mitochondria and induces apoptosis*. Molecular cell, 2006. **21**(4): p. 481-93.

86.   Sung, P.J., et al., *Phosphorylated K-Ras limits cell survival by blocking Bcl-xL sensitization of inositol trisphosphate receptors*. Proc Natl Acad Sci U S A, 2013. **110**(51): p. 20593-8.

87.   Wang, M.T., et al., *K-Ras Promotes Tumorigenicity through Suppression of Non-canonical Wnt Signaling*. Cell, 2015. **163**(5): p. 1237-51.

88.   Rodriguez-Viciana, P. and F. McCormick, *Ras ubiquitination: coupling spatial sorting and signal transmission*. Cancer Cell, 2006. **9**(4): p. 243-4.

89.   Jura, N., et al., *Differential modification of Ras proteins by ubiquitination*. Molecular cell, 2006. **21**(5): p. 679-87.

90.   de la Vega, M., et al., *The deubiquitinating enzyme USP17 blocks N-Ras membrane trafficking and activation but leaves K-Ras unaffected*. The Journal of biological chemistry, 2010. **285**(16): p. 12028-36.

91.   Yang, M.H., et al., *HDAC6 and SIRT2 regulate the acetylation state and oncogenic activity of mutant K-RAS*. Molecular cancer research : MCR, 2013. **11**(9): p. 1072-7.

92.   Knyphausen, P., et al., *Insights into K-Ras 4B regulation by post-translational lysine acetylation*. Biol Chem, 2016.

93.   Yang, M.H., et al., *Regulation of RAS oncogenicity by acetylation*. Proc Natl Acad Sci U S A, 2012. **109**(27): p. 10843-8.

94.   Wurtzel, J.G., et al., *RLIP76 regulates Arf6-dependent cell spreading and migration by linking ARNO with activated R-Ras at recycling endosomes*. Biochemical and biophysical research communications, 2015. **467**(4): p. 785-91.

95.   Furuhjelm, J. and J. Peranen, *The C-terminal end of R-Ras contains a focal adhesion targeting signal*. J Cell Sci, 2003. **116**(Pt 18): p. 3729-38.

96.   Berzat, A.C., et al., *Using inhibitors of prenylation to block localization and transforming activity*. Methods Enzymol, 2006. **407**: p. 575-97.

97.   Oertli, B., et al., *The effector loop and prenylation site of R-Ras are involved in the regulation of integrin function*. Oncogene, 2000. **19**(43): p. 4961-9.

98.   Calvo, F. and P. Crespo, *Structural and spatial determinants regulating TC21 activation by RasGRF family nucleotide exchange factors*. Molecular biology of the cell, 2009. **20**(20): p. 4289-302.

99.   Holly, S.P., M.K. Larson, and L.V. Parise, *The unique N-terminus of R-ras is required for Rac activation and precise regulation of cell migration*. Molecular biology of the cell, 2005. **16**(5): p. 2458-69.

100.   Herrmann, C., G.A. Martin, and A. Wittinghofer, *Quantitative analysis of the complex between p21ras and the Ras-binding domain of the human Raf-1 protein kinase*. The Journal of biological chemistry, 1995. **270**(7): p. 2901-5.

101.   Gorman, C., et al., *Equilibrium and kinetic measurements reveal rapidly reversible binding of Ras to Raf*. The Journal of biological chemistry, 1996. **271**(12): p. 6713-9.

102.   Hwang, M.C., Y.J. Sung, and Y.W. Hwang, *The differential effects of the Gly-60 to Ala mutation on the interaction of H-Ras p21 with different downstream targets*. The Journal of biological chemistry, 1996. **271**(14): p. 8196-202.

103.   Linnemann, T., et al., *Thermodynamic and kinetic characterization of the interaction between the Ras binding domain of AF6 and members of the Ras subfamily*. The Journal of biological chemistry, 1999. **274**(19): p. 13556-62.

104.   Boettner, B., C. Herrmann, and L. Van Aelst, *Ras and Rap1 interaction with AF-6 effector target*. Methods Enzymol, 2001. **332**: p. 151-68.

105.   Linnemann, T., et al., *Interaction between Nef and phosphatidylinositol-3-kinase leads to activation of p21-activated kinase and increased production of HIV*. Virology, 2002. **294**(2): p. 246-55.

106.   Gremer, L., et al., *Duplication of Glu37 in the switch I region of HRAS impairs effector/GAP binding and underlies Costello syndrome by promoting enhanced*

growth factor-dependent MAPK and AKT activation. Human molecular genetics, 2010. **19**(5): p. 790-802.

107. Sydor, J.R., et al., *Transient kinetic studies on the interaction of Ras and the Ras-binding domain of c-Raf-1 reveal rapid equilibration of the complex*. Biochemistry, 1998. **37**(40): p. 14292-9.

108. Sydor, J.R., et al., *Cell-free synthesis of the Ras-binding domain of c-Raf-1: binding studies to fluorescently labelled H-ras*. FEBS Lett, 1999. **452**(3): p. 375-8.

109. Vetter, I.R., et al., *Structural and biochemical analysis of Ras-effector signaling via RalGDS*. FEBS Lett, 1999. **451**(2): p. 175-80.

110. Rudolph, M.G., et al., *Thermodynamics of Ras/effector and Cdc42/effector interactions probed by isothermal titration calorimetry*. The Journal of biological chemistry, 2001. **276**(26): p. 23914-21.

111. Harjes, E., et al., *GTP-Ras disrupts the intramolecular complex of C1 and RA domains of Nore1*. Structure, 2006. **14**(5): p. 881-8.

112. Hunter, J.C., et al., *Biochemical and Structural Analysis of Common Cancer-Associated KRAS Mutations*. Molecular cancer research : MCR, 2015. **13**(9): p. 1325-35.

113. Flex, E., et al., *Activating mutations in RRAS underlie a phenotype within the RASopathy spectrum and contribute to leukaemogenesis*. Human molecular genetics, 2014. **23**(16): p. 4315-27.

114. Herrmann, C., et al., *Differential interaction of the ras family GTP-binding proteins H-Ras, Rap1A, and R-Ras with the putative effector molecules Raf kinase and Ral-guanine nucleotide exchange factor*. The Journal of biological chemistry, 1996. **271**(12): p. 6794-800.

Figure legends
FIGURE 1. Domain organization of RAS effectors and different proteins used in this study. (A) Various domains are highlighted, including RAS association domain (RA) and RAS-binding (RB) domain in blue. The numbers indicate the N- and C-terminal amino acids of the respective effector domain used in this study. Other domains are: C1, cysteine-rich lipid binding; C2, calcium-dependent lipid binding; CRD, cysteine rich domains; DEP, Dishevelled/Egl-10/Pleckstrin; EF, EF-hands; kinase, serine/threonine or phosphoinositide kinase; PH, pleckstrin homology; PI3K, Phosphoinositide 3-kinase family, accessory *domain;* PP, proline-rich region; RA, RAS association; RalGEF, Ral specific guanine nucleotide exchange factor; RASGEF, RAS specific guanine nucleotide exchange factor; RB, RAS binding; REM, RAS exchanger motif; SARAH, Salvador/RASSF/Hippo. (B) Coomassie brilliant blue (CBB) stained SDS-PAGE of purified MBP fusion proteins used in this study.

FIGURE 2. Equilibrium dissociation constants for RAS-effector interaction determined Fluorescence polarization. (A) Fluorescence polarization experiments were conducted by titrating mGppNHp-bound, active forms of RAS proteins (1 µM, respectively) with increasing concentrations of the respective effector domains as MBP fusion proteins. Data of two representative experiments for the interaction of KRAS (upper panel) and RRAS2 (lower panel) with CRAF-RB and PI3Kα-RB, respectively, are shown. All other data are illustrated in Figure S1. (B) Evaluated equilibrium dissociation constants (K_d) in µM shown as bars illustrates a significant difference in the binding properties between the RAS and effector proteins, respectively.

FIGURE 3. Superposition of all available RAS–effector complex structures. Nine structures of RAS-effector domain complexes, found in a PDB search, including HRAS-CRAF (PDB code: 4g0n, 4G3X, 3kud; red), HRAS-BYR2 (PDB code: 1k8r; yellow), RAP1A-CRAF (PDB code: 1GUA; limo), KRAS-ARAF (PDB code: 2mse; magenta), HRAS-RALGDS (PDB code: 1lfd; cyan), HRAS-PI3K (PDB code: 1he8; green), HRAS-PLCε (PDB code: 2c5l; orange), HRAS-RASSF (PDB code: 3ddc; blue), HRAS-GRAB14 (PDB code: 4k81; brown), were overlaid in ribbon presentation. Additional properties outside the interaction interface (box) are indicated.

FIGURE 4. RAS-effector interaction hotspots. (A) Interaction matrix of RAS isoforms and effector proteins. Interaction matrix is launched to demonstrate interaction residues in all available structures (se Figs. 3and S4). Left and upper parts comprise the amino acid sequence alignments of the RAS proteins and the effector domains, respectively. Each element corresponds to a possible interaction of RAS (row; HRAS numbering) and effector (column; CRAF numbering) residues. As indicated, interaction matrix represents five main regions, which cover the main interacting interfaces. (B) The five main regions, comprising the main hotspot for the RAS-effector interaction, are highlighted as ribbon and surface representation in the corresponding colors using an open-book presentation of the structures of HRAS-PLCε (PDB code: 2C5L) and HRAS-CRAF (PDB code: 4G0N).

Table 1. Register of dissociation constants (K_d) determined for the RAS-effector interactions.

RAS	Nnucleotide[a]	Effectors[b]	K_d (µM)	Method[c]	T (°C)	Reference
HRAS	mGTPγS	CRAF-RB	0.005	GDI	37	[100]
	mGDP	CRAF-RB	24.0	GDI	37	[100]
	[³H]GTP	CRAF-RB	0.065	SPA	37	[101]
	[γ³²P]GTP	CRAF-N275	0.029	CPA	4	[102]
	[γ³²P]GTP	RALSGDS-C127	0.028	CPA	4	[102]
	mGppNHp	AF6-RA1	2.4	GDI	37	[103]
		AF6-RA1	2.4	FK	10	[104]
		AF6-RA1	2.8	FK	25	[105]
		CRAF-RB	0.16	FK	25	[105]
		CRAF-RB	0.14	FP	25	[106]
		CRAF-RB	0.22	FP	25	[18]
		CRAF-RB	0.018	GDI	37	[100]
		CRAF-RB	0.16	GDI	25	[107]
		CRAF-RB	0.33	GDI	25	[108]
		RALGDS-RA	2.70	FP	25	[106]
		RALGDS-RA	1.30	FK	25	[105]
		RALGDS-RA	3.50	GDI	37	[109]
		RASSF5-RA	5.20	FP	25	[106]
		RASSF5-RA	0.8	GDI	37	[34]
		RASSF5-RA	0.08	FK	37	[34]
		PLCε-RA2	5.20	FP	25	[106]
	GppNHp	CRAF-RB	0.08	ITC	25	[110]
		AF6-RA1	3.00	ITC	25	[110]
		AF6-RA1	2.20	ITC	25	[24]
		RALGDS-RA	1.0	ITC	25	[110]
		RALGDS-RA	1.0	ITC	25	[24]
		RASSF1-C1-RA	39.0	ITC	25	[24]
		RASSF5-C1-RA	0.40	ITC	25	[111]
		RASSF5-RA	0.21	ITC	25	[111]
		PLCε-RA2	0.82	ITC	25	[24]
		PLCε-RA1/2	0.98	ITC	25	[24]
		AF6-RA1(Y32W)	0.58	WF	10	[104]
KRAS	mGppNHp	CRAF-RB	0.04	GDI	37	[100]
		CRAF-RB	0.102	ITC	25	[17]
	GppNHp	CRAF-RB	0.056	BBA	25	[112]
NRAS	mGppNHp	RAF-RB	0.04	GDI	37	[100]
		PI3Kγ-RB	2.90	FP	20	[35]
RRAS1	mGppNHp	CRAF-RB	252.9	FP	25	[113]
		RALGDS-RA	376.7	FP	25	[113]
		RASSF5-RA	54.6	FP	25	[113]
		PLCε-RA1	306.6	FP	25	[113]
		PI3Kα-RB	330.5	FP	25	[113]
		CRAF-RB	1.10	GDI	37	[114]
RRAS3	GppNHp	AF6-RA1	2.80	ITC	25	[24]
		RALGDS-RA	3.70	ITC	25	[24]
		PLCε-RA1/2	7.50	ITC	25	[24]

[a] Different GTP or GDP analogs bound to HRAS have been used: GppNHp, Guanosine-5'-[(β,γ)-imido]triphosphate; mGDP, N-methylanthraniloyl-guanosine-5'-diphosphate; mGppNHp, N-methylanthraniloyl-GppNHp; mGTPγS, N-methylanthraniloyl-guanosine 5'-[gamma-thio-]triphosphate; [³H]GTP, tritium-labeled GTP; [γ³²P]GTP, gamma 32-phosphate-labeled GTP. [b] RAS binding (RB) and RAS association (RA) of various effectors were used; CRFA-N275 contains the N-terminal 275 aa encompassing RB domain; RALGDS-C127 contains the C-terminal 127 aa encompassing RA domain. PI3Kγ-RB consists of aa 144-1102. [c] BBA, bead–based assay; CPA, co-precipitation assay; FK, fluorescence kinetics; FP, fluorescence polarization; GDI, guanine nucleotide dissociation inhibition; ITC, isothermal titration calorimetry; SPA, scintillation proximity assay; SPR, surface plasmon resonance.

Table 1. Dissociation constants (K$_d$) in µM for the interaction between RAS proteins and effectors

Effector domains[a]	HRAS	KRAS	NRAS	RRAS1	RRAS2
CRAF-RB	0.087	0.142	0.048	2.29	4.09
RASSF5-RA	0.238	0.421	0.442	11.5	10.00
RALGDS-RA	2.50	1.39	2.84	9.71	5.78
PLCε-RA2	3.70	8.90	5.36	114.4	145.4
PI3Kα-RB	84.3	204.7	145.0	11.00	18.10

[a] The effector domain were used in these fluorescence polarization measurement as MBP fusion.

Nakhaeizadeh *et al*., Figure 1
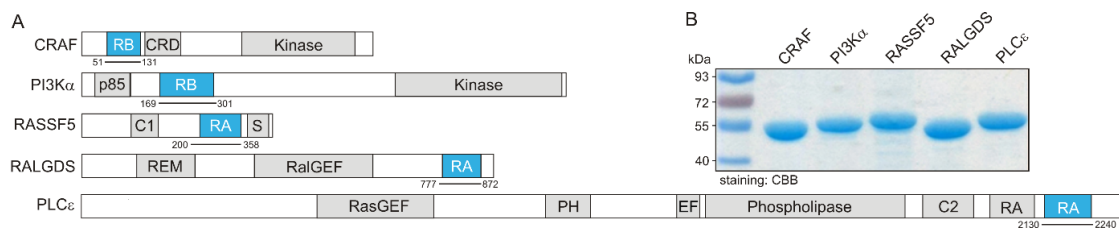
Nakhaeizadeh *et al*., Figure 2
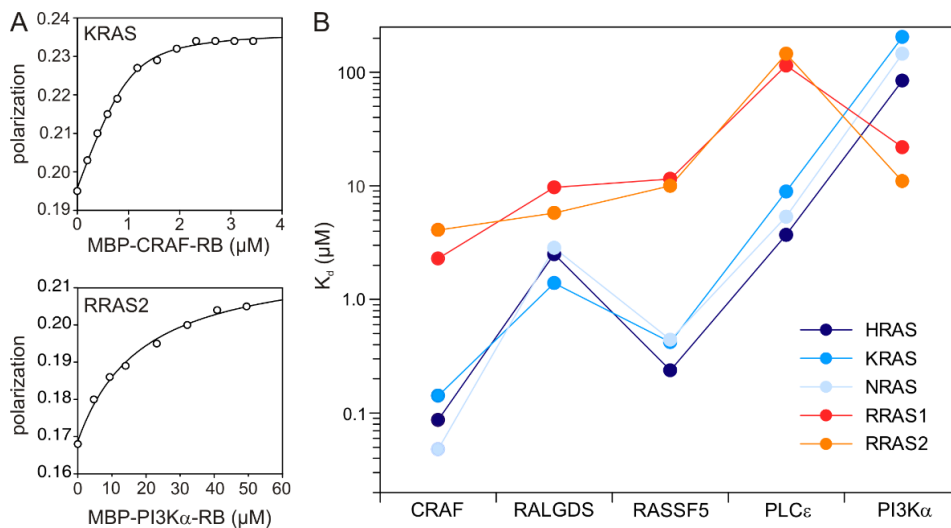
Nakhaeizadeh *et al*., Figure 3

Nakhaeizadeh *et al*., Figure 4

Supporting information
The RAS-effector interface: Isoform-specific differences in the effector binding regions

H. Nakhaeizadeh, E. Amin, S. Nakhaei-Rad, R. Dvorsky, M. R. Ahmadian

Institute of Biochemistry and Molecular Biology II,

Medical Faculty of the Heinrich-Heine University, Düsseldorf, Germany

Table S1. . Published complexes structures of the RAS and Effector proteins.

Proteins	PDB code	Resolution (Å)	Reference
RAP1A(E30D/K31E)-GppNHp-CRAF-RB	1GUA	2.0	[115]
HRAS-GppNHp-RALGDS	1LFD	2.1	[36]
HRAS(G12V)-GppNHp-PI3Kγ-RB(V223K/V326A)	1HE8	3.0	[35]
HRAS-GDP-CRAF-RB(A85K)	3KUD	2.15	[116]
HRAS-GppNHp-Byr2-RB	1K8R	3.0	[117]
HRAS(G12V)-GTP-PLCε(Y2176L)	2C5L	1.9	[33]
HRAS(D30E/E31K)-GppNHp-RASSF5-RA (L285M/K302D)	3DDC	1.8	[118]
HRAS(G12V)-GTP·GRAB14-RA/PH (K272A/E273A)	4K81	2.4	[119]
HRAS-GppNHp-CRAF-RB	4G0N	2.45	[120]
HRAS(Q61L)-GppNHp-CRAF-RB	4G3X	3.25	[120]
KRAS-GppNHp-ARAF-RB	2MSE	NMR	[121]
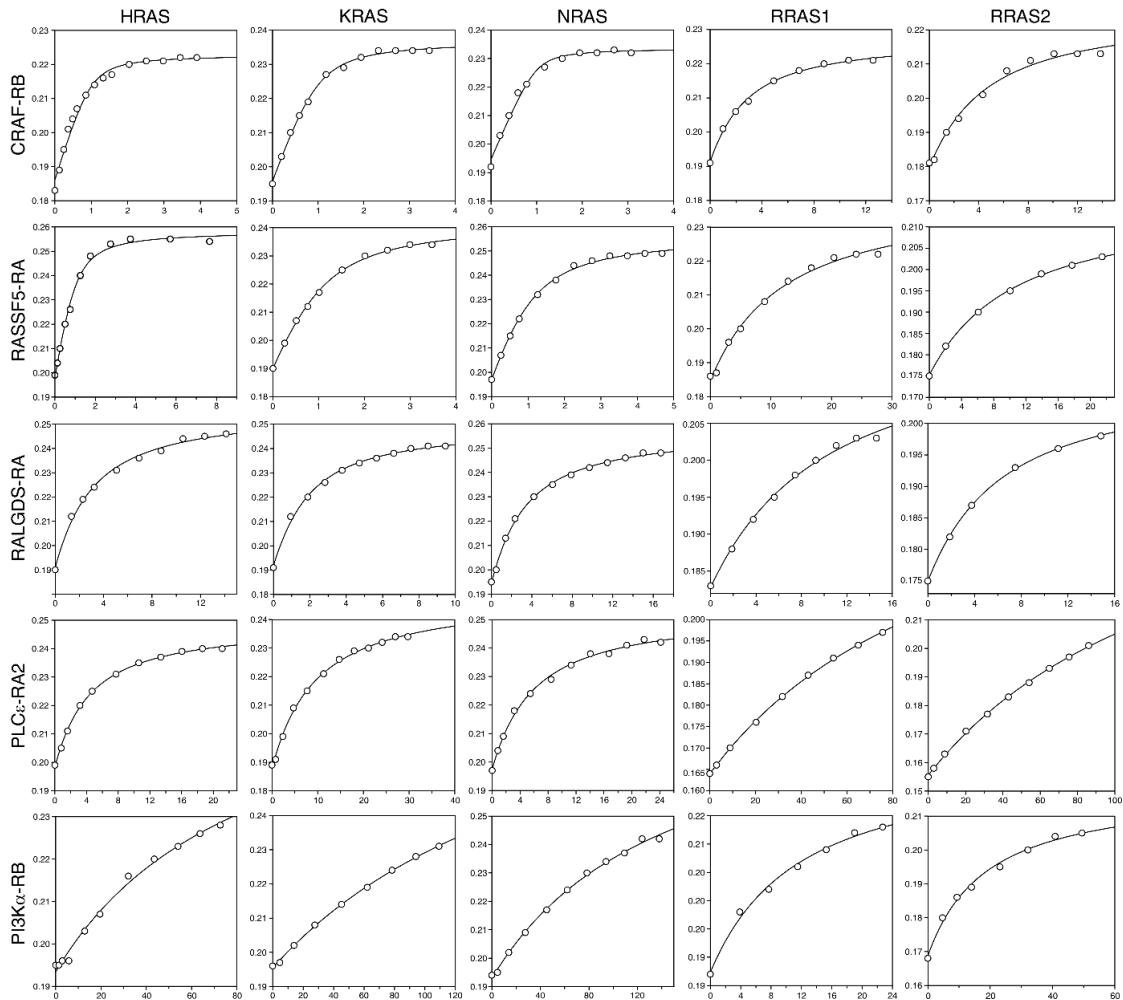
Figure S1. Equilibrium dissociation constants for RAS-effector interaction determined by Fluorescence polarization. Fluorescence polarization experiments were conducted by titrating mGppNHp-bound, active forms of RAS proteins (1 µM, respectively) with increasing concentrations of the respective effector domains, as indicated. The y-axis represents fluorescence polarization and the x-axis the concentration of the effector domain as MBP fusion proteins in µM. Evaluated equilibrium dissociation constants (K_d) are illustrated as bar charts in Figure 2 and summarized in Table 2.

A

```
CRAF-RB    - - - - - - - - - - - - - - - - - - - - - - - - - - - - - - - - - - - - - - - - NT IRVFL - - - - - - - - - - - - - - - - - - 62
ARAF-RB    - - - - - - - - - - - - - - - - - - - - - - - - - - - - - - - - - - - - - - - - TVKVYL - - - - - - - - - - - - - - - - - - 25
PI3Kγ-RB   - - - - - - - KLYAMHPWVTSKPLPEYLWKKIANNCIFIKIH - - - - - - - - - - - - - - - - - - - - - - 175
Byr2-RB    - - - - - - - - - - - - - - - - - - - - - - - - - - - CILRFIA - - - - - - - - - - - - - - - - - - - - 77
RASSF5-RA  PPTIQEIKQKIDSYNSREKHCLGMKLSEDGTYTGFIKVHLKLRRPVTVPAGIRPQSIYDA 259
PLCε-RA2   - - - - - - - - - - - - - - - - - - - - - - - - - - EEESFFVQVHD - - - - - - - - - - - - - - - - - - 2143
RALGDS-RA  - - - - - - - - - - - - - - - - - - - - - - - - - - GDCCIIRVSL - - - - - - - - - - - - - - - - - - 787
GRB14-RA   - - - - - - - - - - - - - - - - - - - - - - - - KKQVIKVYS - - - - - - - - - - - - - - - - - - 114
```

```
CRAF-RB    - - - - - - - - - - - - - - - - - PNKQRTVVNVRNGMSLHDC - - - - - - - - LMKALKVRGLQPECC 95
ARAF-RB    - - - - - - - - - - - - - - - - - PNKQRTVVTVRDGMSVYDS - - - - - - - - LDKALKVRGLNQDCC 59
PI3Kγ-RB   - - - - - - - - - - - - - - - RSTTSQTIKVSPDDTPGAILQSFFTKMAKKK - SLMDIPESQS 216
Byr2-RB    - - - - - - - - - - - - - - CNGQTRAVQSRGDYQKTLA - - - - - - IALKKFSLEDASKFIV 112
RASSF5-RA  IKEVNPAATTDKRTSFYLPLDAIKQMHISSTTTVSEVI - - - - QGLLDKFMVVDNPQK - - - 312
PLCε-RA2   - - - - - - - - - - - - - VSPEQPRTVIKAPRVSTAQDVI - - - - QQTLCKAKYSLSILSNPN 2183
RALGDS-RA  - - - - - - - - - - - - DVDNGNMYKSILVTSQDKAPTVI - - - - RKAMDKHNLDEDEPEDYE 828
GRB14-RA   - - - - - - - - - - - - EDETSRALDVPSDITARDVC - - - QLLILKNHYIDDHSWTLF 152
```

```
CRAF-RB    AVFRLLHEHKGKKARLDWNTDAASLIGEELQVDFL - - - - - - - - - - - - - 131
ARAF-RB    VVYRLIKGRK - - - TVTAWDTAIAPLDGEELIVE - - - - - - - - - - - - - 89
PI3Kγ-RB   EQDFVLRVCGRDEYLVGETPIKNFQWVRHCLKNGEEIHVVLDTPPDP - - - - - - - - - - - 263
Byr2-RB    CVSQSSRIKLITEEEFKQICFNSSSPERDRLIIVPKEKPCPSFEDLRRSWEIELAQPAAL 172
RASSF5-RA  FALFKRIHKDGQVLFQKLSIADYPLYLRLLAGPDTDVLSFVLKEN - - - - - - - - - - - - - 357
PLCε-RA2   PSDYVLLEEVVKDTTNKKTTTPKSSSQRVLLDQECVFQAQSKWKGAGKFILKLKEQVQASR 2243
RALGDS-RA  LLQIISEDHKLKIPENANVFYAMNSAANYDFILLKKR - - - - - - - - - - - - - - - - 864
GRB14-RA   EHLPHIGVERTIEDHELVIEVLSNWGIEEENKLYFRKN - - - - - - - - - - - - - 190
```

B

```
          β1        β2              α1
CRAF-RB   -TIRVFLPNKQRTVVNVRNGMSLHDCLMKALKVRGLQ 92
BRAF-RB   -IVRVFLPNKQRTVVPARCGVTVRDSLKKALMMRGLI 92
ARAF-RB   GTVKVYLPNKQRTVVTVRDGMSVYDSLDKALKVRGLN 55

          α2   β3        β4          α3       β5
CRAF-RB   PECCAVFRLLHEHKGKKARLDWNTDAASLIGEELQVDFL 131
BRAF-RB   PECCAVYRIQ - - -DGEKKPIGWDTDISWLTGEELHVEVL 128
ARAF-RB   QDCCVVYRLI - - -KGRKTVTAWDTAIAPLDGEELIVEVL 91
```

C

```
          α1              β1              β2     β3          α2
p110α-RB  SSPELPKHIYNKLDKGQIVVIWVIVSPNNDKQKYTLKINHDCVP - EQVIAEAIRKKTRSML 233
p110β-RB  HEPSIPENLEDKLYGGKLIVAVHFENC - - - -QDVFSFQVSPNMNP - - -IKVNELAIQKRLTIHG 236
p110γ-RB  TSKPLPEYLWKKIANNCIFIVIHRSTT - - - - - -SQTIKVSPDDTPGAILQSFFTKMAKKKSLMD 260
p110δ-RB  AQTWGPGTLR - -LPNRALLVNVKFEGS - - - -EESFTFQVSTKDVP - - -LALMACALRKKATVFR 229

          β4       α3        α4            β5    α5
p110α-RB  LSSEQLKLCVLEYQGKYILKVCGCDEYFLEKYPLSQYKYIRSCIMLGRMPNLMLMAKES 292
p110β-RB  KEDE - - - - - - - -VSPYDYVLQVSGRVEYVFGDHPLIQFQYIRNCVMNRALPHFILVECCK 288
p110γ-RB  IPES - - - - - - - -QSEQDFVLRVCGRDEYLVGETPIKNFQWVRHCLKNGEEIHVVLDTPPD 312
p110δ-RB  QPLV - - - - - - - -EQPEDYTLQVNGRHEYLYGSYPLCQFQYICSCLHSGLTPHLTMVHSSS 281
```

D

```
          β1          β2          α1              α2
RALGDS-RA
          β1              α1          α2
RASSF5-RA
          β1      β2      α1      α2  α3
PLCε-RA2
          β1      β2      α1
GRB14-RA

RALGDS-RA  DCCIIRVSLDVDNGNMYKSILVTSQDKAPTVIRKAMDKHNLD - - -EDEPE - -D 826
RASSF5-RA  TDKRTSF - YLP - -LDAIKQLHISSTTTVSEVIQ - GLLKKFMV - - -VDNPQ - -K 312
PLCε-RA2   ESFFVQV - HDVSPEQPRTVIKAPRVSTAQDVIQQTLCKAKYSYSILSNPNPSD 2186
GRB14-RA   KKQVIKV - YSE - -DETSRALDVPSDITARDVCQLLILKNHY - - - -IDDHS - - -148

          β3              β4      α3              β5
RALGDS-RA
          β2          β3          α3              β4
RASSF5-RA
          β3              β4      α4              β5
PLCε-RA2
          β3              β4      α2              β5
GRB14-RA

RALGDS-RA  YELLQIISED - - - - - - - - - -HKLKIPENANVFYAMNSA - - -ANYDFILKKR - -864
RASSF5-RA  FALFKRIHKDGQ - - - - - -VLFQKLSIADRPLYLRLLAGP - DTEVLSFVLKENET 359
PLCε-RA2   YVLLEEVVKDTTNKKTTTPKSSQRVLLDQECVFQAQSKW - -KGAGKFILKLKEQ 2238
GRB14-RA   WTLFEHLPH - - - - - - - - - -IGVERTIEDHELVIEVLSNWGIEEENKLYFRKNYA 192
```

Figure S2. Sequence Alignment of the RAS effector domains. The overall amino acid alignment of RB and RA domains (A) was adjusted with structure alignment to increase the identity score. The latter was clearly increased when we separated RB domains of RAF isoforms (B) and the catalytic subunits of PI3K isoforms (C) from the RA domains (D). The five regions, described in Figure 3, are highlighted as arrowheads: R1 in red, R2 in green, R3 in blue, R4 in orange and R5 in purple. The secondary structure elements, the α helices and β sheets, from the RA domains were deduced from the crystal structures of HRAS complexes with RALGDS (PDB code: 1LFD) [36], RASSF5 (PDB code: 3DDC) [118], PLCε (PDB code: 2C5L) [33], and GRB14 (PDB code: 4K81) [119], respectively.
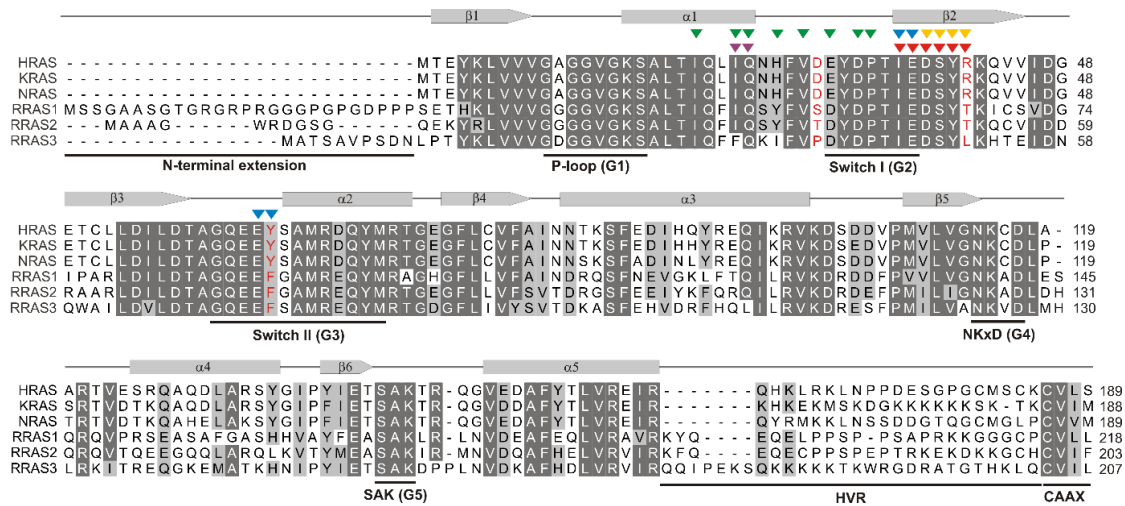
Figure S3. Overall sequence comparison of human RAS proteins. Multiple amino acid sequence alignment of RAS proteins with high similarities has been prepared by clustalW. Interaction regions, R1 to R5, at interface with the RB and RA effector domains are illustrated by arrowhead (color-coding is the same as in Fig. 4: R1 in red; R2 in green; R3 in blue; R4 in purple; R4 in orange). The secondary structure elements, the α helices and β sheets, of the G domain were deduced from the HRAS crystal structure (PDB code: 5P21) [122]. G1 to G5 boxes indicate the presence of five essential GDP/GTP binding (G) motifs. The three amino acid deviations between RAS and RRAS isoforms that are critical selectivity-determining residues for effector binding are highlighted in red.
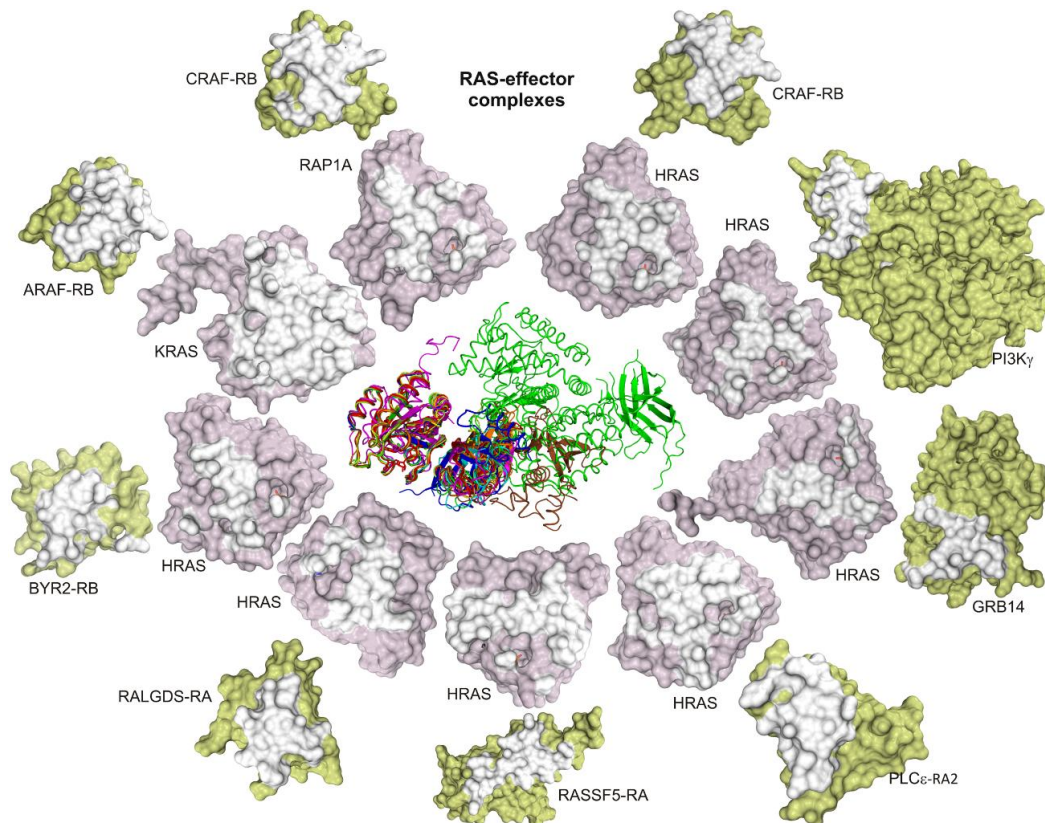
Figure S4. Known structures of the RAS-effector complexes. Nine structures of RAS-effector domain complexes were found in a PDB search, including HRAS-CRAF-RB (PDB code: 4g0n, 4G3X, 3kud), HRAS-BYR2-RB (PDB code: 1k8r), RAP1A-CRAF-RB (PDB code: 1GUA), KRAS-ARAF-RB (PDB code: 2mse), HRAS-RALGDS (PDB code: 1lfd), HRAS-PI3Kγ (PDB code: 1he8), HRAS-PLCε (PDB code: 2c5l), HRAS-RASSF (PDB code: 3ddc), HRAS-GRAB14 (PDB code: 4k81). An overlaid structure in ribbon presentation (central panel) illustrates the overall contacts of these structures (see also Figure 3). The contact sites (with distances of 4 Å or less) were calculated by Pymol and colored in white. RAS proteins are shown in orchid and the effector domains in olive as indicated.

Figure S5. Intermolecular β sheet-β sheet interactions between RAS proteins and their effectors covered by the recognition region R1 in the interaction matrix. Interaction matrix is launched to demonstrate interaction residues in all available structures. Left and upper panels comprises the amino acid sequence alignment of RAS and effector proteins, respectively. Each element corresponds a possible interaction of RAS (row) and effectors (column) residues. Besides, each element involves four sub-elements, which show a combination of main-chain and side-chain interactions, as indicated. Main-chain–main-chain contacts are shown in red.

Supporting References

1. Wittinghofer, A. and C. Herrmann, *Ras-effector interactions, the problem of specificity*. FEBS Lett, 1995. **369**(1): p. 52-6.
2. Gutierrez-Erlandsson, S., et al., *R-RAS2 overexpression in tumors of the human central nervous system*. Mol Cancer, 2013. **12**(1): p. 127.
3. Karnoub, A.E. and R.A. Weinberg, *Ras oncogenes: split personalities*. Nature reviews. Molecular cell biology, 2008. **9**(7): p. 517-31.
4. Herrmann, C., *Ras-effector interactions: after one decade*. Curr Opin Struct Biol, 2003. **13**(1): p. 122-9.
5. Nakhaei-Rad, S., et al., *The Role of Embryonic Stem Cell-expressed RAS (ERAS) in the Maintenance of Quiescent Hepatic Stellate Cells*. The Journal of biological chemistry, 2016. **291**(16): p. 8399-413.
6. Castellano, E. and J. Downward, *Role of RAS in the regulation of PI 3-kinase*. Curr Top Microbiol Immunol, 2010. **346**: p. 143-69.
7. Chan, J.J. and M. Katan, *PLCvarepsilon and the RASSF family in tumour suppression and other functions*. Advances in biological regulation, 2013. **53**(3): p. 258-79.
8. Bunney, T.D. and M. Katan, *PLC regulation: emerging pictures for molecular mechanisms*. Trends Biochem Sci, 2011. **36**(2): p. 88-96.
9. Ferro, E. and L. Trabalzini, *RalGDS family members couple Ras to Ral signalling and that's not all*. Cellular Signalling, 2010. **22**(12): p. 1804-10.
10. Rajalingam, K., et al., *Ras oncogenes and their downstream targets*. Biochimica et biophysica acta, 2007. **1773**(8): p. 1177-95.
11. Desideri, E., A.L. Cavallo, and M. Baccarini, *Alike but Different: RAF Paralogs and Their Signaling Outputs*. Cell, 2015. **161**(5): p. 967-70.
12. Castellano, E. and J. Downward, *RAS Interaction with PI3K: More Than Just Another Effector Pathway*. Genes & cancer, 2011. **2**(3): p. 261-74.
13. Gentry, L.R., et al., *Ral small GTPase signaling and oncogenesis: More than just 15minutes of fame*. Biochimica et biophysica acta, 2014. **1843**(12): p. 2976-2988.
14. Bunney, T.D. and M. Katan, *Phospholipase C epsilon: linking second messengers and small GTPases*. Trends Cell Biol, 2006. **16**(12): p. 640-8.
15. Feig, L.A. and R.J. Buchsbaum, *Cell signaling: life or death decisions of ras proteins*. Curr Biol, 2002. **12**(7): p. R259-61.
16. Bryant, K.L., et al., *KRAS: feeding pancreatic cancer proliferation*. Trends Biochem Sci, 2014. **39**(2): p. 91-100.
17. Cirstea, I.C., et al., *Diverging gain-of-function mechanisms of two novel KRAS mutations associated with Noonan and cardio-facio-cutaneous syndromes*. Human molecular genetics, 2013. **22**(2): p. 262-70.
18. Gremer, L., et al., *Germline KRAS mutations cause aberrant biochemical and physical properties leading to developmental disorders*. Human mutation, 2011. **32**(1): p. 33-43.
19. Lissewski, C., et al., *Copy number variants including RAS pathway genes-How much RASopathy is in the phenotype?* Am J Med Genet A, 2015. **167A**(11): p. 2685-90.
20. McCormick, F., *KRAS as a Therapeutic Target*. Clin Cancer Res, 2015. **21**(8): p. 1797-801.
21. Donninger, H., et al., *Ras signaling through RASSF proteins*. Seminars in cell & developmental biology, 2016.
22. Dhillon, A.S., et al., *MAP kinase signalling pathways in cancer*. Oncogene, 2007. **26**(22): p. 3279-3290.

23.   Repasky, G.A., E.J. Chenette, and C.J. Der, *Renewing the conspiracy theory debate: does Raf function alone to mediate Ras oncogenesis?* Trends Cell Biol, 2004. **14**(11): p. 639-47.

24.   Wohlgemuth, S., et al., *Recognizing and defining true Ras binding domains I: biochemical analysis.* Journal of Molecular Biology, 2005. **348**(3): p. 741-58.

25.   Ahearn, I.M., et al., *Regulating the regulator: post-translational modification of RAS.* Nature reviews. Molecular cell biology, 2012. **13**(1): p. 39-51.

26.   Hennig, A., et al., *Ras activation revisited: role of GEF and GAP systems.* Biol Chem, 2015. **396**(8): p. 831-48.

27.   Fischer, A., et al., *B- and C-RAF display essential differences in their binding to Ras: the isotype-specific N terminus of B-RAF facilitates Ras binding.* The Journal of biological chemistry, 2007. **282**(36): p. 26503-16.

28.   Mott, H.R. and D. Owen, *Structures of Ras superfamily effector complexes: What have we learnt in two decades?* Critical Reviews in Biochemistry and Molecular Biology, 2015. **50**(2): p. 85-133.

29.   Vetter, I.R. and A. Wittinghofer, *The guanine nucleotide-binding switch in three dimensions.* Science, 2001. **294**(5545): p. 1299-304.

30.   Athuluri-Divakar, S.K., et al., *A Small Molecule RAS-Mimetic Disrupts RAS Association with Effector Proteins to Block Signaling.* Cell, 2016. **165**(3): p. 643-55.

31.   Thapar, R., J.G. Williams, and S.L. Campbell, *NMR characterization of full-length farnesylated and non-farnesylated H-Ras and its implications for Raf activation.* Journal of molecular biology, 2004. **343**(5): p. 1391-408.

32.   Drugan, J.K., et al., *Ras interaction with two distinct binding domains in Raf-1 may be required for Ras transformation.* The Journal of biological chemistry, 1996. **271**(1): p. 233-7.

33.   Bunney, T.D., et al., *Structural and Mechanistic Insights into Ras Association Domains of Phospholipase C Epsilon.* Molecular Cell, 2006. **21**(4): p. 495-507.

34.   Stieglitz, B., et al., *Novel type of Ras effector interaction established between tumour suppressor NORE1A and Ras switch II.* EMBO J, 2008. **27**(14): p. 1995-2005.

35.   Pacold, M.E., et al., *Crystal structure and functional analysis of Ras binding to its effector phosphoinositide 3-kinase gamma.* Cell, 2000. **103**(6): p. 931-43.

36.   Huang, L., et al., *Structural basis for the interaction of Ras with RalGDS.* Nat Struct Biol, 1998. **5**(6): p. 422-6.

37.   Nassar, N., et al., *The 2.2 A crystal structure of the Ras-binding domain of the serine/threonine kinase c-Raf1 in complex with Rap1A and a GTP analogue.* Nature, 1995. **375**(6532): p. 554-60.

38.   White, M.A., et al., *Multiple Ras functions can contribute to mammalian cell transformation.* Cell, 1995. **80**(4): p. 533-41.

39.   Khosravi-Far, R., et al., *Oncogenic Ras activation of Raf/mitogen-activated protein kinase-independent pathways is sufficient to cause tumorigenic transformation.* Mol Cell Biol, 1996. **16**(7): p. 3923-33.

40.   Khwaja, A., et al., *Matrix adhesion and Ras transformation both activate a phosphoinositide 3-OH kinase and protein kinase B/Akt cellular survival pathway.* EMBO J, 1997. **16**(10): p. 2783-93.

41.   Vavvas, D., et al., *Identification of Nore1 as a potential Ras effector.* J Biol Chem, 1998. **273**(10): p. 5439-42.

42.   Erijman, A. and J.M. Shifman, *RAS/Effector Interactions from Structural and Biophysical Perspective.* Mini Rev Med Chem, 2016. **16**(5): p. 370-5.

43.   Hall, T.A., *BioEdit: a user-friendly biological sequence alignment editor and analysis program for Windows 95/98/NT.* Nucleic Acids Symposium Series, 1999. **41**: p. 95-98.

44. Pettersen, E.F., et al., *UCSF Chimera—A visualization system for exploratory research and analysis*. Journal of Computational Chemistry, 2004. **25**(13): p. 1605-1612.

45. Cock, P.J., et al., *Biopython: freely available Python tools for computational molecular biology and bioinformatics*. Bioinformatics, 2009. **25**(11): p. 1422-3.

46. DeLano, W.L. *The PyMOL Molecular Graphics System*. 2002; Available from: http://www.pymol.org.

47. Raines, R.T., *Fluorescence polarization assay to quantify protein-protein interactions: an update*. Methods Mol Biol, 2015. **1278**: p. 323-7.

48. Kolch, W., et al., *Raf-1 protein kinase is required for growth of induced NIH/3T3 cells*. Nature, 1991. **349**(6308): p. 426-8.

49. Warne, P.H., P.R. Viciana, and J. Downward, *Direct interaction of Ras and the amino-terminal region of Raf-1 in vitro*. Nature, 1993. **364**(6435): p. 352-5.

50. Zhang, X.F., et al., *Normal and oncogenic p21ras proteins bind to the amino-terminal regulatory domain of c-Raf-1*. Nature, 1993. **364**(6435): p. 308-13.

51. Moodie, S.A., et al., *Complexes of Ras.GTP with Raf-1 and mitogen-activated protein kinase kinase*. Science, 1993. **260**(5114): p. 1658-61.

52. Lu, S., et al., *Drugging Ras GTPase: a comprehensive mechanistic and signaling structural view*. Chem Soc Rev, 2016.

53. Shima, F., et al., *Discovery of small-molecule Ras inhibitors that display antitumor activity by interfering with Ras.GTP-effector interaction*. Enzymes, 2013. **34 Pt. B**: p. 1-23.

54. Beeram, M., A. Patnaik, and E.K. Rowinsky, *Regulation of c-Raf-1: therapeutic implications*. Clin Adv Hematol Oncol, 2003. **1**(8): p. 476-81.

55. Beeram, M., A. Patnaik, and E.K. Rowinsky, *Raf: a strategic target for therapeutic development against cancer*. J Clin Oncol, 2005. **23**(27): p. 6771-90.

56. Ostrem, J.M. and K.M. Shokat, *Direct small-molecule inhibitors of KRAS: from structural insights to mechanism-based design*. Nat Rev Drug Discov, 2016.

57. Cromm, P.M., et al., *Direct Modulation of Small GTPase Activity and Function*. Angew Chem Int Ed Engl, 2015. **54**(46): p. 13516-37.

58. Kurig, B., et al., *Ras is an indispensable coregulator of the class IB phosphoinositide 3-kinase p87/p110gamma*. Proc Natl Acad Sci U S A, 2009. **106**(48): p. 20312-7.

59. Rodriguez-Viciana, P., C. Sabatier, and F. McCormick, *Signaling specificity by Ras family GTPases is determined by the full spectrum of effectors they regulate*. Mol Cell Biol, 2004. **24**(11): p. 4943-54.

60. Nakhaei-Rad, S., et al., *The Function of Embryonic Stem Cell-expressed RAS (E-RAS), a Unique RAS Family Member, Correlates with Its Additional Motifs and Its Structural Properties*. The Journal of biological chemistry, 2015. **290**(25): p. 15892-903.

61. Dvorsky, R. and M.R. Ahmadian, *Always look on the bright site of Rho: structural implications for a conserved intermolecular interface*. EMBO Rep, 2004. **5**(12): p. 1130-6.

62. Jaiswal, M., R. Dvorsky, and M.R. Ahmadian, *Deciphering the molecular and functional basis of Dbl family proteins: a novel systematic approach toward classification of selective activation of the Rho family proteins*. The Journal of biological chemistry, 2013. **288**(6): p. 4486-500.

63. Amin, E., et al., *Deciphering the molecular and functional basis of RhoGAP family proteins: A systematic approach towards selective inactivation of Rho family proteins*. The Journal of biological chemistry, 2016.

64. Spoerner, M., et al., *Dynamic properties of the Ras switch I region and its importance for binding to effectors*. Proc Natl Acad Sci U S A, 2001. **98**(9): p. 4944-9.

65.   Elad-Sfadia, G., et al., *Galectin-1 augments Ras activation and diverts Ras signals to Raf-1 at the expense of phosphoinositide 3-kinase*. J Biol Chem, 2002. **277**(40): p. 37169-75.

66.   Katz, M.E. and F. McCormick, *Signal transduction from multiple Ras effectors*. Curr Opin Genet Dev, 1997. **7**(1): p. 75-9.

67.   Rodriguez-Viciana, P., et al., *Role of phosphoinositide 3-OH kinase in cell transformation and control of the actin cytoskeleton by Ras*. Cell, 1997. **89**(3): p. 457-67.

68.   Vandal, G., B. Geiling, and D. Dankort, *Ras effector mutant expression suggest a negative regulator inhibits lung tumor formation*. PLoS One, 2014. **9**(1): p. e84745.

69.   Wing, M.R., D.M. Bourdon, and T.K. Harden, *PLC-epsilon: a shared effector protein in Ras-, Rho-, and G alpha beta gamma-mediated signaling*. Mol Interv, 2003. **3**(5): p. 273-80.

70.   Wellbrock, C., M. Karasarides, and R. Marais, *The RAF proteins take centre stage*. Nature reviews. Molecular cell biology, 2004. **5**(11): p. 875-85.

71.   Baljuls, A., B.N. Kholodenko, and W. Kolch, *It takes two to tango--signalling by dimeric Raf kinases*. Mol Biosyst, 2013. **9**(4): p. 551-8.

72.   Ahmadian, M.R., et al., *Individual rate constants for the interaction of Ras proteins with GTPase-activating proteins determined by fluorescence spectroscopy*. Biochemistry, 1997. **36**(15): p. 4535-41.

73.   Scheffzek, K., M.R. Ahmadian, and A. Wittinghofer, *GTPase-activating proteins: helping hands to complement an active site*. Trends Biochem Sci, 1998. **23**(7): p. 257-62.

74.   Castellano, E. and E. Santos, *Functional specificity of ras isoforms: so similar but so different*. Genes & cancer, 2011. **2**(3): p. 216-31.

75.   Chavan, T.S., et al., *High-Affinity Interaction of the K-Ras4B Hypervariable Region with the Ras Active Site*. Biophys J, 2015. **109**(12): p. 2602-13.

76.   Abraham, S.J., et al., *The hypervariable region of K-Ras4B is responsible for its specific interactions with calmodulin*. Biochemistry, 2009. **48**(32): p. 7575-83.

77.   Parker, J.A. and C. Mattos, *The Ras-Membrane Interface: Isoform-specific Differences in The Catalytic Domain*. Molecular cancer research : MCR, 2015. **13**(4): p. 595-603.

78.   Abankwa, D., et al., *A novel switch region regulates H-ras membrane orientation and signal output*. EMBO J, 2008. **27**(5): p. 727-35.

79.   Mazhab-Jafari, M.T., et al., *Oncogenic and RASopathy-associated K-RAS mutations relieve membrane-dependent occlusion of the effector-binding site*. Proc Natl Acad Sci U S A, 2015. **112**(21): p. 6625-30.

80.   Rodriguez-Viciana, P., et al., *A phosphatase holoenzyme comprised of Shoc2/Sur8 and the catalytic subunit of PP1 functions as an M-Ras effector to modulate Raf activity*. Molecular Cell, 2006. **22**(2): p. 217-30.

81.   Zhou, M., et al., *VPS35 binds farnesylated N-Ras in the cytosol to regulate N-Ras trafficking*. The Journal of cell biology, 2016. **214**(4): p. 445-58.

82.   Zheng, Z.Y., et al., *CHMP6 and VPS4A mediate the recycling of Ras to the plasma membrane to promote growth factor signaling*. Oncogene, 2012. **31**(43): p. 4630-8.

83.   Jang, H., et al., *Mechanisms of membrane binding of small GTPase K-Ras4B farnesylated hypervariable region*. The Journal of biological chemistry, 2015. **290**(15): p. 9465-77.

84.   Lynch, S.J., et al., *The differential palmitoylation states of N-Ras and H-Ras determine their distinct Golgi subcompartment localizations*. J Cell Physiol, 2015. **230**(3): p. 610-9.

85. Bivona, T.G., et al., *PKC regulates a farnesyl-electrostatic switch on K-Ras that promotes its association with Bcl-XL on mitochondria and induces apoptosis*. Molecular cell, 2006. **21**(4): p. 481-93.

86. Sung, P.J., et al., *Phosphorylated K-Ras limits cell survival by blocking Bcl-xL sensitization of inositol trisphosphate receptors*. Proc Natl Acad Sci U S A, 2013. **110**(51): p. 20593-8.

87. Wang, M.T., et al., *K-Ras Promotes Tumorigenicity through Suppression of Non-canonical Wnt Signaling*. Cell, 2015. **163**(5): p. 1237-51.

88. Rodriguez-Viciana, P. and F. McCormick, *Ras ubiquitination: coupling spatial sorting and signal transmission*. Cancer Cell, 2006. **9**(4): p. 243-4.

89. Jura, N., et al., *Differential modification of Ras proteins by ubiquitination*. Molecular cell, 2006. **21**(5): p. 679-87.

90. de la Vega, M., et al., *The deubiquitinating enzyme USP17 blocks N-Ras membrane trafficking and activation but leaves K-Ras unaffected*. The Journal of biological chemistry, 2010. **285**(16): p. 12028-36.

91. Yang, M.H., et al., *HDAC6 and SIRT2 regulate the acetylation state and oncogenic activity of mutant K-RAS*. Molecular cancer research : MCR, 2013. **11**(9): p. 1072-7.

92. Knyphausen, P., et al., *Insights into K-Ras 4B regulation by post-translational lysine acetylation*. Biol Chem, 2016.

93. Yang, M.H., et al., *Regulation of RAS oncogenicity by acetylation*. Proc Natl Acad Sci U S A, 2012. **109**(27): p. 10843-8.

94. Wurtzel, J.G., et al., *RLIP76 regulates Arf6-dependent cell spreading and migration by linking ARNO with activated R-Ras at recycling endosomes*. Biochemical and biophysical research communications, 2015. **467**(4): p. 785-91.

95. Furuhjelm, J. and J. Peranen, *The C-terminal end of R-Ras contains a focal adhesion targeting signal*. J Cell Sci, 2003. **116**(Pt 18): p. 3729-38.

96. Berzat, A.C., et al., *Using inhibitors of prenylation to block localization and transforming activity*. Methods Enzymol, 2006. **407**: p. 575-97.

97. Oertli, B., et al., *The effector loop and prenylation site of R-Ras are involved in the regulation of integrin function*. Oncogene, 2000. **19**(43): p. 4961-9.

98. Calvo, F. and P. Crespo, *Structural and spatial determinants regulating TC21 activation by RasGRF family nucleotide exchange factors*. Molecular biology of the cell, 2009. **20**(20): p. 4289-302.

99. Holly, S.P., M.K. Larson, and L.V. Parise, *The unique N-terminus of R-ras is required for Rac activation and precise regulation of cell migration*. Molecular biology of the cell, 2005. **16**(5): p. 2458-69.

100. Herrmann, C., G.A. Martin, and A. Wittinghofer, *Quantitative analysis of the complex between p21ras and the Ras-binding domain of the human Raf-1 protein kinase*. The Journal of biological chemistry, 1995. **270**(7): p. 2901-5.

101. Gorman, C., et al., *Equilibrium and kinetic measurements reveal rapidly reversible binding of Ras to Raf*. The Journal of biological chemistry, 1996. **271**(12): p. 6713-9.

102. Hwang, M.C., Y.J. Sung, and Y.W. Hwang, *The differential effects of the Gly-60 to Ala mutation on the interaction of H-Ras p21 with different downstream targets*. The Journal of biological chemistry, 1996. **271**(14): p. 8196-202.

103. Linnemann, T., et al., *Thermodynamic and kinetic characterization of the interaction between the Ras binding domain of AF6 and members of the Ras subfamily*. The Journal of biological chemistry, 1999. **274**(19): p. 13556-62.

104. Boettner, B., C. Herrmann, and L. Van Aelst, *Ras and Rap1 interaction with AF-6 effector target*. Methods Enzymol, 2001. **332**: p. 151-68.

105.   Linnemann, T., et al., *Interaction between Nef and phosphatidylinositol-3-kinase leads to activation of p21-activated kinase and increased production of HIV*. Virology, 2002. **294**(2): p. 246-55.

106.   Gremer, L., et al., *Duplication of Glu37 in the switch I region of HRAS impairs effector/GAP binding and underlies Costello syndrome by promoting enhanced growth factor-dependent MAPK and AKT activation*. Human molecular genetics, 2010. **19**(5): p. 790-802.

107.   Sydor, J.R., et al., *Transient kinetic studies on the interaction of Ras and the Ras-binding domain of c-Raf-1 reveal rapid equilibration of the complex*. Biochemistry, 1998. **37**(40): p. 14292-9.

108.   Sydor, J.R., et al., *Cell-free synthesis of the Ras-binding domain of c-Raf-1: binding studies to fluorescently labelled H-ras*. FEBS Lett, 1999. **452**(3): p. 375-8.

109.   Vetter, I.R., et al., *Structural and biochemical analysis of Ras-effector signaling via RalGDS*. FEBS Lett, 1999. **451**(2): p. 175-80.

110.   Rudolph, M.G., et al., *Thermodynamics of Ras/effector and Cdc42/effector interactions probed by isothermal titration calorimetry*. The Journal of biological chemistry, 2001. **276**(26): p. 23914-21.

111.   Harjes, E., et al., *GTP-Ras disrupts the intramolecular complex of C1 and RA domains of Nore1*. Structure, 2006. **14**(5): p. 881-8.

112.   Hunter, J.C., et al., *Biochemical and Structural Analysis of Common Cancer-Associated KRAS Mutations*. Molecular cancer research : MCR, 2015. **13**(9): p. 1325-35.

113.   Flex, E., et al., *Activating mutations in RRAS underlie a phenotype within the RASopathy spectrum and contribute to leukaemogenesis*. Human molecular genetics, 2014. **23**(16): p. 4315-27.

114.   Herrmann, C., et al., *Differential interaction of the ras family GTP-binding proteins H-Ras, Rap1A, and R-Ras with the putative effector molecules Raf kinase and Ral-guanine nucleotide exchange factor*. The Journal of biological chemistry, 1996. **271**(12): p. 6794-800.

115.   Nassar, N., et al., *Ras/Rap effector specificity determined by charge reversal*. Nat Struct Biol, 1996. **3**(8): p. 723-9.

116.   Filchtinski, D., et al., *What Makes Ras an Efficient Molecular Switch: A Computational, Biophysical, and Structural Study of Ras-GDP Interactions with Mutants of Raf*. Journal of Molecular Biology, 2010. **399**(3): p. 422-435.

117.   Scheffzek, K., et al., *The Ras-Byr2RBD complex: structural basis for Ras effector recognition in yeast*. Structure, 2001. **9**(11): p. 1043-50.

118.   Stieglitz, B., et al., *Novel type of Ras effector interaction established between tumour suppressor NORE1A and Ras switch II*. The EMBO journal, 2008. **27**(14): p. 1995-2005.

119.   Qamra, R. and S.R. Hubbard, *Structural Basis for the Interaction of the Adaptor Protein Grb14 with Activated Ras*. PLoS One, 2013. **8**(8): p. e72473.

120.   Fetics, Susan K., et al., *Allosteric Effects of the Oncogenic RasQ61L Mutant on Raf-RBD*. Structure, 2015. **23**(3): p. 505-516.

121.   Mazhab-Jafari, M.T., et al., *Oncogenic and RASopathy-associated K-RAS mutations relieve membrane-dependent occlusion of the effector-binding site*. Proceedings of the National Academy of Sciences, 2015. **112**(21): p. 6625-6630.

122.   Pai, E.F., et al., *Structure of the guanine-nucleotide-binding domain of the Ha-ras oncogene product p21 in the triphosphate conformation*. Nature, 1989. **341**(6239): p. 209-14.

Chapter 13

NPM interactions with viral proteins

Biophysical Characterization of Nucleophosmin Interactions with Human Immunodeficiency Virus Rev and Herpes Simplex Virus US11
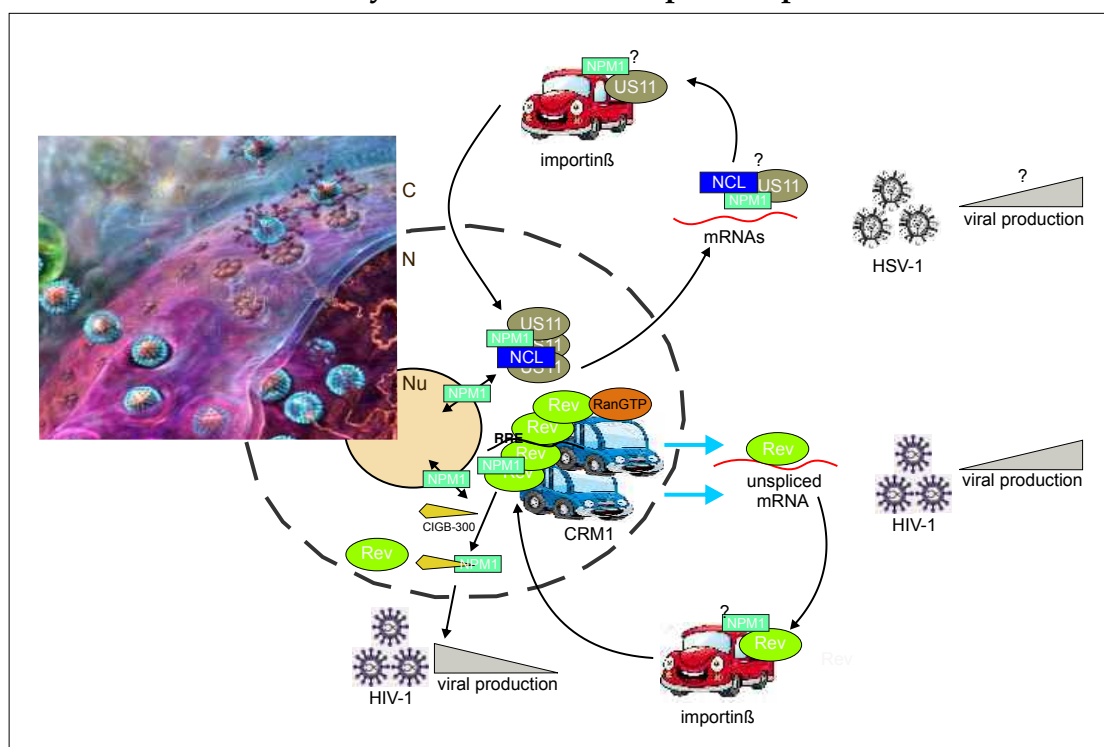
Status:	Published in PLOSE ONE. 2015 Dec 1
Impact factor:	3.23
Own Proportion to this work:	25 %; design and analyse the experiments and discussion

PLOS | ONE

RESEARCH ARTICLE

Biophysical Characterization of Nucleophosmin Interactions with Human Immunodeficiency Virus Rev and Herpes Simplex Virus US11

Kazem Nouri[1], Jens M. Moll[1], Lech-Gustav Milroy[2], Anika Hain[3], Radovan Dvorsky[1], Ehsan Amin[1], Michael Lenders[4], Luitgard Nagel-Steger[5,6], Sebastian Howe[7], Sander H. J. Smits[4], Hartmut Hengel[7,8], Lutz Schmitt[4], Carsten Münk[3], Luc Brunsveld[2], Mohammad R. Ahmadian[1]*

1 Institute of Biochemistry and Molecular Biology II, Medical Faculty, Heinrich-Heine University, Düsseldorf, Germany, **2** Laboratory of Chemical Biology & Institute of Complex Molecular Systems, Department of Biomedical Engineering, Technische Universiteit Eindhoven, Eindhoven, Netherlands, **3** Clinic for Gastroenterology, Hepatology and Infectiology, Medical Faculty, Heinrich-Heine University, Düsseldorf, Germany, **4** Institute of Biochemistry, Heinrich-Heine University, Düsseldorf, Germany, **5** Institute of Complex Systems (ICS-6), Research Centre Jülich, Jülich, Germany, **6** Institute of Physical Biology, Heinrich-Heine University, Düsseldorf, Germany, **7** Institute of Virology, Medical Faculty, Heinrich-Heine University, Düsseldorf, Germany, **8** Institute of Virology, University Medical Center Freiburg, Freiburg, Germany

* reza.ahmadian@uni-duesseldorf.de

Abstract

Nucleophosmin (NPM1, also known as B23, numatrin or NO38) is a pentameric RNA-binding protein with RNA and protein chaperon functions. NPM1 has increasingly emerged as a potential cellular factor that directly associates with viral proteins; however, the significance of these interactions in each case is still not clear. In this study, we have investigated the physical interaction of NPM1 with both human immunodeficiency virus type 1 (HIV-1) Rev and Herpes Simplex virus type 1 (HSV-1) US11, two functionally homologous proteins. Both viral proteins show, in mechanistically different modes, high affinity for a binding site on the N-terminal oligomerization domain of NPM1. Rev, additionally, exhibits low-affinity for the central histone-binding domain of NPM1. We also showed that the proapoptotic cyclic peptide CIGB-300 specifically binds to NPM1 oligomerization domain and blocks its association with Rev and US11. Moreover, HIV-1 virus production was significantly reduced in the cells treated with CIGB-300. Results of this study suggest that targeting NPM1 may represent a useful approach for antiviral intervention.

Introduction

Nucleophosmin (NPM1, also known as B23, numatrin, NO38) is a multifunctional phosphoprotein, predominantly localized in the nucleoli, which participates extensively in RNA regulatory mechanisms including transcription, ribosome assembly and biogenesis, mRNA stability,

translation and microRNA processing [1, 2]. NPM1 (294 amino acids; 37 kDa) consists of an N-terminal oligomerization domain (OD), a central histone binding domain (HBD) and a C-terminal RNA-binding domain (RBD) (Fig 1A) [3]. It also contains nuclear localization signals (NLSs) at the N-terminus, central nuclear exports signals (NESs) and a nucleolar localization signal (NoLS) at the very C-terminus (Fig 1A). NPM1 shuttles between the nucleus and cytoplasm and accordingly, a proportion of nucleolar NPM1 constantly translocates to the nucleoplasm and inner nuclear membrane as well as to the cytoplasm and inner and outer plasma membrane [2, 4, 5]. Due to this ability, NPM1 has been implicated in many stages of viral infection through interaction with a multitude of proteins from heterologous viruses (Table 1), including Human immunodeficiency virus type 1 (HIV-1) Rev [4], Human T-cell leukemia virus type 1 (HTLV-1) Rex [6] and Herpes simplex virus type 1 (HSV-1) UL24 [7].

Rev is 116 amino acid long and its RNA-binding domain is composed of an arginine-rich motif (ARM), which binds to various HIV-1 RNA stem loop structures [8]. The RNA- binding domain of Rev also acts as a nuclear/nucleolar targeting signal, which can deliver cytoplasmic proteins to the nucleus or nucleolus [8, 9]. Many host proteins including DDX1, DDX3, eIF5A, exportin-1, hRIP/Rab, Matrin-3, NPM1, PIMT, and RNA helicase A have been suggested to bind to Rev prior to induction of its nuclear translocation [10–13]. NPM1 interaction with Rev appears to be necessary for nucleolar localization of Rev [4]. In fact, the HIV-1 Rev response element, a segment of viral RNA, represents a nuclear export signal, which triggers, *via* Rev binding, the nucleocytoplasmic shuttling of viral transcripts in infected cells [14]. A similar mechanism is controlled by Rex responsive element [15]. Most interestingly, US11, a protein of HSV-1, has the potential of directly binding to the Rev and Rex response elements and functionally substituting for Rev and Rex functions [4, 14].

HSV-1 virions have four morphologically separate structures, a DNA core, capsid, tegument, and envelope. Tegument proteins fill the space between the capsid and the envelope [16]. US11 is a tegument protein and approximately 600 to 1,000 molecules per virion are released in the target cell upon virus entry [17]. It is a multifunctional protein involved in post-transcriptional regulation of gene expression and in biological processes related to the survival of cells following environmental stress [18, 19]. US11 is localized in the nucleus and the cytoplasm, but especially accumulates in the nucleolus [20, 21]. It has been reported that US11 has RNA-binding activity and can associate strongly with ribosomes and has also been found in rRNA and polysome containing fractions [17, 22]. US11 also interacts with several host proteins, including nucleolin [23], ubiquitous kinesin heavy chain (uKHC) [24], homeodomain-interacting protein kinases 2 (HIPK2) [19], and protein kinase R (PKR) [25], which in turn counteracts the antiviral host defense system. Furthermore, although US11 protein is not essential for viral growth in cell cultures, it plays a vital role in the cells subjected to thermal stress [26], recovery of protein synthesis and survival in heat shock-treated cells [27].

In this study we investigated Rev-NPM1 interaction and found that Rev shows high-affinity binding to two domains of NPM1, OD and HBD, in an RNA-independent manner. Due to the functional homology of US11 with both HIV-1 Rev and HTLV-1 Rex, it was tempting to examine US11 binding to NPM1. The achievements in this study demonstrates, for the first time, a physical interaction between the C-terminal domain of US11 and NPM1^{OD} in an RNA-independent manner. The Rev and US11 association with NPM1 was prevented by a cyclic peptide, CIGB-300, which also bound to NPM1^{OD} but not to the other NPM1 domains. Cell-based experiments revealed a significant reduction of HIV-1 virus production in the presence of CIGB-300. Thus, the association of nucleolar protein NPM1 with the viral proteins Rev and US11 may advance our understanding of HIV and HSV pathology and further implies that NPM1 can be exploited as a therapeutic target for infectious diseases.
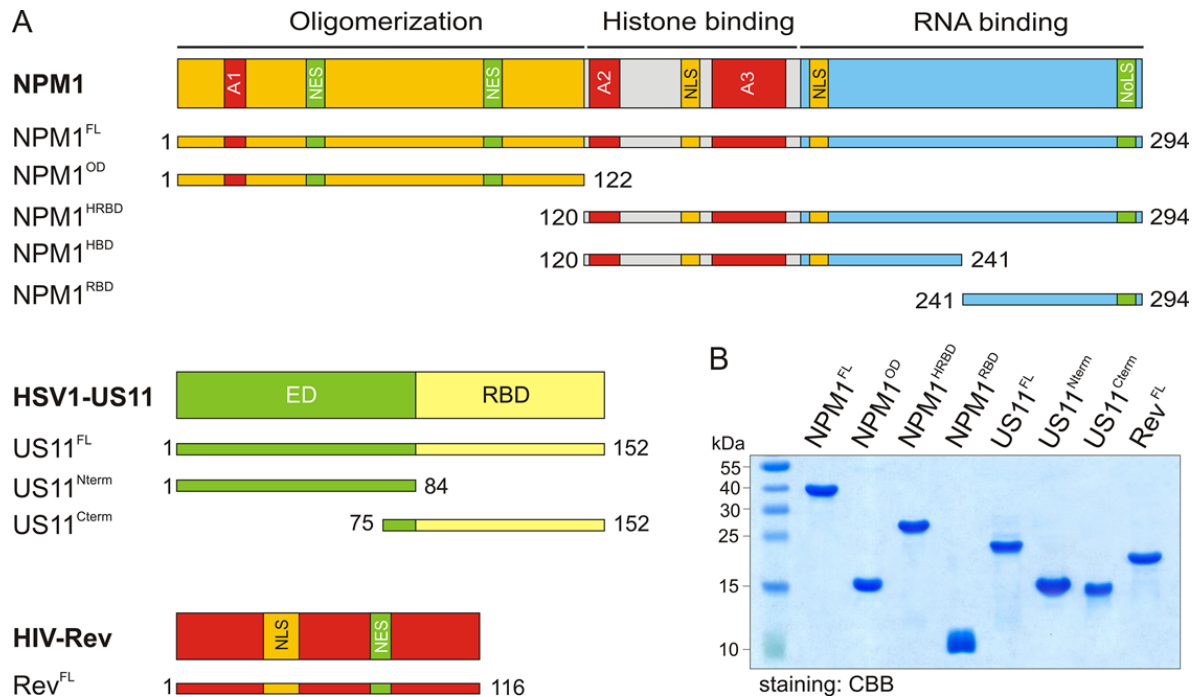
Fig 1. Schematic representation of domain organization, various constructs and proteins of NPM1, HSV-1 US11, and HIV-1 Rev. (A) Domains and various constructs of NPM1, US11 and Rev. The numbers indicate the N- and C-terminal amino acids of the respective constructs used in this study. A1-A3, acidic regions 1–3; Cterm, C-terminal; ED, effector domain; FL, full-length; HRBD, histone and RNA-binding domains; HBD, histone binding domain; NES, nuclear export signal; NLS, nuclear localization signal; NoLS, nucleolar localization signal; Nterm, N-terminal; OD, oligomerization domain; RBD, RNA-binding domain. (B) Coomassie brilliant blue (CBB) stained SDS-PAGE of purified proteins used in this study.

doi:10.1371/journal.pone.0143634.g001

Materials and Methods

Constructs

The coding sequence of NPM1 full-length (NPM1^{FL}, aa 1–294), kindly provided by F. Carrier [28]. Oligomerization domain (NPM1^{OD}, aa 1–122), histone and RNA-binding domains (NPM1^{HRBD}, aa120-294), histone binding domain (NPM1^{HBD}, aa 120–241), RNA-binding domain (NPM1^{RBD}, aa 241–294), HSV-1 US11 full-length (US11^{FL}, aa 1–152), Nterm (US11^{Nterm}, aa 1–84) and Cterm (US11^{Cterm}, aa 79–152) as well as HIV-1 Rev full-length (Rev^{FL}, aa 1–116) were amplified by PCR and cloned into pGEX-4T1-Ntev or pET-23b to obtain GST-fusion or His-tagged proteins. The Myc-tagged HSV-1 US11^{FL} was cloned into pcDNA3.1-Myc for expression in eukaryotic cells. pNL4-3 was used to produce replication competent HIV-1 [29].

Cell culture

COS-7 and HeLa cells were obtained from German Collection of Microorganisms and Cell Cultures (Braunschweig, Germany). TZM-bl Cells were from NIH AIDS reagent program and HOS.CD4.CXCR4 cells were from CFAR (Centers for AIDS Research). All cells were grown in DMEM supplemented with 10% fetal bovine serum (FBS) (Life Technologies) and penicillin/

Table 1. Nucleophosmin involvement in multiple viral infections.

Virus[a]	Partner	Domain	Effect/observation	References
AAV	Rep	n.d.	Viral assembly	[58]
Adenovirus	Core protein V	n.d.	NPM1 re-localization, Replication, Viral assembly	[59, 60]
Adenovirus	Basic core protein	n.d.	Transcription, Replication	[61]
Adenovirus	Core protein V, pre-VII	n.d.	Replication, chromatin assembly	[62, 63]
CHIKV	n.d.	n.d.	n.d.	[64]
EBV	EBNA1	HBD	Transcription	[65, 66]
EBV	EBNA2	OD	Transcription, latency	[67]
EBV	EBNA3	n.d.	Transcription	[68]
EMCV	3BCD	n.d.	Nuclear transport	[69]
HBV	core protein 149	n.d.	Capsid assembly	[70–72]
HBV	X protein	n.d.	n.d.	[73, 74]
HCV	Core protein	n.d.	Transcription	[75]
HDV	Antigen	n.d.	n.d.	[76]
HIV-1	Rev	OD, HBD	n.d.	[4]; this study
HIV-1	Tat	n.d.	NPM1 acetylation, transcription	[77–79],
HRSV	Matrix protein	n.d.	Replication	[80]
HSV-1	UL24	n.d.	NPM1 re-localization	[7]
	US11	OD	n.d.	this study
HTLV-1	Rex	HBD	n.d.	[6]
JEV	Core protein	OD	Replication	[81]
KSHV	LANA	n.d.	NPM1 phosphorylation (T199), latency	[82]
NDV	Matrix protein M	RBD	NPM1 re-localization, Replication	[83]
PEDV	N protein	n.d.	Nucleolar co-localization	[84]

[a] Virus abbreviation: AAS, Adeo-associated virus; EBV, Epstein Barr virus; CHIKV, Chikungunya virus; EMCV, Encephalomyocarditis virus; HBV, Hepatitis B virus; HCV, Hepatitis C virus; HDV, Hepatitis delta virus; HIV-1, Human immunodeficiency virus type 1; HRSV, Human respiratory syncytial virus; HSV-1, Herpes simplex virus type 1; HTLV1, Human T-cell leukemia virus type 1; JEV, Japanese encephalitis virus; KSHV, Kaposi's sarcoma-associated herpes virus; NDV, Newcastle disease virus; PEDV, porcine epidemic diarrhea virus. n.d., not determined.

streptomycin (Life Technologies) as antibiotics. Cells were grown in a humidified CO_2 (5%) atmosphere at 37°C. Trypsin/EDTA was from Genaxxon Bioscience GmbH (Ulm, Germany).

Antibodies and fluorescent probes

Mouse monoclonal anti-NPM1 (ab10530) recognizing the C-terminal 68-amino acids and rabbit monoclonal anti-NPM1 (ab52644) recognizing the N-terminal 122-amino acids were from Abcam (Cambridge, United Kingdom), Rabbit monoclonal anti-myc from Cell Signaling Technology, Inc. (Boston, USA), Alexa fluor 488 mouse anti-rabbit IgG and Alexa fluor 633, and goat anti-mouse IgG from Molecular Probes (Oregon, USA), and normal monoclonal Rabbit IgG (sc-2027) was from Santa Cruz Biotechnology, Texas, USA.

Proteins

For protein expression the *Escherichia coli* strains BL21(DE3), pLysS BL21(DE3), CodonPlus-RIL, or BL21(Rosetta), were transformed and used to purify the respective protein as previously described [30, 31]. All purified proteins were analyzed by SDS-PAGE (Fig 1B) and stored as either tag-fused or cleaved protein at -80°C.

Transient transfection

COS-7 and HeLa cells were transfected using the TurboFect transfection reagent according to the manufacturer's instructions (Thermo Scientific) in 24-well plates or 10 cm dishes by using 0.5 µg or 5 µg plasmid DNA per transfection, respectively.

Confocal laser scanning microscopy

Confocal imaging was performed using a LSM510-Meta confocal microscope (Zeiss, Jena, Germany) as previously reported [5].

Immunoblotting

Proteins were heated in Laemmli sample buffer and subjected to SDS-PAGE. The proteins were transferred to nitrocellulose membranes (Hybond C, GE Healthcare) using Mini Trans-Blot cell (100 volt for 1 h) (BIO-RAD, USA), and immunoblotted using monoclonal primary antibody to mouse NPM1 antibody (Abcam), rabbit NPM1 antibody (Abcam), and rabbit myc antibody (Cell Signaling) for 1 h. After three washing steps, membranes were incubated with polyclonal horseradish peroxidase-coupled secondary antibodies for 1 h and signals were visualized by the ECL detection system (GE Healthcare) and images were collected using the ChemoCam Imager ECL (INTAS science imaging, Germany).

Immunoprecipitation

COS-7 cells were transiently transfected with cDNA encoding Myc-tagged US11. After 48 h, an equal number of the cells were lysed in a buffer, containing 30 mM Tris/HCl, pH 7.5, 150 mM NaCl, 1 mM EDTA, 1% Triton X-100, 2.5 mM Na-pyrophosphate, 1 mM β-glycerophosphate, 1 mM sodium vanadate, and one EDTA-free protease inhibitor cocktail tablet (Roche, Mannheim, Germany). Lysates were centrifuged at 12,000×g for 2 min. The supernatant was precleared with protein G agarose (Roche, Mannheim, Germany) and divided to three parts for IgG control, beads control and IP, and then incubated with an anti-myc antibody (Cell Signaling) overnight at 4°C. Afterwards, protein G-Agarose beads were added to the lysate for 1 h before recovering the beads by centrifugation at 500×g for 5 min at 4°C. The beads were washed 4-times in the lysis buffer, and resuspended in Laemmli sample buffer. Precipitates and total cell lysate were subjected to SDS-PAGE, and Western blotting as described above.

Analytical size exclusion chromatography (aSEC)

The complex formation of NPM1^{OD} and US11^{FL} was analyzed using a superdex 200 10/30 column (GE Healthcare, Uppsala, Sweden) and a buffer, containing 30 mM Tris-HCL (pH 7.5), 150 mM NaCl, 5 mM MgCl$_2$, and 3 mM dithiothreitol. The flow rate was sustained at 0.5 ml/min. Fractions were collected at a volume of 0.5 ml and then peak fractions were visualized by 12.5% SDS-PAGE gel and staining using coomassie brilliant blue (CBB).

Pull-down assay

GST, GST-fused NPM1 and HSV-1 US11 variants as well as HIV-1 Rev were expressed in *E. coli* and purified using standard protocols [30, 31]. In order to obtain prey proteins the GST-tag was cleaved off with purified tobacco etch virus (tev) protease and removed by reverse GSH affinity purification. Pull-down experiments were performed by adding 50 µg purified proteins, e.g. HIV-1 Rev and HSV US11 variants, or COS-7 cell lysate transfected with pcDNA-mycUS11^{FL} to 25 µg of GST-fused NPM1 proteins, immobilized on 100 µl glutathione-conjugated Sepharose 4B beads (Macherey-Nagel, Duren, Germany). The mixture was incubated at

4°C for 1 h in a buffer containing 30 mM Tris/HCl, pH 7.5, 150 mM NaCl, 5 mM MgCl$_2$, and 3 mM Dithiothreitol. In cases of RNase treatments, 70 U RNase A (Qiagen, Hilden, Germany) were added to the same buffer in order to determine an RNA dependent interaction between the NPM1 variants and HIV-1 Rev. After four washing steps with the same buffer, proteins retained on the beads were heat-denatured (7 min at 90°C) and analyzed by SDS-PAGE followed by coomassie brilliant blue (CBB) staining or by Western blotting. Mixed samples prior to pull-down (PD) analysis were used as input controls.

Isothermal titration calorimetry (ITC)

All proteins were prepared in ITC buffer, containing 30 mM Tris-HCl, pH 7.5, 150 mM NaCl, 5 mM MgCl$_2$, and 1 mM Tris (2-carboxyethyl) phosphine (TCEP) on a size exclusion chromatography (SEC) column (Superdex 200, 16/60, GE Healthcare, Uppsala, Sweden). ITC measurements were performed at 25°C using a VP-ITC system (Microcal, Northampton, MA, USA) as previously reported [32]. The final data analysis was carried out using Origin software (Microcal). The experimental data were evaluated using Origin 7.0 software (Microcal) to determine the binding parameters including association constant (K_a), number of binding sites (n), and enthalpy (ΔH). Control measurements were carried out by titrating buffer to the protein.

Analytical ultracentrifugation (AUC)

Sedimentation velocity centrifugation experiments at 50,000 rpm and 20°C were carried out in a Beckman Optima XL-A (Beckman-Coulter, Brea, CA, USA), equipped with absorption optics, and a four-hole rotor. Samples (volume 400 μL) were filled into standard aluminum double sector cells with quartz glass windows. Measurements were performed in absorbance mode at detection wavelengths 230 nm. Radial scans were recorded with 30 μm radial resolution at ~1.5 min intervals. The software package SEDFIT v 14.1 (www.analyticalultracentrifugation.com) was used for data evaluation. After editing time-invariant, noise was calculated and subtracted. In SEDFIT continuous sedimentation coefficient distributions c(s) were determined with 0.05 S resolution and F-ratio = 0.95. Suitable s-value ranges between 0 and 20 S and f/f$_0$ between 1 and 4 were chosen. Buffer density and viscosity had been calculated with SEDNTERP v 20111201 beta (bitcwiki.sr.unh.edu) [33]. The partial specific volume of NPM1^{OD} fragment, NPM1^{FL} and US11^{FL} were calculated according to the method of Cohn and Edsall [34] as implemented in SEDNTERP. NPM1^{OD} was analyzed at 0.25 concentrations in 30 mM Tris-HCl, pH 7.5, 150 mM NaCl, and TCEP (1 mM). After equilibrium was reached, concentration profiles were recorded with 10 μm radial resolution and averaging of seven single registrations per radial value. Equilibria had been established at 14,000, 16,000, 25,000, 42,000 and 50,000 rpm. Data evaluation was performed using SEDPHAT.

Multi angle light scattering (MALS)

MALS experiments were performed as described [35]. Briefly, light scattering measurement of purified NPM1^{OD} alone or combined with US11^{FL} was performed on a MALS instrument (miniDAWN™ TREOS). For exact protein mass calculation, UV absorptions at 280 nm (Agilent Infinity 1260) and refractive index (RI) signals (OptilabRex, Wyatt Technology) were collected. Raw data was analyzed and processed using ASTRA software (Wyatt Technology) to calculate molecular mass averages and polydispersity indexes of analyzed protein samples.

CIGB-300 synthesis

The CIGB-300 peptide was synthesized at room temperature by manual solid-phase peptide synthesis using a Rink Amide resin (0.59 mmol/g loading). Briefly, the resin (200 μmole scale)

was pre-swollen by suspending in 3 mL of NMP for 10 min and the N-terminal Fmoc-protecting group cleaved by treating the resin with 3 mL of a stock solution of 20% piperidine (v/v) in *N*-methyl-2-pyrrolidone (NMP) (2 x 5 min). Each amino acid coupling was performed by pre-mixing 2 mL of a 0.4 M stock solution of *O*-Benzotriazole-*N,N,N′,N′*-tetramethyluronium-hexafluoro-phosphate (HBTU) in NMP with 4 mL of a 0.2 M stock solution of the amino acid building block in NMP, followed by 2 mL of a 1.6 M stock solution of *N,N*-diisopropylethyla-mine (DIPEA) stock solution, also in NMP. The reaction mixture was added immediately to the resin and the reaction vessel agitated at ambient temperature for 30 min. Each amino acid coupling was performed twice. For the coupling of the fluorescein isothiocyanate (FITC) dye, an amino acid linker (Fmoc-O1Pen-OH, Iris Biotech GmbH) was first coupled to the N-terminus, the Fmoc group deprotected under standard conditions, and then the resin was incubated with 7 eq. of FITC and 14 eq. of DIPEA in DMSO at RT for 18 h. The linear peptides (with and without FITC dye) were simultaneously deprotected and cleaved from the Rink Amide resin using a 92.5/2.5/2.5/2.5 (v/v) mixture of trifluoroacetic acid (TFA)/H_2O/triisopropylsilane (TIS)/ ethanedithiol (EDT), and then precipitated in ice-cold diethyl ether. Finally, disulfide formation was performed by stirring the crude peptide in phosphate buffer (pH 7.5) with 1% v/v DMSO at RT for 48 h to afford either CIGB-300 or fluoresceinated CIGB-300 after purification by reverse-phase HPLC using an Alltima HP C18 column (5 μm, length 125 mm, ID: 20 mm) and 0.1% trifluoroacetic acid (TFA) in H_2O/MeCN as mobile phase. The pure peptides were analyzed by LC-MS using a Shimadzu LC Controller V2.0, LCQ Deca XP Mass Spectrometer V2.0, Alltima C18-column 125 x 2.0 mm, Surveyor AS and PDA with solvent eluent conditions: CH_3CN/H_2O/1% TFA. The Rink Amide resin and all amino acid building blocks were purchased from Novabiochem®. HBTU, DIPEA, NMP, HPLC-grade CH_3CN and HPLC-grade TFA were all purchased from Biosolve B.V. Diethyl ether was purchased from Actu-All Chemicals. FITC, ethanedithiol, and triisopropylsilane were all purchased from Sigma-Aldrich. H_2O refers to Millipore-grade distilled water. Summary of LC-MS data (ESI): CIGB-300; $[M+5TFA+3H]^{3+}$: 1210.25 (theoretical), 1210.13 (found); $[M+6TFA+3H]^{3+}$: 1248,26 (theoretical), 1248.20 (found); fluoresceinated CIGB-300; $[M+5TFA+3H]^{3+}$: 1335.61 (theoretical), 1335.73 (found); $[M+6TFA+3H]^{3+}$: 1373.95 (theoretical), 1373,60 (found).

Fluorescence polarization

Fluoresceinated CIGB-300 (also referred to as FITC-labelled CIGB-300) was synthesized as described above. Increasing amounts of different variants of NPM1, GST-Rev, GST-US11 and GST as a negative control were titrated into FITC-labeled CIGB-300 (0.1 μM) in a buffer containing 30 mM Tris/HCl (pH 7.5), 150 mM NaCl, 5 mM $MgCl_2$, 1 mM tris-(2-carboxyethyl) phosphine and a total volume of 200 μl at 25°C using a Fluoromax 4 fluorimeter. Displacement assay was performed by titrating increasing amount of Rev and US11 to the complex of NPM1 and FITC-labelled CIGB-300. The concentration dependent binding curve was fitted using a quadratic ligand binding equation.

Virus production assay

HOS.CD4.CXCR4 were seeded in a 24 well plate with 2.5x10^4 cells per well. One part was treated with 100 μM CIGB-300 peptide for 30 min at 37°C and one part was left untreated. Cells were infected with HIV-1 NL4-3 (MOI 1) and after 6 h cells were washed to remove input virus. Cell culture supernatant was collected 48 h and 72 h after infection. Virus titer in the supernatant was determined by infection of TZM-bl cells and luciferase measurement three days later using the *Steady-Glo Luciferase Assay System* (Promega).

Structural bioinformatics

Model of the complex between NPM1 and CIGB-300 was created in two steps. Tat part of the peptide was first docked to the structure of NPM1 (PDB ID: 4N8M) [36] with the help of Haddock web portal (http://haddocking.org/). Acidic residues on three subunits were defined as active residues for docking while the setup of the Easy interface was used. Docked pose with best score that enables building of cyclic part of the peptide was then used in the second step. Model of the cyclic peptide was first generated and then placed with program CHARMm [37] in different orientations and positions on the surface of NPM1 in a way that enabled its interaction with the Tat portion of the peptide construct. After linking, the geometry of whole complex was optimized by energy minimization applying 500 steps of steepest descent method. Complex with lowest minimized energy was used as a final mode.

Results

HIV-1 Rev directly binds to two distinct regions of NPM1

Previous reports have shown that NPM1 is co-localized and co-immunoprecipitated with HIV-1 Rev in cells [4, 38]. To investigate a direct interaction between NPM1 and Rev, pull-down experiments under cell-free conditions were performed using Rev^{FL} and NPM1 variants as GST-fusion proteins. As indicated in Fig 2A (upper panel), Rev^{FL} interacts with NPM1^{FL}, NPM1^{OD}, NPM1^{HBD} and NPM1^{HRBD}, but not with the NPM1^{RBD}, suggesting that two different regions of NPM1, namely OD and HBD, have tight physical interaction with the HIV-1 Rev. To show whether this interaction is RNA-dependent, the pull-down experiments were performed under the same conditions in the presence of RNase A. As shown in Fig 2A (lower panel), RNase treatment had no effect on HIV-1 Rev association with NPM1. These results clearly indicate that HIV-1 Rev specifically binds to NPM1, and the binding is not RNA-dependent.

Next, we purified all proteins in high quantities (Fig 1B), and after cleaving the tag, isothermal titration calorimetry (ITC) experiments were conducted in order to examine the stoichiometry of binding and to determine the binding affinity of Rev^{FL} for the NPM1 variants. Consistent with the data obtained by pull-down assay, Rev^{FL} revealed variable affinity for the NPM1 variants with calculated dissociation constants (K_d) between 18 and 0.013 µM for 1:1 stoichiometry (Fig 2B and S1 Fig; Table 2). No interaction was detected between Rev^{FL} and NPM^{RBD} (Fig 2C) suggesting that a low micromolar affinity for the interaction between Rev and NPM1^{HRBD} actually stems from the central histone binding domain of NPM1 (NPM1^{HBD}). The obtained dissociation constant (K_d) for the Rev^{FL} and NPM1^{HBD} interaction was 5.8 µM indicating a stronger affinity for Rev^{FL} as compared to that of NPM^{HRBD}, which could be due to a binding site that partially masked by the C-terminal RBD.

HSV-1 US11 associates with NPM1 in cells

The fact that Rev physically binds to NPM1 and US11 alone can fulfill Rex and Rev's function in transactivating envelope glycoprotein gene expression [14], led us to examine a potential US11-NPM1 interaction. We first analyzed the intracellular distribution of endogenous NPM1 and overexpressed myc-US11 in HeLa cells using confocal imaging. Fig 3A shows a nucleolar co-localization of NPM1 and US11 where the overall pattern of these proteins is different. In contrast to a predominant nucleolar localization of NPM1, US11 was found in the cytoplasm and also accumulated, to certain extent, in the nucleoli. To confirm the association of US11 with NPM1, COS-7 cells overexpressing myc-US11 were lysed and endogenous NPM1 was immunoprecipitated. Fig 3B shows that NPM1 co-precipitated with myc-US11 indicating that
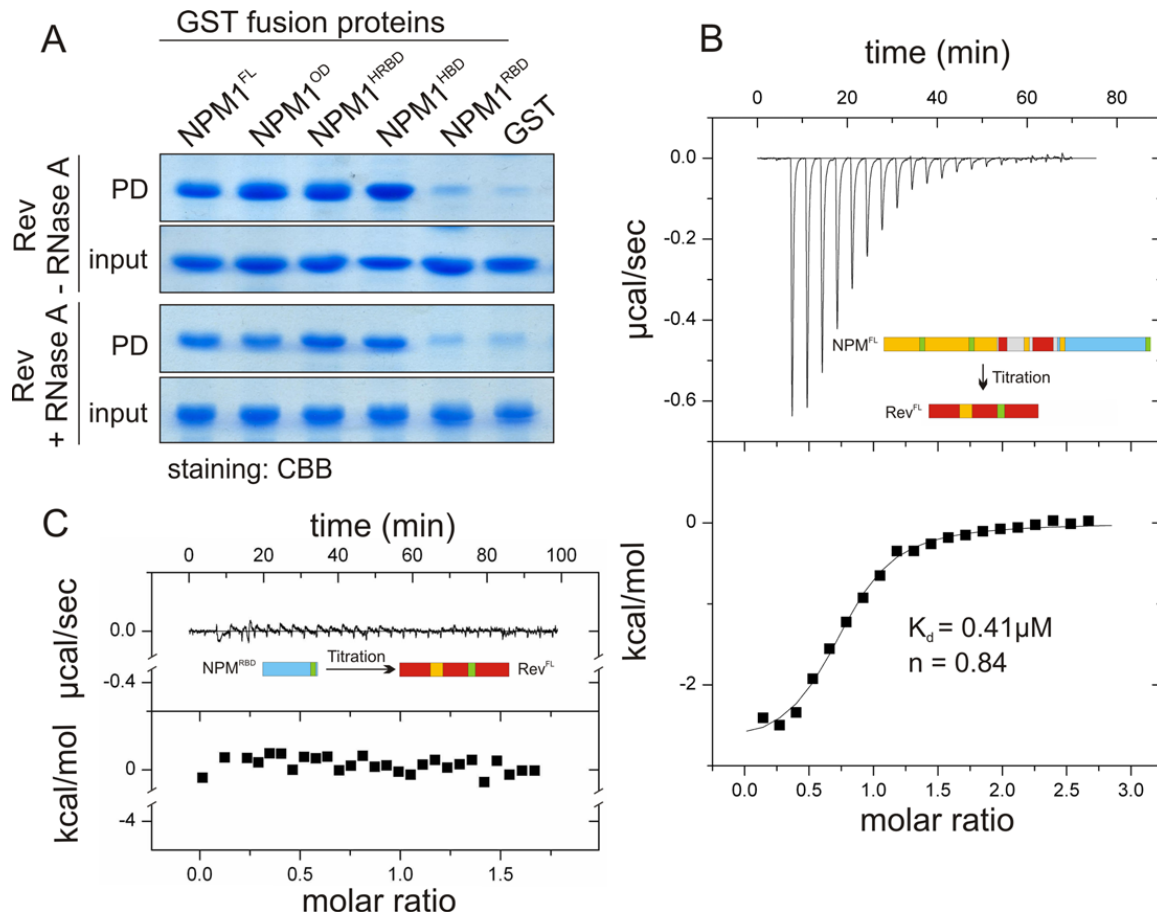
Fig 2. Direct NPM1 interaction with HIV-1 Rev. (A) Qualitative interaction analysis by GST pull-down assay and subsequent CBB staining. NPM1 FL, OD and HRBD, but not RBD, displayed a selective interaction with HIV-1 Rev (upper panel), which was also observed after an RNase A treatment (lower panel). (B) Quantitative interaction analysis by ITC. The binding parameters for the interaction between NPM1^{FL} and Rev were obtained using ITC. Titration of NPM1^{FL} (750 μM) to Rev^{FL} (35 μM) showed an exothermic response (negative peaks) indicating that Rev selectively interacts with NPM1^{FL}. The upper graph shows calorimetric changes plotted versus the time and the lower graph represents the changes in temperature according to the molar ratio of the interacting proteins. (C) No interaction was observed in a control experiments by titrating NPM1^{RBD} (300 μM) to Rev^{FL} (30 μM).

US11 forms a complex with NPM1. We, next, used purified GST-NPM1^{FL} and pulled down myc-US11, transiently overexpressed in COS-7 cells. As shown in Fig 3C, the myc-US11^{FL} clearly bound to NPM^{FL}, but not to the GST control, indicating that there may be a direct interaction between US11 and NPM1.

US11 associates with NPM1^{OD} in its oligomeric state

To clarify whether the interaction observed above is a direct interaction, we used purified, RNase A treated NPM1 and US11 variants from *E. coli*. Fig 4A shows that NPM1^{FL} and NPM1^{OD} but not NPM1^{HRBD} and NPM1^{RBD}, directly interact with US11^{FL}. We repeated the

Table 2. ITC data for HIV-1 Rev[FL] interaction with NPM1 variants.

Protein	K_d (μM)[a]	ΔH (kcal/mol)	TΔS (kcal/mol)	n (sites)
NPM1[FL]	0.41	-16.50±0.47	-0.66	0.84
NPM1[OD]	0.013	-3.79±0.11	-0.58	0.94
NPM1[HRBD]	18	-3.23±0.31	-0.27	0.76
NPM1[HBD]	5.8	-1.71±0.20	-0.71	0.85
NPM1[RBD]	no binding	-	-	-

K_a, association constant; K_d, dissociation constant; ΔH, enthalpy; n, binding stoichiometry (number of binding sites). HIV-1 Rev[FL] did not show any binding to the RNA-binding domain (RBD) of NPM1. All measurements were performed at 25°C.
[a] K_d values were calculated from $K_d = 1/K_a$.

doi:10.1371/journal.pone.0143634.t002

experiments to map the NPM1 binding region of US11 by using purified, GST-fused, N-terminal and C-terminal fragments of US11. As shown in Fig 4A, both US11[Cterm] and US11[Nterm] bound, with the same pattern as US11[FL] bound to NPM1[FL] and NPM1[OD]. However, binding affinities of isolated N- or C-terminal domains of US11 towards NPM1 seemed markedly
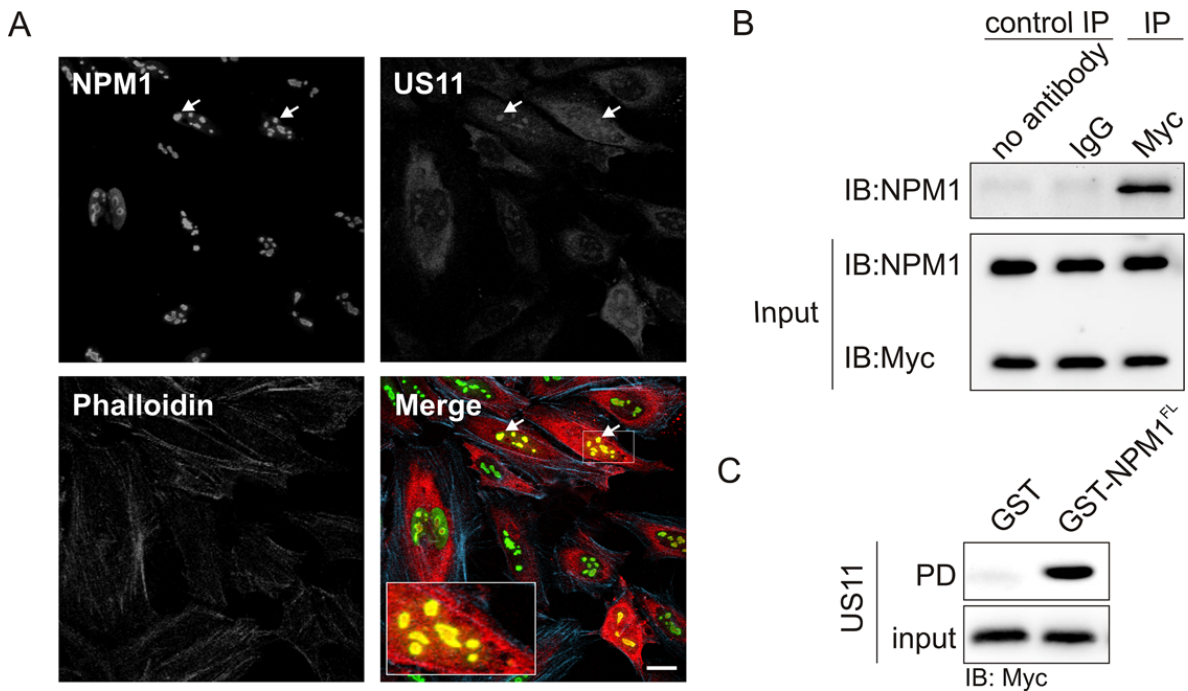
Fig 3. NPM1 association with HSV-1 US11 in the cell. (A) Nucleolar colocalization of endogenous NPM1 with myc-US11. Confocal images of HeLa cells transfected with myc-US11 were obtained by staining endogenous NPM1 (Mouse anti-NPM1 (ab10530)), myc-US11 (anti-myc antibody), and filamentous actin (rhodamine-phalloidin). For clarity, a boxed area in the merged panel shows colocalization of NPM1 and US11 in the nucleolus as pointed by arrows. Scale bar: 20 μm. (B) Myc-US11 associates with endogenous NPM1 in COS-7 cells. NPM1 was co-immunoprecipitated with myc-US11 overexpressed in COS-7 cells using anti-myc antibody. A normal Rabbit IgG and sample without antibody were used as IP controls. Input, 5% of total cell lysate; IP, immunoprecipitation; IB, immunoblotting. (C) Myc-US11[FL] displayed an interaction with NPM1[FL]. Myc-US11[FL] was pulled down with the GST-fusion NPM1[FL], but not with GST, which was used as a negative control. Samples prior pull-down (PD) analysis were used as input control.

doi:10.1371/journal.pone.0143634.g003
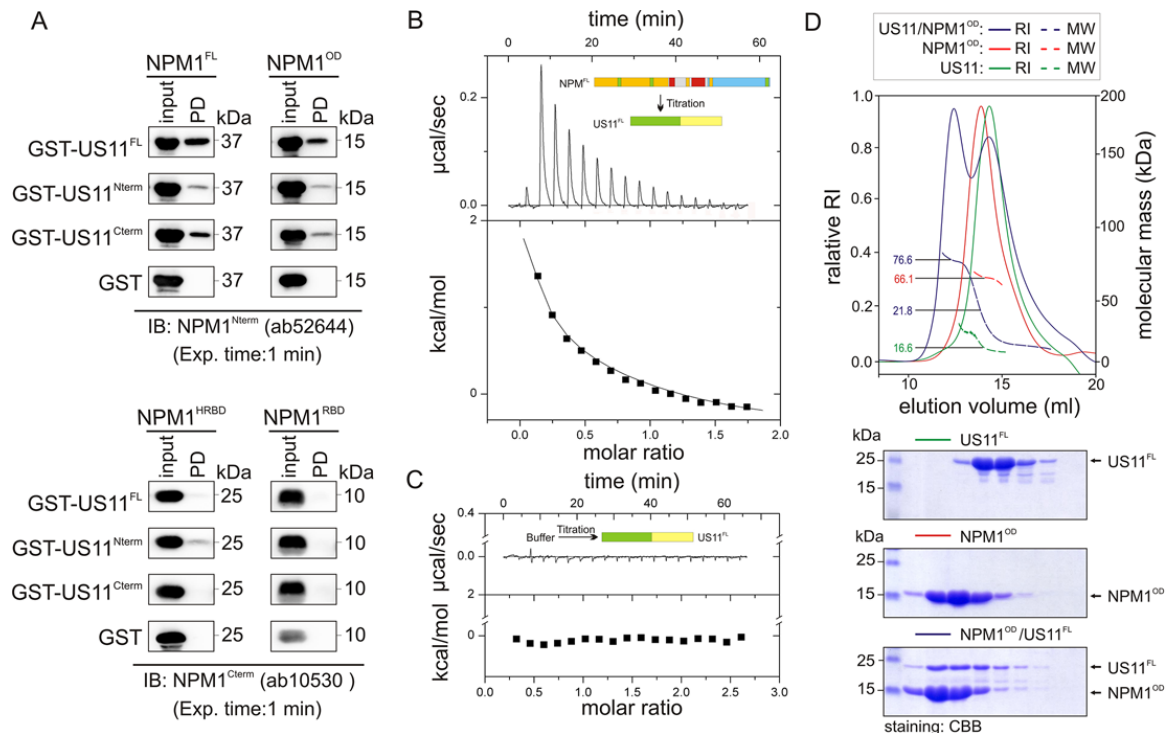
Fig 4. Physical interaction of HSV-1 US11 with NPM1. (A) C-terminal region of US11 largely contributes to NPM1 interaction. Pull-down experiments were conducted with purified proteins in the presence of RNase A by using GST-fused US11^{FL}, US11^{Nterm}, US11^{Cterm}, and GST as a negative control. For the detection of NPM1 variants two different antibodies were used, ab52644 recognized an N-terminal epitope containing in NPM1^{FL} and NPM1^{OD}, and ab10530 recognized a C-terminal epitope containing in NPM1^{HRBD} and NPM1^{RBD}. The same pattern of interaction was obtained for the N-terminal and the C-terminal parts of US11, although the interaction between NPM1^{FL} and NPM1^{OD} with US11^{Nterm} was much weaker than with US11^{Cterm}. The exposure time was 1 min for all the blots. (B-C) US11 binds NPM1 with a binding constant in the low micromolar range. To measure the binding parameter for the NPM1-US11 interaction, 1.2 mM NPM1^{FL} (B) and buffer (C) were titrated to 60 µM US11^{FL}. Both NPM1 and US11 were treated with RNase A. Conditions were the same as described in Fig 2. US11 binding to NPM1 is an endothermic reaction. (D) US11 binds to a pentameric NPM1. aSEC-MALS/RI analysis of NPM1^{OD}, US11^{FL}, and a mixture of both proteins revealed an oligomeric nature of NPM1^{OD} with a molecular weight (MW) of 66.1 kDa corresponding to the pentameric form. Obtained MW for US11 was 16.6 kDa, which matches the theoretical MW of 16.7 kDa for a monomeric US11 (upper panel). SDS-PAGE and CBB staining of the aSEC (Superdex 200, 10/300) elution fractions of NPM1^{OD}, US11^{Fl}, and a mixture of both clearly revealed a NPM1-US11 complex formation (lower panel). Both NPM1 and US11 were treated with RNase A. The MW of this complex corresponds to 76.6 kDa for a pentameric NPM1^{OD}, and a monomeric US11^{FL}. A MW of 21.8 kDa was measured that is estimated to an unbound US11^{FL}.

reduced compared to the full-length protein. In the light of above mentioned, we conclude that NPM1 and US11 physically interact with each other *via* NPM1^{OD} and largely US11^{Cterm}.

Next, ITC measurement was also performed to determine the binding affinity between NPM1 and US11 by titrating NPM1^{FL} (1.2 mM) to US11^{FL} solution (60 µM); both proteins were treated with RNase A. As shown in Fig 4B, the association of NPM1^{FL} with US11^{FL} is endothermic (positive peaks). As a control experiment, buffer was titrated to 60 µM US11^{FL} under the same experimental condition with no calorimetric changes (Fig 4C). Based on ITC analysis we estimated an apparent K_d value of 4 µM. The NPM1^{OD} interaction with US11^{FL} was also analyzed by aSEC combined with MALS, after treating the proteins with RNase A. Fig 4D (lower panel) shows a co-elution of the RNase-treated NPM1^{OD} and US11^{FL} proteins from the Superdex 200 (10/300) column indicating that these proteins form a complex. MALS

Table 3. AUC-SV data for NPM1^FL, NPM1^OD, and US11^FL, respectively.

Proteins	$S_{20,w}$ (S)	Std. dev.	f/f_0	MW (kDa)
NPM1^FL	6.7	0.52	1.5	146
NPM1^OD	4.5	0.14	1.27–1.40	63.3
US11^FL	1.4	0.20	1.4–1.7	15.3

MW, molecular weight; S20,w (S), sedimentation rate at 20°C; f/f0, frictional coefficient. In all three cases the values refer to a single, dominant species, which represented more than 90% of the sample.

doi:10.1371/journal.pone.0143634.t003

analysis revealed that NPM1^OD oligomerized to a pentameric state and formed a 1:1 complex with the monomeric US11^FL (Fig 4D upper panel). To further investigate the oligomerization states of US11 and NPM1, AUC experiments were performed. Results obtained were consistent with the MALS data, and revealed that NPM1^FL and NPM1^OD are pentameric and globular while US11^FL was monomeric and adopts an elongated structure (Table 3 and S2 Fig). Together, the data clearly demonstrates that US11 selectively binds to the N-terminal oligomerization domain of NPM1 in an RNA-independent manner.

Displacement of the NPM1-CIGB-300 complex by Rev and US11

Synthetic peptide CIGB-300 (also called p15-Tat; Fig 5A) has been described as a proapoptotic and anti-cancer peptide, which directly targets and antagonizes NPM1 function in cancer cells [39, 40]. Fluorescence polarization analysis revealed that a FITC-labelled CIGB-300 tightly associates with NPM1^FL and NPM1^OD but not with NPM1^HRBD and NPM1^RBD (Fig 5B). Calculated K_d values for the FITC-labelled CIGB-300 interaction with NPM1^FL and NPM1^OD were 1.4 and 6.6 µM, respectively.

We used the NPM1^FL- FITC-labelled CIGB-300 complex to further investigate NPM1 interactions with Rev and US11. The idea here was that titrating Rev or US11 to the complex may result in displacement of NPM1^FL from the FITC-labelled CIGB-300. Fig 5C shows that increasing concentrations of US11, but not Rev, significantly displaced NPM1^FL from the FITC-labelled CIGB-300 complex. This result was surprising for two reasons: First, Rev binds NPM1 in a higher nanomolar range (Table 2) and should be able to compete with CIGB-300 provided that both bind to the same surface of the NPM1 protein. Interestingly, Rev revealed a 30-fold lower affinity for NPM1^FL as compared to NPM1^OD (Table 2), which may explain why Rev did not displace NPM1^FL from FITC-labelled CIGB-300. Second, US11, which evidently exhibits an approximately 10-fold lower binding affinity for NPM1^FL as compared to Rev, is able to displace NPM1^FL from its complex with the synthetic FITC-labelled CIGB-300 (Fig 5C). To address this issue we repeated the displacement experiments under the same conditions as before but used the FITC-labelled CIGB-300 complex with NPM1^OD instead of NPM1^FL. Data obtained revealed that both Rev and US11 efficiently displace FITC-labelled CIGB-300 by binding to NPM1^OD (Fig 5D), indicating that Rev, US11 and FITC-labelled CIGB-300 have overlapping binding sites on NPM1^OD.

To obtain a first structural assessment of NPM1^OD site targeted by CIGB-300 we conducted a multistage protein-ligand docking approach. Assuming that basic part of CIGB-300 determines the binding, its Tat tail was docked in the first step. In the second step, the cyclic part was placed on the surface of NPM1^OD and linked to the peptide fulfilling geometry and energy criteria. Whole peptide contacted three out of five monomeric units of the pentameric NPM1^OD, but in a way that enables five copies of CIGB-300 to be generated without sterical clashes (Fig 5E). It is important to note that a stoichiometry of 1:1 emerged spontaneously, as

the criteria that five peptides should bind to NPM1^{OD} pentamer was not applied while generating of the model. The feature that CIGB-300 wraps around at least several monomeric units (Fig 5E, middle panel) points to a stabilization effect of bound peptides and is consistent with the model of NPM1 in complex with R-rich proteins, such as p19^{ARF}, ARF6, Rev and the ribosomal protein L5 [36].
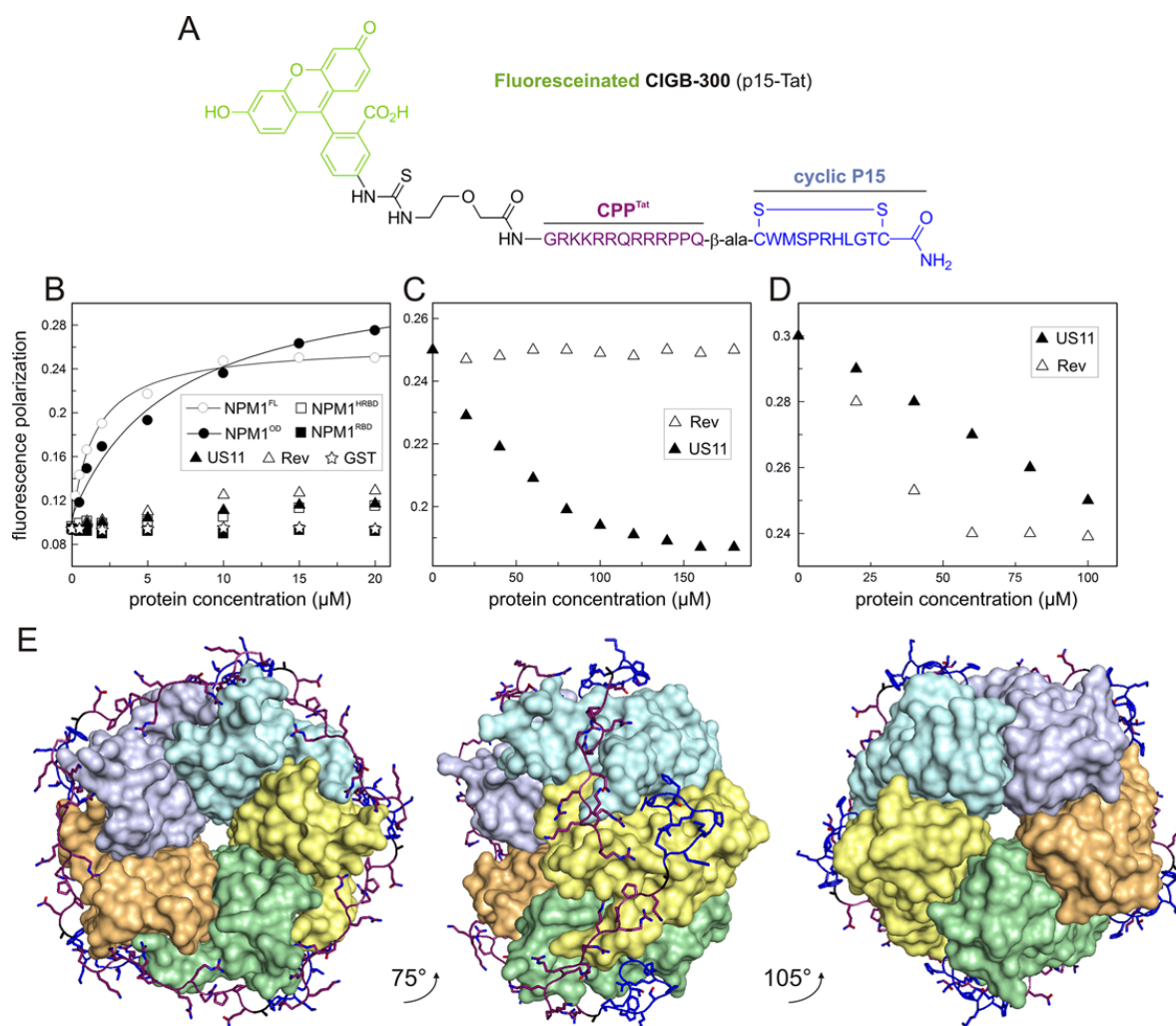

Fig 5. The synthetic peptide CIGB-300 competes with Rev and US11 by binding NPM1^{OD} with high-affinity. (A) CIGB-300 consists of the cyclic P15 (blue) and the Tat (purple) peptides, and labeled with fluorescein (green; FITC). (B) Fluorescence polarization experiments conducted by titrating increasing amounts of NMP1 variants, Rev, US11, and GST to 0.1 μM FITC-labelled CIGB-300 (f CIGB-300). A high affinity interaction with the peptide was only observed for NPM1^{FL} and NPM1^{OD}, resulting from an increase of polarization, but not for Rev, US11, GST, and the other NPM1 variants. (C-D) Contrary to US11, Rev only displaced NPM1^{OD} from its fCIGB-300 complex. Displacement experiments were performed by adding increasing amounts of Rev or US11 to the NPM1^{FL}-fCIGB-300 complex (C) or to the NPM1^{OD}-fCIGB-300 complex (D). (E) A proposed NPM1^{OD}-CIGB-300 docking model of pentameric NPM1^{OD} structure in the complex with CIGB-300. Cyclic part (blue) and basic part (purple) of the peptide shown as sticks and ribbons wraps around several monomeric units of NPM1 represented by surfaces in different colors shown in top view (left), rotated orientation (middle), and the bottom view (right).

HIV-1 production is influenced in CIGB-300 treated cells

In order to investigate the possible role of NPM1-Rev interaction for HIV-1 replication, HOS-CD4.CXCR4 cells were incubated with CIGB-300 for 30 min or left untreated. After removing the peptide, cells were infected with HIV-1 (clone NL4.3, MOI 1). Culture supernatants were collected 48 and 72 h post infection and were quantified by titration on the HIV-1 reporter cells TZM-bl. In cells treated with CIGB-300, the virus production was reduced by 63% and 70% after 48 h and 72 h post infection, respectively (Fig 6). Thus, CIGB-300 may
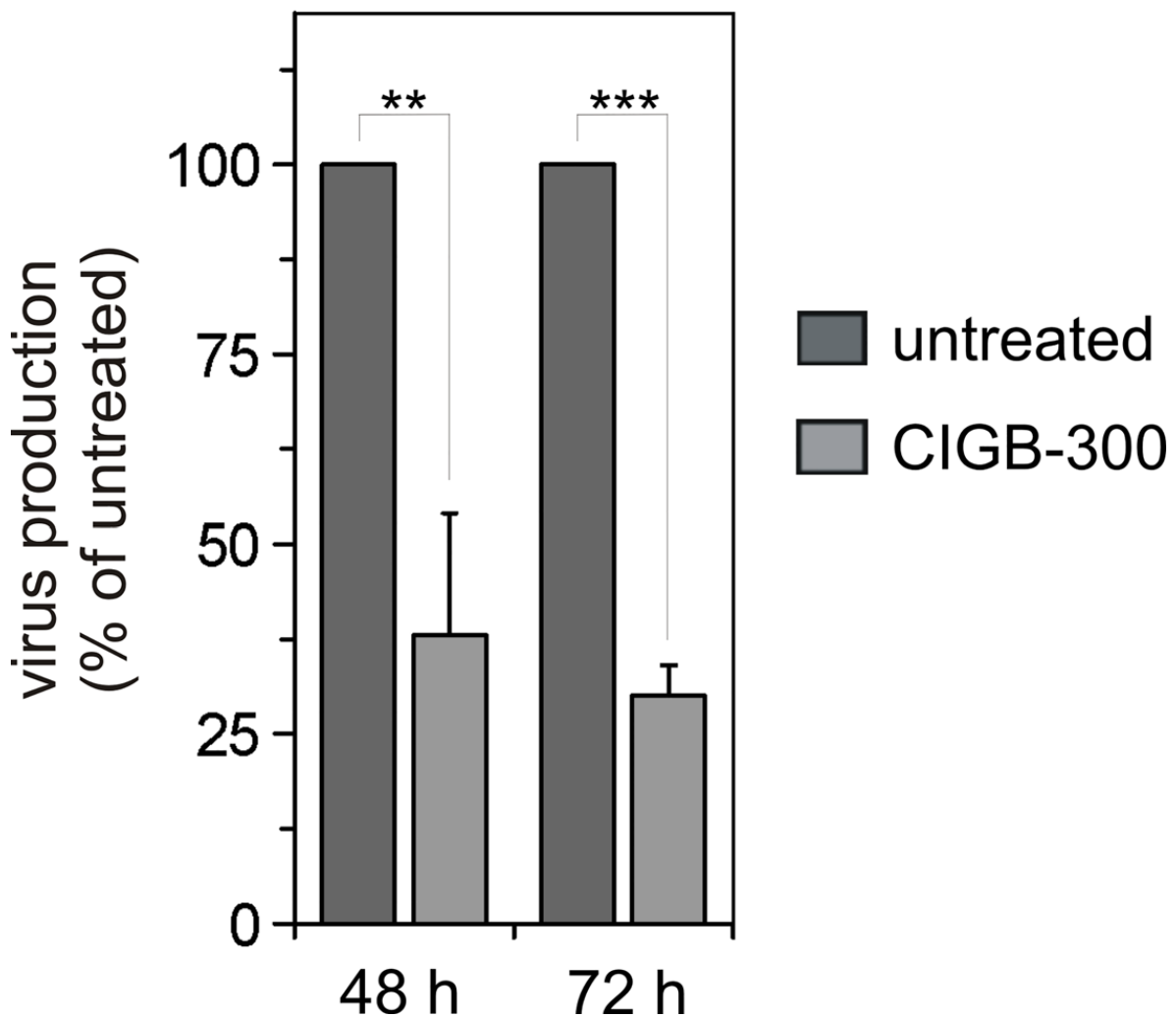
Fig 6. CIGB300 treatment interferes with HIV-1 production. CIGB-300 treated or untreated HOS.CD4.CXCR4 cells were infected with NL4.3 virus at an MOI of 1. Culture supernatant was collected 48 and 72 h post infection and virus titer was determined. The figure shows one representative experiment out of four, in which virus quantification was performed by TZM-bl cell titration. Values are the means ± S.D. of three measurements. Statistical significance (P) was calculated by the Student`s t-test: ***P<0.002; **P<0.02.

doi:10.1371/journal.pone.0143634.g006

interfere with an NPM1-Rev interaction in cells and affect Rev-dependent gene expression and subsequently HIV infection.

Discussion

Since its discovery 34 years ago, intensive research has been performed on NPM1. NPM1 is ubiquitously expressed and significantly upregulated in response to cellular stress signals [18, 19, 41, 42] leading to the alteration of nucleolar structures and its re-localization to other cellular compartments. As a global effector, it has been implicated in maintenance of genomic stability, transcriptional gene regulation, ribosome biogenesis, centrosome duplication, DNA repair, control of cellular senescence, protection against radiation-induced apoptosis, tumor suppression, and has been increasingly emerging as a potential cellular factor for viral infection (see Table 1). Most of these functions have hitherto remained obscure and unexplained.

To shed light on the association of NPM1 with viral proteins, we have investigated its physical interaction with HIV-1 protein Rev and HSV-1 protein US11. Based on our results Rev exhibits affinity towards two NPM1 binding sites: on the pentameric, N-terminal oligomerization domain (NPM1^{OD}) and on the central histone-binding domain (NPM1^{HBD}), while HSV-US11 has only one binding site on NPM1^{OD}. We suggest that the different NPM1 domains interact in a mechanistically different mode with the Rev and US11 proteins. Rev association with NPM1 is the result of presumably an RNA-independent bimodal binding mechanism, according to our data, of (i) a low-affinity binding to the histone-binding domain of NPM1 (K_d = 5.8 µM) and (ii) a very high-affinity binding to oligomerization domain of NPM1 (K_d = 0.013 µM), leading to an overall K_d value of 0.4 µM for the full-length NPM1 (Table 2). In the case of the NPM1-US11 interaction, we observed a strong binding of US11 to NPM1^{OD}, which is most probably achieved *via* its C-terminal RBD (US11^{Cterm}; See Figs 1A and 4A). While the data regarding US11 reports its unprecedented direct interaction with NPM1, our measurements with Rev confirm previously obtained observations. It has been shown that two different transcripts of NPM1, B23.1 and B23.2, prevent the aggregation of Rev *via* their proposed chaperone activity [43]. B23.1, which was also used in this study, is identical to B23.2 but has a 35-amino acid longer C-terminus. As the prevention of Rev aggregation by both constructs was nearly identical, this C-terminus was excluded from the interaction with Rev [43], which is in agreement with our results from PD and ITC experiments (Fig 2 and S1 Fig; Table 2). Our finding of a 1:1 ratio (n≈ 0.84) between NPM1 and Rev obtained by ITC (Table 2) is also consistent with earlier studies that have suggested a stoichiometric interaction between NPM1 and Rev, and a maximal stimulation of the import of Rev into the nucleus by NPM1 at a 1:1 molar ratio [4, 43]. This stoichiometric ratio suggests that NPM1^{FL} exhibits one binding site for one HIV-1 Rev molecule. Since Rev has the tendency to aggregate also under normal physiological conditions [44], it is very likely that NPM1, by acting as a molecular chaperone, increases Rev's solubility and mobility during the import into and throughout the nucleus.

US11 is an abundant HSV-1 protein, which is expressed late during infection [45]. It has been reported that US11 functionally substitutes Rev and Rex proteins by stimulating expression of glycoproteins required for retroviral envelope synthesis [14]. US11 interaction with cellular proteins may, therefore, be required during HSV-1 infection. However, so far, only a few proteins including 2'-5'-oligoadenylate synthetase [46], cellular kinesin light-chain-related protein PAT1 [45], human ubiquitous kinesin heavy chain [24], protein kinase R (PKR) [47], protein activator of the interferon-induced protein kinase (PACT) [48], and nucleolin [23] have been reported. NPM1 and nucleolin are among the most abundant nucleolar proteins [5] with high functional but not structural similarities. They are usually found in the granular

components and dense fibrillar components of nucleoli, have the same distribution as US11 [49], and are re-localized during HSV-1 infection [7, 50]. With NPM1, we have identified in this study a new nucleolar protein partner for US11 and characterized the subdomains responsible for their interactions. US11 has two domains (Fig 1A): An N-terminal domain called effector domain (ED) and a C-terminal RNA-binding domain (RBD). C-terminal domain consisting of 20–24 XPR (X, any amino acid; P, proline; R, arginine) repeats has a polyproline type II helix organization and is usually engaged in interactions with other proteins [15]. US11^{ED} is necessary for transactivation of gene expression, transport, and mRNA translation [15]. Therefore, we designed two deletion variants of US11 (N- and C- terminus) to determine the part involved in the interaction with NPM1. In contrast to nucleolin, which has been reported to interact with the C-terminus of US11 [23], our data clearly shows that both domains are apparently required for the interaction with NPM1. The C-terminal domain of US11, which is involved in the nucleolar localization of US11, binds to NPM1 stronger than the N-terminal domain (Fig 4A). Since C-terminus of US11 is rich in arginine, these results support the idea that arginine-rich motif (R-rich) mediates the interactions with NPM1 [36]. Synthetic peptide CIGB-300 used in our investigation also falls into this category as it is the conjugate of R-rich peptide Tat, and the cyclic peptide (hence is called p15-Tat; Fig 5A). This peptide, which has been described as a proapoptotic peptide with antiproliferative activity *in vitro* and antitumoral activity *in vivo* [51], has been reported to directly bind to NPM1 [39, 40]. We observed in this study that only NPM1^{OD}, but not the other domains of NPM1, associates with fCIGB-300. Interestingly, the K_d value for the fCIGB-300 interaction with NPM1^{FL}, derived from our polarization measurements (Fig 5B), was indicative of almost 5-fold higher affinity than that of fCIGB-300-NPM1^{OD} interaction. This higher affinity can be explained by an avidity effect that originates from core N-terminal domain and the dynamic flexible tails, similarly to the model proposed for nucleoplasmin interaction with histones [52]. NPM1^{OD} is followed by the two highly acidic regions with disordered structure and a C-terminal RBD that folds as a three-helix bundle [53]. The biological significance of the acidic regions (A1-A3; Fig 1A) has not been established. The A1 region in NPM1^{OD} has been recently shown to play a crucial role in the interaction with R-rich motifs of NPM1 binding proteins, such as p19ARF, ARF6, the ribosomal protein L5, and HIV1 Rev [36]. A model of the complex between NPM1^{OD} and CIGB-300 provided insights into different sites for the association of the CIGB-300 peptide, especially the R-rich motif of the CPP^{Tat} contacting negative charges of the A1 region of NPM1^{OD} (Figs 1A and 5E). Additionally, our displacement experiment with Rev indicates that CIGB-300 shares the same binding site on NPM1 and may act as an inhibitor of NPM1-Rev interaction. Most likely for the same reason, we observed a reduced expression of viral production in HIV-1 infected cells treated with the CIGB-300 peptide (Fig 6).

Furthermore, our displacement data shows that the NPM1-US11 interaction was also modulated by CIGB-300 (Fig 5C and 5D). Thus, it is tempting to speculate that US11 and Rev, two functionally homologous viral proteins, share a similar binding site on NPM1 as suggested in this study for CIGB-300. An amino acid sequence analysis revealed clear differences in the R-rich motifs between Rev (^{38}RRNRRRRWRARAR^{48}) and US11, which consists of 21 `XPR´ repeat motifs in US11^{Cterm}. R-rich motifs act as NLS by binding to the nuclear import receptors in nuclear translocation of viral proteins [10, 12, 54, 55]. On the other hand, nucleolar shuttling and accumulation of Rev requires interaction with NPM1 [4, 12]. US11 is similarly shuttling between the nucleus and the cytoplasm in transiently transfected cells and HSV-1-infected cells [20, 56]. Mutagenesis and modeling studies of the C-terminus of US11, containing XPR repeats, have shown that this region is critical for both nucleolar accumulation of US11 and its nucleocytoplasmic export [15, 57]. As mentioned above, CIGB-300 has the cell penetrating peptide Tat with R-rich motif, which corresponds to the presumed nuclear localization signal

(NLS). Tat moves across the nuclear envelope and consequently drives CIGB-300 to the nucleus. Thus, we hypothesize that, (i) R-rich motifs of viral proteins serve as NPM1 binding sites that facilitate their nuclear transport analogous to NLS-importin system, and (ii) NPM1 most likely acts as an auxiliary factor for R-rich motif-containing viral proteins, such as HIV-1 Rev and HSV-1 US11, and achieves their transport into different nuclear compartments and subnuclear domains, leading to nuclear egress of infectious viral particles. Thus, NPM1 seems to represent a key protein in viral infections that is hijacked by invading pathogens to facilitate infection. As a consequence, NPM1 may represent a novel promising target for antiviral therapeutic intervention.

Supporting Information

S1 Fig. Physical interaction of HIV-1 Rev with NPM1. Quantitative interaction analysis were performed by ITC at 25°C by titrating (A) NPM1OD (450 μM) to 30 μM HIV-1 Rev, (B) NPM1HBD (350 μM) to 25 μM HIV-1 Rev and (C) NPM1HRBD (800 μM) to 50 μM HIV-1 Rev, respectively. The upper graph shows calorimetric changes plotted versus the time, and the lower graph represents the changes in temperature according to the molar ratio of the interacting proteins.
(TIF)

S2 Fig. Analytical ultracentrifugation for the determination of the oligomeric state and molecular mass of US11 and NPM1. (A) Sedimentation velocity analysis of US11^{FL} and NPM1^{FL} at 35,000 rpm and 20°C. Graphs show the evaluated c(s) distributions obtained by SEDFIT. For presentation, curves had been normalized to maximum peak height. Results revealed that NPM1^{FL} and US11^{FL} are pentameric and monomeric, respectively. (B) The left panel contains data obtained from the sedimentation velocity analysis of NPM1^{OD}, which shows the population of pentamer, and the right panel are data obtained from sedimentation equilibrium analysis of 0.25 μM NPM1^{OD} at 14000 (purple), 16000 (blue), 25000 (cyan), 42000 (green) and 50000 rpm (yellow) at 20°C. Experimentally determined concentration profiles were fitted globally with a single species model resulting in a molecular mass of 65180 ±640 Da corresponding to a pentamer of NPM1^{OD}. The experimental data together with the fitted concentration profiles are shown on the top, and at the bottom, residuals from the fit are documented.
(TIF)

Author Contributions

Conceived and designed the experiments: KN MRA CM. Performed the experiments: KN JMM AH RD EA ML LNS. Analyzed the data: KN MRA CM LNS RD. Contributed reagents/materials/analysis tools: KN MRA RD EA LGM SH LB HH LS LB SHJS. Wrote the paper: KN MRA.

References

1. Colombo E, Alcalay M, Pelicci PG. Nucleophosmin and its complex network: a possible therapeutic target in hematological diseases. Oncogene. 2011; 30(23):2595–609. doi: 10.1038/onc.2010.646 PMID: 21278791

2. Okuwaki M, Matsumoto K, Tsujimoto M, Nagata K. Function of nucleophosmin/B23, a nucleolar acidic protein, as a histone chaperone. FEBS Lett. 2001; 506(3):272–6. PMID: 11602260

3. Okuwaki M. The Structure and Functions of NPM1/Nucleophsmin/B23, a Multifunctional Nucleolar Acidic Protein. Journal of Biochemistry. 2007; 143(4):441–8. doi: 10.1093/jb/mvm222 PMID: 18024471

4. Fankhauser C, Izaurralde E, Adachi Y, Wingfield P, Laemmli UK. Specific complex of human immunodeficiency virus type 1 rev and nucleolar B23 proteins: dissociation by the Rev response element. Mol Cell Biol. 1991; 11(5):2567–75. PMID: 2017166

5. Taha MS, Nouri K, Milroy LG, Moll JM, Herrmann C, Brunsveld L, et al. Subcellular fractionation and localization studies reveal a direct interaction of the fragile X mental retardation protein (FMRP) with nucleolin. PLoS ONE. 2014; 9(3):e91465. Epub 2014/03/25. doi: 10.1371/journal.pone.0091465 PMID: 24658146; PubMed Central PMCID: PMC3962360.

6. Adachi Y, Copeland TD, Hatanaka M, Oroszlan S. Nucleolar targeting signal of Rex protein of human T-cell leukemia virus type I specifically binds to nucleolar shuttle protein B-23. J Biol Chem. 1993; 268 (19):13930–4. Epub 1993/07/05. PMID: 8314759.

7. Lymberopoulos MH, Bourget A, Abdeljelil NB, Pearson A. Involvement of the UL24 protein in herpes simplex virus 1-induced dispersal of B23 and in nuclear egress. Virology. 2011; 412(2):341–8. doi: 10. 1016/j.virol.2011.01.016 PMID: 21316727

8. Hope TJ. The ins and outs of HIV Rev. Arch Biochem Biophys. 1999; 365(2):186–91. Epub 1999/05/ 18. doi: 10.1006/abbi.1999.1207 PMID: 10328811.

9. Cochrane AW, Perkins A, Rosen CA. Identification of sequences important in the nucleolar localization of human immunodeficiency virus Rev: relevance of nucleolar localization to function. J Virol. 1990; 64 (2):881–5. Epub 1990/02/01. PMID: 2404140; PubMed Central PMCID: PMC249184.

10. Suhasini M, Reddy TR. Cellular proteins and HIV-1 Rev function. Curr HIV Res. 2009; 7(1):91–100. PMID: 19149558

11. Kula A, Guerra J, Knezevich A, Kleva D, Myers MP, Marcello A. Characterization of the HIV-1 RNA associated proteome identifies Matrin 3 as a nuclear cofactor of Rev function. Retrovirology. 2011; 8 (60):1742–4690.

12. Lin MH, Sivakumaran H, Apolloni A, Wei T, Jans DA, Harrich D. Nullbasic, a potent anti-HIV tat mutant, induces CRM1-dependent disruption of HIV rev trafficking. PLoS ONE. 2012; 7(12):e51466. Epub 2012/12/20. doi: 10.1371/journal.pone.0051466 PMID: 23251541; PubMed Central PMCID: PMC3519632.

13. He JJ, Henao-Mejia J, Liu Y. Sam68 functions in nuclear export and translation of HIV-1 RNA. RNA Biol. 2009; 6(4):384–6. PMID: 19535902

14. Diaz JJ, Dodon MD, Schaerer-Uthurralt N, Simonin D, Kindbeiter K, Gazzolo L, et al. Post-transcriptional transactivation of human retroviral envelope glycoprotein expression by herpes simplex virus Us11 protein. Nature. 1996; 379(6562):273–7. PMID: 8538795

15. Schaerer-Uthurralt N, Erard M, Kindbeiter K, Madjar JJ, Diaz JJ. Distinct domains in herpes simplex virus type 1 US11 protein mediate post-transcriptional transactivation of human T-lymphotropic virus type I envelope glycoprotein gene expression and specific binding to the Rex responsive element. J Gen Virol. 1998; 79(Pt 7):1593–602. PMID: 9680120

16. Kelly BJ, Fraefel C, Cunningham AL, Diefenbach RJ. Functional roles of the tegument proteins of herpes simplex virus type 1. Virus Res. 2009; 145(2):173–86. Epub 2009/07/21. doi: 10.1016/j.virusres. 2009.07.007 PMID: 19615419.

17. Roller RJ, Monk LL, Stuart D, Roizman B. Structure and function in the herpes simplex virus 1 RNA-binding protein U(s)11: mapping of the domain required for ribosomal and nucleolar association and RNA binding in vitro. J Virol. 1996; 70(5):2842–51. PMID: 8627758

18. Mulvey M, Arias C, Mohr I. Resistance of mRNA translation to acute endoplasmic reticulum stress-inducing agents in herpes simplex virus type 1-infected cells requires multiple virus-encoded functions. J Virol. 2006; 80(15):7354–63. Epub 2006/07/15. doi: 10.1128/jvi.00479-06 PMID: 16840316; PubMed Central PMCID: PMC1563692.

19. Giraud S, Diaz-Latoud C, Hacot S, Textoris J, Bourette RP, Diaz JJ. US11 of herpes simplex virus type 1 interacts with HIPK2 and antagonizes HIPK2-induced cell growth arrest. J Virol. 2004; 78(6):2984–93. PMID: 14990717

PLOS | ONE

20.   Xing J, Wu F, Pan W, Zheng C. Molecular anatomy of subcellular localization of HSV-1 tegument protein US11 in living cells. Virus Research. 2010; 153(1):71–81. doi: 10.1016/j.virusres.2010.07.009 PMID: 20633584

21.   Salsman J, Zimmerman N, Chen T, Domagala M, Frappier L. Genome-wide screen of three herpesviruses for protein subcellular localization and alteration of PML nuclear bodies. PLoS Pathog. 2008; 4 (7):e1000100. Epub 2008/07/12. doi: 10.1371/journal.ppat.1000100 PMID: 18617993; PubMed Central PMCID: PMC2438612.

22.   Roller RJ, Roizman B. Herpes simplex virus 1 RNA-binding protein US11 negatively regulates the accumulation of a truncated viral mRNA. J Virol. 1991; 65(11):5873–9. PMID: 1656075

23.   Greco A, Arata L, Soler E, Gaume X, Coute Y, Hacot S, et al. Nucleolin Interacts with US11 Protein of Herpes Simplex Virus 1 and Is Involved in Its Trafficking. Journal of Virology. 2011; 86(3):1449–57. doi: 10.1128/jvi.06194-11 PMID: 22130536

24.   Diefenbach RJ, Miranda-Saksena M, Diefenbach E, Holland DJ, Boadle RA, Armati PJ, et al. Herpes simplex virus tegument protein US11 interacts with conventional kinesin heavy chain. J Virol. 2002; 76 (7):3282–91. Epub 2002/03/09. PMID: 11884553; PubMed Central PMCID: PMC136023.

25.   Cassady KA, Gross M. The herpes simplex virus type 1 U(S)11 protein interacts with protein kinase R in infected cells and requires a 30-amino-acid sequence adjacent to a kinase substrate domain. J Virol. 2002; 76(5):2029–35. Epub 2002/02/12. PMID: 11836380; PubMed Central PMCID: PMC135940.

26.   Brown SM, Harland J. Three mutants of herpes simplex virus type 2: one lacking the genes US10, US11 and US12 and two in which Rs has been extended by 6 kb to 0.91 map units with loss of Us sequences between 0.94 and the Us/TRs junction. J Gen Virol. 1987; 68(Pt 1):1–18. PMID: 3027237

27.   Diaz-Latoud C, Diaz JJ, Fabre-Jonca N, Kindbeiter K, Madjar JJ, Arrigo AP. Herpes simplex virus Us11 protein enhances recovery of protein synthesis and survival in heat shock treated HeLa cells. Cell Stress Chaperones. 1997; 2(2):119–31. PMID: 9250403

28.   Yang C, Maiguel DA, Carrier F. Identification of nucleolin and nucleophosmin as genotoxic stress-responsive RNA-binding proteins. Nucleic Acids Res. 2002; 30(10):2251–60. Epub 2002/05/10. PMID: 12000845; PubMed Central PMCID: PMC115285.

29.   Widera M, Erkelenz S, Hillebrand F, Krikoni A, Widera D, Kaisers W, et al. An intronic G run within HIV-1 intron 2 is critical for splicing regulation of vif mRNA. J Virol. 2013; 87(5):2707–20. doi: 10.1128/JVI.02755-12 PMID: 23255806

30.   Jaiswal M, Dubey BN, Koessmeier KT, Gremer L, Ahmadian MR. Biochemical assays to characterize Rho GTPases. Methods Mol Biol. 2012; 827:37–58. Epub 2011/12/07. doi: 10.1007/978-1-61779-442-1_3 PMID: 22144266.

31.   Eberth A, Ahmadian MR. In vitro GEF and GAP assays. Curr Protoc Cell Biol. 2009;Chapter 14:Unit 14 9. Epub 2009/06/06. doi: 10.1002/0471143030.cb1409s43 PMID: 19499504.

32.   Risse SL, Vaz B, Burton MF, Aspenstrom P, Piekorz RP, Brunsveld L, et al. SH3-mediated targeting of Wrch1/RhoU by multiple adaptor proteins. Biol Chem. 2013; 394(3):421–32. Epub 2012/11/28. doi: 10.1515/hsz-2012-0246 PMID: 23183748.

33.   Wennerberg K, Der CJ. Rho-family GTPases: it's not only Rac and Rho (and I like it). J Cell Sci. 2004; 117(Pt 8):1301–12. PMID: 15020670

34.   Lam BD, Hordijk PL. The Rac1 hypervariable region in targeting and signaling: a tail of many stories. Small GTPases. 2013; 4(2):78–89. Epub 2013/01/29. doi: 10.4161/sgtp.23310 PMID: 23354415; PubMed Central PMCID: PMC3747260.

35.   Thakur HC, Singh M, Nagel-Steger L, Kremer J, Prumbaum D, Fansa EK, et al. The centrosomal adaptor TACC3 and the microtubule polymerase chTOG interact via defined C-terminal subdomains in an Aurora-A kinase-independent manner. J Biol Chem. 2014; 289(1):74–88. Epub 2013/11/26. doi: 10.1074/jbc.M113.532333 PMID: 24273164; PubMed Central PMCID: PMC3879581.

36.   Mitrea DM, Grace CR, Buljan M, Yun MK, Pytel NJ, Satumba J, et al. Structural polymorphism in the N-terminal oligomerization domain of NPM1. Proc Natl Acad Sci U S A. 2014; 111(12):4466–71. doi: 10.1073/pnas.1321007111 PMID: 24616519

37.   Brooks BR, Brooks CL III, Mackerell AD Jr, Nilsson L, Petrella RJ, Roux B, et al. CHARMM: the biomolecular simulation program. J Comput Chem. 2009; 30(10):1545–614. Epub 2009/05/16. doi: 10.1002/jcc.21287 PMID: 19444816; PubMed Central PMCID: PMC2810661.

38.   Miyazaki Y, Nosaka T, Hatanaka M. The post-transcriptional regulator Rev of HIV: implications for its interaction with the nucleolar protein B23. Biochimie. 1996; 78(11–12):1081–6. PMID: 9150888

39.   Perera Y, Farina HG, Gil J, Rodriguez A, Benavent F, Castellanos L, et al. Anticancer peptide CIGB-300 binds to nucleophosmin/B23, impairs its CK2-mediated phosphorylation, and leads to apoptosis through its nucleolar disassembly activity. Molecular Cancer Therapeutics. 2009; 8(5):1189–96. doi: 10.1158/1535-7163.mct-08-1056 PMID: 19417160

40. Perera Y, Costales HC, Diaz Y, Reyes O, Farina HG, Mendez L, et al. Sensitivity of tumor cells towards CIGB-300 anticancer peptide relies on its nucleolar localization. J Pept Sci. 2012; 18(4):215–23. Epub 2012/03/13. doi: 10.1002/psc.1432 PMID: 22407768.

41. Kurki S, Peltonen K, Laiho M. Nucleophosmin, HDM2 and p53: players in UV damage incited nucleolar stress response. Cell Cycle. 2004; 3(8):976–9. PMID: 15254398

42. Lindstrom MS, Zhang Y. B23 and ARF: friends or foes? Cell Biochem Biophys. 2006; 46(1):79–90. PMID: 16943625

43. Szebeni A, Olson MO. Nucleolar protein B23 has molecular chaperone activities. Protein Sci. 1999; 8 (4):905–12. PMID: 10211837

44. DiMattia MA, Watts NR, Stahl SJ, Rader C, Wingfield PT, Stuart DI, et al. Implications of the HIV-1 Rev dimer structure at 3.2 A resolution for multimeric binding to the Rev response element. Proc Natl Acad Sci U S A. 2010; 107(13):5810–4. doi: 10.1073/pnas.0914946107 PMID: 20231488

45. Benboudjema L, Mulvey M, Gao Y, Pimplikar SW, Mohr I. Association of the herpes simplex virus type 1 Us11 gene product with the cellular kinesin light-chain-related protein PAT1 results in the redistribution of both polypeptides. J Virol. 2003; 77(17):9192–203. Epub 2003/08/14. PMID: 12915535; PubMed Central PMCID: PMC187382.

46. Sanchez R, Mohr I. Inhibition of cellular 2'-5' oligoadenylate synthetase by the herpes simplex virus type 1 Us11 protein. J Virol. 2007; 81(7):3455–64. PMID: 17229694

47. Khoo D, Perez C, Mohr I. Characterization of RNA determinants recognized by the arginine- and proline-rich region of Us11, a herpes simplex virus type 1-encoded double-stranded RNA binding protein that prevents PKR activation. J Virol. 2002; 76(23):11971–81. Epub 2002/11/05. PMID: 12414939; PubMed Central PMCID: PMC136894.

48. Peters GA, Khoo D, Mohr I, Sen GC. Inhibition of PACT-mediated activation of PKR by the herpes simplex virus type 1 Us11 protein. J Virol. 2002; 76(21):11054–64. Epub 2002/10/09. PMID: 12368348; PubMed Central PMCID: PMC136652.

49. Besse S, Diaz JJ, Pichard E, Kindbeiter K, Madjar JJ, Puvion-Dutilleul F. In situ hybridization and immuno-electron microscope analyses of the Us11 gene of herpes simplex virus type 1 during transient expression. Chromosoma. 1996; 104(6):434–44. Epub 1996/03/01. PMID: 8601338.

50. Lymberopoulos MH, Pearson A. Involvement of UL24 in herpes-simplex-virus-1-induced dispersal of nucleolin. Virology. 2007; 363(2):397–409. Epub 2007/03/10. doi: 10.1016/j.virol.2007.01.028 PMID: 17346762.

51. Perea SE, Reyes O, Baladron I, Perera Y, Farina H, Gil J, et al. CIGB-300, a novel proapoptotic peptide that impairs the CK2 phosphorylation and exhibits anticancer properties both in vitro and in vivo. Molecular and Cellular Biochemistry. 2008; 316(1–2):163–7. doi: 10.1007/s11010-008-9814-5 PMID: 18575815

52. Taneva SG, Bañuelos S, Falces J, Arregi I, Muga A, Konarev PV, et al. A Mechanism for Histone Chaperoning Activity of Nucleoplasmin: Thermodynamic and Structural Models. Journal of Molecular Biology. 2009; 393(2):448–63. doi: 10.1016/j.jmb.2009.08.005 PMID: 19683001

53. Gallo A, Lo Sterzo C, Mori M, Di Matteo A, Bertini I, Banci L, et al. Structure of Nucleophosmin DNA-binding Domain and Analysis of Its Complex with a G-quadruplex Sequence from the c-MYC Promoter. Journal of Biological Chemistry. 2012; 287(32):26539–48. doi: 10.1074/jbc.M112.371013 PMID: 22707729

54. Jeang KT, Xiao H, Rich EA. Multifaceted activities of the HIV-1 transactivator of transcription, Tat. J Biol Chem. 1999; 274(41):28837–40. Epub 1999/10/03. PMID: 10506122.

55. Cardarelli F, Serresi M, Bizzarri R, Giacca M, Beltram F. In vivo study of HIV-1 Tat arginine-rich motif unveils its transport properties. Mol Ther. 2007; 15(7):1313–22. Epub 2007/05/17. doi: 10.1038/sj.mt.6300172 PMID: 17505482.

56. Attrill HL, Cumming SA, Clements JB, Graham SV. The herpes simplex virus type 1 US11 protein binds the coterminal UL12, UL13, and UL14 RNAs and regulates UL13 expression in vivo. J Virol. 2002; 76 (16):8090–100. Epub 2002/07/23. PMID: 12134014; PubMed Central PMCID: PMC155164.

57. Catez F, Erard M, Schaerer-Uthurralt N, Kindbeiter K, Madjar JJ, Diaz JJ. Unique Motif for Nucleolar Retention and Nuclear Export Regulated by Phosphorylation. Molecular and Cellular Biology. 2002; 22 (4):1126–39. doi: 10.1128/mcb.22.4.1126–1139.2002 PMID: 11809804

58. Bevington JM, Needham PG, Verrill KC, Collaco RF, Basrur V, Trempe JP. Adeno-associated virus interactions with B23/Nucleophosmin: identification of sub-nucleolar virion regions. Virology. 2007; 357 (1):102–13. Epub 2006/09/09. doi: 10.1016/j.virol.2006.07.050 PMID: 16959286; PubMed Central PMCID: PMC1829415.

59. Matthews DA. Adenovirus protein V induces redistribution of nucleolin and B23 from nucleolus to cytoplasm. J Virol. 2001; 75(2):1031–8. Epub 2001/01/03. doi: 10.1128/jvi.75.2.1031–1038.2001 PMID: 11134316; PubMed Central PMCID: PMC113999.

60. Ugai H, Dobbins GC, Wang M, Le LP, Matthews DA, Curiel DT. Adenoviral protein V promotes a process of viral assembly through nucleophosmin 1. Virology. 2012; 432(2):283–95. Epub 2012/06/22. doi: 10.1016/j.virol.2012.05.028 PMID: 22717133; PubMed Central PMCID: PMC3423539.

61. Okuwaki M, Iwamatsu A, Tsujimoto M, Nagata K. Identification of nucleophosmin/B23, an acidic nucleolar protein, as a stimulatory factor for in vitro replication of adenovirus DNA complexed with viral basic core proteins. J Mol Biol. 2001; 311(1):41–55. Epub 2001/07/27. doi: 10.1006/jmbi.2001.4812 PMID: 11469856.

62. Samad MA, Okuwaki M, Haruki H, Nagata K. Physical and functional interaction between a nucleolar protein nucleophosmin/B23 and adenovirus basic core proteins. FEBS Lett. 2007; 581(17):3283–8. Epub 2007/07/03. doi: 10.1016/j.febslet.2007.06.024 PMID: 17602943.

63. Samad MA, Komatsu T, Okuwaki M, Nagata K. B23/nucleophosmin is involved in regulation of adenovirus chromatin structure at late infection stages, but not in virus replication and transcription. J Gen Virol. 2012; 93(Pt 6):1328–38. Epub 2012/02/18. doi: 10.1099/vir.0.036665–0 PMID: 22337638.

64. Abraham R, Mudaliar P, Jaleel A, Srikanth J, Sreekumar E. High throughput proteomic analysis and a comparative review identify the nuclear chaperone, Nucleophosmin among the common set of proteins modulated in Chikungunya virus infection. J Proteomics. 2015; 120:126–41. Epub 2015/03/19. doi: 10.1016/j.jprot.2015.03.007 PMID: 25782748.

65. Malik-Soni N, Frappier L. Proteomic profiling of EBNA1-host protein interactions in latent and lytic Epstein-Barr virus infections. J Virol. 2012; 86(12):6999–7002. Epub 2012/04/13. doi: 10.1128/jvi.00194-12 PMID: 22496234; PubMed Central PMCID: PMC3393576.

66. Malik-Soni N, Frappier L. Nucleophosmin contributes to the transcriptional activation function of the Epstein-Barr virus EBNA1 protein. J Virol. 2014; 88(4):2323–6. Epub 2013/11/29. doi: 10.1128/jvi.02521-13 PMID: 24284322; PubMed Central PMCID: PMC3911533.

67. Liu CD, Chen YL, Min YL, Zhao B, Cheng CP, Kang MS, et al. The nuclear chaperone nucleophosmin escorts an Epstein-Barr Virus nuclear antigen to establish transcriptional cascades for latent infection in human B cells. PLoS Pathog. 2012; 8(12):e1003084. Epub 2012/12/29. doi: 10.1371/journal.ppat.1003084 PMID: 23271972; PubMed Central PMCID: PMC3521654.

68. Bazot Q, Deschamps T, Tafforeau L, Siouda M, Leblanc P, Harth-Hertle ML, et al. Epstein-Barr virus nuclear antigen 3A protein regulates CDKN2B transcription via interaction with MIZ-1. Nucleic Acids Res. 2014; 42(15):9700–16. Epub 2014/08/06. doi: 10.1093/nar/gku697 PMID: 25092922; PubMed Central PMCID: PMC4150796.

69. Aminev AG, Amineva SP, Palmenberg AC. Encephalomyocarditis viral protein 2A localizes to nucleoli and inhibits cap-dependent mRNA translation. Virus Res. 2003; 95(1–2):45–57. Epub 2003/08/19. PMID: 12921995.

70. Ning B, Shih C. Nucleolar localization of human hepatitis B virus capsid protein. J Virol. 2004; 78 (24):13653–68. Epub 2004/11/27. doi: 10.1128/jvi.78.24.13653–13668.2004 PMID: 15564475; PubMed Central PMCID: PMC533942.

71. Lee SJ, Shim HY, Hsieh A, Min JY, Jung G. Hepatitis B virus core interacts with the host cell nucleolar protein, nucleophosmin 1. J Microbiol. 2009; 47(6):746–52. Epub 2010/02/04. doi: 10.1007/s12275-009-2720-z PMID: 20127469.

72. Jeong H, Cho MH, Park SG, Jung G. Interaction between nucleophosmin and HBV core protein increases HBV capsid assembly. FEBS Lett. 2014; 588(6):851–8. Epub 2014/01/28. doi: 10.1016/j.febslet.2014.01.020 PMID: 24462683.

73. Li WH, Miao XH, Qi ZT, Ni W, Zhu SY, Fang F. Proteomic analysis of differently expressed proteins in human hepatocellular carcinoma cell lines HepG2 with transfecting hepatitis B virus X gene. Chin Med J (Engl). 2009; 122(1):15–23. Epub 2009/02/04. PMID: 19187611.

74. Ahuja R, Kapoor NR, Kumar V. The HBx oncoprotein of hepatitis B virus engages nucleophosmin to promote rDNA transcription and cellular proliferation. Biochim Biophys Acta. 2015; 1850(8):1783–95. Epub 2015/04/29. doi: 10.1016/j.bbamcr.2015.04.012 PMID: 25918010.

75. Mai RT, Yeh TS, Kao CF, Sun SK, Huang HH, Wu Lee YH. Hepatitis C virus core protein recruits nucleolar phosphoprotein B23 and coactivator p300 to relieve the repression effect of transcriptional factor YY1 on B23 gene expression. Oncogene. 2006; 25(3):448–62. Epub 2005/09/20. doi: 10.1038/sj.onc.1209052 PMID: 16170350.

76. Huang WH, Yung BY, Syu WJ, Lee YH. The nucleolar phosphoprotein B23 interacts with hepatitis delta antigens and modulates the hepatitis delta virus RNA replication. J Biol Chem. 2001; 276(27):25166–75. PMID: 11309377

77. Marasco WA, Szilvay AM, Kalland KH, Helland DG, Reyes HM, Walter RJ. Spatial association of HIV-1 tat protein and the nucleolar transport protein B23 in stably transfected Jurkat T-cells. Arch Virol. 1994; 139(1–2):133–54. Epub 1994/01/01. PMID: 7826206.

78. Li YP. Protein B23 is an important human factor for the nucleolar localization of the human immunodeficiency virus protein Tat. J Virol. 1997; 71(5):4098–102. Epub 1997/05/01. PMID: 9094689; PubMed Central PMCID: PMC191564.

79. Gadad SS, Rajan RE, Senapati P, Chatterjee S, Shandilya J, Dash PK, et al. HIV-1 infection induces acetylation of NPM1 that facilitates Tat localization and enhances viral transactivation. J Mol Biol. 2011; 410(5):997–1007. Epub 2011/07/19. doi: 10.1016/j.jmb.2011.04.009 PMID: 21763502.

80. Oliveira AP, Simabuco FM, Tamura RE, Guerrero MC, Ribeiro PG, Libermann TA, et al. Human respiratory syncytial virus N, P and M protein interactions in HEK-293T cells. Virus Res. 2013; 177(1):108–12. Epub 2013/07/31. doi: 10.1016/j.virusres.2013.07.010 PMID: 23892143.

81. Tsuda Y, Mori Y, Abe T, Yamashita T, Okamoto T, Ichimura T, et al. Nucleolar protein B23 interacts with Japanese encephalitis virus core protein and participates in viral replication. Microbiol Immunol. 2006; 50(3):225–34. Epub 2006/03/21. PMID: 16547420.

82. Sarek G, Jarviluoma A, Moore HM, Tojkander S, Vartia S, Biberfeld P, et al. Nucleophosmin phosphorylation by v-cyclin-CDK6 controls KSHV latency. PLoS Pathog. 2010; 6(3):1000818.

83. Duan Z, Chen J, Xu H, Zhu J, Li Q, He L, et al. The nucleolar phosphoprotein B23 targets Newcastle disease virus matrix protein to the nucleoli and facilitates viral replication. Virology. 2014;452–453:212–22. Epub 2014/03/13. doi: 10.1016/j.virol.2014.01.011 PMID: 24606698.

84. Lv M, Chen J, Shi H, Chen X, Fan X, Shen S, et al. Co-localization analysis between porcine epidemic diarrhea virus nucleocapsid protein and nucleolar phosphoprotein B23.1. Wei Sheng Wu Xue Bao. 2011; 51(5):643–7. Epub 2011/08/02. PMID: 21800627.

Chapter 14

Discussion

Members of the RAS superfamily of small GTPases (small G-proteins, or the Ras superfamily proteins), are involved in nearly every aspect of cell biology. Small GTPases typically function as nodal points that integrate broad upstream regulatory inputs and distribute broad effector outputs (Reiner et al., 2016). RHO and RAS as two main families tune timing of signal transduction and regulate mainly actin dynamics and proliferation, respectively, by cycling as molecular switches between active and inactive states. Their abnormal activation plays a crucial role especially in cardiovascular diseases and cancer. Human proteome consists of 26 RAS, 20 RHO, 70 RHOGEF, 66 RHOGAP and more than 100 RHO effector proteins. This makes the molecular pathways multifaceted. Explicate the interaction networks of these GTPases guides to new strategies to treat diseases. In chapter 2 described briefly the regulation mechanism of RHO family protein and pointed out the importance of their regulation investigations. In chapter 3, we summarized the function and regulation of ROCK, which is the most important drug target in cardiovascular diseases. RHOA-ROCK regulates a wide range of fundamental cell functions, such as contraction, motility, proliferation, and apoptosis. Hyper-activation of this pathway has been observed in cancer, neurodegenerative diseases, and notably in major cardiovascular disorders, including hypertension, atherosclerosis, cerebral cavernous malformations, post-angioplasty restenosis, pulmonary hypertension, and cardiac hypertrophy (Amin et al., 2013). Over the past 20 years development of pharmacological inhibitors interfering with RHOA-ROCK signal transduction were very well investigated. A large number of studies have shown that statins, GGTIs, FIs and kinase inhibitors are valuable inhibitors of RHO-ROCK pathways. Nevertheless, in one hand, targeting protein prenylation inhibits large number of different prenylated proteins and in the other hand, the majority of kinase inhibitors are ATP competitors towards catalytic active sites of kinase domains and lack selectivity. Therefore, specific targeting of RHO-ROCK signal transduction remained to be investigated. Identification of new mechanisms may offer great potential for defining new drug target sites and for attempting a novel strategy for more selective therapeutic intervention. It is of major importance to note that numerous proteins directly or indirectly control the activity of RHO-ROCK signaling pathways. Understanding the mechanisms underlying the negative regulation of RHO-ROCK signaling could lead to the development of novel therapeutic approaches for the treatment of these diseases.

14.1   RHO-RAS interplay

RHO proteins mostly regulate cytoskeleton dynamics while RAS proteins differently control cell differentiation and proliferation. However, there are crosstalks between these pathways. chapter 4 describes a central role of p120RASGAP, a multifunctional regulatory signaling molecule, which links RAS and RHO pathways by physically binding via its SH3 domain to and inhibiting the RHOGAP activity of the tumor suppressor protein DLC1. This effect keeps RHO pathways in an ON status. In the same time, p120RASGAP via its GAP domain switches RAS signal transduction off. Furthermore, p120RASGAP interacts to p190 and p200 RHOGAPs, leading to their recruitment and activation. This nicely illustrates the interdependence of the RAS and RHO signaling pathways and underlines the multifaceted nature of regulatory proteins beyond their critical GAP functions. Cancer cells proliferate uncontrollably and in metastasis stages do metastasis, which further emphasizes critical crosstalks of RAS and RHO proteins. Previously, it has been shown that anticancer phytochemical Rocaglamide (Roc-A) inhibits cell growth and induce apoptosis (Li-Weber, 2015). The mechanism is through inhibition of RAS/RAF kinase pathway by inhibiting prohibitin (Polier et al., 2012). Interestingly, as described in chapter 5, Roc-A inhibits cancer cell migration as well. Mechanistically, Roc-A treatment induces F-actin based morphological changes leading to membrane protrusions. Notably, this effect is emerging from decrease in the activities of the small GTPases RHOA, RAC1 and CDC42. Additional investigations under cell-free conditions clearly demonstrate that this inhibition does not origin from GEFs, GAPs or GDIs. Thus, evidences shows that this inhibition may emerge from early upstream events. Taken together, our results provide evidence that Roc-A may be a lead candidate for a new class of anticancer drugs that inhibit metastasis formation.

14.2   (Dys)Regulation of RHO pathways in cardiovascular system

Among various cardiovascular disorders, endothelial dysfunction is one of the early phases of vascular diseases such as atherosclerosis. In one hand, endothelium functions as a barrier between blood and underlying tissues in vessels and in the other hand regulates trafficking of materials. Any dysfunction could leads to diverse pathological consequences and activation of severe reactions, such as platelet activation and formation of thrombosis. It has been intensively investigated that RHOA and RAC1, among the 20 RHO GTPases, especially regulate endothelial barrier function. It is proposed that RHOA activation decreases and RAC1 activation increases barrier function. But, based on recent publications as there are different types of endothelial cells with diverse functionalities and environment, it seems that this regulation is very complex. In this dissertation, we focus on different points of regulation pathways in endothelial cells. The endothelium is a target for many inflammatory and thrombogenic mediators, which can result in barrier disruption and increased permeability to plasma proteins. Thrombin is a protease that is produced on the surface of injured endothelium from prothrombin circulating in blood and causes disturbance of endothelial barrier function. Consequently, thrombin stimulates the release of inflammatory mediators and vasodilatation agents (Bogatcheva et al., 2002). In addition, thrombin induces leukocyte adhesion on the EC surface and their subsequent penetration into the

underlying tissues. In spite of this, the exact mechanism of its function has not been fully understood yet. p115RHOGEF, a specific GEF for RHOA, plays a critical role in increasing endothelial permeability (EP) stimulated by thrombin (Holinstat et al., 2003). In chapter 6, we used different fluorescence labeling strategies and measured rate constants of all diverse steps of p115-catalyzed nucleotide exchange reactions. This set of complete data led us to estimate exact timing of RHOA activation. To do so we needed cellular concentration of proteins and compounds involved in this mechanism. We have been used endothelial cells isolated from human umbilical cords. In the other hand, recombinant proteins have been expressed in E. coli and purified with affinity chromatography techniques. We used purified proteins to assess specificity of antibodies as well as calibration curves for protein concentrations. Our kinetic data presents an estimation of RHOA activation timing more close to cellular conditions and provides valuable pieces for further system biology studies on signaling pathways. RHOGAP proteins in the opposite site of RHOGEFs have an adjusting function for ECs. Among 66 human RHOGAPs only a few of them are studies in ECs (Buul et al., 2014). P190RHOGAP is the most studied one and it has been shown that its activity enhance endothelial barrier by deactivation of RHOA (Grinnell et al., 2012). So, first we addressed the question how is the specificity and selectivity of RHOGAPs on RHO proteins regulated? In chapter 7 we have chosen representatives among all human RHOGAPs and after recombinant protein expressions and purifications we measured the activity of 14 GAPs on 12 RHO proteins. Our experiments exhibit broad range of catalytic efficiencies and illustrate differential specificities of RHOGAPs towards RHO proteins. Availability of large structural data guided us to investigate evidences of GAP specificities for RHO proteins. We used python capabilities to analyze protein sequences and structures. A python code searches in Uniprot, finds all human proteins containing RHOGAP domain, extracts corresponding sequences and aligns them (Appendix A). Another code takes sequence alignments and PDB code of structures and summarizes interface contacts of complexes in the form of a matrix. Conformational differences in the variable loop of GAP domains contribute to the observed activity changes. In contrast to GEF domains of RhoGEFs (Jaiswal et al., 2013), the GAP domains lack high selectivity for RHO family proteins. Notably, p190 GAP domain displayed high affinities for both RHOA and RHOD in vitro but no activities in HEK 293 cells. In contrast, full-length p190RHOGAP exhibited specificity only for RhoA in HEK 293 cells but not for RhoD. Altogether, we conclude that domains other than GAP domains within RhoGAPs play a major role in conferring substrate specificity and fine-tune their catalytic efficiency and specificity in cells. Further experiment needs to test its effect in endothelial context and investigate its functions. As discussed for example GEFs like p115 and GAPs like p190 regulate activation state of RHO proteins like RHOA. Active RHOA binds and trigger ROCK activation. ROCK is a main regulator of actin-myosin contraction by phosphorylation and inactivation of MLCP and also phosphorylatoin of MLC. Its hyper-activation leads to various cardiovascular diseases such as cerebral vasospasm and hypertension. It has been proposed that ROCK is in an auto-inhibited structure and is released by RHO activation. Also an oligomerization state of this protein is controversial. Recently, protein-protein interactions are found to be a specific target for drug discovery. However, this approach needs a comprehensive understanding of the mechanism of these interactions. Therefore, elucidating the mechanism of ROCK activation opens a window for new class of drug discoveries. In chapter 8 using electron microscopy, we provide structural insights of ROCK full-length in vitro demonstrating an elongated parallel dimer. Sedimentation assay by extracted liposomes shows that ROCK tightly binds to specific lipids, such PIP3. In

another hand, ROCK shows considerable kinase activity and it is not changed significantly in the present of RHOA and/or liposomes. We propose that other proteins, such as scaffold proteins, may modulate auto-inhibited conformation of ROCK in the cellular context. Contraction and relaxation of actomyosins are balanced by MLC phosphorylation triggered by Ca^{2+}. ROCK sensitizes myofilaments to Ca^{2+} and slows down relaxation through phosphorylation of MLCP Figure 1.10 (Solaro, 2000). This vasoactive effect leads to hypertension. Several pathways contribute to this effect. It is known that exposure of vessels to Angiotensin II produced by kidneys increases the blood pressure partly by modifying contraction relaxation states of vessels. In chapter 9, we found that deficiency of CNTF, as a cytokine receptor, protects mice against Angiotensin II-dependent hypertension. The results suggest that CNTF has a major impact on blood pressure regulation induced by Ang-II. It seems that this effect is modulated the Ang-II response via a JAK2/STAT3-dependent mechanism. Phosphorylation of JAK2/STAT3 pathway phosphorylates MLCP probably through activation of RHO/ROCK pathway. Thus, CNTF could be an important regulatory cytokine in the pathogenesis of Ang-II-dependent hypertension. The spatial and temporal organization of molecules within a cell is critical for coordinating many distinct cellular activities. Increasing number of biological processes have been found in which scaffold proteins, statically or dynamically, play a central role in modulating protein-protein interactions (Good et al., 2011; Garbett et al., 2014). Especially for polarized cells, like endothelial cells, the presence of scaffolding proteins is pronounced. It is known that IQGAP has a key scaffolding role to modulate endothelial barrier function. IQGAP binds to RAC1 and CDC42 but not RHOA and preserves the active form of RAC1/DCD42 in place of adherent junctions of endothelial barrier. This reflexes enhancement in barrier function by promoting cortical actin polymerization. However, the exact mechanism of this binding is not well understood. In chapter 10 we identified the binding modes of IQGAP to RAC1/CDC42. We propose that the ability of IQGAP1 to interact with RHO proteins is based on a multiple-step binding process, which is a prerequisite for the dynamic functions of IQGAP1 as a scaffolding protein and a critical mechanism in temporal regulation and integration of IQGAP1-mediated cellular responses. Platelets are involved in the formation of blood clots which cause heart attacks and strokes (Gregg et al., 2003). Over endothelial injury and release of substances like Thrombin and Von Willebrand factor (vWF) or exposure of extracellular matrix (fibrinogen, collagen) to the lumen, platelets are sensitized and undergo activation and aggregation. These processes are regulated by RHO GTPases. It has been shown that RAC1 pathway regulates platelet activation. Previously, it has been studied that NSC23766 and EHT1864 inhibits platelet activation by inhibiting RAC1. In **??** interestingly we have shown that these compounds also inhibit thrombin induced activation and aggregation of RAC1-deficient mouse platelets. We illustrated that this effect arises partly from inhibition of PAK1, a RAC1 effector. These compounds inhibit auto-phosphorylation of PAK1 full length in vitro. It significantly distinguishes off-target effects of these inhibitors, at least in part because of RAC1-independent inhibition of PAK1/PAK2 activation.

14.3   Specificity of RAS pathways

HRAS, KRAS and NRAS are classical RAS proteins that initiate signaling of MAPK pathways. In humans, mutations in genes of this particular pathway cause congenital disorders such as

Costello, LEOPARD and Noonan syndromes, associated with hypertrophic cardiomyopathy (Aoki et al., 2008). Moreover, over expression of RAS proteins in the heart result in cardiac hypertrophy with diastolic dysfunction (Hunter et al., 1995; Sharma, 2015). Thus, understanding the molecular mechanism of processes triggered by RAS proteins has of major importance. Five main effectors of RAS proteins are CRAF, PI3K, PLCε, RALGDS and RASSF5. In chapter 12 we studied the binding affinities of HRAS, KRAS, NRAS, RRAS1 and RRAS2 to the effectors. By analyzing the available structural data, we identified distinct regions at the interface of RAS-effector complexes responsible for binding of RAS proteins exclusively by RB or RA domains. Recent studies has been shown that activating mutations in RAF1 are strongly associated with hypertrophic cardiomyopathy (Yin et al., 2015). Our data provides insights to elucidate the impact of such mutations on interaction with RAS proteins. As we discussed above, the critical role of scaffolding proteins in signal transduction was mentioned. NPM is known to regulate centrosome duplication triggered by RAN activation (Wang, Budhu et al. 2005). NPM is identified as a new class of KRAS regulators that modulates signal transduction via the MAPK pathway (Inder et al., 2010). In chapter 13 we provide structural and biochemical insights into NPM interactions with viral proteins, such as HIV Rev and HSV US11, a mechanism promoting infections. All together, our investigations clearly show that RAS and RHO GTPase pathways play decisive role in regulation biological processes. Additional investigations are needed, especially the less characterized members of the families, in order to identify new targets and target sites for more selective therapies against various diseases, especially cardiovascular disorders.

Appendix A

Alignment extraction from Uniprot

```python
from Bio.Seq import Seq
from Bio.Alphabet import IUPAC
from bioservices.apps.fasta import FASTA
from bioservices import UniProt
from Bio.Align.Applications import ClustalwCommandline


u = UniProt()
print "enter domain name:"
domain_name = raw_input()
print "reviewed? yes/no:"
rev_answ = raw_input()
data_gff = u.search("Domain:%(0)s+and+taxonomy:9606+and+reviewed:%(1)s" % {'0': domain_name
, '1': rev_answ}, frmt="gff")
f = open('gff.txt', 'w')
print >> f, 'gff.txt', data_gff;  # or f.write('...\n')
f.close()

data_table = u.search("Domain:%(0)s+and+taxonomy:9606+and+reviewed:%(1)s" % {'0':
domain_name , '1': rev_answ}, frmt="tab", columns="entry name,id, length, genes")


f = open('table.txt', 'w')
print >> f, 'table.txt', data_table;  # or f.write('...\n')
f.close()

f = open('doamin_sequences.fasta', 'w') # determine residue number of doamins
for line in file('gff.txt', 'r'):
    if "Note=%s"% domain_name in line:
    if "ID=PRO" not in line:
        ID = line.split()[0]
        start = (line.split()[3])
        x = int(start) - 1
        end = line.split()[4]
        y = int(end) - 1
        seq = u.get_fasta_sequence(ID)     # retrive sequences
        seq2 = seq[x:y]
        f.write('>'+ID+'['+start+'-'+end+']'+'\n'+seq2+'\n')

f.close()

import subprocess
from Bio.Align.Applications import ClustalwCommandline                # clustalW alignment
cline = ClustalwCommandline("clustalw", infile="doamin_sequences.fasta")
stdout, stderr = cline()

from Bio import AlignIO
align = AlignIO.read("doamin_sequences.aln", "clustal")
print(align)
```

Bibliography

Ahmadian, M. R., U. Hoffmann, R. S. Goody, and A. Wittinghofer (1997a). "Individual Rate Constants for the Interaction of Ras Proteins with GTPase-Activating Proteins Determined by Fluorescence Spectroscopy". In: *Biochemistry* 36.15, pp. 4535–4541.

Ahmadian, M. R., P. Stege, K. Scheffzek, and A. Wittinghofer (1997b). "Confirmation of the arginine-finger hypothesis for the GAP-stimulated GTP-hydrolysis reaction of Ras". In: *Nature Structural Biology* 4.9, pp. 686–689.

Aittaleb, M., C. A. Boguth, and J. J. G. Tesmer (2010). "Structure and Function of Heterotrimeric G Protein-Regulated Rho Guanine Nucleotide Exchange Factors". In: *Molecular Pharmacology* 77.2. 19880753[pmid] 3550156[PII] Mol Pharmacol, pp. 111–125.

Amado-Azevedo, J., E. T. Valent, and G. P. Van Nieuw Amerongen (2014). "Regulation of the endothelial barrier function: a filum granum of cellular forces, Rho-GTPase signaling and microenvironment". In: *Cell and Tissue Research* 355.3, pp. 557–76.

Amin, E., B. N. Dubey, S. C. Zhang, L. Gremer, R. Dvorsky, J. M. Moll, et al. (2013). "Rho-kinase: regulation, (dys)function, and inhibition". In: *Biological chemistry* 394.11. Amin, Ehsan Dubey, Badri Nath Zhang, Si-Cai Gremer, Lothar Dvorsky, Radovan Moll, Jens M Taha, Mohamed S Nagel-Steger, Luitgard Piekorz, Roland P Somlyo, Avril V Ahmadian, Mohammad R Biol Chem. 2013 Nov 1;394(11):1399-1410. doi: 10.1515/hsz-2013-0181., pp. 1399–1410.

Amin, E., M. Jaiswal, U. Derewenda, K. Reis, K. Nouri, K. T. Koessmeier, et al. (2016). "Deciphering the molecular and functional basis of RhoGAP family proteins: A systematic approach towards selective inactivation of Rho family proteins". In: *Journal of Biological Chemistry*.

Aoki, Y., T. Niihori, Y. Narumi, S. Kure, and Y. Matsubara (2008). "The RAS/MAPK syndromes: novel roles of the RAS pathway in human genetic disorders". In: *Human Mutation* 29.8, pp. 992–1006.

Aslan, J. E. and O. J. T. McCarty (2013). "Rho GTPases in platelet function". In: *Journal of Thrombosis and Haemostasis* 11.1, pp. 35–46.

Bennett, B. D., E. H. Kimball, M. Gao, R. Osterhout, S. J. Van Dien, and J. D. Rabinowitz (2009). "Absolute metabolite concentrations and implied enzyme active site occupancy in Escherichia coli". In: *Nature Chemical Biology* 5.8, pp. 593–9.

Bid, H. K., R. D. Roberts, P. K. Manchanda, and P. J. Houghton (2013). "RAC1: An Emerging Therapeutic Option for Targeting Cancer Angiogenesis and Metastasis". In: *Molecular Cancer Therapeutics* 12.10. 24072884[pmid] Mol Cancer Ther,

Bishop, A. L. and A. Hall (2000). "Rho GTPases and their effector proteins". In: *Biochemical Journal* 348.2, p. 241.

Bogatcheva, N. V., J. G. Garcia, and A. D. Verin (2002). "Molecular mechanisms of thrombin-induced endothelial cell permeability". In: *Biochemistry* 67.1, pp. 75–84.

Boriack-Sjodin, P. A., S. M. Margarit, D. Bar-Sagi, and J. Kuriyan (1998). "The structural basis of the activation of Ras by Sos". In: *Nature* 394.6691. Using Smart Source Parsing Jul 23, pp. 337–43.

Bos, J. L., H. Rehmann, and A. Wittinghofer (2007). "GEFs and GAPs: critical elements in the control of small G proteins". In: *Cell* 129.5. Bos, Johannes L Rehmann, Holger Wittinghofer, Alfred Cell. 2007 Jun 1;129(5):865-77., pp. 865–77.

Boulter, E., R. Garcia-Mata, C. Guilluy, A. Dubash, G. Rossi, P. J. Brennwald, et al. (2010). "Regulation of Rho GTPase crosstalk, degradation and activity by RhoGDI1". In: *Nat Cell Biol* 12.5. 10.1038/ncb2049, pp. 477–483.

Braun, A. C., J. Hendrick, S. A. Eisler, S. Schmid, A. Hausser, and M. A. Olayioye (2015). "The Rho-specific GAP protein DLC3 coordinates endocytic membrane trafficking". In: *Journal of Cell Science* 128.7. Braun, Anja C Hendrick, Janina Eisler, Stephan A Schmid, Simone Hausser, Angelika Olayioye, Monilola A England J Cell Sci. 2015 Apr 1;128(7):1386-99. doi: 10.1242/jcs.163857. Epub 2015 Feb 11., pp. 1386–99.

Brossier, N. M., A. M. Prechtl, J. F. Longo, S. Barnes, L. S. Wilson, S. J. Byer, et al. (2015). "Classic Ras Proteins Promote Proliferation and Survival via Distinct Phosphoproteome Alterations in Neurofibromin-Null Malignant Peripheral Nerve Sheath Tumor Cells". In: *Journal of Neuropathology and Experimental Neurology* 74.6, p. 568.

Bulgin, R., B. Raymond, J. A. Garnett, G. Frankel, V. F. Crepin, C. N. Berger, et al. (2010). "Bacterial Guanine Nucleotide Exchange Factors SopE-Like and WxxxE Effectors". In: *Infection and Immunity* 78.4. 1250-09[PII] 20123714[pmid] Infect Immun, pp. 1417–1425.

Burns, M. E. and E. N. Pugh (2010). "Lessons from Photoreceptors: Turning Off G-Protein Signaling in Living Cells". In: *Physiology* 25.2, pp. 72–84.

Buul, J. D. van, D. Geerts, and S. Huveneers (2014). "Rho GAPs and GEFs Controling switches in endothelial cell adhesion". In: *Cell Adhesion and Migration* 8.2, pp. 108–124.

Carbone, M. L., J. Brégeon, N. Devos, G. Chadeuf, A. Blanchard, M. Azizi, et al. (2015). "Angiotensin II Activates the RhoA Exchange Factor Arhgef1 in Humans". In: *Hypertension* 65.6, pp. 1273–1278.

Castellano, E. and J. Downward (2011a). "RAS Interaction with PI3K: More Than Just Another Effector Pathway". In: *Genes and cancer* 2.3. Castellano, Esther Downward,

Julian Genes Cancer. 2011 Mar;2(3):261-74. doi: 10.1177/1947601911408079., pp. 261–74.

Castellano, E. and J. Downward (2011b). "Role of RAS in the Regulation of PI 3-Kinase". In: *Phosphoinositide 3-kinase in Health and Disease: Volume 1*. Ed. by C. Rommel, B. Vanhaesebroeck, and K. P. Vogt. Berlin, Heidelberg: Springer Berlin Heidelberg, pp. 143–169.

Chen, X. L., J.-O. Nam, C. Jean, C. Lawson, C. T. Walsh, E. Goka, et al. (2012). "VEGF-Induced Vascular Permeability Is Mediated by FAK". In: *Developmental Cell* 22.1, pp. 146–157.

Cherfils, J. and M. Zeghouf (2013). "Regulation of small GTPases by GEFs, GAPs, and GDIs". In: *Physiol Rev* 93.1. Cherfils, Jacqueline Zeghouf, Mahel Research Support, Non-U.S. Gov't Review United States Physiological reviews Physiol Rev. 2013 Jan;93(1):269-309. doi: 10.1152/physrev.00003.2012., pp. 269–309.

Cherfils, J. and P. Chardin (1999). "GEFs: structural basis for their activation of small GTP-binding proteins". In: *Trends in Biochemical Sciences* 24.8, pp. 306–311.

Chistiakov, D. A., A. N. Orekhov, and Y. V. Bobryshev (2015). "Endothelial Barrier and Its Abnormalities in Cardiovascular Disease". In: *Frontiers in Physiology* 6.365.

Coleman, M. L., C. J. Marshall, and M. F. Olson (2004). "RAS and RHO GTPases in G1-phase cell-cycle regulation". In: *Nat Rev Mol Cell Biol* 5.5. 10.1038/nrm1365, pp. 355–366.

Consortium, T. U. (2015). "UniProt: a hub for protein information". In: *Nucleic Acids Research* 43.D1, pp. D204–D212.

Cook, D. R., K. L. Rossman, and C. J. Der (2014). "Rho guanine nucleotide exchange factors: regulators of Rho GTPase activity in development and disease". In: *Oncogene* 33.31. Using Smart Source Parsing Jul 31; doi: 10.1038/onc.2013.362. Epub 2013 Sep 16, pp. 4021–35.

Couzens, A. L., V. Saridakis, and M. P. Scheid (2009). "The hydrophobic motif of ROCK2 requires association with the N-terminal extension for kinase activity". In: *The Biochemical journal* 419.1. Couzens, Amber L Saridakis, Vivian Scheid, Michael P England Biochem J. 2009 Apr 1;419(1):141-8. doi: 10.1042/BJ20081376., pp. 141–8.

Cullere, X., S. K. Shaw, L. Andersson, J. Hirahashi, F. W. Luscinskas, and T. N. Mayadas (2005). "Regulation of vascular endothelial barrier function by Epac, a cAMP-activated exchange factor for Rap GTPase". In: *Blood* 105.5, pp. 1950–1955.

Donninger, H., M. L. Schmidt, J. Mezzanotte, T. Barnoud, and G. J. Clark (2016). "Ras signaling through RASSF proteins". In: *Seminars in Cell and Developmental Biology*.

Dovas, A. and J. R. Couchman (2005). "RhoGDI: multiple functions in the regulation of Rho family GTPase activities". In: *Biochemical Journal* 390.Pt 1. bj3900001[PII] 16083425[pmid] Biochem J, pp. 1–9.

Droppelmann, C. A., D. Campos-Melo, K. Volkening, and M. J. Strong (2014). "The emerging role of guanine nucleotide exchange factors in ALS and other neurodegenerative diseases". In: *Frontiers in Cellular Neuroscience* 8.282.

Elvers, M. (2016). "RhoGAPs and Rho GTPases in platelets". In: *Hämostaseologie* 36.3, pp. 168–177.

Esters, H., K. Alexandrov, A. Iakovenko, T. Ivanova, N. Thoma, V. Rybin, et al. (2001). "Vps9, Rabex-5 and DSS4: proteins with weak but distinct nucleotide-exchange activities for Rab proteins". In: *Journal of molecular biology* 310.1, pp. 141–56.

Etienne-Manneville, S. and A. Hall (2002). "Rho GTPases in cell biology". In: *Nature* 420.6916. 10.1038/nature01148, pp. 629–635.

Fiegen, D., R. Dvorsky, and M. R. Ahmadian (2006). "Structural Principles of Ras Interaction with Regulators and Effectors". In: *RAS Family GTPases*. Ed. by C. Der. Dordrecht: Springer Netherlands, pp. 45–66.

Fritz, R. D. and O. Pertz (2016). "The dynamics of spatio-temporal Rho GTPase signaling: formation of signaling patterns". In: *F1000Research* 5.

Gandhi, S. P. and C. F. Stevens (2003). "Three modes of synaptic vesicular recycling revealed by single-vesicle imaging". In: *Nature* 423.6940, pp. 607–613.

Garbett, D. and A. Bretscher (2014). "The surprising dynamics of scaffolding proteins". In: *Molecular Biology of the Cell* 25.16. 25122925[pmid] E14-04-0878[PII] Mol Biol Cell, pp. 2315–2319.

Garcia-Mata, R., E. Boulter, and K. Burridge (2011). "The 'invisible hand': regulation of RHO GTPases by RHOGDIs". In: *Nature reviews. Molecular cell biology* 12.8, pp. 493–504.

Geissbuehler, M., Z. Kadlecova, H.-A. Klok, and T. Lasser (2012). "Assessment of transferrin recycling by Triplet Lifetime Imaging in living cells". In: *Biomedical Optics Express* 3.10. 172898[PII] 23082293[pmid] Biomed Opt Express, pp. 2526–2536.

Giannotta, M., M. Trani, and E. Dejana (2013). "VE-Cadherin and Endothelial Adherens Junctions: Active Guardians of Vascular Integrity". In: *Developmental Cell* 26.5, pp. 441–454.

Goggs, R., C. M. Williams, H. Mellor, and A. W. Poole (2015). "Platelet Rho GTPases–a focus on novel players, roles and relationships". In: *Biochemical Journal* 466.3, pp. 431–442.

Goicoechea, S. M., S. Awadia, and R. Garcia-Mata (2014). "I'm coming to GEF you: Regulation of RhoGEFs during cell migration". In: *Cell Adhesion and Migration* 8.6, pp. 535–549.

Goldfarb, M., K. Shimizu, M. Perucho, and M. Wigler (1982). "Isolation and preliminary characterization of a human transforming gene from T24 bladder carcinoma cells". In: *Nature* 296.5856. Using Smart Source Parsing Apr 1, pp. 404–9.

Good, M. C., J. G. Zalatan, and W. A. Lim (2011). "Scaffold Proteins: Hubs for Controlling the Flow of Cellular Information". In: *Science (New York, N.Y.)* 332.6030. 21551057[pmid] Science, pp. 680–686.

Gordon, M., M. El-Kalla, and S. Baksh (2012). "RASSF1 Polymorphisms in Cancer". In: *Molecular biology international* 2012. Gordon, Marilyn El-Kalla, Mohamed Baksh, Shairaz Mol Biol Int. 2012;2012:365213. doi: 10.1155/2012/365213. Epub 2012 May 31., p. 365213.

Gregg, D. and P. J. Goldschmidt-Clermont (2003). "Platelets and Cardiovascular Disease". In: *Circulation* 108.13, e88–e90.

Grinnell, K. L. and E. O. Harrington (2012). "Interplay between FAK, PKCdelta, and p190RhoGAP in the regulation of endothelial barrier function". In: *Microvascular Research* 83.1. Grinnell, Katie L Harrington, Elizabeth O R01 HL067795/HL/NHLBI NIH HHS/ R01 HL067795-09/HL/NHLBI NIH HHS/ Microvasc Res. 2012 Jan;83(1):12-21. doi: 10.1016/j.mvr.2011.04.005. Epub 2011 Apr 22., pp. 12–21.

Guilluy, C., J. Bregeon, G. Toumaniantz, M. Rolli-Derkinderen, K. Retailleau, L. Loufrani, et al. (2010). "The Rho exchange factor Arhgef1 mediates the effects of angiotensin II on vascular tone and blood pressure". In: *Nature Medicine* 16.2. Guilluy, Christophe Bregeon, Jeremy Toumaniantz, Gilles Rolli-Derkinderen, Malvyne Retailleau, Kevin Loufrani, Laurent Henrion, Daniel Scalbert, Elizabeth Bril, Antoine Torres, Raul M Offermanns, Stephan Pacaud, Pierre Loirand, Gervaise Nat Med. 2010 Feb;16(2):183-90. doi: 10.1038/nm.2079. Epub 2010 Jan 24., pp. 183–90.

Guo, Z., M. R. Ahmadian, and R. S. Goody (2005). "Guanine nucleotide exchange factors operate by a simple allosteric competitive mechanism". In: *Biochemistry* 44.47, pp. 15423–9.

Guo, Z., X. Hou, R. S. Goody, and A. Itzen (2013). "Intermediates in the Guanine Nucleotide Exchange Reaction of Rab8 Catalyzed by Rabin8/GRAB". In: *The Journal of biological chemistry*.

Ha, B. H., M. J. Davis, C. Chen, H. J. Lou, J. Gao, R. Zhang, et al. (2012). "Type II p21-activated kinases (PAKs) are regulated by an autoinhibitory pseudosubstrate". In: *Proceedings of the National Academy of Sciences of the United States of America* 109.40. 22988085[pmid] 201214447[PII] Proc Natl Acad Sci U S A, pp. 16107–16112.

Harvey, J. J. (1964). "An Unidentified Virus Which Causes the Rapid Production of Tumours in Mice". In: *Nature* 204. Using Smart Source Parsing Dec 12, pp. 1104–5.

Hedman, A. C., J. M. Smith, and D. B. Sacks (2015). "The biology of IQGAP proteins: beyond the cytoskeleton". In: *EMBO Reports* 16.4, pp. 427–46.

Holinstat, M., N. Knezevic, M. Broman, A. M. Samarel, A. B. Malik, and D. Mehta (2006). "Suppression of RhoA activity by focal adhesion kinase-induced activation of p190RhoGAP: role in regulation of endothelial permeability". In: *Journal of biological chemistry* 281.4, pp. 2296–305.

Holinstat, M., D. Mehta, T. Kozasa, R. D. Minshall, and A. B. Malik (2003). "Protein Kinase Cα-Induced p115RhoGEF Phosphorylation Signals Endothelial Cytoskeletal Rearrangement". In: *Journal of Biological Chemistry* 278.31, pp. 28793–28798.

Hunter, J. J., N. Tanaka, H. A. Rockman, J. Ross, and K. R. Chien (1995). "Ventricular Expression of a MLC-2v-ras Fusion Gene Induces Cardiac Hypertrophy and Selective Diastolic Dysfunction in Transgenic Mice". In: *Journal of Biological Chemistry* 270.39, pp. 23173–23178.

Hutchinson, J. P. and J. F. Eccleston (2000). "Mechanism of nucleotide release from Rho by the GDP dissociation stimulator protein". In: *Biochemistry* 39.37, pp. 11348–59.

Inder, K. L., M. M. Hill, and J. F. Hancock (2010). "Nucleophosmin and nucleolin regulate K-Ras signaling". In: *Communicative and Integrative Biology* 3.2. 20585519[pmid] 1942-0889-3-2-26[PII] Commun Integr Biol, pp. 188–190.

Ito, Y., K. Yamasaki, J. Iwahara, T. Terada, A. Kamiya, M. Shirouzu, et al. (1997). "Regional polysterism in the GTP-bound form of the human c-Ha-Ras protein". In: *Biochemistry* 36.30. Using Smart Source Parsing Jul 29, pp. 9109–19.

Itzen, A., A. Rak, and R. S. Goody (2007). "Sec2 is a highly efficient exchange factor for the Rab protein Sec4". In: *Journal of molecular biology* 365.5, pp. 1359–67.

Jaffe, A. B. and A. Hall (2005). "RHO GTPASES: Biochemistry and Biology". In: *Annual Review of Cell and Developmental Biology* 21.1, pp. 247–269.

Jaiswal, M., R. Dvorsky, and M. R. Ahmadian (2013). "Deciphering the molecular and functional basis of Dbl family proteins: a novel systematic approach toward classification of selective activation of the Rho family proteins". In: *Journal of biological chemistry* 288.6, pp. 4486–500.

Jaiswal, M., L. Gremer, R. Dvorsky, L. C. Haeusler, I. C. Cirstea, K. Uhlenbrock, et al. (2011). "Mechanistic insights into specificity, activity, and regulatory elements of the regulator of G-protein signaling (RGS)-containing Rho-specific guanine nucleotide exchange factors (GEFs) p115, PDZ-RhoGEF (PRG), and leukemia-associated RhoGEF (LARG)". In: *The Journal of biological chemistry* 286.20, pp. 18202–12.

Karnoub, A. E. and R. A. Weinberg (2008). "Ras oncogenes: split personalities". In: *Nat Rev Mol Cell Biol* 9.7. 10.1038/nrm2438, pp. 517–531.

Katz, M. E. and F. McCormick (1997). "Signal transduction from multiple Ras effectors". In: *Current Opinion in Genetics and Development* 7.1, pp. 75–79.

Kelly, M. L., A. Astsaturov, and J. Chernoff (2013). "Role of p21-activated kinases in cardiovascular development and function". In: *Cellular and Molecular Life Sciences* 70.22, pp. 4223–4228.

Kirsten, W. H., V. Schauf, and J. McCoy (1970). "Properties of a murine sarcoma virus". In: *Bibliotheca haematologica* 36. Using Smart Source Parsing, pp. 246–9.

Klebe, C., H. Prinz, A. Wittinghofer, and R. S. Goody (1995). "The kinetic mechanism of Ran–nucleotide exchange catalyzed by RCC1". In: *Biochemistry* 34.39, pp. 12543–52.

Komarova, Y. and A. B. Malik (2010). "Regulation of endothelial permeability via para-cellular and transcellular transport pathways". In: *Annual Review of Physiology* 72, pp. 463–93.

Konstantinopoulos, P. A., M. V. Karamouzis, and A. G. Papavassiliou (2007). "Post-translational modifications and regulation of the RAS superfamily of GTPases as anticancer targets". In: *Nature reviews. Drug discovery* 6.7. Konstantinopoulos, Panagiotis A Karamouzis, Michalis V Papavassiliou, Athanasios G England Nat Rev Drug Discov. 2007 Jul;6(7):541-55., pp. 541–55.

Kyriakis, J. M. (2009). "Thinking outside the box about Ras". In: *The Journal of biological chemistry* 284.17. Kyriakis, John M J Biol Chem. 2009 Apr 24;284(17):10993-4. doi: 10.1074/jbc.R800085200. Epub 2008 Dec 17., pp. 10993–4.

Lawson, C. D. and K. Burridge (2014). "The on-off relationship of Rho and Rac during integrin-mediated adhesion and cell migration". In: *Small GTPases* 5. 2013SGTP0008R[PII] 24607953[pmid] Small GTPases, e27958.

Lazer, G. and S. Katzav (2011). "Guanine nucleotide exchange factors for RhoGTPases: Good therapeutic targets for cancer therapy?" In: *Cellular Signalling* 23.6, pp. 969–979.

Lenzen, C., R. H. Cool, H. Prinz, J. Kuhlmann, and A. Wittinghofer (1998). "Kinetic analysis by fluorescence of the interaction between Ras and the catalytic domain of the guanine nucleotide exchange factor Cdc25Mm". In: *Biochemistry* 37.20. Using Smart Source Parsing May 19, pp. 7420–30.

Lin, M.-Y., Y.-M. Lin, T.-c. Kao, H.-H. Chuang, and R.-H. Chen (2011). "PDZ-RhoGEF ubiquitination by Cullin3-KLHL20 controls neurotrophin-induced neurite outgrowth". In: *The Journal of cell biology* 193.6, pp. 985–994.

Liu, C.-A., M.-J. Wang, C.-W. Chi, C.-W. Wu, and J.-Y. Chen (2004). "Rho//Rhotekin-mediated NF-[kappa]B activation confers resistance to apoptosis". In: *Oncogene* 23.54, pp. 8731–8742.

Liu, P., H. Cheng, T. M. Roberts, and J. J. Zhao (2009). "Targeting the phosphoinositide 3-kinase pathway in cancer". In: *Nature reviews. Drug discovery* 8.8, pp. 627–44.

Loirand, G., E. Scalbert, A. Bril, and P. Pacaud (2008). "Rho exchange factors in the cardiovascular system". In: *Current Opinion in Pharmacology* 8.2, pp. 174–180.

Matallanas, D., M. Birtwistle, D. Romano, A. Zebisch, J. Rauch, A. von Kriegsheim, et al. (2011). "Raf family kinases: old dogs have learned new tricks". In: *Genes and cancer* 2.3. Matallanas, David Birtwistle, Marc Romano, David Zebisch, Armin Rauch, Jens von Kriegsheim, Alexander Kolch, Walter Genes Cancer. 2011 Mar;2(3):232-60. doi: 10.1177/1947601911407323., pp. 232–60.

Mateer, S. C., L. E. Morris, D. A. Cromer, L. B. Bensenor, and G. S. Bloom (2004). "Actin filament binding by a monomeric IQGAP1 fragment with a single calponin homology domain". In: *Cell Motility and the Cytoskeleton* 58.4, pp. 231–41.

Maurya, M. R. and S. Subramaniam (2010). "Chapter 8 - Computational Challenges in Systems Biology". In: *Systems Biomedicine*. Ed. by E. T. Liu and D. A. Lauffenburger. San Diego: Academic Press, pp. 175–223.

Mehta, D., A. Rahman, and A. B. Malik (2001). "Protein Kinase C-α Signals Rho-Guanine Nucleotide Dissociation Inhibitor Phosphorylation and Rho Activation and Regulates the Endothelial Cell Barrier Function". In: *Journal of Biological Chemistry* 276.25, pp. 22614–22620.

Mikelis, C. M., T. R. Palmby, M. Simaan, W. Li, R. Szabo, R. Lyons, et al. (2013). "PDZ-RhoGEF and LARG Are Essential for Embryonic Development and Provide a Link between Thrombin and LPA Receptors and Rho Activation". In: *Journal of Biological Chemistry* 288.17, pp. 12232–12243.

Mittal, R., M. R. Ahmadian, R. S. Goody, and A. Wittinghofer (1996). "Formation of a Transition-State Analog of the Ras GTPase Reaction by Ras·GDP, Tetrafluoroaluminate, and GTPase-Activating Proteins". In: *Science* 273.5271, pp. 115–117.

Mohan, S., D. Das, R. J. Bauer, A. Heroux, J. K. Zalewski, S. Heber, et al. (2013). "Structure of a Highly Conserved Domain of Rock1 Required for Shroom-Mediated Regulation of Cell Morphology". In: *PLoS One* 8.12, e81075.

Moy, A. B., J. E. Bodmer, K. Blackwell, S. Shasby, and D. M. Shasby (1998). "cAMP protects endothelial barrier function independent of inhibiting MLC dependent tension development". In: *American Journal of Physiology - Lung Cellular and Molecular Physiology* 274.6, p. L1024.

Nakano-Kobayashi, A., N. N. Kasri, S. E. Newey, and L. Van Aelst (2009). "The Rho-linked mental retardation protein OPHN1 controls synaptic vesicle endocytosis via endophilin A1". In: *Curr Biol* 19.13. Using Smart Source Parsing Jul 14; doi: 10.1016/j.cub.2009.05.022. Epub 2009 May 28, pp. 1133–9.

Nakhaei-Rad, S., H. Nakhaeizadeh, S. Götze, C. Kordes, I. Sawitza, M. J. Hoffmann, et al. (2016). "The role of embryonic stem cell-expressed RAS (ERAS) in the maintenance of quiescent hepatic stellate cells". In: *Journal of Biological Chemistry*.

Namekata, K., A. Kimura, K. Kawamura, C. Harada, and T. Harada (2014). "Dock GEFs and their therapeutic potential: Neuroprotection and axon regeneration". In: *Progress in Retinal and Eye Research* 43, pp. 1–16.

Narumiya, S., M. Tanji, and T. Ishizaki (2009). "Rho signaling, ROCK and mDia1, in transformation, metastasis and invasion". In: *Cancer and Metastasis Reviews* 28.1, pp. 65–76.

Neel, N. F., T. D. Martin, J. K. Stratford, T. P. Zand, D. J. Reiner, and C. J. Der (2011). "The RalGEF-Ral Effector Signaling Network: The Road Less Traveled for Anti-Ras Drug Discovery". In: *Genes and cancer* 2.3, pp. 275–287.

Nieuw Amerongen, G. P. van and V. W. M. van Hinsbergh (2002). "Targets for pharmacological intervention of endothelial hyperpermeability and barrier function". In: *Vascular Pharmacology* 39.4–5, pp. 257–272.

Nobes, C. D. and A. Hall (1999). "Rho GTPases Control Polarity, Protrusion, and Adhesion during Cell Movement". In: *The Journal of cell biology* 144.6, pp. 1235–1244.

Owen, D., L. J. Campbell, K. Littlefield, K. A. Evetts, Z. Li, D. B. Sacks, et al. (2008). "The IQGAP1-Rac1 and IQGAP1-Cdc42 Interactions: INTERFACES DIFFER BETWEEN THE COMPLEXES". In: *Journal of Biological Chemistry* 283.3, pp. 1692–1704.

Pacold, M. E., S. Suire, O. Perisic, S. Lara-Gonzalez, C. T. Davis, E. H. Walker, et al. (2000). "Crystal structure and functional analysis of Ras binding to its effector phosphoinositide 3-kinase gamma". In: *Cell* 103.6. Using Smart Source Parsing Dec 8, pp. 931–43.

Pai, E. F., U. Krengel, G. A. Petsko, R. S. Goody, W. Kabsch, and A. Wittinghofer (1990). "Refined crystal structure of the triphosphate conformation of H-ras p21 at 1.35 A resolution: implications for the mechanism of GTP hydrolysis". In: *The EMBO journal* 9.8. Using Smart Source Parsing Aug, pp. 2351–9.

Parri, M. and P. Chiarugi (2010). "Rac and Rho GTPases in cancer cell motility control". In: *Cell Communication and Signaling* 8.1, pp. 1–14.

Parrini, M. C. (2012). "Untangling the complexity of PAK1 dynamics: The future challenge". In: *Cellular logistics* 2.2, pp. 78–83.

Pasqualucci, L., P. Neumeister, T. Goossens, G. Nanjangud, R. S. K. Chaganti, R. Kuppers, et al. (2001). "Hypermutation of multiple proto-oncogenes in B-cell diffuse large-cell lymphomas". In: *Nature* 412.6844. 10.1038/35085588, pp. 341–346.

Polier, G., J. Neumann, F. Thuaud, N. Ribeiro, C. Gelhaus, H. Schmidt, et al. (2012). "The Natural Anticancer Compounds Rocaglamides Inhibit the Raf-MEK-ERK Pathway by Targeting Prohibitin 1 and 2". In: *Chemistry and Biology* 19.9, pp. 1093–1104.

Post, A., W. J. Pannekoek, B. Ponsioen, M. J. Vliem, and J. L. Bos (2015). "Rap1 Spatially Controls ArhGAP29 To Inhibit Rho Signaling during Endothelial Barrier Regulation". In: *Molecular and Cellular Biology* 35.14, pp. 2495–502.

Post, A., W.-J. Pannekoek, S. H. Ross, I. Verlaan, P. M. Brouwer, and J. L. Bos (2013). "Rasip1 mediates Rap1 regulation of Rho in endothelial barrier function through ArhGAP29". In: *Proceedings of the National Academy of Sciences of the United States of America* 110.28, pp. 11427–32.

Pulciani, S., E. Santos, A. V. Lauver, L. K. Long, K. C. Robbins, and M. Barbacid (1982). "Oncogenes in human tumor cell lines: molecular cloning of a transforming gene from human bladder carcinoma cells". In: *Proc Natl Acad Sci U S A* 79.9. Using Smart Source Parsing May, pp. 2845–9.

Raftopoulou, M. and A. Hall (2004). "Cell migration: Rho GTPases lead the way". In: *Developmental Biology* 265.1, pp. 23–32.

Rane, C. K. and A. Minden (2014). "P21 activated kinases". In: *Small GTPases* 5.1, e28003.

Reiner, D. J. and E. A. Lundquist (2016). "Small GTPases". In: *WormBook : the online review of C. elegans biology*, pp. 1–99.

Rensland, H., A. Lautwein, A. Wittinghofer, and R. S. Goody (1991). "Is there a rate-limiting step before GTP cleavage by H-ras p21?" In: *Biochemistry* 30.46. Using Smart Source Parsing Nov 19, pp. 11181–5.

Ridley, A. J. (2013). "RhoA, RhoB and RhoC have different roles in cancer cell migration". In: *Journal of Microscopy* 251.3, pp. 242–249.

Rittinger, K. (2009). "Snapshots Form a Big Picture of Guanine Nucleotide Exchange". In: *Science Signaling* 2.91, pe63–pe63.

Rodrigues, S. F. and D. N. Granger (2015). "Blood cells and endothelial barrier function". In: *Tissue Barriers* 3.1-2, e978720.

Rossman, K. L., C. J. Der, and J. Sondek (2005). "GEF means go: turning on RHO GTPases with guanine nucleotide-exchange factors". In: *Nat Rev Mol Cell Biol* 6.2. 10.1038/nrm1587, pp. 167–180.

Rumbaut, R. and P. Thiagarajan (2010). "Platelet Adhesion to Vascular Walls". In: *Platelet-Vessel Wall Interactions in Hemostasis and Thrombosis*. San Rafael (CA): Morgan and Claypool Life Sciences. Chap. 3.

Sahai, E. and C. J. Marshall (2002). "RHO-GTPases and cancer". In: *Nat Rev Cancer* 2.2. 10.1038/nrc725, pp. 133–142.

Sasaki, T. and Y. Takai (1998). "The Rho Small G Protein Family-Rho GDI System as a Temporal and Spatial Determinant for Cytoskeletal Control". In: *Biochemical and Biophysical Research Communications* 245.3, pp. 641–645.

Scheffzek, K., M. R. Ahmadian, W. Kabsch, L. Wiesmuller, A. Lautwein, F. Schmitz, et al. (1997). "The Ras-RasGAP complex: structural basis for GTPase activation and its loss in oncogenic Ras mutants". In: *Science* 277.5324. Using Smart Source Parsing Jul 18, pp. 333–8.

Scheffzek, K., M. R. Ahmadian, and A. Wittinghofer (1998). "GTPase-activating proteins: helping hands to complement an active site". In: *Trends in Biochemical Sciences* 23.7, pp. 257–62.

Schiller, M. R. (2006). "Coupling receptor tyrosine kinases to Rho GTPases—GEFs what's the link". In: *Cellular Signalling* 18.11, pp. 1834–1843.

Schmidt, V. A. (2012). "Watch the GAP: Emerging Roles for IQ Motif-Containing GTPase-Activating Proteins IQGAPs in Hepatocellular Carcinoma". In: *International Journal of Hepatology* 2012, p. 8.

Schofield, A. V. and O. Bernard (2013). "Rho-associated coiled-coil kinase (ROCK) signaling and disease". In: *Critical reviews in biochemistry and molecular biology* 48.4. Schofield, Alice V Bernard, Ora England Crit Rev Biochem Mol Biol. 2013 Jul-Aug;48(4):301-16. doi: 10.3109/10409238.2013.786671. Epub 2013 Apr 19., pp. 301–16.

Sharma, K. H. (2015). *Pathophysiology, pharmacotherapy, cardiovascular disease*. Vol. 47. Indian Journal of Pharmacology. IJPharm-47-700[PII] Indian J Pharmacol. India: Medknow Publications and Media Pvt Ltd, pp. 700–701.

Shih, C. and R. A. Weinberg (1982). "Isolation of a transforming sequence from a human bladder carcinoma cell line". In: *Cell* 29.1. Using Smart Source Parsing May, pp. 161–9.

Siddiqui, M. R., Y. A. Komarova, S. M. Vogel, X. Gao, M. G. Bonini, J. Rajasingh, et al. (2011). "Caveolin-1-eNOS signaling promotes p190RhoGAP-A nitration and endothelial permeability". In: *Journal of Cell Biology* 193.5, pp. 841–50.

Slattum, G., K. M. McGee, and J. Rosenblatt (2009). "P115 RhoGEF and microtubules decide the direction apoptotic cells extrude from an epithelium". In: *The Journal of cell biology* 186.5, pp. 693–702.

Solaro, R. J. (2000). "Myosin Light Chain Phosphatase". In: *A Cinderella of Cellular Signaling* 87.3, pp. 173–175.

Szulcek, R., C. M. Beckers, J. Hodzic, J. de Wit, Z. Chen, T. Grob, et al. (2013). "Localized RhoA GTPase activity regulates dynamics of endothelial monolayer integrity". In: *Cardiovascular Research* 99.3, pp. 471–482.

Takenouchi, T., R. Kosaki, T. Niizuma, K. Hata, and K. Kosaki (2015). "Macrothrombocytopenia and developmental delay with a de novo CDC42 mutation: Yet another locus for thrombocytopenia and developmental delay". In: *American Journal of Medical Genetics Part A* 167.11, pp. 2822–2825.

Takenouchi, T., N. Okamoto, S. Ida, T. Uehara, and K. Kosaki (2016). "Further evidence of a mutation in CDC42 as a cause of a recognizable syndromic form of thrombocytopenia". In: *American Journal of Medical Genetics Part A* 170.4, pp. 852–855.

Tcherkezian, J. and N. Lamarche-Vane (2007). "Current knowledge of the large RhoGAP family of proteins". In: *Biology of the cell / under the auspices of the European Cell Biology Organization* 99.2. Tcherkezian, Joseph Lamarche-Vane, Nathalie England Biol Cell. 2007 Feb;99(2):67-86., pp. 67–86.

Tian, Y., X. Tian, G. Gawlak, N. Sarich, D. B. Sacks, A. A. Birukova, et al. (2016). "Role of IQGAP1 in endothelial barrier enhancement caused by OxPAPC". In: *American journal of physiology. Lung cellular and molecular physiology* 26.00095.

Tian, Y., X. Tian, G. Gawlak, J. J. 3. O'Donnell, D. B. Sacks, and A. A. Birukova (2014). "IQGAP1 regulates endothelial barrier function via EB1-cortactin cross talk". In: *Molecular and Cellular Biology* 34.18, pp. 3546–58.

Vega, F. M. and A. J. Ridley (2008). "Rho GTPases in cancer cell biology". In: *FEBS Letters* 582.14, pp. 2093–2101.

Vetter, I. R. and A. Wittinghofer (2001). "The guanine nucleotide-binding switch in three dimensions". In: *Science* 294.5545. Using Smart Source Parsing Nov 9, pp. 1299–304.

Viaud, J., F. Gaits-Iacovoni, and B. Payrastre (2012). "Regulation of the DH–PH tandem of guanine nucleotide exchange factor for Rho GTPases by phosphoinositides". In: *Advances in Biological Regulation* 52.2, pp. 303–314.

Vigil, D., J. Cherfils, K. L. Rossman, and C. J. Der (2010). "Ras superfamily GEFs and GAPs: validated and tractable targets for cancer therapy?" In: *Nature reviews. Cancer* 10.12, pp. 842–57.

Vouret-Craviari, V., P. Boquet, J. Pouysségur, and E. Van Obberghen-Schilling (1998). "Regulation of the Actin Cytoskeleton by Thrombin in Human Endothelial Cells: Role of Rho Proteins in Endothelial Barrier Function". In: *Molecular Biology of the Cell* 9.9, pp. 2639–2653.

Wang, Z., M. Fu, L. Wang, J. Liu, Y. Li, C. Brakebusch, et al. (2013). "p21-Activated Kinase 1 (PAK1) Can Promote ERK Activation in a Kinase-independent Manner". In: *Journal of Biological Chemistry* 288.27, pp. 20093–20099.

Li-Weber, M. (2015). "Molecular mechanisms and anti-cancer aspects of the medicinal phytochemicals rocaglamides (=flavaglines)". In: *International Journal of Cancer* 137.8, pp. 1791–1799.

Wen, W., W. Liu, J. Yan, and M. Zhang (2008). "Structure basis and unconventional lipid membrane binding properties of the PH-C1 tandem of rho kinases". In: *The Journal of biological chemistry* 283.38. Wen, Wenyu Liu, Wei Yan, Jing Zhang, Mingjie J Biol Chem. 2008 Sep 19;283(38):26263-73. doi: 10.1074/jbc.M803417200. Epub 2008 Jul 18., pp. 26263–73.

Wennerberg, K., K. L. Rossman, and C. J. Der (2005). "The Ras superfamily at a glance". In: *Journal of Cell Science* 118.Pt 5. Wennerberg, Krister Rossman, Kent L Der, Channing J England J Cell Sci. 2005 Mar 1;118(Pt 5):843-6., pp. 843–6.

Wilde, M., M. Klausberger, D. Palmberger, W. Ernst, and R. Grabherr (2014). "Tnao38, high five and Sf9—evaluation of host–virus interactions in three different insect cell lines: baculovirus production and recombinant protein expression". In: *Biotechnology Letters* 36.4, pp. 743–749.

Williams, C. M., M. T. Harper, R. Goggs, T. G. Walsh, S. Offermanns, and A. W. Poole (2015). "Leukemia-associated Rho guanine-nucleotide exchange factor is not critical for RhoA regulation, yet is important for platelet activation and thrombosis in mice". In: *Journal of Thrombosis and Haemostasis* 13.11, pp. 2102–2107.

Wing, M. R., D. M. Bourdon, and T. K. Harden (2003). "PLC-epsilon: a shared effector protein in Ras-, Rho-, and G alpha beta gamma-mediated signaling". In: *Molecular Interventions* 3.5. Using Smart Source Parsing Aug, pp. 273–80.

Winter, J. J., M. Anderson, K. Blades, C. Brassington, A. L. Breeze, C. Chresta, et al. (2015). "Small molecule binding sites on the Ras:SOS complex can be exploited for inhibition of Ras activation". In: *Journal of Medicinal Chemistry* 58.5. Using Smart Source Parsing Mar 12; doi: 10.1021/jm501660t. Epub 2015 Feb 26, pp. 2265–74.

Wittinghofer, A. and I. R. Vetter (2011). "Structure-function relationships of the G domain, a canonical switch motif". In: *Annual Review of Biochemistry* 80. Wittinghofer, Alfred

Vetter, Ingrid R Annu Rev Biochem. 2011;80:943-71. doi: 10.1146/annurev-biochem-062708-134043., pp. 943–71.

Wittinghofer, A., K. Scheffzek, and M. R. Ahmadian (1997). "The interaction of Ras with GTPase-activating proteins". In: *FEBS Letters* 410.1, pp. 63–67.

Yin, J. C., M. Platt, X. Wu, J. A. Simpson, T. Araki, and B. G. Neel (2015). "Abstract 20130: Hypertrophic Cardiomyopathy in RAF1 Mutant-associated Noonan Syndrome Requires Complex Cellular Interplay". In: *Circulation* 132.Suppl 3, A20130–A20130.

Zhang, S.-C., K. Nouri, E. Amin, M. S. Taha, H. Nakhaeizadeh, S. Nakhaei-Rad, et al. (2014). "Classical Rho Proteins: Biochemistry of Molecular Switch Function and Regulation". In: pp. 327–340.

Zhang, W., Y. Huang, and S. J. Gunst (2016). "p21-Activated kinase (Pak) regulates airway smooth muscle contraction by regulating paxillin complexes that mediate actin polymerization". In: *The Journal of Physiology* 594.17, pp. 4879–4900.

Zhao, Z.-s. and E. Manser (2005). "PAK and other Rho-associated kinases – effectors with surprisingly diverse mechanisms of regulation". In: *Biochemical Journal* 386.2, p. 201.

Zong, H., K. Kaibuchi, and L. A. Quilliam (2001). "The Insert Region of RhoA Is Essential for Rho Kinase Activation and Cellular Transformation". In: *Molecular and Cellular Biology* 21.16. 0046[PII] 11463812[pmid] Mol Cell Biol, pp. 5287–5298.